UPS (uninterruptible power supply)/stationary batteries: Long idle periods at full SOC; rapid discharge when required (discharge time in the range of 10 min to 1 h, in some applications even longer); designs for lifetimes of up to 20 years available and market grows strongly in connection with the expansion of telecommunications and computer systems. The electrodes are thicker than for SLI applications to withstand corrosion for long periods.

Traction batteries: Application in fork-lift trucks, traction engines, underground mining vehicles and so on; designed for daily complete cycling with moderate currents and regular and controlled complete charging and cycle lifetimes of 1000 to 2000 cycles with 80% DOD can be achieved. The most common electrode technology in these applications is tubular-plate. Flooded batteries show longer lifetimes than VRLA and are widely used.

Electric-vehicle batteries: Widely fluctuating current profile; partial recharging phases (regenerative braking); inadequate lifetimes to date; expanding market and strong competition from other types of battery technology (see Table 18.3). Low gravimetric energy density is a major drawback in this application. Lead acid batteries based on thin pasted lead foils and wounded design are currently under development and are already available in the market from some manufacturers to serve hybrid vehicles[11] that are seen at the moment as a more realistic option than purely battery-powered electric vehicles. Wounded cells have very high power capability and therefore can serve electric motors for accelerating and regenerative breaking.

Batteries for photovoltaic systems: Operating conditions corresponding to the load profiles illustrated in Section 18.3; complete charging very seldom and many partial cycles. Two classes of so-called "solar batteries" are in the market. One class is the modified SLI battery with typically thicker grids than those used in SLI batteries, quite cheap (often from local production in developing countries [17]) but with limited lifetime. The other class of "solar batteries" are modifications from high-quality batteries originally used for cycling or standby applications. In general, flooded batteries show better lifetimes in autonomous power supply systems than VRLA batteries. On the other hand, VRLA batteries have significant advantages concerning electrolyte spillage, maintenance and transport and very little release of corrosive and explosive gases. This reduces the requirements on the battery housing significantly. Therefore, a final choice must be made according to the specific application and the boundary conditions.

Operational experience, however, reveals that the lifetime of batteries in stand-alone applications based on solar energy is in general unsatisfactory compared to battery lifetimes in traditional applications. Batteries in solar home systems normally have to be exchanged after 2 to 3 years and batteries in hybrid systems after 3 to 8 years. Lifetime extensions to 5 years in solar home systems and 10 years in hybrid systems are achievable with advanced batteries designed for the purposes of autonomous power supply systems and appropriate system designs and operation strategies.

[11] Hybrid vehicles have a conventional motor but with less power than in traditional cars. Acceleration is supported by electric motors powered by the batteries. The batteries are charged during regenerative breaking and from the main motor. This concept allows the conventional motor to run with small variations in power and therefore at higher efficiencies. Fuel consumption was reduced with this concept in prototypes down to 2 l/100 km.

Downloaded from https://onlinelibrary.wiley.com/doi/ by <Shibboleth-member@purdue.edu, Wiley Online Library on [25/08/2024]. See the Terms and Conditions (https://onlinelibrary.wiley.com/terms-and-conditions) on Wiley Online Library for rules of use; OA articles are governed by the applicable Creative Commons License

Downloaded from https://onlinelibrary.wiley.com/doi/ by <Shibboleth-member@purdue.edu, Wiley Online Library on [25/08/2024]. See the Terms and Conditions (https://onlinelibrary.wiley.com/terms-and-conditions) on Wiley Online Library for rules of use; OA articles are governed by the applicable Creative Commons License

18.4.7.3 Discharge capacity

The capacity that can be withdrawn from lead acid batteries depends strongly on the discharge conditions.

For stationary batteries usually the C_{10} or C_8 capacity, for starter batteries usually the C_{20} capacity and for traction batteries usually the C_5 capacity is specified. Solar batteries often are rated as C_{100} and C_{120} at 100 or 120-h discharge current, respectively. Typical end-of-discharge voltage is 1.8 V/cell or 1.85 V/cell for C_{10}, C_{20} and C_{100}. For C_5, 1.7 V/cell is commonly used. All other ratings and voltage limits can be found as well.

The measured and the practical capacity increase when the discharge current decreases. If a battery is discharged with a lower current than the rated current, a higher capacity than the rated capacity can be withdrawn. If the state of charge is specified with respect to the rated capacity (a reasonable convention), negative values for the state of charge can arise. This is the reason Figure 18.6 displays negative states of charge.

Figure 18.16 shows the voltage during discharge as a function of the discharged capacity at different discharge currents. The lead acid batteries' capacity depends very much on the discharge current.

As a rule of thumb, it can be assumed that a battery with a nominal capacity of 100 Ah at C_{10} has approximately 50 Ah at C_1 and approximately 130 Ah at C_{100}. Please note the fact that the corresponding currents I_1 and I_{100} are not equivalent to $10 \times I_{10}$ res. $0.1 \times I_{10}$. In this example, I_1 is 50 A and I_{100} is 1.3 A.

With respect to the electrical properties, the temperature influences the inner resistance (increasing conductivity of the electrolyte with increasing temperature), the diffusion

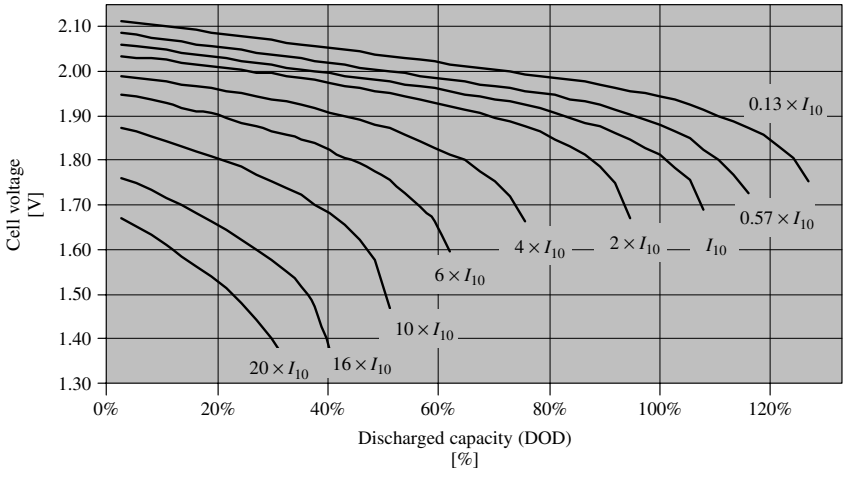


Figure 18.16 Voltage during constant discharge as a function of the discharged capacity at different discharge currents (tubular-plate lead acid battery, C_{10} capacity defined at I_{10} and 1.8 V), data from Berndt D, *Blei-Akkumulatoren (Varta)*, VDI-Verlag, 11. Auflage, Düsseldorf (1986) [18]

processes and the reaction at the electrochemical double layer. Therefore, the capacity of lead acid batteries depends strongly on the temperature. The capacity increases almost linearly by approximately 0.6%/K with an increase in temperature. The capacity decreases in the same way with decreasing temperatures. Depending on the battery technology, the temperature coefficient can be as high as 1.0%/K.

18.4.7.4 Ageing processes and their influence on the battery properties

A comparison with other battery systems, for example, NiCd batteries, reveals that the relatively short lifetime of lead acid batteries is a significant disadvantage. However, the operating behaviour of the batteries is already affected during the lifetime by the processes responsible for ageing. Thus, it is helpful to be aware of the most important ageing processes and to avoid the conditions that accelerate them.

18.4.7.4.1 Acid stratification

Acid stratification is not an ageing process but affects the operating behaviour of the battery. On one hand it reduces the available capacity and changes the current/voltage characteristics. On the other hand it leads to inhomogeneous current distribution at the electrodes. The latter effect accelerates sulphation (Section 18.4.7.4.2), which is a major ageing effect. Therefore, acid stratification is a reason for ageing and not an ageing effect by itself. Acid stratification in flooded batteries can be removed immediately by stirring the electrolyte.

Because the electrolyte functions as an active component of the electrode reaction, local variations in the density can arise, with the result that the acid density decreases in the upper part of the cell and increases in the lower part. The potential difference associated with the concentration difference leads to discharging of the lower section of the electrodes, which can result in irreversible ageing effects (e.g. sulphation).

In batteries with liquid electrolytes, the acid stratification can be eliminated by deliberate overcharging, associated with gas production. The same mixing effect can be achieved by active circulation of the electrolyte. Such electrolyte stirring systems are made from an air bubbling system (Figure 18.22).

Electrolyte stratification can also occur in batteries with immobilised electrolytes. In a gel battery, the effect is very small and therefore is of little relevance. In AGM batteries, the strength of acid stratification depends very much on the quality of the glass mat. Large battery cells from AGM technology are mounted vertically to avoid any acid stratification. While purchasing the batteries, it is important to check the manufacturer's specifications regarding vertical installation of the battery. The problem with VRLA batteries is that an existing acid stratification cannot be removed.

From theoretical consideration [19, 20], it is obvious that small currents in conjunction with acid stratification lead to a significant undercharging of the lower part of the electrodes. This effect is getting more and more pronounced with smaller battery currents. When an acid stratification occurs, the upper part of the electrodes is charge preferential and the lower part is discharge preferential. This results in differences in the local state of charge between the upper and the lower part of up to 30%. During the limited charging

Downloaded from https://onlinelibrary.wiley.com/doi/ by <Shibboleth-member@purdue.edu>, Wiley Online Library on [25/08/2024]. See the Terms and Conditions (https://onlinelibrary.wiley.com/terms-and-conditions) on Wiley Online Library for rules of use; OA articles are governed by the applicable Creative Commons License

times, the upper part can reach a very high state of charge while the lower part is by far not completely charged. This means, that the lower part of the electrode is cycled in lower states of charge than from the average state of charge of the electrode. Further, the lower part is cycled without a full charge for extended periods.

These findings are confirmed twofold by experimental results. On one hand, it was possible to show experimentally the effect of inhomogeneous current distribution and the state of charge within the electrode as a function of the charge/discharge currents [20]. On the other hand, almost all physicochemical analysis of lead acid batteries from PV systems at the end of their lifetime shows a high degree of sulphation in the lower part of the electrodes [21, 22].

Another problem related to acid stratification in batteries with liquid electrolytes is that a measurement of the acid density, made at the only accessible position above the electrodes, does not give any direct information on the battery's state of charge.

As an example, Figure 18.17 shows the correlation between the acid density above the electrodes in a flooded battery and the battery's state of charge for a battery from a PV system, with a large number of partial cycles.[12] Without acid stratification, a measured acid density of, for example, 1.18 g/cm^3 corresponds to a real state of charge of approximately

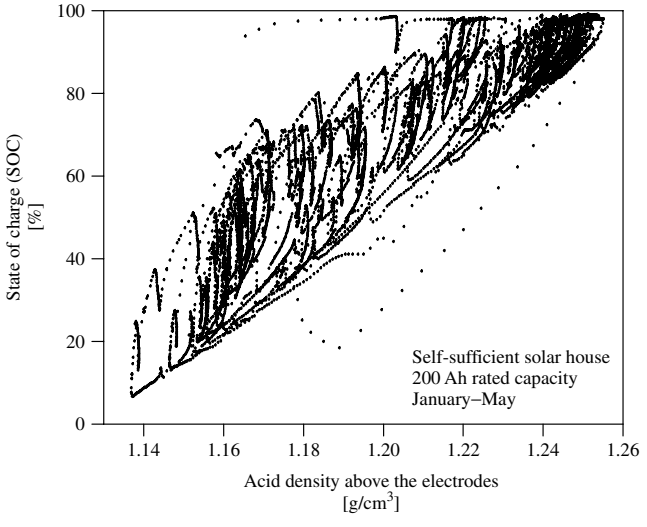


Figure 18.17 Acid density above the electrodes versus the actual state of charge, measured over five months for a battery from a photovoltaic system (200 Ah cells, simulated acid densities based on measured initial data 10-minute average values)

[12] Figure 18.17 is based on a detailed battery model including modelling of the vertical acid-density distribution. The model was verified by measurements in a battery. The model and verification are described in [19]. Therefore, the state of charge and the acid density above the electrode displayed in Figure 18.18 are calculated by the model. The calculations are based on detailed measurements of the battery current, voltage and temperature in the system.

Petitioner Canadian Solar (USA) Inc., Ex. 1035, p. 2224

Downloaded from https://onlinelibrary.wiley.com/doi/ by <Shibboleth-member@purdue.edu, Wiley Online Library on [25/08/2024]. See the Terms and Conditions (https://onlinelibrary.wiley.com/terms-and-conditions) on Wiley Online Library for rules of use; OA articles are governed by the applicable Creative Commons License

30%, whereas it can range between approximately 30% and 75% if the acid is stratified. This measurement only allows a lower limit to be estimated. A measurement of the acid density above the electrodes can lead to appreciable errors in determining the state of charge and thus in associated operation-management measures.

18.4.7.4.2 Sulphation

When the electrodes are discharged, the active masses, PbO_2 and Pb, are transformed into $PbSO_4$. The size of the sulphate formed depends on the strength of the discharge current – high discharge currents result in small sulphate crystals. If a battery is not recharged soon after its discharge, the sulphate crystals grow as a result of recrystallisation processes. The rate of recrystallisation is linearly correlated with the solubility of sulphate ions. Unfortunately, the solubility of sulphate ions increases with decreasing acid concentration [15]. Therefore, periods of low states of charge (and hence low acid concentrations and high sulphate solubility) harm the battery by accelerating the growth of large sulphate crystals. During subsequent charging, large sulphate crystals with their relatively smaller active surface are re-dissolved more slowly than smaller ones, so that sulphate crystals are still present when charging is nearly finished. Figure 18.18 illustrates that for the same volume, small crystals have a larger surface area than large ones (two-dimensional representation of the three-dimensional effect).

During the course of the operation, these remaining sulphate crystals can accumulate, reducing the active mass and thus the accessible capacity [23]. Sulphation can be reduced to a minimum if each discharging process is rapidly followed by sufficiently complete charging. The effect of acid stratification is that complete charging is seldom achieved for the lower part of the electrode, so that strong sulphation occurs there. This sulphation effect can be clearly seen in the cross-sections of Figure 18.19.

As a result of sulphation, the amount of active material available for normal charging and discharging operations decreases. This reduces the capacity, and the voltage during discharge is also shifted to lower values. If sulphation is too pronounced (as in the lower section shown in Figure 18.19), larger areas of the electrodes can become completely inactive.

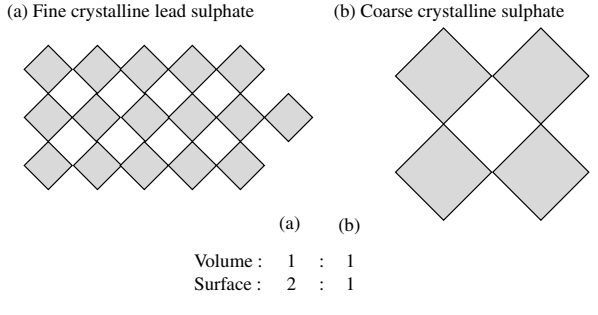


Figure 18.18 An example illustrating the effect of the crystal size on the active surface area of the electrodes. Mass ratio a:b = 1:1, surface area ratio a:b = 2:1

Downloaded from https://onlinelibrary.wiley.com/doi/ by <Shibboleth-member@purdue.edu>, Wiley Online Library on [25/08/2024]. See the Terms and Conditions (https://onlinelibrary.wiley.com/terms-and-conditions) on Wiley Online Library for rules of use; OA articles are governed by the applicable Creative Commons License

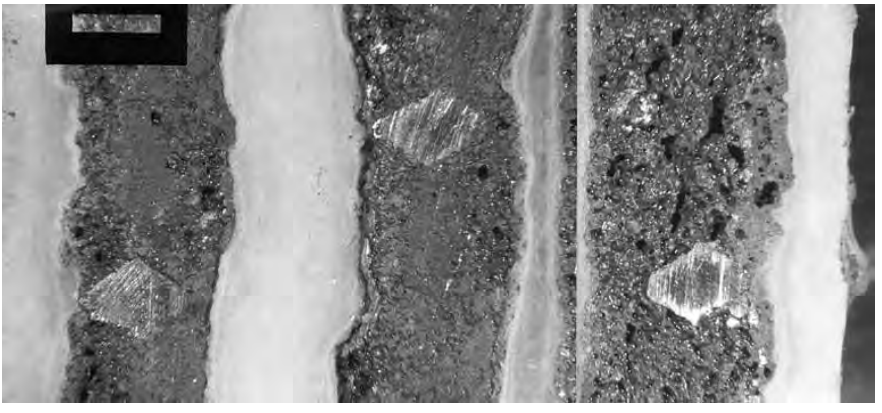


Figure 18.19 Cross-section of a negative flat-plate electrode after 3.5 years of operation in a photovoltaic system. The sections were taken from the upper, central and lower parts of the electrode (from left to right, respectively). Sulphation is clearly indicated in the lower section by the very coarse pores between large crystals, and by the noticeable broadening of the electrode, due to the difference in the specific volumes of Pb and $PbSO_4$ (Photo source: ZSW)

18.4.7.4.3 Corrosion

The high positive potential at the positive electrode results in the corrosion of the lead grid [24]. On one hand, this causes the cross-section of the grid to decrease, so that the grid resistance increases. On the other hand, a layer consisting of lead dioxide, lead oxide and lead sulphate forms between the grid and the active material, which also raises the contact resistance. This becomes evident during charging and discharging as an increased ohmic voltage drop. Figure 18.20 shows the cross-section of a tubular electrode from a battery after 3.5 years of operation. The lead core (grid rod in the centre of the tube) has almost completely disappeared due to corrosion.

The corrosion rate depends on the acid density, the electrode potential, the temperature, the grid alloy, the active material coverage [25] and a most important factor, the manufacturing quality of the grid. Corrosion is particularly pronounced for cell voltages below 2.0 V and above 2.4 V [24]. Corrosion is minimal for cell voltages around 2.23 V. Corrosion is an irreversible ageing effect and increases the internal resistance of the battery. An indirect consequence is that the current distribution becomes more inhomogeneous in the vertical direction, so that sulphation is accelerated in the lower parts of the electrodes. In batteries for PV systems, thicker grids are used to reduce the effect of corrosion and thus extend the lifetime.

18.4.7.4.4 Erosion

Both electrodes are subjected to strong mechanical loads during cycle operation. The reason is that up to 50% of the active material is converted to lead sulphate during discharge. Lead sulphate has a volume per mole, which is 1.94 times larger than lead dioxide and 2.4 times larger than lead.

Downloaded from https://onlinelibrary.wiley.com/doi/ by <Shibboleth-member@purdue.edu, Wiley Online Library on [25/08/2024]. See the Terms and Conditions (https://onlinelibrary.wiley.com/terms-and-conditions) on Wiley Online Library for rules of use; OA articles are governed by the applicable Creative Commons License

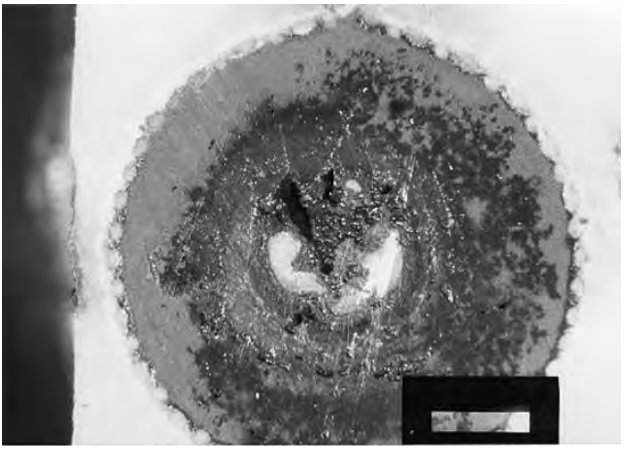


Figure 18.20 Cross-section through a tubular electrode of a battery after 3.5 years of operation. The lead rod (light-coloured area in the centre) has almost completely disintegrated as a result of corrosion. The diameter of the electrode is 8 mm. (Photo source: ZSW)

These large changes in volume act to loosen the active material. This effect increases with increasing depth of discharge. Thus, deep discharge with low currents has an additional negative effect on sulphation. Once the active material has become loose, it can be separated from the electrode, for example, by gas movement, and gathers as sludge at the base of the battery. If the volume below the electrodes that contains the sludge is not large enough, there is a danger of short circuits between the electrodes.

The erosion effect is much less pronounced in sealed batteries, as the electrodes there can be mounted under pressure. The pressure compensates the forces arising from the volume change and increases the stability of the active masses.

The available active mass at the electrodes is reduced by the loss due to erosion. This corresponds directly to a reduction in the accessible capacity. Accordingly, the battery will be discharged earlier.

18.4.7.4.5 Short circuits

In addition to the danger of short circuits in the sludge volume of batteries with liquid electrolytes, there are two further risks for short circuits.

The plate connectors from the positive electrode above the active material are also subject to corrosion. This results in detachment of large corrosion flakes, which can fall onto the electrodes and cause short circuits. This risk can be eliminated by including separators that extend upward well over the electrodes.

Further, there is a risk for all battery types that dendrites (microscopic short circuits) may grow from the positive to the negative electrode through the separators. These dendrites are so fine that they are usually not visible even when the battery is investigated

Downloaded from https://onlinelibrary.wiley.com/doi/ by <Shibboleth-member@purdue.edu>, Wiley Online Library on [25/08/2024]. See the Terms and Conditions (https://onlinelibrary.wiley.com/terms-and-conditions) on Wiley Online Library for rules of use; OA articles are governed by the applicable Creative Commons License

in the laboratory. Their growth is accelerated by long periods at a low state of charge and thus low acid concentrations. As described in Section 18.4.7.4.2, the solubility of $PbSO_4$ increases at low acid concentrations. For example, the solubility of $PbSO_4$ is 2 mg/l at a sulphuric acid density of 1.28 g/cm^3, and is already 35 mg/l at a density of 1.02 g/cm^3. The higher the solubility the higher is the rate of recrystallisation and hence the rate of formation of large sulphate crystals and dendrites. The danger of dendrite growth can be counteracted by thicker separators and by operating the battery at high states of charge.

In general, a short circuit is a defect that causes a sudden and complete breakdown in the battery. Short circuits can occur from dendrites between the electrodes and the sludge in flooded batteries from active material accumulated as a result of active-material shedding under the electrodes. If the amount of material exceeds the free-electrolyte height under the electrodes, short circuits occur through the "mud". Microscopic short circuits through the separator affect particularly the self-discharging properties of a battery.

18.4.7.4.6 Reverse charging

If a battery is subjected to a discharging current even after the battery has been fully discharged, the potential changes its sign.

Reverse charging of an individual cell can occur in strings of series-connected cells. The battery voltage and therefore the depth of discharge protection are controlled on the basis of overall string voltage. A single cell within the string may have lower capacity due to manufacturing deviations or due to accelerated ageing. In consequence, the low-capacity cell can be over-discharged resulting in reverse charging.

In case of reverse charging, PbO_2 is formed at the original Pb electrode and vice versa. Although this type of reverse charging can sometimes increase the capacity for a short time, it is certainly detrimental to the cell lifetime in the long term. The main cause of damage is the oxidation of additives in the lead sponge of the negative electrode, which are included to maintain the high porosity of the electrode. If these additives are destroyed, large lead crystals form in the negative electrode resulting in a loss of internal surface area and therefore in an irreversible loss of capacity.

The danger of reverse charging can be reduced if the voltage of the individual cells is monitored and used as the criterion to end discharging (rather than the total voltage of the battery). Alternatively, it can be prevented by allowing charge equalisation between the cells of a series connection [12].

18.4.7.4.7 Ice formation

Figure 18.21 shows the dependence of the freezing point of diluted sulphuric acid on the electrolyte concentration. Ice must be prevented from forming in a battery under all circumstances, as it is then practically impossible to operate the battery (in particular, a frozen battery can hardly be charged) and it is possible that the cell housing may burst (battery breakdown and contamination of the surroundings with sulphuric acid).

For operating modes with very low discharge currents, or if the deep-discharge protection is inactive or non-existent, it is possible to reach extremely deep discharge,

Downloaded from https://onlinelibrary.wiley.com/doi/ by <Shibboleth-member@purdue.edu, Wiley Online Library on [25/08/2024]. See the Terms and Conditions (https://onlinelibrary.wiley.com/terms-and-conditions) on Wiley Online Library for rules of use; OA articles are governed by the applicable Creative Commons License

Petitioner Canadian Solar (USA) Inc., Ex. 1035, p. 2228

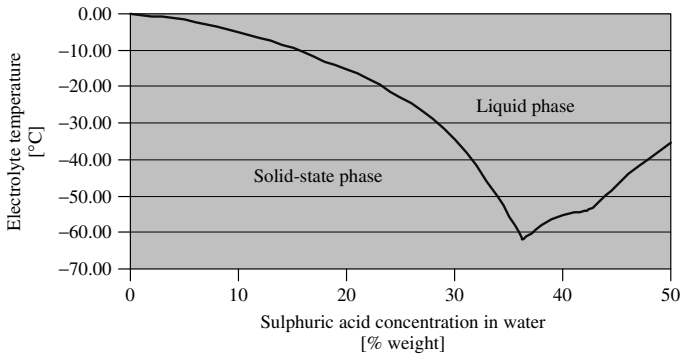


Figure 18.21 Freezing point of diluted sulphuric acid as a function of the acid concentration

as the voltage does not break down until very late in the process. Batteries that are subjected to temperatures below the freezing point should be dimensioned such that after withdrawing $1.3 \times C_{100}$ or $1.7 \times C_{10}$, the acid density is still so high that freezing is not expected, according to Figure 18.21.

18.4.7.5 Battery peripherals

For proper battery operation, several battery peripherals must be used. The following gives a brief description of the most important devices.

Charge controller: Charge controllers are responsible for the charging strategies and the deep-discharge protection. They limit the power from the PV generator if necessary. More details on the operation strategies are given in Section 18.4.7.6 and on the hardware in Chapter 19.

Chargers: Chargers are AC/DC converters that use the power from motor generators to recharge the battery. They need a charge control as well to avoid overcharging of the battery. The charging regime should be the same as for charge controllers.

Charge equaliser: In long strings of series-connected cells, problems with individual cells like overcharging and reverse charging can occur owing to differences in the ageing processes or tolerances in the production. Charge equalisers avoid the detrimental effects by individual treatment of the cells. More details are given in [13] and in Chapter 19.

Monitoring: To get actual information of the state of the battery, monitoring systems can be used. A wide range of commercial products is available. They range from simple voltage monitoring of the complete battery to complete monitoring of temperature, current and voltage of individual blocks and cells as well as impedance of the battery.

State-of-charge meters: For proper battery operation (Section 18.4.7.6) and for the orientation of the user, it is helpful to have proper information on the actual state of charge of the battery. Several devices and algorithms are available, but only very few are really suited to autonomous power supply systems [26].

Downloaded from https://onlinelibrary.wiley.com/doi/ by <Shibboleth-member@purdue.edu>, Wiley Online Library on [25/08/2024]. See the Terms and Conditions (https://onlinelibrary.wiley.com/terms-and-conditions) on Wiley Online Library for rules of use; OA articles are governed by the applicable Creative Commons License

Electrolyte-agitation systems: To avoid the detrimental effects of acid stratification in flooded batteries, electrolyte-agitation systems are an effective solution. Figure 18.22 shows a battery with an agitation system. Most systems are based on compressed air that is pumped to the bottom of the cells. The ascending air bubbles cause an electrolyte circulation and mixing.

Recombinators: To reduce the loss of water from flooded batteries, recombinators are used. They consist of a catalyser that recombines the hydrogen and oxygen gas evolving from flooded batteries. Figure 18.22 shows a battery with recombinators.

18.4.7.6 Operation strategies

The operation strategy and the charging strategy have an important impact on the battery lifetime. Therefore, in the following paragraphs some ideas on appropriate strategies are discussed.

In most PV systems, the system and the battery control are realised through the charge controllers; in some cases energy management systems take over this job. The battery requires proper handling of frequent full charges, gassing for electrolyte-stirring in flooded batteries, control of end-of-charge voltage and deep-discharge protection.



Figure 18.22 Flooded, tubular-plate battery (2 × 240 Ah in parallel connection, 12 V) with gas recombinators for reduction of water loss through gassing and an electrolyte-stirring system to avoid acid stratification (only connected to the right hand unit), the membrane air pump is mounted on the wall, operation of the pump: twice a day for 15 min, (Picture courtesy Fraunhofer ISE)

Petitioner Canadian Solar (USA) Inc., Ex. 1035, p. 2230

Downloaded from https://onlinelibrary.wiley.com/doi/ by <Shibboleth-member@purdue.edu, Wiley Online Library on [25/08/2024]. See the Terms and Conditions (https://onlinelibrary.wiley.com/terms-and-conditions) on Wiley Online Library for rules of use; OA articles are governed by the applicable Creative Commons License

Downloaded from https://onlinelibrary.wiley.com/doi/ by <Shibboleth-member@purdue.edu>, Wiley Online Library on [25/08/2024]. See the Terms and Conditions (https://onlinelibrary.wiley.com/terms-and-conditions) on Wiley Online Library for rules of use; OA articles are governed by the applicable Creative Commons License

18.4.7.6.1 Charging

As a result of the specific operating conditions, full charging occurs very rarely. Charge and discharge cycles follow each other very frequently. Long charging times at constant power supply as available in grid-connected systems do not occur. Nevertheless, field experience showed that full charging is necessary to achieve long battery lifetimes.

The most common charging strategy is the constant current/constant voltage mode (*IU* or cccv, Figure 18.23(a)). In autonomous power supply systems, this means that the battery is charged with the fully available power until the battery voltage reaches the defined end-of-charge voltage. From this moment, the charging power to the battery is limited in a way that this voltage limit is not exceeded (constant voltage mode). The voltage drops at the moment when the battery charging is not high enough (due to decreasing power generation or increasing load) to maintain the battery voltage at the given limit. Most charge regulators and battery chargers use this charging procedure.

A more advanced charging method is shown in Figure 18.23(b). The charging starts with a constant current/constant voltage charging, but the maximum voltage is reduced after a certain time to a lower limit (IU_0U). This allows higher voltages during the first constant–voltage phase, but avoids negative effects like gassing and corrosion due to long durations of the high voltage. Therefore, this charging method allows overall faster charging but avoids hazardous conditions in the battery. More and more sophisticated charge controllers in the market use this charging procedure.

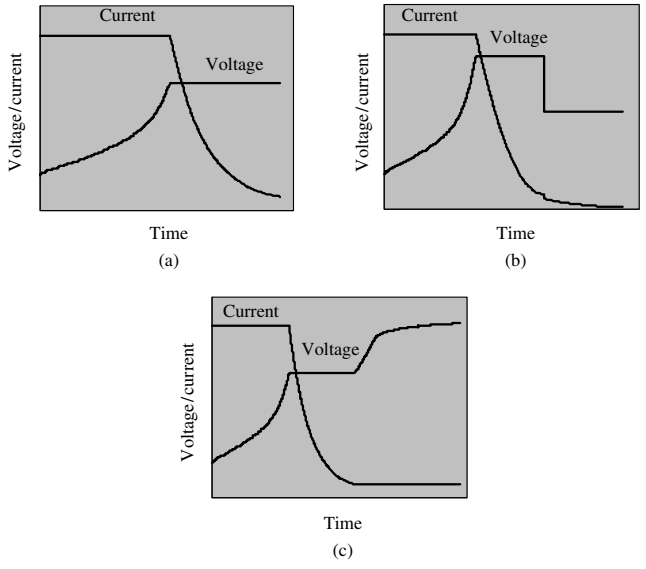


Figure 18.23 Schematics of different charge regimes. (a) Current and voltage during a constant current/constant voltage charge *IU* or cccv; (b) a constant current/constant voltage charge with two end-of-charge voltage limits IUU_0; and (c) a constant current/constant voltage charge followed by a limited constant current phase IUI_a are shown

Especially for VRLA batteries, it turned out that longer lifetimes can be achieved with the constant current/constant voltage/constant current (IUI_a) charging as shown in Figure 18.23(c) ([4]). After the current drops during the constant-voltage phase below the limit for I_a charging, the charging is continued for a limited time or amount of charge with a constant current. The voltage is not limited during this phase, but the I_a current must be limited in the range of I_{50} to I_{100}. No commercial device in PV applications uses such a scheme these days.

It is necessary to take into account that the batteries in PV systems hardly ever get fully charged due to the limited charging time per day [4]. Therefore, the term full charge has to be distinguished in a real full charge, defined by the point at which the complete active material is converted into charged material, and a practical or solar full state of charge (Figure 18.3). The latter is defined by the maximum state of material conversion that can be achieved during a sunny summer day or the maximum operation time of the back-up generator that is accepted by the system operator. A "solar full charge" requires at least 5 h at a battery voltage of 2.4/cell.

In hybrid systems, a solar full charging can be achieved by operation of the back-up generator or from the PV generator. Full charging every four weeks is recommended. A detailed analysis of the operational data from systems showed that this has little impact on the overall energy balance, but is obviously enhancing the battery lifetime.

For batteries in systems of Class 1, according to Figure 18.6 an end-of-charge voltage of 2.4 V/cell is appropriate. However, the duration per day at this voltage should be limited to two hours. During the rest of the day (if the charging power is available), the battery voltage should be limited to 2.3 V/cell (charging regime as in Figure 18.23(b)).

In systems of Classes 2, 3 and 4, the end-of-charge voltage should be 2.45 V/cell also limited to 2 hours per day. An end-of-charge voltage of 2.35 V/cell for the rest of the day is appropriate (charging regime as in Figure 18.23(b)).

The values are valid for flooded and for VRLA batteries. In addition, for flooded batteries an increase of the end-of-charge voltage up to 2.6 V/cell periodically for a maximum of 5 hours per 14 days is appropriate. This causes gassing and therefore stirring of the electrolyte. Nevertheless, an active electrolyte-stirring system as shown in Figure 18.22 is the best and most efficient solution.

A significant lifetime extension can be achieved if the battery is charged to a really full SOC at least twice a year. This can be achieved by charging the battery normally to a solar-full SOC followed by a complete discharge with approximately I_{10}. The discharge must be followed by a recharge according to the IUI_a charging regime (Figure 18.23c) where the battery gets charged with 110 to 120% of the ampere-hour capacity taken from the battery in the previous discharge or the nominal capacity (whatever value is higher).

The end-of-charge voltage limit depends on the battery-operating condition and on the temperature. All values for the voltage limits given here are for a battery temperature of 25°C. At increasing temperatures, the voltage must be reduced by 4 to 5 mV/(K*cell) but not below 2.25 V/cell. At temperatures below 25°C, the voltage must be increased accordingly but not above 2.6 V/cell. To protect DC loads or electronic devices connected directly to the DC bus bar, it might be necessary to limit the maximum voltage accordingly.

Downloaded from https://onlinelibrary.wiley.com/doi/ by <Shibboleth-member@purdue.edu>, Wiley Online Library on [25/08/2024]. See the Terms and Conditions (https://onlinelibrary.wiley.com/terms-and-conditions) on Wiley Online Library for rules of use; OA articles are governed by the applicable Creative Commons License

Downloaded from https://onlinelibrary.wiley.com/doi/ by <Shibboleth-member@purdue.edu>, Wiley Online Library on [25/08/2024]. See the Terms and Conditions (https://onlinelibrary.wiley.com/terms-and-conditions) on Wiley Online Library for rules of use; OA articles are governed by the applicable Creative Commons License

18.4.7.6.2 Deep-discharge protection

Lead acid batteries suffer from deep discharge for several reasons. An increasing depth of discharge results in a decreasing acid concentration and due to the increased sulphate solubility in accelerated sulphation (Section 18.4.7.4.2), corrosion (Section 18.4.7.4.3) and higher sensitivity to freezing (Section 18.4.7.4.7). Further, the mechanical stress is increased because of the changes in the specific volume of the active materials and in long battery strings, the risk of reverse charging of single cells (Section 18.4.7.4.6) increases.

Therefore, the maximum depth of discharge should be limited during normal operation.[13]

While choosing the appropriate DOD for the operation strategy, the data-sheet information given by the manufacturers should be analysed. They often give the number of cycles during the lifetime of a battery as a function of the depth of discharge. However, for the system design the number of cycles is not the most important parameter. The level of capacity throughput that can be realised during the battery lifetime is of more relevance. A cycle with 50% DOD means that only 50% of the capacity is used and therefore the overall capacity throughput for, for example, 200 cycles with 50% DOD is equivalent to 100 cycles with 100% DOD. However, from the point of view of the system design a battery which is limited to 50% DOD during normal operation must have double the size with respect to a battery with 100% DOD during normal operation. This is worthy of mention because batteries are always limited by the capacity throughput on one hand and by operation life on the other hand. Therefore, it makes no sense to operate a battery which is, for example, rated for 10 000 cycles at 20% DOD in autonomous power supply systems even though this might promise the highest capacity throughput. Assuming that on a daily basis 10 000 cycles take place, it would take more than 25 years to achieve this. However, the battery lifetime would not last that long due to other ageing processes.

Figure 18.24 shows for two different batteries the cycle life as a function of the DOD (data taken from data sheets) and the resulting capacity throughput. It is obvious that for the battery Type 2, the capacity throughput is almost independent of the DOD but for battery Type 1 there is a strong dependency leading to higher throughputs at lower DODs.

For practical purposes, the following "rules" can be used, which have proved their suitability in the field. In Classes 1 and 2 (Section 18.3.2), the maximum DOD should be 60 to 70% and in Classes 3 and 4, 80 to 90%. The lower values are for flooded batteries and the higher values are for VRLA batteries. Low-cost "solar batteries" should be operated to a maximum of 50% DOD. It is very important to take into account that the mentioned values for the DOD are given on the basis of the C_{10} capacity. Using, for example, 80% of the C_{100} capacity means using more than 100% of the C_{10} capacity and this is hazardous.

Control of the maximum DOD can be realised either by deep-discharge disconnecting voltage or on the basis of the state of charge. Most commercial charge controllers

[13] As stated in the subsection on charging, a complete discharge of the battery to 100% DOD twice a year is of benefit to the battery. This is not in contradiction to a limited DOD during normal operation. The defined discharge is done within a short time and is followed directly by complete recharging of the battery. In normal operation, discharge times and duration in deep states of charge can be very long and the next full charging may occur only weeks or month later.

Petitioner Canadian Solar (USA) Inc., Ex. 1035, p. 2233

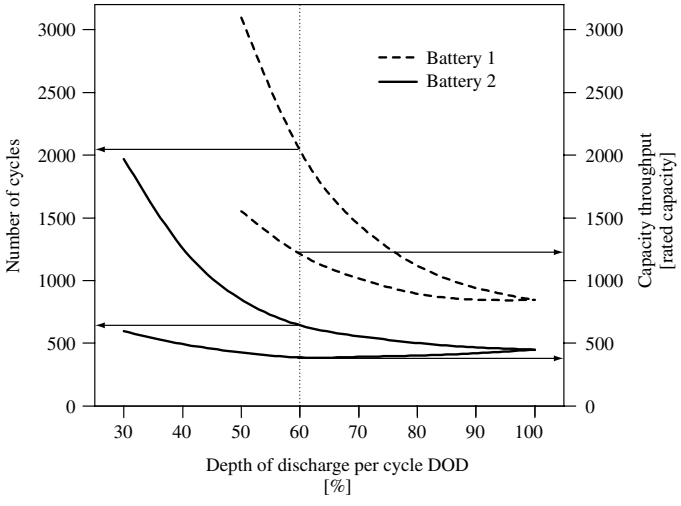


Figure 18.24 Number of cycles and overall charge transfer (capacity throughput) in units of the rated capacity during the battery lifetime as a function of the depth of discharge during cycling. Data from data sheets from battery manufacturers

Table 18.5 Typical end-of-discharge voltages up to which 100% of the C_{10} capacity has been discharged from the battery at different discharge currents at room temperature

$I_{discharge}$	U [V/cell]
$1.0 \times I_{10}$	1.80–1.85
$0.5 \times I_{10}$	1.85–1.90
$0.2 \times I_{10}$	1.90–1.95
$0.1 \times I_{10}$	1.95–2.00

control the maximum DOD by the voltage. The drawback of this method is that the discharged capacity up to a certain voltage limit depends very much on the discharge current. Table 18.5 shows typical end-of-discharge voltages up to which 100% of the C_{10} capacity has been discharged from the battery. This shows the problem of an efficient DOD control. If the maximum DOD is assured by a high voltage limit even at small currents (e.g. 1.95 V/cell), the available capacity at higher currents is very limited [27]. Figure 18.25 shows a more pronounced version of the problem. A given voltage limit might be appropriate for one battery type, but for another with the same technology (flat plates, lead acid and flooded electrolyte) the discharge curve looks quite different and the same voltage limit results in significant differences in the maximum DOD with respect to the minimum SOC defined to protect the battery as shown in the figure. The difference

Petitioner Canadian Solar (USA) Inc., Ex. 1035, p. 2234

Downloaded from https://onlinelibrary.wiley.com/doi/ by <Shibboleth-member@purdue.edu, Wiley Online Library on [25/08/2024]. See the Terms and Conditions (https://onlinelibrary.wiley.com/terms-and-conditions) on Wiley Online Library for rules of use; OA articles are governed by the applicable Creative Commons License

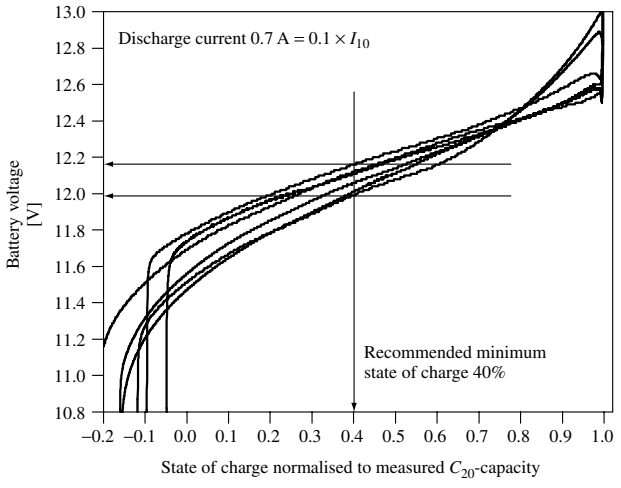


Figure 18.25 Discharge curves of six batteries rated for the same capacity, with the same technology (flat plate, flooded lead acid and all batteries new). The voltage is shown as a function of the state of charge of the batteries. The state of charge is calculated on the basis of the discharge ampere-hour and the nominal (not measured) capacity. Capacity tests were performed with $0.1 \times I_{10}$. The voltage is given for a 12-V block battery made from 6 cells connected in series (a typical design as used for SLI batteries for cars)

in SOC for the same voltage limit could be as high as 25%. Taking into account different battery technologies, the differences in SOC are even higher. In autonomous power supply systems, low and high currents occur (Figure 18.5, [9]).

Two solutions for the problem are available. One is a current-compensated end-of-discharge voltage threshold and the other is the use of state-of-charge determination. The latter solution is the most appropriate for autonomous power supply systems. There are various methods for state-of-charge determination in lead acid batteries, which are appropriate for autonomous power supply systems [26].

18.5 SECONDARY ELECTROCHEMICAL BATTERY SYSTEMS WITH EXTERNAL STORAGE

The secondary batteries described in Section 18.4 use electrodes both as part of the electron-transfer process and to store the energy via electrode solid-state reactions. Consequently, both energy storage capacity and the power rating are intimately related to the electrodes' size and shape.

Electrochemical batteries with external storage overcome this drawback. The reaction occurs within an electrochemical cell and the energy is stored in two tanks separated from the electrochemical cell. The electrochemical cell has two compartments, one for each storage medium, physically separated by an ion-exchange membrane. This allows the designing of the battery power and the energy content separately.

Downloaded from https://onlinelibrary.wiley.com/doi/ by <Shibboleth-member@purdue.edu>, Wiley Online Library on [25/08/2024]. See the Terms and Conditions (https://onlinelibrary.wiley.com/terms-and-conditions) on Wiley Online Library for rules of use; OA articles are governed by the applicable Creative Commons License

Here, a distinction between the so-called redox-flow batteries in which salts are dissolved in liquid electrolytes and the hydrogen/oxygen storage systems based on the electrolyser and the fuel cell will be made.

The costs for the converters and therefore the power sizing are independent of the storage size. Therefore, these systems show an economy of scale concerning the energy storage. The larger is the storage, the lower are the specific storage costs. This makes the systems interesting for seasonal storage or other long-term storage applications.

18.5.1 Redox-flow Batteries

In redox-flow batteries, the active material is made from salts dissolved in a liquid electrolyte. The electrolyte is stored in tanks. As the solubility of the salts is typically not very high, the energy density is in the range of lead acid batteries. The electrochemical charge/discharge reactions take place in the converter, which determines the power of the system. Therefore, redox-flow batteries belong to the group of batteries with external storage. Redox-flow batteries were already under investigation for stationary applications in the 1970s and 1980s. An overview of these activities can be found in [28]. Owing to problems with the materials, the investigations were almost stopped but were again started in the last year.

Redox-flow batteries work with electrolytes in two circulations. Each circulation contains a redox system whose valence is changed during charging and discharging. The change in the valence of the two redox systems should take place at preferably high potential difference as this forms the equilibrium voltage of the battery. Figure 18.26 shows the principle of the redox-flow battery with the vanadium battery (equation (18.14)) as an example. The valence of all ions during each step can be seen in the figure.

Several different combinations of salts were and still are under investigation.

Fe-Cr	$Fe^{3+} + Cr^{2+} \rightleftarrows Fe^{2+} + Cr^{3+}$	(18.12)
Br_2Cr	$Br_2 + 2Cr^{2+} \rightleftarrows 2Br^{-} + 2Cr^{3+}$	(18.13)
Vanadium	$V^{5+} + V^{2+} \rightleftarrows V^{4+} + V^{3+}$	(18.14)
Regenesys	$3NaBr + Na_2S_4 \rightleftarrows 2Na_2S_2 + NaBr_3$	(18.15)

Several problems with redox-flow batteries have occurred and are still unsolved. The stability of the separator and the mixing of the electrolytes through the separators are severe problems. Therefore, the vanadium system became the centre of interest in the last few years as the materials and electrolytes are similar for the positive and the negative electrodes. Therefore, a crossing of ions through the separator just causes coulomb losses, but causes no deterioration of the electrolytes.

Defining the specific energy densities is difficult because of the independent sizing of the converter and the storage. Typical values for 20 kW/20 kWh vanadium redox-flow batteries are about 20 Wh/kg and 50 W/kg. For mobile applications in electrical cars, this is not enough, but for stationary, especially in load levelling, applications it is an interesting option. Figure 18.27 shows a prototype of a redox battery at laboratory scale

Downloaded from https://onlinelibrary.wiley.com/doi/ by <Shibboleth-member@purdue.edu, Wiley Online Library on [25/08/2024]. See the Terms and Conditions (https://onlinelibrary.wiley.com/terms-and-conditions) on Wiley Online Library for rules of use; OA articles are governed by the applicable Creative Commons License

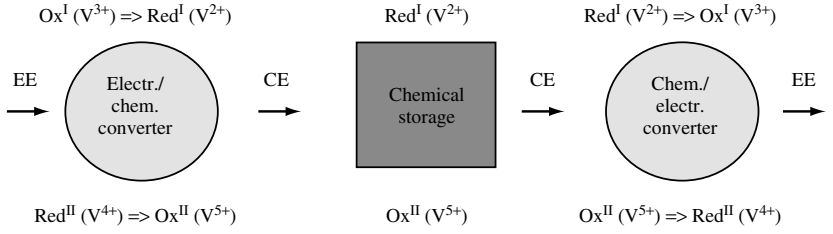


Figure 18.26 General concept of a redox-flow battery with two electrolyte/active mass circulations. The circulation in the upper row is equivalent to the negative electrode, the lower row denotes the positive electrode. In brackets, the vanadium battery is given as an example. The figure is based on an idea from [29] (EE: electrical energy, CE: chemical energy)

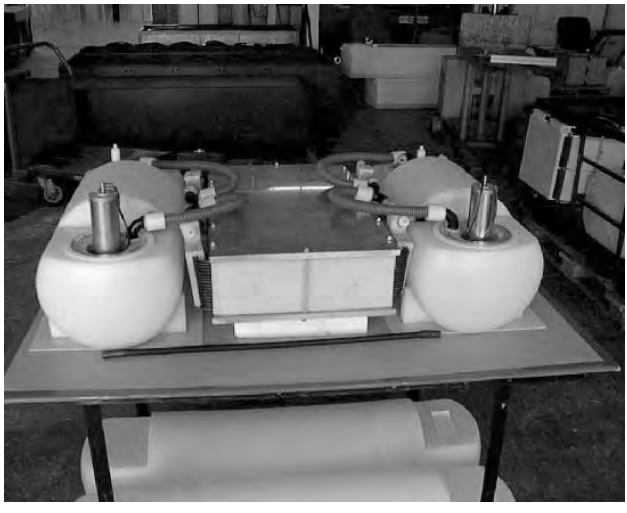


Figure 18.27 Prototype of a vanadium redox-flow battery with 32 cells and 14 Ah (Picture Courtesy by ZSW [29])

and Figure 18.28 shows a schematic of a redox-flow battery in the megawatt hour. As there have been no commercial products in operation for a long time, data on lifetimes are hardly available. Theoretically, long lifetimes can be expected as no part of the system undergoes structural changes as they occur in most other battery technologies. In literature, data for a vanadium battery with more than 13 000 cycles have been reported [30]. In any case, a regeneration of the electrolyte/active mass is possible. The influence of vanadium batteries on the environment is described in [31]. No material loss or "down cycling" of the electrolyte including the vanadium occurs.

What is true for the lifetime is also true for the costs. Rough estimations show, for the vanadium battery, costs of approximately 200 €/kWh for batteries with more than

Downloaded from https://onlinelibrary.wiley.com/doi/ by <Shibboleth-member@purdue.edu>, Wiley Online Library on [25/08/2024]. See the Terms and Conditions (https://onlinelibrary.wiley.com/terms-and-conditions) on Wiley Online Library for rules of use; OA articles are governed by the applicable Creative Commons License

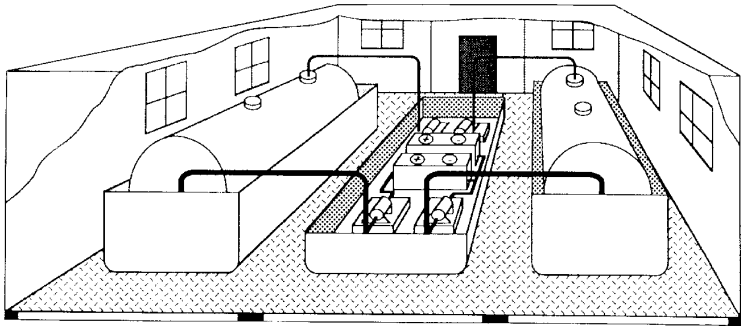


Figure 18.28 Schematic of a redox-flow battery in the megawatt hour range [29]

20 h of discharge time at full power [29]. As no mass production is established, these data are subject to speculations on the mid-term achievable cost figures.

The energy efficiency for the vanadium battery has been demonstrated to be 80 to 85% for the cell itself. As the system requires peripherals (mainly pumps for the electrolytes), the system efficiency can be in the range of 75%, which is considerably better in comparison with the hydrogen system described in Section 18.5.2. No self-discharge of the electrolytes in the tanks occurs. An optimum operation temperature for redox-flow batteries is defined by an optimum of the solubility of all the salts in the electrolyte while avoiding any recrystallisation of a salt.

18.5.2 Hydrogen/Oxygen Storage Systems

The other major technology with external storage is the use of liquid water (discharged state) and its gaseous components hydrogen and oxygen (charged state) [32].

Water can be split into hydrogen and oxygen gas by the fundamental reaction (18.16).

$$2H_2 + O_2 \rightleftarrows 2H_2O \tag{18.16}$$

Electrolysis of water starts at 1.23 V/cell. A hydrogen storage system consists of three major components that are listed below:

1. An electrolyser for the production of the gases from electric power,
2. Gas storage for the hydrogen and, depending on the system's design, for the oxygen. Hydrogen is commonly stored either in pressure tanks or metal-hydride tanks.
3. A fuel cell to reconvert the gases into water and electric power. Hydrogen is taken from the storage and oxygen either from gas storage or from air.

Electrolyser/fuel cell systems have been demonstrated; the technology, however, still has to go through a long process of maturation until it reaches the market at acceptable costs and with high reliability.

Downloaded from https://onlinelibrary.wiley.com/doi/ by <Shibboleth-member@purdue.edu, Wiley Online Library on [25/08/2024]. See the Terms and Conditions (https://onlinelibrary.wiley.com/terms-and-conditions) on Wiley Online Library for rules of use; OA articles are governed by the applicable Creative Commons License

Downloaded from https://onlinelibrary.wiley.com/doi/ by <Shibboleth-member@purdue.edu>, Wiley Online Library on [25/08/2024]. See the Terms and Conditions (https://onlinelibrary.wiley.com/terms-and-conditions) on Wiley Online Library for rules of use; OA articles are governed by the applicable Creative Commons License

18.5.2.1 Electrolyser

Electrolysers are needed to produce hydrogen and oxygen gas from water by using electric power. Electrolysis is used in many industrial processes apart from hydrogen production. Two technologies for low-temperature water electrolysis are available today:

- Alkaline electrolysers
- Polymer electrolyte membrane (PEM) electrolysers.

In addition, high-temperature steam electrolysers are under investigation, which are in general good for higher efficiencies (see [33]).

Special electrolysers can release the gases already under pressure without using an additional compressor. PEM electrolysers can have efficiencies of 80 to 85%. They are commercially available, but are very expensive because only a few units are sold and expensive materials (membrane, catalysts) are needed. Presently, there is no important market for PEM electrolysers in the kW range. However, larger alkaline electrolysers for use with wind or water power plants are commercial and in operation. Reference [34] gives an overview on a research project on electrolysers operated by wind turbines.

18.5.2.2 Gas storage

Three major technologies for hydrogen gas storage are available today:

1. Pressure tanks (low pressure up to 30 bar, medium pressure up to 200 bar and high pressure up to 700 bar).
2. Metal hydrides with adsorption of hydrogen.
3. Liquid hydrogen storage (only for large scale applications).

Low-pressure tanks can be used in conjunction with pressure electrolysers. Specially designed electrolysers [35] produce hydrogen and oxygen at 30 bar without any compressor and therefore a minimum of energy loss due to compression. Medium-pressure tanks or bottles can be fitted to compressors. Today, hydrogen mechanical compressors with a high efficiency for small gas volumes are hardly available. Presently, no compressors for hydrogen with flow rates below approximately 10 Nm^3/h are available.[14] Another technology for gas compression is thermal compression with metal hydrides. The pressure in a metal-hydride storage unit increases significantly with an increase in temperature. As different metal alloys have different pressure/temperature curves, gas compression in a multi-stage process is possible. High-pressure gas bottles from composite materials are under development and in operation in R&D and demonstration projects.

Metal hydride is an interesting material for hydrogen storage. The hydrogen is adsorbed within the highly porous metal hydride. In fully loaded metal-hydride tanks, 1 to 2% of the overall weight is hydrogen. The volumetric energy density of metal hydrides is comparable with a 200 bar pressure bottle. The pressure in a metal-hydride tank depends

[14] Nm^3 is the typical dimension for a gas amount. It is a gas in a volume of 1 m^3 at a pressure of 1 bar and a temperature of 0°C.

on the temperature, the alloy and the state of charge. For outdoor applications, it is important to be aware that the pressure in the metal-hydride tank at constant hydrogen load approximately doubles with an increase of 20 K in temperature.

The energy content of 1 Nm^3 of hydrogen gas is approximately 3.5 kWh. Depending on the fuel cell system and power-converter efficiency, between 1 and 1.8 kWh of net energy can be drawn from 1 Nm^3 of hydrogen gas.

A standard 200 bar pressure bottle contains 8.8 Nm^3 of hydrogen gas. The cost for metal-hydride storage systems is currently in the range of 500 to 1500 € per Nm^3.

For oxygen storage, currently only pressure tanks are commercially available. Materials with adsorption properties for oxygen are under investigation. A reduction in volume by a factor of 3 has been achieved.

Nanotubes for hydrogen storage are under investigation. After a very optimistic period some years ago, the optimism has been reduced, but meanwhile there are several activities to investigate this technology which promises very low costs.

18.5.2.3 Fuel cell

As fuel cells can only replace batteries in conjunction with the hydrogen gas generation, only the polymer electrolyte or proton exchange membrane fuel cell (PEMFC) is considered here. A very comprehensive overview of all the fuel cell technologies is given in [36].

The basic reactions are given in equations (18.17) and (18.18).

$$\text{Anode reaction} \qquad H_2 \rightarrow 2H^+ + 2e^- \tag{18.17}$$

$$\text{Cathode reaction} \qquad 1/2O_2 + 2H^+ + 2e^- \rightarrow H_2O \tag{18.18}$$

Figure 18.29 shows a schematic of a PEM fuel cell. If hydrogen and oxygen are stored, a closed-loop operation with water and gases can be realised. Then, the water demand for refilling is limited. If air is used instead of pure oxygen, the water produced in the fuel cell process gets lost with the air throughput. The water household of the membrane is one of the most challenging problems in fuel cell operation and control.

PEMFCs operate best at temperatures between 60 and 90°C. The fuel cell stack itself can operate at an efficiency of 50 to 60%. The overall fuel system has additional components beside the stack like air compressors, electronics, valves and security devices. They cause a self-consumption of the fuel cell system and therefore reduce the overall efficiency to 35 to 50%. The efficiency is higher if pure oxygen is used instead of air, but this requires an additional oxygen tank. The stack efficiency is calculated from the ratio of the fuel cell voltage during power generation and the electrochemical potential of the reactants, which is 1.23 V. The coulomb efficiency is considered as 100% even though some gas losses synonymous with coulomb losses due to the penetration of gas through the membrane occur as well.

A big advantage of fuel cells in comparison with motor generators are the high efficiency even at partial loads. Usually the stack efficiency increases with decreasing power output.

Downloaded from https://onlinelibrary.wiley.com/doi/ by <Shibboleth-member@purdue.edu, Wiley Online Library on [25/08/2024]. See the Terms and Conditions (https://onlinelibrary.wiley.com/terms-and-conditions) on Wiley Online Library for rules of use; OA articles are governed by the applicable Creative Commons License

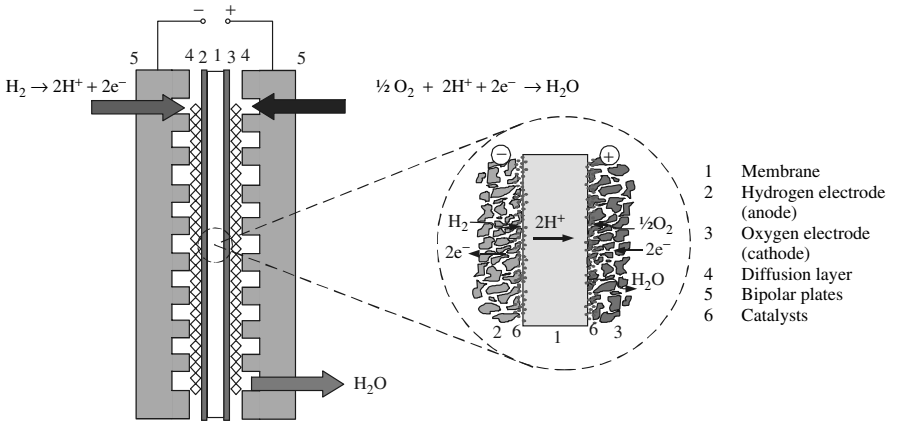


Figure 18.29 Schematic of a polymer electrolyte membrane fuel cell (PEMFC)

The current/voltage characteristic of a fuel cell is quite similar to the characteristic of a PV cell. Unlike secondary electrochemical batteries, the voltage depends very much on the current. To supply a load with a constant voltage, power electronics are necessary. The power electronics are also needed to adjust the point on the I/V curve corresponding to the actual power demand. Therefore, the operation of a fuel cell in applications with varying load demands without power electronics is impossible. Charging of a battery with a fuel cell is in principle possible. However, the fuel cell must not exceed certain current limits for a safe operation. Power electronics that limit current and voltage according to the requirements are highly recommended. Power electronics are necessary in any case if a controlled charge of a battery according to one of the charging regimes given in Figure 18.23 is necessary.

Presently, no cost figures for marketable fuel cells can be given as all available PEM fuel cells are prototypes for R&D and demonstration. However, there is a huge bunch of activities in fuel cell research. They are mainly driven by the automobile industry and by the combined heat and power generation CHP space-heating applications. The target figures for fuel cell systems in these applications are approximately 100 euro/kW for automobiles and 1000 euro/kW for CHP space-heating systems.

18.5.2.4 Applications

Hydrogen storage systems have a low overall efficiency. Even under the assumption of a fuel cell system efficiency of 50%, an electrolyser system efficiency of 85%, no energy losses for the hydrogen storage and efficiencies of 97% each for the two power-converting steps, an overall storage system efficiency of 40% maximum is achievable. Compared with approximately 90% efficiency in lead acid or lithium batteries, this is rather small and rules out the hydrogen system as the principle and only energy storage unit in autonomous power supply systems. This will be the fact as long as the power production is as expensive as it is now. Secondly, the specific storage costs per kilowatt

Downloaded from https://onlinelibrary.wiley.com/doi/ by <Shibboleth-member@purdue.edu>, Wiley Online Library on [25/08/2024]. See the Terms and Conditions (https://onlinelibrary.wiley.com/terms-and-conditions) on Wiley Online Library for rules of use; OA articles are governed by the applicable Creative Commons License

hour with the hydrogen system must come down to the values of today's lead acid batteries and thirdly, the technical reliability of the complex hydrogen system must be as high as with conventional batteries. The hydrogen storage system is far away from all these goals and these goals will be hardly achieved within the next decade.

One interesting line of development is the reversible fuel cell RFC. RFCs fulfil the functionality of the electrolyser and the fuel cell at the same time. As the process is completely reversible, this is an obvious solution. Technical problems concerning the catalysts and the gas and water management within the cell have to be solved [37]. No commercial products for field applications are available in this technology today.

Applications in autonomous power supply systems will have a combined storage system made from a conventional battery and the hydrogen system. Figure 18.30 shows a principle system design as it is currently under development within an R&D project [38]. The hydrogen system here substitutes the conventional motor generator, which is used today in hybrid systems to bridge the energy gap between summer and winter. A conventional lead acid battery (five days of autonomy) is assisted by the hydrogen storage systems. During summer, the energy excess from the PV generator is used to produce hydrogen in the electrolyser (oxygen is released to the atmosphere). The hydrogen is stored in a metal-hydride tank. During winter, in long periods with low energy supply

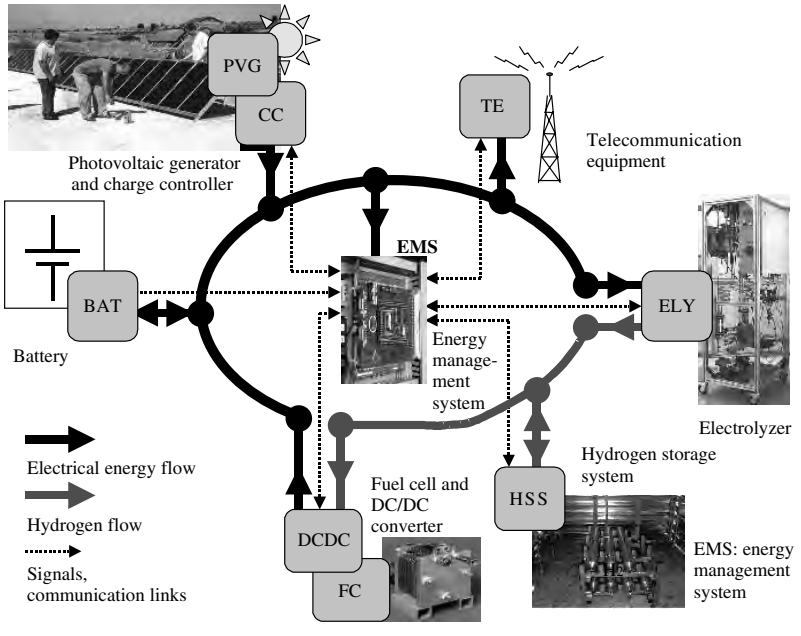


Figure 18.30 Example of an autonomous power supply system for telecommunication with a PVgenerator, a lead acid battery for short-term storage (five days of autonomy) and a hydrogen storage system for seasonal energy storage. The system and components have been developed by partners in the EC co-financed project FIRST [38]

Petitioner Canadian Solar (USA) Inc., Ex. 1035, p. 2242

Downloaded from https://onlinelibrary.wiley.com/doi/ by <Shibboleth-member@purdue.edu, Wiley Online Library on [25/08/2024]. See the Terms and Conditions (https://onlinelibrary.wiley.com/terms-and-conditions) on Wiley Online Library for rules of use; OA articles are governed by the applicable Creative Commons License

from the PV generator the fuel cell takes the oxygen from the air and the hydrogen from the tank to produce electrical power.

This concept allows operating the system with very high reliability with respect to the power supply throughout the year without any conventional fuel. The shift of energy from the summer to the winter is beneficial, as, otherwise, in Central Europe a larger PV generator or motor generator would be required to fulfil the energy requirements during winter. Numerous other systems of this type for different applications have been developed and installed by R&D projects within the last decade (e.g. [39–41]).

18.6 INVESTMENT AND LIFETIME COST CONSIDERATIONS

While designing an autonomous power supply system, it is essential to face the lifetime costs rather than looking only into the initial investment costs. The battery has major impacts on the system design, system operation and overall costs.

- The battery causes a considerable part of the initial investment costs.
- The size of the battery influences significantly the solar fraction of the power supply system.
- Typically, more than two-thirds of the energy flow in an autonomous power supply system goes across the storage system. Therefore, the battery acts as an important consumer of electrical energy due to its efficiency of less than 100%.
- The battery voltage influences the selection of the electronic components or vice versa.
- The battery is subject to ageing. Ageing depends very much on the operating conditions of the battery. Operating conditions depend on system sizing and control strategy.
- The lifetime of the battery determines the running costs through the replacement investment.
- The battery needs regular maintenance.
- Depending on the type of the battery, the different requirements of the battery room have to be considered. The requirements are defined in the standards.

These facts are valid for all battery technologies. For the system design, the characteristics of the chosen battery technology must be taken into account. For the following considerations, only lead acid batteries are taken into account.

Investment costs for lead acid batteries depend very much on the technology and the quality of the battery. Typical costs for end users are in the range of 75 to 250 €/kWh. Lifetimes are – depending on the operation conditions – 3 to 8 years. Depending on the sizing of the system (days of autonomy) and the lifetime, the battery will be subjected to 100 to 1000 capacity throughputs. This results in electricity costs of 0.20 to 0.75 €/kWh dedicated to the storage unit. Additional costs occur for the peripherals, the charge controllers res. chargers and maintenance.

Lead acid batteries need maintenance once or twice a year to check the cell connectors, to measure all cell or block voltages to identify weak cells, to clean the tops of the batteries to avoid creeping currents between the poles, to refill water for flooded batteries

Downloaded from https://onlinelibrary.wiley.com/doi/ by <Shibboleth-member@purdue.edu>, Wiley Online Library on [25/08/2024]. See the Terms and Conditions (https://onlinelibrary.wiley.com/terms-and-conditions) on Wiley Online Library for rules of use; OA articles are governed by the applicable Creative Commons License

and to check the general state of the battery. The set points of the charge controllers or the battery management should be checked. For a 48 V battery system with single cells, 30 to 60 min for the maintenance are necessary.

Figure 18.31 gives an example of the cost share of the battery in a PV battery system. The system is designed to supply power with 100% reliability at a location in Mexico. The left-side graphs show a system that was designed to minimise the initial investment costs under the given boundary conditions. The right-side graphs show the results of a minimisation of the lifetime costs. The calculation includes the initial investment costs, maintenance, repair and replacement of the components, capital costs and other operating costs. It can be seen from the graphs that the lifetime costs are 288% or 248% of the costs for the initial investment. Sizing of the system with respect to lifetime costs resulted, in this example, in an overall cost reduction of 14%. It is interesting to see that this was achieved by approximately 20% higher investments in the PV generator. This allows on one hand a reduction of battery size by approximately 25% and on the other hand the larger PV generator allows a more frequent complete charging of the battery and therefore a lifetime extension. This altogether resulted in a cost reduction for the battery of more than 40% and – as mentioned above – for the overall system of 14%.

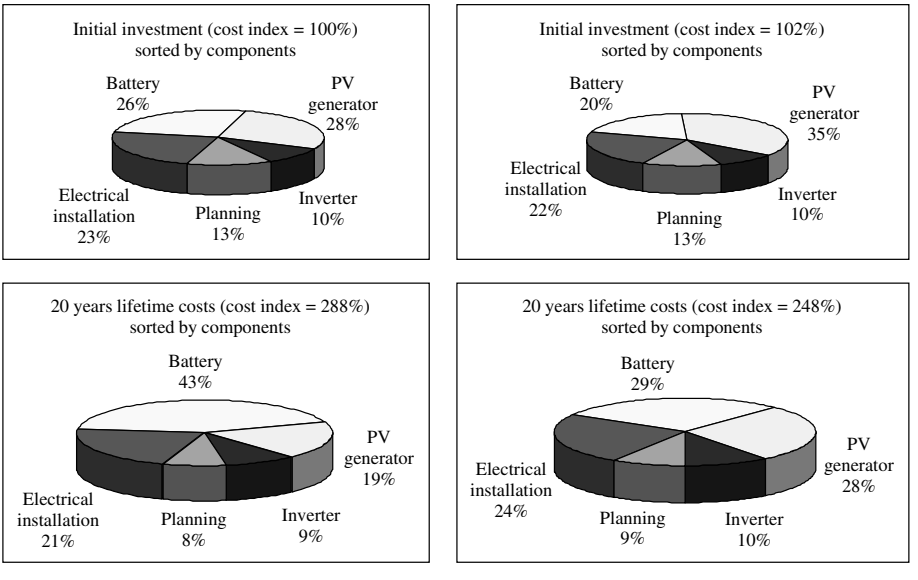


Figure 18.31 Comparison of costs for a PV battery system derived under different assumptions. Left-side graphs show the costs for the system optimised by initial investment costs, right-side graphs show the costs for a system optimised by lifetime costs. The overall costs for the initial investments (upper graphs) and the overall lifetime costs (lower graphs) calculated according to the annuity method are normalised to the initial investment costs for the system optimised by initial investment (cost index = 100%). Location, Mexico; annual power consumption, 1500 kWh; effective interest rate, 6%; lifetime of components: PVgenerator 20 years, electronic components 15 years, battery according to sizing and operating conditions, calculations and optimisation done with the simulation tool TALCO[42]

Downloaded from https://onlinelibrary.wiley.com/doi/ by <Shibboleth-member@purdue.edu, Wiley Online Library on [25/08/2024]. See the Terms and Conditions (https://onlinelibrary.wiley.com/terms-and-conditions) on Wiley Online Library for rules of use; OA articles are governed by the applicable Creative Commons License

Downloaded from https://onlinelibrary.wiley.com/doi/ by <Shibboleth-member@purdue.edu>, Wiley Online Library on [25/08/2024]. See the Terms and Conditions (https://onlinelibrary.wiley.com/terms-and-conditions) on Wiley Online Library for rules of use; OA articles are governed by the applicable Creative Commons License

This example is just to illustrate the importance of an integrated system planning and design. Powerful tools are necessary and available [42]. The battery is the component with the highest cost share in autonomous power supply systems. Other than in photovoltaics, cost reductions on battery investment costs will be small within the next few years as lead acid batteries are already a commercial product today with a market of more than 10 billion euro per year in the different applications. Cost reductions can occur from improved lifetimes and optimised operation strategies. These figures also show that little tolerance for higher battery costs is given. This is important for the estimation of the market entry of other or new storage technologies. Higher specific costs per kilowatt hour of energy supply and significantly lower efficiency than that achieved today with lead acid batteries will hardly be accepted by a commercial market.

18.7 CONCLUSION

Even though there is a wide range of possible solutions for storage in autonomous power supply systems, the economic boundary conditions focus all solutions on lead acid batteries. This will not change significantly for some years. Their electrical properties are very good. Nevertheless, they have a bad reputation among system designers and operators, which is mainly due to the fact that batteries have a limited lifetime. Owing to their electrochemical nature, they have very complex operation and ageing patterns. Technically speaking, batteries have several time constants. Rapid levelling out of microcycles occurs in the millisecond range, diffusion processes in the seconds and minutes range, state of charge in the hour and day range and ageing effects in the day, month and year range. Batteries have a memory with regard to operation conditions. Faults in the operation can often hardly be repaired, but might show their negative impact much later. Further, currently no method exists that allows a determination of the state of health of the battery within minutes. Nevertheless, it is most likely that lead acid batteries will be the leading storage technologies in autonomous power supply systems for many years to come. This will be especially true if the still available improvements in the lead acid technology concerning lifetime in autonomous power supply systems can be realised.

Mainly lithium batteries have enormous growth rates in the portable market segment. Today, it is difficult to forecast the costs for larger units in terms of capacity for lithium batteries – actual forecasts expect costs in the range of 150 €/kWh and from the technical parameters the lithium batteries are most suited to autonomous power supply systems.

Double-layer capacitors will have their market in applications with very high power demands in the range of a few seconds or less and most probably in combination with an electrochemical battery.

In general, a battery is considered to be “used up” when it has less than 80% of the rated capacity guaranteed by the manufacturer. Nevertheless, this usually does not mean that the battery is completely non-functional. From field experience, it is well known that batteries can be used easily down to 50% of the rated capacity. However, the users must be aware that the days of autonomy are reduced according to the capacity loss and the power available from the battery is reduced due to ageing.

In hybrid systems, the solar fraction reduces with decreasing battery capacity. However, as ageing proceeds, the danger of the so-called "fatal defect" increases. This results in a more or less sudden breakdown of the battery, and can create considerable problems for the user. They are usually due to short circuits, caused by erosion sludge, corrosion flakes from the poles or dendrite growth between the electrodes. This risk should be considered when the decision is made about replacing a battery with clearly reduced capacity.

The operation strategy has a significant effect on the battery lifetime. It is necessary to take this into consideration when planning and designing an autonomous power supply system. Some additional investments in the battery peripherals will result in significant savings within the system lifetime. Frequent additional full charging and deep-discharge protection on the basis of a state-of-charge determination are highly recommended.

Hydrogen storage systems and redox batteries are options for the future, but the hydrogen storage systems have a fundamental drawback concerning the efficiency and the complexity of the system. Nevertheless, important impulses for their development will come from load-levelling applications in grids with a high penetration of renewable energy sources.

Further development on the conventional battery systems is necessary and will happen within the coming years. After almost one century (1880–1980) with no sustainable market entry of different fundamental battery technologies, we have seen within the last decade great achievements with nickel-metal hydride and lithium batteries, which were not expected. Further, improved battery technologies and a more integral system design and operation resulting in longer lifetimes will allow a decrease in the specific costs for electrical energy storage within the next decade by approximately a factor of two. Further cost reduction can hardly be seen from today's point of view.

REFERENCES

1. Garche J, Döring H, Harnisch P, *Workshop Fortschrittliche Back-up- und Speichersysteme für regenerative Energieversorgungsanlagen*, Forschungsverbund Sonnenenergie, 51–72 (Köln, 1996).
2. Linden D, *Handbook of Batteries*, 2nd Edition, McGraw-Hill, New York (1995).
3. Berndt D, *Maintenance-Free Batteries – A Handbook of Battery Technology*, John Wiley & Sons, Chichester, UK (1993).
4. Wagner R, Sauer D, *J. Power Sources* **95**, 141 (2001).
5. Sauer D *et al*., "State of Charge – What do we Really Speak About?" *INTELEC '99*, Electronic proceedings of the conference, Copenhagen (1999).
6. Bopp G *et al*., "Hybrid Photovoltaic-Diesel-Battery Systems for Remote Energy Supply", *Proc. NORTH SUN '97* (Espoo, Finland, June 1997).
7. Sauer D *et al*., *J. Power Sources* **64**, 197–201 (1997).
8. Bopp G *et al*., *13th European Photovoltaic Solar Energy Conference*, Vol. 2, 1763–1769 (Nice, France, 1995).
9. Sauer D *et al*., *14th European Photovoltaic Solar Energy Conference*, 1348–1353 (Barcelona, Spain, 1997).

Downloaded from https://onlinelibrary.wiley.com/doi/ by <Shibboleth-member@purdue.edu, Wiley Online Library on [25/08/2024]. See the Terms and Conditions (https://onlinelibrary.wiley.com/terms-and-conditions) on Wiley Online Library for rules of use; OA articles are governed by the applicable Creative Commons License

10. Ruddell A *et al*., *J. Power Sources* **112**, 531–546 (2002).
11. Reilly J, in Besenhard J, Ed, *Metal Hydrid Electrodes in Handbook of Battery Materials*, 209, Wiley-VCH, Weinheim, Germany (1999).
12. Schmidt H, Siedle C, Anton L, Tuphorn H, *Proc. 30th ISATA Conference*, 581–588 (Florence, 1997).
13. Anton L, Schmidt H, 5. Design & Elektronik Entwicklerforum, 103–116 München, Germany, (1998).
14. Maxell Europe GmbH, *Lithium Ion Rechargeable Batteries*, Product explanation.
15. Bode H, *Lead-Acid Batteries*, John Wiley & Sons, New York (1977).
16. Hollenkamp A, *J. Power Sources* **59**, 87–98 (1996).
17. Preiser K *et al*., *14th European Photovoltaic Solar Energy Conference*, Vol. II, 1692–1695 (Barcelona, Spain, 1997).
18. Berndt D, *Blei-Akkumulatoren (Varta)*, VDI-Verlag, 11. Auflage, Düsseldorf (1986).
19. Sauer D, *J. Power Sources* **64**, 181–187 (1997).
20. Mattera F, Sauer D, Desmettre D, Rosa M, *Acid Stratification and Vertical Current Distribution: An Experimental and Theoretical Explanation of a Major Ageing Effect of Lead-Acid Batteries in PV Systems*, Extended Abstract for LABAT99, Sofia (1999).
21. McCarthy S, Kovach A, Wrixon G, "Operational Experience with Batteries in the 16 PV Pilot Plants", *9th European Photovoltaic Solar Energy Conference*, 1142–1145 (Freiburg, Germany, 1989).
22. Döring H, Jossen A, Köstner D, Garche J, 10. *Symposium Photovoltaische Solarenergie*, 549–553 (Staffelstein, Germany, 1995).
23. Bohmann J, Hullmeine U, Voss E, Winsel A, *Active Material Structure Related to Cycle Life and Capacity*, Final Report, ILZRO Project LE-277 (1982).
24. Lander J, *J. Electrochem. Soc.* **103**, 1–8 (1965).
25. Garche J, *J. Power Sources* **53**, 85–92 (1995).
26. Piller S, Perrin M, Jossen A, "Methods for State-of-Charge Determination and their Applications", *Int. Power Sources Symposium* (2001).
27. Kuhmann J, Paradzik T, Preiser K, Sauer D, 13. *Symposium Photovoltaische Solarenergie*, 97–101 Staffelstein (1998).
28. Bartolozzi M, *J. Power Sources* **27**, 219–234 (1989).
29. Garche J *et al*., *Study on New Battery Systems and Double Layer Capacitors*, Internal study in German language for German project EDISON, Financed by BMWi, Compiled by Centre for Solar Energy and Hydrogen Research Baden Württemberg (ZSW), Ulm, Germany (2000).
30. Tokuda N *et al*., *SEI Tech. Rev.* **45**, R22-1–R22-7 (1988).
31. Ryhd C, *J. Power Sources* **80**, 21–29 (1999).
32. Rzayeva M, Salamov O, Kerimov M, *Int. J. Hydrogen Energy* **26**, 195–201 (2001).
33. Pham A, "High Efficient Steam Electrolyzer", *Proc. 2000 DOE Hydrogen Program Review*, NREL/CP-570-28890 (2000).
34. Menzl F, Wenske M, Lehmann J, XII. *WHEC Buenos Aires 1998 Proc.*, 757–765 (1998).
35. Heinzel A, Ledjeff K, in Kreysa G, Jüttner K, Eds, *Elektrochemische Energiegewinnung*, DECHEMA- Monographien, Vol. 128, 595–601, Verlag Chemie, Weinheim, Germany (1993).
36. Fuel Cell handbook, 5th Edition, Online version at *http://216.51.18.233/fchandbook.pdf* , Compiled for the U.S. Department of Energy by EG & G Services (2000).
37. Rau A, Heinzel A, *Reversibles Electrolyse-/Brennstoffzellen-System zur Energiespeicherung, Tagung der Gesellschaft Deutscher Chemiker e.V.*, Fachgruppe Angewandte Elektrochemie, Ulm, Germany (2000).
38. Vegas A *et al*., "The FIRST Project-Fuel Cell Innovative Remote Systems for Telecom", *12th Annual U.S. Hydrogen Meeting* (Washington, DC, 2001).

Downloaded from https://onlinelibrary.wiley.com/doi/ by <Shibboleth-member@purdue.edu, Wiley Online Library on [25/08/2024]. See the Terms and Conditions (https://onlinelibrary.wiley.com/terms-and-conditions) on Wiley Online Library for rules of use; OA articles are governed by the applicable Creative Commons License

39. Armbruster A *et al*., *13th European Photovoltaic Solar Energy Conference*, 360–363 (Nizza, 1995).
40. Brinner A *et al*., *Int. J. Hydrogen Energy* **17**, 187–198 (1992).
41. Barthels H *et al*., *Int. J. Hydrogen Energy* **23**, 295–301 (1998).
42. Puls H, Sauer D, Bopp G, *Proc. 17th European Photovoltaic Solar Energy Conference and Exhibition*, 2673–2678 (Munich, Germany, 2001).

Downloaded from https://onlinelibrary.wiley.com/doi/ by <Shibboleth-member@purdue.edu, Wiley Online Library on [25/08/2024]. See the Terms and Conditions (https://onlinelibrary.wiley.com/terms-and-conditions) on Wiley Online Library for rules of use; OA articles are governed by the applicable Creative Commons License

19

Power Conditioning for Photovoltaic Power Systems

Jürgen Schmid[1] and Heribert Schmidt[2]

[1]*ISET, Universität Institut für Solare Energieversorgung technik e.V. Kassel,*
[2]*Fraunhofer Institut für Solare Energiesysteme, Freiburg*

In PV systems, power conditioning units are used to provide a match between the specific characteristics of the PV generator and the connected balance of system (BOS) components. Furthermore, they take over the control of other BOS components, for example, batteries or back-up generators.

In general, the characteristic curve of a PV generator varying with solar radiation and temperature does not match the characteristic curve of the load. In those cases, the power conditioning unit effects a transformation of the load's voltage and current in such a way, that the PV generator is operated at its optimum operation voltage V_{MPP} even under changing boundary conditions.

In the following chapter, the characteristics of the most common power conditioning units – charge controllers, DC/DC converters and inverters – are described.

In almost every stand-alone system, a charge controller is required to optimally operate the storage battery within safe limits as prescribed by the manufacturer.

The matching of PV generator and the load can be achieved by means of DC/DC converters which can be integral part of a charge controller, an inverter or a DC pump, but can also be a separate BOS component.

If in stand-alone systems the load requires an AC voltage, inverters are used to convert the DC power supplied by the PV generator or the storage battery into AC power. Inverters are mandatory in grid-connected PV systems. Here, besides high efficiency, reliability and power quality, safety is an important issue and has to be dealt with.

Handbook of Photovoltaic Science and Engineering. Edited by A. Luque and S. Hegedus
© 2003 John Wiley & Sons, Ltd ISBN: 0-471-49196-9

Downloaded from https://onlinelibrary.wiley.com/doi/ by <Shibboleth-member@purdue.edu, Wiley Online Library on [25/08/2024]. See the Terms and Conditions (https://onlinelibrary.wiley.com/terms-and-conditions) on Wiley Online Library for rules of use; OA articles are governed by the applicable Creative Commons License

19.1 CHARGE CONTROLLERS AND MONITORING SYSTEMS FOR BATTERIES IN PV POWER SYSTEMS

In PV-powered systems, batteries are still the component with the lowest average lifetime. Compared to solar modules, which in principle have an infinite economic lifetime and in many cases offer a guarantee period of 25 years, the lifetime of batteries is much lower. The maximum lifetime found in practice is around 8 to 10 years; in most cases it is in the range of 3 to 6 years and in some cases even lower. The upper limit will be determined by normal ageing; the shorter lifetimes are mostly caused by inappropriate treatment or unsuitable control strategies. This topic is discussed in Chapter 18.

Looking at the battery cost in a typical PV diesel system, one can find that its share of the initial costs is around 15%. Because of repeated replacement of exhausted batteries, this initial share grows to more than 35% or even 50% over the expected 25-year service life of the system. Compared to this, the costs for solar modules and other balance-of-system components become small.

To achieve minimum lifetime costs and satisfying operation of the PV system, equipping the battery with appropriate peripherals is money well spent. Some examples, such as systems to automatically mix the electrolyte to prevent acid stratification or automatic water-topping systems, are explained in Chapter 18. Besides this, the application of appropriate operation modes is a crucial factor.

In this chapter, the technical realisation of the key component, the "charge controller", will be described. Furthermore, a new system to operate long battery strings optimally will be introduced.

19.1.1 Charge Controllers

The fundamental task of a charge controller is to operate the battery within the safe limits defined with respect to overcharging and deep discharging by the battery manufacturer or by the operation mode.

Compared to conventional battery chargers powered by the public grid, the situation is much more complex in PV systems. Here, charging power and energy are limited and depend on the varying insolation and load demand. Well-known charging strategies such as constant-current–constant-voltage charging (CC/CV) or more complex charging strategies, cannot be applied one to one. For example, in PV systems the charging current varies according to the insolation. Nevertheless, the term used is "constant current charging". Also, regular full charging of the battery – which is very important for a long service life – cannot be guaranteed.

Furthermore, very high energy efficiency is crucial for all balance-of-system components in PV systems. Most grid-powered battery chargers offer only unsatisfactory efficiency values.

In the following sections, the fundamental technical concepts of charge controllers [1, 2] as well as the associated control strategies will be explained. In addition, a list of criteria will be given that should be taken into account when developing or selecting charge controllers.

Downloaded from https://onlinelibrary.wiley.com/doi/ by <Shibboleth-member@purdue.edu, Wiley Online Library on [25/08/2024]. See the Terms and Conditions (https://onlinelibrary.wiley.com/terms-and-conditions) on Wiley Online Library for rules of use; OA articles are governed by the applicable Creative Commons License

Downloaded from https://onlinelibrary.wiley.com/doi/ by <Shibboleth-member@purdue.edu>, Wiley Online Library on [25/08/2024]. See the Terms and Conditions (https://onlinelibrary.wiley.com/terms-and-conditions) on Wiley Online Library for rules of use; OA articles are governed by the applicable Creative Commons License

19.1.1.1 Self-regulating PV systems

In small systems, such as house-number illumination or power supplies for measurement systems, a charge controller can be avoided in special cases.

This is, for example, true for NiCd batteries, when the current provided by the PV module is lower than the continuous charging current accepted by the battery. Also, such "self-regulating" systems have been used in the past for systems in the 50-W range such as light buoys.

In these systems illustrated in Figure 19.1, only a series diode is needed to block reverse currents from flowing into the module at night. To prevent overcharging of the battery, specially tailored PV modules with, for example, 30 crystalline-silicon cells will be used for 12-V lead acid batteries. With this low number of cells, the operating point will move into the steeply sloping part of the module's $I-V$ curve when the battery is fully charged.

To make this kind of system operate reliably, the load profile as well as the insolation and temperature at the place of operation must be known accurately. Because cheap and reliable charge controllers are available today in the market, such "self-regulating" systems should be avoided.

In all cases, deep-discharge protection according to Section 19.1.1.6 should be implemented.

19.1.1.2 Linear charge controllers

When PV applications commenced, the well-known principles of conventional linear charge controllers were adapted to photovoltaics. These principles do not take advantage of the special properties of solar cells, for example, that they are infinitely tolerant to short circuits. Therefore, the initial linear charge controllers have been replaced by the switching charge controllers described below.

Meanwhile, novel integrated voltage controllers have appeared in the market, which make the principle of linear charge controllers a reasonable option in the power range up to about 50 W like in Solar Home Systems (SHS).

In a linear charge controller, the charging current will be adjusted by a final controlling element that acts continuously and is located either in series or in parallel with

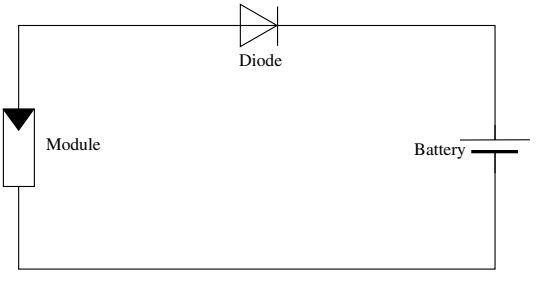


Figure 19.1 "Self-regulating" PV system without a charge controller

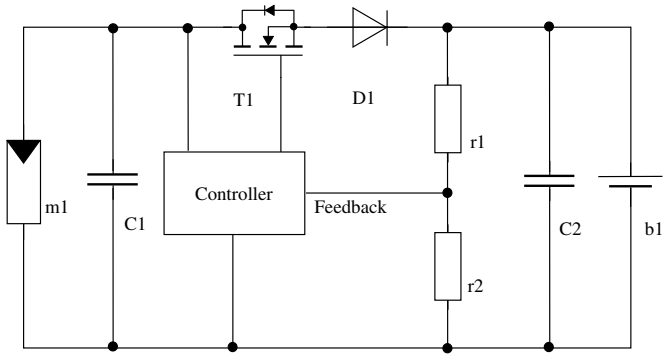


Figure 19.2 Linear charge controller based on the integrated voltage controller MIC 5158 (MICREL) labelled controller with an external power MOS-FET

the solar generator. By driving the controlling element appropriately, the battery voltage can be prevented from exceeding the end-of-charge limit.

Figure 19.2 shows the block circuit diagram of a linear series charge controller. In the constant-current (CC) phase, in which the battery voltage is below the end-of-charge voltage, the control element MOS-FET T1 is fully conducting. The solar generator and the battery are directly coupled via the blocking diode D1. The operating point of the solar generator is determined by the instantaneous insolation and the battery voltage. The power losses inside the control element are almost negligible in this phase. Additional power losses are caused by the voltage drop across the blocking diode D1, which in most cases will be a Shottky diode with a very low forward voltage drop. To minimise the power losses, the blocking diode can be replaced by a second MOS-FET connected back-to-back in series with T1. With such designs, care has to be taken that both MOS-FETs turn off during the night, and that no reverse current flows into the solar generator!

It is important to note that in most cases the energy gained by the reduction of power losses is not relevant for the function of the PV system. In fact, the goal is to reduce the voltage drop across the controller, which finally leads to a saving of one or two solar cells in the module.

As soon as the end-of-charge voltage has been reached, the gate voltage for the MOS-FET T1 will be reduced by the controller. Now, the output voltage is kept constant while the charging current will drop slowly according to the battery's increasing state of charge. In contrast to the first charging phase, now the difference between the solar generator voltage and the battery voltage will occur at the transistor terminals and cause some heat dissipation.

In Figure 19.3, the operating points for three different charging currents are shown as an example. The shaded areas are proportional to the power dissipated in the control element. As can be seen, this power is in the range between approximately one-fourth and one-tenth of the instantaneous maximum power point (MPP) power of the generator. The resulting heat must be dissipated by appropriate heat sinks. This is a clear disadvantage compared to the switching charge controllers described below. On the other hand, there are

Downloaded from https://onlinelibrary.wiley.com/doi/ by <Shibboleth-member@purdue.edu, Wiley Online Library on [25/08/2024]. See the Terms and Conditions (https://onlinelibrary.wiley.com/terms-and-conditions) on Wiley Online Library for rules of use; OA articles are governed by the applicable Creative Commons License

Petitioner Canadian Solar (USA) Inc., Ex. 1035, p. 2252

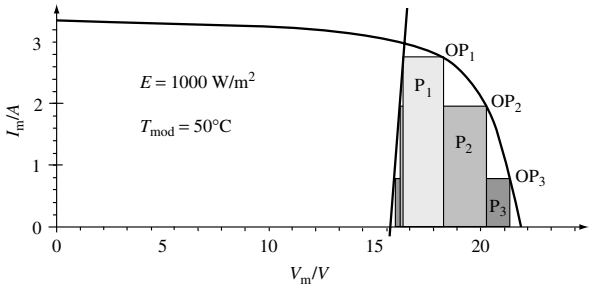


Figure 19.3 $I-V$ curve of a 36-cell PV module and characteristic curve of a 12-V lead acid battery with 3-m input lead (1.5 mm^2 cross-section) for three different charging currents. The shaded areas show the power dissipated in the control element

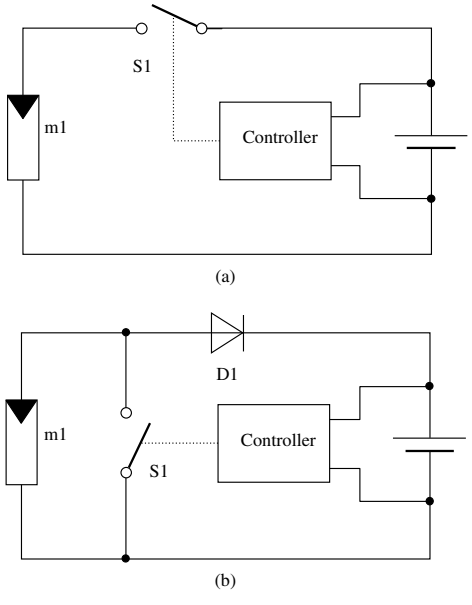


Figure 19.4 Principle of (a) series and (b) shunt controllers

no problems with electromagnetic compatibility (EMC), and the battery will be charged with a life-extending CC without micro-cycles.

19.1.1.3 Switching controllers

The above-mentioned disadvantage of intensive heat dissipation in linear charge controllers can be overcome with switching controllers. In these controllers, the control element is either fully closed (conducting) or fully open (blocking). Under ideal conditions,

Downloaded from https://onlinelibrary.wiley.com/doi/ by <Shibboleth-member@purdue.edu>, Wiley Online Library on [25/08/2024]. See the Terms and Conditions (https://onlinelibrary.wiley.com/terms-and-conditions) on Wiley Online Library for rules of use; OA articles are governed by the applicable Creative Commons License

the power losses are zero in both cases because either voltage or current at the control element is zero.

Once again, it must be pointed out that the additional energy gained in this way is normally not relevant for the functioning of the PV system. By contrast, the reduction of heat generation leads to savings in component costs (heat sinks) and to an increased reliability due to lower component temperatures.

In a series controller as shown in Figure 19.4(a), the charging current will be controlled by an element switched in series with the solar generator.

In early charge controllers, relays were used as switching elements, but today semiconductor switches like MOS-FETs are used in almost every application.

One advantage of the series controllers is that in addition to PV generators, they can be used for other power sources that are not being tolerant to short circuits such as wind turbines. Furthermore, the voltage stress for the switch is lower compared to the shunt controller described below. With a fully charged battery, the solar generator operates in the open-circuit mode. In this operation mode, no module overloading due to partial shading can occur. On the other hand, the solar generator current is fully turned on and off, which can lead to greater EMC problems compared to shunt controllers.

In the past, the series controller was accused of having fundamentally higher losses. This is no longer true since low-resistive semiconductor switching elements have been used – the losses can be even lower than for shunt controllers. Furthermore, some early series controllers did not start with completely flat batteries because they did not have enough energy to activate the series switch. This problem can easily be solved by powering the controller from the PV module instead of from the battery.

A parallel or shunt controller as shown in Figure 19.4(b) makes use of the electrical characteristic of PV modules that they are infinitely tolerant to short circuits.

In the constant-current charging phase, the module current flows through the blocking diode D1 into the battery. When the end-of-charge voltage has been reached, the PV generator is short-circuited by the switch S1. The blocking diode now prevents the reverse current flowing from the battery into the switch. Furthermore, it suppresses the discharging currents into the PV generator during the night.

In contrast to the series controller, this kind of charge controller will also reliably start charging with a fully discharged battery, because the switch can be energised only when the battery is fully charged.

The hybrid charge controller is a modified shunt controller, in which the blocking diode is bypassed by a second transistor in the charging phase. This reduces the power dissipation in the controller, which leads to smaller heat sinks and lower thermal stress. Furthermore, the reduction of the voltage drop supports the use of cost-optimised PV modules with a smaller number of series-connected cells, for example, 30 to 33 crystalline-silicon cells for 12-V systems.

Another variant of the shunt controller is the partial-shunting controller according to Figure 19.5. Here, only some of the series-connected modules are shunted via taps.

Downloaded from https://onlinelibrary.wiley.com/doi/ by <Shibboleth-member@purdue.edu, Wiley Online Library on [25/08/2024]. See the Terms and Conditions (https://onlinelibrary.wiley.com/terms-and-conditions) on Wiley Online Library for rules of use; OA articles are governed by the applicable Creative Commons License

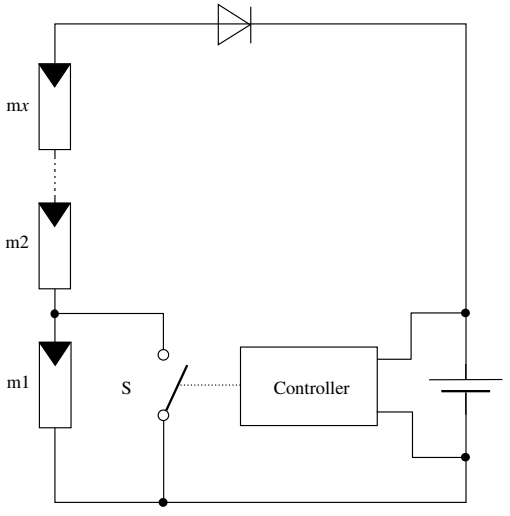


Figure 19.5 Partial-shunting controller for high-voltage systems

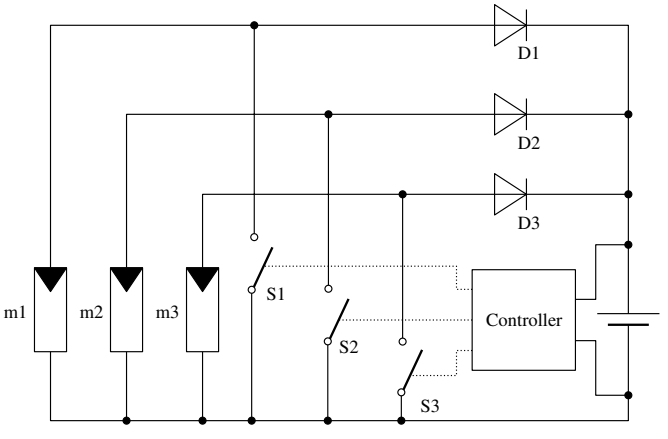


Figure 19.6 Sub-array switching controller for high-power systems

In consequence, the remaining generator voltage is too low to further charge the battery. The advantage of partial shunting is the reduced voltage stress for the switch in high-voltage systems. On the other hand, a tap and additional wiring are needed.

In high-power systems, sub-array switching according to Figure 19.6 is used for charge control. The PV generator is set up as a number of sub-arrays (strings), and each of these strings is connected to the battery via its own control element (e.g. blocking diode and switch).

Downloaded from https://onlinelibrary.wiley.com/doi/ by <Shibboleth-member@purdue.edu, Wiley Online Library on [25/08/2024]. See the Terms and Conditions (https://onlinelibrary.wiley.com/terms-and-conditions) on Wiley Online Library for rules of use; OA articles are governed by the applicable Creative Commons License

Two different control strategies are used. The multiple switches can be driven in parallel, turning the full array current on and off in one step. A preferred strategy is to drive the switches in a certain sequence that allows stepwise adjustment of the charging current.

With all of the switching controllers described above, the designer or end user has to be aware that the solar generator is directly coupled with the battery and the load. If the battery connection is interrupted (maintenance work, lead breakage, blowing of the battery fuse etc.), the full open-circuit voltage of the PV generator can be applied to the load and may destroy it! To prevent damage, either the loads must be able to withstand the high voltage or the controller must be designed to avoid voltages higher than the rated output. This can be achieved, for example, by rapid over-voltage detection and load cut-off.

19.1.1.4 Control strategies

When the end-of-charge voltage is reached for the first time, the battery is not yet fully charged. The missing 5 to 10% of charge can be added to the battery by keeping it at the end-of-charge voltage level for a prolonged period. In this constant-voltage (CV) phase, the charging current will slowly decrease. How can such a charging regime be implemented by a series or shunt controller as described above, which can only switch all of the PV generator current on and off? Two techniques are used in practice to approximate the ideal CC/CV charging mode.

In a two-position controller, the charging current is dropped to zero by either opening the series switch or closing the shunt switch as soon as the end-of-charge voltage has been reached. As a result, the battery-terminal voltage decreases. The charging current is enabled again when the battery voltage drops below a threshold that is between 5 and 50 mV/cell lower than the end-of-charge voltage.

This sequence gets repeated periodically and the charging pulses become shorter and shorter, while the intervals in between become longer, as the battery's state of charge increases as shown in Figure 19.7. The average charging current decreases, while the terminal voltage is more or less constant. The period of the cycle described above is

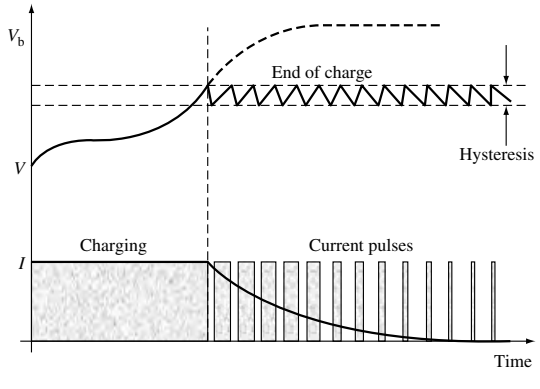


Figure 19.7 Battery voltage and current during charging

Petitioner Canadian Solar (USA) Inc., Ex. 1035, p. 2256

Downloaded from https://onlinelibrary.wiley.com/doi/ by <Shibboleth-member@purdue.edu, Wiley Online Library on [25/08/2024]. See the Terms and Conditions (https://onlinelibrary.wiley.com/terms-and-conditions) on Wiley Online Library for rules of use; OA articles are governed by the applicable Creative Commons License

not constant and depends on the battery capacity, the state of charge, the charging or discharging current as well as the voltage hysteresis. It can vary from milliseconds to minutes. If mechanical relays are used as switching elements, the period should not be shorter than 1 to 5 min.

The second control regime found in practice is pulse-width modulation (PWM). In principle, it works like the two-step controller described above, but the switching frequency of the control element is fixed and determined by a clock generator. The typical frequency is about 100 Hz. In the CC phase, the switch is permanently closed and the full charging current flows into the battery. When approaching the end-of-charge voltage, the duty cycle (the ratio between the charging time and the cycle period) will be reduced towards zero by the pulse-width modulator. As mentioned above, the average charging current will drop and the battery voltage is kept constant.

One advantage of PWM controllers is that the switching frequency is known and constant. EMC problems can be solved more easily, and also monitoring of the average charging current becomes simpler.

19.1.1.5 Matching DC/DC converter, MPP trackers

Both the battery voltage and the PV generator voltage vary over a wide range during operation due to the changing state of charge and boundary conditions such as temperature and insolation. When directly coupled, this leads to a certain mismatch between the actual and the optimum operation voltage (MPP voltage) of the solar generator and therefore causes energy losses.

The mismatch can be overcome by introducing a matching DC/DC converter (MDC) that de-couples the characteristic curves of the PV generator and the battery. The power stage of these converters corresponds to the well-known topologies such as buck, boost or inverting converters. The control section is specially tailored to the PV conditions and consists of two control loops: one for the input and the other for the output. As long as the end-of-charge voltage has not been reached, the input voltage controller keeps the PV generator voltage at a constant level by appropriate adjustment of the DC/DC converter's switching regime (PWM). The voltage level can either be fixed (CV mode) or can track the actual MPP by an appropriate searching strategy (MPP tracking, MPPT). When the end-of-charge voltage is reached, the output voltage controller takes over and keeps the battery voltage at a constant level. The PV generator's operating point then shifts towards open-circuit conditions.

Numerous strategies and algorithms have been developed to find and track the MPP of a solar generator. They can be grouped into two categories:

- Indirect MPP trackers
  This type of MPP tracker estimates the MPP voltage by means of simple assumptions and measurements.
  Some examples from practice include the following:
  - The operating voltage of the solar generator can be adjusted seasonally. Higher MPP voltages can be expected in winter due to lower cell temperatures and vice versa.
  - The operating voltage can be adjusted according to the module temperature.

Downloaded from https://onlinelibrary.wiley.com/doi/ by <Shibboleth-member@purdue.edu>, Wiley Online Library on [25/08/2024]. See the Terms and Conditions (https://onlinelibrary.wiley.com/terms-and-conditions) on Wiley Online Library for rules of use; OA articles are governed by the applicable Creative Commons License

– The operating voltage can be derived from the instantaneous open-circuit voltage by multiplication with a constant factor, for example, 0.8 for crystalline silicon solar cells. The open-circuit voltage is measured periodically (e.g. every two seconds) by disconnecting the load for one millisecond.

The advantage of the above-mentioned procedures is simplicity, but they only give an estimate of the optimum operating point. They are not able to adapt to changing solar generator characteristics due to ageing or soiling.

- Direct MPP trackers
  In these systems, the optimum operating voltage is derived from measured currents, voltages or the power of the PV generator. Therefore, they are able to react to changes in the generator's performance.
  Some examples include the following:
  – Periodic scanning of a part of the $I-V$ curve. Here, the operating voltage of the module is varied within a given voltage window by means of the DC/DC converter. The maximum module power is determined and then the operating voltage is adjusted to the corresponding voltage level. In practice, it is much easier to measure the output current of the DC/DC converter and to maximise it. This leads to the same result as above.
  – "Mountain-climb algorithm". Here, the operating voltage is periodically changed in small steps. The increment can either be constant or can be adapted to the instantaneous operating point as shown in Figure 19.8. If the module's power (and therefore the charging current) increases from one step to the next, the search direction is retained; otherwise it is reversed. In this way, the MPP is found and the operating point oscillates around the actual MPP.

The above-mentioned losses due to mismatch are mostly overestimated. Particularly, if the components are chosen properly (e.g. modules with 30 to 33 cells for 12-V systems), the energy losses are on the order of a few percent when using direct coupling

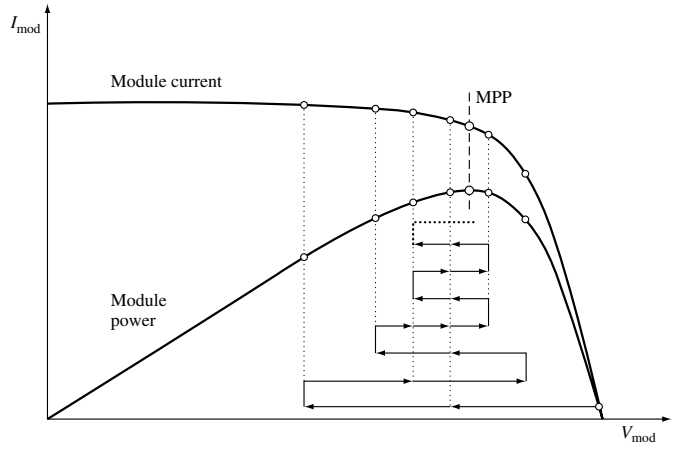


Figure 19.8 Working principle of the "Mountain-climb" MPP-tracking algorithm

Petitioner Canadian Solar (USA) Inc., Ex. 1035, p. 2258

Downloaded from https://onlinelibrary.wiley.com/doi/ by <Shibboleth-member@purdue.edu, Wiley Online Library on [25/08/2024]. See the Terms and Conditions (https://onlinelibrary.wiley.com/terms-and-conditions) on Wiley Online Library for rules of use; OA articles are governed by the applicable Creative Commons License

instead of ideal matching! Besides this fact, it should be considered whether the additional energy gained by optimum matching is relevant to the function of the system at all. For example, the battery in a typical Solar Home System will be fully charged before noon and the excess solar energy will be dissipated.

In general, caution is indicated if the inventors or the manufacturers claim a tremendous energy gain by the use of MPP trackers!

Nevertheless, there are three advantages in using charge controllers with matching DC/DC converters:

- In the case of long wires from the PV generator to the battery, the generator voltage can be chosen much higher than the battery voltage, resulting in lower currents and therefore lower wiring losses.
- In small applications, the PV module can consist of only a few, large cells instead of numerous small cells connected in series. This reduces production costs, the impact of cell mismatch and the sensitivity to partial shading.
- More complex charging-current profiles can be realised by means of a DC/DC converter.

19.1.1.6 Deep-discharge protection

To achieve a maximum service life, deep discharging of batteries as well as prolonged periods with a low state of charge should be avoided. Therefore, the load has to be disconnected automatically from the battery as soon as the state of charge falls below a certain level. The load should be reconnected to the battery only when a sufficient state of charge has been reached.

Different criteria for detecting the deep-discharge condition have been explained in Chapter 18. In commercial products, the battery voltage will be used as a criterion for load disconnection. As soon as the battery voltage drops below a determined level, the load will be disconnected via a (bi-polar) relay or a semiconductor switch. Also, a control signal can be output to shut down balance-of-system components like inverters.

More complex charge controllers are able to generate a warning signal when the deep-discharge condition is being approached. Also, different loads can be disconnected according to a given priority. Charge controllers including an energy-management systems (EMS) are used to start back-up generators such as diesel or gas generators, depending on the battery's instantaneous state of charge. Additional parameters like load demand, weather conditions and so on can be considered.

There should be an appropriate delay time $t_{\mathrm{d\ off}}$ of 10 to 60 s between the undershooting of the end-of-discharge level and the actual disconnection of the load as shown in Figure 19.9. This ensures that undesirable disconnection of loads with large starting currents, for example, motors, refrigerators, washing machines and so on can be avoided. As the end-of-discharge voltage threshold depends on the instantaneous battery current, some advanced charge controllers offer a current-dependent adaptation of the disconnect threshold.

The ideal solution would be deep-discharge protection based on the actual state of charge of the battery. As systems or algorithms for accurately measuring the state of charge

Downloaded from https://onlinelibrary.wiley.com/doi/ by <Shibboleth-member@purdue.edu>, Wiley Online Library on [25/08/2024]. See the Terms and Conditions (https://onlinelibrary.wiley.com/terms-and-conditions) on Wiley Online Library for rules of use; OA articles are governed by the applicable Creative Commons License

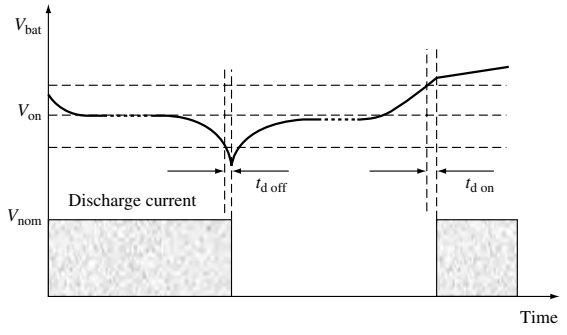


Figure 19.9 Changes in the battery voltage and load current during discharge

under the complex boundary conditions in PV systems are still under development, this type of controller is not yet in the market. For safety reasons, deep-discharge protection systems based on algorithms should be combined with a redundant control system based on simple voltage thresholds as described above!

The voltage threshold for reconnection of the load must be adjusted properly. If it is too low, the battery's open-circuit voltage will overshoot the threshold and the load will be reconnected periodically. In spite of the protection system, the battery will be deeply discharged and damaged. A time delay $t_{d\ on}$ as described above is also appropriate for guaranteeing a minimum state of charge before load reconnection.

In contrast to the end-of-charge threshold, the end-of-discharge threshold should not be temperature-compensated.

19.1.1.7 Monitoring systems and interfaces

Successful functioning of most PV systems strongly depends on the co-operation of the user. Reliable and meaningful information to the user about the current status of the system – the battery in particular – is therefore crucial. It would be ideal to have a "fuel gauge" that enables the system operator to plan the future energy demand. Such systems to monitor the state of charge have been discussed in Chapter 18.

As a minimum, the charge controller should be equipped with a display, for example, a light-emitting diode (LED) that indicates the conditions "Battery can be further discharged (green)" and "Battery is fully discharged (red)". Other conditions like "Battery close to end-of-discharge" can be helpful. Furthermore, an experienced operator can draw a lot of information from a meter showing the battery's voltage and current as shown in Figure 19.10.

All user interfaces should be ergonomic and provide only that information really required by the operator.

Energy-management systems are equipped with (potential free) inputs and outputs to communicate with external components, for example, to remotely start a diesel generator. In addition, standard interfaces such as RS 232, RS 485 or CAN-Bus can be integrated

Downloaded from https://onlinelibrary.wiley.com/doi/ by <Shibboleth-member@purdue.edu, Wiley Online Library on [25/08/2024]. See the Terms and Conditions (https://onlinelibrary.wiley.com/terms-and-conditions) on Wiley Online Library for rules of use; OA articles are governed by the applicable Creative Commons License

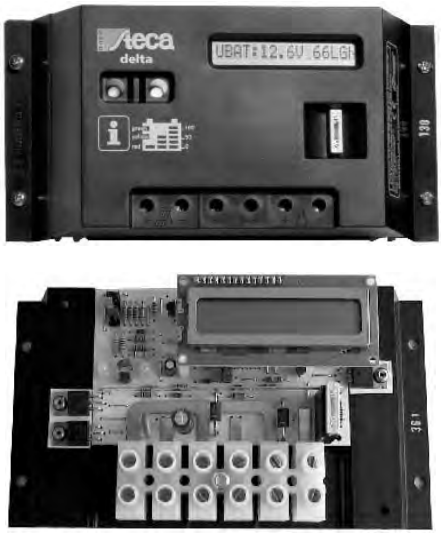


Figure 19.10 Charge controller with integrated voltage and current meter (Courtesy: STECA Solarelektronik, Germany)

to parameterise the controller, to read out the status of the system or to download operation data from the built-in data logger. Another feature is to communicate with external balance-of-system components via power line transmission.

In Solar Home Systems, the charge controller can act as an energy meter or can be used to automatically debit energy costs from a pre-paid card.

19.1.1.8 Design criteria and appraisal factors for charge controllers

The following summary of requirements is intended to support a designer or a purchaser of a charge controller. Which of these requirements must be met has to be decided specifically for each individual application.

The values of voltage thresholds and so on are related to lead acid batteries.

1. Charging phase.

- The end-of-charge voltage threshold should be adjustable according to the battery in use (2.3–2.5 V/cell at 25°C). To prevent extreme misadjustment, the setting range should not extend beyond these limits.
- The end-of-charge voltage can automatically be adapted to the system voltage (e.g. 12 V or 24 V).
- If the battery temperature is expected to deviate more than ±10°C from the average temperature under operation, the end-of-charge voltage should have a temperature compensation (approximately −4 to −6 mV/K per cell). If the temperature deviation is smaller, temperature compensation is not mandatory and the threshold should be set

Downloaded from https://onlinelibrary.wiley.com/doi/ by <Shibboleth-member@purdue.edu>, Wiley Online Library on [25/08/2024]. See the Terms and Conditions (https://onlinelibrary.wiley.com/terms-and-conditions) on Wiley Online Library for rules of use; OA articles are governed by the applicable Creative Commons License

according to the average battery temperature. Fail-safe behaviour is crucial in case of a temperature-monitoring malfunction, for example, due to broken sensor wires.

- The thresholds must be stable over temperature and time.
- If relays are used as control elements, the minimum switching period should be 1 to 5 min.
- The charge controller should be able to charge totally flat batteries. As a minimum requirement, charging should start from a cell voltage of 1.5 V.
- The battery voltage can be monitored by separate sensor wires. This is recommended if the battery wiring is long and of low cross-section. Fail-safe behaviour is crucial in case of broken sensor wires.
- The charge controller should be able to automatically perform gassing charging or equilibration charging according to the manufacturer's recommendations.
- It must be possible to prevent gassing charging in case of valve-regulated batteries (Gel- or AGM-VRLA batteries).
- The output voltage must be limited to safe values in the case of system operation without a battery, for example, due to unintended disconnection of the battery, wire breakage or blowing of the battery's fuse.

2. Deep-discharge protection.

- Deep-discharge protection is mandatory for a long service life. Only when the function of the system is more important than the battery life (e.g. in SOS telephones), deep-discharge protection can be omitted.
- The threshold voltages should be adjustable in a range of 1.5 to 2.0 V/cell. The adjustment range should not extend beyond this range to prevent extremely incorrect settings.
- The threshold should not be temperature-compensated.
- The threshold must be stable over temperature and time.
- The threshold can automatically adapt to the instantaneous battery current.
- The threshold can be based on the battery's actual state of charge.
- A time delay of 10 to 60 s should be implemented between undershooting of the threshold and the actual load disconnection.
- A warning signal can be given out when the deep-discharge condition is approached, for example, switch on a yellow LED 30 min before load disconnection at full load.
- Load disconnection can be performed according to load priorities.
- After load disconnection, only minimum current ($<I_{10.000}$) should be drawn from the battery. This can be achieved by appropriate design, for example, displaying of the current system status only on demand.
- The threshold for load reconnection should be relatively high, for example, >2.1 V/cell.
- A time delay of 10 to 60 s should be implemented between overshooting of the reconnection voltage threshold and the actual reconnection of the load.

3. Efficiency.

- The parasitic consumption of the charge controller should be less than 0.2% of the PV generator's power, for example, <8 mA in a 12-V/50-W controller.

Downloaded from https://onlinelibrary.wiley.com/doi/ by <Shibboleth-member@purdue.edu>, Wiley Online Library on [25/08/2024]. See the Terms and Conditions (https://onlinelibrary.wiley.com/terms-and-conditions) on Wiley Online Library for rules of use; OA articles are governed by the applicable Creative Commons License

- The voltage drop measured between the PV input terminal and the battery terminal should be less than 4% at full charging current, for example, approximately 0.5 V in a 12-V system.
- The voltage drop measured between the battery terminal and the load terminal should be less than 4% at full load current, for example, approximately 0.5 V in a 12-V system.
- The above-mentioned figures lead to an efficiency of >96% under rated charging as well as discharging conditions.

4. Safety aspects and compliance to codes.

- The charge controller must be protected against the reverse polarity of the input voltage and the battery voltage, for example, by a combination of fuses and diodes. Also, interchange of the inputs and outputs must not lead to damage.
- The charge controller must permanently withstand the maximum possible open-circuit voltage of the PV generator. This occurs at maximum insolation and minimum module temperature.
- Inputs and outputs must be protected against transient over-voltages by appropriate voltage arresters, for example, varistors.
- The charge controller must be designed according to the ambient temperatures at the usage site.
- The housing for the charge controller must withstand the environmental stress at the usage site, for example, protection level IP 00 inside a control cabinet, or IP 65 for outdoor applications.
- The electronic components should be protected by lacquer or encapsulation.
- The terminals should be generously dimensioned and robust. Cage clamps are a preferred solution.
- The charge controller must comply with relevant codes concerning electric safety and electromagnetic compatibility (EMC). It must have a Communautés Européennes (CE) label.

19.1.2 Charge Equaliser for Long Battery Strings

19.1.2.1 Introduction

All electrochemical storage systems react sensitively to operating states that do not conform to their specifications, such as overcharging, deep discharge or reversed polarity. The general observations are that the lifetime is shortened, the storage capacity and the efficiency are diminished and more maintenance is required. Further, detrimental conditions can arise with some batteries, for example, lithium-ion batteries, which lead to destruction or even explosion.

Thus, the manufacturers specify the allowable charging and discharging voltages, currents and also temperatures very precisely for individual cells – for the voltages, tolerances on the order of 1% are no exception.

However, on proceeding from the individual cell to series connection of several cells or groups of cells, which are usually needed, a well-known phenomenon is observed: in all applications, from laptops through PV systems and electric vehicles to

Downloaded from https://onlinelibrary.wiley.com/doi/ by <Shibboleth>-member@purdue.edu, Wiley Online Library on [25/08/2024]. See the Terms and Conditions (https://onlinelibrary.wiley.com/terms-and-conditions) on Wiley Online Library for rules of use; OA articles are governed by the applicable Creative Commons License

un-interruptible power supplies and grid back-up systems, each individual cell in the series connection behaves differently. This individualisation results from differences in cell capacity, self-discharge rate, charging factor and so on. They are determined by production conditions, ageing and temperature and cannot be avoided on principle.

Conventional charge controllers are not able to recognise this variation in the behaviour of the cells, so that the undesirable operating conditions listed above arise. In practice, it is evident that the "weakest link in the chain" determines the quality of the whole string, and that the deviating performance of a single cell can lead to a chain reaction.

The problem of increasing divergence in individual cell properties within a battery has been known since the beginning of battery technology, so that over the years a number of different procedures to solve the problem have been developed. Most of them are based on the dissipation of the surplus energy of fully charged cells in a bypass element. This approach is not suitable for applications in which highest efficiency is crucial, such as PV systems. Furthermore, it is effective only with a fully charged battery – it has no impact when the battery is being discharged.

On the basis of experience with numerous PV systems, active, non-dissipative charge-equalising systems have been developed. In contrast to conventional dissipative systems, here the surplus energy from cells having a higher state of charge is redistributed among the remaining cells. As indicated in Figure 19.11, this redistribution occurs not only during or at the end of charging but also constantly during discharging.

As a result, cells with a lower capacity are supported by the other cells during discharge. Their relative state of charge decreases evenly with that of the cells with higher capacity. In this way, the entire available capacity of all cells can be used. During charging, some of the charging current is redistributed from weaker cells to stronger ones, so that these are charged with a higher current, resulting in faster charging.

The energy redistribution also allows cells with larger capacity tolerances to be connected together in series. Costly selection of matched cells during battery construction can thus be avoided. In extreme cases, it is even possible to sustain operation with a mixture of new cells and old cells after the replacement of defective cells. Additionally,

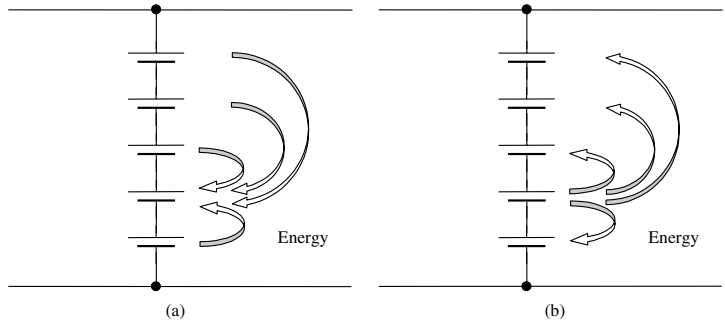


Figure 19.11 (a) Support for a weak cell during discharge by redistribution of energy from stronger cells. (b) Protection against overcharging

Downloaded from https://onlinelibrary.wiley.com/doi/ by <Shibboleth-member@purdue.edu, Wiley Online Library on [25/08/2024]. See the Terms and Conditions (https://onlinelibrary.wiley.com/terms-and-conditions) on Wiley Online Library for rules of use; OA articles are governed by the applicable Creative Commons License

it has been shown that the energy efficiency can increase as overcharging or reverse charging is prevented.

19.1.2.2 The T-CHEQ principle

Several different procedures for active charge equalisation were developed and publicised under the name "CHarge EQualizer" (CHEQ) [1].

The "T-CHEQ" principle is based on a multiple-gate forward converter as shown in Figure 19.12. It can be used over a wide power range, but is particularly suited to higher power values. Here, the cells are coupled magnetically via coils, which are wound around a common core. The coils are periodically connected to the single cells with alternating polarity via semiconductor switches. As the same voltage is induced in all the coils due to the tight coupling, an equalising current automatically flows into or out of the cells if there is any deviation from the average cell voltage. It is advantageous that all cells can be treated simultaneously. Furthermore, this device can be extended to a battery charger by feeding energy into an additional coil wound around the core.

19.1.2.3 Operating experience

The working principle of active charge equalisation has been proven in numerous laboratory tests and pilot installations.

A typical charging cycle from a long-term test with a T-CHEQ system is shown in Figure 19.13. The battery was charged according to a CC/CV charging profile with a

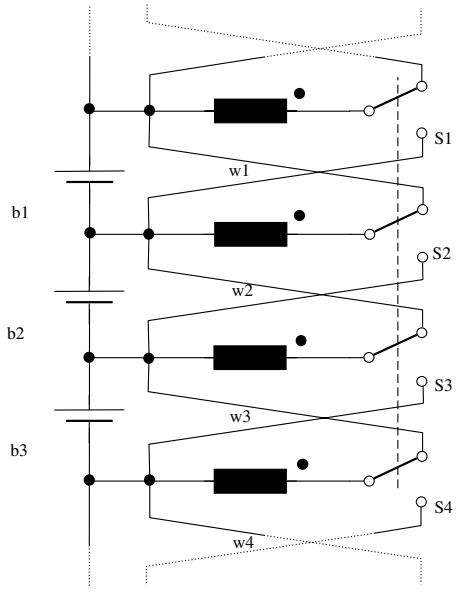


Figure 19.12 CHarge EQualizer with transformer coupling (T-CHEQ)

Downloaded from https://onlinelibrary.wiley.com/doi/ by <Shibboleth-member@purdue.edu>, Wiley Online Library on [25/08/2024]. See the Terms and Conditions (https://onlinelibrary.wiley.com/terms-and-conditions) on Wiley Online Library for rules of use; OA articles are governed by the applicable Creative Commons License

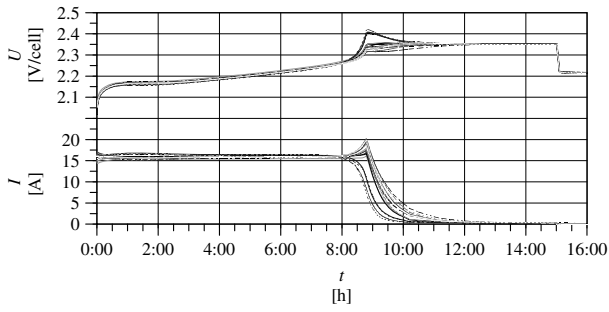


Figure 19.13 Voltages and currents of 16 series-connected cells during charging with an activated T-CHEQ

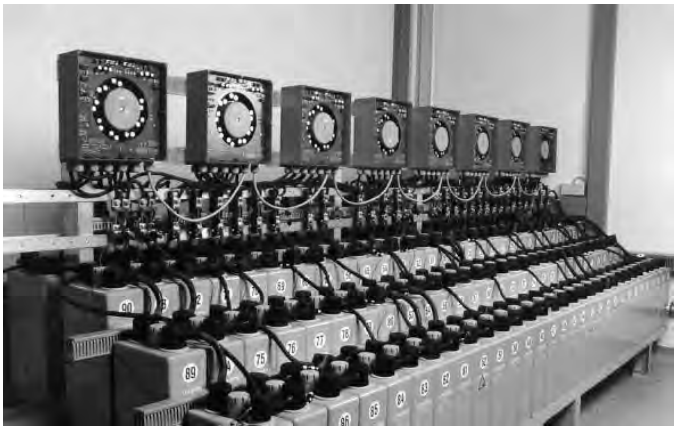


Figure 19.14 Experimental set-up with a 342-V/200-Ah sealed lead acid battery with eight cascaded T-CHEQs

charging current of 16 A and an end-of-charge voltage of 2.35 V/cell. The upper curves in Figure 19.13 show the 16 individual cell voltages and the lower curves show the corresponding cell currents. The cells with a lower capacity are the first to be fully charged – their voltage increases above the average voltage. As a result, the T-CHEQ draws some of the charging current from these cells and directs it to the cells with a lower state of charge. After 9 h, some cells are effectively charged only with 5 to 10 A, whereas the charging current for others is around 20 A. At the end of the charging phase, the T-CHEQ achieves a convergence of all the cell voltages and all the cells are fully charged.

Investigations of a 342-V/200-Ah sealed lead acid battery (VRLA, Gel-type) with eight cascaded T-CHEQs (Figure 19.14) show that such high system voltages can be operated without any difficulties. This type of battery is very sensitive to overcharging due to its demobilised electrolyte.

Petitioner Canadian Solar (USA) Inc., Ex. 1035, p. 2266

Downloaded from https://onlinelibrary.wiley.com/doi/ by <Shibboleth-member@purdue.edu, Wiley Online Library on [25/08/2024]. See the Terms and Conditions (https://onlinelibrary.wiley.com/terms-and-conditions) on Wiley Online Library for rules of use; OA articles are governed by the applicable Creative Commons License

19.2 INVERTERS

19.2.1 General Characteristics of PV Inverters

Since the production cost of PV electricity is several times more expensive than conventional electric energy, conversion efficiency becomes predominant to the economics of the total PV system. As a consequence extremely high efficiency not only in the nominal power range but also under a part-load condition is a requirement for PV inverters in grid-connected as well as in stand-alone systems. Since some characteristics of both types of applications are different, they will be highlighted separately in the following chapter.

19.2.2 Inverters for Grid-connected Systems

This configuration consists mainly of the following components: the PV generator, the inverter, the safety devices and, in many cases, the electric meter as shown in Figure 19.15.

The actual power fed into the grid can be estimated by multiplying the actual power of the PV generator with the actual efficiency of the inverter if we neglect the losses in the safety device and in the meter. More important is the energy produced by the system after a certain period of time, for example, after one year of operation. In this case the mean efficiency of the inverter taking into account all load conditions throughout the year becomes important. As a first step the inverter must allow the PV generator to operate in the MPP by adjusting the corresponding operation voltage as shown in Figure 19.16.

Many inverters adjust this operation voltage continuously to the actual MPP. This operation is called maximum power point tracking (MPPT). The method most commonly used to perform the MPPT is to change the actual input voltage in such a way that maximum power is obtained (Figure 19.8). The effect of continuous MPPT is often overestimated. Simulation has shown that for grid-connected PV systems, CV operation leads only to losses between 1 and 2% when properly adjusted [1, 2].

For optimum use of the PV energy, MPPT and CV operation can be seen as equivalent. As a matter of their operation principle, single-phase inverters, which are most common in small-scale PV systems ($P \leq 5$ kW$_P$), lead to deviations from the MPP due to DC ripple, which is explained as follows: when injecting AC power into the grid, the feed-in current should be in phase with the grid's voltage, which means that the power factor equals one as shown in Figure 19.17.

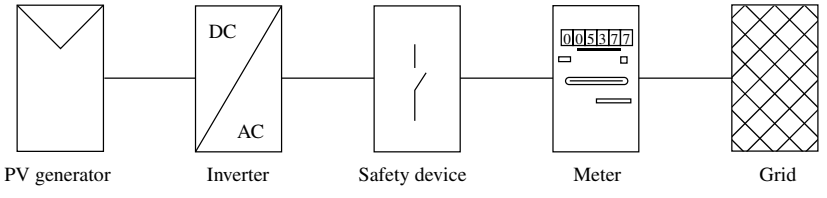


Figure 19.15 General structure of a grid-connected PV system

Downloaded from https://onlinelibrary.wiley.com/doi/ by <Shibboleth-member@purdue.edu>, Wiley Online Library on [25/08/2024]. See the Terms and Conditions (https://onlinelibrary.wiley.com/terms-and-conditions) on Wiley Online Library for rules of use; OA articles are governed by the applicable Creative Commons License

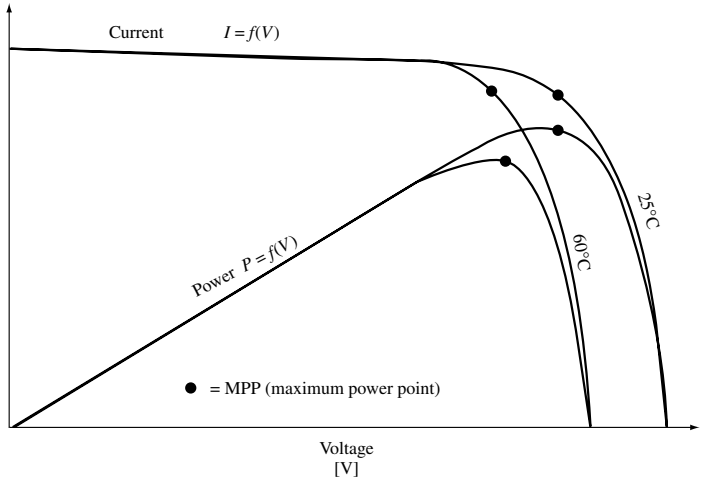


Figure 19.16 Maximum power point (MPP) for different module temperatures

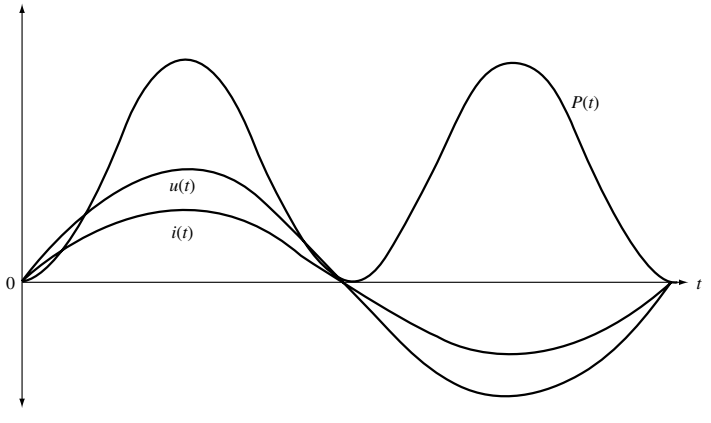


Figure 19.17 Pulsewise injection of power into single-phase grids needs energy storage

As a consequence, the actual power injected into the grid becomes

$$\begin{aligned} P(t) &= u(t) \cdot i(t) \\ &= u_o \cdot \sin(\omega t) \cdot i_o \cdot \sin(\omega t) \\ &= u_o \cdot i_o \cdot \sin^2(\omega t) \\ &= ui[1 + \sin(2\omega t)] \end{aligned}$$

These power pulses with a frequency of 100 Hz are also shown in Figure 19.17. Since the PV generator provides continuous and quasi-constant power and since power injection

Downloaded from https://onlinelibrary.wiley.com/doi/ by <Shibboleth-member@purdue.edu, Wiley Online Library on [25/08/2024]. See the Terms and Conditions (https://onlinelibrary.wiley.com/terms-and-conditions) on Wiley Online Library for rules of use; OA articles are governed by the applicable Creative Commons License

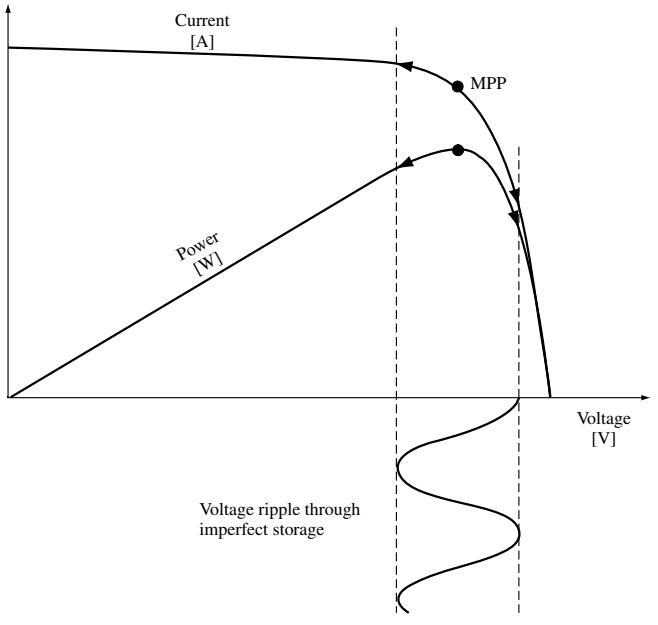


Figure 19.18 Deviations from the MPP through DC voltage ripple caused by the working principle of single-phase inverters

into the grid is pulsewise, each single-phase inverter needs a storage element that can be realised either using a capacitor or an inductor [3]. Since for economic reasons these storage elements must be limited, a voltage ripple can be found with all single-phase inverters at the DC side. This ripple forces the PV generator to deviate from the MPP as shown in Figure 19.18.

Well-designed single-phase inverters show DC voltage ripple with a negligible influence on MPP deviations. It should be noted at this point that three-phase inverters inject a continuous power into the grid, which eliminates the need for this kind of storage.

19.2.3 Inverters for Stand-alone Operation

Typical inverters for this type are often supplied by batteries. They have to provide constant voltage and frequency to the loads irrespective of the actual load profile. In case of reactive loads they have to provide and to absorb reactive power.

In hybrid PV systems, they should be able to operate in a bi-directional mode. This means that they should be able to recharge the battery in case of surplus power at the AC side.

Basically, both inverter types for a grid-connected and stand-alone operation have very similar hardware elements with respect to power electronics. Differences are found in inverter control.

Downloaded from https://onlinelibrary.wiley.com/doi/ by <Shibboleth-member@purdue.edu>, Wiley Online Library on [25/08/2024]. See the Terms and Conditions (https://onlinelibrary.wiley.com/terms-and-conditions) on Wiley Online Library for rules of use; OA articles are governed by the applicable Creative Commons License

19.2.4 Inverter Principles

19.2.4.1 General aspects

Basically, inverters convert direct current (DC) into alternating current (AC) by inversion of the DC polarity in the rhythm of the desired AC frequency (Figure 19.19). The symbol used to describe an inverter is shown in Figure 19.20.

19.2.4.2 Square-wave-type inverters

A simple version of such an inverter is shown in Figure 19.21.

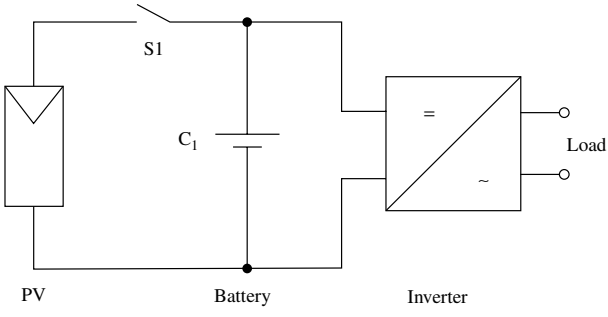


Figure 19.19 Typical configuration for stand-alone AC power supply systems

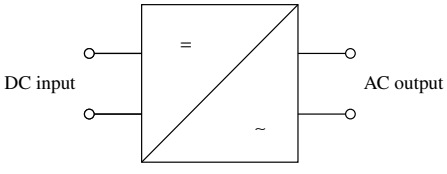


Figure 19.20 Symbol used to describe inverters

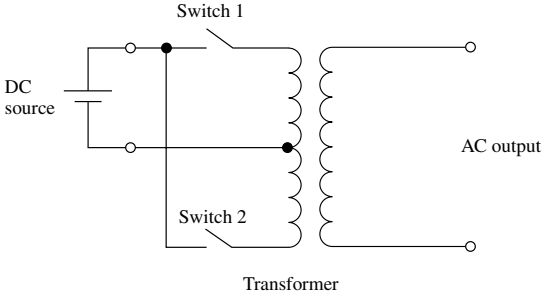


Figure 19.21 Layout of a simple inverter with square-wave AC output

Petitioner Canadian Solar (USA) Inc., Ex. 1035, p. 2270

Downloaded from https://onlinelibrary.wiley.com/doi/ by <Shibboleth-member@purdue.edu, Wiley Online Library on [25/08/2024]. See the Terms and Conditions (https://onlinelibrary.wiley.com/terms-and-conditions) on Wiley Online Library for rules of use; OA articles are governed by the applicable Creative Commons License

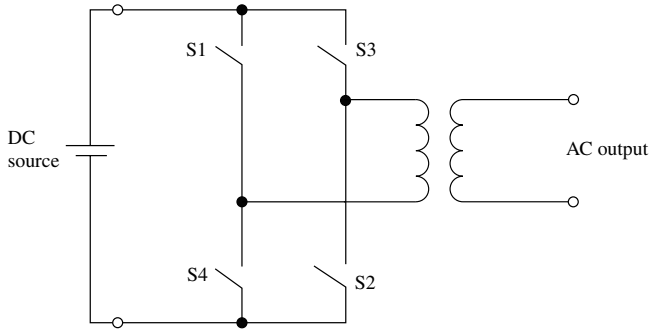


Figure 19.22 H-bridge-type inverter

AC at the primary windings of the transformer is produced by alternatively closing the switches 1 and 2. If switch 1 is closed, switch 2 is open and vice versa. The resulting AC output voltage is of the square-wave type, which may be used for resistive-type loads such as incandescent light bulbs and so on. The two primary windings of the transformer can be reduced to one if two more switches are used as shown in Figure 19.22.

In this configuration, the switches are opened and closed pairwise in such a way that the groups S1 and S2 and the groups S3 and S4 open and close alternately. At the output of the H-bridge formed by the switches S1 through S4, AC is already available. The transformer is only necessary in case of a voltage transformation.

19.2.4.3 Inverters with sinusoidal AC output

Since many consumers and the public grid operate on the basis of sinusoidal voltage, high-quality inverters should also be able to provide this type of AC output. This voltage form can be produced by voltage-transformation principles. Two of the most common transformation principles, namely, the step-down and the step-up converter and a combination of both will be highlighted as well as a digital synthesis one.

19.2.4.3.1 Step-down converter (Buck converter)

With the help of these converters, the input DC voltage, which is, for example, generated by the PV generator (V_{PV}) as represented in Figure 19.23, can be stepped down.

If the switch S_1 is turned on at t_0, the diode D is reverse-biased and a circuit current arises (Figure 19.24). The current ($= i_L$) does not increase immediately but rather rises with a rate imposed by the inductor L:

$$\frac{di_L}{dt} = \frac{V_{PV} - V_{load}}{L}$$

Meanwhile, the inductor stores energy in a magnetic form. If S_1 is turned off after $t = t_1$, the load is separated from the supplied system. The current is, however, maintained by the stored energy in the inductor L and flows through the freewheeling

Downloaded from https://onlinelibrary.wiley.com/doi/ by <Shibboleth>-member@purdue.edu, Wiley Online Library on [25/08/2024]. See the Terms and Conditions (https://onlinelibrary.wiley.com/terms-and-conditions) on Wiley Online Library for rules of use; OA articles are governed by the applicable Creative Commons License

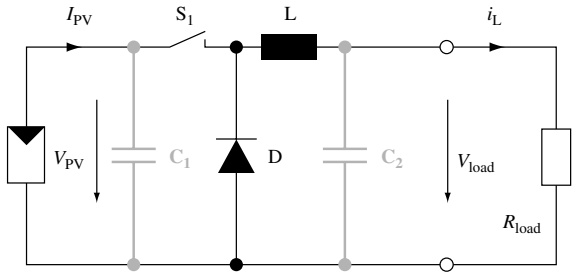


Figure 19.23 Equivalent circuit diagram of a step-down converter

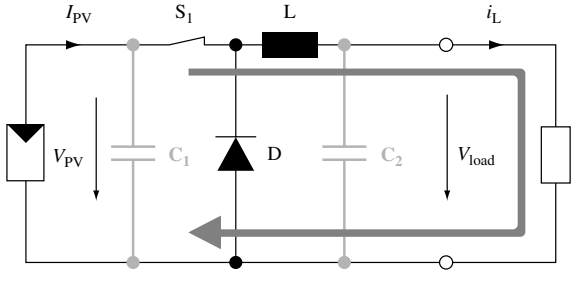


Figure 19.24 Step-down converter during "on" state

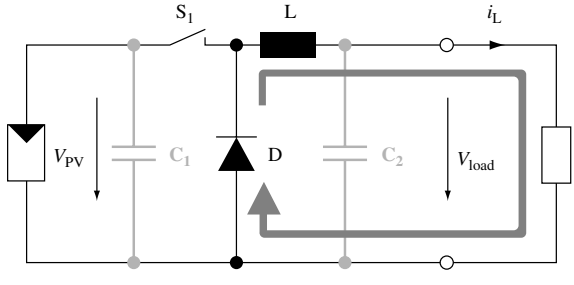


Figure 19.25 Step-down converter during "off" state

diode instead (Figure 19.25). Neglecting the voltage drop across the diode, the current falls down, however, due to the following equation:

$$\frac{\mathrm{d}i_L}{\mathrm{d}t} = -\frac{V_{load}}{L}$$

The capacitor C_1 is used to support the supply voltage (V_{PV}). In principle, S_1 is turned on and off with a switching frequency (i.e. with "t_{on}" and "t_{off}"). With regard to Ohm's law, the behaviour of the load voltage can be obtained from the load current ($= i_L$).

Petitioner Canadian Solar (USA) Inc., Ex. 1035, p. 2272

Downloaded from https://onlinelibrary.wiley.com/doi/ by <Shibboleth-member@purdue.edu, Wiley Online Library on [25/08/2024]. See the Terms and Conditions (https://onlinelibrary.wiley.com/terms-and-conditions) on Wiley Online Library for rules of use; OA articles are governed by the applicable Creative Commons License

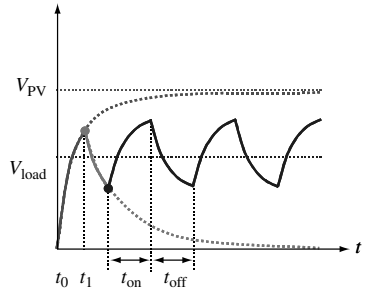


Figure 19.26 Behaviour of the load voltage of a step-down converter

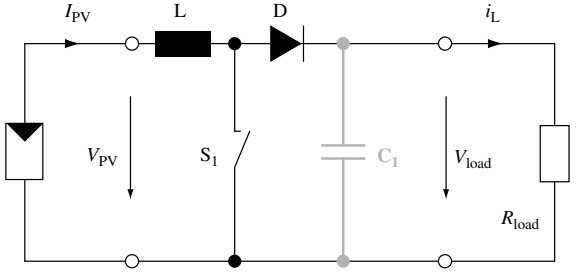


Figure 19.27 Equivalent circuit diagram of a step-up converter

As shown in Figure 19.26, the resulting load voltage obviously has a ripple, which can be smoothed by the additional capacitor C_2. Anyway, its average value (V_{load}) is lower than V_{PV}. In case the switching frequency is increased, for example, up to the kilohertz range, then the necessary inductance can be reduced considerably.

The resulting voltage transformation can be described by the relation of the switching time as follows:

$$\frac{V_{load}}{V_{PV}} = \frac{t_{on}}{t_{off} + t_{on}}$$

19.2.4.3.2 Step-up converter (Boost converter)

By rearrangement of the components of the step-down converter, a step-up converter can be obtained (Figure 19.27). Contrarily, here V_{PV} is stepped up. At a steady state as S_1 is still "off", V_{load} is equal to the V_{PV}, neglecting the voltage across diode.

As shown in Figure 19.28, during "on" state, without C_1 the load voltage drops immediately to zero. The circuit current ($= i_L$) flows through the inductor L and S_1 and rises according to the following equation:

$$\frac{di_L}{dt} = \frac{V_{PV}}{L}$$

Downloaded from https://onlinelibrary.wiley.com/doi/ by <Shibboleth-member@purdue.edu>, Wiley Online Library on [25/08/2024]. See the Terms and Conditions (https://onlinelibrary.wiley.com/terms-and-conditions) on Wiley Online Library for rules of use; OA articles are governed by the applicable Creative Commons License

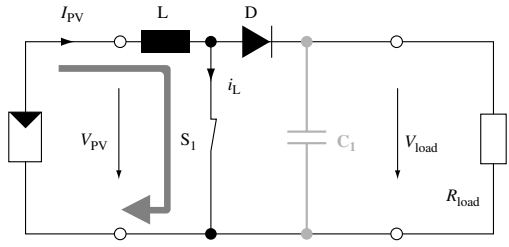


Figure 19.28 Step-up converter during "on" state

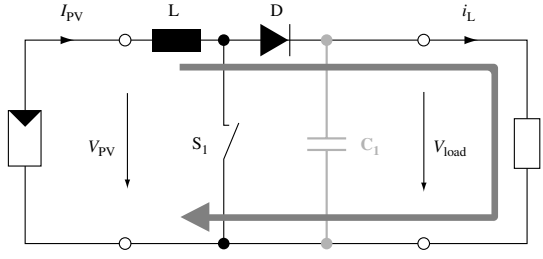


Figure 19.29 Step-up converter during "off" state

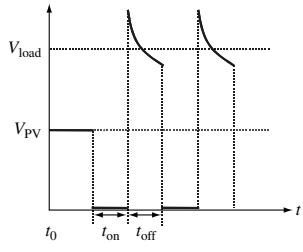


Figure 19.30 Behaviour of the load voltage of a step-up converter

After S_1 is switched off (Figure 19.29), the induced voltage in the inductor adds itself to V_{PV}, which then lies across the load. i_L flows through the inductor and further to the load. Thereby, it falls down gradually because $V_{load} > V_{PV}$:

$$\frac{di_L}{dt} = \frac{V_{PV} - V_{load}}{L}$$

The proceeding of the load voltage is illustrated in Figure 19.30. The diode D protects against a short circuit (i.e. discharge) of the charged capacitor C_1, which is assumed to be so big that it can smooth the load voltage completely.

Downloaded from https://onlinelibrary.wiley.com/doi/ by <Shibboleth-member@purdue.edu, Wiley Online Library on [25/08/2024]. See the Terms and Conditions (https://onlinelibrary.wiley.com/terms-and-conditions) on Wiley Online Library for rules of use; OA articles are governed by the applicable Creative Commons License

The resulting voltage transformation then becomes

$$\frac{V_{\text{load}}}{V_{\text{PV}}} = \frac{t_{\text{off}} + t_{\text{on}}}{t_{\text{off}}}$$

19.2.4.3.3 Step-down/step-up converter (Buck/Boost or inverting converter)

This circuit (Figure 19.31) enables both step down and step up of a DC voltage. During the "on" state, the energy given by the source (PV generator, in this case) is stored in the inductor L (Figure 19.32). The stored energy in the inductor L is then delivered to R_{load} during the "off" state (Figure 19.33). With the help of the diode D, the current flows through the inductor L only in one direction during both "on" and "off" states. As a result, V_{load} obviously has an opposite polarity to V_{PV}. Therefore, the circuit is also called an inverting converter. Equations describing the proceeding of the circuit currents can be derived in the same way to both converters mentioned before and will not be done here. As stated earlier, the capacitor C_1 supports the supply voltage V_{PV} and C_2 smoothes V_{load}. In conclusion, the amplitude of V_{load} can be either lower or higher than V_{PV} depending on the adjusted t_{on} and consequently t_{off} [4]:

$$\frac{V_{\text{load}}}{V_{\text{PV}}} = \frac{t_{\text{on}}}{t_{\text{off}}}$$

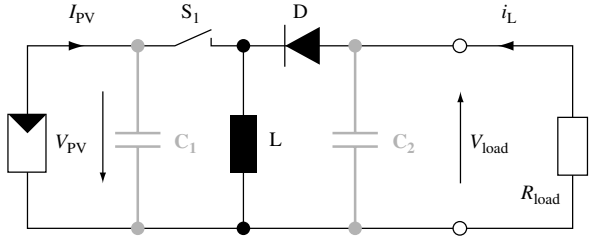


Figure 19.31 Equivalent circuit diagram of a step-down/step-up converter

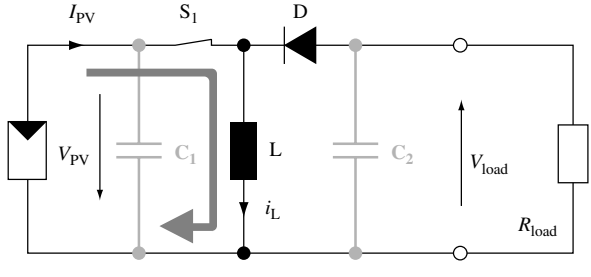


Figure 19.32 Step-down/step-up converter during "on" state

Downloaded from https://onlinelibrary.wiley.com/doi/ by <Shibboleth-member@purdue.edu>, Wiley Online Library on [25/08/2024]. See the Terms and Conditions (https://onlinelibrary.wiley.com/terms-and-conditions) on Wiley Online Library for rules of use; OA articles are governed by the applicable Creative Commons License

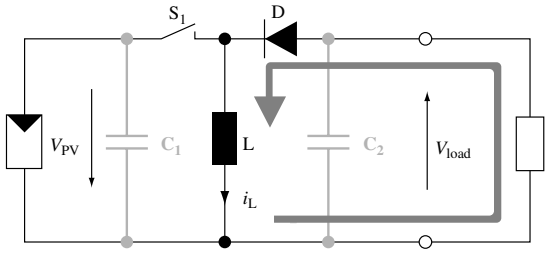


Figure 19.33 Step-down/step-up converter during "off" state

19.2.4.3.4 Combination of a step-down converter with an inverter

The combination of a step-down converter with a voltage inversion is shown in Figure 19.34. It should be noted that in this configuration the voltage of the DC input sources must always be equal to or bigger than the AC peak voltage.

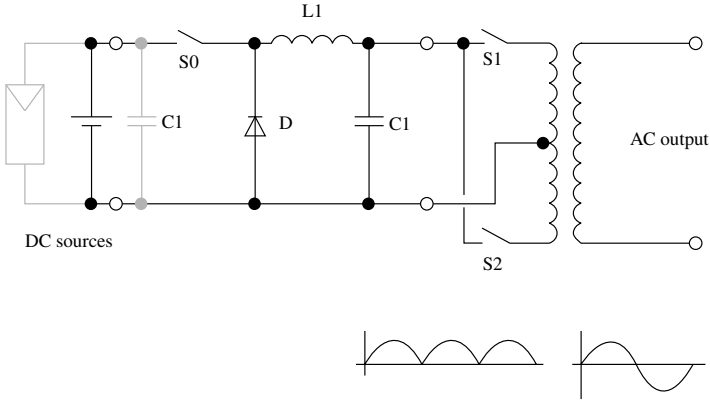


Figure 19.34 The combination of a step-down converter with inverters allows to produce sine-shaped AC output voltage. Wave shapes correspond to the voltage at the terminals over them

19.2.4.3.5 Voltage shaping by digital synthesis

In a further concept, the step-down converter can be replaced by digital synthesis as shown in Figure 19.34. In this concept, the desired voltage is obtained by binary addition of individual voltage sources [5–7]. Depending on the sum of these sources, the sine-shape can be approximated.

When using 5 sources, 32 voltage steps according to 2^5 adjustable levels can be obtained as shown in Figure 19.35. The resulting total harmonic distortion (THD)[1] can be kept well below 5%.

[1] Definition of THD: sum of the amplitudes of all harmonic frequencies compared to the amplitude of the fundamental signal (the 50- or 60-Hz frequency).

Petitioner Canadian Solar (USA) Inc., Ex. 1035, p. 2276

Downloaded from https://onlinelibrary.wiley.com/doi/ by <Shibboleth-member@purdue.edu, Wiley Online Library on [25/08/2024]. See the Terms and Conditions (https://onlinelibrary.wiley.com/terms-and-conditions) on Wiley Online Library for rules of use; OA articles are governed by the applicable Creative Commons License

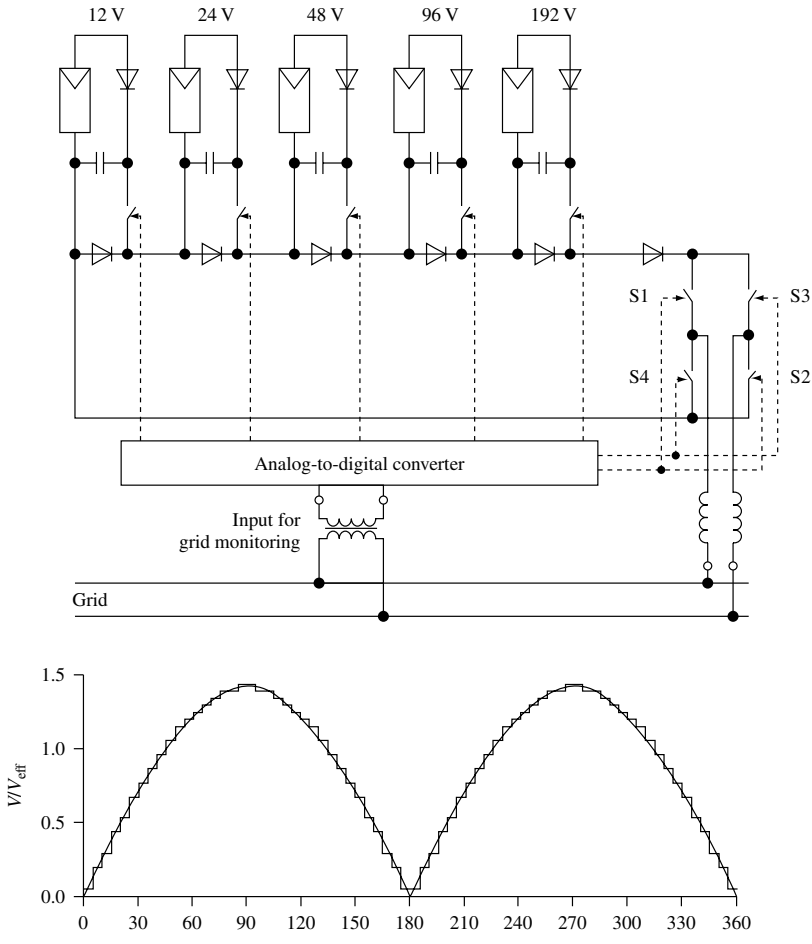


Figure 19.35 Digital waveform synthesis inverter

This concept provides extremely high efficiency since no induction coils or other magnetic elements are required (see Figure 19.35). One disadvantage that can be seen in the use of multiple voltage sources is the increase in cabling needs between the PV generator and the inverter.

In this concept the switches (transistors) S1 through S4 are needed to invert every second sine half-wave to arrive at AC. If using voltage sources with such voltages that they can sum up with the peak voltage of the desired AC output as

$$\sum_{i=1}^{n} V_i = 1.1\sqrt{2}V_{\mathrm{AC}} = 358 \text{ Volts} \quad \text{for 230 V AC (+10\% tolerance)}$$

Downloaded from https://onlinelibrary.wiley.com/doi/ by <Shibboleth-member@purdue.edu, Wiley Online Library on [25/08/2024]. See the Terms and Conditions (https://onlinelibrary.wiley.com/terms-and-conditions) on Wiley Online Library for rules of use; OA articles are governed by the applicable Creative Commons License

no transformer is needed, which increases the efficiency of this concept further, especially under part-load conditions.

19.2.4.3.6 Integration of the step-down principle into the inverting process

The four switches of the H-type bridge itself can also be used to form the desired sine-shape of the AC output. In this case a choke has to be inserted between the bridge and the AC output as shown in Figure 19.36. As has been shown in the concepts before, the switches S1 and S2 and therefore S3 and S4 act synchronously, but their switching frequency becomes very much higher than the desired AC output frequency that is called the fundamental frequency. During the first half-period of the fundamental frequency (10 ms for 50 Hz), the switches S1 and S2 change their on and off state in such a way that the relation t_{on}/t becomes proportional to the actual desired voltage similar to the step-down converter principle shown in Figure 19.23. In fact, the step-down converter principle has been extended to work under both positive and negative polarities.

The configuration shown in Figure 19.36 has become popular since only a very few components are needed, resulting in high efficiency and low cost. One possible disadvantage of this concept is the high DC input voltage necessary for proper working, for example, 358 V DC for 230 V at the AC side. Adding a transformer between the load and the inverter's output allows reducing the DC input voltage according to its transformation ratio. This combination can be found in many products that are in the market today. Compared to the transformer-less version, separation of the potential between source and load becomes feasible. Reduced efficiency and increased investment costs are the consequences, however.

The concept shown in Figure 19.36 allows further operation in a reversed power flow. This situation may occur for inverters in the stand-alone mode if the load is of a reactive type or if surplus power from the AC side is used to charge the battery. In both cases, the variable AC voltage must be transformed to the DC voltage level, which is always higher than any value of the AC voltage as shown in Figure 19.37. By combining S2 and D3 in Figure 19.36, a complete step-up converter can be realised for the positive part of the AC voltage. For the negative part, the combination of S1 and D4 forms the step-up converter for inverse power flow.

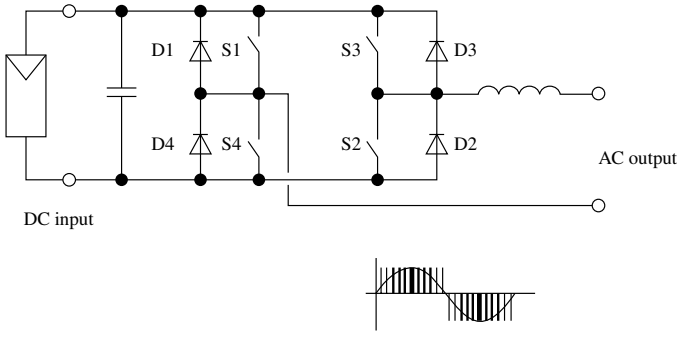


Figure 19.36 Pulse-width modulated (7-phase chopping) H-type bridge inverter

Downloaded from https://onlinelibrary.wiley.com/doi/ by <Shibboleth-member@purdue.edu>, Wiley Online Library on [25/08/2024]. See the Terms and Conditions (https://onlinelibrary.wiley.com/terms-and-conditions) on Wiley Online Library for rules of use; OA articles are governed by the applicable Creative Commons License

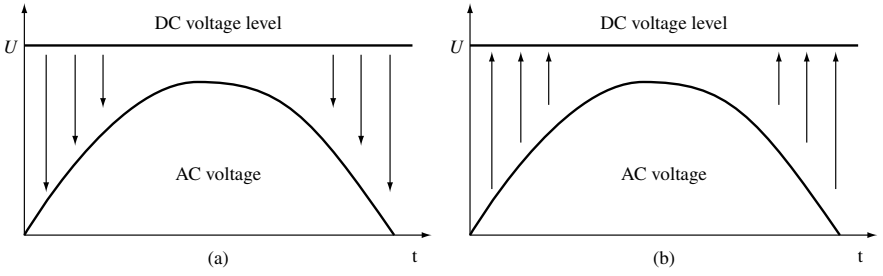


Figure 19.37 (a) Step-down conversion in the forward power-flow mode. (b) Step-up conversion in the reverse power-flow mode

19.2.4.3.7 Bi-directional step-up/step-down conversion

The concept described above allows reversed power flow only in cases in which the DC voltage level is always higher than the peak voltage of the AC side, which means that $U_{DC} \geq 358$ V for 230 V AC. However, there are two possibilities to lower the DC voltage level, that is, to install a transformer at the AC side or to install a bi-directional DC-DC converter at the DC side. Since a conventional step-down converter, as was described earlier, is not able to act as a step-up converter in the reversed power-flow mode, either two converters in anti-parallel mode or a different conversion concept would be necessary. One topology developed by Cuk [8] in 1977, which is able to fulfil these requirements, is given in Figure 19.38.

This conversion principle is in fact able to perform step-up as well as step-down conversion in both directions. The relation between the input voltage U_1 and the output voltage U_2 becomes:

$$U_2 = U_1 \cdot \frac{t_{on}}{(t_{off} + t_{on}) \cdot \left(1 - \frac{t_{on}}{(t_{off} - t_{on})}\right)}$$

Switches S1 and S2 operate complementarily, for example, if S1 is on, S2 is off and vice versa.

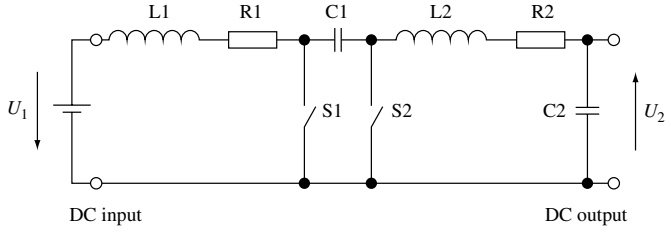


Figure 19.38 Bi-directional Cuk converter

Downloaded from https://onlinelibrary.wiley.com/doi/ by <Shibboleth>-member@purdue.edu, Wiley Online Library on [25/08/2024]. See the Terms and Conditions (https://onlinelibrary.wiley.com/terms-and-conditions) on Wiley Online Library for rules of use; OA articles are governed by the applicable Creative Commons License

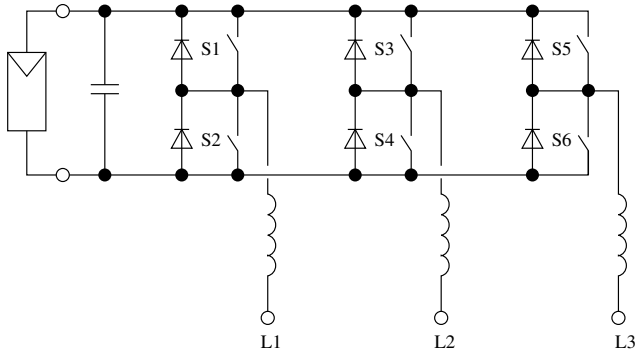


Figure 19.39 Three-phase PWM inverter

19.2.4.3.8 Three-phase configuration

The configuration shown in Figure 19.36 is also very well suited to be expanded into a three-phase version as given in Figure 19.39 [4].

This type of inverter is normally suited to a power range above 5 kW. Connection efforts at the AC side are somewhat higher since three terminals have to be dealt with. The most striking advantage of a three-phase concept can be seen in the fact that the power output and, thus, the power input are absolutely constant. As a consequence, no storage capacitor at the DC input side is needed.

This concept can also be combined with a three-phase transformer in a way as has been described earlier.

This inverter type is most commonly used in PV pumping systems. In contrast to most other applications, PV pump inverters operate with variable frequency and voltage at the AC output side. As an example, a typical characteristic of a centrifugal pump system is given in Figure 19.40.

The figure shows the pump head as a function of mass flow. The parameters are pump speed equivalent to the frequency and system efficiency.

Since the sinusoidal shape is obtained by a step-down process, as was described earlier, lowering of the AC voltage can be easily performed by the same configuration. In addition, MPP tracking can easily be performed by adjusting the frequency and proportionally the AC voltage in such a way that the PV generator can provide maximum power. In Figure 19.41, a typical PV pump system configuration is shown.

19.2.4.3.9 High-frequency concepts

If electric isolation between DC input and AC output is requested and if the bulky 50-Hz transformer should be avoided, high-frequency (HF) transformer concepts may be used. Three topologies using HF concepts will be described in this section.

In the first concept, the configuration as described in Figure 19.34 is used to operate with a high frequency (some 100 kHz) using an HF transformer. The HF square-wave

Downloaded from https://onlinelibrary.wiley.com/doi/ by <Shibboleth-member@purdue.edu, Wiley Online Library on [25/08/2024]. See the Terms and Conditions (https://onlinelibrary.wiley.com/terms-and-conditions) on Wiley Online Library for rules of use; OA articles are governed by the applicable Creative Commons License

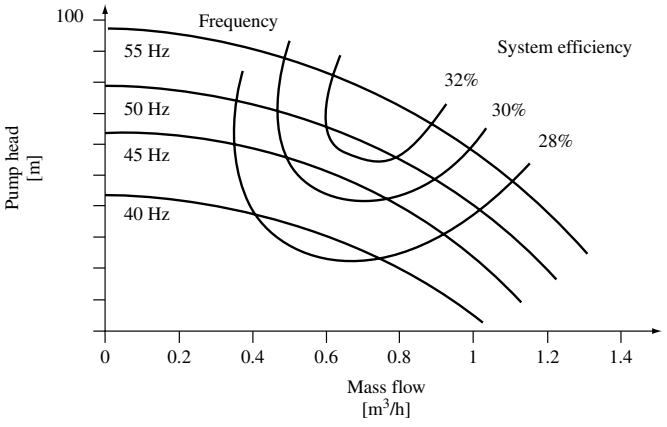


Figure 19.40 Characteristic of a centrifugal pump system

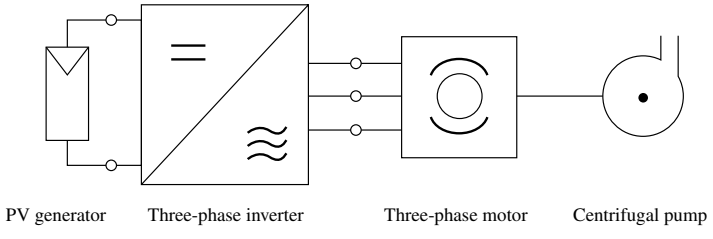


Figure 19.41 Typical layout of an AC PV pumping system

AC output is then rectified as shown in Figure 19.42, providing the desired DC voltage necessary for PWM inversion according to the H-type Bridge explained in Figure 19.36.

Compared to the low-frequency concepts, it becomes obvious that the savings using the HF transformer are widely being compensated by extra components. This might be one of the reasons HF concepts have not widely been used in inverters offered to the market so far.

When operating the high-frequency concept, as described in Figure 19.42, in the PWM mode, in which the desired low frequency is used for modulation, a PWM series of unipolar half-waves result after the rectifier at the secondary windings of the HF transformer. By means of the combination of L and C_2, a unipolar series of sine-shaped half-waves result, which are finally inverted with the H-type bridge as described in Figure 19.43. The 100-Hz pulsewise power injection requests an adequate storage element, which is realized by means of the capacitor C_1. It should be noted that this storage function is realized with C_2 in the topology presented previously in Figure 19.42.

Finally, an HF concept is presented in which AC is directly produced at the secondary side of the HF transformer. In this case, the non-controlled rectifier shown in

Downloaded from https://onlinelibrary.wiley.com/doi/ by <Shibboleth-member@purdue.edu, Wiley Online Library on [25/08/2024]. See the Terms and Conditions (https://onlinelibrary.wiley.com/terms-and-conditions) on Wiley Online Library for rules of use; OA articles are governed by the applicable Creative Commons License

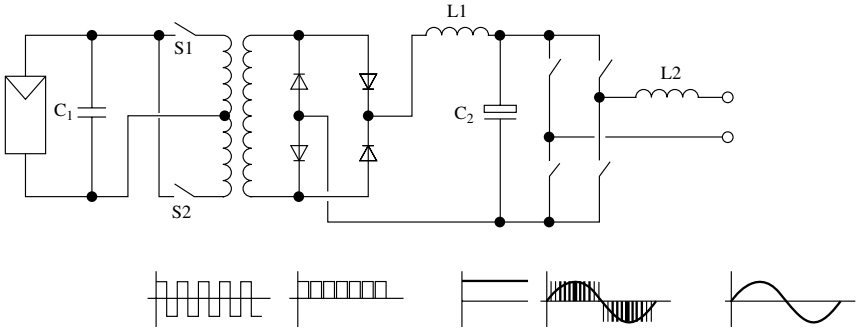


Figure 19.42 HF transformer combined with PWM H-type bridge inverter

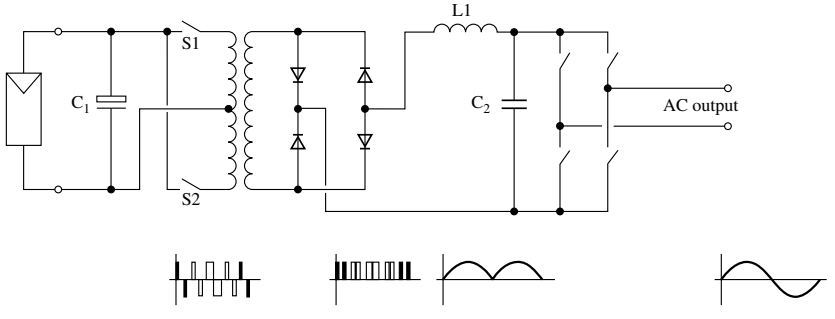


Figure 19.43 HF transformer combined with PWM high-frequency generator at the input side and a low-frequency H-type bridge at the output side

Figure 19.43 has been replaced by active switches combining the functions of rectification and inversion. This configuration is shown in Figure 19.44. It should be noted that in this case, the switches in the H-type bridge have to be operated in the rhythm of the high frequency in contrast to the configuration according to the topology shown in Figure 19.43. Since transistors switched with higher frequencies have higher losses as well as higher investment costs, the benefit of saving the passive rectifier used in the concept given in Figure 19.43 might be compensated by these facts to a certain extent.

19.2.5 Power Quality of Inverters

When dealing with power quality, a distinction has to be made between stand-alone and grid-connected applications.

In a stand-alone operation, the output waveform becomes important for many applications. Square-wave inverters, according to the working principle shown in Figure 19.21 or Figure 19.22, may be used to power resistive-type loads such as light bulbs or similar objects. When feeding power to reactive-type loads such as motors, proper operation

Downloaded from https://onlinelibrary.wiley.com/doi/ by <Shibboleth> -member@purdue.edu, Wiley Online Library on [25/08/2024]. See the Terms and Conditions (https://onlinelibrary.wiley.com/terms-and-conditions) on Wiley Online Library for rules of use; OA articles are governed by the applicable Creative Commons License

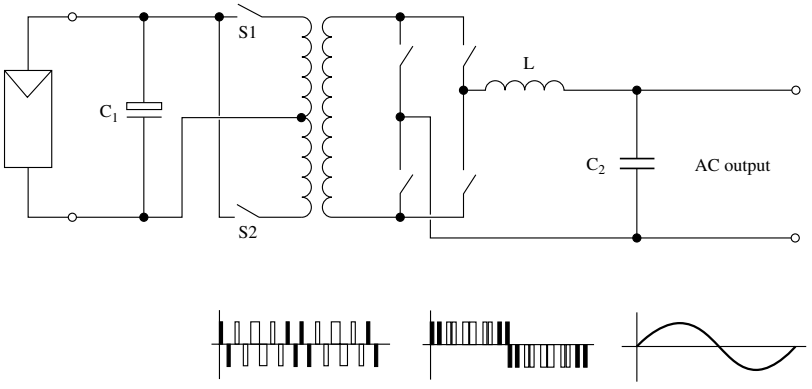


Figure 19.44 Direct AC synthesis at the secondary winding of the HF transformer. The PWM high-frequency signal is inverted in the low-frequency rhythm and smoothed by means of L and C_2. C_1 is needed to store the input energy in the rhythm, which equals twice the low frequency

might become difficult and losses inside the load created by the square-wave character of the supply might occur [9]. For these load-types, ideal sinusoidal voltage supply would be best. In reality, a compromise between this ideal voltage that results in high expenses and a lower quality for cheaper investments must be found.

The deviation from the ideal sinusoidal voltage is normally described as total harmonic distortion (THD). THD is usually defined as the ratio of the square root of the sum of the squares of the rms values of the harmonics to the rms value of the fundamental. This ratio is usually converted to percent or decibels (dB). As an example, the third harmonic and their influence on the shape of the fundamental waveform are given in Figure 19.45.

For high-quality power supply, the THD of the output voltage should be less than 5%, which corresponds with the quality of the public grid.

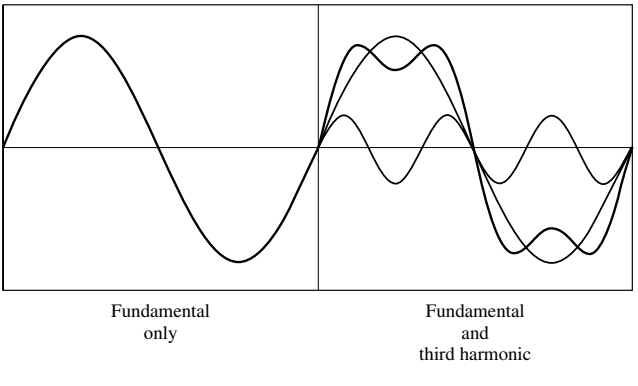


Figure 19.45 Influence of harmonics on the waveform

Downloaded from https://onlinelibrary.wiley.com/doi/ by <Shibboleth-member@purdue.edu, Wiley Online Library on [25/08/2024]. See the Terms and Conditions (https://onlinelibrary.wiley.com/terms-and-conditions) on Wiley Online Library for rules of use; OA articles are governed by the applicable Creative Commons License

As a second and very important power-quality element for stand-alone applications, the ability to provide and to absorb reactive power should be mentioned. Typical loads requesting reactive power are electric motors. Under these load conditions, the load current is no longer in phase with the voltage as shown in Figure 19.46.

Proper handling of reactive power is only possible with appropriate topologies as have been described and presented in Figures 19.36 and 19.37. In some inverter designs, handling of reactive power is limited depending on the load type. In this case, the acceptable power factor, which corresponds with the cosine of the phase-angle difference between voltage and current, is defined and the maximum power of the inverter is given in kilovolt amperes (kVA) instead of kilowatts (kW). The energy of the reactive power, which is to be absorbed and afterwards re-injected into the load, is normally stored in capacitors of appropriate size.

If all the elements in the inverter allow for reverse power flow, a bi-directional inverter is obtained, which can be used to charge the battery, when surplus power at the AC side is available. The combination of a Cuk converter shown in Figure 19.38 with a H-type bridge given in Figure 19.22 allows for such a concept.

Finally, stand-alone inverters should also be able to blow fuses in cases in which a short current occurs in loads. This requirement is perfectly fulfilled with only a few inverters. The reason can be seen in the high current needed to blow fuses. Depending on the reaction time, this current can be as high as five times the nominal one as shown in Figure 19.47.

Some inverters produce this high current by reducing the AC output voltage significantly. The resulting flicker observed for loads not to be separated by the fuse in question may be accepted in most cases.

Since the output voltage of grid-connected inverters has to correspond with the grid's voltage, the quality of the current that is to be injected into the grid becomes important. Under ideal circumstances, this current should be in phase with the grid's voltage (power factor = 1). The deviation from this power factor becomes therefore important for the description of the power quality. All modern transistor-based inverters have a power factor near unity at nominal load, with a tendency towards smaller values under part load (Figure 19.48).

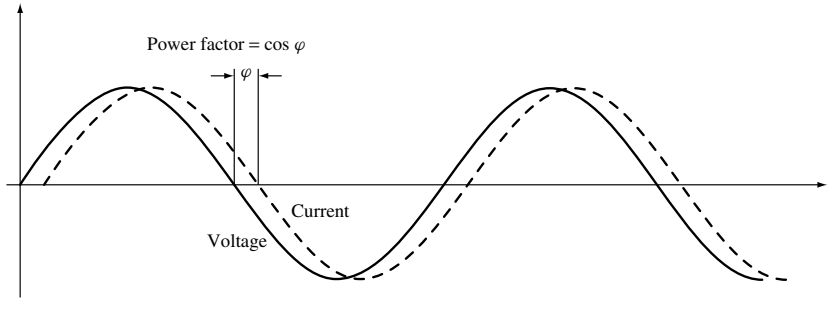


Figure 19.46 Power factors ≠ 1 produced by reactive (inductive or capacitive) loads

Downloaded from https://onlinelibrary.wiley.com/doi/ by <Shibboleth-member@purdue.edu>, Wiley Online Library on [25/08/2024]. See the Terms and Conditions (https://onlinelibrary.wiley.com/terms-and-conditions) on Wiley Online Library for rules of use; OA articles are governed by the applicable Creative Commons License

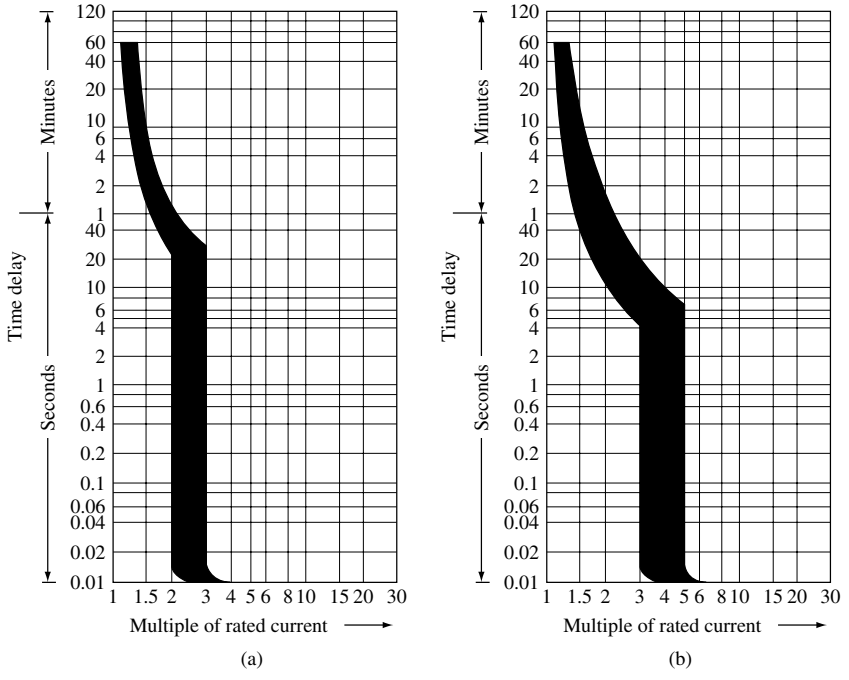


Figure 19.47 Current–time diagram for different fuse types: (a) characteristic left and (b) characteristic right (DIN EN 60898, DIN EN 62019)

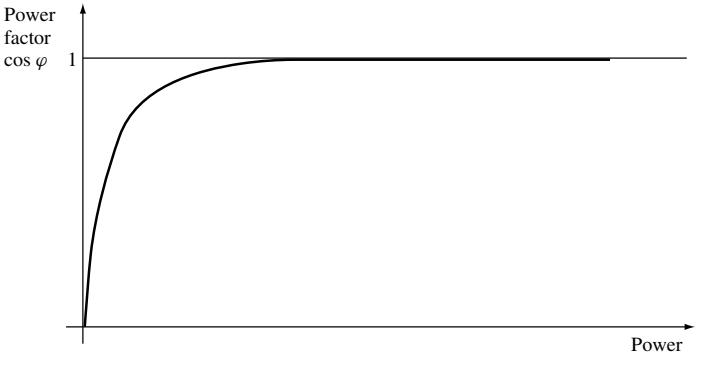


Figure 19.48 Power factor as a function of the output power of a typical grid-connected inverter

For grid-connected inverters' the THD of the current injected into the grid is used to describe the inverters' quality. The THD of the injected current, which is defined in the same way as was done for the voltage. A high-quality grid-connected inverter shows a THD in the current that is below 5%.

Downloaded from https://onlinelibrary.wiley.com/doi/ by <Shibboleth> -member@purdue.edu, Wiley Online Library on [25/08/2024]. See the Terms and Conditions (https://onlinelibrary.wiley.com/terms-and-conditions) on Wiley Online Library for rules of use; OA articles are governed by the applicable Creative Commons License

19.2.6 Active Quality Control in the Grid

Since the power factor in modern grid-connected inverters can be adjusted by internal control, this kind of inverters can be used to compensate reactive power flow in the grid, which otherwise must be performed by extra compensation units such as inductors or capacitors. This ability can either be fixed to a constant value or, in case of an appropriate communication system, be controlled by the grid operator according to the actual needs.

As a further means of power quality improvement, high-quality inverters are able to compensate deviations in the sinusoidal voltage of the grid. As shown in Figure 19.49, the inverter injects surplus power into the grid to compensate for the actual deficit in the voltage.

In a later stage of PV use, inverters will have to prevent grid overloading. Grid-connected inverters can easily handle this kind of power control by changing the DC input voltage from the MPP in such a way that the PV generator reduces power production to the desired level. This request may come in a situation in which several hundreds of megawatts of PV power are fed into a local system. To allow for such ability, the grid operator must be able to communicate with these inverters.

As a consequence, it can be stated that high-quality inverters will be able to improve the power quality in the grid by adjusting the power factor, by reducing the THD and by stabilising power flow through power control. To realise these functions, appropriate control and the availability of a communication element becomes necessary. A few inverters in the market already show these features today.

19.2.7 Safety Aspects with Grid-connected Inverters

An important issue for grid-connected systems is associated with islanding protection. Islanding may occur, if a part of the local grid is switched off, for example, for maintenance reasons and if the injected power is equal to the actual load in the separated part of the grid. This situation is shown in Figure 19.50.

The situation described above becomes very unlikely since not only the effective power but the reactive power as well must be equal between production and consumption.

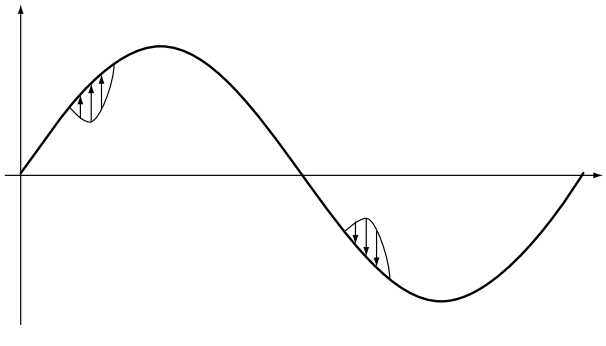


Figure 19.49 Inverter injects surplus power

Downloaded from https://onlinelibrary.wiley.com/doi/ by <Shibboleth-member@purdue.edu, Wiley Online Library on [25/08/2024]. See the Terms and Conditions (https://onlinelibrary.wiley.com/terms-and-conditions) on Wiley Online Library for rules of use; OA articles are governed by the applicable Creative Commons License

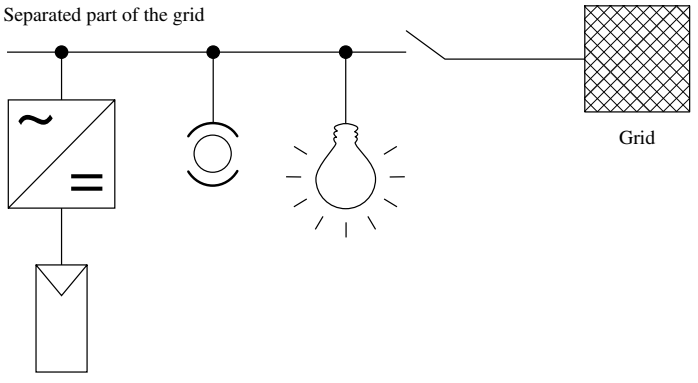


Figure 19.50 After switch-off, the separated part of the grid may continue operation, if the injected power by the PV system equals the actual load

As a first measure, frequency and voltage monitoring will identify by far most situations in grids turned off since the smallest deviations in production or in consumption will lead to changes in frequency or voltage or in both of them. The experience with big wind farms has shown that limitation of voltage or frequency may lead to undesired results, however.

In case of heavy loads on the grid, both the voltage and the frequency may fall below the set point. In this situation, cut-off of power sources takes place when they would be needed urgently to support the grid. As a further method to identify islanding conditions, monitoring of the grid's impedance is being performed by injecting power peaks, which do not correspond with the fundamental frequency (50 or 60 Hz), by the inverter into the grid and by monitoring this influence on the grids voltage shape. This method is currently accepted by German safety code.

This code, which applies to grid-connected single-phase PV systems smaller than 5 kW, requests a separation from the grid, if the impedance of the grid exceeds 1.75 ohms or if a jump in the impedance $\geq$0.5 ohms occurs. Reconnection to the grid is allowed for grid impedance smaller than 1.25 ohms. There are two independent monitoring and switching systems that have been requested. One of the two systems must act on a mechanical switch, for example, a relay, while for the second system, the semiconductors of the inverter output bridge are accepted. Figure 19.51 explains this configuration.

In addition to the monitoring of the grid impedance, frequency deviations above $\pm$0.2 Hz or voltage differences bigger than -15 or $+10\%$ must lead to a separation of the grid as well. The safety protection device can either be integrated into the inverter or installed separately between the inverter and the grid. The latter may be used preferably in combination with small-scale inverters, for example, module-integrated ones. In these cases, the investment cost for integrating the unit in each of the small inverters with a power of not more than a few hundred watts may not be economic. In case of a separate installation, one supervision unit could be used to protect several small module-integrated inverters. As an alternative, also accepted as a safety device, voltage monitoring of all three phases of the grid, which lead to a separation, if one of the three phases becomes

Downloaded from https://onlinelibrary.wiley.com/doi/ by <Shibboleth-member@purdue.edu, Wiley Online Library on [25/08/2024]. See the Terms and Conditions (https://onlinelibrary.wiley.com/terms-and-conditions) on Wiley Online Library for rules of use; OA articles are governed by the applicable Creative Commons License

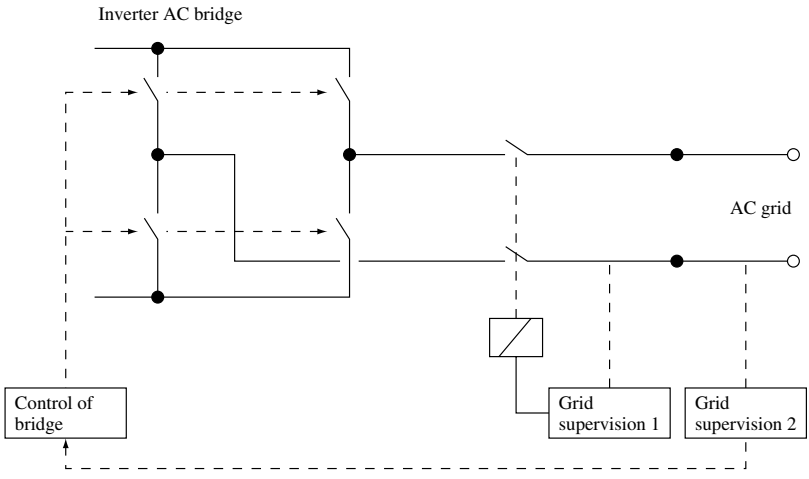


Figure 19.51 Two independent grid-supervision units for safety against islanding (DIN VDE 0126)

zero, can be used in Germany. In case of a single-phase grid, as is the case in many rural areas of the world, this method cannot be applied, however.

There is a limitation to be expected, if a big number of inverters are monitoring the grid in this way. In this case, interference between the different inverters may lead to unspecific interpretation of the grid's response. It might become necessary therefore to equip all inverters with communication capabilities. This feature would allow switching off all relevant inverters by the grid operator if needed. As a further benefit, power-quality improvements controlled by the grid operator will become feasible as well.

19.3 ACKNOWLEDGEMENT

Heribert Schmidt of the Fraunhofer ISE, Freiburg, authored Section 19.1, *Charge Controllers and Monitoring Systems for Batteries in PV Power Systems*. Jurgen Schmidt, of the ISET/Universität Kassel, authored Section 19.2, *Inverters*.

REFERENCES

1. Nekrasov P, "Partial Shunt Regulation", *Proc. 14th Annual Meeting of the Astronautical Society* (May 13–15, 1968).
2. Salim A, "A Simplified Minimum Power Dissipation Approach to Regulate the Solar Array Output Power in a Satellite Power Subsystem", *Proc. 11th Intersociety Energy Conversion Engineering Conference Proceedings*, Vol. II (Nevada, Sept. 12–17, 1976).
3. Siedle Ch, *Vergleichende Untersuchungen von Ladungsausgleicheinrichtungen zur Verbesserung des Langzeitverhaltens vielzelliger Batteriebänke (Comparative investigations of CHarge EQualizers to improve the long-term performance of multi-cell battery banks)*, Doctoral thesis, Reihe 21, Nr. 245, ISBN 3-18-324521-3, Düsseldorf VDI-Verlag (1998).
4. Appelbaum J, Gabbray D, *IEEE Trans. Aerospace Electron. Syst.* AES 21, 484–489 (1985).

Downloaded from https://onlinelibrary.wiley.com/doi/ by <Shibboleth-member@purdue.edu, Wiley Online Library on [25/08/2024]. See the Terms and Conditions (https://onlinelibrary.wiley.com/terms-and-conditions) on Wiley Online Library for rules of use; OA articles are governed by the applicable Creative Commons License

5. Gonzalez G, Hill G, Ross Jr. R, *Photovoltaic Array – Power Conditioner Interface Characteristics*, DOE/JPL-1012-79, Prepared for U.S. Department of Energy (1979).
6. Schmid J, Schmidt H, "Inverters for Photovoltaic Systems", *5th Contractors Meeting Commission of the European Communities DG XVII*, ISPRA (Italy, May 22–24, 1991).
7. Schmid J, Schätzle R, "Simple Transformer-less Inverter with Automatic Grid Tracking and Negligible Harmonic Content for Utility Interactive Photovoltaic Systems", *Proc. 4th EC Photovoltaic Solar Energy Conference*, 316 (Stresa, 1982).
8. Dickerson A, "*Proof of Feasibility of a Novel Inverter for Photovoltaic Power Conditioning*", draft final report, Contract 21-3517, Received from Cal Poly State University, San Luis Obispo, CA (Sept. 1985).
9. Cuk S, Middlebrook R, "A New Optimum Topology Switching DC-to-DC Converter", *Power Electronic Specialists Conference* (1977).

Downloaded from https://onlinelibrary.wiley.com/doi/ by <Shibboleth-member@purdue.edu, Wiley Online Library on [25/08/2024]. See the Terms and Conditions (https://onlinelibrary.wiley.com/terms-and-conditions) on Wiley Online Library for rules of use; OA articles are governed by the applicable Creative Commons License

20

Energy Collected and Delivered by PV Modules

Eduardo Lorenzo

Instituto de Energía Solar – Universidad Politécnica de Madrid, Madrid, Spain

20.1 INTRODUCTION

This chapter deals with two different questions: "How much solar radiation reaches the surface of a photovoltaic (PV) collector?" and "What is the conversion efficiency of this solar radiation into electricity?" Both questions are analysed from the PV-system designer's point of view, whose ultimate interests, depending on the type of application, are the determination of the PV collector surface needed to provide a certain required service, and the estimation of the average electricity yield from a certain PV array.

The input information available for the PV designer is usually restricted to the 12 monthly mean values of global horizontal irradiation, that characterise the solar climate of the location, and to the electrical characteristics of the PV modules under Standard Test Conditions (STC), as provided by its manufacturers. This chapter contains a whole set of procedures applicable to most PV engineering practical problems using only this input information. In particular, models to predict the long-term evolution of the solar radiation incident over any arbitrarily oriented surface, and also models to anticipate the electricity output of PV arrays operating in other than STC are described. Looking for practical usefulness, the chapter is, as far as possible, self-contained and the formulae are presented in such a way, that they can be applied directly to practical problems, even if sometimes empirical or cumbersome expressions have to be introduced. Some examples intended to clarify the proper use of the formulae have also been included.

The two above-mentioned questions intrinsically differ in nature. The random character of the solar radiation over the Earth implies that answers to the first question are never more than future predictions, unavoidably associated with a degree of uncertainty (even if very good past solar radiation data are available). This uncertainty is more than is commonly assumed, and represents a serious limit to the accuracy (or, more strictly, to

Handbook of Photovoltaic Science and Engineering. Edited by A. Luque and S. Hegedus
© 2003 John Wiley & Sons, Ltd ISBN: 0-471-49196-9

Downloaded from https://onlinelibrary.wiley.com/doi/ by <Shibboleth> -member@purdue.edu, Wiley Online Library on [25/08/2024]. See the Terms and Conditions (https://onlinelibrary.wiley.com/terms-and-conditions) on Wiley Online Library for rules of use; OA articles are governed by the applicable Creative Commons License

the significance) of the results of any PV design exercise, irrespective of the complexity of the radiation and PV array models supporting the particular design tool. This means that for stand-alone PV systems, reliability can only be properly estimated for Loss of Load Probabilities greater than 10^{-2}. For grid-connected systems, it implies that yield predictions should be understood to have an uncertainty that can reach up to $\pm 30\%$, for monthly values, and $\pm 10\%$ for annual ones.

Regarding the behaviour of PV modules in arbitrary operating conditions, an $I-V$ model based on the incident irradiance and ambient temperature is presented. Particular attention is paid to the consideration of incidence angle effects, which can be significant in several real situations. Further refinements to incorporate the effects of wind speed, solar spectrum and low irradiance effects are also described. These second-order effects help to explain temporary differences between predicted and observed values, but are of minor importance when long-term energy production calculations are considered.

Finally, some problems related to relevant applications are particularly addressed: the reliability of stand-alone PV systems, the case of Solar Home Systems (SHS) (characterised by a large variety of individual real energy consumption values in contrast to only a few standard ones for design purposes), and the energy yield of grid-connected PV systems.

20.2 MOVEMENT BETWEEN SUN AND EARTH

Although the movement of the sun relative to a fixed point on the Earth seems very familiar, because the sun is fortunately there everyday, the mathematics that governs it is surprisingly complex. In fact, the understanding of such movement was among the longest scientific adventures of mankind. It seems that the very first sundials were built in the Babylonian time (1800 BC), and that the attempts to explain the evolution of the "gnomon" shadow led to the first proposed models of the Sun–Earth movement, which in turn led to the beginning of geometry, in Greece [1]. Figure 20.1 pays a fully

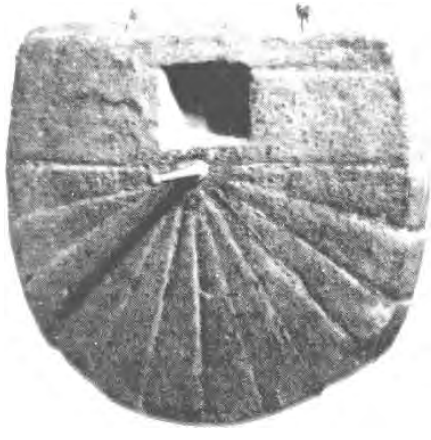


Figure 20.1 Sundial about 2000 years old

Downloaded from https://onlinelibrary.wiley.com/doi/ by <Shibboleth-member@purdue.edu, Wiley Online Library on [25/08/2024]. See the Terms and Conditions (https://onlinelibrary.wiley.com/terms-and-conditions) on Wiley Online Library for rules of use; OA articles are governed by the applicable Creative Commons License

Petitioner Canadian Solar (USA) Inc., Ex. 1035, p. 2291

deserved homage to such a glorious background. However, it was not until the seventeenth century, when Kepler published *Astronomia Nova* (1609) and *Harmonice mundi* (1618), that such movement was completely explained. And then the explanation spread only very slowly. For example, Galileo in his *Dialogo sopra y due massimi del mundo*, published in 1632 (just one year before the famous ecclesiastic sentence condemning him for publicly defending the heliocentric system formerly proposed by Copernicus), still promoted the idea of the planets revolving around the sun in circular orbits, fully ignoring Kepler's work.

Fortunately for us, such discussions ended a long time ago. Today, it is well established that the Earth goes around the sun in an elliptic orbit with the sun at one of the foci. The plane containing this orbit is called the *ecliptic plane* and the time that the Earth takes to complete this orbit leads to the definition of the year. The distance from the sun to the Earth, r, is given by

$$r = r_0 \left[1 + 0.017 \sin \left(\frac{360(d_n - 93)}{365} \right) \right] \tag{20.1}$$

where d_n is the day number counted from the beginning of the year. It is worth noting that the eccentricity of the ecliptic is only 0.017, that is, very small. Because of that, the deviation of the orbit from the circular is also very small, and it is normally adequate to express the distance just in terms of its mean value r_0, equal to 1.496×10^8 km, and is usually referred to as *one astronomical unit*, 1 AU. For most engineering applications, a very simple and useful expression for the so-called eccentricity correction factor is

$$\varepsilon_0 = (r_0/r)^2 = 1 + 0.033 \cos \left(\frac{360 d_n}{365} \right) \tag{20.2}$$

The Earth also spins once a day on its own central axis, the *polar axis*. The polar axis orbits around the sun, maintaining a constant angle of 23.45° with the ecliptic plane. This inclination is what causes the sun to be higher in the sky in the summer than in the winter. It is also the cause of longer summer sunlight hours and shorter winter sunlight hours. Figure 20.2 shows the Earth's orbit around the sun, with the inclined polar axis; and Figure 20.3 adds some details for a particular day and a particular geographic latitude, ϕ. It is important to note that the angle between the equatorial plane and a straight line drawn between the centre of the Earth and the centre of the sun is constantly changing over the year. This angle is known as the *solar declination*, δ. For our present purposes, it may be considered as approximately constant over the course of any one day. The maximum variation in δ over 24 h is less than 0.5°. If angles north of the equator are considered as positive and south of the equator are considered negative, the solar declination can be found from

$$\delta = 23.45^\circ \sin \left[\frac{360(d_n + 284)}{365} \right] \tag{20.3}$$

On the *spring equinox* (20th/21st March) and the *autumn equinox* (22nd/23rd September), the line between the Sun and the Earth passes through the equator. Consequently, $\delta = 0$, the length of day and night is equal all over the Earth, and the sun rises and sets precisely in the east and west, respectively. On the *summer solstice* (21st/22nd June) $\delta = 23.45^\circ$,

Downloaded from https://onlinelibrary.wiley.com/doi/ by <Shibboleth-member@purdue.edu, Wiley Online Library on [25/08/2024]. See the Terms and Conditions (https://onlinelibrary.wiley.com/terms-and-conditions) on Wiley Online Library for rules of use; OA articles are governed by the applicable Creative Commons License

Petitioner Canadian Solar (USA) Inc., Ex. 1035, p. 2292

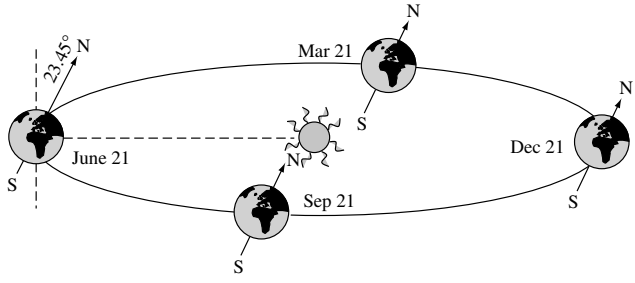


Figure 20.2 The orbit of the Earth around the sun

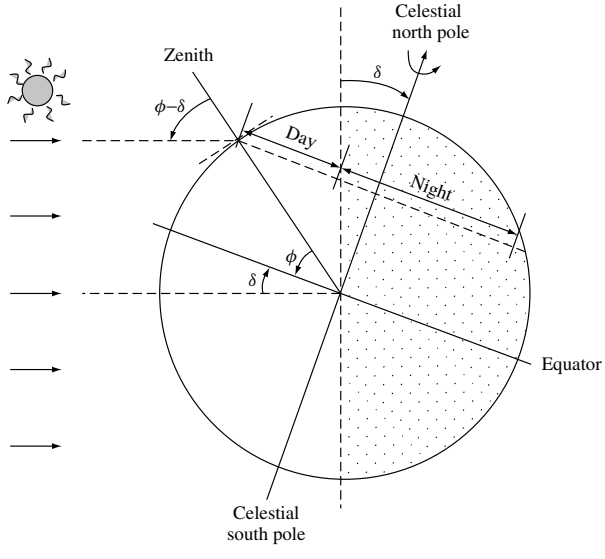


Figure 20.3 Relative Earth–Sun position at noon of a negative declination day (winter in the Northern Hemisphere, and summer in the Southern Hemisphere)

the sun is situated directly above the Tropic of Cancer, and sunrise and sunset are displaced towards the north-east and north-west, respectively. In the Northern Hemisphere, the summer solstice is when the longest day and shortest night of the whole year occur. In the Southern Hemisphere, it is the opposite. On the *winter solstice* (21st/22nd December) $\delta = -23.45^\circ$, the sun is directly above the Tropic of Capricorn, and sunrise and sunset are displaced towards the south-east and south-west, respectively. In the Northern Hemisphere, this is the shortest day and longest night of the whole year, and again, the opposite is true in the Southern Hemisphere.

A classic way of representing the sky is as a sphere centred on a fixed point of the Earth, as indicated in Figure 20.4. This is known as the *celestial sphere*. Each of its

Petitioner Canadian Solar (USA) Inc., Ex. 1035, p. 2293

Downloaded from https://onlinelibrary.wiley.com/doi/ by <Shibboleth-member@purdue.edu, Wiley Online Library on [25/08/2024]. See the Terms and Conditions (https://onlinelibrary.wiley.com/terms-and-conditions) on Wiley Online Library for rules of use; OA articles are governed by the applicable Creative Commons License

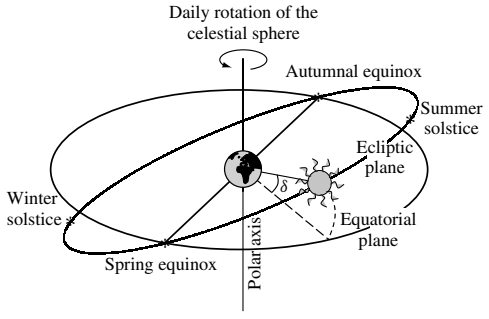


Figure 20.4 The celestial sphere and the ecliptic plane

points represents a direction towards the sky as seen from the Earth. The intersection of the celestial sphere with the equatorial plane defines the *celestial equator*. The points of intersection with the polar axis are called the *celestial poles*. Using this form of representation, the movement of the Earth around the stationary sun may instead be seen as a movement of the Sun with the Earth taken as fixed. The sun then travels through a great circle of the celestial sphere, the *ecliptic*, which forms an angle of 23.45° with the celestial equator. The sun completes this circuit once a year while the celestial sphere rotates once a day around the Earth (regarded as fixed). In this way, the sun marks out a circle around the Earth. The diameter of the circle changes daily, reaching a maximum on the equinoxes and a minimum on the solstices. The rotation of the sun around the ecliptic is in the opposite direction to that of the celestial sphere around the Earth.

Now, landing on a particular location on the Earth's surface, where a PV system is going to be used, it is convenient to specify the position of the sun by means of two angles that refer to the horizontal plane and to the vertical. The vertical intersects the celestial sphere at points known as the zenith and the nadir. Figure 20.5 attempts to visualise these concepts. The *solar zenith angle*, θ_{ZS}, is between the vertical and the incident solar beam; and the *solar azimuth*, ψ_S, is between the meridians of the location and the sun. The complement of the zenith angle is called the *solar altitude*, γ_S, and represents the angle between the horizon and the solar beam in a plane determined by the zenith and the sun. In the Northern (Southern) Hemisphere, the solar azimuth is referenced to south (north) and is defined as positive towards the west, that is, in the evening, and negative towards the east, that is, in the morning.

At any given moment, the angular coordinates of the sun with respect to a point of geographic latitude ϕ (north positive, south negative) are calculated from the equations:

$$\cos\theta_{ZS} = \sin\delta\sin\phi + \cos\delta\cos\phi\cos\omega = \sin\gamma_S \tag{20.4}$$

and

$$\cos\psi_S = \frac{(\sin\gamma_S\sin\phi - \sin\delta)}{\cos\gamma_S\cos\phi}[\text{sign}(\phi)] \tag{20.5}$$

where ω is called the true solar time, or local apparent time, or solar hour, and is the difference between noon and the selected moment of the day in terms of a 360° rotation

Downloaded from https://onlinelibrary.wiley.com/doi/ by <Shibboleth-member@purdue.edu, Wiley Online Library on [25/08/2024]. See the Terms and Conditions (https://onlinelibrary.wiley.com/terms-and-conditions) on Wiley Online Library for rules of use; OA articles are governed by the applicable Creative Commons License

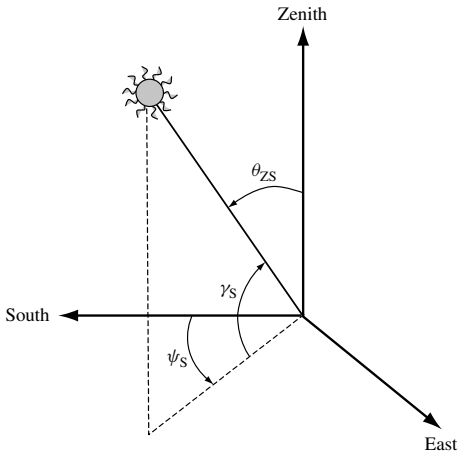


Figure 20.5 Position of the sun relative to a fixed point on the Earth

in 24 h. $\omega = 0$ at the midday of each day, and is counted as negative in the morning and positive in the afternoon. [sign(ϕ)] means "1" for northern latitudes and "−1" for southern latitudes. The true solar time ω is related to the local official time, *TO*, also called local standard time (the time shown by a clock) by the equation

$$\omega = 15 \times (TO - AO - 12) - (LL - LH) \tag{20.6}$$

where *LL* is the local longitude and *LH* is the reference longitude of the local time zone (positive towards the west and negative towards the east of the Greenwich Meridian). *AO* is the time by which clocks are set ahead of the local time zone. In the European Union, *AO* is usually one hour during winter and autumn, and two hours during spring and summer. In this equation ω, *LL* and *LH* are given in degrees, while *TO* and *AO* are given in hours.

Figure 20.6 presents the sun's trajectory on the celestial sphere for (a) a winter and a summer day and (b) the corresponding plots of solar altitude versus azimuth. We will return to such plots later on.

Equation (20.4) may be used to find the *sunrise angle*, ω_S, since at sunrise $\gamma_S = 0$. Hence

$$\omega_S = -\arccos(-\tan\delta \tan\phi) \tag{20.7}$$

In accordance with the sign convention, ω_S is always negative. Obviously, the sunset angle is equal to $-\omega_S$ and the length of the day is equal to $2 \times abs(\omega_S)$. In the polar regions, during the winter the sun does not rise ($\tan\delta \tan\phi > 1$) and equation (20.7) has no real solution. However, for computing purposes, it is convenient to set $\omega_S = 0$. Similarly, during the summer, $\omega_S = -\pi$ is a practical solution for the continuous day. It is also interesting to note that just at noon, $\omega = 0$, and the solar altitude is equal to the latitude

Petitioner Canadian Solar (USA) Inc., Ex. 1035, p. 2295

Downloaded from https://onlinelibrary.wiley.com/doi/ by <Shibboleth-member@purdue.edu, Wiley Online Library on [25/08/2024]. See the Terms and Conditions (https://onlinelibrary.wiley.com/terms-and-conditions) on Wiley Online Library for rules of use; OA articles are governed by the applicable Creative Commons License

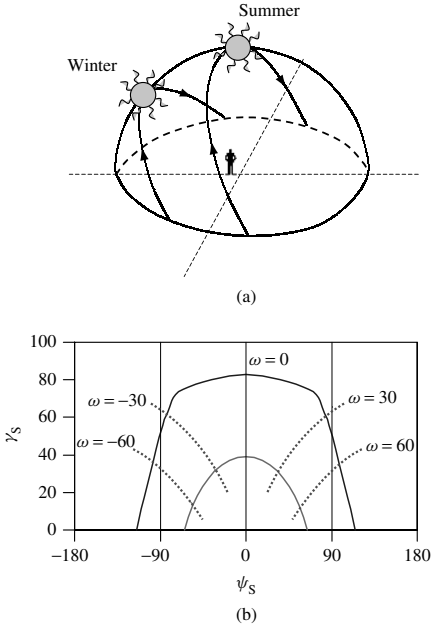


Figure 20.6 (a) Sun's trajectory corresponding to a winter and to a summer day represented over the celestial sphere. (b) The solar altitude γ_S is plotted against the solar azimuth ψ_S. The solar time ω is also shown

complement plus the declination

$$\omega = 0 \Rightarrow \gamma_S = \frac{\pi}{2} - \phi + \delta \tag{20.8}$$

It should be noted that equation (20.5) is indeterminate for $\gamma_S = \pi/2$ and for $\phi = \pi/2$. In the first case, the sun is just on the vertical, so that ψ_S is meaningless. In the second, the sun's position is given by $\gamma_S = \delta$ and $\psi_S = \omega$.

It should now be said that equations (20.1–20.3 and 20.6) derive from considering the angular velocity of the Earth through its elliptic orbit as constant, which is sufficiently accurate for most PV engineering applications. In particular, for all designs involving flat-plate PV modules, typical accuracy is about 1°. However, if desired, more accurate expressions are obtained when taking into account that the well-known Kepler's second law governs this angular velocity [2].

Another word of caution is necessary here. All the above-presented equations refer to a baseline year composed of 365 days, while the time length of the real year is 365 days, 5 h, 48 min and 45.9 s. As is well known, the difference is compensated by adding a day in the leap years. For most PV engineering applications, the same number corresponding to the precedent may be associated to this additional day, that is, $d_n = 59$ for both 28th and 29th of February. However, for some demanding applications, such as

Downloaded from https://onlinelibrary.wiley.com/doi/ by <Shibboleth-member@purdue.edu, Wiley Online Library on [25/08/2024]. See the Terms and Conditions (https://onlinelibrary.wiley.com/terms-and-conditions) on Wiley Online Library for rules of use; OA articles are governed by the applicable Creative Commons License

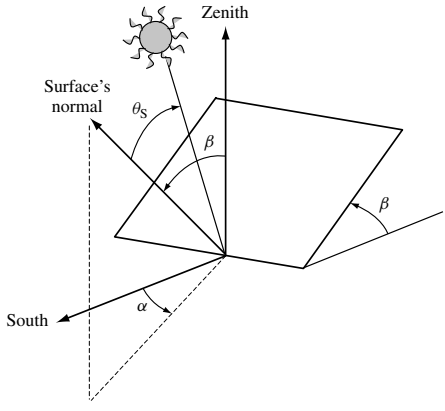


Figure 20.7 Receiver position (slope β and azimuth α) and sun's rays incidence angle θ_S

highly accurate trackers for concentrators, more precise equations may be necessary to calculate the relative Earth–Sun position. The interested reader is encouraged to consult Reference [3]. It describes an accurate algorithm and provides a software file for its implementation.

Equations (20.4) and (20.5) give the angles θ_{ZS} and ψ_S relative to a horizontal surface. However, most practical applications require the position of the sun relative to an inclined plane to be determined. The position of a surface (Figure 20.7) may generally be described by its slope β (the angle formed with the horizontal) and the azimuth α of the normal to the surface. The angle of solar incidence between the sun's rays and the normal to the surface may be calculated from

$$\cos\theta_S = \sin\delta\sin\phi\cos\beta - [\text{sign}(\phi)]\sin\delta\cos\phi\sin\beta\cos\alpha + \cos\delta\cos\phi\cos\beta\cos\omega + [\text{sign}(\phi)]\cos\delta\sin\phi\sin\beta\cos\alpha\cos\omega + \cos\delta\sin\alpha\sin\omega\sin\beta \quad (20.9)$$

Although this expression appears quite complicated, it is very convenient to use in most instances. In the case of surfaces tilted towards the equator (facing south in the Northern Hemisphere, or facing north in the Southern Hemisphere), $\alpha = 0$, and it simplifies to

$$\cos\theta_S = [\text{sign}(\phi)]\sin\delta\sin(abs(\phi) - \beta) + \cos\delta\cos(abs(\phi) - \beta)\cos\omega \quad (20.10)$$

20.3 SOLAR RADIATION COMPONENTS

Figure 20.8 helps to illustrate the following brief explanation of the different components of solar radiation that reach a terrestrial flat-plate PV surface

To a good approximation, the sun acts as a perfect emitter of radiation (black body) at a temperature close to 5800 K. The resulting power incident on a unit area perpendicular to the beam outside the Earth's atmosphere, when it is 1 AU from the sun, is known as the *solar constant*

$$B_0 = 1367 \text{ W/m}^2 \quad (20.11)$$

Downloaded from https://onlinelibrary.wiley.com/doi/ by <Shibboleth-member@purdue.edu, Wiley Online Library on [25/08/2024]. See the Terms and Conditions (https://onlinelibrary.wiley.com/terms-and-conditions) on Wiley Online Library for rules of use; OA articles are governed by the applicable Creative Commons License

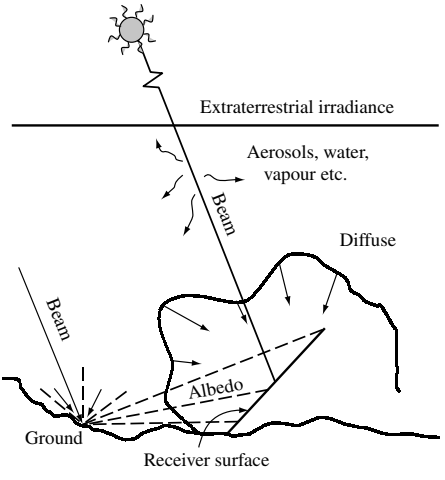


Figure 20.8 Different components of solar radiation

The radiation falling on a receiver situated beyond the Earth' atmosphere, that is, *extraterrestrial radiation*, consists almost exclusively of radiation travelling along a straight line from the sun. Since the intermediate space is almost devoid of material that might scatter or reflect the light, it appears virtually black, apart from the sun and faint points of light corresponding to the stars.

As the solar radiation passes through the Earth's atmosphere, it is modified by interaction with components present there. Some of these, such as clouds, reflect radiation. Others, for example, ozone, oxygen, carbon dioxide and water vapour, have significant absorption at several specific spectral bands. Water droplets and suspended dust also cause scattering. The result of all these processes is the decomposition of the solar radiation incident on a receiver at the Earth's surface into clearly differentiated components. *Direct or Beam radiation*, made up of beams of light that are not reflected or scattered, reaches the surface in a straight line from the sun. *Diffuse radiation*, coming from the whole sky apart from the sun's disc, is the radiation scattered towards the receiver. *Albedo radiation* is radiation reflected from the ground. The total radiation falling on a surface is the sum of these (direct + diffuse + albedo) and is termed *global radiation*.

It is intuitively obvious that the directional properties of the diffuse radiation depend to a large extent on the position, form and composition of the water vapor and dust responsible for scattering. The angular distribution of the diffuse radiation is therefore a complex function that varies with time. Diffuse radiation is essentially anisotropic. The amount of albedo radiation is greatly affected by the nature of the ground, and a wide range of features (snow, vegetation, water etc.) occur in practice.

In the following discussion, the word *radiation* will be used as a general term. To distinguish between power and energy, more specific terminology will be used. *Irradiance* means density of power falling on a surface, and is measured in W/m^2 (or similar); whereas *irradiation* is the density of the energy that falls on the surface over some

Downloaded from https://onlinelibrary.wiley.com/doi/ by <Shibboleth>-member@purdue.edu, Wiley Online Library on [25/08/2024]. See the Terms and Conditions (https://onlinelibrary.wiley.com/terms-and-conditions) on Wiley Online Library for rules of use; OA articles are governed by the applicable Creative Commons License

period of time, for example, hourly irradiation or daily irradiation, and is measured in Wh/m^2. Furthermore, only the symbols B_0, B, D, R and G will be used, respectively, for extraterrestrial, direct, diffuse, albedo and global irradiance, whereas a first subscript, h or d, will be used to indicate hourly or daily irradiation. A second subscript, m or y, will refer to monthly or yearly averaged values. Furthermore, the slope and orientation of the concerned surface are indicated among brackets. For example, $G_{\mathrm{dm}}(20,40)$ refers to the monthly mean value of the daily global irradiation incident on a surface tilted $\beta = 20^\circ$ and oriented $\gamma = 40^\circ$ towards the west. For surfaces tilted towards the equator ($\gamma = 0$), only the slope will be indicated. For example, $B(60)$ refers to the value of the direct irradiance incident on a surface tilted $\beta = 60^\circ$ and oriented towards the south (in the Northern Hemisphere).

An important concept characterising the effect of atmosphere on clear days is the *air mass*, defined as the relative length of the direct-beam path through the atmosphere compared with a vertical path directly to sea level, which is designed as AM. For an ideal homogeneous atmosphere, simple geometrical considerations lead to

$$AM = \frac{1}{\cos\theta_{\mathrm{ZS}}} \tag{20.12}$$

which is generally sufficient for most engineering applications. If desired, more accurate expressions, considering second-order effects (curvature of the Earth, atmospheric pressure etc.), are available [4].

At the standard atmosphere $AM\,1$, after absorption has been accounted for, the normal irradiance is generally reduced from B_0 to 1000 W/m^2, which is just the value used for the standard test of PV devices (see Chapter 16). Obviously, that can be expressed as $1000 = 1367 \times 0.7^{AM}$. For general AM values, a reasonable fit to observed clear days data is given by [5].

$$G = B_0 \cdot \varepsilon_0 \times 0.7^{AM^{0.678}} \tag{20.13}$$

A particular example can help to clarify the use of these equations, by calculation of the sun co-ordinates and the global irradiance on a surface perpendicular to the sun, and also on a horizontal surface, over two geographic positions defined by $\phi = 30^\circ$ and $\phi = -30^\circ$, at 10:00 (solar time) on 14 April, being a clear day. The solution is as follows:

$$\begin{aligned}
&14\ \text{April} \Rightarrow d_{\mathrm{n}} = 104;\ \varepsilon_0 = 0.993;\ \delta = 9.04^\circ\\
&10{:}00\ \text{h} \Rightarrow \omega = -30^\circ\\
&\phi = 30^\circ \Rightarrow \cos\theta_{\mathrm{ZS}} = 0.819 \Rightarrow \theta_{\mathrm{ZS}} = 35^\circ \Rightarrow \cos\psi_{\mathrm{S}} = 0.508 \Rightarrow \psi_{\mathrm{S}} = -59.44^\circ\\
&\qquad\qquad \Rightarrow AM = 1.222 \Rightarrow G = 902.4\ \mathrm{W/m^2}\\
&\qquad\qquad \Rightarrow G(0) = G \cdot \cos\theta_{\mathrm{ZS}} = 739\ \mathrm{W/m^2}\\
&\phi = -30^\circ \Rightarrow \cos\theta_{\mathrm{ZS}} = 0.662 \Rightarrow \theta_{\mathrm{ZS}} = 48.54^\circ \Rightarrow \cos\psi_{\mathrm{S}} = 0.403 \Rightarrow \psi_{\mathrm{S}} = -66.28^\circ\\
&\qquad\qquad \Rightarrow AM = 1.510 \Rightarrow G = 846.9\ \mathrm{W/m^2}\\
&\qquad\qquad \Rightarrow G(0) = G \cdot \cos\theta_{\mathrm{ZS}} = 561\ \mathrm{W/m^2}
\end{aligned}$$

Downloaded from https://onlinelibrary.wiley.com/doi/ by <Shibboleth-member@purdue.edu>, Wiley Online Library on [25/08/2024]. See the Terms and Conditions (https://onlinelibrary.wiley.com/terms-and-conditions) on Wiley Online Library for rules of use; OA articles are governed by the applicable Creative Commons License

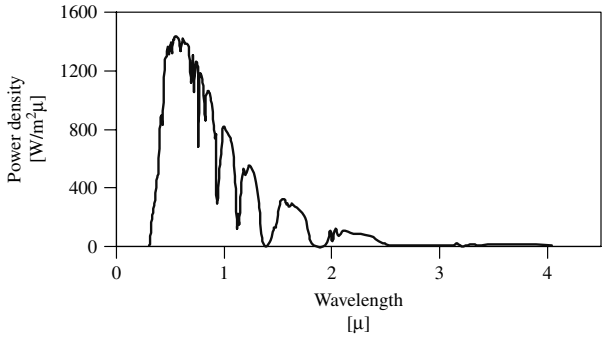


Figure 20.9 *AM* 1.5 solar spectrum, for an irradiance $G = 1000$ W/m^2

When solar radiation enters the Earth's atmosphere, not only the irradiance but also the spectral content is affected. Figure 20.9 shows the *AM* 1.5 spectrum, which is considered for standard test of PV devices. Figure 16.1 shows other spectra for comparison. In general, increasing air mass displaces the solar spectrum towards the red. This is why the sky becomes so nice at nightfall.

Of course, PV devices are sensitive to the spectrum, as discussed in Chapters 3, 9, 12 and 16. However, this is of little importance from the PV engineering point of view, compared to changes in total radiation incident on the PV modules. Because of that, in what follows, we will omit the detailed treatment of the spectral composition of sunlight. Additional comments will be given later on in this chapter.

20.4 SOLAR RADIATION DATA AND UNCERTAINTY

The amount of global radiation that reaches the receiver is extremely variable. On the one hand, even the extraterrestrial radiation experiences regular daily and yearly variations due to the apparent motion of the sun. These variations are predictable and can be theoretically determined just by geometrical considerations. For example, the extraterrestrial irradiance over a horizontal surface is given by

$$B_0(0) = B_0 \varepsilon_0 \cos\theta_{ZS} \tag{20.14}$$

which when integrated over the day, leads to [6]

$$B_{0d}(0) = \frac{T}{\pi} B_0 \varepsilon_0 \left[-\frac{\pi}{180} \omega_S \cdot \sin\delta \cdot \sin\phi - \cos\delta \cos\phi \sin\omega_S \right] \tag{20.15}$$

where T is the day length, that is, 24 h. The monthly average of this quantity, named $B_{0dm}(0)$, is of particular practical importance. Obviously

$$B_{0dm}(0) = \frac{1}{d_{n2} - d_{n1} + 1} \sum_{d_{n1}}^{d_{n2}} B_{0d}(0) \tag{20.16}$$

Downloaded from https://onlinelibrary.wiley.com/doi/ by <Shibboleth-member@purdue.edu>, Wiley Online Library on [25/08/2024]. See the Terms and Conditions (https://onlinelibrary.wiley.com/terms-and-conditions) on Wiley Online Library for rules of use; OA articles are governed by the applicable Creative Commons License

Table 20.1 Declination and extraterrestrial irradiation values for the characteristic day of each month

Month	Date	d_n	δ [degrees]	$B_{0d}(0) = B_{0dm}(0)$, in [Wh/m^2]			
				$\phi = 30^\circ$	$\phi = 60^\circ$	$\phi = -30^\circ$	$\phi = -60^\circ$
January	17	17	−20.92	5 907	949	11 949	11 413
February	14	45	−13.62	7 108	2 235	11 062	9 083
March	15	74	−2.82	8 717	4 579	9 531	5 990
April	15	105	+9.41	10 225	7 630	7 562	3 018
May	15	135	+18.79	11 113	10 171	5 948	1 225
June	10	161	+23.01	11 420	11 371	5 204	605
July	18	199	+21.00	11 224	10 741	5 530	878
August	18	230	+12.78	10 469	8 440	6 921	2 294
September	18	261	+1.01	9 121	5 434	8 835	4 937
October	19	292	−11.05	7 436	2 726	10 612	8 226
November	18	322	−19.82	6 056	1 114	11 754	10 983
December	13	347	−23.24	5 498	613	12 174	12 177

where d_{n1} and d_{n2} are the day numbers of the first and last day of the month, respectively. It is useful to know that, for a given month, there is a day for which $B_{0d}(0) = B_{0dm}(0)$. It can be demonstrated that this day is the one whose declination equals the mean declination for the month. Table 20.1 shows the day number of this day and the corresponding value of $B_{0dm}(0)$ for each month of the year at several latitudes.

We have also shown that the effect of clear cloudless skies can be predictably accounted for by a single geometrical parameter, namely, the Air Mass (equation 20.12). On the other hand, there are random variations caused by climatic conditions: cloud cover, dust storms and so on so that the PV systems design should rely on the input of measured data close to the site of the installations and averaged over a long time. This is routinely done by the National Meteorological Services (or similar services), which use a variety of instruments and procedures, from direct sunlight measurements (pyranometers, pyrheliometers etc.) to correlations with other meteorological variables (hours of sunshine, cloudiness, tone of satellite photographs etc). Then, they are treated to derive some representative parameters, which are made publicly available by different ways: World radiation databases [7, 8], Regional [9], National [10–12] and local [13] Radiation Atlas, web sites [14, 15] and so on. The 12 monthly mean values of global horizontal daily irradiation, $G_{dm}(0)$, today represent the most widely available information concerning the solar radiation resource, and that is likely to remain in the years to come. It is important to note that solar radiation unavoidably represents a large source of uncertainty for PV systems designers, as revealed by the significant disparity between different information sources. As a representative example, we will consider the case of Madrid.

The Spanish National Meteorological Institute has been recording daily values of hours of sunshine from 1951 to 1980, and hourly global horizontal irradiation data since 1973. This means that the Madrid solar radiation data bank is today composed of more than 50 years of daily indirect observations and more than 25 years of hourly direct ones. Such comprehensive data may appear very gratifying. However, an in-depth examination of the data bank reveals several difficulties: significant data gaps (the most important extends from June 1988 to July 1989); changes of the sensor's calibration constant (in

Downloaded from https://onlinelibrary.wiley.com/doi/ by <Shibboleth-member@purdue.edu, Wiley Online Library on [25/08/2024]. See the Terms and Conditions (https://onlinelibrary.wiley.com/terms-and-conditions) on Wiley Online Library for rules of use; OA articles are governed by the applicable Creative Commons License

Downloaded from https://onlinelibrary.wiley.com/doi/ by <Shibboleth-member@purdue.edu, Wiley Online Library on [25/08/2024]. See the Terms and Conditions (https://onlinelibrary.wiley.com/terms-and-conditions) on Wiley Online Library for rules of use; OA articles are governed by the applicable Creative Commons License

1977, the IPS-1956 reference was substituted by the WRP); and inconsistencies between global, direct and diffuse irradiation values due to mistakes in graphic record evaluation. All these difficulties must be overcome when computing statistical representative values. Different researchers use different procedures (for example, when considering a set of data of doubtful quality, one can opt to use it directly, or to estimate a best value, or simply to neglect it), arriving at different results. Furthermore, different researches use different data recording periods for computing representative values (because solar radiation data are being constantly and routinely recorded, this is usually the case). The astonishing result is that a large disparity in representative values is found for the same location, when different publications are consulted. Table 20.2 presents the $G_{dm}(0)$ values for Madrid according to different publications. Large disparities are evident and deserve further comment, because they translate into serious practical consequences. For example, for sizing the PV generator of a stand-alone PV system, it is customary to select the so-called worst month, that is, the month with the lowest value of $G_{dm}(0)$. It is clear that irrespective of the selected sizing methodology, the choice of the particular solar radiation database for Madrid involves PV array size differences up to 12% [(1.58–1.77)/1.58], far beyond the claimed accuracy of most presently available PV sizing methods.

It is important to note that, despite the above-mentioned difficulties, concerning rough solar radiation data, the uncertainty does not derive primarily from a lack of perfect precision in the measuring instruments, but rather from the random nature of the solar radiation, that is, from the overall statistical fluctuations in the collection of finite number of counts over finite intervals of time. This leads us to the question of the real representativeness of the data, or, in more strict terms, to the "confidence" we have that average values, based on past observations of solar radiation, are a correct prediction of the future solar radiation. A close look at the rough recorded data can help to elucidate this question. Figure 20.10 shows the January $G_{dm}(0)$ values corresponding to the years 1979 to 1986, for which very accurate data – let us say, 3% of accuracy – are available, according to Reference [16]. The average value is $\overline{G_{dm}}(0) = 1.99$ kWh/m^2. We could then give this value as our estimate for the future. However, if someone now asked the question, "What is the probability that the future $G_{dm}(0)$ will be exactly 1.99 kWh/m^2?", we would have to answer – somewhat uncomfortably – that the probability is no doubt close to zero. However, we would have to hasten to add that if we relax the prediction rigour, just saying that the future $G_{dm}(0)$ values will be within the range of 1.55 to 2.58 kWh/m^2, as in Figure 20.10, then the probability is high. Note that this range represents ±26% of the

Table 20.2 Values of the mean global daily irradiations $G_{dm}(0)$, in kWh/m^2, in Madrid according to different publications

Ref	Jan	Feb	Mar	Apr	May	June	July	Aug	Sep	Oct	Nov	Dec	Year
[7]	1.86	2.94	3.78	5.22	5.80	6.53	7.22	6.42	4.69	3.17	2.08	1.64	4.29
[16]	1.99	2.64	4.32	5.32	6.28	7.29	7.47	6.62	5.11	3.40	2.16	1.72	4.53
[94]	2.29	2.81	4.48	5.25	6.60	7.24	7.55	6.33	5.22	3.62	2.10	1.64	4.60
[10]	2.0	2.8	4.4	5.4	6.6	7.4	7.8	7.0	5.4	3.6	2.6	1.8	4.7
[9]	1.73	2.63	4.15	5.45	6.17	6.69	7.22	6.49	4.80	3.16	1.99	1.77	4.36
[95]	2.0	2.91	3.92	5.34	6.31	6.95	7.09	6.31	4.73	3.30	2.18	1.74	4.41
[96]	2.13	2.75	4.55	5.10	6.58	7.43	7.42	6.48	5.00	3.39	2.13	1.58	4.55
[14]	1.94	2.76	4.05	4.84	5.79	6.47	7.05	6.24	4.87	3.07	1.98	1.61	4.23

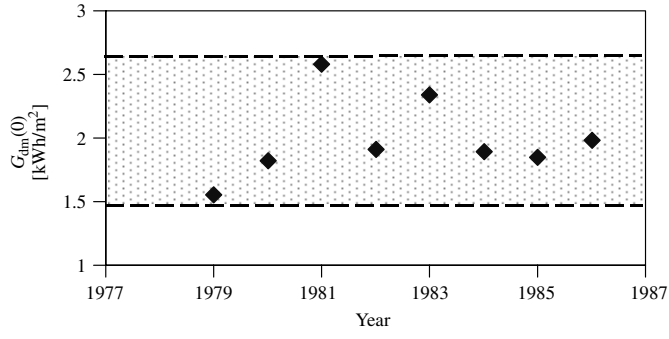


Figure 20.10 January means of the global horizontal irradiation $G_{dm}(0)$ in Madrid, for the years 1979 to 1986, in kWh/m^2

average value, much larger than the accuracy of the original data! Then, our questioner's retort would probably be, "How 'high' is the probability and how 'large' is the range?".

Basic statistical theory [17] gives proper answers to this question. For example, if we desire a 99% probability (the *confidence coefficient*) we must keep a $\pm 3\sigma$ range (the *confidence interval*) around the average value, in which σ is the *standard deviation* of the past observed values. In our example, $\sigma = 0.31$ kWh/m^2, so that $\pm 3\sigma$ represents $\pm 47\%$ of the average value. Still larger than the previously considered range, noted by the band of Figure 20.10! In order to keep on intervals of practical use, a $\pm 2\sigma$ interval is often employed. The corresponding confidence interval is 95%. In our example, $\pm 2\sigma$ represents $\pm 31\%$. Using the 2σ confidence level, the correct way to state the daily global irradiation prediction for the next January would be to say

$$1.37 \text{ kWh/m}^2 \leq G_{dm}(0) \leq 2.61 \text{ kWh/m}^2$$

or

$$G_{dm}(0) = 1.99 \text{ kWh/m}^2 \pm 31\%$$

Probably, surprised by such large uncertainty ($\pm 31\%$ seems badly matched and inconsistent with the "high accuracy" image generally associated with modern computational technology), our questioner would retort, "How can this uncertainty be reduced?" In fact, the only way is by enlarging the number of years of the future for which the prediction applies. That is, to give an estimate not for the next January, but for the average value of the following Januarys. Then, it can be shown that the confidence interval becomes reduced by a factor of $1/\sqrt{N}$, N being the number of future years for which the prediction is extended. Coming back to our example, and considering a future length of 10 years, the correct prediction would be

$$1.79 \text{ kWh/m}^2 \leq G_{dm}(0) \leq 2.19 \text{ kWh/m}^2$$

or

$$G_{dm}(0) = 1.99 \text{ kWh/m}^2 \pm 10\%$$

Downloaded from https://onlinelibrary.wiley.com/doi/ by <Shibboleth-member@purdue.edu, Wiley Online Library on [25/08/2024]. See the Terms and Conditions (https://onlinelibrary.wiley.com/terms-and-conditions) on Wiley Online Library for rules of use; OA articles are governed by the applicable Creative Commons License

Downloaded from https://onlinelibrary.wiley.com/doi/ by <Shibboleth-member@purdue.edu, Wiley Online Library on [25/08/2024]. See the Terms and Conditions (https://onlinelibrary.wiley.com/terms-and-conditions) on Wiley Online Library for rules of use; OA articles are governed by the applicable Creative Commons License

And still, we are disregarding the instrumental errors – at least ±3% in the best series of solar radiation data – and the causes of variability that can be hidden on a series of only 20 years of data. For example, the ones associated with the Global Climatic Change due to the global emissions of CO_2. As a matter of fact, it should be noted that some of the $G_{dm}(0)$ values listed in Table 20.2 for January fall outside this range.

Table 20.3 shows the uncertainty parameters for each month and for the entire year for Madrid, based on data of Reference [16]. It is worth observing that monthly uncertainty is greater in winter than in summer (this is because summer solar radiation is dominated by clear days, essentially governed by the predictable extraterrestrial radiation, while winter solar radiation is strongly influenced by cloudy days, which are governed by random atmospheric phenomena). Besides, uncertainty becomes substantially lower when the whole year is considered (this is because yearly data result from greater aggregates than monthly data, and it is a basic law that the greater the aggregation, the lower the dispersion of the corresponding results). Later on, we will analyse the implications for different PV applications. It should be said that the IES experience in designing PV systems for different locations around the world has led us to believe that the above-described, concerning solar radiation data sources for Madrid, far from being a particular case, is rather representative of a general situation. For example, the December mean daily global horizontal irradiation in New York is $G_{dm}(0) = 1.36$ kWh/m^2 according to Reference [7], 1.47 kWh/m^2 according to Reference [14], and 1.6 kWh/m^2 according to Reference [15]. The interested reader is encouraged to also consult Reference [18].

It is rather obvious that, whatever the detailed methodology, the PV-system design is essentially a prediction exercise extended over the expected system lifetime. From the previous considerations, it follows that such a prediction exercise is unavoidably associated with a rather large degree of uncertainty. Irrespective of whether good historical data are available and whether more complex models are used, any attempt to overcome such uncertainty is simply wrong. We should insist on that because, unfortunately, many authors often forget it when proposing PV-system design tools. This false sense of predictability and regularity in the solar radiation is, to a certain extent, being boosted by the proliferation of software-based tools, that are able to perform extremely detailed simulations with large sequences of solar radiation data. The great "accuracy" of their calculations tends to confer an impressive "scientific" appearance to these tools, and foster the tendency to believe that their results are superior to others. However, the truth is that such great accuracy is statistically meaningless, and that, much more simple design methodologies can yield results of similar confidence. We should keep this idea in mind all through this chapter.

Table 20.3 Solar radiation parameters for Madrid. Mean G_{dm} and standard deviation values σ are given in kWh/m^2, while $2\sigma/G_{dm}$ is given in %

	Jan	Feb	Mar	Apr	May	June	July	Aug	Sep	Oct	Nov	Dec	Mean
G_{dm}	1.99	2.64	4.32	5.32	6.28	7.29	7.47	6.62	5.11	3.4	2.16	1.72	4.53
σ	0.31	0.31	0.36	0.39	0.64	0.34	0.31	0.18	0.36	0.39	0.36	0.17	0.08
$2\sigma/G_{dm}$	31	23	17	15	20	9	8	8	14	23	34	20	4

20.4.1 Clearness Index

The relation between the solar radiation at the Earth's surface and the Extraterrestrial radiation gives a measure of the atmospheric transparency. This way, a *clearness index*, K_{Tm}, is calculated for each month:

$$K_{\mathrm{Tm}} = \frac{G_{\mathrm{dm}}(0)}{B_{0\mathrm{dm}}(0)} \tag{20.17}$$

Note that the clearness index is physically related not only to the radiation path through the atmosphere, that is, with the *AM* value, but also with the composition and the cloud content of the atmosphere. Liu and Jordan [19] have demonstrated that, irrespective of latitude, the fractional time during which daily global radiation is equal to or less than a certain value is directly dependent on this parameter. Because of that, K_{Tdm} can properly characterise the solar climate of a particular location. This provides the basis for estimating solar radiation on inclined surfaces.

20.5 RADIATION ON INCLINED SURFACES

To eliminate the effects of varying local features, such as obstructions that cast shadows and the specific ground covering, solar radiation is routinely measured on horizontal surfaces free of obstacles. Consequently, solar radiation data are most often given in the form of global radiation on a horizontal surface. Since PV modules are usually positioned at an angle to the horizontal plane, the radiation input to the system must be calculated from the data.

The assessment of radiation arriving on an inclined surface, using as input global horizontal data, raises two main problems: to separate the global horizontal radiation into their direct and diffuse components; and, from them, to estimate the radiation components falling on an inclined surface. In general, these problems may be posed for different time scales, for example, daily irradiation, hourly irradiation and so on. Individual or time-averaged values may be sought. Here, we will first focus on the monthly average daily irradiation values. This is not only convenient for presentation purposes, but also coherent with solar radiation data availability, and particularly suited to afford most PV engineering practical problems. Additional comments for other cases will also be given afterwards.

20.5.1 Estimation of the Direct and Diffuse Components of Horizontal Radiation, Given the Global Radiation

The underlying concept is the one originally proposed by Liu and Jordan [19]. It consists of establishing empirical correlation between the *diffuse fraction of horizontal radiation*, $F_{\mathrm{Dm}} = D_{\mathrm{dm}}(0)/G_{\mathrm{dm}}(0)$, (diffuse radiation/global radiation) and the *clearness index* (global radiation/extraterrestrial radiation) defined in equation (20.17). Note that the clearer the atmosphere, the higher the radiation and the lower the diffuse content. Hence, F_{Ddm} and K_{Tdm} are expected to be negatively correlated. Actual analytical expressions are established from the comparison of simultaneous measurements of global and diffuse radiation

Downloaded from https://onlinelibrary.wiley.com/doi/ by <Shibboleth-member@purdue.edu>, Wiley Online Library on [25/08/2024]. See the Terms and Conditions (https://onlinelibrary.wiley.com/terms-and-conditions) on Wiley Online Library for rules of use; OA articles are governed by the applicable Creative Commons License

performed in certain places. Liu and Jordan were, in fact, very clever in selecting the clearness index (which they called the cloudiness index) to characterise the solar climate at a particular location, because the division by the extraterrestrial radiation eliminates the radiation variations due to the apparent motion of the sun. This way, the correlation between F_{Dm} and K_{Tm} becomes independent of latitude effects, and, in principle, tends to be of universal validity.

Various empirical formulae are available. Using data from ten locations situated between 40°N and 40°S, Page [20] recommended a liner equation that has been frequently identified as the one giving the best results.

$$F_{\mathrm{Dm}} = 1 - 1.13K_{\mathrm{Tm}} \tag{20.18}$$

Figure 20.11 plots equation (20.18) and a set of experimental points, obtained in Madrid, from 1977 to 1988.

Example: Determination of direct and diffuse components of the global radiation for the month of June in a location having a latitude $\phi = 30°$ and a mean global horizontal daily irradiation $G_{\mathrm{dm}}(0) = 6100$ Wh/m^2. The solution is

$\phi = 30$ and June $\Rightarrow B_{0\mathrm{dm}}(0) = 11\,420$ Wh/m^2 (See Table 20.1)

$G_{\mathrm{dm}}(0) = 6100$ Wh/m^2 $\Rightarrow K_{\mathrm{Tm}} = 0.534 \Rightarrow F_{\mathrm{Dm}} = 0.396 \Rightarrow D_{\mathrm{dm}}(0) = 2418$ Wh/m^2

$\Rightarrow B_{\mathrm{dm}}(0) = 3682$ Wh/m^2

Empirical correlations between the diffuse fraction of the horizontal irradiation and the clearness index can also be derived for an individual day (April 14 is, for example, an individual day, while generic April is a monthly mean day). They should be described here because they have been the object of extensive research in the general solar radiation community and, as a result they have received large attention in the available literature, and they are often employed in today's available PV engineering software tools. However, it should be advised that their advantage for PV design purposes is far from clear. As a matter of fact, the electrical behaviour of PV generators is mainly governed by the linear

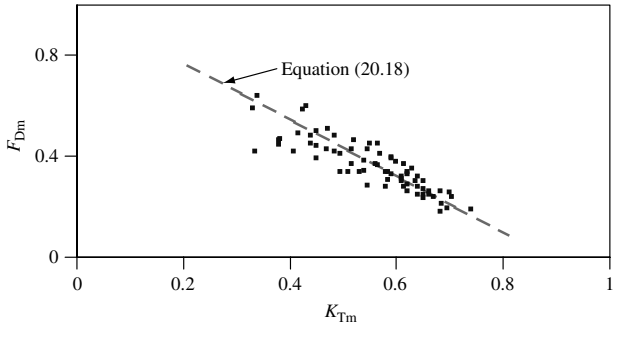


Figure 20.11 The diffuse fraction of the mean daily global irradiation F_{Dm} is plotted against the clearness index K_{Tm}. The cluster of points refers to measured values in Madrid from 1977 to 1988

Downloaded from https://onlinelibrary.wiley.com/doi/ by <Shibboleth-member@purdue.edu, Wiley Online Library on [25/08/2024]. See the Terms and Conditions (https://onlinelibrary.wiley.com/terms-and-conditions) on Wiley Online Library for rules of use; OA articles are governed by the applicable Creative Commons License

dependence incident irradiance. It follows that the mean power they deliver during a period of time tends to be equal to the delivered power when they are illuminated with the mean irradiance during such time. Second-order effects, associated to ambient temperature or operation voltage fluctuations, do not significantly alter this idea, provided that they are adequately considered, as discussed afterwards. Because of that, rather few benefits, in terms of long-term performance predictions, should be expected from analysing all the days of a month instead of only the mean day of such a month. The reason for the popularity of individual day analysis in recently available software tools, lies more with fashion and prestige than with increasing energy yield prediction certainty.

Figure 20.12 shows the experimental values of $F_{Dd} = D_d(0)/G_d(0)$ versus $K_{Td} = G_d(0)/B_{0d}(0)$, obtained in Madrid, from 1977 to 1988. Each point derives from the simultaneous measurement of the diffuse and the global horizontal irradiation along a particular day. Note that the general trend is consistent with the principle that the clearer the atmosphere, the lower the diffuse content. A third-order or fourth-order polynomial in K_{Td} is generally used to model the diffuse fraction F_{Dd}. A correlation between F_{Dd} and K_{Td} was first developed by Liu and Jordan [19]. However, it was derived from diffuse radiation data that were not compensated for by shadow-band effects (the shadow band is a device added to a pyranometer, to exclude the direct radiation from the sun. Hence, it allows for the measurement of diffuse radiation. However, the shadow-band screens the sensor not only from the sun but also from a portion of the diffuse radiation coming in from the sky, so that, a correction must be made to the measurement). Not surprisingly, later revisions by other authors concluded that the Liu and Jordan correlation underestimates diffuse radiation.

The most frequently referred correlation for daily values is that put forward by Collares Pereira and Rabl [21], using data from five stations located in the United States. It is expressed as

$$F_{Dd} = 0.99 \text{ for } K_{Td} \leq 0.17$$
$$F_{Dd} = 1.188 - 2.272K_{Td} + 9.473K_{Td}^2 - 21.856K_{Td}^3 + 14.648K_{Td}^4 \quad (20.19)$$

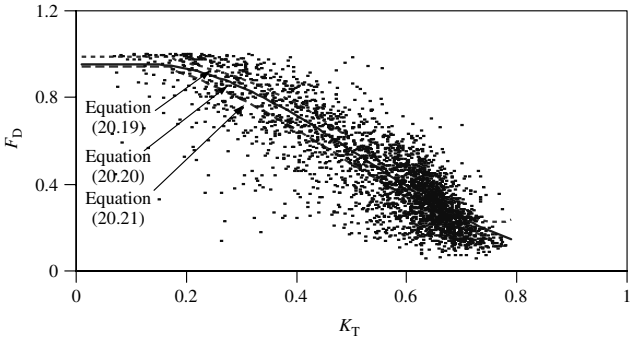


Figure 20.12 The diffuse fraction of the individual daily global irradiation F_{Dd} is plotted against the clearness index K_{Td}. The cluster of points refers to measured values in Madrid from 1977 to 1988

Downloaded from https://onlinelibrary.wiley.com/doi/ by <Shibboleth-member@purdue.edu, Wiley Online Library on [25/08/2024]. See the Terms and Conditions (https://onlinelibrary.wiley.com/terms-and-conditions) on Wiley Online Library for rules of use; OA articles are governed by the applicable Creative Commons License

Downloaded from https://onlinelibrary.wiley.com/doi/ by <Shibboleth-member@purdue.edu, Wiley Online Library on [25/08/2024]. See the Terms and Conditions (https://onlinelibrary.wiley.com/terms-and-conditions) on Wiley Online Library for rules of use; OA articles are governed by the applicable Creative Commons License

Despite independence of latitude, other second-order factors can affect the observed correlations, leading to a certain site dependence. For example, at very high latitudes, perennial snow cover could significantly increase diffuse radiation caused by multiple reflections between the ground and cloud cover. Also, atmospheric humidity tends to increase scattering, in relative terms. Hence, for a given clearness index, locations with low humidity will tend to have the lowest diffuse radiation content. Because of that, and because radiation data are still being accumulated and revised, new correlations are continuously enlarging the available literature. A recent study [22], devoted to the development of solar radiation models for the Mediterranean area, has found about 250 different correlations in the literature. The same study, extended to more than 150 000 pairs of data from eleven different stations of the European network, has proposed the following expression

$$\begin{aligned} F_{\mathrm{Dd}} &= 0.952 \text{ for } K_{\mathrm{Td}} \leq 0.13 \\ F_{\mathrm{Dd}} &= 0.868 + 1.335K_{\mathrm{Td}} - 5.782{K_{\mathrm{Td}}}^2 + 3.721{K_{\mathrm{Td}}}^3 \\ &\qquad \text{for } 0.13 < K_{\mathrm{Td}} \leq 0.8 \\ F_{\mathrm{Dd}} &= 0.141 \text{ for } K_{\mathrm{Td}} > 0.8 \end{aligned} \tag{20.20}$$

Local correlations that are derived from the data of only one site can also be found. As an example, Macagnan [16] proposed the following for Madrid

$$\begin{aligned} F_{\mathrm{Dd}} &= 0.942 \text{ for } K_{\mathrm{Td}} \leq 0.18 \\ F_{\mathrm{Dd}} &= 0.974 + 0.326K_{\mathrm{Td}} - 3.896{K_{\mathrm{Td}}}^2 + 2.661{K_{\mathrm{Td}}}^3 \\ &\qquad \text{for } 0.18 < K_{\mathrm{Td}} \leq 0.79 \\ F_{\mathrm{Dd}} &= 0.115 \text{ for } K_{\mathrm{Td}} > 0.79 \end{aligned} \tag{20.21}$$

Such diversity of correlations can again perplex our hypothetical questioner, who would ask, "What correlation should I use?" Hence, it is worth to study further the implications of using one or the other.

On the one hand, it should be remembered that the uncertainty associated with the variability of observed individual data, as described in the previous section for global radiation, also applies here. The cluster of (F_{Dd}, K_{Td}) points in Figure 20.12 reveals that, for a given K_{Td}, very different F_{Dd} values can be found in reality. For example, the observed range for $K_{\mathrm{Td}} = 0.5$ is $0.1 \leq F_{\mathrm{Td}} \leq 0.7$, that is $\pm 75\%$ around the mean value. In more strict terms, a measure of the dispersion of expected observations around the prediction derived from a particular correlation, is given by the so-called Root Mean Square Error, or Standard Error of Estimate, s_{e}. As with the standard deviation, $\pm 2s_{\mathrm{e}}$ is the interval, around the predicted value, for 95% confidence. In general, s_{e} are larger than 25%, which means that, regardless of the selected correlation, we would nearly always expect real values of diffuse irradiation for individual days falling between $\pm 50\%$ of the predictions. It is also interesting to observe that the dispersion associated with individual days (Figure 20.12) is significantly larger than the dispersion associated with monthly means (Figure 20.11).

On the other hand, when long-term performance predictions are concerned – which is the standard case on PV design – the implications of using different correlations are in

fact very modest. As a representative exercise, we have calculated the daily irradiation incident on a surface tilted to the latitude in Djelfa-Algeria ($\phi = 34.6^\circ$), for a winter day ($d_n = 17$) and for a summer day ($d_n = 161$), using the different correlations defined by equations (20.19–20.21). Djelfa and Madrid are relatively similar on geographical altitude and solar climate. Hence, it is reasonable to assume that the same local correlation could be applied to both places. $G_d(0) = 2778$ and 6972 Wh/m^2 for the winter and for the summer day, respectively. This radiation data has been obtained from Reference [7], by assuming that the value of the global irradiation during these days coincides with the corresponding monthly averages. Details of the calculating procedure will be given in the next section, but they are not relevant for the present discussion. The results are as follows:

$$d_n = 17 \Rightarrow B_{0d}(0) = 5177 \text{ Wh/m}^2$$
$$G_d(0) = 2778 \text{ Wh/m}^2 \Rightarrow K_{Td} = 0.537$$

Eq.	F_{Dd}	$D_d(0)$ in [Wh/m^2]	$G_d(\phi)$ in [Wh/m^2]
20.19	0.5301	1472	3946
20.20	0.5067	1408	4008
20.21	0.4351	1209	4185

$$d_n = 161 \Rightarrow B_{0d}(0) = 11\,525 \text{ Wh/m}^2$$
$$G_d(0) = 6972 \text{ Wh/m}^2 \Rightarrow K_{Td} = 0.605$$

Eq.	F_{Dd}	$D_d(0)$ in [Wh/m^2]	$G_d(\phi)$ in [Wh/m^2]
20.19	0.4034	2813	5988
20.20	0.4031	2811	5988
20.21	0.3345	2332	5940

Significant differences are observed in the estimation of the diffuse component of the horizontal irradiation. However, the noticeable key point is that these differences are significantly lessened in the estimation of the global irradiation. For example, for the winter day, differences on the diffuse component reach 22% while differences on the global radiation are lower than 6%.

Now, it is worth noting that, to a certain extent, we can cite a physical reason for the differences, considering the primary role of scattering in the diffusion of solar radiation. Equation (20.19) was derived from northern latitudes, with higher air masses than the Mediterranean region (higher air mass means higher scattering and, consequently, higher diffuse radiation content), and Madrid is a relatively high altitude site (670 m over the sea level) and its climate is essentially dry (both, higher altitude and lesser humidity

Downloaded from https://onlinelibrary.wiley.com/doi/ by <Shibboleth-member@purdue.edu, Wiley Online Library on [25/08/2024]. See the Terms and Conditions (https://onlinelibrary.wiley.com/terms-and-conditions) on Wiley Online Library for rules of use; OA articles are governed by the applicable Creative Commons License

means lesser scattering). Note that the correlative order of the results agrees with this physical explanation.

To summarize, an adequate answer to our hypothetical questioner is as follows:

1. Most PV engineering problems are properly solved using a monthly mean analysis. Then, equation (20.18) is the recommended choice.
2. If you require a day-to-day analysis, the choice of a particular diffuse-to-global correlation is not really critical. You can simply adhere to the widely extended practise of trusting on the "universal" character of equation (20.19). But, if you are interested in a specific site, you can perform slightly better by choosing a more site-specific correlation, providing it is derived from solar radiation measurements in a place having a similar climate to the concerned site.
3. Whichever possibility you choose, you must take a very important precaution. If your results are going to be compared with the results of another calculation (for example, comparing different PV module orientations for the same application), then be sure that they both use the same assumptions, correlations, model and data. Otherwise, the differences in the results would be completely meaningless. Although this caveat should be obvious, it still should be mentioned, because the literature contains several examples of different results derived from different correlations that were proposed as the basis of optimisation design exercises [23].

Finally, it should be mentioned that not only daily but also hourly based correlations have been proposed. These are correlations between the diffuse fraction of the hourly horizontal global irradiation, $F_{\mathrm{Dh}} = D_{\mathrm{h}}(0)/G_{\mathrm{h}}(0)$, and the hourly clearness index, $K_{\mathrm{Th}} = G_{\mathrm{h}}(0)/B_{0\mathrm{h}}(0)$. However, none of the hourly based correlations proposed so far is really satisfactory [6, 22], so that the associated complexity is not justified. Hence, they will be not considered here.

20.5.2 Estimation of the Hourly Irradiation from the Daily Irradiation

In some cases, the treatment of solar radiation is more easily understood at the instant time scale, that is, at the radiance level. Because irradiation over an hour (in $\mathrm{Wh/m^2}$) is numerically equal to the mean irradiance during this hour (in $\mathrm{W/m^2}$), irradiance values can be, to a certain extent, assimilated to hourly irradiation values. However, since the availability of hourly irradiation data is limited, the problem is how to estimate the hourly irradiation, given the daily irradiation.

To introduce the solution to this problem, it is highly instructive to observe that, in terms of extraterrestrial horizontal radiation, the ratio between irradiance, $B_0(0)$, and daily irradiation, $B_{0\mathrm{d}}(0)$, can be theoretically determined from equations (20.4), (20.14) and (20.15).

$$\frac{B_0(0)}{B_{0\mathrm{d}}(0)} = \frac{\pi}{T} \times \frac{\cos\omega - \cos\omega_{\mathrm{S}}}{\left(\dfrac{\pi}{180}\omega_{\mathrm{S}}\cos\omega_{\mathrm{S}} - \sin\omega_{\mathrm{S}}\right)} \tag{20.22}$$

where the sunrise angle, ω_{S}, is expressed in degrees and T, the day length, is usually expressed in hours.

Downloaded from https://onlinelibrary.wiley.com/doi/ by <Shibboleth-member@purdue.edu>, Wiley Online Library on [25/08/2024]. See the Terms and Conditions (https://onlinelibrary.wiley.com/terms-and-conditions) on Wiley Online Library for rules of use; OA articles are governed by the applicable Creative Commons License

From the examination of data from several stations, it has been repeatedly noted [19, 24] that, considering long-term averages of terrestrial radiation, the correspondence between the measured ratio of diffuse irradiance to diffuse daily irradiation, $r_D = D(0)/D_d(0)$, and this theoretical expression for extraterrestrial radiation (equation 20.22) is quite good, while the correspondence between the measured ratio of global irradiance to global daily irradiation, $r_G = G(0)/G_d(0)$, and this expression, although not perfect, is quite close, so that a slight modification is required to fit the observed data. The following expressions apply [21]:

$$r_D = \frac{D(0)}{D_d(0)} = \frac{B_0(0)}{B_{0d}(0)} \tag{20.23}$$

and

$$r_G = \frac{G(0)}{G_d(0)} = \frac{B_0(0)}{B_{0d}(0)}(a + b\cos\omega) \tag{20.24}$$

where a and b are obtained from the following empirical formulae:

$$a = 0.409 - 0.5016 \times \sin(\omega_S + 60) \tag{20.25}$$

and

$$b = 0.6609 + 0.4767 \times \sin(\omega_S + 60) \tag{20.26}$$

Note that r_D and r_G have units of T^{-1}, and that they can be extended to calculate irradiations during short periods centred on the considered instant, ω. For example, if we wish to evaluate the irradiation over one hour between 10:00 and 11:00 (in solar time), we set $\omega = -22.5^\circ$ (the centre time of the considered period is 10:30, i.e. one hour and half, or 22.5°, before noon) and $T = 24$ h. If we wish to evaluate the irradiation over one minute, we just have to express T in minutes, that is, we set it to 1440, the number of minutes in a day.

An example can help in the use of these equations: the calculation of the irradiance components at several moments along the 15 April in Portoalegre–Brasil ($\phi = -30^\circ$), knowing the global daily irradiation, $G_d(0) = 3861$ Wh/m^2. The results are as follows:

$$d_n = 105 \Rightarrow B_{0d}(0) = 7562 \text{ Wh/m}^2 \Rightarrow K_{Td} = 0.5106 \Rightarrow F_{Dd} = 0.423$$
$$\Rightarrow D_d(0) = 1633 \text{ Wh/m}^2$$
$$\omega_S = -84.51^\circ$$
$$\frac{\pi}{180}\omega_S \cos\omega_S - \sin\omega_S = 0.8542$$
$$a = 0.6172$$
$$b = 0.4672$$
$$r_D = 0.0922(\cos\omega + 0.0967) \text{ h}^{-1}$$
$$r_G = r_D(a + b\cos\omega)$$

Downloaded from https://onlinelibrary.wiley.com/doi/ by <Shibboleth-member@purdue.edu, Wiley Online Library on [25/08/2024]. See the Terms and Conditions (https://onlinelibrary.wiley.com/terms-and-conditions) on Wiley Online Library for rules of use; OA articles are governed by the applicable Creative Commons License

ω°	r_D [h^{-1}]	r_G [h^{-1}]	$D(0)$ in [Wm^{-2}]	$G(0)$ in [Wm^{-2}]	$B(0)$ in [Wm^{-2}]
ω_s	0	0	0	0	0
±60	0.0618	0.0529	100.94	204.25	103.31
±30	0.1177	0.1211	192.24	467.58	275.34
0	0.1382	0.1508	225.73	582.24	356.51

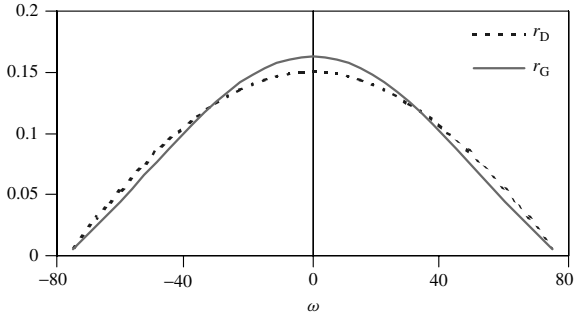


Figure 20.13 Plots of irradiance to daily irradiation ratios, for both diffuse and global radiation, r_D and r_G, along the day at a latitude $\phi = -30^\circ$ for 15 April

Figure 20.13 plots r_D and r_G versus the solar time, along the day. It is interesting to observe that r_G is slightly more sharp-pointed than r_D. This is because, due to air mass variations, beam transmittance is higher at noon that at any other moment of the day. Obviously, integrating the areas below both, r_D and r_G must be equal to one. As already mentioned, for this calculation it can be assumed that the irradiation over one hour (in Wh/m^2) is numerically equal to the mean irradiance during this hour and also equal to the irradiance at the instant half way through the hour. For example, the global irradiance at noon, $G(0) = 580.4$ W/m^2 can be identified with the hourly irradiation from 11:30 to 12:30, $G_h(0) = 580.4$ Wh/m^2. This assumption does not introduce significant errors and it greatly simplifies the calculations by eliminating the need to evaluate integrals with respect to time, which, otherwise, can be quite tedious.

From these equations, it can be deduced that, on any day of the year and anywhere in the world, 90% of the total global horizontal irradiation is received during a period centred around midday and of length equal to two-thirds the total sunlight day length. Consequently, a stationary receiver tilted to the equator ($\alpha = 0$) captures all the useful energy in this period. The same need not be true, however, of receivers that track the sun.

20.5.3 Estimation of the Radiation on Surfaces on Arbitrary Orientation, Given the Components Falling on a Horizontal Surface

The most obvious procedure for calculating the global irradiance on an inclined surface, $G(\beta, \alpha)$, is to obtain separately the direct, diffuse and albedo components, $B(\beta, \alpha)$,

Downloaded from https://onlinelibrary.wiley.com/doi/ by <Shibboleth-member@purdue.edu>, Wiley Online Library on [25/08/2024]. See the Terms and Conditions (https://onlinelibrary.wiley.com/terms-and-conditions) on Wiley Online Library for rules of use; OA articles are governed by the applicable Creative Commons License

$D(\beta, \alpha)$ and $R(\beta, \alpha)$, respectively. Once these are known

$$G(\beta, \alpha) = B(\beta, \alpha) + D(\beta, \alpha) + R(\beta, \alpha) \tag{20.27}$$

20.5.3.1 Direct irradiance

Straightforward geometrical considerations lead to

$$B(\beta, \alpha) = B \max(0, \cos\theta_S) \tag{20.28}$$

where B is the direct irradiance falling on a surface perpendicular to the sun's rays, and $\cos\theta_S$ is the angle of incidence between the sun's rays and the normal to the surface, given by equation (20.9). B can be obtained from the corresponding value on a horizontal surface

$$B = \frac{B(0)}{\cos\theta_{ZS}} \tag{20.29}$$

Note that when the sun is illuminating the back of the surface (for example, during all morning on a vertical surface oriented to the west) $|\theta_S| > \pi/2$. Then, $\cos\theta_S < 0$ and $B = 0$. This way, the factor $\max(0, \cos\theta_S)$ reflects that the irradiance incident on the back surface of PV modules is normally not utilised.

20.5.3.2 Diffuse irradiance

We can assume that, when the sun is occulted, the sky is composed of elemental solid angles, such as $d\Omega$ (Figure 20.14) from which a diffuse radiance $L(\theta_Z, \psi)$ is emanated towards the horizontal surface. The term radiance is taken to mean the flux of energy per unit solid angle crossing a surface normal to the direction of the radiation. It is expressed in W/m^2.steradian.

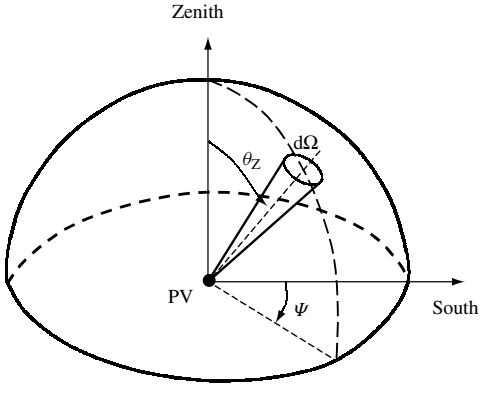


Figure 20.14 Angular co-ordinates, θ_Z and ψ, of an elemental solid angle of the sky

Downloaded from https://onlinelibrary.wiley.com/doi/ by <Shibboleth-member@purdue.edu, Wiley Online Library on [25/08/2024]. See the Terms and Conditions (https://onlinelibrary.wiley.com/terms-and-conditions) on Wiley Online Library for rules of use; OA articles are governed by the applicable Creative Commons License

Then, the horizontal irradiance is equal to the integration of the contribution of each solid angle, and can be written as

$$D(0) = \int_{\text{sky}} L(\vartheta_Z, \psi) \cos \vartheta_Z \, d\Omega \tag{20.30}$$

where the integral is extended to the whole sky, that is, $0 \leq \theta_Z \leq \pi/2$ and $0 \leq \psi \leq 2\pi$.

When we are dealing with an inclined surface, a similar reasoning leads to

$$D(\beta, \alpha) = \int_{\propto} L(\vartheta_Z, \psi) \cos \vartheta'_Z \, d\Omega \tag{20.31}$$

where ϑ'_Z is the incident angle from the solid angle element to the inclined surface, and $\propto$ means the integral is extended to the non-obstructed sky. The general solution of this equation is difficult because, under realistic skies, the radiance is not uniform and varies with the sky condition. For example, the form, brightness and position of clouds strongly affect the directional properties of the radiance.

The distribution of radiance over the sky is not measured routinely. Nevertheless, a number of authors [25, 26] have developed instruments to measure it and have presented results for different sky conditions. Some general patterns may be discerned from these.

With clear skies, the maximum diffuse radiance comes from the parts of the sky close to the sun and to the horizon. The minimum radiances come from a region at an angle of 90° to the solar zenith (Figure 20.15). The diffuse radiation coming from the region close to the sun is called *circumsolar radiation* and is mainly due to the dispersion by aerosols. The angular extent of the sun's aureole depends mainly on the turbidity of

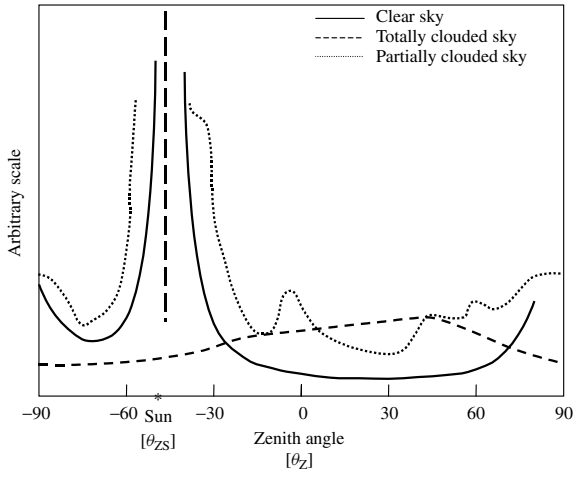


Figure 20.15 Typical angular distribution of the sky irradiance. The values are taken along the length of the meridian containing the sun, $\psi = \psi_S$

Downloaded from https://onlinelibrary.wiley.com/doi/ by <Shibboleth-member@purdue.edu, Wiley Online Library on [25/08/2024]. See the Terms and Conditions (https://onlinelibrary.wiley.com/terms-and-conditions) on Wiley Online Library for rules of use; OA articles are governed by the applicable Creative Commons License

the atmosphere and on the zenith angle of the sun. The increase in diffuse radiance near the horizon is due to the albedo radiation of the Earth and is called *horizon brightening*.

The radiance distributions associated with overcast skies are very well described by Kondratyev: "*for dense non-transparent cloudiness, the azimuthal dependence of diffuse radiation intensity is very weak. There is a slight monotonic increase of the radiance from the horizon upward towards the zenith*" [27].

Some models can be derived from these general ideas. The simplest model makes use of the assumption that the sky radiance is isotropic, that is, every point of the celestial sphere emits light with equal radiance, $L(\theta_Z, \psi) = \text{constant}$. The solution of equations (20.30 and 20.31) leads then to

$$D(\beta, \alpha) = D(0)\frac{1 + \cos\beta}{2} \tag{20.32}$$

Because of its simplicity, this model has achieved great popularity, despite the fact that it systematically underestimates diffuse irradiance on surfaces tilted to the equator.

The opposite approach assumes that all the diffuse radiation is circumsolar, that is, from the sun. This is really a case of treating diffuse radiation as though it were direct, and leads to

$$D(\beta, \alpha) = \frac{D(0)}{\cos\theta_{ZS}} \max(0, \cos\theta_S) \tag{20.33}$$

This model also has the advantage of being very simple to use, but in general it overestimates diffuse irradiances.

In general, better results are obtained with so called anisotropic models. Hay and Davies [28] proposed to consider the diffuse radiation as composed by a circumsolar component coming directly from the direction of the sun, and an isotropic component coming from the entire celestial hemisphere. Both components are weighted according to the so-called anisotropy index, k_1, defined as

$$k_1 = \frac{B(0)}{B_0(0)} = \frac{B}{B_0\varepsilon_0} \tag{20.34}$$

The solution of equation (20.31) is now

$$D(\beta, \alpha) = D^I(\beta, \alpha) + D^C(\beta, \alpha) \tag{20.35}$$

where

$$D^I(\beta, \alpha) = D(0)(1 - k_1)\frac{1 + \cos\beta}{2} \tag{20.36}$$

and

$$D^C(\beta, \alpha) = \frac{D(0)k_1}{\cos\theta_{ZS}} \max(o, \cos\theta_S) \tag{20.37}$$

respectively, define the contribution of the isotropic and of the circumsolar components.

Downloaded from https://onlinelibrary.wiley.com/doi/ by <Shibboleth-member@purdue.edu, Wiley Online Library on [25/08/2024]. See the Terms and Conditions (https://onlinelibrary.wiley.com/terms-and-conditions) on Wiley Online Library for rules of use; OA articles are governed by the applicable Creative Commons License

Downloaded from https://onlinelibrary.wiley.com/doi/ by <Shibboleth>-member@purdue.edu, Wiley Online Library on [25/08/2024]. See the Terms and Conditions (https://onlinelibrary.wiley.com/terms-and-conditions) on Wiley Online Library for rules of use; OA articles are governed by the applicable Creative Commons License

Note than k_1 is just the ratio between a pyrheliometer's reading and the solar constant, once corrected by the eccentricity due to the ecliptic orbit of the Earth around the sun. This way, k_1 can be understood as a measure of the instantaneous atmospheric transmittance for direct irradiance. When the sky is completely clouded over, $k_1 = 0$ and the above equation becomes the same as that for the simple isotropic model. This anisotropic model is an excellent compromise between simplicity and precision. It has been well-validated against measurements performed at different worldwide locations, and has been extensively used, for example, for the elaboration of the European Atlas of the Solar Radiation [9].

Also, very commonly employed, in particular with digital machines, is the model that has been put forward by Perez [29, 30]. It divides the sky into three zones acting as diffuse radiation sources: a circumsolar region, a horizontal band and the rest of the celestial hemisphere. The relative contributions of each component is modulated by means of empirical factors determined from the study of data from 18 measurement stations at 15 sites in North America and Europe. The Perez model used to perform slightly better than others [31], because the larger number of modulating factors allows for the consideration of a larger number of different sky conditions.

20.5.3.3 Albedo irradiance

The reflectivity of most types of ground is rather low. Consequently, the contribution of the albedo irradiance falling on a receiver is generally small. (An exception occurs in the case of snow.) There is therefore no point in developing very sophisticated models for albedo. It is usual to assume that the ground is horizontal and of infinite extent and that it reflects isotropically. On this basis, the albedo irradiance on an inclined surface is given by

$$R(\beta, \alpha) = \rho G(0) \frac{1 - \cos \beta}{2} \tag{20.38}$$

where ρ is the reflectivity of the ground and depends on the composition of the ground. When the value of ρ is unknown, it is common to take $\rho = 0.2$

It is now opportune to go forward with the example of the previous section, by calculating the irradiance components over a surface tilted to the latitude, the 15 April in Portoalegre-Brazil. Using equations (20.34) to (20.37) to deal with diffuse radiation and $\rho = 0.2$, the results, expressed in W/m^2, are as follows:

ω	k_1	$D^{\mathrm{I}}(\phi)$	$D^{\mathrm{C}}(\phi)$	$B(\phi)$	$R(\phi)$	$G(\phi)$
ω_s	0	0	0	0	0	0
$\pm 60^\circ$	0.2205	73.40	31.80	147.56	2.73	255.49
$\pm 30^\circ$	0.3082	124.14	76.94	357.14	6.26	564.48
0°	0.3403	138.97	98.09	455.31	7.80	700.18

It becomes clear that the albedo can be generally neglected in PV calculations.

Downloaded from https://onlinelibrary.wiley.com/doi/ by <Shibboleth-member@purdue.edu, Wiley Online Library on [25/08/2024]. See the Terms and Conditions (https://onlinelibrary.wiley.com/terms-and-conditions) on Wiley Online Library for rules of use; OA articles are governed by the applicable Creative Commons License

20.5.3.4 Daily irradiation

The most accurate way of calculating $G_{dm}(\beta, \alpha)$ from $G_{dm}(0)$ is, first, to calculate the hourly horizontal irradiation components $G_{hm}(0)$, $D_{hm}(0)$ and $B_{hm}(0)$; second, to transpose them to the inclined surface $G_{hm}(\beta, \alpha)$, $D_{hm}(\beta, \alpha)$ and $B_{hm}(\beta, \alpha)$; and, finally, to integrate during the day.

Such a procedure, summarised in Figure 20.16, allows us to account for the anisotropic properties of diffuse radiation, and leads to good results whatever the orientation of the inclined surface. However, it is laborious to apply and a computer must be used. It is interesting to mention that, for the case of surfaces tilted to the equator ($\alpha = 0$), frequently encountered in photovoltaic applications, if the diffuse radiation is taken to be isotropic, the following expression may be applied

$$G_d(\beta, 0) = B_d(0) \times RB + D_d(0)\frac{1 + \cos\beta}{2} + \rho G_d(0)\frac{1 - \cos\beta}{2} \tag{20.39}$$

where the factor RB represents the ratio between the daily direct irradiations on an inclined surface and on an horizontal surface, and may be approximated by setting it equal to the corresponding ratio between daily extraterrestrial irradiations on similar surfaces. Hence, RB is given as follows:

$$RB = \frac{\omega_{SS}\frac{\pi}{180}[\text{sign}(\phi)]\sin\delta\sin(|\phi| - \beta) + \cos\delta\cos(|\phi| - \beta)\sin\omega_{SS}}{\omega_S\frac{\pi}{180}\sin\delta\sin\phi + \cos\delta\cos\phi\sin\omega_S} \tag{20.40}$$

where ω_{SS} is the sunrise angle on the inclined surface, which is given by

$$\omega_{SS} = \max[\omega_S, -\arccos(-[\text{sign}(\phi)]\tan\delta\tan(abs(\phi) - \beta))] \tag{20.41}$$

It is interesting to observe that for the equinox days, $\delta = 0 \Rightarrow \omega_S = \omega_{SS}$ and equation (20.40) becomes $RB = \cos[abs(\phi) - \beta]/\cos\phi$.

Example: Estimate the average daily irradiation in January at Changchun–China ($\phi = 43.8^\circ$) over a fixed surface facing south and tilted at an angle $\beta = 50^\circ$ with respect to the horizontal, knowing that the mean value of the global horizontal irradiation is $G_{dm}(0) = 1861$ Wh/m^2 and the ground reflection $\rho = 0.2$. The solution is as follows:

January $\Rightarrow d_n = 17; \delta = -20.92^\circ$

$\phi = 43.8^\circ \Rightarrow \omega_S = -68.50$ and $B_{0d}(0) = 3586$ Wh/m^2 $\Rightarrow K_{Tm} = 0.519$

$\Rightarrow F_{Dm} = 0.414$

$D_{dm}(0) = 770$ Wh/m^2; $B_{dm}(0) = 1091$ Wh/m^2

$\arccos(-\tan\delta\tan(\phi - \beta)) = -92.38^\circ \Rightarrow \omega_{SS} = -68.5^\circ \Rightarrow RB = 2.741$

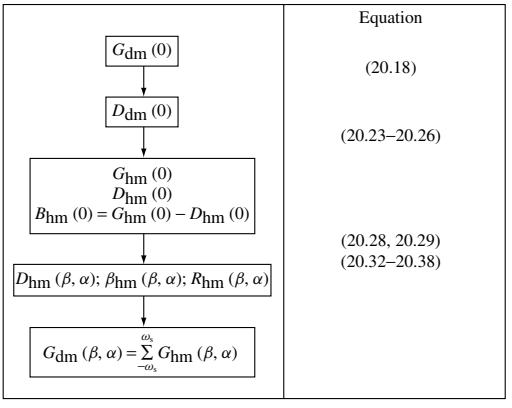


Figure 20.16 Diagram explaining the calculation of the daily irradiation on an inclined surface $G_{dm}(\beta, \alpha)$ from the corresponding horizontal value $G_{dm}(0)$

$$D_{dm}(50) = 633 \text{ Wh/m}^2; B_{dm}(50) = 2990 \text{ Wh/m}^2; R_{dm}(50) = 66 \text{ Wh/m}^2$$
$$G_{dm}(50) = 3689 \text{ Wh/m}^2$$

It is worth mentioning that a more detailed calculation, following the procedure outlined in Figure 20.16, would lead to $G_{dm}(50) = 3956$ Wh/m^2. That means the error associated to equation (20.40) is below 8%. This difference is mainly due to the different consideration of the diffuse radiance distribution.

20.6 DIURNAL VARIATIONS OF THE AMBIENT TEMPERATURE

The behaviour of the photovoltaic modules depends, to some extent, on the ambient temperature. Just as it is for solar radiation, sometimes it is necessary to determine how this parameter varies throughout the day. The data available as a starting point for this calculation are, in general, the maximum and minimum temperature of the day, T_{aM} and T_{am}, respectively.

A model that is simple but, nevertheless, gives a good fit to the experimental values is obtained from the fact that the temperature evolves in a similar manner to the global radiation but with a delay of about 2 h. This fact allows the following three principles to be deduced

- T_{am} occurs at sunrise ($\omega = \omega_S$).
- T_{aM} occurs two hours after midday ($\omega = 30°$).
- Between these two times, the ambient temperature develops according to two semi cycles of a cosine function: one from dawn to midday, and the other between midday and sunrise of the following day.

Downloaded from https://onlinelibrary.wiley.com/doi/ by <Shibboleth-member@purdue.edu>, Wiley Online Library on [25/08/2024]. See the Terms and Conditions (https://onlinelibrary.wiley.com/terms-and-conditions) on Wiley Online Library for rules of use; OA articles are governed by the applicable Creative Commons License

The following set of equations based on the above, permits the ambient temperature throughout a day j to be calculated as follows:

For $-180 < \omega \leq \omega_S$

$$T_a(j, \omega) = T_{aM}(j-1) - \frac{T_{aM}(j-1) - T_{am}(j)}{2}[1 + \cos(a\omega + b)] \tag{20.42}$$

with $a = \dfrac{-180}{\omega_S + 330}$ and $b = -a\omega_S$

For $\omega < \omega_S \leq 30$

$$T_a(j, \omega) = T_{am}(j) + \frac{T_{aM}(j) - T_{am}(j)}{2}[1 + \cos(a\omega + b)] \tag{20.43}$$

with $a = \dfrac{180}{\omega_S - 30}$ and $b = -30a$

For $30 < \omega \leq 180$

$$T_a = T_{aM}(j) - \frac{T_{aM}(j) - T_{am}(j+1)}{2}[1 + \cos(a\omega + b)] \tag{20.44}$$

with $a = \dfrac{180}{\omega_S + 330}$ and $b = -(30a + 180)$

To apply these equations, it is necessary to know the maximum temperature on the previous day, $T_{aM}(j-1)$, and the minimum temperature of the following day, $T_{am}(j+1)$. If these data are unavailable, then it can be assumed, without introducing too much error, that they equal those for the day in question.

20.7 EFFECTS OF THE ANGLE OF INCIDENCE AND OF THE DIRT

The reflectance and transmittance of optical materials depends on the angle of incidence. Glass covers of solar collectors are not an exception and therefore the optical input of photovoltaic modules is affected by their orientation with respect to the sun, due to the angular variation of the glass reflection. Theoretical models, based on the well-known Fresnel formulae, have been developed for clean surfaces. The most popular formulation is from ASHRAE [32]. For a given incidence angle, θ_S, it can be described by the simple expression

$$FT_B(\theta_S) = 1 - b_0\left(\frac{1}{\cos\theta_S} - 1\right) \tag{20.45}$$

where $FT_B(\theta_S)$ is the relative transmittance, normalised by the total transmittance for normal incidence, and b_0 is an adjustable parameter that can be empirically determined for each type of photovoltaic module. If this value is unknown, a general value $b_0 = 0.07$ may be used. The effect of the angle of incidence on the successfully collected solar radiation can be calculated by applying equation (20.45) to the direct and circumsolar irradiances, and by considering an approximated value, $FT = 0.9$, for the isotropic diffuse and reflected radiation terms. Figure 20.17 shows a plot of $FT_B(\theta_S)$ versus θ_S. It presents

Petitioner Canadian Solar (USA) Inc., Ex. 1035, p. 2319

Downloaded from https://onlinelibrary.wiley.com/doi/ by <Shibboleth-member@purdue.edu, Wiley Online Library on [25/08/2024]. See the Terms and Conditions (https://onlinelibrary.wiley.com/terms-and-conditions) on Wiley Online Library for rules of use; OA articles are governed by the applicable Creative Commons License

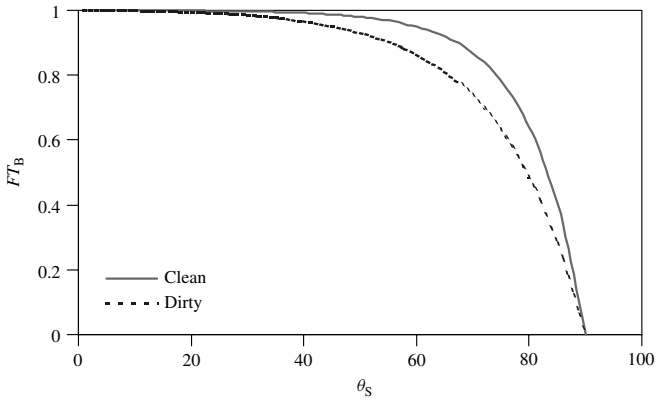


Figure 20.17 The relative transmittance FT_B is plotted against the angle of incidence θ_S, for a clean surface and also for a dust-covered surface

a pronounced knee close to 60°. In practical terms, that means the effects of the angle of incidence are negligible for all the θ_S values well below this figure. For example, $FT_B(40^\circ) = 0.98$.

The ASHRAE model is simple to use but has noticeable disadvantages. It cannot be used for $\theta_S > 80^\circ$, and, still worse, it cannot take into consideration the effects of dust. Dust is always present in real situations, and not only reduces the transmittance at normal incidence but also influences the shape of $FT_B(\theta_S)$. Figure 20.17 shows that the relative transmittance decreases because of dust at angles from about 40 to 80°. Real $FT_B(\theta_S)$ are best described [33] by

$$FT_B(\theta_S) = 1 - \frac{\exp\left(-\frac{\cos\theta_S}{a_r}\right) - \exp\left(-\frac{1}{a_r}\right)}{1 - \exp\left(-\frac{1}{a_r}\right)} \tag{20.46}$$

where a_r is an adjust parameter mainly associated with the degree of dirtiness, as shown in Table 20.4. Note that the degree of dirtiness is characterised by the corresponding relative normal transmittance, $T_{dirt}(0)/T_{clean}(0)$. Equation (20.46) applies for direct and circumsolar radiation components. The angular losses for isotropic diffuse and albedo radiation components are, respectively, approximated by [33]

$$FT_D(\beta) = 1 - \exp\left[-\frac{1}{a_r}\left[c_1\left(\sin\beta + \frac{\pi - \beta\cdot\frac{\pi}{180} - \sin\beta}{1+\cos\beta}\right) + c_2\left(\sin\beta + \frac{\pi - \beta\frac{\pi}{180} - \sin\beta}{1+\cos\beta}\right)^2\right]\right] \tag{20.47}$$

Downloaded from https://onlinelibrary.wiley.com/doi/ by <Shibboleth-member@purdue.edu, Wiley Online Library on [25/08/2024]. See the Terms and Conditions (https://onlinelibrary.wiley.com/terms-and-conditions) on Wiley Online Library for rules of use; OA articles are governed by the applicable Creative Commons License

Table 20.4 Recommended parameters for angular losses calculation

Dirtiness degree	$T_{dirt}(0)/T_{clean}(0)$	a_r	c_2
Clean	1	0.17	−0.069
Low	0.98	0.20	−0.054
Medium	0.97	0.21	−0.049
High	0.92	0.27	−0.023

and

$$FT_R(\beta) = 1 - \exp\left[-\frac{1}{a_r}\left[c_1\left(\sin\beta + \frac{\beta\cdot\frac{\pi}{180} - \sin\beta}{1-\cos\beta}\right) + c_2\left(\sin\beta + \frac{\beta\cdot\frac{\pi}{180} - \sin\beta}{1-\cos\beta}\right)^2\right]\right] \tag{20.48}$$

where $c_1 = 4/(3\pi)$ and c_2 is linearly related to a_r. Table 20.4 also presents some values of these parameters for several dirtiness degrees.

It must be noted that $FT_B(0) = 1$. That means, this function does not include the dirt effect on the relative normal transmittance but only the angular losses relative to normal incidence. In other words, the "effective" direct irradiance reaching the solar cells of a PV module, should be computed as

$$B_{eff}(\beta,\alpha) = B(\beta,\alpha) \times \frac{T_{dirt}(0)}{T_{clean}(0)} \times FT_B(\theta_S) \tag{20.49}$$

and similar expressions should be used for the diffuse and albedo irradiance (or hourly irradiation) components.

Following the example of 15 April in Portoalegre-Brazil, we can now calculate the effective irradiances over a surface tilted to the latitude, neglecting the albedo, supposing a medium dirtiness degree and by applying $FT_B(\theta_S)$ not only to the direct radiation but also to the circumsolar component of the diffuse radiation. Obviously, $FT_D(\beta)$ is applied to the isotropic component of the diffuse radiation. The results are as follows:

$$FT_D(\phi) = 0.934$$

ω°	$FT_B(\theta_S)$	$B_{eff}(\phi)$, [Wm^{-2}]	$D_{eff}(\phi)$ [Wm^{-2}]	$G_{eff}(\phi)$ [Wm^{-2}]	ΔG_{eff} [%]
ω_S	0	0	0	0	0
±60	0.913	80.84	126.39	207.23	−11.3
±30	0.991	249.63	249.74	499.37	−6.8
0	0.999	332.13	296.37	628.50	−6.1

Downloaded from https://onlinelibrary.wiley.com/doi/ by <Shibboleth-member@purdue.edu, Wiley Online Library on [25/08/2024]. See the Terms and Conditions (https://onlinelibrary.wiley.com/terms-and-conditions) on Wiley Online Library for rules of use; OA articles are governed by the applicable Creative Commons License

The last column of this table describes the losses due to both dirt and angular effects. Taking into consideration that dirt reduces normal transmittance by a factor of 3% ($T_{\text{dirt}}(0)/T_{\text{clean}}(0) = 0.97$), it can be noted that pure angular losses dominate for $|\omega| > 30^{\circ}$.

Finally, it should be stressed that angular-dependent reflection is often neglected in PV simulations. However, they become significant in many practical situations, for example, where vertical (façade-integrated PV generators) or horizontal (N–S horizontal trackers) surfaces are concerned. Furthermore, they help to explain the observed low irradiance effects in PV module performance. This is because low irradiance just happens when the incidence angle is large or when solar radiation is mainly diffuse. In both cases, angular losses are particularly important. As a matter of fact, the failure to consider angular losses has been signalled as the main cause of error in some energy models [34].

20.8 SOME CALCULATION TOOLS

20.8.1 Generation of Daily Radiation Sequences

Long series (many years) of daily irradiation data are sometimes required for particular purposes, for example, when studying the long-term reliability of stand-alone photovoltaic systems. However, long series of historical data are scarce and hard to obtain. This leads to the need for methods that are able to generate a series starting from widely available information, such as the 12 long-term average monthly mean values of the daily irradiation, $G_{\text{dm}}(0)$. The idea is that the generated series must keep some statistical properties believed to be universal, as they are also found in historical data, when available. In particular, the persistence of solar radiation, that is, the dependence of today's irradiation on the irradiation of the precedent days, is adequately described by a first-order autoregressive process [35]. Moreover, the probability function of the daily clearness index for any given period has a form associated with only its average value for the period. Several methods for the generation of daily irradiation sequences are available in the literature [36]. The method proposed by Aguiar [37] is the most widely used today.

20.8.2 The Reference Year

As already mentioned, the most widely available information related to the solar radiation resource at a given location is the set of 12 monthly mean values of global horizontal daily irradiation, $G_{\text{dm}}(0)$. The methods presented above allow estimation of all the radiation components incident on any surface of arbitrary orientation and at any moment of the average year, and even at any moment of a long sequence of years. This can be applied to all the problems related to the design of photovoltaic systems: sizing, prediction of energy yields, impact of shadowing, optimisation of tilt angles and so on.

Nevertheless, the solar radiation is still the object of systematic recording, and more and more irradiance and irradiation data are being accumulated and put at public disposal. Such data whether in the form of crude recorded data or in the form of elaborate mathematical tools, attempt to properly represent the climate of the concerned location. The most widely used is the so-called Reference Year, also called the Typical Meteorological Year [18], *TMY*, or the Standard Year. The *TMY* for a location is a hypothetical

Downloaded from https://onlinelibrary.wiley.com/doi/ by <Shibboleth-member@purdue.edu>, Wiley Online Library on [25/08/2024]. See the Terms and Conditions (https://onlinelibrary.wiley.com/terms-and-conditions) on Wiley Online Library for rules of use; OA articles are governed by the applicable Creative Commons License

year in which months are real months, but are chosen from different years from the whole period for which data are available. In practice [38], the months are chosen such that the monthly mean of the daily global irradiation on the horizontal represents an average value for all values contained in the database. For example, January of 1986 was chosen for the *TMY* of Madrid, because it had a value of $G_{dm}(0) = 1.98$ kWh/m^2, the closest to the average value of $G_{dm}(0) = 1.99$ kWh/m^2 for all the months of January on record [16].

The most widely used *TMY* for photovoltaic applications is set in a one-hour time scale. Hence, it contains 4380[1] values of global horizontal irradiation. Ambient temperature values are also specified for each hour. This huge number of initial data can lead to the impression that the corresponding results should be much more accurate than those obtained when simply using the 12 $G_{dm}(0)$ values as input. However, this impression is largely wrong. On the one hand, because the representativeness of any data – it should be again remembered – is limited by the random nature of the solar radiation, small differences in the results are scarcely meaningful. On the other hand, because the results obtained from the 12 $G_{dm}(0)$ values and from the *TMY* are very similar, provided the initial data are coherent (i.e. the monthly means in the *TMY* coincides with the 12 $G_{dm}(0)$ values) and that the selected correlations and diffuse radiation models to transpose from horizontal to inclined surfaces are the same. The physical reasons for this lie in the quasi-linear power-irradiance relationship in most PV devices, and in the fact, initially shown by Liu and Jordan [19], that the solar climate of a particular location can be well characterised by only the monthly mean daily clearness index. As already mentioned, they have demonstrated that, irrespective of latitude, the fractional time during which daily global radiation is equal to or less than a certain value depends only on this parameter. Surely, to go into this question in-depth would increase the reader's boredom which is probably already large enough; hence, we will restrict ourselves to describing a representative case from our own experience:

> In 1992, the Solar Energy Institute in the University of Madrid, IES-UPM, was involved in the design of the 1 MW PV plant in Toledo, Spain. It was the biggest European PV project at that time, so very careful studies were required at the initial project stage. Fortunately, a large historical database, containing 20 years of hourly irradiation data, was available from a nearby meteorological station, and was directly used to calculate the expected energy yields. Both static and sun-tracked photovoltaic arrays were analysed while taking into account detailed features such as shadowing from adjacent rows, back-tracking features and so on. Moreover, the same calculation was also performed using as input the *TMY*, previously derived from the historical radiation sequence, and also using as the only input the 12 $G_{dm}(0)$ values and computing for just the mean day of each month. The results from the three calculation procedures never differed more than 2%! As a matter of fact, the results were much more sensitive to the considerations of the solar angle of incidence effects [39] described below.

A clever friend, not involved in this project but being aware of this anecdote, posed the questions: Then why go into such exhaustive detail when they give similar results?

[1] There are 8760 hours per year, and the sun shines exactly half of the year in any location, hence there are 4380 hours of sunshine per year.

Downloaded from https://onlinelibrary.wiley.com/doi/ by <Shibboleth-member@purdue.edu>, Wiley Online Library on [25/08/2024]. See the Terms and Conditions (https://onlinelibrary.wiley.com/terms-and-conditions) on Wiley Online Library for rules of use; OA articles are governed by the applicable Creative Commons License

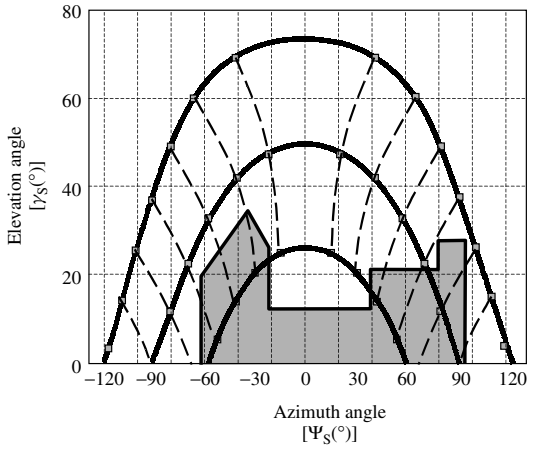


Figure 20.18 Sun's trajectory map corresponding to a latitude $\phi = 40.5°$, with a skyscraper superimposed on the map. For example, on the winter solstice, shadows occur from sunrise to about 10:30 (solar time) and from 14:30 to sunset

Why not just be simple? The proper answers are best found in human psychology. Many people simply desire not to believe in some ideas. Hence, the ones daring to declare them are automatically impelled to provide strong arguments in favour of such ideas. To a large extent, this is usually the case when defending the argument that modern complex software tools do not necessarily yield better results than simple (but judicious) traditional methods. That was the position of the IES-UPM in 1992, and today for the author of this chapter the position remains the same.

20.8.3 Shadows and Trajectory Maps

Surroundings of photovoltaic modules can include trees, mountains, chimneys, walls, other PV modules and so on. Because of that, photovoltaic modules cannot always be positioned entirely free of shadows. This reduces their potential energy yield, and must be taken into account when designing photovoltaic systems. Equations (20.3 to 20.5) allow the plotting of the trajectories of the sun, in terms of elevation versus azimuth angles, as already explained in Figure 20.6.

These types of diagrams are called sun trajectory maps. They are a very useful tool for determining the duration and effect of shadowing cast by any obstacle. A correctly placed theodolite can measure the azimuth and elevation angles of the most relevant points (corners, peaks etc.) of any kind of obstacle. The *local horizon* can then be superimposed on the trajectory map, as Figure 20.18 shows. The effect of the shadow is calculated with the assumption that the direct and circumsolar radiations are zero when the sun is below the local horizon. Unless the shadows are very large, the effect of the local horizon on the diffuse radiation (other than the circumsolar component) can be neglected. Several tools have been proposed [40, 41] to simplify the practise of this calculation.

Downloaded from https://onlinelibrary.wiley.com/doi/ by <Shibboleth-member@purdue.edu>, Wiley Online Library on [25/08/2024]. See the Terms and Conditions (https://onlinelibrary.wiley.com/terms-and-conditions) on Wiley Online Library for rules of use; OA articles are governed by the applicable Creative Commons License

20.9 IRRADIATION ON MOST WIDELY STUDIED SURFACES

This section analyses some important features of the radiation available on commonly studied surfaces. As already mentioned, the methods presented before conform to a complete package, allowing the calculation of the irradiation incident over any arbitrary surface over any period of time, using the horizontal data as input. This can no doubt be a tedious task, so specific commercial software packages have been developed [42, 43]. However, for many practical engineering problems, more direct and simple tools can be developed. In particular, it is possible to develop analytical expressions that can be simply solved by only hand calculations. In order to apply the discussion in the previous sections, let us analyse the particular case of the yearly mean daily irradiation collected at four different places on a fixed surface, tilted towards the equator ($\alpha = 0$) and inclined at an angle β to the horizontal, $G_{dy}(\beta)$. Figure 20.19 plots, for each place, such value in relation to its maximum and versus the inclination angle referred to as the absolute value of the latitude, that is, $G_{dy}(\beta - |\phi|)/G_{dy}(\beta_{opt})$, being β_{opt} the inclination angle associated to the maximum value of $G_{dy}(\beta)$. The calculation procedure had followed the lines described in Figure 20.16. Solar radiation data has been obtained from Reference [7]. Several aspects need to be outlined.

On the one hand, a great similarity between all the curves is noticeable. Despite large differences in latitude and clearness index of the selected locations, the shape of the curve and also the inclination angle maximising the collection of radiation are very similar for the four selected places. Furthermore, this angle is relatively close to the latitude. It is important to mention that the extension of this exercise to many other places all around the world verifies that this great similarity is nearly universal. In fact, we have performed a specific exercise covering 30 different places distributed from $\phi = 80^\circ$ to $\phi = -78.2^\circ$ (see list in Table 20.5). We limit Figure 20.19 to only four curves for presentation purposes. A physical explanation of this similitude can be argued observing that, irrespective of the latitude, all the surfaces tilted towards the equator and inclined at an angle equal to the absolute value of the latitude are parallel all over the Earth, and also parallel to the Earth's rotation axis. Therefore, in the absence of the atmosphere, on

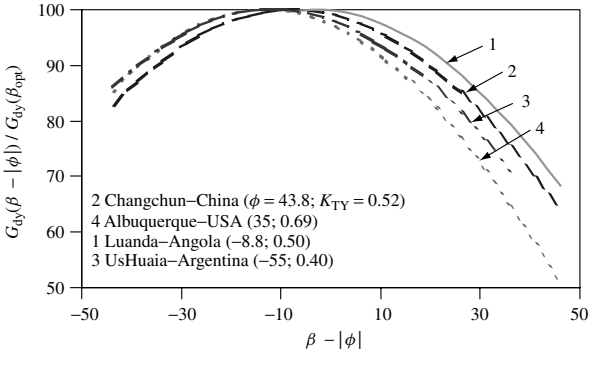


Figure 20.19 Yearly energy collection versus inclination angle for surfaces tilted towards the equator. The percentage of relative collection, with respect to the maximum, $G_{dy}(\beta - |\phi|)/G_{dy}(\beta_{opt})$ is plotted against the difference between the tilt angle and the latitude $\beta - |\phi|$

Petitioner Canadian Solar (USA) Inc., Ex. 1035, p. 2325

Downloaded from https://onlinelibrary.wiley.com/doi/ by <Shibboleth-member@purdue.edu, Wiley Online Library on [25/08/2024]. See the Terms and Conditions (https://onlinelibrary.wiley.com/terms-and-conditions) on Wiley Online Library for rules of use; OA articles are governed by the applicable Creative Commons License

Downloaded from https://onlinelibrary.wiley.com/doi/ by <Shibboleth-member@purdue.edu, Wiley Online Library on [25/08/2024]. See the Terms and Conditions (https://onlinelibrary.wiley.com/terms-and-conditions) on Wiley Online Library for rules of use; OA articles are governed by the applicable Creative Commons License

Table 20.5 Annual radiation availability on different surfaces, for 30 different places all around the world. Various tracking options (1 axis, 2 axis, etc.) described in Section 20.9.2

Location	Lat. ϕ°	$B_{0dy}(0)$ [Wh/m^2]	Clearness index K_{Ty}	Ratios to global horizontal yearly irradiation					
				2 axis	1 Az-axis	1 Ho-axis	1 Po-axis	Fixed β_{opt}	2 axis Conc.
Ice-Island-Arctic	80	4261	0.580	2.75	2.54	1.97	2.60	1.67	2.26
S. Petersburg-Russia	59.9	5703	0.453	1.72	1.64	1.43	1.61	1.18	1.21
Hamburg-Germany	53.6	6437	0.412	1.49	1.42	1.28	1.39	1.11	0.97
Freiburg-Germany	48	7075	0.428	1.42	1.36	1.26	1.33	1.07	0.93
Nantes-France	47.2	7164	0.468	1.50	1.44	1.31	1.41	1.10	1.03
Olympia-USA	46.6	7230	0.437	1.41	1.35	1.27	1.32	1.05	0.93
Changchun-China	43.8	7531	0.510	1.60	1.53	1.35	1.51	1.16	1.13
Sapporo-Japan	43	7615	0.421	1.41	1.35	1.22	1.31	1.09	0.89
Madrid-Spain	40.4	7880	0.544	1.53	1.46	1.36	1.45	1.08	1.12
Seoul-Korea	37.5	8161	0.440	1.39	1.32	1.23	1.30	1.07	0.89
Albuquerque-USA	35	8391	0.687	1.66	1.55	1.47	1.58	1.09	1.37
Djelfa-Algeria	34.6	8427	0.584	1.53	1.44	1.45	1.37	1.06	1.15
El Paso-Mexico	31.5	8691	0.689	1.61	1.49	1.45	1.53	1.07	1.33
Shanghai-China	31.2	8716	0.487	1.36	1.29	1.25	1.27	1.02	0.91
Cairo-Egypt	30.6	8764	0.637	1.53	1.43	1.39	1.46	1.05	1.20
Delhi-India	28.6	8919	0.630	1.56	1.44	1.40	1.47	1.07	1.23
Karachi-Pakistan	24.8	9189	0.560	1.48	1.36	1.35	1.39	1.04	1.13
Morelia-Mexico	19.7	9494	0.415	1.20	1.14	1.14	1.08	0.98	0.70
Dakar-Senegal	14.7	9729	0.599	1.38	1.23	1.31	1.29	0.98	1.04
Bangkok-Thailand	13.7	9768	0.490	1.27	1.16	1.21	1.14	0.98	0.83
Claveria-Philippines	8.6	9924	0.513	1.27	1.13	1.23	1.16	0.95	0.86
Colombo-Sri Lanka	6.9	9961	0.529	1.28	1.12	1.23	1.16	0.96	0.76
Medellin-Colombia	6.2	9974	0.469	1.22	1.08	1.18	1.08	0.95	0.76
Luanda-Angola	−8.8	9918	0.497	1.26	1.12	1.21	1.13	0.95	0.83
El Alto-Bolivia	−16.4	9652	0.579	1.39	1.25	1.31	1.29	0.99	1.04
Sao Paulo-Brazil	−23.5	9267	0.427	1.25	1.19	1.17	1.14	0.99	0.76
Porto Alegre-Brazil	−30	8805	0.505	1.38	1.30	1.26	1.29	1.02	0.93
Bariloche-Argentina	−41.1	7801	0.566	1.58	1.50	1.40	1.50	1.07	1.18
Ushuaia-Argentina	−55	6263	0.402	1.62	1.55	1.30	1.51	1.19	1.07
Little America-Antartic	−78.2	4306	0.577	2.67	2.48	1.87	2.52	1.55	2.12

the equinox days, they receive identical solar irradiation, $B_{0d}(|\phi|)|_{\delta=0}$. And the same is true for surfaces equally tilted with respect to the latitude angle, $B_{0d}(\beta - |\phi|)|_{\delta=0}$. For other than equinox days, this is not exactly true, because sunrise time (and, therefore, the length of daytime and, in turn, the daily extraterrestrial irradiation) depends on latitude, as described by equation (20.7). However, the yearly ratio between extraterrestrial irradiation collected on both inclinations, $B_{0dy}(\beta - |\phi|)/B_{0dy}(|\phi|)$ tends to remain constant. Now, when accounting for the Earth's atmosphere, such site independence is not necessarily maintained, because of the different climatic conditions, that is, the different annual clearness index K_{Ty}, from one site to another. Obviously, the collection of diffuse radiation is less sensitive to inclination angle variations than the collection of direct radiation. Because of this, the lower the K_{Ty} value (the higher the F_{dy}), the slightly less is sharp-pointed curve that should be expected. Figure 20.19 reveals that this tendency is, in fact, very weak, so that the site independence clearly dominates and the function $G_{dy}(\beta - |\phi|)/G_{dy}(\beta_{opt})$ can be properly considered as being a universal invariant.

On the other hand, the smooth form of the curves of Figure 20.19 suggests that it may be possible to describe them analytically, thus avoiding the need to use a computer each time a particular value is required. A convenient way of doing it is, first, analysing the correspondence between the optimal inclination angle and latitude. It is worth noting that the larger the latitude, the larger the difference between summer daytime and winter daytime and, in turn, the larger the difference between the summer and the winter irradiation. Therefore, it can be anticipated that as latitude increases, the optimal inclination angle should progressively give priority to the collection of summer over the collection of winter. This can be observed in Figure 20.20, where the values of $\beta_{\text{opt}} - |\phi|$ have been plotted against the latitude, for the 30 above-mentioned different locations.

It is useful to fit a linear equation to these values

$$\beta_{\text{opt}} - |\phi| = 3.7 - 0.31|\phi| \quad \text{or} \quad \beta_{\text{opt}} = 3.7 + 0.69|\phi| \tag{20.50}$$

where β and ϕ are given in degrees. It is worth mentioning that the observed dispersion of the cluster of points around equation (20.50) (also depicted in Figure 20.20) is, in fact, of negligible importance, due to the very low sensibility of the energy collection to deviations from the optimal inclination angle. For example, the point corresponding to Delhi ($\phi = 28.6^\circ$) – marked as ♥ in the figure – indicates a value of $\beta_{\text{opt}} = 29.6^\circ$, while equation (20.50) leads to $\beta_{\text{opt}} = 23.4^\circ$. The 6.2° of difference can appear relatively large ($\approx$20%), but a detailed simulation exercise would disclose that $G_{\text{dy}}(23.4^\circ)/G_{\text{dy}}(29.6^\circ)$ is 99%, that is, such a difference is irrelevant when translated into energy content. A similar reasoning also justifies the validity of the usual assumption $\beta_{\text{opt}} = \phi$. Now, a second-order polynomial describes very well the curves of Figure 20.19.

$$\frac{G_{\text{dy}}(\beta)}{G_{\text{dy}}(\beta_{\text{opt}})} = 1 + p_1(\beta - \beta_{\text{opt}}) + p_2(\beta - \beta_{\text{opt}})^2 \tag{20.51}$$

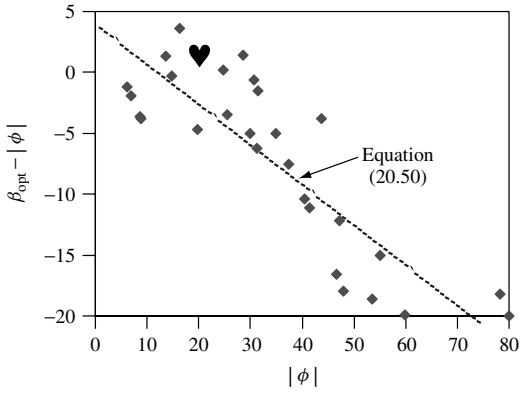


Figure 20.20 Optimal inclination angle versus latitude. The difference between $\beta_{\text{opt}} - |\phi|$ is plotted against the latitude $|\phi|$. The cluster of points corresponds to the different places listed in Table 20.5

Petitioner Canadian Solar (USA) Inc., Ex. 1035, p. 2327

Downloaded from https://onlinelibrary.wiley.com/doi/ by <Shibboleth-member@purdue.edu, Wiley Online Library on [25/08/2024]. See the Terms and Conditions (https://onlinelibrary.wiley.com/terms-and-conditions) on Wiley Online Library for rules of use; OA articles are governed by the applicable Creative Commons License

where p_1 and p_2 are the adjusted parameters for which values are 4.46×10^{-4} and -1.19×10^{-4}, respectively. The corresponding value of the so-called correlation coefficient, R^2, is greater than 0.98, indicating that equations (20.50) and (20.51) adjust very well to the simulated values. This way, the results of a rather complex calculation, involving a lot of tedious steps, can be described by means of two simple mathematical expressions. Apart from simplicity and elegance, all the information has been condensed into just four numbers and an equation that have the advantage of having a continuous slope, which can be useful in many calculations. It is worth mentioning that these equations can also be used to calculate the value of $G_{dy}(\beta_{opt})$ from the data corresponding to the horizontal surface, which is the most usually available information.

Example: Estimation of the optimal tilt angle and the corresponding yearly irradiation in Sapporo-Japan knowing the latitude, $\phi = 43^\circ$, and the annual average of the daily global horizontal irradiation, $G_{dy}(0) = 3220$ Wh/m^2. The solution is

Equation (20.50), $\phi = 43^\circ \Rightarrow \beta_{opt} = 33.37^\circ$

Equation (20.51), $\beta = 0^\circ \Rightarrow G_{dy}(0)/G_{dy}(\beta_{opt}) = 0.8526$

$$\Rightarrow G_{dy}(\beta_{opt}) = 1.1729 \times G_{dy}(0) = 3776 \text{ Wh/m}^2.$$

The total yearly irradiation is $365 \times G_{dy}(0) = 1379$ kWh/m^2.

It is worth mentioning that a more careful calculation, using the 12 values of the monthly mean irradiation and following the procedure described in Figure 20.16, would lead to $G_{dy}(\beta_{opt}) = 3663$ Wh/m^2. This means, that the error associated to equation (20.51) is below 3%.

Attempting to help in the following discussion, Table 20.5 presents the results of a detailed simulation exercise devoted to the calculation of the annual radiation availability on horizontal surfaces, optimally tilted fixed surfaces and several types of tracking surfaces. The exercise has been extended to 30 different places distributed around the World. The hope is that the readers could find here a relatively similar location, both in latitude and clearness index, to the location of their interest. The yearly means of the daily global horizontal irradiation, $G_{dy}(0)$, can be obtained by multiplying the corresponding values of the extraterrestrial radiation and the clearness index. (column 3 × column 4). Then, these horizontal $G_{dy}(0)$ values are used as reference for the irradiation availability in all the other considered surfaces. In particular, column 8 of this table gives the ratio between the global irradiation on a fixed and optimally tilted surface to the global horizontal irradiation, $G_{dy}(\beta_{opt})/G_{dy}(0)$. Hence, the irradiation on the optimally tilted surface is given by the product (column 3 × column 4 × column 8).

20.9.1 Fixed Surfaces

The integration of PV generators in buildings, presently in vogue in many industrialised countries, led to the use of a large range of different orientations and tilt angles. PV module orientations from east to west, and tilt angles from horizontal to vertical are found in practise. Then, it is worth extending the previous exercise to surfaces other than those

Downloaded from https://onlinelibrary.wiley.com/doi/ by <Shibboleth-member@purdue.edu, Wiley Online Library on [25/08/2024]. See the Terms and Conditions (https://onlinelibrary.wiley.com/terms-and-conditions) on Wiley Online Library for rules of use; OA articles are governed by the applicable Creative Commons License

tilted towards the equator, that is, to $\alpha \neq 0$, and also to dirty surfaces. E. Caamaño [44] has proposed the following solution:

$$\frac{G_{\text{effdy}}(\beta, \alpha)}{G_{\text{dy}}(\beta_{\text{opt}})} = g_1(\beta - \beta_{\text{opt}})^2 + g_2(\beta - \beta_{\text{opt}}) + g_3 \tag{20.52}$$

where

$$g_i = g_{i1} \cdot |\alpha|^2 + g_{i2} \cdot |\alpha| + g_{i3}; i = 1, 2, 3 \tag{20.53}$$

being the values of the coefficients as show in Table 20.6, for medium dirty surfaces. The sub-index "eff" in the left term of equation (20.52) indicates that the dirt effect on the relative normal transmittance is also being included, in order to facilitate the direct application of the equation to real cases.

Let us continue with the example of Sapporo-Japan, by calculating the effective irradiation available on the following surfaces:

1. Optimally oriented, $\alpha = 0$, and optimally tilted, $\beta = \beta_{\text{opt}}$
   Equation (20.53), $\alpha = 0 \Rightarrow g_i = g_{i3}$
   Equation (20.52), $\beta = \beta_{\text{opt}} \Rightarrow G_{\text{effdy}}(\beta_{\text{opt}}) = 0.9314\ G_{\text{dy}}(\beta = \beta_{\text{opt}}) = 3517\ \text{Wh/m}^2$
   Note that the total losses due to the optical effects of the angle of incidence (≈7%) are larger than pure normal transmittance losses (≈3%)
2. Tilted 20° with respect to the horizontal, $\beta = 20°$, and oriented 30° towards the west, $\alpha = 30° \Rightarrow g_1 = -1.032 \times 10^{-4}$; $g_2 = 1.509 \times 10^{-4}$; $g_3 = 0.9057$
   $\beta - \beta_{\text{opt}} = -13.37° \Rightarrow G_{\text{effdy}}(20, 30) = 0.8853 \cdot G_{\text{dy}}(\beta_{\text{opt}}) = 3343\ \text{Wh/m}^2$
   It is worth mentioning that a similar calculation, but without considering the angular losses, would lead to $G_{\text{dy}}(20, 30) = 0.936 \cdot G_{\text{dy}}(\beta_{\text{opt}}) = 3533\ \text{Wh/m}^2$
3. A vertical facade, $\beta = 90°$, oriented towards the south-east, $\alpha = -45°$.
   $\alpha = -45° \Rightarrow g_1 = -0.885 \times 10^{-4}$; $g_2 = -2.065 \times 10^{-4}$; $g_3 = 0.8761$
   $\beta - \beta_{\text{opt}} = 56.63° \Rightarrow G_{\text{effdy}}(90, -45) = 0.5806 \cdot G_{\text{dy}}(\beta_{\text{opt}}) = 2192\ \text{Wh/m}^2$

It is opportune to mention again the relatively weak sensitivity of the annual capture of energy to the inclination angle. A value of 0.2% loss for each degree of deviation from the optimum value is a rough approximation. This is true to an even greater extent in the case of azimuthal orientation, where only a 0.08% loss occurs for each degree of deviation from the south. This means that many existing surfaces (roofs, car parks etc.) are suitable for PV modules integration, even if their orientation differs considerably from

Table 20.6 Coefficients used to solve equation (20.52). Values are given for the representative case of medium dirtiness degree ($T_{\text{dirt}}(0)/T_{\text{clean}}(0) = 0.97$)

Coefficients	$T_{\text{dirt}}(0)/T_{\text{clean}}(0) = 0.97$		
	$i = 1$	$i = 2$	$i = 3$
g_{1i}	8×10^{-9}	3.8×10^{-7}	-1.218×10^{-4}
g_{2i}	-4.27×10^{-7}	8.2×10^{-6}	2.892×10^{-4}
g_{3i}	-2.5×10^{-5}	-1.034×10^{-4}	0.9314

Petitioner Canadian Solar (USA) Inc., Ex. 1035, p. 2329

Downloaded from https://onlinelibrary.wiley.com/doi/ by <Shibboleth-member@purdue.edu, Wiley Online Library on [25/08/2024]. See the Terms and Conditions (https://onlinelibrary.wiley.com/terms-and-conditions) on Wiley Online Library for rules of use; OA articles are governed by the applicable Creative Commons License

the optimum. This also means there is no need to carry out expensive civil works to level the site of PV arrays, despite it being an extended custom in large PV plants.

The case of stand-alone systems designed to feed equipment having a constant consumption throughout the year is an especially interesting one, and deserves particular mention. The design criterion here is to maximise the energy captured during the period of least radiation, rather than throughout the year. As might be expected, such receivers are positioned perpendicular to the winter sunlight, which leads to recommend a tilt angle $\beta \approx \phi + 10^{\circ}$.

20.9.2 Sun-tracking Surfaces

At the moment, tracking mechanisms are little used in photovoltaics, but in the future they are likely to become much more common, mainly associated with relatively big grid-connected PV plants, where these mechanisms have already demonstrated very high reliability. As a particular example, the 100 kWp tracking system at the Toledo-PV plant [39] is in routine operation with 100% of availability from 1994 (about 66 000 h when writing this chapter).

Tracking about two axes maintains the receiver surface always perpendicular to the sun ($\beta = \theta_{ZS}$; $\alpha = \psi_S$). Hence, it allows collecting the maximum amount of energy possible. Mainly depending on the clearness index, the comparison with an optimally tilted fixed surface leads to the ratio $G_{dy}(2\text{ axes})/G_{dy}(\beta_{opt})$ varying from 1.25 to 1.55 (column 4 divided by column 8 of Table 20.5). However, it is expensive to implement, because it uses relatively complicated mechanisms and takes up a great deal of space, due to the shadows cast. For these reasons, several types of one-axis trackers are usually preferred.

Azimuthal one-axis trackers rotate around their vertical axis, in such a way that the azimuth of the receiver PV surface is always the same as that of the sun's azimuth. Meanwhile, the tilt angle keeps constant ($\beta = \beta_{cons}$ and $\alpha = \psi_S$). The incidence angle is given by the difference between the surface's tilt angle and the solar zenith angle ($\theta_S = \theta_{ZS} - \beta_{cons}$). Obviously, the amount of collected radiation depends on the inclination of the surface, being the maximum for a value close to the latitude. Again, the sensitivity of the annual capture of energy to this inclination angle is relatively low. A typical value of approximately 0.4% loss from each degree of deviation from the optimum inclination can be assumed. Note that an azimuthal tracker tilted to the latitude collects up to 95% of the yearly irradiation corresponding to the case of two-axes tracking (column 5 divided by column 4 of Table 20.5).

One-axis trackers turning around a single axis–oriented N–S and tilted at an angle β_{NS} to the horizontal are also of great interest. It can be seen that, in order to minimise the solar incident angle, the rotation angle of the axis, $\psi_{NS} - 0$ at noon – must be

$$\tan \psi_{NS} = \frac{\sin \omega}{\cos \omega \cos \beta_{\Delta} - [\text{sign}(\phi)] \tan \delta \sin \beta_{\Delta}} \tag{20.54}$$

where $\beta_{\Delta} = \beta_{NS} - abs(\phi)$. The corresponding solar incident angle is given by

$$\cos \theta_S = \cos \psi_{NS} (\cos \delta \cos \omega \cos \beta_{\Delta} - [\text{sign}(\phi)] \sin \delta \sin \beta_{\Delta}) + \sin \psi_{NS} \cos \delta \sin \omega \tag{20.55}$$

Downloaded from https://onlinelibrary.wiley.com/doi/ by <Shibboleth-member@purdue.edu>, Wiley Online Library on [25/08/2024]. See the Terms and Conditions (https://onlinelibrary.wiley.com/terms-and-conditions) on Wiley Online Library for rules of use; OA articles are governed by the applicable Creative Commons License

A common configuration, called *polar tracking*, is when the axis is inclined just to the latitude. Then, the rotation axis is parallel to the rotation axis of the Earth, and the equations (20.54 and 20.55) become reduced to $\psi_{NS} = \omega$, and $\theta_S = \delta$. Because of the variation of the declination during the year, the cosines of the solar incident angle ranges between 0.92 and 1, having an annual mean value of about 0.95. This way, the polar tracker also collects about 95% of the energy corresponding to the two-axes case (column 7 divided by column 4 of Table 20.5). It is interesting to note that a polar tracker turns just at the same angular speed as that of a standard clock.

Another common configuration is when the axis is just horizontal. Horizontal one-axis trackers are of particularly simple construction and do not cast shadows in the N–S direction. This encompasses significant radiation reduction when compared with two-axis tracking (column 6 divided by column 4 of Table 20.5), but still significant radiation increase when compared with optimally tilted fixed surfaces (column 6 divided by column 8 of Table 20.5). Because of this, they are today the most common tracking solution in large PV plants: PVUSA [45], Toledo [39] and so on. And the same is true for solar thermal plants. We should remember that the very first solar tracker used in any significant way for power generation was just a N–S-oriented horizontal one-axis tracker associated to a parabolic reflecting trough, constructed in 1912 by Frank Shumann and C.V. Boys to power a 45-kW steam-pumping plant in Meadi, Egypt [46]. The tracking surface covered an area of 1200 m^2. The plant was a technical success, that is, reliable trackers existed already at the time, but it was shut down in 1915 due to the onset of World War I and cheaper fuel prices. The world's largest solar plant, at the well-known Luz solar field, erected in California from 1984 to 1986, also employs this type of tracking and, again, with great technical success [47]. The surface position and the solar incident angle are given by

$$\beta = \arctan\left|\frac{\sin\psi_S}{\tan\gamma_S}\right| \tag{20.56}$$

and

$$\cos\theta_S = \cos\delta \cdot [\sin^2\omega + (\cos\phi\cos\omega + \tan\delta\sin\phi)^2]^{1/2} \tag{20.57}$$

Finally, it is worth commenting that large PV generators have several rows of modules mounted above the ground. The distance between rows affects the energy produced by the PV generator. If the separation is increased, fewer shadows are cast by some rows on the others and more energy is produced. But it also affects the cost, as greater separations lead to more land being occupied, longer cables and more expensive civil works. Therefore, there is an optimum separation, giving the best trade-off between greater energy and lower cost. There is a widely held view that tracking generally requires much more land than static arrangements. However, it should be outlined that this is not necessarily the case when horizontal one-axis tracking is concerned. The interested reader is encouraged to refer to [48], which deals in detail with tracking and shadowing in large PV arrays.

20.9.3 Concentrators

PV concentrators are able to capture only direct-beam solar radiation and require tracking mechanisms to keep in focus the solar cells. Therefore, they are best suited to sunny

Downloaded from https://onlinelibrary.wiley.com/doi/ by <Shibboleth-member@purdue.edu, Wiley Online Library on [25/08/2024]. See the Terms and Conditions (https://onlinelibrary.wiley.com/terms-and-conditions) on Wiley Online Library for rules of use; OA articles are governed by the applicable Creative Commons License

Petitioner Canadian Solar (USA) Inc., Ex. 1035, p. 2331

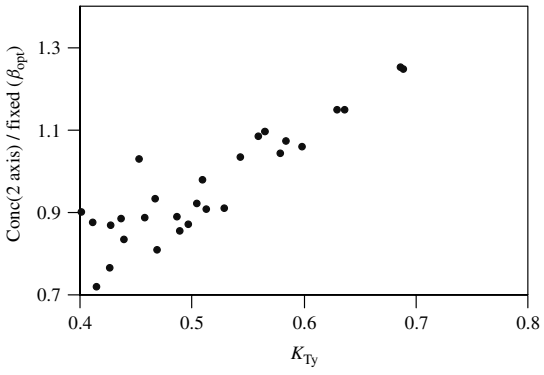


Figure 20.21 Comparison of annual average solar radiation available for fixed flat-plate conventional PV modules, and two-axis tracking PV concentrators. The y-axis is (column 10)/(column 9) and the x-axis column 4 of Table 20.5

sites with low scattering (or low diffuse radiation) and good solar resources. Figure 20.21 compares the amount of normal direct radiation for a PV concentrator mounted on a two-axis tracker, with the amount of global radiation, collected by a conventional flat-plate PV collector, at a fixed optimal tilt. The data represents the 30 locations in Table 20.5. The ratio between both quantities, $B_{dy}(\perp)/G_{dy}(\beta_{opt})$, (column 9 divided by column 8 of Table 20.5) is plotted against the annual clearness index. As a general rule, two-axis tracking concentrators collect more radiation than fixed flat-plate modules in places where $K_{Ty} > 0.55$.

20.10 PV GENERATOR BEHAVIOUR UNDER REAL OPERATION CONDITIONS

A problem that the engineer frequently has to solve is the prediction of the electrical behaviour of a PV generator, given the information about the generator's construction, geographic location, and the local weather. In particular, this represents the base for predicting the generator energy delivery, which is a critical step of any PV-system design. This leads to the question of establishing a PV module rating condition, at which power performance and other characteristics are specified and, defining a method for calculating performance at the prevailing environmental conditions such as solar irradiance, ambient temperature, wind speed and so on.

Traditionally, PV modules are being rated under the so-called Standard Test Conditions (STC) (Irradiance: 1000 W/m^2; Spectrum: *AM* 1.5; and Cell Temperature: 25°C). In the following, we will use the superscript * to refer to these conditions. The most usual case is to know just the values of the short-circuit current, I^*_{SC}, the open-circuit voltage, V^*_{OC} and the maximum power, P^*_M, which are always included in the manufacturer's data sheets. Furthermore, the characterisation of the PV module is completed by measuring the *nominal operating cell temperature* (*NOCT*), defined as the temperature reached by the cells when the PV module is submitted to an irradiance of 800 W/m^2 and

Downloaded from https://onlinelibrary.wiley.com/doi/ by <Shibboleth-member@purdue.edu>, Wiley Online Library on [25/08/2024]. See the Terms and Conditions (https://onlinelibrary.wiley.com/terms-and-conditions) on Wiley Online Library for rules of use; OA articles are governed by the applicable Creative Commons License

an ambient temperature of 20°C. However, performance predictions based on STC are being continuously questioned, mainly because the resulting annual energy efficiencies are significantly lower than the power efficiencies defined, using STC. Certainly, PV users can be astonished on learning that the real efficiency of the PV module they have purchased, once installed at home, has only about 70% of the STC efficiency they have read in the manufacturer's information. This could lead to a feeling of having been deceived. This frustration can even increase in the case of fraud, that is, if the actual STC power performance of the delivered PV module is below the value declared by the module's manufacturer, which, unfortunately, has sometimes been the case [49, 50].

All together, these facts have stimulated several authors to propose other methods for PV module rating and energy performance estimation, more oriented to give buyers clear and more accurate information about the energy generation of PV modules (see Chapter 16 for a detailed description on rating module performance). This is still an open question, and it is difficult to predict the extent to which these new models would be incorporated in future PV engineering practices. Most of these methods require extending testing to other-than-STC, and rely on a relatively large number of parameters that should be empirically determined. Surely, the use of a large number of parameters would potentially allow for more accurate energy modelling. But it is not clear as to what extent the possible improvements would compensate for the associated increase of complexity derived from the experimental determination of such parameters. The proponents of new methods tend to argue that their procedures can be easily implemented. (Their papers used to include sentences like ... *the entire test procedure for outdoor measurements, including the set-up, takes approximately three hours* ... [51]). But, at the same time, the PV module manufacturers are very reluctant to incorporate troublesome novelties into their module characterisation procedures already established at factory PV. This dilemma is, in fact, easily understandable considering the inherent difficulties associated with the adoption of any innovation. This was magnificently explained by Maquiavelo in his famous work *The Prince*, written in 1513:(... *There is nothing more difficult to plan, more doubtful of success ... than the creation of a new order of things* ...).

Together, claims of low PV modules energy performance, and the flourishing of proposals for new rating methodologies have led, no doubt, to significant confusion in today's PV community, making risky this author's task of selecting a particular methodology for recommending to his PV colleagues. However, it is this author's opinion that, at least in the case of crystalline silicon, energy performance modelling based on only a few parameters obtained at STC, and always included in the manufacturer's data sheets, can lead to adequate predictions, providing that some judicious considerations are made. Obviously, precautions to assure that actual STC power of the purchased PV modules correspond with the manufacturer's declarations are a different matter [52].

It must be remembered that crystalline silicon solar cells remain the workhorse for PV power generation, despite significant advances in other PV devices. For example, c-Si technology increased its world market share [53], from 84.4% in 1999 to 86.4% in 2000. This predominance means that actual information concerning in-field c-Si PV modules performance is particularly consistent, which is not typically the case where other materials are concerned. Because of this, dealing with c-Si PV modules is, by far, the simplest and easiest case for PV designers. This is why, despite the above-mentioned confusion, the

Downloaded from https://onlinelibrary.wiley.com/doi/ by <Shibboleth-member@purdue.edu, Wiley Online Library on [25/08/2024]. See the Terms and Conditions (https://onlinelibrary.wiley.com/terms-and-conditions) on Wiley Online Library for rules of use; OA articles are governed by the applicable Creative Commons License

author dares to detail here a rather simple methodology that allows the estimation of the $I-V$ curve of c-Si PV modules operating in any prevailing environmental condition, exclusively using as input the values of I_{SC}^*, V_{OC}^* and P_M^*. In principle, such methodology can be extended to other-than-c-Si materials, and additional comments to do this are also included in the text that follows. However, the reader should be advised that the much less available experience with these materials encompasses significant increase in uncertainty.

20.10.1 The Selected Methodology

In a previous chapter (see Chapter 3), it has been shown that the characteristic $I-V$ of a solar cell can be expressed with sufficient accuracy by

$$I = I_L - I_0\left(\exp\frac{V+IR_S}{V_t} - 1\right) - \frac{V+IR_S}{R_P} \tag{20.58}$$

where I_L, I_0, R_S and R_P are the photo-generated current, the dark current, the series resistance and the parallel resistance, respectively. The voltage V_t equals mkT/e (we recall that for $m = 1$, $V_t \approx 25$ mV at 300 K). This expression gives an adequate representation of the intrinsic behaviour of a typical c-Si solar cell. Nonetheless, it cannot be used directly to obtain the required predictions, because some parameters, I_L and I_O in particular, cannot be established from the usually available information, often restricted to the values of I_{SC}^*, V_{OC}^*, and P_M^*, which are always included on the manufacturers' data sheets.

This difficulty is effectively overcome when the following assumptions, which are generally valid for c-Si PV cells and modules, are made:

- The effect of parallel resistance is negligible.
- The photo-generated current and the short-circuit current are equal.
- $\exp((V + IR_S)/V_t) \gg 1$ under all working conditions.

This allows equation (20.58) to be written as

$$I = I_{SC} - I_O\exp\left(\frac{V+IR_S}{V_t}\right) \tag{20.59}$$

which, with $I = 0$, leads to the following expression for the open-circuit voltage:

$$V_{OC} = V_t\ln\left(\frac{I_{SC}}{I_O}\right) \tag{20.60}$$

whence

$$I_O = I_{SC}\exp\left(-\frac{V_{OC}}{V_t}\right) \tag{20.61}$$

Substituting equation (20.61) in (20.59), we arrive at

$$I = I_{SC}\left[1 - \exp\left(\frac{V - V_{OC} + IR_S}{V_t}\right)\right] \tag{20.62}$$

Downloaded from https://onlinelibrary.wiley.com/doi/ by <Shibboleth-member@purdue.edu, Wiley Online Library on [25/08/2024]. See the Terms and Conditions (https://onlinelibrary.wiley.com/terms-and-conditions) on Wiley Online Library for rules of use; OA articles are governed by the applicable Creative Commons License

This is a very useful expression. As we shall see, the values of all the parameters on the right-hand side are easily obtained allowing immediate application of the expression. An inconsistency arises in the sense that $I(V = 0) \neq I_{SC}$. Nevertheless, in all solar cells of practical use, we find that $V_{OC} \gg IR_S \Rightarrow I(V = 0) \approx I_{SC}$, which therefore makes this objection irrelevant. The expression can be inconvenient to use in the sense that I is implicit (it appears on both sides of the equation), theoretically making it necessary to solve the equation iteratively. However, for voltages close to the maximum-power point, a reasonably accurate solution can be obtained with only one iteration by setting $I = 0.9 \times I_{SC}$ in the second term.

The calculation of the maximum power can, in principle, be carried out by considering that the power is given by the product $P = VI$. The values of I_M and V_M, defining the maximum-power operation point, can be obtained from the usual condition for a maximum, $dP/dV = 0$. However, the implicit nature of the resulting expression makes it very cumbersome to use. It would be better to look for a simpler method, based on the existing relationship between the fill factor and the open-circuit voltage. According to M.A. Green [54] an empirical expression describing this relation is

$$FF = \frac{V_M I_M}{V_{OC} I_{SC}} = \frac{P_M}{V_{OC} I_{SC}} = FF_0(1 - r_s) \tag{20.63}$$

where

$$FF_0 = \frac{v_{OC} - \ln(v_{OC} + 0.72)}{v_{OC} + 1} \tag{20.64}$$

and $v_{OC} = V_{OC}/V_t$ and $r_s = R_S/(V_{OC}/I_{SC})$ are defined as the normalised voltage and the normalised resistance, respectively. It is interesting to note that the series resistance at STC can be deduced from the manufacturer's data by the expression

$$R_S = \left(1 - \frac{FF}{FF_0}\right) \frac{V_{OC}}{I_{SC}} \tag{20.65}$$

The values of V_M and I_M are in turn given by [55]

$$\frac{V_M}{V_{OC}} = 1 - \frac{b}{v_{OC}} \ln a - r_s(1 - a^{-b}) \text{ and } \frac{I_M}{I_{SC}} = 1 - a^{-b} \tag{20.66}$$

where:

$$a = v_{OC} + 1 - 2v_{OC}r_s \text{ and } b = \frac{a}{1 + a} \tag{20.67}$$

This set of expressions is valid for $v_{OC} > 15$ and $r_s < 0.4$. The typical accuracy is better than 1%. Their application to a photovoltaic generator is immediate, if all their cells are supposed to be identical, and if the voltage drops in the conductors connecting the modules are negligible.

Now, for the prediction of the $I-V$ curve of a PV generator operating on arbitrary conditions of irradiance and temperature, a good balance between simplicity and exactness is obtained through the following additional assumptions.

Petitioner Canadian Solar (USA) Inc., Ex. 1035, p. 2335

Downloaded from https://onlinelibrary.wiley.com/doi/ by <Shibboleth-member@purdue.edu, Wiley Online Library on [25/08/2024]. See the Terms and Conditions (https://onlinelibrary.wiley.com/terms-and-conditions) on Wiley Online Library for rules of use; OA articles are governed by the applicable Creative Commons License

Downloaded from https://onlinelibrary.wiley.com/doi/ by <Shibboleth-member@purdue.edu, Wiley Online Library on [25/08/2024]. See the Terms and Conditions (https://onlinelibrary.wiley.com/terms-and-conditions) on Wiley Online Library for rules of use; OA articles are governed by the applicable Creative Commons License

- The short-circuit current of a solar cell depends exclusively and linearly on the irradiance. That is,

$$I_{SC}(G) = \frac{I^*_{SC}}{G^*} G_{eff} \tag{20.68}$$

where G_{eff} is the "effective" irradiance. This concept must take into consideration the optical effects related to solar angle of incidence, as described in Section 20.7. Effects, as described by equations (20.46–20.59), are as follows:

- The open-circuit voltage of a module depends exclusively on the temperature of the solar cells T_c. The voltage decreases linearly with increasing temperature. Hence,

$$V_{OC}(T_c) = V^*_{OC} + (T_c - T^*_c)\frac{dV_{OC}}{dT_c} \tag{20.69}$$

where the voltage temperature coefficient, dV_{OC}/dT_c is negative. The measurement of this parameter used to be included in PV modules characterisation standards [51, 56] and the corresponding value must, in principle, be also included on the manufacturer's data sheets. For crystalline silicon cells, dV_{OC}/dT_c is typically -2.3 mV per °C and per cell.

- The series resistance is a property of the solar cells, unaffected by the operating conditions.
- The operating temperature of the solar cell above ambient is roughly proportional to the incident irradiance. That is,

$$T_c = T_a + C_t G_{eff} \tag{20.70}$$

where the constant C_t has the value:

$$C_t = \frac{NOCT\,(^\circ\mathrm{C}) - 20}{800\ \mathrm{W/m^2}} \tag{20.71}$$

The values of *NOCT* for modules currently on the market varies from about 42 to 46°C, implying a value of C_t between 0.027 and 0.032°C/(W/m^2). When *NOCT* is unknown, it is reasonable to approximate $C_t = 0.030$°C/(W/m^2). This *NOCT* value corresponds to mounting schemes allowing the free air convection in both sides of the PV modules, which cannot be the case on roof-mounting arrays, that restrict some of the airflow. Then, it has been shown [57] that the *NOCT* increases by about 17°C if some kind of back ventilation is still allowed and up to 35°C if the modules are mounted directly on a highly insulated roof.

Example: To illustrate the use and the usefulness of the equations of the above sections, we shall analyse the electrical behaviour of a PV generator rated at 1780 W (STC), made up of 40 modules, arranged 10 in series × 4 in parallel. The conditions of operation are $G_{eff} = 700$ Wm^{-2} and $T_a = 34$°C. It is known that the modules have the following characteristics under STC: $I^*_{SC} = 3$ A, $V^*_{OC} = 19.8$ V and $P^*_M = 44.5$ W. Further, it is known that each module consists of 33 cells connected in series and that $NOCT = 43$°C.

The calculations consist of the following steps:

1. Determination of the characteristic parameters of the cells that make up the generator under STC (equations 20.63–20.67):

33 cells in series ⇒ Per cell: $I_{SC}^* = 3$ A, $V_{OC}^* = 0.6$ V and $P_M^* = 1.35$ W
Assuming m = 1; $V_t(V) = 0.025 \times (273 + 25)/300 = 0.0248\ V \Rightarrow v_{OC} = 0.6/0.0248 = 24.19 > 15$
Then, $FF_0 = (24.19 - \ln(24.91))/25.19 = 0.833$; $FF = 1.35/(0.6 \times 3) = 0.75$
And $r_s = 1 - 0.75/0.833 = 0.0996 < 0.4 \Rightarrow R_S = 0.0996 \times 0.6/3 = 19.93$ mΩ

$$a = 20.371; b = 0.953 \Rightarrow V_M/V_{OC} = 0.787 \text{ and } I_M/I_{SC} = 0.943$$

It is worth noting that these values lead to a value of $FF = 0.742$, slightly different from the starting value. This error shows the precision available by the method, better than 1% in this instance. Sometimes values of $m = 1.2$ or 1.3 give a better approximation.

2. Determination of the temperature of the cells under the considered operating conditions (equations 20.70 and 20.71):

$$C_t = 23/800 = 0.0287°\text{C m}^2/\text{W} \Rightarrow T_c = 34 + 0.0287 \times 700 = 54.12°\text{C}$$

3. Determination of the characteristic parameters of the cells under the operating conditions being considered (equations 20.68 and 20.69):

$$I_{SC}(700\ \text{W/m}^2) = 3 \times (700/1000) = 2.1\ \text{A}$$
$$V_{OC}(54.12°\text{C}) = 0.6 - 0.0023 \times (54.12 - 25) = 0.533\ \text{V}$$

With R_S considered constant, these values lead to:

$$V_t = 27.26\ \text{mV}; v_{OC} = 19.55; r_s = 0.0785; FF_0 = 0.805; FF = 0.742; P_M = 0.83\ \text{W}$$

4. Determination of the characteristic curve of the generator, (I_G, V_G):
Number of cells in series 330; Number of cells in parallel: 4. Then:
$I_{SCG} = 4 \times 2.1\ \text{A} = 8.4\ \text{A}$; $V_{OCG} = 330 \times 0.533\ \text{V} = 175.89\ \text{V}$; $R_{SG} = 1.644\ \Omega$; $P_{MG}^* = 1095.6$ W

$$I_G(A) = 8.4\left[1 - \exp\frac{V_G(V) - 175.89 + 1.644 \cdot I_G(A)}{9.00}\right]$$

To calculate the value of the current corresponding to a given voltage, we may solve this equation iteratively, substituting I_G for $0.9\ I_{SCG}$ on the first step. Only one iteration is required for $V_G \leq 0.8\ V_{OCG}$. By way of example, the reader is encouraged to do it for $V_G = 140$ V and $V_G = 150$ V. The solution is $I_G(140\ \text{V}) = 7.77$ A and $I_G(150\ \text{V}) = 6.77$ A.

5. Determination of the maximum power point:

$$a = 17.48; b = 0.9458; V_M/V_{OC} = 0.7883; I_M/I_{SC} = 0.9332$$
$$V_M = 138.65\ \text{V}; I_M = 7.84\ \text{A}, P_M = 1087\ \text{W}.$$

Note that the ratio $P_M/P_M^* = 0.661$, while the ratio $G_{eff}/G^* = 0.7$. This indicates a decrease in efficiency at the new conditions compared to STC, primarily due to the greater solar cell temperature, $T_c < T_c^*$. An efficiency temperature coefficient can now be

Petitioner Canadian Solar (USA) Inc., Ex. 1035, p. 2337

Downloaded from https://onlinelibrary.wiley.com/doi/ by <Shibboleth-member@purdue.edu, Wiley Online Library on [25/08/2024]. See the Terms and Conditions (https://onlinelibrary.wiley.com/terms-and-conditions) on Wiley Online Library for rules of use; OA articles are governed by the applicable Creative Commons License

obtained by

$$\frac{1}{\eta^*}\cdot\frac{\mathrm{d}\eta}{\mathrm{d}T_\mathrm{c}}=\left(\frac{P_\mathrm{M}}{P_\mathrm{M}^*}\cdot\frac{G^*}{G_\mathrm{eff}}-1\right)\cdot\left(\frac{1}{T_\mathrm{c}-T_\mathrm{c}^*}\right)=-0.004/^\circ\mathrm{C}$$

This means the efficiency decrease is about 0.4% per degree of temperature increase, which can be considered as representative for c-Si.

It should be noted that, depending on the input data availability, other PV- generator modelling possibilities exist. For example, commonly I_M^* and V_M^* are given in the specifications in addition to their product P_M^*. Then, the series resistance can directly be estimated from equation (20.62). This leads to

$$R_\mathrm{S}^*=\frac{V_\mathrm{OC}^*-V_\mathrm{M}^*+V_\mathrm{t}\ln\left(1-\dfrac{I_\mathrm{M}^*}{I_\mathrm{SC}^*}\right)}{I_\mathrm{M}^*} \tag{20.72}$$

20.10.2 Second-order Effects

The model presented in the previous section is based only on standard and widely available information, which is an undeniable advantage, in particular for PV-system design. Furthermore, it is simple to use. However, it can be argued that such simplicity is at the price of neglecting the following:

- The effects of the parallel resistance
- The influence of the cell temperature in the short-circuit current.
- The influence of the irradiance in the open-circuit voltage.
- The non-linearity due to low irradiance.
- The spectral effects.
- The effects of wind.

It should be recognised that differences between expected and real energies delivered by PV modules are often mentioned in the literature [58]. Hence, it is worth reviewing the importance of each one of these previously neglected factors, with the aim of clarifying possible error sources. Many of these factors are discussed further in Chapter 16.

The influence of the parallel resistance is, to a great extent, compensated here, by the particular way of estimating the series resistance of a PV module, which assures that the maximum power of the modelled curve coincides exactly with that corresponding to the real one. Because of this, the accuracy of the model tends to be very good just around the maximum-power operation point, that is, just on the voltage region of interest.

The short-circuit current tends to increase slightly with increasing temperature. This can be attributed, in part, to increased light absorption, since semiconductor band gaps generally decrease with temperature, and, in part, to increased diffusion lengths of the

Downloaded from https://onlinelibrary.wiley.com/doi/ by <Shibboleth>-member@purdue.edu, Wiley Online Library on [25/08/2024]. See the Terms and Conditions (https://onlinelibrary.wiley.com/terms-and-conditions) on Wiley Online Library for rules of use; OA articles are governed by the applicable Creative Commons License

minority carriers. This can be considered by adding a linear term to equation (20.68). Thus

$$I_{SC}(G, T_c) = I^*_{SC} \cdot \frac{G}{G^*} \cdot \left[1 + (T_c - T^*_c)\frac{dI_{SC}}{dT_c}\right] \tag{20.73}$$

where the temperature coefficient dI_{SC}/dT_c depends on the semiconductor type and on the manufacturing process, but it is always quite small. Typical experimental values are below 3.10^{-4} (A/A)/°C [51, 59]. For a solar cell operating at 70°C, that represents only 0.13% of I_{SC} increase. Hence, ignoring this dependence has no practical effects, in all the cases.

The open-circuit voltage tends to increase with the illumination level. The ideal diode equation (see equation (20.60)) shows there is a logarithmic dependence. Then, this effect can be considered by adding a logarithmic term to equation (20.69). Thus

$$V_{OC}(T_c, G) = V^*_{OC} + (T_c - T^*_c)\frac{dV_{OC}}{dT_c} + V_t \cdot \ln\left(\frac{G_{eff}}{G^*}\right) \tag{20.74}$$

Note that the relative influence of this new term increases with decreasing irradiance. For example, for $G_{eff} = 500$ W/m^2 and $G_{eff} = 200$ W/m^2, it represents about 3 and 7%, respectively. Hence, its importance when predicting the energy delivered by PV modules depends on the irradiance distribution of the irradiation content. Obviously, it is more important for northern than for southern countries. For example, in Freiburg-Germany ($\phi = 48°$) about 50% of yearly irradiation is collected below 600 W/m^2 and 18% below 200 W/m^2. Meanwhile in Jaen-Spain ($\phi = 37.8°$) about 30% of yearly irradiation is collected below 600 W/m^2 and only 6% below 200 W/m^2. Moreover, it should be understood that very low irradiances are sometimes rejected by PV-system requirements. For example, in grid-connected systems, DC power from PV modules must be large enough to compensate for the inverter losses. Otherwise, the PV system becomes a net energy consumer.

While this logarithmic term does account for some variation in open-circuit voltage as irradiance changes, it does not adequately predict the rapid decrease observed at values of irradiance less than about 200 W/m2, which causes a noticeable efficiency decrease below this value. The use of a second logarithmic term has been proposed [60] to also consider this low irradiance effect. Thus

$$V_{OC}(T_c, G) = \left[V^*_{OC} + \frac{dV_{OC}}{dT_c}(T_c - T^*_c)\right]\left[1 + \rho_{OC} \ln\left(\frac{G_{eff}}{G_{OC}}\right) \ln\left(\frac{G_{eff}}{G^*}\right)\right] \tag{20.75}$$

where ρ_{OC} and G_{OC} are empirically adjusted parameters. Values of $\rho_{OC} = -0.04$ and $G_{OC} = G^*$ have proven adequate for many silicon PV modules.

The sun spectrum shifts over time, due to changes in atmosphere composition, and changes in the distance the light has to travel through the atmosphere. This can affect the response of PV devices, especially if they have a narrow spectral response. Martin and Ruiz have proposed [61] a model based on the parameterisation of the atmosphere by means of the clearness index and the air mass, and this considers independently the spectrum of each radiation component: direct, diffuse and albedo. It can be described by

Downloaded from https://onlinelibrary.wiley.com/doi/ by <Shibboleth-member@purdue.edu, Wiley Online Library on [25/08/2024]. See the Terms and Conditions (https://onlinelibrary.wiley.com/terms-and-conditions) on Wiley Online Library for rules of use; OA articles are governed by the applicable Creative Commons License

Downloaded from https://onlinelibrary.wiley.com/doi/ by <Shibboleth-member@purdue.edu>, Wiley Online Library on [25/08/2024]. See the Terms and Conditions (https://onlinelibrary.wiley.com/terms-and-conditions) on Wiley Online Library for rules of use; OA articles are governed by the applicable Creative Commons License

modifying the equation (20.68). Thus

$$I_{SC} = \frac{I^*_{SC}}{G^*}(B_{eff} \cdot f_B + D_{eff} \cdot f_D + R_{eff} \cdot f_R) \tag{20.76}$$

where f_B, f_D and f_R obeys to the general form

$$f = c \cdot \exp[a(K_T - 0.74) + b(AM - 1.5)] \tag{20.77}$$

and a, b and c are empirically adjusted factors, for each module type and for each radiation component. Note that 0.74 and 1.5 are just the values of the atmospheric parameters corresponding to the STC. Table 20.7 shows the recommended values of these parameters for crystalline, c-Si, and amorphous a-Si modules. The usefulness of this table can be extended to other PV materials, by linear interpolation on the energy band gap, E_g, between E_g(c-Si) = 1.12 eV and E_g(a-Si) = 1.7 eV. For example, E_g(a-SiGe) = 1.4 eV $\Rightarrow$ estimated value of c is equal to 0.8.

Spectral effects used to be small on a yearly basis. Spectral losses with respect to STC are typically below 2% with semiconductors with broad spectral sensitivity, and below 4% for the others. However, on an hourly basis, spectral effects up to 8% can be encountered.

The PV module cell temperature is a function of the physical variables of the PV cell material, the module and its configuration, the surrounding environment and the weather conditions. It results from the balance of energy inputs and outputs through radiation, convection, conduction and power generation. Today, the more widely extended model, based on the *NOCT* concept and described by equations (20.70 and 20.71), lump the contributions together in an overall heat-loss coefficient, resulting in a liner relationship between module temperature and irradiance under steady-state conditions. This implies accepting that the heat transfer process between the solar cell and the ambience is essentially dominated by the conduction through the encapsulating materials, and neglecting the wind effects on convection. This model is simple to use and requires only standard available input information, which are undeniable advantages for the PV designer. But it can lead to significant errors in cell temperature estimation for non-steady-state conditions [62] (observed thermal time constant of PV modules is about 7 minutes), and for high wind speeds. That has stimulated several authors to develop new thermal models for PV systems, based not only on irradiance but also on wind speed. For example, Sandia

Table 20.7 Coefficient for spectral response modelling, for c-Si and a-Si modules

	B		D		R	
	c-Si	a-Si	c-Si	a-Si	c-Si	a-Si
c	1.029	1.024	0.764	0.840	0.970	0.989
a	−3.13E-01	−2.22E-01	−8.82E-01	−7.28E-01	−2.44E-01	−2.19E-01
b	5.24E-03	9.20E-03	−2.04E-02	−1.83E-02	1.29E-02	1.79E-02

Table 20.8 Temperature coefficients for module and cell temperature estimation, for two typical module designs

Type	T_1 [°C]	T_2 [°C]	b	ΔT [°C]
Glass/cell/glass	25.0	8.2	−0.112	2
Glass/cell/tedlar	19.6	11.6	−0.223	3

Laboratories proposed [63] a two components thermal model given by

$$T_c = T_m + \frac{G_{eff}}{G^*}\Delta T, \text{ where } T_m = T_a + \frac{G_{eff}}{G^*}[T_1 \exp(b \cdot \omega_S) + T_2] \tag{20.78}$$

In this equation, T_m is the back-surface module temperature, in °C; ω_S is the wind speed measured at standard 10 m height, in m.s^{-1}; T_1 is an empirical coefficient determining the upper temperature limit at low wind speeds; T_2 is an empirical coefficient determining the lower temperature limit at high wind speeds; b is an empirical coefficient determining the rate at which the module temperature drops as wind speed increases and ΔT is also an empirical coefficient related to the temperature gap along the back encapsulation material. Table 20.8 gives the parameters found to have good agreement with measured temperatures, for two different module types.

However, the real usefulness of all these second-order corrections (equations 20.74–20.77) for temperature and wind speed is far from clear, because wind speed is difficult to predict, and also because cell temperature errors becomes more tolerable when translated into PV module power generation. For example, for a solar cell operating around 50°C, an error of 20% on the estimation of its cell temperature (≈10°C) reflects in an error of only 0.4% (≈10°C × 2.3(mV/°C)/600 mV) in the estimation of the corresponding power.

20.11 RELIABILITY AND SIZING OF STAND-ALONE PV SYSTEMS

The merit of a stand-alone PV system depends on how reliably it supplies electricity to the load. It is customary to quantify this reliability in terms of the Loss of Load Probability (*LLP*), defined as the ratio between the energy deficit and the energy demand, both referring to the load, over the total operation time of the installation. Thus,

$$LLP = \frac{\int_t \text{energy deficit}}{\int_t \text{energy demand}} \tag{20.79}$$

It should be noted that, because of the random nature of solar radiation, the value of *LLP* is always greater than zero, even if the PV system never actually breaks down. The available literature shows a large consensus over the expression of reliability in terms

Petitioner Canadian Solar (USA) Inc., Ex. 1035, p. 2341

Downloaded from https://onlinelibrary.wiley.com/doi/ by <Shibboleth-member@purdue.edu, Wiley Online Library on [25/08/2024]. See the Terms and Conditions (https://onlinelibrary.wiley.com/terms-and-conditions) on Wiley Online Library for rules of use; OA articles are governed by the applicable Creative Commons License

Downloaded from https://onlinelibrary.wiley.com/doi/ by <Shibboleth-member@purdue.edu, Wiley Online Library on [25/08/2024]. See the Terms and Conditions (https://onlinelibrary.wiley.com/terms-and-conditions) on Wiley Online Library for rules of use; OA articles are governed by the applicable Creative Commons License

of energy shortage probability, but different names can be found for the *LLP*: Deficit of Energy [64], Loss of Power Probability [65] and Loss of Power Supply Probability [66]. Moreover, the Load Coverage Rate [67] or Solar Fraction [68], *SF*, defined as the fraction of energy load covered by the PV system is also used to quantify reliability. Clearly, $SF = 1 - LLP$.

The "size" of a PV system means the size of both the generator (PV modules) and the accumulator (batteries or other storage device). It is useful to relate these sizes to the size of the load, in terms of average daily energies. Thus, the generator capacity, C_A, is defined as the ratio of the average daily energy output of the generator divided by the average daily energy consumption of the load. The accumulator capacity, C_S, is defined as the maximum energy that can be extracted from the accumulator divided by the average daily energy consumption of the load. Thus,

$$C_A = \frac{\eta_G \cdot A_G \cdot \overline{G_d}}{L} \text{ and } C_S = \frac{C_u}{L} \tag{20.80}$$

where A_G and η_G are the area and conversion efficiency of the photovoltaic generator, respectively, $\overline{G_d}$ is the mean value of the daily irradiation on the surface of the generator, L is the mean value of the daily energy consumed by the load and C_u is the useful energy storage capacity of the accumulator. More strictly, η_G should be the path efficiency from the array to the load, and C_u is the product of the nominal capacity (which refers to the whole energy that can be extracted from the accumulator if no particular limitations were imposed) and the maximum allowable depth of discharge. We will deal with the practical meaning of such parameters later. Meanwhile, it is worth pointing out that C_A depends on the local solar climate conditions. Therefore, the same photovoltaic generator, connected to the same load, may seem big in one place and small in another where there is less radiation.

Figure 20.22 shows how the energy generation varies over an assumed period of j days, for a given location and load, and for two different sizes of the generator ($C_{A1} < C_{A2}$). The shaded areas underneath the line $y = 1$, illustrate the temporal deficits of energy generation that need to be compensated by extraction of energy from the accumulator. It can be observed that the larger the generator, the lower the deficit and, hence, the smaller the required accumulator. Two ideas are now intuitively apparent: the first is that it is possible to find different combinations of C_A and C_S that lead to the same value of *LLP*; the second is that the larger the photovoltaic system, the better the reliability, that is, the lower the value of *LLP*, but also the greater the cost.

A certain degree of reliability is (or should be) a requirement depending on the typology of the load. For example, reliability requirements of telecommunication equipment are usually higher than that required by domestic appliances (higher reliability means lower *LLP* values). The problem confronting the PV engineer then takes the following "theoretical" form: Which combination of C_A and C_S achieves the desired *LLP* with minimum cost? Since cost estimation is a classic economic problem discussed widely in the literature, the PV-sizing problem is mainly rooted in the relationship between C_A, C_S and *LLP*. Later, C_A and C_S must be translated into the number and power of PV modules and battery capacity.

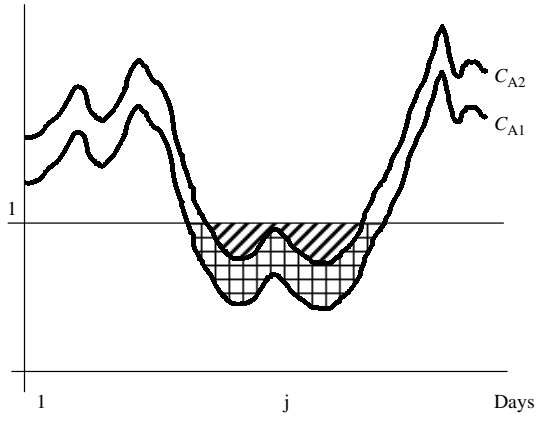


Figure 20.22 Time variation of the generated daily energy, relative to load, for two PV generators for which $C_{A1} < C_{A2}$. The shadowed areas represent the corresponding energy deficits to be covered by the storage device

In essence, any PV- sizing method involves four different steps:

- obtaining solar radiation site information,
- preparation of global horizontal daily irradiation sequences,
- transposition from horizontal to inclined radiation values,
- simulation of PVsystem behaviour, in order to quantify *LLP* corresponding to pairs of C_A and C_S values.

The first three steps have already been discussed in previous sections of this chapter. We will now deal with the last step, with the following assumptions: first, the daily energy consumption is constant all through the year; second, all the daily consumption occurs at night (i.e. after the energy generation time ends); and, third, the components of the PV system are ideal and can be linearly modelled. This is adequate for analysing the "pure" sizing problem, that is, the relation between C_A, C_S and *LLP*. Non-linearities and non-ideal effects (for example, battery efficiency) are better taken into account by the use of proper correction factors when translating C_A and C_S values into nominal PV array power and battery capacity. It is interesting to note that short-term (hourly) variations of demanded energy have no effect on *LLP* [64, 69], provided that $C_S > 2$, which is usually the case. The above- described assumption leads to particularly simple calculations. The state of charge, *SOC*, of the accumulator at sunset of day j is given by

$$SOC_j = \min\left\{SOC_{j-1} + \frac{C_A \cdot G_{dj}}{C_S \cdot \overline{G_d}} - \frac{1}{C_S}; 1\right\} \tag{20.81}$$

where G_{dj} is the total irradiation for day j, and

$$LLP = \frac{\sum_{1}^{N} E_{LACK}\, j}{N \cdot L} \tag{20.82}$$

Downloaded from https://onlinelibrary.wiley.com/doi/ by <Shibboleth-member@purdue.edu, Wiley Online Library on [25/08/2024]. See the Terms and Conditions (https://onlinelibrary.wiley.com/terms-and-conditions) on Wiley Online Library for rules of use; OA articles are governed by the applicable Creative Commons License

where N is the number of days for which the simulation is carried out, and E_{LACK} is the daily energy deficit, given by

$$E_{\mathrm{LACK}}j = \max\left\{\frac{1}{C_{\mathrm{S}}} - SOC_j; 0\right\} \tag{20.83}$$

This equation implies that an energy deficit occurs only when the stored energy at the end of the day $SOC_j \cdot C_{\mathrm{S}} \cdot L$ does not suffice to cover the daily load L. Note that $SOC_j \cdot C_{\mathrm{S}} \cdot L < L \Rightarrow (1/C_{\mathrm{S}} - SOC_j) > 0$.

Because information on the daily irradiation used to be expressed in terms of mean monthly values, a different value of C_{A} may be worked out for each month. In what follows, we shall use for C_{A} just the value corresponding to the worst month. Thus,

$$\overline{G_{\mathrm{d}}} = \min\{G_{\mathrm{dm}}(\beta, \alpha)\}; (\mathrm{m} = 1, \ldots, 12) \tag{20.84}$$

Computed results can be arranged and presented graphically. Figure 20.23 presents some examples of the so-called "reliability maps".

The shape of such curves prompts the thought that it should be possible to describe them in an analytical form. Several attempts at proposing analytical methods based on this idea have been made [64, 70–76] allowing sizing of PV systems by means of straightforward, simple calculations. For example, at the IES-UPM we have concluded [76] that all these curves conform to the relationship

$$C_{\mathrm{A}} = f \cdot C_{\mathrm{S}}^{-u} \tag{20.85}$$

where f and u are two parameters that depend on the value of *LLP* and on the location. These parameters do not have particular physical meaning, and their determination previously requires a lot of simulations to be carried out. However, they allow a large number of simulated results to be condensed into just a few sizing parameters. Advanced simulation software tools have also been developed and are being marketed today [42, 43].

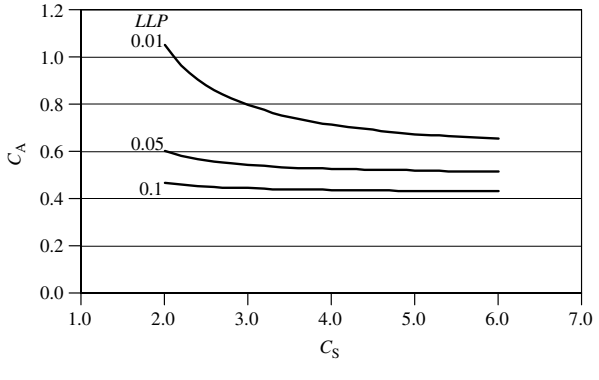


Figure 20.23 Reliability maps: Generator capacity C_{A} versus storage capacity C_{S} with the reliability *LLP* as parameter

Downloaded from https://onlinelibrary.wiley.com/doi/ by <Shibboleth-member@purdue.edu>, Wiley Online Library on [25/08/2024]. See the Terms and Conditions (https://onlinelibrary.wiley.com/terms-and-conditions) on Wiley Online Library for rules of use; OA articles are governed by the applicable Creative Commons License

It must be stressed that, whatever the detailed methodology, PV-system sizing relies on future prediction (the expected system lifetime) based on past observations of the solar radiation. Basic statistical laws imply that such prediction exercises are unavoidably associated with a degree of uncertainty, as mentioned before. This implies a basic limit of accuracy for PV sizing. We will try to clarify this aspect with an example.

We will suppose that 20 years of daily irradiation data measured in a certain location with a great level of accuracy are available. We will call them the "historical sequence". This allows us first, to establish the statistical characteristics of the radiation (mean value, standard deviation, etc.); and, second, to make detailed simulations of a PV system's behaviour over these particular years. Thus, we can map with high precision the reliability associated with different system sizes, for this particular historical sequence. As a simulation exercise, the accuracy of the result is limited only by the precision of the initial measurements, which have been assumed to be very good. However, when using such a sequence for sizing a future system, another limitation arises simply because the solar radiation in the future will not exactly repeat the same pattern as in the past. In fact, it is extremely unlikely in terms of daily sequences. All that can be expected is that the future solar radiation sequence will keep some statistical properties whose validity is known to be general, which opens the door for the generation of a vast collection of hypothetical solar radiation sequences with the same occurrence probability as the historical one. Then, a different reliability map can be associated with each of these radiation sequences, by means of the above-mentioned simulation exercise. Obviously, the similarity between the different maps can be understood as a measure of the uncertainty associated with the prediction. Figure 20.24 shows the result of superimposing such maps. The example is for Madrid, generating different solar radiation sequences following the above-mentioned Aguiar's method [37]. It is clear that precautions must be taken with predictions for $LLP < 10^{-2}$. For example, for $LLP = 10^{-3}$ and $C_S = 3$, we can find C_A values from 1.1 to 1.5. Other authors [70, 77] have presented similar results. We must conclude that the validity of PV-sizing methodologies is generally restricted to the range $1 > LLP > 10^{-2}$, that is, to solar coverage below 99%. Beyond this limit, sizing results are statistically of doubtful quality, although unfortunately, they are often found in the literature and in simulation software tools marketed today.

It must be stressed that this basic uncertainty cannot be overcome either by reducing the simulation time-step (hourly instead of daily values) or by incorporating more complex models of the elements of the PV systems (non-linear $I-V$ models of PV generators, battery efficiency dependence with SOC etc.). In fact, the reduction of the considered simulation period can only worsen the situation. It can be shown that the validity of sizing results based only on the TMY (avoiding the generation of large-radiation sequences) is restricted to the range $1 > LLP > 10^{-1}$, independent of any other consideration [78]. Appropriately, Marion and Urban [18], when presenting USA TMY s, advises "... *Because they represent typical rather than extreme conditions, they are not suited for designing systems to meet the worst-case conditions occurring at a location*".

On the other hand, such basic uncertainty can help to explain why the result of the different PV-sizing methods can be inconsistent; and also why the accuracy gains associated with the consideration of second-order effects when modelling the PV system are likely to be insignificant. In other words, such modelling can be useful for studying some PV-system features (optimal number of solar cell per module, optimal charge regulation

Downloaded from https://onlinelibrary.wiley.com/doi/ by <Shibboleth-member@purdue.edu, Wiley Online Library on [25/08/2024]. See the Terms and Conditions (https://onlinelibrary.wiley.com/terms-and-conditions) on Wiley Online Library for rules of use; OA articles are governed by the applicable Creative Commons License

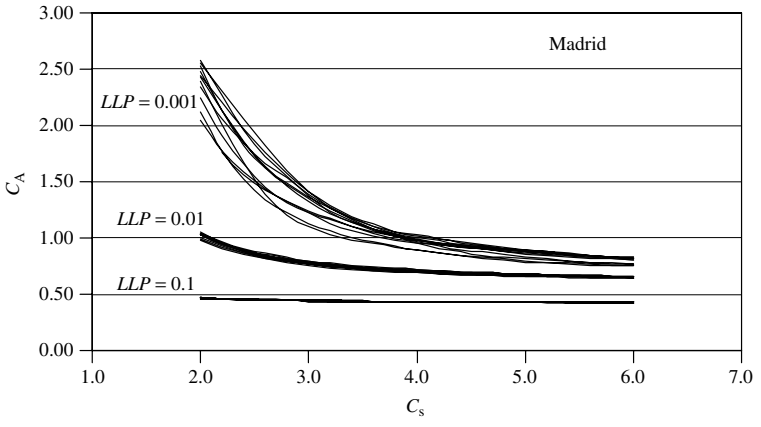


Figure 20.24 Simulated reliability maps, C_A versus C_S, with the historical and with 12 generated solar radiation sequences for three different reliability *LLP* values

algorithms etc.); but it is of little value when considering the pure size problem, for which a judicious and rather simple hypothesis suffices. A similar conclusion is presented in Kaiser and Sauer [79], from a comparison of the long-term energy yield of stand-alone PV systems simulated with both simple and detailed models. The authors observe that the range of uncertainty due to possible fluctuations of the radiation-time series is significantly larger than the those corresponding to changes in the PV-system component modelling, and conclude "*The results make it clear that exact simulation models can provide exact numbers, but do not automatically allow exact predictions*".

This can also help explain why PV-system sizing simply based on guesswork remains widely practiced in current engineering practices. This prevents any quantitative relationships between C_A, C_S and *LLP* being established. The size of the generator is instead chosen to ensure that the energy produced during the design period (most often, the worst month) exceeds the demand of the load by a margin that depends on the designer's experience. A similar procedure is used to size the accumulator. In summary,

$$C_A = F_{S1} \text{ and } C_S = F_{S2} \tag{20.86}$$

where F_{S1} and F_{S2} are arbitrary factors. For example, $C_A = 1.1$ and $3 \leq C_S \leq 5$ are common values for rural electrification purposes [80]. $1.2 \leq C_A \leq 1.3$ and $5 \leq C_S \leq 8$ are common ranges on the so-called professional market [71]: telecommunication and so on.

It is worth pointing out that this rather unscientific way of proceeding does not necessarily give bad results, in terms of reliability and cost. As a matter of fact, a proper combination of expertise and common sense often leads to very good results. Today, PV systems have the reputation of being reliable, even in those sectors where high reliability is an established requirement, such as telecommunications and cathodic protection. This helps explain why reliability quantification is generally considered irrelevant in real

Downloaded from https://onlinelibrary.wiley.com/doi/ by <Shibboleth-member@purdue.edu, Wiley Online Library on [25/08/2024]. See the Terms and Conditions (https://onlinelibrary.wiley.com/terms-and-conditions) on Wiley Online Library for rules of use; OA articles are governed by the applicable Creative Commons License

engineering practice, and mainly good for academic discussion; and why the actual use of PV-sizing methodologies is mainly aimed at giving a pseudo-scientific appearance to commercial activities. Our own experiences at IES-UPM contain several cases of perplexed PV clients requesting our opinion on the big PV-system sizing differences among different PV contractor estimates that they have received for a given location and application. Obviously, simplistic relations like equation (20.86) do not help the PV professional to adopt rigorous sizing procedures. However, we still believe such rigorous procedures should play an important role in future. This is because a professional's credibility benefits from reliability quantification (the use of the Mean Time Between Failures concept in the conventional electricity sector is a good example of this); and also because the usefulness of such methods extends beyond pure sizing problems. Additional comments are given in the following section.

It must be mentioned that in the common case of PV arrays directly coupled to batteries, that is without maximum power-tracking devices, energy balance analysis can be done by means of simple ampere balances, initially supposing that the working voltage is always the nominal one, V_{NOM}, at which it equals the maximum power point voltage of the generator. Therefore,

$$L = V_{\mathrm{NOM}} \cdot Q_{\mathrm{L}} \text{ and } \eta_{\mathrm{G}} \cdot A_{\mathrm{G}} = \frac{V_{\mathrm{NOM}} \cdot I_{\mathrm{M}}^{*}}{G^{*}} \tag{20.87}$$

which leads to

$$C_{\mathrm{A}} = \frac{I_{\mathrm{M}}^{*} \cdot G_{\mathrm{dm}}(\beta, \alpha)}{Q_{\mathrm{L}} \cdot G^{*}} \text{ and } C_{\mathrm{S}} = \frac{Q_{\mathrm{B}}}{Q_{\mathrm{L}}} \tag{20.88}$$

where Q_{L} is the amount of charge (expressed in ampere-hours) drawn daily by the load, that characterises the required PV array, and Q_{B} is the useful ampere-hour capacity of the battery, which is equal to the product of the nominal capacity by the maximum depth of discharge. This approximation, in spite of appearing oversimplified, gives very good results and simplifies the task of deducing the number of PV modules to be installed.

20.12 THE CASE OF SOLAR HOME SYSTEMS

Global market indicators [81, 82] lead to the estimate that about 1.3 million home systems for lighting, radio and television are currently in operation, totalling 40 MWp, and large rural electrification programmes comprising some thousands of SHSs are increasingly becoming a part of the rural market. Thus, SHS represent the most widespread PV application nowadays, and the trend is likely to continue.

Standardisation of equipment and its mass production represent efficient ways to obtain low prices and high technical quality. In consequence, SHS designers have to fix a single "standard" value of energy consumption for a large number of different families. It must be noted that such standardisation is a requirement imposed by the technology itself in order to reduce cost and guarantee quality, but it does not correspond well with the idea of needs at the individual level. PV history shows some interesting cases [83, 84]. For example, in Reference [83] it is stated that "... *an interesting aspect,*

Petitioner Canadian Solar (USA) Inc., Ex. 1035, p. 2347

Downloaded from https://onlinelibrary.wiley.com/doi/ by <Shibboleth-member@purdue.edu, Wiley Online Library on [25/08/2024]. See the Terms and Conditions (https://onlinelibrary.wiley.com/terms-and-conditions) on Wiley Online Library for rules of use; OA articles are governed by the applicable Creative Commons License

clearly confirmed by the operating results of ENEL plants, is that the intake power by this type of user . . . is rarely the same on any given day, and it is linked to the particular lifestyle of the people involved, to periods of absence and to the number of occupants of the houses being supplied, and so on". Apart from PV, other types of rural electrification also provide examples. Figure 20.25 shows the distribution of the individual monthly electricity consumption measured along four years in the 63 dwellings of Iferd, a Moroccan village where a small diesel generator set provides 3 h of electricity per day (consumers are metered and pay for their energy use). The large observed spread leads one to question the real meaning of reliability parameters such as *LLP*, and the real usefulness of rigorous PV-sizing methodologies.

It appears that "standard" *LLP* values derived from sizing methodologies are scarcely representative of the realities in the field. The relationship between reliability and load, that is, the function $LLP = LLP(L)$ for a given PV system, can be explored just by extending the previously described simulation procedure to a large number of cases. A certain baseline case has been, first, established by fixing the PV array power and the battery capacity values, C_A and C_S, for a given load, L_{BASE}, and a given reliability, $LLP = 0.1$. Then, the load has been varied from 0.8 L_{BASE} to 1.2 L_{BASE} and the corresponding reliability has been calculated. Figure 20.26 shows the result. Roughly speaking, we can say that an approximately logarithmic relationship exists in such a way that *LLP* decreases one order of magnitude for each 30% of load reduction. This result, together with the observation that real L values are generally found within the range -50% to $+100\%$ of the mean, let us conclude that real individual *LLP* values can vary more than three orders of magnitude (for example, from 10^{-1} to 10^{-4}) in the context of the same SHS project. This nullifies any attempt at finding a single representative

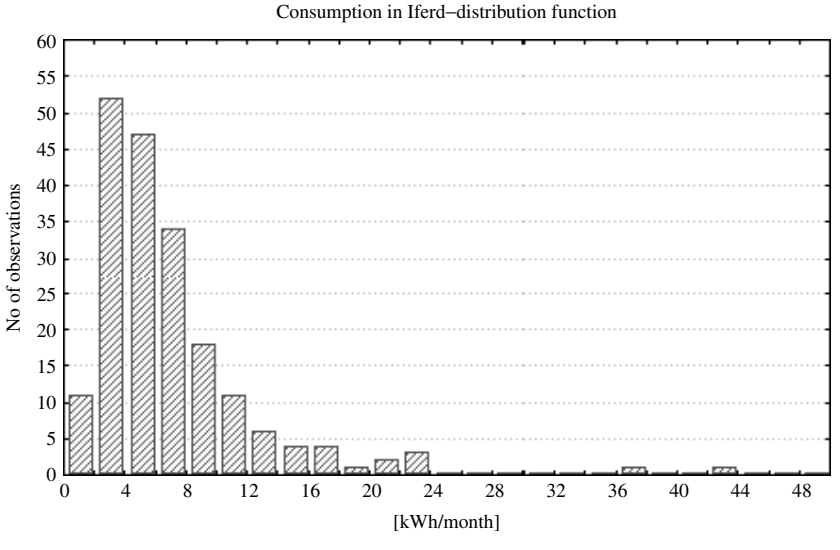


Figure 20.25 Distribution function of monthly electricity consumption in all the Iferd dwellings

Downloaded from https://onlinelibrary.wiley.com/doi/ by <Shibboleth-member@purdue.edu, Wiley Online Library on [25/08/2024]. See the Terms and Conditions (https://onlinelibrary.wiley.com/terms-and-conditions) on Wiley Online Library for rules of use; OA articles are governed by the applicable Creative Commons License

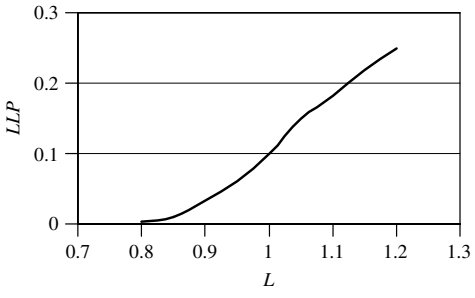


Figure 20.26 Reliability *LLP* as a dependent variable on the consumption *L* for a given PV array and capacity values

LLP value. It is worth mentioning that the same is not true when centralised electricity generators are considered (PV or not), because the total energy consumed by all the families involved shows a much lower standard deviation than that corresponding to the individual consumptions (roughly, the standard deviation becomes reduced by a factor of $1/\sqrt{N}$, N being the number of families), so that it is possible to find single L and *LLP* representative values for the whole served population.

However, even in extremely varying applications, such as SHS, PV-sizing methods based on reliability can be of great help if large-scale programmes become a future reality. This will probably require the development of rigorous engineering: standardisation of different levels of service, technical quality controls and so on. For example, PV-sizing methods based on *LLP* represent an interesting possibility of comparing different alternatives (different offers from various manufactures) on an objective basis, as the *LLP* value respectively associated to each alternative, for the same considered energy service [78].

It is worth considering the question: "How much electricity has to be provided to a rural house in a developing country to be socially and economically acceptable?" Although this question is always at the origin of any PV rural electrification programme, its answer in terms of watthour/day, is far from being clear. Energy consumption data, based on practical experience in developing countries, are scarce in the literature [84], which is paradoxical considering that many thousands of SHS are currently operating in developing countries. Instead, there are a great number of consumption scenarios where, although starting from very different hypothesis concerning the number of appliances and the length of time they are in use, the SHSs finally selected have an installed power of about 40 to 50 Wp. This is because past in-field experience has shown PV designers that such systems are generally well accepted by the rural users, while the same is not always the case when small (20–30 Wp) PV modules are concerned. This way, the SHS scenarios elaborated by PV designers must therefore be interpreted as explanation exercises, rather than as designs for systems starting from an evaluation of actual needs (see Chapter 23 for discussion of rural electrification programmes). So, we must conclude that energy scenarios for rural electrification purposes are still an open question, which need to be explored in-depth.

Downloaded from https://onlinelibrary.wiley.com/doi/ by <Shibboleth-member@purdue.edu, Wiley Online Library on [25/08/2024]. See the Terms and Conditions (https://onlinelibrary.wiley.com/terms-and-conditions) on Wiley Online Library for rules of use; OA articles are governed by the applicable Creative Commons License

Petitioner Canadian Solar (USA) Inc., Ex. 1035, p. 2349

20.13 ENERGY YIELD OF GRID-CONNECTED PV SYSTEMS

The output of grid-connected PV systems is the output from the PV array less the losses in the inverter. The output from the PV array has been considered in detail in this chapter, and the performance of inverters is described in Chapter 19. As far as inverters are concerned, it is important to account for the fact that the instantaneous efficiency, η_y, depends on the ratio between the actual power delivered to the grid P_{AC}, and the rated power of the inverter, P_{IMAX}. This dependence may be represented by [85]

$$\eta_i = \frac{p}{p + k_0 + k_{i1}p + k_{i2}p^2} \tag{20.89}$$

where $p = P_{AC}/P_{IMAX}$ and k_0, k_{i1} and k_{i2} are parameters characteristic of the inverter defining its electrical behaviour. k_0 is the quiescent power consumption, k_{i1} represents the losses that depend linearly on the current (voltage drop across diodes, etc.) and k_{i2} represents the losses that depend on the square of the current (resistive losses, etc.). These parameters can be obtained from the inverter efficiency curve. Depending on quality level, input voltage and rated power, the loss parameters of existing inverters have a spread of more than a factor of 10. Average values, in percentage, are $k_0 = 2$, $k_{i1} = 2.5$ and $k_{i2} = 8$, leading to 85% typical energy efficiency. Very good inverters reduce these values to $k_0 = 0.35$, $k_{i1} = 0.5$ and $k_{i2} = 1.$, leading to 95% typical energy efficiency.

To describe the effect of no-load shut-off, the standby self-consumption k_0' is used. It is the value to which the operating self-consumption (k_0) is reduced during shut-off ($k_0' < k_0$). Reduction of self-consumption improves the low- and medium-power efficiency, which is most important for PV applications. The loss fractions due to self-consumption sum up to considerable losses in PV systems. In comparison, the sum of the load dependent losses (due to k_1 and k_2) is 1.5 to 7 times smaller.

Standard methods for performance analysis of PV grid-connected plants have been introduced in the JRC Ispra Guidelines [86] and extended and improved by HTA Burgdorf [87]. Global performance is appropriately described by the so-called *performance ratio* (*PR*), which is the ratio of AC energy delivered to the grid, E_{AC}, to the energy production of an ideal, loss-less PV plant with 25°C cell temperature and the same solar irradiation. This gives a good indication of how much of the ideally available PV energy has actually been used. It is given by

$$PR = \frac{E_{AC}}{\dfrac{G_y(\beta, \alpha)}{G^*} \cdot P_M^*} \tag{20.90}$$

Other interesting parameters are the *Reference Yield*, $Y_r = G_y(\beta, \alpha)/G^*$, the *Array Yield*, $Y_a = E_{DC}/P_M^*$, where E_{DC} is the DC energy generated by the PV array, and the *Final Yield*, $Y_f = E_{AC}/P_M^*$. All the three have units of time, and allow us to distinguish between the losses due to the PV array, and the losses associated to the inverter and to the operation of the system. Capture losses, $L_C = Y_r - Y_a$, are defined as the energy losses, expressed in hours per day of PV array operation at STC power output, caused by: cell temperatures

Downloaded from https://onlinelibrary.wiley.com/doi/ by <Shibboleth-member@purdue.edu>, Wiley Online Library on [25/08/2024]. See the Terms and Conditions (https://onlinelibrary.wiley.com/terms-and-conditions) on Wiley Online Library for rules of use; OA articles are governed by the applicable Creative Commons License

Table 20.9 Power distribution of the yearly irradiation for a low and a high latitude location

Location	$G_y(\beta_{opt})$ [kWh/m^2]	Percent of irradiation in different ranges of irradiance in [W/m^2]				
		<200	200–500	500–800	>800	Total
Jaen	2040	5.8	23.6	44.7	25.9	100
Copenhagen	1190	13.9	30.7	35.7	19.7	100

higher than 25°C, losses in wiring and protection diodes, poor module performance at low irradiance, partial shading, snow and ice coverage, module mismatch, operation of the array at a voltage other than its maximum power point, and spectral and angular losses. *System losses*, $L_S = Y_a - Y_f$, are the losses due to inverter inefficiencies. It must be noted that $PR = Y_f/Y_r$.

Energy losses in good PV grid-connected systems are about $L_C = 15\%$ and $L_S = 7\%$, which lead to $PR \approx 0.78$. However, reported experimental values have ranged from 0.65 to 0.72. The main reason for such *PR* reduction is that the actual power of installed PV arrays is often below the rated power declared by the manufactures [88].

The power distributions of solar irradiation are different for varied geographical latitudes. In places of high latitude, with very cloudy weather, the solar irradiation is almost evenly distributed over a wide range of power scale; while in low latitude places, with predominantly clear sky, the higher power range is enhanced. Table 20.9 presents the distribution in different irradiance classes of the total yearly irradiation over an optimally tilted surface, as obtained from the *TMY* of Copenhagen [89] ($\phi = 55.7°$) and Jaen-Spain [90] ($\phi = 37.8°$). Surprisingly, the energy content at low irradiances ($G < 200$ W/m^2) is relatively low in both places. This may appear counter-intuitive, but it is easily understood when considering the difference between time and energy distribution. For example, in Copenhagen, the low irradiance (<200 W) accounts for only 13.9% of the total annual irradiation, despite it occurring during 2461 h/year, which represents 55% of the total daily time. That leads one to question the idea, sometimes defended in PV literature [91], that PV module performance at low irradiances is very relevant for cloudy climates. As a matter of fact, empirical evidence that efficiency at low light levels is scarcely relevant is found in the literature [92].

However, because the most commonly occurring irradiation corresponds to medium irradiances, an energetic advantage can be obtained by selecting the inverter size smaller than the PV generator peak power, that is, $P_{IMAX} < P_M^*$. The corresponding reduction of relative inverter self-consumption and losses may compensate the possible energy loss by an inverter power limit lower than the maximum PV output power. Recommended values of P_{IMAX}/P_M^* range from 0.6 (high latitudes) to 0.8 (low latitudes) [85, 93].

20.14 CONCLUSIONS

Methods to estimate all the solar radiation components incident on any arbitrarily oriented surface and at any time of the year have been presented. The only required input

Downloaded from https://onlinelibrary.wiley.com/doi/ by <Shibboleth-member@purdue.edu, Wiley Online Library on [25/08/2024]. See the Terms and Conditions (https://onlinelibrary.wiley.com/terms-and-conditions) on Wiley Online Library for rules of use; OA articles are governed by the applicable Creative Commons License

Downloaded from https://onlinelibrary.wiley.com/doi/ by <Shibboleth-member@purdue.edu, Wiley Online Library on [25/08/2024]. See the Terms and Conditions (https://onlinelibrary.wiley.com/terms-and-conditions) on Wiley Online Library for rules of use; OA articles are governed by the applicable Creative Commons License

information is the 12 monthly mean values of the daily global horizontal irradiation. Several sources of solar radiation data are available. The corresponding values, for the same location and the same month, can significantly differ from one source to another. The corresponding uncertainty does not derive primarily from a lack of precision in the measuring instruments, but from the random nature of the solar radiation. The intrinsic uncertainty of solar radiation represents an important limit to the significance of the results of any PV design exercise, irrespective of the complexity of the model supporting the particular design tool. Because of this, rather simple design methodologies can yield results of similar confidence that results from sophisticated ones. The annual solar radiation availability on horizontal surfaces, optimally tilted fixed surfaces and several types of tracking surfaces has been calculated for 30 different places distributed all over the world. The hope is that the readers could find here a similar location, both in latitude and clearness index, to the location of their interest.

On the other hand, the PV module's conversion efficiency of solar radiation into electricity has also been considered. A model for predicting the $I-V$ characteristic of a PV generator at any prevailing condition such as solar irradiance, ambient temperature, wind speed and so on, have been described. The only required input data are the short-circuit current, the open- circuit voltage and the maximum power under the STC, and the Nominal Operating Cell Temperature. All these data are commonly found in the manufacturer's standard information. Particular attention has been paid to the consideration of the dust and angle of incidence effects.

Some relevant aspects related to the design of the more important PV applications have been disclosed. It has been stressed that, whatever the detailed methodology, stand-alone PV-system sizing relies on future prediction (the expected system lifetime) based on past observations of the solar radiation data. The corresponding uncertainty, unavoidably associated with the random nature of the solar radiation, encompasses that simulation models can provide exact numbers but not automatically exact predictions. Concerning SHS, by far the most widespread PV application nowadays (in terms of the number of systems currently in operation), the difficulties for deriving representative standard energy consumption values have been pointed out. Finally, energy performance ratios for grid-connected PV systems have been defined.

ACKNOWLEDGEMENTS

Montse Rodrigo has been extremely kind in preparing all the figures. The comments of the editor have been extremely valuable. The writing of this chapter has been at the expense of many hours away from my loved ones. I must thank the large tolerance and patience of Leda and Cristina Celena.

REFERENCES

1. Serres M *et al*., *Éléments d'Histoire des Sciences*, Chap. 3, Ed Bordas, Paris, 77–117 (1989).
2. Spencer J, *Search* **2**, 172–178 (1971).
3. Blanco M, Alarcón D, López T, Lara M, *Sol. Energy* **70**, 431–441 (2001).
4. Kasten F, *Arch. Meteorol. Geophys. Bioklimatol.* **14**, 206–223 (1966).

5. Meinel A, Mainel M, *Applied Solar Energy, An Introduction*, Addison-Wesley, Reading, MA (1976).
6. Iqbal M, *An Introduction to Solar Radiation*, Academic Press, Ontario (1983).
7. International H-World Database, *Mean Values of Solar Irradiation on Horizontal Surface*, Ed Progensa, Sevilla, Spain (1993).
8. SOLMET, *Solar Radiation-Surface Meteorological Observations*, National Climatic Data Center, TD-9724, Asheville, NC (1979).
9. Palz W, Greif J, *European Solar Radiation Atlas*, Commission of the European Communities, Ed Springer, Germany (1996.)
10. Font Tullot I, *Atlas de la Radiación Solar en España*, Ed Instituto Nacional de Meteorología, Madrid, Spain (1984).
11. Capderou M, *Atlas Solaire de l'Algerie*, Ed EPAU, Alger (1985).
12. Colle S, Pereira E, *Atlas de Irradiaçao Solar do Brasil*, INM, Labsolar EMC-UFSC (1998).
13. *Atlas de radiació solar a Catalunya*, Institut Catalá d'Energia, Barcelona, Spain (1996).
14. NASA Surface Meteorology and Solar Energy Data Set. Available at *eosweb.larc.nasa.gov/sse*.
15. National Solar Radiation Data Base. Available at *rredc.nrel.gov/solar*.
16. Macagnan M, Lorenzo E, Jimenez C, *Int. J. Sol. Energy* **16**, 1–14 (1994).
17. Papoulis A, *Probability, Random Variables and Stochastic Processes*, McGraw-Hill, New York (1965).
18. Marion W, Urban K, *User's Manual for TMY2s*, Report to DOE DE-AC36-83CH10093, NREL (1995).
19. Liu B, Jordan R, *Sol. Energy* **4**, 1–19 (1960).
20. Page J, *Proc. U.N. Conf. New Sources Energy*, 378–390 (1961).
21. Collares-Pereira M, Rabl A, *Sol. Energy* **22**, 155–164 (1979).
22. Miguel A *et al*., *Sol. Energy* **70**, 143–153 (2001).
23. Egido M, Lorenzo E, *Sol. Energy Mater. Sol. Cells* **26**, 51–69 (1992).
24. Willier A, *Arch. Meteorol. Geophys. Bioklimatol.* **7**, 197–204 (1956).
25. Hopkinson R, *J. Opt. Soc. Am.* **44**, 455–459 (1954).
26. McArthur L, Hay J, *J. Appl. Meteorol.* **20**, 421–429 (1981).
27. Kondratyev K, *Radiation in the Atmosphere*, Academic Press, New York, NY (1969).
28. Hay J, McKay D, *Int. J. Sol. Energy* **3**, 203–240 (1985).
29. Perez R *et al*., *Sol. Energy* **36**, 481–497 (1986).
30. Perez R *et al*., *Sol. Energy* **39**, 221–231 (1987).
31. Siala F, Rosen M, Hooper F, *J. Sol. Energy Eng.* **112**, 102–109 (1990).
32. Standard ASHRAE 93-77, *Methods of Testing to Determine the Thermal Performance of Solar Collectors*, American Society of Heating, Refrigeration, and Air Conditioning Engineers, New York (1977).
33. Martin N, Ruiz J, *Sol. Energy Mater. Sol. Cells* **70**, 25–38 (2001).
34. Bottenberg W, "Module Performance Ratings: Tutorial on History and Industry Needs", *PV Performance, Reliability and Standards Workshop*, 5–42, NREL, Vail, CO (1999).
35. Amato U *et al*., *Sol. Energy* **37**, 179–194 (1986).
36. Graham V *et al*., *Sol. Energy* **40**, 83–92 (1988).
37. Aguiar R, Collares-Pereira M, Conde J, *Sol. Energy* **40**, 269–279 (1988).
38. Benseman R, Cook F, *N Z J. Sci.* **12**, 296–708 (1960).
39. Lorenzo E, Maquedano C, *Proc. 13th Euro. Conf. Photovoltaic Solar Energy Conversion*, 2433–2436 (1995).
40. Quaschning V, Hanitsch R, *Proc. 13th Euro. Conf. Photovoltaic Solar Energy Conversion*, 683–686 (1995).
41. Skiba M *et al*., *Proc. 16th Euro. Conf. Photovoltaic Solar Energy Conversion*, 2402–2405 (2000).
42. Castro M *et al*., *Era Sol.* **87**, 5–17 (1998).

Downloaded from https://onlinelibrary.wiley.com/doi/ by <Shibboleth-member@purdue.edu, Wiley Online Library on [25/08/2024]. See the Terms and Conditions (https://onlinelibrary.wiley.com/terms-and-conditions) on Wiley Online Library for rules of use; OA articles are governed by the applicable Creative Commons License

43. Kaiser R, Reise C, *PV System Simulation Programmes*, Internal Report for the IEA SHCP Task 16, Fraunhofer-FISE, Freiburg (1996).
44. Caamaño E, Lorenzo E, *Prog. Photovolt.* **4**, 295–305 (1996).
45. Jennings C, Farmer B, Townsend T, Hutchinson P, Gough J, Shipman D, *Proc. 25th IEEE Photovoltaic Specialist Conf.*, 1513–1516 (1996).
46. Butti K, Perlin J, *A Golden Thread: 2500 Years of Solar Architecture and Technology*, Ed Cheshire, Palo Alto, NY (1980).
47. de Laquil III P., Kearney D, Geter M, Diver R, in Johansson T, Kelly H, Reddy A, Willians R, Eds, *Renewable Energy: Sources for Fuels and Electricity*, Chap. 5, Island Press, Washington, DC, 213–236 (1993).
48. Lorenzo E, Macagnan M, *Prog. Photovolt.* **2**, 45–55 (1994).
49. Zilles R, Ribeiro C, Moszkowicz M, *Proc. 2nd WCE Photovoltaic Solar Energy Conversion*, 2009–2012 (1998).
50. Durisch W, Tille D, Wörz A, Plapp W, *Appl. Energy* **65**, 273–284 (2000).
51. Eikelboom J, Jansen M, *Characterisation of PV Modules of New Generations*, ECN-C-00-067, Report to NOVEM Contract 146.230-016.1, Available at *www.ecn.com* (2000).
52. Caamaño E, Lorenzo E, Zilles R, *Prog. Photovolt.* **7**, 137–149 (1999).
53. Schmela M, *PHOTON Int.* **3-2001**, 32–35 (2001).
54. Green M, *Solar Cells*, Chap. 5, Prentice Hall, Kensington, 95–98 (1982).
55. Araujo G, Sanchéz E, *Sol. Cells* **5**, 377–386 (1982).
56. King D, Kratochvil J, Boyson W, *Proc. 26th IEEE Photovoltaic Specialist Conf.*, 1113–1116 (1997).
57. Fuentes M, *Proc. 17th IEEE Photovoltaic Specialist Conf.*, 1341–1346 (1984).
58. Chianese D, Cerenghetti N, Rezzonico R, Travaglini G, *Proc. 16th Euro. Conf. Photovoltaic Solar Energy Conversion*, 2418–2421 (2000).
59. Scheiman D, Jenkins P, Brinker D, Appelbaum J, *Prog. Photovolt.* **4**, 117–127 (1996).
60. Smiley E, Stamenic L, Jones J, Stojanovic M, *Proc. 16th Euro. Euro. Conf. Photovoltaic Solar Energy Conversion*, 2002–2004 (2000).
61. Martin N, Ruiz J, *Prog. Photovolt.* **7**, 299–310 (1999).
62. Jones A, Underwood C, *Sol. Energy* **70**, 349–359 (2001).
63. King L, Kratochvil J, Boyson E, Bower W, *Proc. 2nd World Conf. Photovoltaic Solar Energy Conversion*, 1947–1952 (1998).
64. Gordon J, *Sol. Cells* **20**, 295–313 (1987).
65. Cowan W, *Proc. 12th Euro. Conf. Photovoltaic Solar Energy Conversion*, 403–407 (1994).
66. Abouzahr Y, Ramakumar R, *IEEE Trans. Energy Conversion* **5**(3), 445–452 (1990).
67. Negro E, *Proc. 13th Euro. Conf. Photovoltaic Solar Energy Conversion*, 687–690 (1995).
68. Kaiser R *Photovoltaic Systems*, Chap. Fraunhofer-FISE, Freiburg, Germany (1995).
69. Boland J, Marjolijn D, *Sol. Energy* **71**, 187–198 (2001).
70. Chapman R, *Sol. Energy* **43**, 71–76 (1989).
71. Macomber H, Ruzek I, Costello F, *Photovoltaic Stand-Alone Systems: Preliminary Engineering Design Handbook*, Prepared for NASA, Contract DEN 3-195 (1981).
72. Barra L, Catalanotti S, Fontana F, Lavorante F, *Sol. Energy* **33**, 509–514 (1984).
73. Bucciarelli L, *Sol. Energy* **32**, 205–209 (1984).
74. Bartoli B *et al*., *Appl. Energy* **18**, 37–47 (1984).
75. Sidrach-de-Cardona M, Mora Ll, *Sol. Energy Mater. Sol. Cells* **55**, 199–214 (1998).
76. Egido M, Lorenzo E, *Sol. Energy Mater. Sol. Cells* **26**, 51–69 (1992).
77. Klein S, Beckman W, *Sol. Energy* **39**, 499–512 (1987).
78. Lorenzo E, Narvarte L, *Prog. Photovolt*, **8**, 391–409 (2000).
79. Kaiser R, Sauer D, *Proc. 12th Euro. Conf. Photovoltaic Solar Energy Conversion*, 457–460 (1994).
80. Universal Technical Standard for Solar Home Systems, Thermie B SUP 995-96, EC-DGXVII (1998).

Downloaded from https://onlinelibrary.wiley.com/doi/ by <Shibboleth-member@purdue.edu>, Wiley Online Library on [25/08/2024]. See the Terms and Conditions (https://onlinelibrary.wiley.com/terms-and-conditions) on Wiley Online Library for rules of use; OA articles are governed by the applicable Creative Commons License

81. Maycock P, *Renewable Energy World* **2**, 72–76 (1999).
82. Nieuwenhout F *et al*., *Prog. Photovolt.* **9**, 455–474 (2001).
83. Belli G, Iliceto A, Previ A, *Proc. 11th Euro. Conf. Photovoltaic Solar Energy Conversion*, 1571–1574 (1992).
84. Morante F, Zilles R, *Prog. Photovolt.* **9**, 379–388 (2001).
85. Jantsch M, Schmidt H, Schmid J, *Proc. 11th Euro. Conf. Photovoltaic Solar Energy Conversion*, 1589–1593 (1992).
86. *Guidelines for the Assessment of PV Plants. Document B: Analysis and Presentation of Monitoring Data*, Issue 4.1, JRC of the Commission of the European Communities, Ispra, Italy (1993).
87. Haeberlin H, Beutler C, *Proc. 13th Euro. Conf. Photovoltaic Solar Energy Conversion*, 934–937 (1995).
88. Rindelhardt U, Teichmann G, Decker B, Grochowski J, *Proc. 14th Euro. Conf. Photovoltaic Solar Energy Conversion*, 2652–2655 (1997).
89. Katic Y, Jensen B, *Proc. 16th Euro. Conf. Photovoltaic Solar Energy Conversion*, 2830–2833 (2000).
90. Nofuentes G, *Contribución al desarrollo de aplicaciones fotovoltaicas en edificios*, Ph.D. thesis, Presented at the Polytechnical University of Madrid, Madrid (2001).
91. Mason N, Bruton T, Heasman K, *Proc. 14th Euro. Conf. Photovoltaic Solar Energy Conversion*, 2021–2024 (1997).
92. Wilk H, *Proc. 14th Euro. Conf. Photovoltaic Solar Energy Conversion*, 297–300 (1997).
93. Macagnan M, Lorenzo E, *Proc. 11th Euro. Conf. Photovoltaic Solar Energy Conversion*, 1167–1170 (1992).
94. Bourges B, *Climatic Data Handbook for Europe*, Ed Kluwer Academic Publishers, The Netherlands (1992).
95. Herrero M, *Soleamiento y Energía Solar*, Ed University of Valencia, Spain (1985).
96. PVSYST 3.1, *www.pvsyst.com* (2000).

Downloaded from https://onlinelibrary.wiley.com/doi/ by <Shibboleth-member@purdue.edu, Wiley Online Library on [25/08/2024]. See the Terms and Conditions (https://onlinelibrary.wiley.com/terms-and-conditions) on Wiley Online Library for rules of use; OA articles are governed by the applicable Creative Commons License

21

Economic Analysis and Environmental Aspects of Photovoltaic Systems

Richard A. Whisnant[1], Stephen A. Johnston[2] and James H. Hutchby[3]

[1]*Parameters, Inc., Cary, North Carolina,* [2]*Research Triangle Institute, Research Triangle Park, North Carolina* [3]*Semiconductor Research Corporation, Research Triangle Park, North Carolina*

Photovoltaic (PV) systems provide electric energy, and the range of uses for electricity and the situations in which it is employed are enormous. Moreover, there are numerous other well-developed and widely used technologies for supplying electricity. Conventional fossil-fuel and hydroelectric generation are presently far more widely deployed than PV. The question arises, then, of how PV systems can penetrate the world's electric supply in competition with these alternatives, or, more narrowly, how a PV system can compete with other electricity sources for a specified application. At this point in time, there are many PV systems that do compete successfully in applications for which they are particularly suited. In other applications, PV systems have been deployed with the support of financial subsidies from private or public sources in order to either satisfy defined energy needs or to demonstrate the potential for PV systems. In all cases, it is useful to understand the economic viability, whether present or future, of any PV system in a given application. It is the purpose of this chapter to define and illustrate methods of defining the economics of PV systems as measured by conventional financial criteria and the cost of delivered energy. The cost of delivered energy is a fundamental characteristic of PV systems, and it can be influenced by the design and performance of the system, as well as by the sources and costs of capital to fund the system. The choice to deploy PV in a given situation is also influenced by other issues, including competition from the established electric supply, financial risk, and environmental, political, and humanitarian concerns.

Handbook of Photovoltaic Science and Engineering. Edited by A. Luque and S. Hegedus
© 2003 John Wiley & Sons, Ltd ISBN: 0-471-49196-9

Downloaded from https://onlinelibrary.wiley.com/doi/ by <Shibboleth-member@purdue.edu, Wiley Online Library on [25/08/2024]. See the Terms and Conditions (https://onlinelibrary.wiley.com/terms-and-conditions) on Wiley Online Library for rules of use; OA articles are governed by the applicable Creative Commons License

21.1 BACKGROUND

A rational decision to develop, supply, or utilize PV systems calls for consideration of many factors in an organized manner so as to address the broad issue of whether photovoltaics is a good choice for the person or institution making the decision. Electric energy today can be provided from many sources that are both nonrenewable (including coal, oil, natural gas, nuclear) and renewable (such as wind, biomass, hydro, PV). PV systems compete, in the broadest sense of the word, against the other sources. The competition encompasses financial, reliability, environmental, and performance considerations, and the weight given to these factors will depend on the decision maker's priorities. The values of the parameters in the decision process are defined by well-developed and widely available energy-supply technologies. Economic analysis in the developed world usually focuses on which supply technology best meets the well-defined economic criteria for a given application or class of applications. The preponderance of the use of electric energy in the developed world is available from an electric supply grid, and the competitiveness of PV systems is often evaluated in that context. There are some off-grid demands that can be supplied by PV systems, and for which they are technically well qualified. In the United States, such applications include remote vacation homes or public buildings, navigation buoy signals, communications repeaters, outdoor signage, and irrigation pumping.

In less-developed areas of the world, which for the present discussion mean areas without electric-power grids, the context of the decision process is different. PV systems in such areas are often termed *remote* or *village* systems. They may be deployed in individual homes, small businesses, or may serve a community with local distribution of energy. The competition faced by PV systems in these settings is usually from diesel oil–powered generators (nonrenewable source) or from small renewable sources (such as wind, hydro, biomass). The factors in the decision to deploy PV systems may include factors common to developed regions, though there may be fewer energy alternatives, and generally the individual system capacities are much smaller than in developed regions. However, in less-developed regions of the world, certain other factors may assume greater importance. The viability of the systems is a serious issue if the infrastructure for their installation and maintenance is lacking. Conversely, the provision of that infrastructure to provide installation and maintenance may be a more significant concern than in developed regions. It may also vary among energy technologies, and to that extent it is a competitive factor. For example, diesel generators must be supplied with fuel on a periodic basis, and they have moving parts that must periodically be repaired or replaced. PV systems do not require fuel supply and have no moving parts to repair. However, this does not mean that they would never need repair or replacement.

The financial considerations in a decision to deploy PV can be quite different in developed regions than in the undeveloped regions. In a developed country, the economic units (e.g. individuals, families, businesses, government operations) have a cash flow and well-defined energy needs. The question that they must answer periodically is what source of energy will they choose from among competing alternatives that are highly developed and more or less readily available. The question can be addressed in a quantitative fashion, at varying levels of sophistication, and the resources are available to implement the choice. In undeveloped regions, the situation is more likely that the economic units are individuals or very small businesses with little or no cash flow. The question for these regions is whether any electric energy is at all affordable and where do the resources to pay for

Downloaded from https://onlinelibrary.wiley.com/doi/ by <Shibboleth-member@purdue.edu, Wiley Online Library on [25/08/2024]. See the Terms and Conditions (https://onlinelibrary.wiley.com/terms-and-conditions) on Wiley Online Library for rules of use; OA articles are governed by the applicable Creative Commons License

Downloaded from https://onlinelibrary.wiley.com/doi/ by <Shibboleth>-member@purdue.edu, Wiley Online Library on [25/08/2024]. See the Terms and Conditions (https://onlinelibrary.wiley.com/terms-and-conditions) on Wiley Online Library for rules of use; OA articles are governed by the applicable Creative Commons License

it come from. The purely financial comparison of electricity sources by private entities often becomes subservient to public economic-development initiatives, and national and international politics may play a strong role. The choice of electric energy sources for the classes of applications must still be made, and the cost of energy delivered, in the sense employed for developed regions may still be computed, but generally not by individuals or small economic units, because they will not pay for them.

21.2 ECONOMIC ANALYSIS

Once the technical requirements of a PV application have been stated and a PV system design completed, the economic analysis can be carried out. The economic assessment includes both costs and benefits of the system. The methodology for this assessment constitutes a major portion of this chapter.

21.2.1 Key Concepts

The purchase of a PV system represents an expenditure of capital resources at a given time with the expectation of benefits in the form of electric energy delivered over some future period, which is generally the life of the PV system. Other benefits, such as reductions in greenhouse gases, might be quantified. For large systems, the construction expenditures may occur over more than one year. The future benefits, primarily the value of the electricity generated, may be realized over a 10- to 30-year period. Thus, the basic issue is how to measure the value of future benefits from a present expenditure. Further, the issue is how to compare that value for a PV system with a consistently defined value for an alternative system such as a diesel-electric system, a fuel cell, or electricity from the grid. Salvage value at the end of the system life is also a future benefit. In many cases, there will not only be future benefits but future costs as well. The cost of maintenance and the replacement of failed modules are primary examples. In addition, qualitative benefits, such as energy independence or reduction in the risk of future escalation of energy costs, may enter the decision process, although they are not dealt with here.

We generally recognize intuitively that the value of a cost or benefit in the future is not equal to the same cost or benefit today. If we were to receive $100, we would rather get it today than five years from now. Why? Perhaps because we could buy something today with the money and enjoy its use for the next five years, rather than wait to enjoy it. More practically, we could put the $100 in a savings account and it would be worth perhaps $125 in 5 years; so the value of money possessed now as opposed to later can be measured in this simple way. All of this goes to say that there is a "time value of money," and defining that time value pervades the whole process of economic analysis for PV systems. These expenditures and benefits, as measured in monetary terms, are usually called *cash flows*.

As suggested above, the purchase and operation of a PV system involves a stream of cash flows over a period of years, and economic assessment requires some consistent measure of these cash flows to be made. It may in some instances require the comparison of the value associated with that stream with the value of a different stream for a competing system. For a PV system, such a stream might look like what is shown in Figure 21.1. Outflows, such as the purchase cost and maintenance costs, are shown as negative, while

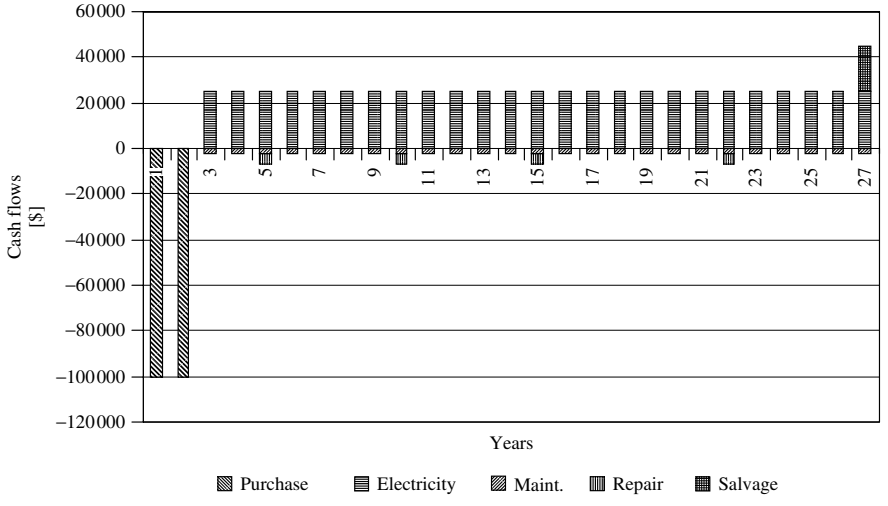


Figure 21.1 Example of PV system cash flows

inflows, such as the value of electricity produced and the salvage value, are shown as positive. In Figure 21.1, it is assumed that the system construction covers 2 years and outlays are \$100 000 in each year; the value of electricity generated is \$25 000 per year for the next 25 years; annual maintenance costs are \$2000; there are replacement costs of \$5000 in Years 5, 10, 15, and 20; and the salvage value is \$20 000 at the end of Year 27. For a PV system, the value of the generated electricity is usually determined by the avoided cost of the electricity that would otherwise need to be purchased. Note that the annual electricity production in kilowatt hour from the PV system is implicitly included in this example through the determination of the electricity cost stream. If the PV system is remotely situated, the PV electricity might alternatively be valued by its contribution to its end-use activity, though this valuation may be easier said than done.

To put a single value on these cost and benefit streams occurring over time, the usual approach is to refer all costs and benefits to a selected point in time, usually the present time, sum the values for the given streams, and compare the sums. These sums are called the *present value* or *present worth* of the systems. To compare two or more systems with one another, the present worth of each is computed to provide an economic comparison.

A sum received or spent at the present time has a present worth, P. A sum spent or received at a future time n years hence has a future worth, F. If P is invested at an interest rate of i percent per year, then its future worth at the end of the first year is

$$F = P + Pi = P(1 + i)$$

The future worth at the end of the second year is

$$F = [P(1 + i)](1 + i) = P(1 + i)^2$$

Petitioner Canadian Solar (USA) Inc., Ex. 1035, p. 2359

Downloaded from https://onlinelibrary.wiley.com/doi/ by <Shibboleth-member@purdue.edu, Wiley Online Library on [25/09/2024]. See the Terms and Conditions (https://onlinelibrary.wiley.com/terms-and-conditions) on Wiley Online Library for rules of use; OA articles are governed by the applicable Creative Commons License

and the future worth after n years is

$$F = P(1+i)^n \tag{21.1}$$

Conversely, the present worth of a future sum is given by

$$P = F(1+i)^{-n} \tag{21.2}$$

Equation (21.2) shows that the present worth of a sum received n years in the future is reduced by the factor $(1+\mathrm{i})^n$.

When equations (21.1 and 21.2) refer to the money deposited at interest, the factor i is the interest rate offered by the bank, but when an investment in an energy system is being considered, the factor i is referred to as a *discount rate*. The discount rate is the value that the system owner puts on the capital invested in the system, and is often called the opportunity cost of the investor; that is, the rate of return foregone on the next most attractive investment.

In Figure 21.1, the annual delivered energy values of \$25 000 constitute a uniform stream of cash flows. The sum of the future worth of each of these annual amounts, a, is, from equation (21.1)

$$F = a[1 + (1+i) + (1+i)^2 + \cdots + (1+i)^{n-1}]$$

This relationship can be shown to be equivalent to [1]

$$F = a[(1+i)^n - 1] \div i \tag{21.3}$$

By combining equations (21.2 and 21.3), the present worth of a uniform series of amounts a can be stated as

$$P = a\frac{[(1+i)^n - 1]}{[i(1+i)^n]} \tag{21.4}$$

Consider the application of equations (21.2–21.4) to the simplified example of cash flows in Figure 21.1. The value of the PV system as measured by present worth at the beginning of Year 3, the time the system begins to produce electricity, is P_s.

$$P_\mathrm{s} = P_\mathrm{investment} + P_\mathrm{electricity} + P_\mathrm{maintenance} + P_\mathrm{replacement} + P_\mathrm{salvage} \tag{21.5}$$

Equation (21.5) implies that each of the components of P_s is referred to the same point in time, beginning of Year 3, and can therefore be summed. Table 21.1 summarizes the computation of P_s. Assume that the two \$100 000 investments are made as of the beginning of Years 1 and 2, and that all other amounts are as of year-end. Assume a discount rate, i, of 8%. Note that in Table 21.1 expenditures, or outflows, are shown as negative numbers and benefits, or inflows, are shown as positive. The appropriate equation for each category is indicated and the value of the exponent, n, required to reference the present-worth values to the beginning of Year 3 is also given. Note that cash flows that occur later in the system life contribute less to the system present worth, relative to their current values, than those that occur earlier.

Downloaded from https://onlinelibrary.wiley.com/doi/ by <Shibboleth-member@purdue.edu, Wiley Online Library on [25/08/2024]. See the Terms and Conditions (https://onlinelibrary.wiley.com/terms-and-conditions) on Wiley Online Library for rules of use; OA articles are governed by the applicable Creative Commons License

Table 21.1 Present worth of PV system cash flows shown in Figure 21.1 (discount rate = 8%)

Cash flow		Present worth		
Category	Amount [$]	n	Equation	P [$]
Year 1 investment	−100 000	2	(21.1)	$P_{\text{investment}} = -116\,640$
Year 2 investment	−100 000	1	(21.1)	$P_{\text{investment}} = -108\,000$
Annual electricity, Years 3–27	25 000	25	(21.4)	$P_{\text{electricity}} = 266\,869$
Replacement, Year 5	−5 000	5	(21.2)	$P_{\text{replacement}} = -3403$
Replacement, Year 10	−5 000	10	(21.2)	$P_{\text{replacement}} = -2316$
Replacement, Year 15	−5 000	15	(21.2)	$P_{\text{replacement}} = -1576$
Replacement, Year 20	−5 000	20	(21.2)	$P_{\text{replacement}} = -1073$
Annual maintenance, Years 3–27	−2 000	25	(21.4)	$P_{\text{maintenance}} = -21\,350$
Salvage value, Year 27	20 000	25	(21.2)	$P_{\text{salvage}} = 2920$
Total			(21.5)	$P_{\text{s}} = 15\,431$

This PV system present worth is positive, and thus the system can be said to have a net benefit of $15 431 measured at the beginning of Year 3. Whether this is an acceptable economic choice would depend on the economic criteria of the system purchaser. This subject will be discussed again later.

There are instances when the annual amounts a in equation (21.4) are not uniform (constant) over all periods, but escalate at a constant rate, e. That is, if c is defined as the amount for the first year, the amount for the second year is $c(1+e)$, and the amount for the third year is $c(1+e)^2$. An obvious instance of where such a series of cash flows might arise would be in accounting for the effect of inflation on the value of avoided electricity. In this instance, the present worth of the series of cash flows can be expressed [1], when $e > i$, as

$$P = \frac{c}{1+i}\left\{\frac{(1+x)^n - 1}{x}\right\} \tag{21.6}$$

where x is defined by

$$\frac{1+e}{1+i} = 1 + x \tag{21.6a}$$

If the escalation rate is less than the discount rate, $e < i$, then

$$P = \frac{c}{1+e}\left\{\frac{(1+x)^n - 1}{x(1+x)^n}\right\} \tag{21.7}$$

where x is defined by

$$\frac{1+e}{1+i} = \frac{1}{1+x} \tag{21.7a}$$

If the escalation rate equals the discount rate, $e = i$, then

$$P = cn/(1+e) = cn/(1+i) \tag{21.8}$$

When a financial evaluation of a PV system project is defined, such as the one in Figure 21.1, it is important to be clear about how inflation will be taken into account.

Downloaded from https://onlinelibrary.wiley.com/doi/ by <Shibboleth-member@purdue.edu>, Wiley Online Library on [25/08/2024]. See the Terms and Conditions (https://onlinelibrary.wiley.com/terms-and-conditions) on Wiley Online Library for rules of use; OA articles are governed by the applicable Creative Commons License

When Figure 21.1 was defined, inflation was not mentioned, and the cash flows shown for the electricity value were constant over a number of years. Such a problem statement is consistent with a "real dollar" or "constant worth dollar" or just "constant dollar" approach. In this view, all monetary values are stated in terms of their purchasing power at the point in time at which the present worth of the system will be calculated. The computation of the present worth is a little simpler for a constant-dollar formulation, but that approach can mask some real-world inflationary effects. For example, the inflation of avoided electricity prices may be different from the inflation of labor required for maintenance or components used in replacing failed modules. When explicitly taking inflation into account, the monetary amounts in the cash flows are stated in terms of the actual dollar transactions at the time at which they occur. These amounts are called *actual dollars, then-current dollars*, or just *current dollars*.

Since the calculation of present worth measures is usually carried out for the purpose of comparing system alternatives, it can be argued that useful comparisons can be made in either constant-dollar or current-dollar terms. Where the differences in system measures turn out to be relatively large, that argument is likely to be valid, because the difference in the systems is obvious. However, there may be instances in which the outcome could be skewed if inflation is not properly calculated.

Thus far, the discussion has assumed present worth calculations either on a constant-dollar basis or on a current-dollar basis with inflation at a constant rate. It is also possible that a constant inflation rate does not adequately represent the future. If the inflation rate (or the discount rate) varies over the period of the analysis, then, practically speaking, one is forced to calculate separately the present worth of each future cash transaction and add the terms to get a system present worth.

It needs to be emphasized here that the computation of a present-worth measure for some energy alternatives requires the projection of cash flows (transactions) up to 30 years into the future, and thus the result depends not just on the proper application of computational methods, but on the assumptions and information that go into this projection. The cash flows to be projected include energy prices, materials costs, labor costs, cost of capital, and related factors. This requirement often leads to the parameterization of critical factors and economic analysis under a range of scenarios rather than a single set of assumptions. Fortunately, the effect of the discount rate is to reduce the impact of projections far into the future relative to those in the near term.

Now, let us consider a more general statement of cash flow that supports the definition of additional economic measures of PV systems. The statement assumes that a PV system will be purchased, installed, and operated over a period of years by a profit-making organization. For a given year, n, the net cash flow based on returns to equity capital is [2]

$$X_n = (R_n - C_n - I_n) - (R_n - C_n - I_n - D_n)T - K_n + S_n + B_n - P_n \pm W_n \qquad (21.9)$$

The terms of equation (21.9) are as follows.

R_n = gross revenue due to the system in the year n; typically the value of the electricity generated.

Downloaded from https://onlinelibrary.wiley.com/doi/ by <Shibboleth-member@purdue.edu, Wiley Online Library on [25/08/2024]. See the Terms and Conditions (https://onlinelibrary.wiley.com/terms-and-conditions) on Wiley Online Library for rules of use; OA articles are governed by the applicable Creative Commons License

C_n = cost associated with the operation and maintenance of the system in year n; including labor, materials, and replacement parts.
I_n = debt interest paid in year n on funds borrowed (B defined below) to fund the system.
D_n = tax depreciation in year n for the system, assuming that the taxation applicable to the owner allows deduction of depreciation for tax purposes, calculated as allowed by the tax law.
T = incremental (marginal) tax rate for the owner; the second term in parentheses in equation (21.9) represents the taxes on income paid by the owner.
K_n = capital expenditure in year n; the total amount spent on capital assets.
S_n = salvage value received in year n.
B_n = amount of money borrowed in year n from external sources and used to fund capital expenditures.
P_n = payment of principal on debt capital (B) in year n.
W_n = net increase in working capital in year n; has a negative sign if an increase in working capital is required; working capital represents the funds employed for such items as payroll, inventories, and accounts receivable.

The definition of net cash flow on an equity capital basis is used here because profit-making organizations tend to judge their financial performance based on returns on equity capital.

The annual net cash flow in equation (21.9) for each year in a PV project life must be used with equation (21.10) to calculate a system present worth that is comparable to the result P_s shown in Table 21.1.

$$NPW = \sum_{n=0}^{L} \frac{X_n}{(1+m)^n} \tag{21.10}$$

where

X_n = annual net cash flow from equation (21.9).
L = system life or the life of the project for evaluation purposes.
m = the minimum acceptable rate of return on equity capital.

The quantity m is equivalent mathematically to the discount rate i used earlier (e.g. equations (21.1–21.3), but m has the additional stipulation that it represents a requirement of the system owner for returns on equity. It may or may not be the opportunity cost. It may represent a hurdle rate set to determine what the owner requires in order to take the financial risk represented by the project.

In Table 21.1, the present worth of each component (investment, annual electricity, replacement, maintenance, and salvage) was calculated over the project life, and the component present worth figures were added to get a system present worth. Equation (21.9) adds the figures for all components (investment, annual electricity, replacement, maintenance, and salvage) in any given year to get the annual net cash flow for that year. Then, the annual net cash flows are discounted in equation (21.10) to get the system

Petitioner Canadian Solar (USA) Inc., Ex. 1035, p. 2363

Downloaded from https://onlinelibrary.wiley.com/doi/ by <Shibboleth-member@purdue.edu, Wiley Online Library on [25/08/2024]. See the Terms and Conditions (https://onlinelibrary.wiley.com/terms-and-conditions) on Wiley Online Library for rules of use; OA articles are governed by the applicable Creative Commons License

present worth, which is called net present worth (NPW). Thus, the order of computation is different in Table 21.1 from that of equations (21.9 and 21.10), but the result is the same. Equations (21.9 and 21.10) are just a more general expression of the computational process than Table 21.1.

Note also that if the PV system owner is selling electricity and thus has a revenue (income) stream, that revenue is taxable as per equation (21.9). However, if the PV system owner is not selling electricity, then the electricity has a value to the owner and the term R in equation (21.9) can be used in the calculation of the system worth, but the taxation term is zero because $T = 0$. (The case of $T = 0$ is implicit in Table 21.1.)

Several other measures of system worth can be defined using the annual net cash flow defined by equation (21.9).

$$0 = \sum_{n=0}^{L} \frac{X_n}{(1 + IRR)^n} \tag{21.11}$$

where

IRR = internal rate of return.

Equation (21.11) is solved iteratively for the value of internal rate of return (IRR) that satisfies the equation. To determine if the investment in the PV system is acceptable, the IRR must be compared to a hurdle rate set by the owner. This rate may or may not be the owner's opportunity cost.

A less-sophisticated economic measure is the simple payback period defined by

$$0 = \sum_{n=0}^{\mathrm{PB}} X_n \tag{21.12}$$

where

PB = payback period in years.

The payback period is the number of years required for the inflows to equal the outflows. It is the time required to recover the initial investment in the system. This measure is referred to as *simple* because it does not consider the time value of money (there is no discounting). It also does not consider cash flows beyond the time when the investment is recovered. Simple payback is probably more useful, for example, to the homeowner who does not have the same tax and profit considerations as the business owner.

A measure of the intermediate complexity and usefulness is the discounted payback period, defined as

$$0 = \sum_{n=0}^{\mathrm{DPB}} \frac{X_n}{(1 + m)^n} \tag{21.13}$$

where

DPB = discounted payback period.

The discounted payback period (DPB) does consider the time value of money, but does not consider the cash flow after the recovery of the initial investment.

Downloaded from https://onlinelibrary.wiley.com/doi/ by <Shibboleth-member@purdue.edu, Wiley Online Library on [25/08/2024]. See the Terms and Conditions (https://onlinelibrary.wiley.com/terms-and-conditions) on Wiley Online Library for rules of use; OA articles are governed by the applicable Creative Commons License

Finally, there is another method of valuing PV systems that uses some of the same mathematical techniques as the above measures, but expresses the result differently; namely, the levelized energy cost (LEC) or levelized bus bar energy cost (LBEC). This approach is particularly appropriate to energy providers such as electric utilities. This method provides a unit cost of electricity in \$/kWh that is constant over time (i.e. levelized) and expressed in monetary units at the beginning of a commercial operation. The LEC method is useful to utilities, who sell electricity on a \$/kWh basis, since it is easy to compare the computed LEC to the costs of electricity from other conventional or renewable sources. This method can also be adapted for nonutility system owners.

The LEC method is based on the same discounted cash-flow concepts illustrated by Table 21.1 and equations (21.1–21.8). These latter results represent the total discounted worth of a PV system over its economic life stated in dollars, and these dollars implicitly incorporate the annual PV energy produced. The LEC method, in effect, takes a present worth of the cost (but not revenue) streams as in equation (21.9) and computes a stream of constant annual values having the same present worth. This annual value is divided by the rated annual energy production of the system to get an annualized cost of electricity.

$$LEC = \frac{(NPW_C)(CRF)}{E} \tag{21.14}$$

where CRF is called the capital recovery factor, defined as

$$CRF = \frac{m(1+m)^n}{(1+m)^n - 1} = \frac{a}{P} \tag{21.15}$$

The capital recovery factor (CRF) is the inverse of the present worth of a uniform series defined in equation (21.4). NPW_C is computed from equation (21.10), which, in turn, is based on equation (21.8) with revenues, R, set to zero. The numerator of equation (21.14) is the annualized value of the costs associated with the system construction and operation, that is, it defines a uniform annual series of costs that have the same present value as NPW_C. The term E is the annual energy in kilowatt hour generated by the system.

21.2.2 General Methodology

A general methodology for the economic assessment of PV systems is illustrated in Figure 21.2. The assessment begins in Step 1, system design, which must be done prior to an economic analysis. For an assessment addressing multiple systems and/or applications, the methodology of Figure 21.2 must be carried out for each system of interest and the results summed to determine the economic potential.

Steps 2, 3, 4: system cost. In determining system cost, completeness and accuracy in individual component costs lead to a good estimate of system cost. Figure 21.2 suggests two paths to estimate system cost. If the system design is based on the currently available technology, then defining a complete bill of materials and then obtaining quotations from the vendors is the path to be followed. If the cell/module technology is to be projected into the future, or if a current technology is not in volume production so that its costs are not available, then the price can be predicted from the modeling of the manufacturing process.

Downloaded from https://onlinelibrary.wiley.com/doi/ by <Shibboleth-member@purdue.edu, Wiley Online Library on [25/08/2024]. See the Terms and Conditions (https://onlinelibrary.wiley.com/terms-and-conditions) on Wiley Online Library for rules of use; OA articles are governed by the applicable Creative Commons License

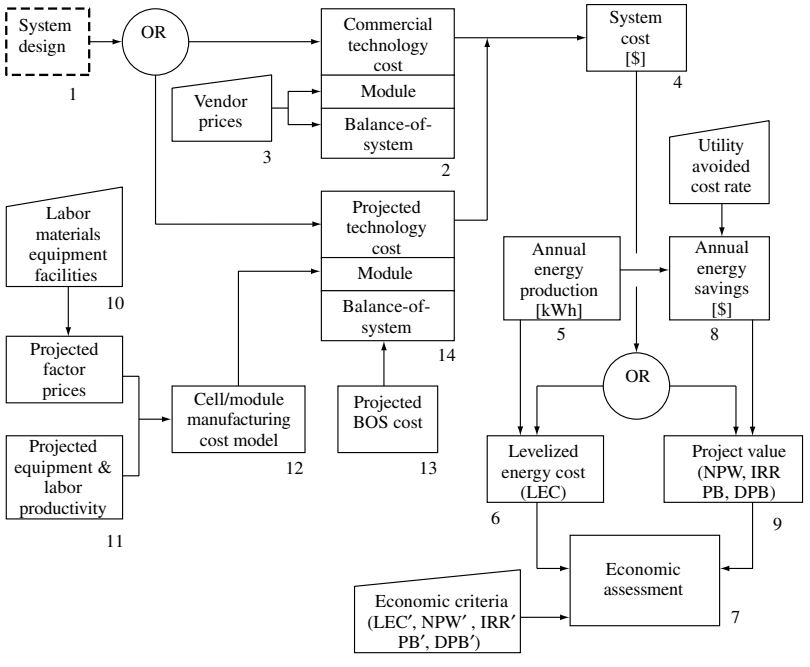


Figure 21.2 Economic assessment

Such a modeling procedure is discussed later in this section. For either path, the system components and materials, aside from the cells and modules, are in general commercially available and the prices can be obtained from manufacturers and distributors. A limited number of cells and modules are also commercially available. System components are particular to the design, and the following list suggests the major components whose costs are required. Detail part specifications and costs are needed in many cases for accurate costing.

- PV cells
- PV modules
- Module support structure
- Tracking structure/drives/controls
- Heliostats
- Foundations and structures
- Cooling system
- Interconnection wiring and terminations
- Power-conditioning unit
- Transfer switching and metering
- Substation equipment
- Land

Downloaded from https://onlinelibrary.wiley.com/doi/ by <Shibboleth> -member@purdue.edu, Wiley Online Library on [25/08/2024]. See the Terms and Conditions (https://onlinelibrary.wiley.com/terms-and-conditions) on Wiley Online Library for rules of use; OA articles are governed by the applicable Creative Commons License

- Site improvements (grading, roads, fencing, buildings)
- Installation labor and management
- Financing cost during construction
- Shipping
- Taxes
- Licenses, permits.

For large systems whose installation may extend over months or years, a schedule of installation and expenditures will also be needed to properly compute economic measures as defined previously.

Steps 10, 11, 12, 13, 14, 4: system cost (manufacturing-cost modeling). Figure 21.2 shows two paths to determine the system cost. The path utilizing commercial technology has been addressed in the figure. When a PV cell/module technology that is not commercially available is to be considered, predictions of the cell and/or module cost are required. One approach to predicting the cell/module costs is shown in Figure 21.2 (Step 12) as a cell/module-manufacturing cost model. Such a model was developed at the Research Triangle Institute under the sponsorship of the Electric Power Research Institute (EPRI), and was used over a period of years in studies of the cell and module costs [3]. This modeling approach, which eventually came to be called Strategic Analysis of Manufacturing Product and Price (STAMPP), is briefly described here to illustrate how cell/module costs can be predicted.

The objective of STAMPP is to model the operations of a cell- or module-manufacturing firm in such a way that the annual required revenue of the firm is calculated for a specified annual production volume. The required revenue divided by the production volume gives a required unit price for the cell or module. The term *required price* is used because all direct and indirect costs and after-tax profit are included in the revenue. The required price is thus the minimum price for which the product could be sold while returning the specified margin of profit. However, the market would always determine the actual selling price. A further objective of the model is to facilitate the parametric analysis of a wide range of cost factors so that the cost drivers can be identified and their effect on the required price of a cell or module design can be explored for a specified manufacturing process.

The firm is described in the model by a fixed organization whose top management levels are filled by a fixed number of people. The lower levels of the organization, including supervisors, production, and support staff are filled by a number of employees, which is scaled to the manufacturing requirements. Hours of operation, meteorological data for heating/cooling loads, and other firm-level financial and operating data are included among the input.

The physical operations of manufacturing are modeled in STAMPP using the concept of a "workstation". A workstation is defined as a collection of one or more identical machines, each performing the same operations in parallel. The user specifies the direction of workflow among the workstations.

The user defines the operations performed at a workstation on a per-machine basis. The model calculates the number of machines for each workstation based on a specified

Downloaded from https://onlinelibrary.wiley.com/doi/ by <Shibboleth-member@purdue.edu, Wiley Online Library on [25/08/2024]. See the Terms and Conditions (https://onlinelibrary.wiley.com/terms-and-conditions) on Wiley Online Library for rules of use; OA articles are governed by the applicable Creative Commons License

annual volume of the final product and the workstation characteristics. The workstation is characterized by the nominal operating parameters of one of its machines, which are defined as long-term average values. The quantity of work done at each workstation is determined by the model from a process balance using as inputs the total annual product volume from the last workstation, and individual machine parameters including

- form conversion factor (input/output units),
- yield (number of good units out per unit time/ideal production rate),
- machine ideal production rate,
- machine availability.

The quantity of required materials is determined from the workstation-level, per-product-unit consumption factors and the workstation product quantity, and the quantity of labor of specified types is determined from per-machine labor requirements. Total materials, labor, utilities, and floor-space requirements are summed for the firm, and their costs are calculated using these quantities and unit costs input to a cost catalog. Unit costs of process equipment and facilities are used to compute the capital investment for the plant.

Using the calculated production costs, the model produces a corporate income statement and balance sheet. These reports are based on accepted accounting procedures. The income statement provides the revenue to calculate the product cost. The data in both reports can be compared to the data for typical real businesses to assess the appropriateness of the modeling from a business point of view. On the manufacturing side, reports are provided that summarize the equipment, labor, materials, floor space, and utilities required in terms of both quantity and cost. Also reported are personnel and associated costs for administrative functions. The result is a complete picture of all aspects of the cost structure underlying the required product price. In the subsequent section, outputs from the model are shown to illustrate an economic assessment of a PV power plant.

Step 5: annual energy production. Within the assessment framework of Figure 21.2, the annual energy production for the system will be calculated from local solar data and the performance parameters of the system (as described elsewhere). For a private user, the energy considered here is the *useful* energy; that is, the energy actually consumed by the load plus any energy sold back to a utility. For a utility, all of the energy produced is useful.

Step 6: levelized energy cost (LEC). LEC is defined in equation (21.14) as a constant annual cost ($/kWh) over a specified period of years whose present worth is the same as that of the cost stream associated with its production. The cost stream was defined in equation (21.9). LEC incorporates the cost of capital and the annual energy production. LEC is typically computed by utilities, but could also be used by private PV system owners.

Step 7: economic assessment. The final step in this assessment methodology is to decide if the value of the economic measure computed is an acceptable value when compared to an economic criterion. Where LEC is the economic measure, it is compared with the cost of electricity (LEC′) from other sources calculated in the same manner. For a private user, the comparison value might be that of electricity from, for example, a diesel-electric generator or a fuel cell. For a utility, this comparison may entail the consideration of the

Downloaded from https://onlinelibrary.wiley.com/doi/ by <Shibboleth-member@purdue.edu, Wiley Online Library on [25/08/2024]. See the Terms and Conditions (https://onlinelibrary.wiley.com/terms-and-conditions) on Wiley Online Library for rules of use; OA articles are governed by the applicable Creative Commons License

system-capacity expansion for a given load growth in order to determine the alternative cost of electricity, or a simpler approach might be just the utility's cost of peaking power. The problem with the simpler approach is that it may not adequately consider issues such as reserve capacity.

Step 8: annual energy value. In order to calculate the project value measures in Step 9, the value of the annual energy production is needed. For grid-connected, customer-side systems, the value is the cost avoided by not purchasing the annual energy produced (Step 5). The value is calculated from the electric utility rate and the energy production. Where the rate is multitiered or has seasonal components, the energy production as a function of time would need to be taken into account in order to value the energy properly.

Step 9: project value. Several financial measures for PV systems have been defined in equations (21.10 to 21.13): NPW($), IRR(%), PB(years), and DPB(years). Each one depends on the net equity cash flow, X_n, defined by equation (21.9), which includes a revenue term, R, which is the value of the electricity purchase avoided by the use of the PV system. The annual electric energy produced by the PV system is implicitly included in R.

When the computed economic measure is NPW, IRR, PB or DPB, it is compared to the threshold (NPW′, IRR′, PB′, DPB′) values that the owner considers appropriate. If the owner is a commercial firm, the NPW or IRR measures would typically be used. If the decision is between two competing energy sources, say, PV and a fuel cell, the one with the higher NPW or IRR would be preferable. It should be noted that since the fuel-cell system is dispatchable (i.e. provides energy at any time on demand), the PV system is not comparable unless it includes storage. The two systems must be designed to meet the same load profile in order to be compared by a single measure such as NPW or IRR. If the decision for the commercial user is just whether to buy a PV system for a stated purpose, the issue then is whether the NPW or IRR is greater than some threshold value. In this instance, the PV system competes for capital with other capital needs of the firm, and the threshold may be set by considering the NPW or IRR associated with alternative capital expenditures. The firm may even look at the decision in both ways: is the PV system the best choice from among several systems *and* is it a better use of capital than nonenergy expenditures.

The payback (PB) and discounted payback (DPB) measures are more typically appropriate to homeowners or others without tax considerations in the purchase decision, although nothing prevents others from considering these criteria. The payback for the PV system can be compared to the life of the system as a decision criterion. If the payback is shorter than the life, then in a simple view the energy is free after the payback period. Another use of the payback measures is to compare two or more systems by calculating their payback; the one with the shortest payback is preferred.

21.2.3 Case Studies

To illustrate some of the methodologies for the economic analysis of PV systems, brief summaries of three studies in which the authors participated are presented here. Each study considered PV technology operated in a large-scale (25–50 MW) electric-utility setting. The first study [3] compared the required module price in $\$/W_p$ of several Si-cell technologies. The second study [4] covered silicon and copper indium diselenide (CIS)

Downloaded from https://onlinelibrary.wiley.com/doi/ by <Shibboleth-member@purdue.edu, Wiley Online Library on [25/08/2024]. See the Terms and Conditions (https://onlinelibrary.wiley.com/terms-and-conditions) on Wiley Online Library for rules of use; OA articles are governed by the applicable Creative Commons License

technology, and the third [5] compared the 500X concentrator systems with Si technology to GaAs technology in plants of the same annual energy capacity. All three studies modeled the cell- and module-manufacturing processes using the STAMPP model, and included both flat-plate and 500X concentrator collectors.

Financial studies of complex systems require extensive data input, and can produce volumes of data output. Restriction of space in this chapter limits the details that can be provided to only a small fraction of what was there in the original studies. The numerical values of inputs and outputs are based on the time at which the studies were performed, so the objective is to illustrate methodology and relative technology comparisons, not to give current quantitative cost results.

21.2.3.1 Module price for silicon technology

From the beginning of the photovoltaic commercialization efforts in the 1970s, crystalline-silicon-cell technology has been dominant. The availability of refined silicon wafers resulting from semiconductor development, the availability of mature processing equipment developed by that industry, and the simplicity of the Si-cell fabrication technology relative to thin-film Si or compound semiconductors such as gallium arsenide or copper indium diselenide were, and still are, major factors that influence the role of silicon in photovoltaics. The first cost analysis conducted by the authors [3], which was also the genesis of the STAMPP program defined earlier, compared silicon-module prices fabricated by several different methods. (In [3], the STAMPP model was called IMCAP, but the model is essentially the same.) While the results discussed here were determined in 1986, there still are some relevant and useful lessons to be learned from the comparison of different cell- and module-fabrication methods, and the focus here is on these rather than on current absolute cost of cells and modules.

Five different cell technologies and modules fabricated from them were examined in this study:

- Flat-plate modules using silicon cells from single-crystal Czochralski wafers.
- Flat-plate modules using silicon cells fabricated on silicon dendritic web substrate.
- Flat-plate modules using single-junction amorphous-silicon cells (a-Si:H) grown on glass.
- Flat-plate modules using tandem-junction amorphous-silicon cells (a-Si:H/a-SiGe:H) grown on glass.
- 500X Fresnel lens concentrator module using high-performance cells from float-zone single-crystal silicon wafers.

The concentrator module incorporated cells under separate development by the study sponsor and the cell fabrication was not modeled with STAMPP. The cells were treated as a purchased item. All of the manufacturing processes were defined to produce annually modules with a total rating of 25 MW.

The module prices computed for this study were intended to give a comparison of significantly different cell technologies and to provide a perspective on how low the prices might fall in the future. The cost of materials and other items for a base case

Downloaded from https://onlinelibrary.wiley.com/doi/ by <Shibboleth-member@purdue.edu>, Wiley Online Library on [25/08/2024]. See the Terms and Conditions (https://onlinelibrary.wiley.com/terms-and-conditions) on Wiley Online Library for rules of use; OA articles are governed by the applicable Creative Commons License

Table 21.2 Key technical and financial parameters [3]

Parameter	Process case			
	Technology	Base	Pessimistic	Optimistic
Module efficiency (%)	Czochralski	15.0	12.0	17.0
	Dendritic web	15.0	12.0	17.0
	Concentrator	19.42	17.09	21.75
	a-Si:H	10.0	6.0	12.0
Silicon price ($)	Czochralski	40/kg	75/kg	25/kg
	Dendritic web	40/kg	75/kg	25/kg
	Concentrator	2.00/cell	4.00/cell	1.00/cell
	a-Si:H (silane)	618/kg	2000/kg	150/kg
Glass ($/m^2)	All	10.76	13.46	8.07
Wafer/Kerf Thk. (mil)	Czochralski	12/10	14/12	10/6
Web pull rate (cm^2/min)	Dendritic web	20	8	30
Plasma deposition rate (Å/s)	a-Si:H	10	2	40
		Financial case		
Return on equity (%)	All	18	22	15
Debt/equity ratio	All	0.3	0.2	0.5
Debt interest rate (%)	All	14	16	12
Average cost of capital (%) (derived from other inputs)	All	17.1	21.0	13.5

Copyright © 2002. Electric Power Research Institute. EPRI AP-4369. Photovoltaic Manufacturing Cost Analysis; A Required Price Approach, Vol. 1, 2. Reprinted with Permission

were selected and reviewed by several organizations involved in the study, and it was recognized that the resulting module-price predictions were lower than those achieved at the time of the study, or, for the most part, even today. They represented a potential level of the price for high volume production with high conversion efficiencies. After determining with the model the key price drivers for each technology, other cases were defined to examine the effect of different values of the key drivers. Two cases, defined as optimistic and pessimistic and shown in Table 21.2, were used to compare with the base case. Base, pessimistic, and optimistic cases relating to material-cost parameters (process case) and cost-of-money parameters (financial case) were defined. Table 21.2 shows only the "key" parameters of the defined cases, that is, the parameters from the cases that had the greatest effect on price.

The range of required module prices associated with the full set of process-case parameters is provided in Figure 21.3 for all of the cell technologies. Within each of the process cases, the spread in module prices among the technologies is about 2:1, so that achievement of important processing parameters and conversion efficiencies has a large impact on their ultimate relative prices.

The effect of the financial case parameters on module price was determined to be in the range of about ±5% of the base case for all of the technologies. For example, Table 21.3 gives the required module prices for the Czochralski modules for each case. The range of prices for the process cases due to variation in material costs ($3.46–$1.22) is much greater than the variation due to the financial-case parameters ($1.98–$1.80).

Downloaded from https://onlinelibrary.wiley.com/doi/ by <Shibboleth-member@purdue.edu, Wiley Online Library on [25/08/2024]. See the Terms and Conditions (https://onlinelibrary.wiley.com/terms-and-conditions) on Wiley Online Library for rules of use; OA articles are governed by the applicable Creative Commons License

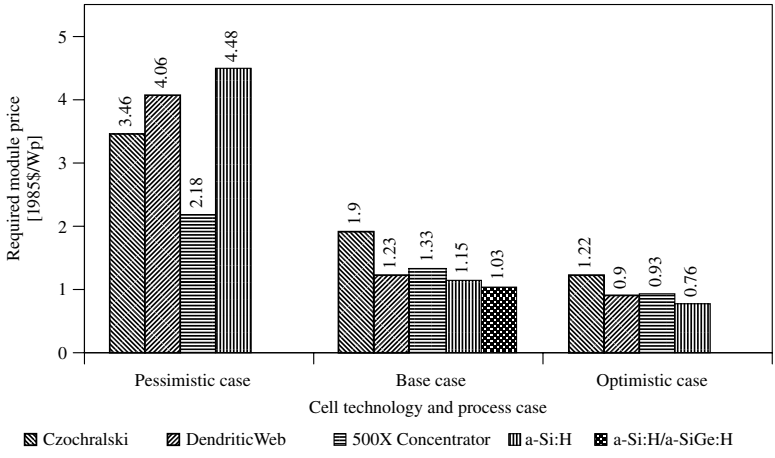


Figure 21.3 Required module price for silicon-cell technologies [3]. Copyright © 2002. Electric Power Research Institute. EPRI AP-4369. Photovoltaic Manufacturing Cost Analysis; A Required Price Approach, Vol. 1, 2. Reprinted with Permission

Table 21.3 Czochralski module prices for process and financial cases (1985$/W$_p$)

		Process cases		
		Pessimistic	Base	Optimistic
Financial cases	Pessimistic		1.98	
	Base	3.46	1.90	1.22
	Optimistic		1.80	

This relationship results from the fact that material costs are a large fraction of the required module price, 44.2% for the Czochralski base case, whereas the cost of the required capital for machinery and equipment, which is usable over several years, is a much smaller fraction of the price.

A sensitivity diagram, such as Figure 21.4 for the Czochralski module, illustrates the relative effect of individual process or financial-parameter values on the required module price. Here, the module-price variations for each parameter are plotted with respect to the parameter expressed as a percent of its base-case value. The slopes of the lines are then the price sensitivity to each parameter. For the Czochralski module, the price is most sensitive to the achieved conversion efficiency and the unit cost of the silicon boule. The price is much less sensitive to the unit cost of the glass sheet, wafer thickness, and return on equity (a financial parameter equivalent to the profit for the module manufacturer). Sensitivities for the other cell technologies follow a similar pattern.

One of the most useful results of the study is the illustration of the trade-off between the silicon-utilization and cell-conversion efficiency as reflected in the module price. Figure 21.5 shows the effect of efficiency on the base-case prices for all five cell

Downloaded from https://onlinelibrary.wiley.com/doi/ by <Shibboleth-member@purdue.edu, Wiley Online Library on [25/08/2024]. See the Terms and Conditions (https://onlinelibrary.wiley.com/terms-and-conditions) on Wiley Online Library for rules of use; OA articles are governed by the applicable Creative Commons License

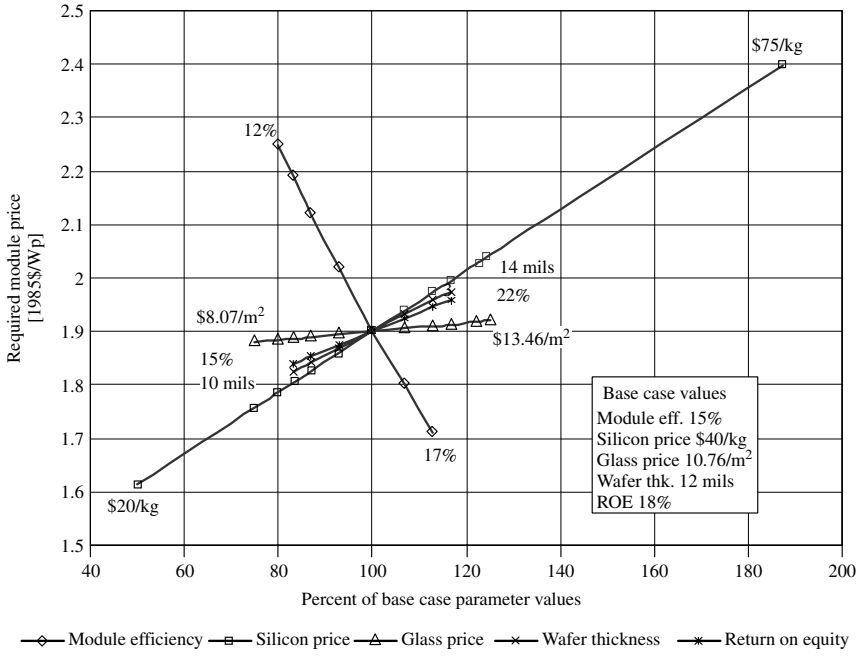


Figure 21.4 Sensitivity of Czochralski required module price to selected parameters [3]. Copyright © 2002. Electric Power Research Institute. EPRI AP-4369. Photovoltaic Manufacturing Cost Analysis; A Required Price Approach, Vol. 1, 2. Reprinted with Permission

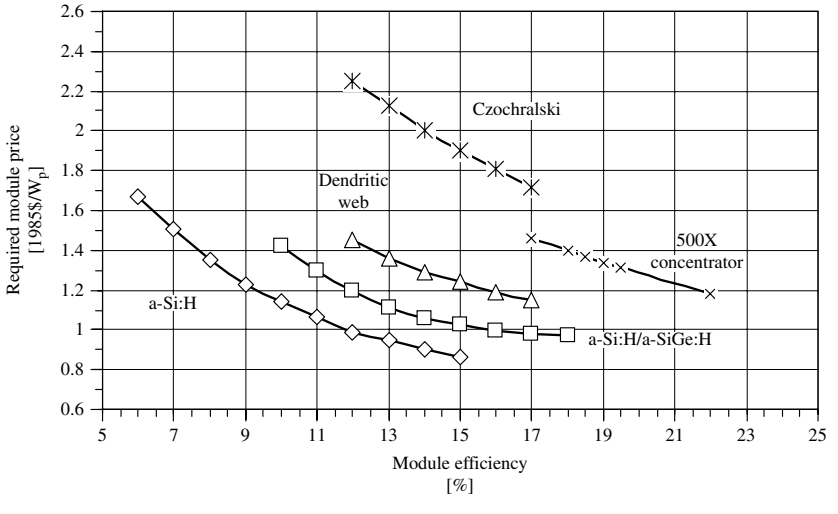


Figure 21.5 Effect of cell technology and efficiency on module price

Downloaded from https://onlinelibrary.wiley.com/doi/ by <Shibboleth-member@purdue.edu, Wiley Online Library on [25/08/2024]. See the Terms and Conditions (https://onlinelibrary.wiley.com/terms-and-conditions) on Wiley Online Library for rules of use; OA articles are governed by the applicable Creative Commons License

technologies. Silicon requirements vary significantly with the choice of a cell technology and its associated cell-fabrication process. Cell-conversion efficiency is also significantly different among the cells made by different processes, and these efficiency differences are inherent in the cell structures. For example, the amorphous cells require much less silicon than Czochralski cells, but the latter have higher efficiency and require less module area to achieve the same rated capacity. How the module prices of the two cell technologies compare is also dependent on the cost of their fabrication processes. Some processing steps are unique to each cell or module as required by their structures and materials, but in other steps the processing is essentially the same. For example, the single- and tandem-junction thin-film cells have many common processing steps. Also, the encapsulation steps for several of these modules are the same.

The similarities and differences in the five cell/module technologies have important implications on cost, measured as $\$/W_p$. In the case of cells fabricated from either Czochralski wafers or dendritic web substrates, the use of silicon for dendritic web cells is less than 20% of that used for Czochralski cells, and silicon is the single most costly material in both processes.

The dendritic web thickness was taken as about 5 mils, whereas the wafer thickness was 12 mils, and the wafers must be sawed from a boule with a kerf loss of 10 mils and an area loss because the boule is round. Dendritic webs are formed in a long strip with no kerf loss and very little area loss. The formation of the dendritic web substrate and the wafer is the primary difference in the two cell/module processes; the remaining steps to produce the cells and modules are essentially the same. The cell efficiency was taken as the same for the Czochralski and dendritic web modules.

Amorphous-silicon cells are produced by an entirely different process that results in a silicon cell that is about 1000 times thinner than the other two flat-plate cells. The "silicon" consumption (actually silane gas) is reduced to the point at which the glass substrate on which the cells are grown is the most costly item of material. However, a-Si cell efficiency has proved to be lower than that for the crystalline cells. In this study, base-case module efficiency using crystalline cells was taken as 15%, and the efficiency for the a-Si module was taken as 10%. For the tandem-junction a-Si cell/module, additional film-growth steps are added to the process, which consumes additional silane, but the material cost is still small. The efficiency for the tandem cell was taken as 15%. The module-fabrication steps are also different from the crystalline-cell modules because all of the cells for a module are deposited on one piece of glass, and cell interconnections are defined by scribing rather than soldering copper straps between cells.

For the concentrator module, the cell is fabricated on Si wafers on equipment comparable to the Czochralski flat-plate cell, but its fabrication was not modeled for this study. There are some cell-design differences that change the cell fabrication somewhat. Instead of modeling with STAMPP, a base-case cell cost of \$2/cell was used for a 1-cm square cell. For comparison, the Czochralski and dendritic web cells were 10-cm square. The fabrication of the 48-cell Fresnel module was modeled as an automated parts fabrication and assembly operation. Since the concentration ratio for the module was 500X, the basic trade-off between the concentrator and flat-plate modules is the more complex mechanical structure of the concentrator with much less silicon-cell area compared to the simpler flat-plate structure with more silicon-cell area. The concentrator also had a

Downloaded from https://onlinelibrary.wiley.com/doi/ by <Shibboleth-member@purdue.edu, Wiley Online Library on [25/08/2024]. See the Terms and Conditions (https://onlinelibrary.wiley.com/terms-and-conditions) on Wiley Online Library for rules of use; OA articles are governed by the applicable Creative Commons License

base-case conversion efficiency of 19.2%. Inherent in the comparison is also the difference in solar insolation applicable to the two technologies.

The required module prices in Figure 21.5 show a significant overlap of all of the cell technologies except Czochralski, which is consistently higher than the others. It is clear that the module-price, in $\$/W_p$, comparison among any of the four less-expensive modules depends greatly on the efficiency achieved. A horizontal line representing, for example, $\$1.20/W_p$ corresponds to about a 9% efficient single-junction amorphous module, but requires about 12% efficiency for the tandem-junction amorphous module, because the latter is more expensive to produce. The same rationale applies to the dendritic web and concentrator modules. The module price range for the Czochralski single-crystal wafer cells does not overlap the other cells, and, for the input data used in the study, it would always be more costly than the others. In hindsight, single-crystal and polycrystalline cells continue to be the most prevalent commercial technology, which perhaps is due to their having achieved more of their performance potential in volume production than have the other technologies. The wafer-cell technologies have simplicity on their side, even at the disadvantage of higher silicon use.

21.2.3.2 Cost of electricity for utility-scale PV plants

A study by the EPRI [4] encompassed both manufacturing-cost modeling and financial analysis for utility-scale PV plants. The study included three systems: a heliostat field focused on a central receiver incorporating a water-cooled silicon-cell array, a field of Fresnel lens concentrator arrays using silicon cells, and a field of fixed-tilt flat-plate module arrays using CIS cells. Brief results of the Fresnel system are given here to illustrate module-price analysis and system-cost development. Total energy costs for all three plants are also given later to illustrate the economic analysis for the three systems.

An extensive design study defined a 50-MW Fresnel system, and included specifications for a 500X Fresnel concentrator module having 48 Fresnel lenses per module, each lens being about 45-inches square with one back-contact Si cell mounted below it. A glass secondary lens was mounted between the Fresnel lens and the cell. The cell efficiency was taken as 27.4%, and module efficiency as 20.7%. Each cell had a passive heat dissipator on the back surface of the assembly. The basic module structural element was a molded plastic box supporting 4 cell/lens units, and 12 of these were assembled into a module (i.e. 48 cells/module). Sixty of these modules were mounted on a tracking structure to form an array. The total array field had 3390 arrays and the plant covered 700 acres.

Manufacturing of the cell and module assembly was modeled with the STAMPP program described previously. It was assumed that the modules would be produced over two years. The Stanford Advanced Back Contact cells were fabricated on 150-mm silicon wafers using conventional cell-fabrication processes. Table 21.4 summarizes the results of the module-cost modeling for a base case, whose results were input to the plant cost computation. The top section of the table shows some basic operating and financial parameters for the module business, and gives the computed module required price as \$320.08 each (1990\$), or $\$1.30/W_p$. Such a cost was indeed optimistic for the time the study was conducted, but it did represent a relatively high annual production volume. A significant amount of automation was employed, especially in the assembly of the module. A breakdown of module cost (taken from the income statement of the business) is shown in

Downloaded from https://onlinelibrary.wiley.com/doi/ by <Shibboleth-member@purdue.edu, Wiley Online Library on [25/08/2024]. See the Terms and Conditions (https://onlinelibrary.wiley.com/terms-and-conditions) on Wiley Online Library for rules of use; OA articles are governed by the applicable Creative Commons License

Downloaded from https://onlinelibrary.wiley.com/doi/ by <Shibboleth-member@purdue.edu, Wiley Online Library on [25/08/2024]. See the Terms and Conditions (https://onlinelibrary.wiley.com/terms-and-conditions) on Wiley Online Library for rules of use; OA articles are governed by the applicable Creative Commons License

Table 21.4 Fresnel module price summary, base case [4]

Annual plant production (module/year)	101 700
Unit price (1990$/module)	320.076
Base year	1989
Simulation length (years)	10
Plant capacity factor (%)	100.000
Annual plant operating time (h/year)	8519
Maximum number of shifts per working day	3
Required return on investment (fraction)	0.200
Debt to equity ratio (fraction)	0.250
Combined fed/state income tax rate (fraction)	0.340

Product price components in first full year of production (end of year dollars)

Component	1990$/module	% of total
Annual sales	320.076	100.00
Annual manufacturing expense	289.366	90.41
Annual direct material expense	219.758	68.66
Annual direct labor expense	14.592	4.56
Annual manufacturing overhead	55.016	17.19
Net annual work-in-process	0.297	0.09
Net finished goods inventory	0.000	0.00
Selling & administrative expense	9.155	2.86
Corporate income taxes payable	6.679	2.09
Excess revenue (interest earned)	12.966	0.50
Annual net income	1.612	4.05

Initial work station equipment cost ($1989)	4 260 447
Initial facility cost ($1989)	3 158 375
Total manufacturing area (sq ft)	39 453
Total nonmanufacturing area (sq ft)	11 532
Total facility area (sq ft)	50 985
Total land cost ($1989)	124 036
Total direct manufacturing labor (# workers)	56
Total indirect manufacturing labor (# workers)	19
Total indirect nonmanufacturing labor (# workers)	43
Total plant labor (# workers)	118

Copyright © 2002. Electric Power Research Institute. EPRI TR-101255. Engineering and Economic Evaluation of Central-Station Photovoltaic Power Plants. Reprinted with Permission

the center section of Table 21.4. Direct manufacturing costs are about 90% of the total cost, with materials accounting for 69%. The 17% contribution of manufacturing overhead is composed of manufacturing supervision labor, equipment and facilities depreciation, plus other smaller items, but about half of the 17% is the R&D budget assigned to the business, which corresponds to 8.5% of sales. In the bottom section of Table 21.4 are the costs of process equipment and buildings, and the number of people employed in the business.

Any study of future costs benefits from an examination of the sensitivity of the result to different values of critical input parameters, because it contributes to understanding the

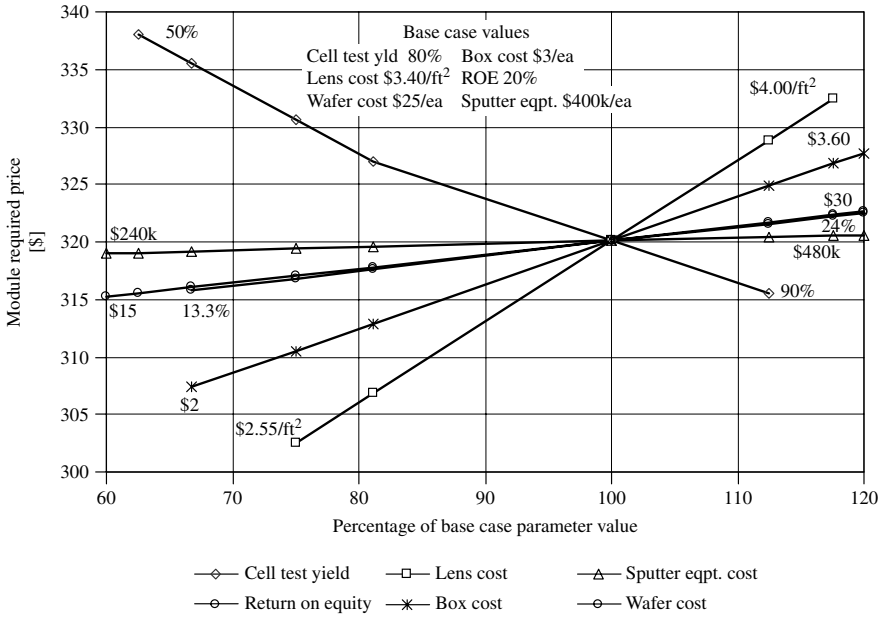


Figure 21.6 Effect of selected parameters on Fresnel module price (1990$) [4]. Copyright © 2002. Electric Power Research Institute. EPRI TR-101255. Engineering and Economic Evaluation of Central-Station Photovoltaic Power Plants. Reprinted with Permission

risk in the choice of inputs. Figure 21.6 shows the effect of different values of certain materials, equipment, and financial costs on module required price. Cost components are plotted on the abscissa as a percentage of their base case value, which means that the slope of the lines represents a relative sensitivity of module price to the parameter change (absolute values at the extremes are also shown for reference). The output of the STAMPP model identified the Fresnel lens and the molded box as the two largest material costs, at 31% and 17% of material costs, respectively. Silicon wafers, at 5%, were another significant cost. Sensitivities to a fairly wide range of these costs are shown, with the extreme variation in module price being less than 6%. By way of comparison, the price of the most expensive cell-processing equipment, sputtering, had a much smaller impact on module cost. This is a typical result in such studies, resulting from the depreciation of the equipment over several years. Cost of money, represented by return on equity (ROE), has about the same impact as wafer cost. Process yield for each workstation is a parameter in STAMPP. For cell manufacturing, the yield at cell test is critical, and the base case cell yield for the study was 80%. Figure 21.6 shows cell yield to have a large impact relative to some other parameters.

The total capital cost of the Fresnel lens plant in Table 21.5 reflects the accounting system of the study sponsor, EPRI. The $\$1.62/W_p$ cost of the PV modules includes shipping and installation, and is 50% of the total system capital cost. The installed array-structure cost brings the total collector cost to about 73.5% of the system cost. The power conditioning and balance-of-plant costs add another 5.5%, leaving about 20% of the cost

Petitioner Canadian Solar (USA) Inc., Ex. 1035, p. 2377

Downloaded from https://onlinelibrary.wiley.com/doi/ by <Shibboleth-member@purdue.edu, Wiley Online Library on [25/08/2024]. See the Terms and Conditions (https://onlinelibrary.wiley.com/terms-and-conditions) on Wiley Online Library for rules of use; OA articles are governed by the applicable Creative Commons License

Table 21.5 Total capital requirements for central station plants [4] 3rd Quarter 1990$, Carrisa Plains Site

	Fresnel lens		Central receiver		CIS flat plate	
	[$(10^6)]	[$/Watt]	[$(10)^6]	[$/Watt]	[$(10^6]	[$/Watt]
Buildings, site improvement	1.20	0.02	1.9	0.04	1.23	0.02
Array structure	37.92	0.76			13.38	0.27
PV modules	80.80	1.62			66.91	1.38
Heliostat system			53.30	1.07		
Receiver system			18.80	0.38		
Receiver tower			6.30	0.13		
Power conditioning unit	5.92	0.12	4.30	0.09	5.85	0.12
Balance of plant	3.09	0.06	16.40	0.33	7.06	0.14
Master control system	0.12	0.00	0.80	0.02	0.08	0.00
Total field cost	129.10	2.58	101.80	2.04	94.50	1.91
Engineering. & const. Management	5.20	0.10	6.10	0.12	2.80	0.06
Owner's costs	5.40	0.11	5.40	0.11	2.90	0.06
Contingencies	14.20	0.29	19.70	0.39	9.80	0.20
Total plant cost	153.90	3.08	133.00	2.66	110.00	2.22
Escalation (mixed year dollars)	(2.90)	(0.06)	(2.50)	(0.05)	(2.10)	(0.04)
Total cash expended (mixed year dollars)	151.00	3.02	130.50	2.61	107.90	2.18
Allowance for funds during const. (mixed year dollars)	6.80	0.14	5.80	0.12	4.80	0.10
Total plant investment	157.80	3.16	136.30	2.73	112.70	2.27
Preproduction costs	3.20	0.06	2.90	0.06	2.30	0.05
Inventory capital	0.80	0.02	0.70	0.01	0.60	0.01
Land	0.20	0.00	0.30	0.01	0.20	0.00
Total capital requirement	162.00	3.24	140.00	2.80	116.00	2.34

Copyright © 2002. Electric Power Research Institute. EPRI TR-101255. Engineering and Economic Evaluation of Central-Station Photovoltaic Power Plants. Reprinted with Permission

associated with engineering, construction management, cost of money, contingencies, and so on. The contingency item accounts for uncertainties in system performance and unaccounted costs in the design. Later systems of the same design may avoid some of the contingency cost. The total system cost in Table 21.5 is equivalent to the present worth of capital expenditures during the construction of the systems. The central receiver plant and the CIS flat plate plant both turn out to have less-expensive collector costs than the Fresnel lens plant, and the resultant total capital requirements are also less by 14% and 28%, respectively. The central receiver plant has a forced convection, water-cooling system that adds significantly to the system cost relative to the other two plants.

The remaining steps in computing LEC (see equation (21.14)) are summarized in Table 21.6. The typical energy output was calculated from solar-insolation data and the performance parameters of the systems using computer codes. The energy outputs for

Downloaded from https://onlinelibrary.wiley.com/doi/ by <Shibboleth-member@purdue.edu, Wiley Online Library on [25/08/2024]. See the Terms and Conditions (https://onlinelibrary.wiley.com/terms-and-conditions) on Wiley Online Library for rules of use; OA articles are governed by the applicable Creative Commons License

Table 21.6 Annual performance and energy cost summary for central station plants [4] Constant 1990$, Carrisa Plains Site

	Fresnel lens	Central receiver	CIS flat plate
Average annual performance			
Energy output (MWh)	140 100	125 000	112 000
Capacity factor	32.0%	28.5%	25.8%
Annual energy efficiency	18.8%	11.3%	9.9%
Annual expenses (10^6)			
Capital charge	16.69	14.42	11.95
Operation & maintenance expense	0.61	1.197	0.18
Total	17.30	16.39	12.13
30-year levelized energy cost ($/kWh)			
Capital charge	0.119	0.115	0.106
Operation & maintenance costs	0.004	0.016	0.002
Total ($/kWh)	0.123	0.131	0.106

Copyright © 2002. Electric Power Research Institute. EPRI TR-101255. Engineering and Economic Evaluation of Central-Station Photovoltaic Power Plants. Reprinted with Permission

the systems reflect both the efficiencies and the collector characteristics of the different system designs. The annual capital charge is the annualized amount of the total capital requirement, using a CRF of 10.2%. Levelized energy cost is the total annual expense divided by the annual energy output. It is interesting that the lowest LEC corresponds to the CIS flat-plate system that has the lowest efficiency and incorporates the simplest collector technology. (Cell efficiency for the CIS cell was taken as 15%.) The relationship among the LECs for the systems also points out that cell and module efficiencies, while very important in system performance, do not by themselves determine energy cost. Other system-design factors are also very important, and within limits, override the effect of efficiency on energy cost.

21.2.3.3 Gallium arsenide cells in power systems

GaAs cells have been developed and used extensively for space applications, but traditionally have been considered too expensive for terrestrial applications despite their high efficiency. These compound semiconductor cells are fabricated by epitaxial growth, either on GaAs wafers or on Ge wafers, the latter being a more recent development. The cost of GaAs wafers is a major factor in the cost of cells, and Ge wafers are projected to be less expensive by more than an order of magnitude. The question that arises is whether GaAs cells could be competitive with Si cells for utility-scale terrestrial systems, particularly if grown on Ge wafers. To address this question, the cost study in the previous section, as it relates to the Fresnel lens plant, was extended to determine the cost of energy for the same plant using GaAs cells of several different designs [5].

Two cells were considered: a single-junction GaAs cell, and a tandem-junction GaInP/GaAs cell. These GaAs cells are designed as concentrator cells, and could be considered for the same kinds of applications as the Si concentrator cells in the Fresnel lens

Petitioner Canadian Solar (USA) Inc., Ex. 1035, p. 2379

Downloaded from https://onlinelibrary.wiley.com/doi/ by <Shibboleth-member@purdue.edu, Wiley Online Library on [25/08/2024]. See the Terms and Conditions (https://onlinelibrary.wiley.com/terms-and-conditions) on Wiley Online Library for rules of use; OA articles are governed by the applicable Creative Commons License

Table 21.7 GaAs cell and module price (1994$) [5]

Cell/wafer	Cell efficiency	$/Module (48 cells)	$/48 cells
SJ/GA-SC	25	741.14	459.94
	30	741.54	460.50
SJ/Ge-SC	25	447.01	156.52
	30	450.40	159.11
SJ/Ge-PC	25	404.19	111.28
	30	407.58	113.79
TJ/GA-SC	30	745.96	464.68
	35	748.56	466.99
TJ/Ge-SC	30	456.33	164.51
	35	456.31	164.90
TJ/Ge-PC	30	413.50	119.11
	35	413.49	119.51

Note: SJ = single junction; TJ = tandem junction; SC = single-crystal; wafer PC = polycrystalline wafer. © 1994 IEEE

module of the prior study [4]. The manufacturing processes for each cell were defined using three different wafers: single-crystal GaAs, single-crystal Ge, and polycrystalline Ge. Modules incorporating each of the six combinations were modeled using the same STAMPP model as for the Fresnel lens module in the prior study. Further, a range of cell efficiencies for the GaAs cells was examined because the GaAs technology was not as well developed as the Si technology. In order to compare the annual energy production from GaAs plants with Si plants, the number of modules required for a 50-MW plant was calculated and the cost of modules computed with STAMPP at the required volume, as shown in Table 21.7. The total capital requirements, as shown in Table 21.5 for the Si plant and adjusted to 1994$, were then scaled appropriately for the number of GaAs modules.

The price of GaAs cells, whether single- and tandem-junction, shown in Table 21.7 is heavily influenced by the choice of GaAs or Ge substrate. Cells grown on Ge-PC wafers are roughly four times less expensive than cells grown on GaAs-SC wafers. However, the prices of modules incorporating these cells differ by only a little less than a factor of two due to the fact that several substantial module-cost components are the same regardless of the cell structure. The least expensive module cost of $413.50 in Table 21.7 for TJ/Ge-PC cells compares to the $328.42 for a module incorporating Si cells (see Table 21.4, escalated to 1994$). Cell efficiency for the same cell structure in Table 21.7 has little effect on module price. Indeed, module price is, in some cases, just slightly higher for the higher efficiency cell than the lower one (e.g. SJ/Ge-PC at 25% versus 30%). This is a result of the modeling procedure in which the number of modules produced was just sufficient for the 50-MW power plant, being fewer at higher cell efficiency, and the allocation of elements of cost by the STAMPP model to a fewer number of modules.

The reduction in cell and module prices in Table 21.7 reflects a span of about 15:1 in wafer costs between GaAs-SC and Ge-PC wafers, as indicated in Table 21.8. When GaAs cells are grown on the GaAs wafer, the cost of the wafers is almost 60% of the module materials cost, but when a Ge-PC wafer is used, then the wafer contributes to only

Downloaded from https://onlinelibrary.wiley.com/doi/ by <Shibboleth-member@purdue.edu, Wiley Online Library on [25/08/2024]. See the Terms and Conditions (https://onlinelibrary.wiley.com/terms-and-conditions) on Wiley Online Library for rules of use; OA articles are governed by the applicable Creative Commons License

Table 21.8 Module materials cost drivers, GaAs tandem-junction cells [5]

	Substrate (GaAs & Ge = 4″, Si = 6″)			
	GaAs	Single-crystal Ge	Polycrystalline Ge	Si
Wafer cost/each	$360.46	$64.37	$23.62	$29.94
Material	*Percentage of total module materials cost*			
Wafer	59.8	20.4	8.6	5.3
Module box ($3.59/each)	6.9	13.2	15.1	17.4
Heat sink ($0.52/each)	4.0	7.7	8.8	10.1
Fresnel lens ($4.07/ft^2)	12.2	23.3	26.8	14.3

Source: © 1994 IEEE

about 9% of the module materials cost. The latter case is very similar to the materials cost contributions for the Si module, where the wafer cost is not the largest single contributor. Using Ge wafers would thus be a major step in making GaAs cells competitive.

When the module prices in Table 21.7 are incorporated into the 50-MW power plant, capital requirements (Table 21.5) by adjusting these costs for the changes in field size resulting from the GaAs conversion efficiencies, the cost of energy generated, expressed as LEC, can be calculated for the various cell structures in Table 21.7 (see Figure 21.7). These GaAs-based energy-production costs are compared to that of Si-based energy-production costs from the previous study [4] as summarized in Table 21.6. Since none of the GaAs module prices, ranging from $741 to $413, is as low as the Si module price of $328, the LECs in Figure 21.7 essentially show the trade-off of the more efficient (27.5% to 35%) but higher cost GaAs modules with the less efficient (27.4%) but lower

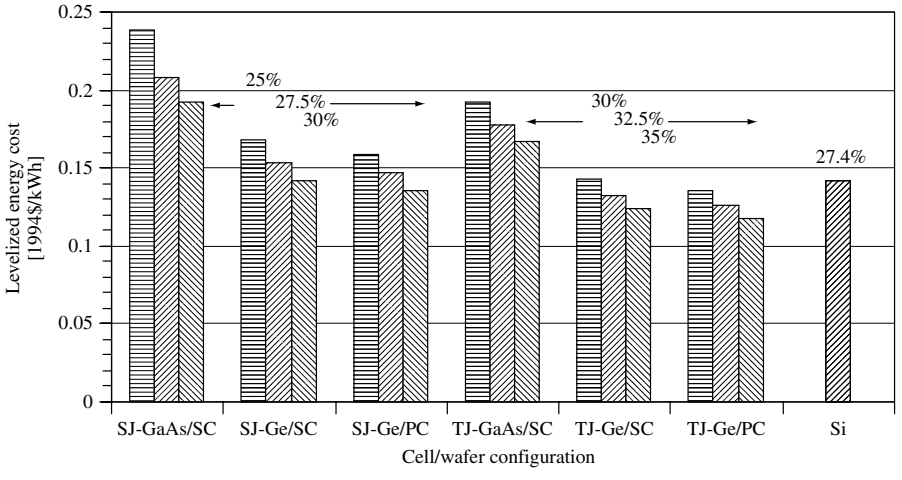


Figure 21.7 Cost of energy produced by 50 MW central station Fresnel lens plants using GaAs cells [5]. © 1994 IEEE

Downloaded from https://onlinelibrary.wiley.com/doi/ by <Shibboleth-member@purdue.edu>, Wiley Online Library on [25/08/2024]. See the Terms and Conditions (https://onlinelibrary.wiley.com/terms-and-conditions) on Wiley Online Library for rules of use; OA articles are governed by the applicable Creative Commons License

cost Si modules. The most costly GaAs technology (SJ/GA-SC), even at its highest projected efficiency of 30%, has an LEC of $0.192/kWh compared to the LEC of the Si technology of $0.142/kWh. The least-costly GaAs technology (TJ/Ge-PC) has an LEC of $0.118/kWh at its highest efficiency of 35%, which is less than the Si LEC. The slightly more costly TJ/GA-SC technology still has a lower LEC ($0.124/kWh at 35%) than the Si module, and this GaAs structure using the single-crystal wafer is more likely to achieve the 35% efficiency than the polycrystalline wafer cell.

21.3 ENERGY PAYBACK AND AIR POLLUTION REDUCTION

PV systems convert the free solar energy resource into valuable electric energy. However, it has long been noted that energy is consumed in the manufacture of PV conversion hardware. That is, there is an energy cost to produce energy. The mining, refining, and purification of semiconductor materials is energy intensive, and energy is consumed in the manufacture of all the other materials in a PV system, such as glass, steel, aluminum, copper, and plastic. In addition to the energy content of the materials incorporated directly in the module, support structures, and balance of system (BOS) components, there is an energy content in the equipment that produces all the PV system components. Energy is also consumed in transporting and erecting a PV system at its operating site. During the life of a PV system, usually taken as 20 to 30 years, energy is produced as a return on the energy "invested" in its creation. The long-raised question is: how much more energy does the PV system generate than it takes to produce it; or, is there a net energy benefit to society from PV systems? The answer is usually stated as "energy payback," which is the number of years that is required to repay the energy content of the PV system with its delivered electricity. Energy payback for PV systems, measured in years, should ideally be a small fraction of the system life in years. In fairness to PV, it should also be noted that fossil energy systems, in addition to the energy consumed as they operate to produce electricity, also have an energy content in their power-plant hardware. In addition, the fuel itself has an energy content associated with the exploration, development, recovery, and transportation to the generation site. Thus, the terms of comparison for energy payback between PV and other systems need to be carefully defined if they are to be meaningful.

The energy-payback question needs to be differentiated from whether a PV system pays for itself economically (financially), which is a primary subject of this chapter. The question of economic benefit is adequately answered when the cost of all materials, equipment of production, and capital are accounted for. These costs include the cost of the energy content of all the elements of the system. Given that economic criteria are met, the energy payback question is essentially an ecological one; that is, does the creation of PV systems that generate substantially more energy than is consumed to produce them represent a wise use of fossil resources? A related issue is the reduction in greenhouse gases that results from the generation of electricity with PV rather than with fossil-fuel-based generation. If governments impose financial penalties on fossil generation or give credits for solar generation, then financial benefits can be introduced into the economic evaluation. To a degree this is implicit in the process when, for example, the cost of exhaust scrubbers for fossil plants is included in the economic comparison. Moreover, if solar energy is the source for producing PV systems, the ecological consequences are

Downloaded from https://onlinelibrary.wiley.com/doi/ by <Shibboleth-member@purdue.edu, Wiley Online Library on [25/08/2024]. See the Terms and Conditions (https://onlinelibrary.wiley.com/terms-and-conditions) on Wiley Online Library for rules of use; OA articles are governed by the applicable Creative Commons License

diminished. Given the small amount of PV generation capacity in service today relative to other electric generation capacity, the primary concern for energy payback is in long-term energy planning in relation to ecological impact.

The issue of energy payback has been examined quantitatively, and a good bibliography is given in [6]. Energy payback is determined by the four basic factors mentioned below:

- The design of the PV system, including all components
- The location of the system
- The life of the PV system
- The portion of the manufacturing energy-consumption chain included in the payback.

System design determines the system conversion efficiency and system power level, as well as defining the energy content of the hardware. The system location determines the incident energy for the system, which, coupled with the system life, determines the total energy delivered by the PV system. The total energy content of the PV system depends on just how far back in the energy chain the analysis goes. For example, does the chain go back to the mining, transportation, refining, and fabricating of a material, and include every piece of equipment used at every link of the chain? In most cases, PV material energy content is based on prior studies of the energy content of basic materials. Special considerations are sometimes incorporated; for example, much of the crystalline PV production is currently based on using scrap-refined Si from the microelectronics industry, so it may be reasonable to ignore the energy content of the scrap material.

In a summary of energy payback studies, the US National Renewable Energy Laboratory (NREL), states that "(E)nergy payback estimates for rooftop PV systems boils down to 4, 3, 2, and 1 years: 4 years for systems using current multicrystalline-silicon PV modules, 3 years for current thin-film modules, 2 years for future multicrystalline modules, and 1 year for future thin-film modules." These data assume a 30-year life. Multicrystalline modules have a longer energy payback because they have a much larger content of silicon than thin-film modules. Shorter payback for future modules is predicated on improved manufacturing processes and higher efficiencies.

NREL credits these results to the Dutch researcher Erik Alsema [7]. His data are based on estimates of 600 kWh/m^2 for the near-future, frameless, single-crystal silicon PV modules and 420 kWh/m^2 for multicrystalline modules. With a 12% conversion efficiency and a solar insolation level of 1700 kWh/m^2/year, Alsema calculated the 4-year payback for current multicrystalline modules. The future payback of 2 years for multicrystalline modules was based on a 14% efficiency and solar-grade silicon feedstock.

For thin-film modules, amorphous-silicon paybacks are a good proxy for all material systems (including copper indium diselenide, cadmium telluride) because the major energy content is in the substrate, usually glass, and the deposition process plus other facilities. The films are so thin that they have relatively little energy content [8].

Knapp and Jester [6] examine the energy payback for both actual copper indium diselenide (CIS) and single-crystal silicon processes and modules produced using measured data. The data that were collected from plants operated by Siemens Solar Industries and reported in [6] assume that the CIS plant operated at capacity. Energy content of

Downloaded from https://onlinelibrary.wiley.com/doi/ by <Shibboleth-member@purdue.edu, Wiley Online Library on [25/08/2024]. See the Terms and Conditions (https://onlinelibrary.wiley.com/terms-and-conditions) on Wiley Online Library for rules of use; OA articles are governed by the applicable Creative Commons License

production equipment, production facilities, and transportation of goods to and from the facility were excluded from the result. Using a solar insolation of 1700 kWh/m^2/year, and assuming an 80% correction for the system losses, the single-crystal silicon module had an energy payback of 4.1 years and the CIS module's payback was 2.2 years.

Given the predicted energy paybacks of, say, 1 to 5 years for PV systems, and their life of up to 30 years, payback is not a negligible factor in the overall energy-planning process, but neither is it a prohibitive one. Gradual improvements in conversion efficiency and improvements in manufacturing techniques can further reduce its impact over time.

The literature that addresses energy payback also addresses the contribution of PV systems in reducing greenhouse gases [7, 8]. "An average US household uses 830 kWh of electricity per month. On an average, producing 1000 kWh of electricity with solar power reduces emissions by nearly 8 pounds of sulfur dioxide, 5 pounds of nitrogen oxides, and more than 1400 pounds of carbon dioxide. During its 28 years of clean energy production, a rooftop system with 2-year payback and meeting half of a household's electricity use would avoid conventional electrical plant emissions of more than half a ton of sulfur dioxide, one-third of a ton of nitrogen oxides, and 100 tons of carbon dioxide." (Though not stated, we assume these comparisons are of solar versus coal-fueled generation.) Again, if the cost of removing these from the conventional emissions is quantified, the cost saving can be included in an economic assessment.

21.4 PROSPECTS FOR THE FUTURE

Photovoltaic cells, modules, and systems have undergone intensive development in the 25 years immediately prior to the twenty-first century. Significant improvements in performance and reductions in cost per unit area have been made. The variety of PV cells and module technologies commercially available or under development has expanded greatly, although crystalline-silicon technology still predominates. Cost-effective applications that capitalize on the unique characteristics of PV systems have been implemented. Many other applications have been installed that benefited from subsidies from utilities, government, or economic-development institutions. A lot of progress has been made, and yet PV supplies only a tiny fraction of the electric generation market.

A recent survey [9] by *Photon International* magazine puts the annual worldwide production of Photovoltaics at 401.4 MW_p in the year 2001. There are about 59 PV module manufacturers worldwide. However, the industry has lost more than US$3 billion over its first 25 years, according to the President and CEO of Siemens Solar in 1998[10]. He further states that two-thirds of the industry is still dependent on some kind of subsidy. Europe, Japan, and the United States each supply major portions of this production. The corporate landscape has been in a constant state of change over these years. Many small companies started up and a few large corporations entered the business. Many of the smaller firms have been absorbed by large corporate conglomerates, but a few have managed to stay in the business and grow. In recent years, some of the world's major corporations have become major players in the PV industry. The top ten producers in 2001 were listed as follows [9]:

1. Sharp (a major Japanese electronic-equipment maker, their solar cells are primarily integral to electronics products) 74.0 MW_p

Downloaded from https://onlinelibrary.wiley.com/doi/ by <Shibboleth-member@purdue.edu>, Wiley Online Library on [25/08/2024]. See the Terms and Conditions (https://onlinelibrary.wiley.com/terms-and-conditions) on Wiley Online Library for rules of use; OA articles are governed by the applicable Creative Commons License

2. BP Solar (a unit of British Petroleum, that merged with the US firm Solarex and presently has plants in US, Spain, Australia, and India) 54.4 MW_p
3. Kyocera (a major Japanese electronics, equipment, and materials company) 54.0 MW_p
4. Siemens and Shell Solar GmbH (investments by German/Dutch conglomerate Shell and Siemens AG whose main production is in the US) 48.3 MW_p
5. AstroPower (independent US manufacturer) 26.0 MW_p
6. RWE Solar (a unit of the German Utility RWE that merged with ASE Americas 22.7 MW_p
7. Isofoton (independent Spanish manufacturer of PV and solar thermal technology) 18.7 MW_p
8. Sanyo (a major Japanese maker of electronic consumer products, semiconductors, batteries, etc; PV products made by Solec International division) 16.0 MW_p
9. Mitsubishi (a Japanese conglomerate providing a wide range of products and services) 14.0 MW_p
10. Photowatt (a unit of Matrix Solar Technologies, owned by a Canadian corporation ATS) 13.5 MW_p.

Despite the changes in the makeup of the industry, progress has been sustained by gains in performance and reductions in cost. PV module prices in $/$W_p$ declined by an order of magnitude over the nearly 20-year period ending in 1994[11]. This experience, shown in Figure 21.8, is based primarily on data for crystalline-silicon modules, but is said to be representative of other flat-plate module technologies as well. The projection beyond 1994 is based on a fit of the data for module price versus cumulative

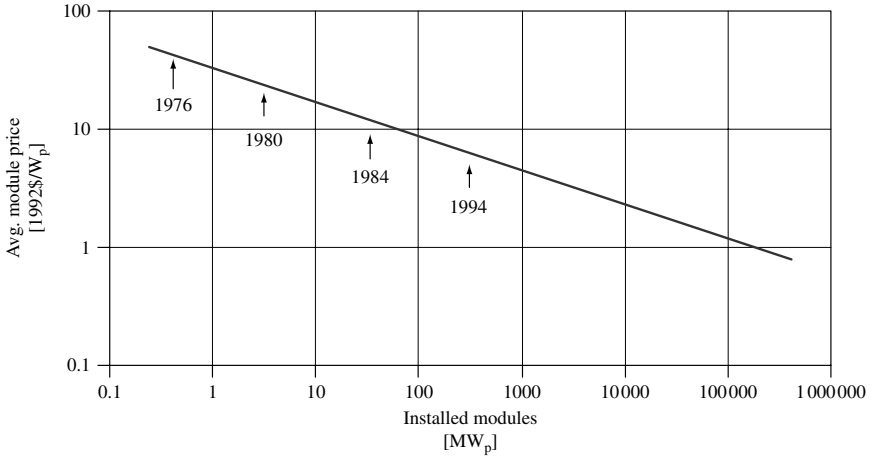


Figure 21.8 PV module price trends. Adapted from [11]. Copyright © 2002. Electric Power Research Institute. EPRI TR-109496. Renewable Energy Technology Characterizations, Topical Report

Downloaded from https://onlinelibrary.wiley.com/doi/ by <Shibboleth-member@purdue.edu>, Wiley Online Library on [25/08/2024]. See the Terms and Conditions (https://onlinelibrary.wiley.com/terms-and-conditions) on Wiley Online Library for rules of use; OA articles are governed by the applicable Creative Commons License

production. Significant departures from the projection might result from new technological development, such as thin-film modules or concentrator technology.

Some recent experiences [12] with PV systems with capacities in the range of 70 to 236 kW_p showed that system costs dropped by 14% from 1996–1997 to 1998–1999 ($9.77/$W_p$ to $8.46/$W_p$). These systems included both fixed and one-axis tracking systems, which were mounted both on buildings and on the ground, and included modules and inverters from several manufacturers. Three of the most recent projects had installed costs below $7/$W_p$.

Siemens has stated [10] that it is planning on a long-term annual growth rate of 15% for installed PV. Their projection is that a 15% to 25% rate would result in PV contributing to 1% of the world's electricity between 2025 and 2040, which they estimate as 300 TWh in 2025. They state that one-third of this energy could provide for the basic needs of two-billion people not served by a grid.

Another view of the potential for PV can be gained from some figures published by the US government. Recent progress and long-term goals for the US PV program [13] are shown in Table 21.9. Meeting these goals would increase cumulative US sales by the year 2030 to 20 times the year 2000 level, and correspond to about a 12% compounded annual rate of sales growth. The average annual sales from 1996 to 2000 would be about 65 MW/year, and from 2001 to 2030 would be roughly 315 MW/year. The US share of the world market for PV was about 41% in 1995[13]. If this share was maintained till 2030, the cumulative capacity would be about 25 GW. Assuming an average of 2000 h/year of sunlight, the annual generated energy would be 50 TWh by 2030. This is substantially lower than the Siemens estimate given above, but the difference is largely explained by the difference in the 12% annual growth rate and the Siemens estimate of 15% to 25%. Starting at the same 500-MW cumulative sales in 2000, using a constant 41% market share and 2000 h/year of sunlight, a 15% growth rate results in about 80 TWh/year of generated energy. Using a 25% growth rate, the energy is about 645 TWh. There is obviously a lot of uncertainty in making such projections, and the truth no doubt lies somewhere in the range of these estimates.

Some additional insight into the potential contribution of PV to the world's electric-energy needs can be had from data published by the US Energy Information Administration [14]. The world's net electricity consumption in 1999 was 12 833 TWh. Of this total, industrialized countries consume 59%, eastern Europe and the former Soviet Union, consume 11%, and developing countries account for 30%. If the cumulative PV capacity

Table 21.9 Photovoltaic progress and program goals (1995$) US department of energy [13]

	1991	1995	2000	2010–2030
Electricity price (¢/kWh)	40–75	25–50	12–20	<6
Module efficiency[a] (%)	5–14	7–17	10–20	15–25
System cost ($/$W_p$)	10–20	7–15	3–7	1–1.5
System lifetime (years)	5–10	10–20	>20	>30
US cumulative sales (MW)	75	175	400–600	>10 000

[a]Range of efficiencies for commercial flat-plate and concentrator technologies

Downloaded from https://onlinelibrary.wiley.com/doi/ by <Shibboleth-member@purdue.edu, Wiley Online Library on [25/08/2024]. See the Terms and Conditions (https://onlinelibrary.wiley.com/terms-and-conditions) on Wiley Online Library for rules of use; OA articles are governed by the applicable Creative Commons License

in 2000 was 1220 MW (500 MW divided by 41%), an estimate of the energy generated will be 2.4 TWh, or about 0.02% of the world consumption. The projected average annual growth of electricity consumption over the period 1999 to 2020 in [14] is 2.7% worldwide, resulting in consumption of 22 230 TWh in 2020. Extrapolating this to 2025 as 25 398 TWh, the contribution of PV at 300 TWh would be 1.2%. While this is a small fraction, it still could, as the Siemens article points out, make a significant contribution to the lives of people where conventional grid-connected electricity is not available.

Looking at these varied projections of growth in PV sales, it is clear that the penetration of the future electricity market by PV systems is difficult to predict. It depends on many factors whose outcomes are uncertain, among them being the following factors:

- Continued progress in performance and cost reduction of PV systems. This is perhaps the most certain of the factors to be achieved, assuming that the deep-pocket firms now engaged in PV system development continue to be involved. Participation by government and industry associations through support of research and development will also contribute to this factor.
- Increase in the cost of fossil fuels. Numerous predictions made in the past of the cost of oil rising well above US$30 per barrel have failed to materialize on any consistent basis. The price of oil is a strong determinant of the cost of electricity that competes with PV electricity. The price of oil, largely determined by the international cartel, can only be raised so far without decreasing their market size. Major new fields in the Caspian Sea area or elsewhere will be an influence if they materialize, but such finds will become less likely over time.
- Increases in environmental costs for fossil-fuel-based electricity. Global warming concerns may prompt added costs of production due to greenhouse gas control or regulatory constraints or restrictions on competing uses, especially as the energy use of developing nations goes up. These factors will make PV more competitive.
- Accommodation of users to the variable character of the PV source. PV delivers energy when the sun shines, but there is much demand at other times. This characteristic can be overcome by the integration of PV into utilities, by sharing PV capacity among groups of users (a utility of a different sort), by adding storage to the PV system (e.g. electric storage batteries, hydrogen production and storage, hydroelectric storage), or by lifestyle changes. All of these are possible, but each accommodation has its own barriers.
- The need for off-grid electric power is very large and the capacity required for individual sites is usually small. PV systems are more modular than almost any other source, and they provide insurance against rising fossil-fuel prices. If ways can be found to make them affordable, PV has an enormous off-grid market.

All of these projections suggest that PV systems will continue to increase their market penetration and make a useful contribution to energy supply over the next several decades. The likelihood of their becoming an economically significant fraction of the energy supply, say 5% or more, within the next 20 to 30 years appears to be small at this point. Such an event will require fundamental changes in the way energy is delivered, and those changes will have to be driven by economic and environmental forces beyond the control of the PV industry.

Downloaded from https://onlinelibrary.wiley.com/doi/ by <Shibboleth-member@purdue.edu, Wiley Online Library on [25/08/2024]. See the Terms and Conditions (https://onlinelibrary.wiley.com/terms-and-conditions) on Wiley Online Library for rules of use; OA articles are governed by the applicable Creative Commons License

REFERENCES

1. Smith G, *Engineering Economy: Analysis of Capital Expenditures*, 2nd Edition, Chap. 4, The Iowa State University Press, Ames, IA (1977).
2. Stevens Jr. G, *The Economic Analysis of Capita Investments for Managers & Engineers*, Chap. 5, Reston Publishing, Reston, VA (1983).
3. Whisnant R, Wright S, Champagne P, Brookshire K, *Photovoltaic Manufacturing Cost Analysis; A Required Price Approach*, Vol. 1, 2, EPRI AP-4369, Electric Power Research Institute, Palo Alto, CA (1986).
4. Stolte W, *Engineering and Economic Evaluation of Central-Station Photovoltaic Power Plants*, TR-101255, Electric Power Research Institute, Palo Alto, CA (1992).
5. Whisnant R *et al*., "Silicon and GaAs/Ge Concentrator Power Plants: A Comparison of Cost of Energy Produced", *Proc. IEEE First World Conference on PV Energy Conversion*, 1103–1106 (1994).
6. Knapp K, Jester T, "An Empirical Perspective on the Energy Payback Time for Photovoltaic Modules", *Proc. Solar 2000 Conference* (Madison, WI, 2000).
7. Alsema E, "Energy Requirements and CO_2 Mitigation Potential of PV Systems", *Workshop, Proceedings, Photovoltaics and the Environment* (Keystone, CO, 1998).
8. *Energy Payback: Clean Energy from PV*, NREL Report No. FS-520-24619, National Renewable Energy Laboratory, Golden, CO (1999).
9. Schmela M, *World production for solar cells grew 40% in 2001*, Photon International (magazine), 38–43 (March 2002).
10. Oswald G, "The PV Industry Moving into the Solar Century", *2nd World Congress on Photovoltaic Energy Conversion* (Vienna, Austria, 1998).
11. DeMeo E, Galdo J, *Renewable Energy Technology Characterizations*, Topical Report, TR-109496, U.S. Department of Energy, Electric Power Research Institute, Washington, DC, USA (1997).
12. *Large Systems Cost Report: Cost Analysis for 70 kW and Larger TEAM-UP PV Installations*, Solar Electric Power Association, Washington, DC (2000).
13. *Photovoltaics the Power of Choice: The National Photovoltaics Program Plan for 1996–2000*, U.S. Department of Energy, Washington, DC.
14. *International Energy Outlook 2001*, U.S. Energy Information Administration, Washington, DC (2001).

Downloaded from https://onlinelibrary.wiley.com/doi/ by <Shibboleth-member@purdue.edu>, Wiley Online Library on [25/08/2024]. See the Terms and Conditions (https://onlinelibrary.wiley.com/terms-and-conditions) on Wiley Online Library for rules of use; OA articles are governed by the applicable Creative Commons License

22
PV in Architecture

Tjerk H. Reijenga

BEAR Architecten, Gouda, Netherlands

22.1 INTRODUCTION

22.1.1 Photovoltaics (PV) as a Challenge for Architects and Engineers

What is happening in the built environment around us? We are witnessing an essential change in society. Governments are spending hundreds of millions of dollars on research, development and the demonstration of renewable energy. Big oil companies such as BP Amoco and Shell have invested more than a billion dollars in solar energy. Current developments show that renewables, such as solar energy systems, will be incorporated into our daily life in the near future, as conventional energy sources become depleted and environmental concerns grow [1].

Within a short period of time, solar systems will become an integral part of our society and thus our environment. There are large incentives for urban planners and architects to incorporate these techniques into their design. New products are emerging yet need further development to fully meet the architectural needs of sustainable buildings. Architects therefore need to start thinking about this new Smart Solar Architecture.

The European Commission has issued the "White Paper for a Community Strategy and Action Plan, Energy, for the future: Renewable Sources of Energy" [2]. This White Paper sets a target of 12% for the contribution of renewable energy sources to the total energy consumption in the European Union by 2010. The "Campaign for Take-Off" was launched in 1999 and aims to facilitate the success of the Strategy for Renewable Energy Sources up to the year 2003. One of the proposed key sectors to be promoted during the campaign is PV systems – 1 million systems in total.

The 450 MWp rooftop system campaign in the European Union can be achieved by installing 150 000 systems at an average capacity of 3 kWp each. The 150 MWp

Handbook of Photovoltaic Science and Engineering. Edited by A. Luque and S. Hegedus
© 2003 John Wiley & Sons, Ltd ISBN: 0-471-49196-9

Downloaded from https://onlinelibrary.wiley.com/doi/ by <Shibboleth-member@purdue.edu, Wiley Online Library on [25/08/2024]. See the Terms and Conditions (https://onlinelibrary.wiley.com/terms-and-conditions) on Wiley Online Library for rules of use; OA articles are governed by the applicable Creative Commons License

building facades program in the commercial sector can be realized by installing 5000 systems, assuming an average size of 30 kWp per building. With an additional capacity of 50 MWp for stand-alone systems the total target for installed PV for Europe will be 650 MWp (approx. 6 500 000 m^2).

22.1.2 Definition of Building Integration

A large part of the future PV market will be associated with building applications, especially in Europe and Japan where the population density is high and the land is valuable [3]. In areas with less population, it will be possible to find land for ground-mounted PV structures (Figure 22.1) [4].

Building-integrated, grid-connected PV systems have the following advantages [5]:

- There is no additional requirement for land.
- The cost of the PV wall or roof can be offset against the cost of the building element it replaces.
- Power is generated on site and replaces electricity that would otherwise be purchased at commercial rates.
- Connecting to the grid means that the high cost of storage is avoided and security of supply is ensured.

Additional benefits of public awareness are [6] as follows:

- Architecturally elegant, well-integrated systems will increase market acceptance.
- Building-integrated PV (BIPV) systems provide building owners with a highly visible public expression of their environmental commitment (Figure 22.2).



Figure 22.1 The 1 MWp ground-mounted system in Toledo, Spain. Reproduced with permission by BEAR Architecten T. Reijenga

Downloaded from https://onlinelibrary.wiley.com/doi/ by <Shibboleth-member@purdue.edu>, Wiley Online Library on [25/08/2024]. See the Terms and Conditions (https://onlinelibrary.wiley.com/terms-and-conditions) on Wiley Online Library for rules of use; OA articles are governed by the applicable Creative Commons License



Figure 22.2 Integrated façade system with 14 kWp amorphous silicon modules made by Energy Photovoltaics (EPV) in New Jersey, USA on top of a skyscraper at Four Times Square, New York, USA. The PV modules are the dark regions on the facade near the top. Reproduced from Kiss G, *Proc. 2nd WC Photovoltaic Solar Energy Conversion*, 2452–2455 (1998) with permission by Gregory Kiss [7]

The way people deal with photovoltaics in architecture differs from country to country. This depends on the scale, culture and type of financing for building projects. In countries such as Denmark, the Netherlands and the United Kingdom, where public housing is very common, serial production is strongly emphasized in housing projects. Professionals such as project developers and architects implement the housing construction process, in which the main opportunities are for PV roof integration in single-family terraced houses and for façade and roof integration in apartment buildings.

In countries where the government has little influence on house building, the building process is a private initiative. Integration of PV systems in buildings can be carried out by professionals but, on the smaller scale of a single-family house, the motivation must come from the private owner. In these countries, most building-integrated PV systems are found in commercial and industrial buildings in which building professionals are involved. With these types of buildings, PV systems are integrated both into façades and roofs. There is a significant market for private homeowners who buy small-scale (less than 500 Wp) PV systems and mount them somewhere on their house.

The aim of integrating PV systems into buildings is to reduce the requirement for land and the costs [8]. This could be the cost of the support construction and the cost of building elements, such as tiles. It is more efficient to integrate a PV system when constructing the building, rather than mounting it afterwards.

A definition for Building Integration is hard to formulate, as it concerns the physical integration of a PV system into a building, but it also covers the overall image of the PV system in the building. For the architect, the aesthetic aspect, rather than the physical integration, is the main reason for talking about building integration. The optimal situation is a physically and aesthetically well-integrated BIPV system. In fact, many examples of physical integration show a lack of aesthetic integration. Visual analysis of PV systems in buildings shows that the look of a poorly designed building does not improve, simply

Downloaded from https://onlinelibrary.wiley.com/doi/ by <Shibboleth-member@purdue.edu, Wiley Online Library on [25/08/2024]. See the Terms and Conditions (https://onlinelibrary.wiley.com/terms-and-conditions) on Wiley Online Library for rules of use; OA articles are governed by the applicable Creative Commons License

by adding a well-designed PV system. On the other hand, a well-designed building with a nicely integrated PV system will be accepted by everybody.

The following section aims to explain some basic thoughts about PV to non-designers, from an architectural and design point of view.

Note: All specified power of PV systems is the power under standard test conditions and tilt which may be greater than the power delivered when installed in nonoptimum orientation required by the BIPV application.

22.2 PV IN ARCHITECTURE

22.2.1 Architectural Functions of PV Modules

Basically there are three locations for integrating PV systems into buildings. The main locations are the roof and façade, with all other locations being known as *building components*.

A PV system can be integrated into the roof in several ways. One choice is for the integrated system to be part of the external skin and therefore be part of an impermeable layer in the construction. In the 1990s, several building projects were constructed on the basis of this principle (Figure 22.3) [9]. The other choice for roof mounting the PV system is above the impermeable layer. This is a more secure option but not without some risk, as the impermeable layer has to be pierced in order to mount the system on the roof. Using PV modules as roof covering reduces the amount of building materials needed, which is very favorable for a sustainable building and can help reduce costs. In addition to covering the complete roof with modules, there are also many products for small-scale use, for example, PV shingles and tiles. The small scale of these products (from 2 cells on a tile to around 20 cells on a look-alike tile) makes them very convenient for use in existing buildings or as do-it-yourself products.



Figure 22.3 Roof integration in a renovation project with the Shell Solar/BOAL profiles in Leiden (NL), providing a 2.1 kWp system per house. The PV roof is an impermeable layer. Reproduced from Maycock P *et al*., *Building with Photovoltaics*, 78–81, Ten Hagen & Stam, Den Haag (1995) with permission by NOVEM, R Schropp [10]

Downloaded from https://onlinelibrary.wiley.com/doi/ by <Shibboleth-member@purdue.edu, Wiley Online Library on [25/08/2024]. See the Terms and Conditions (https://onlinelibrary.wiley.com/terms-and-conditions) on Wiley Online Library for rules of use; OA articles are governed by the applicable Creative Commons License



Figure 22.4 Solar office in Doxford Sunderland (UK) with a transparent double-glazing PV system integrated in the façade. The 73 kWp PV system is manufactured by Saint Gobain and mounted in Schüco window frames. Reproduced with permission by Dennis Gilbert

Transparent PV modules used as roofing materials serve as water and sun barriers and also transmit daylight (see Figure 22.4). In glass-covered areas, such as sunrooms and atriums, sun protection on the roof is necessary in order to avoid overheating in summer. The PV cells absorb 70 to 80% of the sun radiation. The space between the cells transmits enough diffused daylight to achieve a pleasant lighting level in the area. PV cells were used in this way at the Centre for Sustainability De Kleine Aarde in Boxtel (NL) [11] and the Brundtland Centre (DK). Using transparent PV modules in the Solar Office in Doxford (UK), has resulted in a similar contrast in the façade [12]. In order to increase the usage of daylight in the workplaces, transparent PV modules have been used instead of glass.

Of course, PV cells convert sunlight into electricity (with typical efficiencies of 6–15%) with the remainder of the solar energy being converted into heat. At the project "Haus der Zukunft" in Linz (AT), this residual heat is also used to warm the home [13]. An air cavity has been created underneath the PV modules, through which warm air (heated by PV modules) is exhausted. The hybrid collector provides warm air to the heating system in the home, which in this case, makes it a cost-effective use of the collector.

At the Netherlands Energy Research Foundation (ECN) in Petten (NL), Building 42 has a conservatory with 43 kWp BP solar roof-integrated transparent laminates that reduce light and sun transmission by around 70% as compared to glass. The conservatory therefore acts as a big parasol over the offices, protecting them from the sun while still providing enough daylight (Figure 22.5) [14].

Facades are basically constructed using *in situ* bricklaying or concrete constructions, prefab elements or structural metal facades that are mounted in place. Concrete constructions form the structural layer and are covered with insulation and a protective cladding [15]. This cladding can be wood, metal sheets, panels, glass or PV modules. For luxury office buildings, which often have expensive cladding, cladding with PV modules is not more expensive than other commonly used materials, for example, natural stone

Downloaded from https://onlinelibrary.wiley.com/doi/ by <Shibboleth> -member@purdue.edu, Wiley Online Library on [25/09/2024]. See the Terms and Conditions (https://onlinelibrary.wiley.com/terms-and-conditions) on Wiley Online Library for rules of use; OA articles are governed by the applicable Creative Commons License



Figure 22.5 Interior view of the conservatory with integrated 43 kWp transparent BP solar modules in ECN Building 42 in Petten (NL). Reproduced with permission by BEAR Architecten T. Reijenga

and expensive special glass. This cladding costs around \$1000/m^2, which is comparable to the cost of the PV module today.

Structural glazing or structural facades are constructed using highly developed profile systems, which can be filled with all types of sheeting, such as glass or frameless PV modules. Facades are very suitable for all types of sunshades, louvers and canopies [16]. There is a logical combination between shading a building in summer and producing electricity at the same time. Architects recognize this and many examples of PV shading systems can be seen around the world (Figure 22.6). A canopy (entrance protection) on the sunny side of a building is a good place for BIPV systems (Figure 22.7) thus providing shade, protection from rain, as well as electricity.

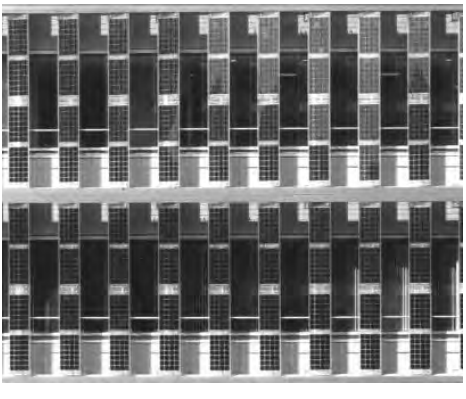


Figure 22.6 Solar shading (PV modules as part of a vertical louver system) on the west façade of the SBIC office building in Tokyo (JA). The transparent vertical louvers, with a total capacity of 20.1 kWp, were manufactured by Atlantis Switzerland. Reproduced with permission by Jiro Ono

Downloaded from https://onlinelibrary.wiley.com/doi/ by <Shibboleth-member@purdue.edu, Wiley Online Library on [25/08/2024]. See the Terms and Conditions (https://onlinelibrary.wiley.com/terms-and-conditions) on Wiley Online Library for rules of use; OA articles are governed by the applicable Creative Commons License

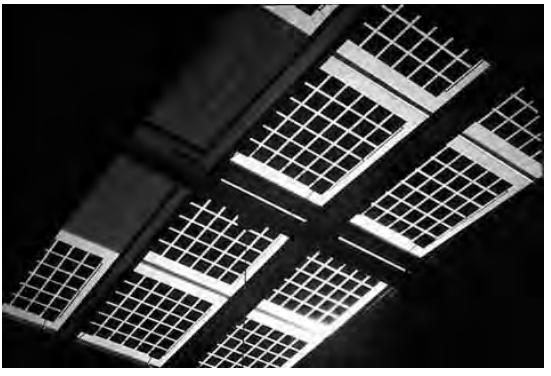


Figure 22.7 This system is the 1.25 kWp canopy with Atlantis transparent modules at the Thoreau Center in San Francisco, CA (USA). The canopy protects the entrance against the rain and wind but daylight is still allowed through via the transparent modules. Reproduced from Eiffert P, Kiss G, *Building-Integrated Photovoltaic Designs for Commercial and Institutional Structures – A Sourcebook for Architects*, 7–10, NREL, Golden, CO (2000) with permission by NREL USA [17]

22.2.2 PV as Part of "Green Design"

The government's role in promoting and supporting sustainable energy (PV systems) strongly influences the extent to which these systems are used in buildings. In countries with less government intervention, the power companies play a bigger role. Even without financial support, the government can encourage sustainable energy, for example, by demanding better performance for buildings. By introducing certain performance goals, sustainable energy and solar energy PV systems might be considered.

There is a growing interest in "green" products such as organic food, organic fibers as well as green buildings. Insurance companies and financial markets are becoming aware of "green" financing, which requires a different design approach from architects. "Green" design is the basic reason for integrating PV systems into buildings.

22.2.3 PV Integrated as Roofing Louvres, Facades and Shading

For architects, the application of PV systems must be part of a whole (holistic) approach. A high-quality PV system can provide a substantial part of the building's energy needs if the building has been designed in the right way. In general, the energy consumption of buildings needs to be cut down by at least 50% compared to a typical but inefficiently designed building.

In a holistic approach, integrating a PV system not only means replacing a building material but also aesthetically integrating it into the design. The integration also takes over other functions of the building's skin. Mounted on a sloped roof, profile systems mean that PV modules can be part of the watertight skin. The system can also be mounted above an impermeable roof foil, thereby protecting the foil against UV light and direct sun. This extends the life span of the foil. This kind of system is also available for flat roofs. The Powerlight Company from Berkeley, CA (USA) introduced a PV system into

Downloaded from https://onlinelibrary.wiley.com/doi/ by <Shibboleth-member@purdue.edu>, Wiley Online Library on [25/08/2024]. See the Terms and Conditions (https://onlinelibrary.wiley.com/terms-and-conditions) on Wiley Online Library for rules of use; OA articles are governed by the applicable Creative Commons License

the market that is glued on expanded polystyreen (XPS) insulation material. This type of warm roof construction (construction on the warm side of the insulation) system is very well suited to renovating large flat roofs (Figure 22.8).

The designer may well use building elements such as canopies and shading systems to integrate PV systems, but will need to look in detail at shading and PV technology to understand the details of how to design this PV integration. One of the first things that the designer will discover is the fact that an efficient PV system is not automatically a good shading system. In general, a PV system on louvres will need a certain mutual distance between the louvers to prevent shading of the cells, which may let too much sun through at a lower sun angle in spring and fall (Figure 22.9).



Figure 22.8 Powerguard flat-roof PV system including thermal insulation at the Coastguard building in Boston, MA (USA). The 3 kWp system has a special wind-tunnel-tested profile at the edge to keep the system on the roof in heavy winds. Adapted from Eiffert P, Kiss G, *Building-Integrated Photovoltaic Designs for Commercial and Institutional Structures – A Sourcebook for Architects*, 42–44, NREL, Golden, CO (2000). Reproduced with permission by NREL USA [18]



Figure 22.9 Colt shading system that is optimized for sun control. The distance between the louvers with PV modules cause shading on 50% of the PV cells; 47 kWp PV system at Stadtwerke in Winterthur (CH). Reproduced with permission by BEAR Architecten T. Reijenga

Downloaded from https://onlinelibrary.wiley.com/doi/ by <Shibboleth-member@purdue.edu, Wiley Online Library on [25/08/2024]. See the Terms and Conditions (https://onlinelibrary.wiley.com/terms-and-conditions) on Wiley Online Library for rules of use; OA articles are governed by the applicable Creative Commons License

Heat load and daylight control systems can be combined with the integration of PV systems. Moreover, when the designer studies these aspects in detail, he or she will discover that PV systems can also be part of the thermal envelope or thermal system (Figure 22.10) [19]. Another example is the refurbishment of Building 31 in Petten (NL) [20]. In this project, the PV system is integrated into a louver system that supports the 35 kWp Shell Solar modules, to keep out the summer heat and give less glare, and improve daylight conditions inside. To prevent shading of the modules by the upper louver, the dimensions of the louvers have to be almost twice the size of the modules (Figure 22.11) (Diagram 1) [21].

Orientation is a major design issue for (green) buildings. The heat load of a building, the need for shading and the design of facades all depend on the orientation.



Figure 22.10 Daylight control at the Kaiser fashion house in Freiburg (D). This 4 kWp PV system on louvers is mounted in front of the glass façade and prevents glare inside. The PV louvers are in the center of the figure. Reproduced with permission by BEAR Architecten T. Reijenga



Figure 22.11 South façade of ECN Building 31 in Petten (NL). The shading structure supports the 35 kWp Shell Solar modules. Reproduced with permission by BEAR Architecten T. Reijenga

Downloaded from https://onlinelibrary.wiley.com/doi/ by <Shibboleth-member@purdue.edu, Wiley Online Library on [25/08/2024]. See the Terms and Conditions (https://onlinelibrary.wiley.com/terms-and-conditions) on Wiley Online Library for rules of use; OA articles are governed by the applicable Creative Commons License

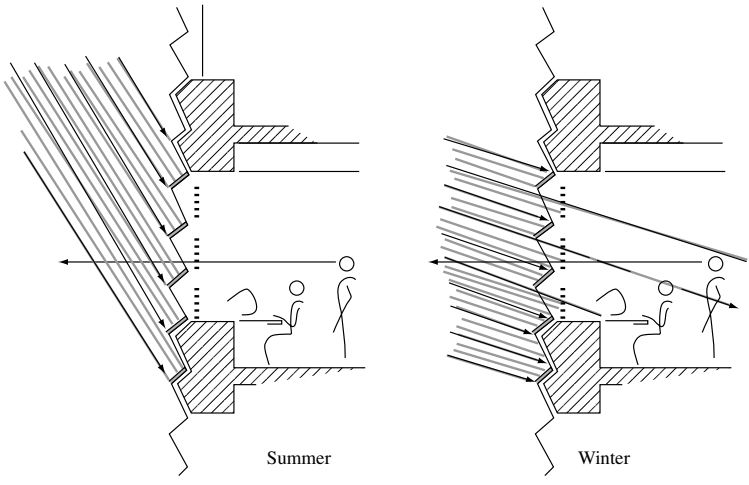


Diagram 1 Shading system with high angle (summer) and low angle (winter). In a fixed position designed for high angle of summer sun the system will be inefficient for the winter period. Reproduced with permission by BEAR Architecten, NL

Orientation is also important for PV systems. Facade systems might be suitable in certain countries, especially at a northern (above 50°N) or a southern (below 50°S) latitude. When shading of the facade cannot be prevented, and for the countries in between these latitudes, sloped surfaces facing the sun or even horizontal surfaces might be more suitable. The designer's final choice will be based on orientation, amount of total annual (sun)light on the PV module, shading from surrounding buildings and the aesthetics of the design. An important issue for the designer is to appreciate the blue, gray or black cells and to become familiar with finding integration opportunities in the first draft design. Ideally, a PV system should not be added to a building but designed as part of the building.

22.2.4 Well-integrated Systems

How can we discuss whether a BIPV system is well integrated? [22] A group of architects within the IEA PVPS (PV Power Systems) Task 7 workgroup discussed this subject and came up with several criteria for judging the aesthetic qualities of BIPV projects [23].

In order to decide which BIPV systems are of a high quality, we need to distinguish between the following:

- technical quality of the BIPV system, that is, the technical aspects of PV, cables and inverters,
- building quality of the BIPV system. Here we look for the quality of the system as a building element (part of the roof or the façade that is replaced by modules). The module and its integration must meet typical building standards, such as an impermeable layer or a structure strong enough to withstand wind or snow loads,

Petitioner Canadian Solar (USA) Inc., Ex. 1035, p. 2398

Downloaded from https://onlinelibrary.wiley.com/doi/ by <Shibboleth-member@purdue.edu, Wiley Online Library on [25/08/2024]. See the Terms and Conditions (https://onlinelibrary.wiley.com/terms-and-conditions) on Wiley Online Library for rules of use; OA articles are governed by the applicable Creative Commons License

Downloaded from https://onlinelibrary.wiley.com/doi/ by <Shibboleth-member@purdue.edu, Wiley Online Library on [25/08/2024]. See the Terms and Conditions (https://onlinelibrary.wiley.com/terms-and-conditions) on Wiley Online Library for rules of use; OA articles are governed by the applicable Creative Commons License

- aesthetic quality of the BIPV system. This is the least scientific and most subjective part of judging BIPV systems. But the reality is that architecturally elegant, well-integrated systems will increase market acceptance.

Both the technical and building qualities of the PV system have been considered as preconditions. All installations in a building must function correctly.

Aesthetic quality is not a precondition. Although the discussion of architectural values is very broad, high-quality architecture or poor architecture is generally recognizable.

The criteria formulated by the IEA PVPS Task 7 workgroup for evaluating the aesthetic quality of building-integrated PV systems are [24, 25]

- natural integration,
- designs that are architecturally pleasing,
- good composition of colors and materials,
- dimensions that fit the gridula,[1] harmony, composition,
- PV systems that match the context of the building,
- well-engineered design,
- use of innovative design.

These architectural criteria need to be explained particularly to nonarchitects and manufacturers developing photovoltaic systems for integration into roofs and façades, who often believe that their systems fit perfectly. Some architectural journals,[2] however, have criticized PV projects in, for example, the 250 kWp project in Sloten, Amsterdam (NL) [26] and the 1.3 MWp project in Nieuwland, Amersfoort (NL) [27]. The average architect is not yet convinced of the "beauty" of a PV system on his building. All the more reason this book should show appealing examples and critically judge PV products.

The Lafarge Braas PV 700 roof tile system is a good example of how manufacturers look at their product. This system can be placed invisibly in between the flat Lafarge Stonewold tiles (Figure 22.12) [28].

However, in product advertisements, the manufacturer has chosen tiles with contrasting colors instead of harmonious colors, thus ignoring the fact that integration, in most situations, should be discreet. After commercial introduction, the system was prepared for use with a standard roofing tile. This corrugated tile is an even bigger contrast to the flat PV elements. Technically speaking, this high-quality product has been integrated. Aesthetically, however, the product has not been integrated because of the contrast. Therefore, the architect, building inspectors and clients might reject a PV system incorporating this product.

Explanation of the criteria

- *Natural integration*: This means that the PV system seems to form a logical part of the building (Figure 22.13). The system adds the finishing touch to the building. The

[1] Gridula is not a common word outside architectural vocabulary. It means the grid that is used for the design that is a (sometimes hidden) part of the building.
[2] Archis February 1998.



Figure 22.12 This sustainable WWF (World Wildlife Fund) project in Harderwijk (NL) has a roof with a thermal solar collector on top and a 460 Wp PV 700 system underneath. The PV 700 system fits almost invisibly in between the tiles. Reproduced with permission by BEAR Architecten T. Reijenga



Figure 22.13 A naturally integrated PV system that is clearly part of the building. This system is located in Poitiers (FR). Reproduced with permission by ECN J. Beurskens

PV system does not have to be that obvious. In renovation situations, the result should look as though the PV system was there before the renovation.

- *Architecturally pleasing*: The design has to be architecturally pleasing (Figure 22.14). The building should look attractive and the PV system should noticeably improve the design. This is a very subjective issue, but there is no doubt that people find some buildings more pleasing than others.
- *Good composition of colors and materials*: The color and texture of the PV system should be consistent with the other materials (Figure 22.15).
- *Fit the gridula, harmony, and composition*: The dimensions of the PV system should match the dimensions of the building (Figure 22.16). This will determine the dimensions

Downloaded from https://onlinelibrary.wiley.com/doi/ by <Shibboleth-member@purdue.edu, Wiley Online Library on [25/08/2024]. See the Terms and Conditions (https://onlinelibrary.wiley.com/terms-and-conditions) on Wiley Online Library for rules of use; OA articles are governed by the applicable Creative Commons License



Figure 22.14 Corridor in the Centre for Sustainability De Kleine Aarde in Boxtel (NL). The space is unheated and naturally ventilated. The 6.7 kWp PV system with transparent modules has a double function and reduces the heat load by around 70%. Reproduced from Reijenga T, Böttger W, *Proc. 2nd WC Photovoltaic Solar Energy Conversion*, 2748–2751 (1998) with permission by NOVEM, R Schropp [11]



Figure 22.15 The 80.5 kWp Atlantis Sunslates on the roof of the historic horse stables in Bern (CH). The color and texture matches so well that this PV system was allowed on a protected historic building. Reproduced with permission by Atlantis Solar Systems Ltd

of the modules and the building grid lines used (grid = modular system of lines and dimensions used to structure the building).

- *Matching the context of the building*: The entire appearance of the building should be consistent with the PV system used (Figure 22.17). In a historic building, a tile-type system will look better than large modules. A high-tech PV system, however, would fit better in a high-tech building.
- *Well engineered*: This does not concern the waterproofing or reliability of the construction. However, it does concern the elegance of the details (Figure 22.18). Did the

Downloaded from https://onlinelibrary.wiley.com/doi/ by <Shibboleth> -member@purdue.edu, Wiley Online Library on [25/08/2024]. See the Terms and Conditions (https://onlinelibrary.wiley.com/terms-and-conditions) on Wiley Online Library for rules of use; OA articles are governed by the applicable Creative Commons License



Figure 22.16 The cube at the Discovery Science Center in Santa Ana, Los Angeles, CA (USA). The 20 kWp PV system fits the gridula of this huge structure and there is harmony between the PV modules and the structure behind. Some 494 Thin-film Millienna photovoltaic modules from BP Solar were used on the solar cube. Reproduced from Eiffert P, Kiss G, *Building-Integrated Photovoltaic Designs for Commercial and Institutional Structures – A Sourcebook for Architects*, 48, 49, NREL, Golden, CO (2000) with permission by BEAR Architecten T. Reijenga [29]



Figure 22.17 The 180 kWp Sofrel flat-roof system on the UBS Bank near Lugano (CH) matches the context of the roof, which fits between different installations, high-tech chimneys and the tight rhythm of the flat-roof PV system on the roof. Here the BIPV is mainly aesthetically and not physically integrated. Reproduced from Maycock P *et al*., *Building with Photovoltaics*, 78–81, Ten Hagen & Stam, Den Haag (1995) with permisson by UBS Switzerland [10]

designers pay attention to detail? Has the amount of material been minimized? These considerations will determine the influence of the working details.

- *Innovative design*: PV systems have been used in many ways but there are still countless new ways to be developed. This is all the more reason to consider this criterion as well.

Downloaded from https://onlinelibrary.wiley.com/doi/ by <Shibboleth-member@purdue.edu, Wiley Online Library on [25/08/2024]. See the Terms and Conditions (https://onlinelibrary.wiley.com/terms-and-conditions) on Wiley Online Library for rules of use; OA articles are governed by the applicable Creative Commons License



Figure 22.18 The Schüco façade in the Solar office in Doxford, Sunderland (UK) is well engineered. Reproduced with permission by BEAR Architecten T. Reijenga

22.2.5 Integration of PV Modules in Architecture

The integration of PV systems in architecture can be divided into five categories:

1. Applied invisibly
2. Added to the design
3. Adding to the architectural image
4. Determining architectural image
5. Leading to new architectural concepts.

These categories have been classified according to the increasing extent of architectural integration. However, a project does not necessarily have to be of a lesser quality just because PV modules have been applied invisibly. A visible PV system is not always appropriate, especially in renovation projects with historic architectural styles. The challenge for architects, however, is to integrate PV modules into buildings properly. PV modules are new building materials that offer new designing options. Applying PV modules in architecture should therefore lead to new designs. In some of the selected projects, the design was based on this principle.

1. *Applied invisibly*: The PV system has been incorporated invisibly (and is therefore not architecturally 'disturbing') (Figure 22.19). The PV system harmonizes with the total project. An example is the Maryland project in the USA (Figure 22.20), where the architect tried to integrate PV modules into the design invisibly. This solution was chosen because the entire project concerned historic architecture. A modern high-tech PV module look would not be appropriate for this architectural style.
2. *Added to the design*: The PV system is added to the design (Figure 22.21). Building integration is not really used here, but this does not necessarily mean that architectural

Downloaded from https://onlinelibrary.wiley.com/doi/ by <Shibboleth-member@purdue.edu, Wiley Online Library on [25/08/2024]. See the Terms and Conditions (https://onlinelibrary.wiley.com/terms-and-conditions) on Wiley Online Library for rules of use; OA articles are governed by the applicable Creative Commons License



Figure 22.19 Modern style houses in the 1.3 MW project in Amersfoort (NL). The architect thought that the modules did not blend in with the design. He chose an "invisible" solution with a flat-roof system. The PV system is not visible from the surrounding streets. Reproduced with permission by REMU J. van IJken



Figure 22.20 Houses at the National Research Home Park in Bowie, MA (USA) in historic style. The roofs are Unisolar standing-seam roofs with thin film (amorphous silicon). Reproduced with permission by NREL USA

integration is also lacking. The "added" PV system is not always visible either (Figure 22.22).

3. *The PV system adds to the architectural image*: The PV system has been integrated beautifully into the total design of the building, without changing the project's image (Figure 22.23). In other words, the contextual integration is very good (Figure 22.24).

Downloaded from https://onlinelibrary.wiley.com/doi/ by <Shibboleth-member@purdue.edu, Wiley Online Library on [25/08/2024]. See the Terms and Conditions (https://onlinelibrary.wiley.com/terms-and-conditions) on Wiley Online Library for rules of use; OA articles are governed by the applicable Creative Commons License



Figure 22.21 The IES building in Madrid (E) has a 6.6 kWp PV system that was added shortly after the building was finished. The modules are mounted on the façade above the windows and keep out the sun. Reproduced with permission by BEAR Architecten T. Reijenga



Figure 22.22 These houses in Amersfoort Nieuwland (NL) have a roof with a white foil on top. The architect chose a color contrasting with the color of the modules to show that the PV system is an addition to his design. Reproduced with permission by REMU J. van IJken

4. *The PV system determines the architectural image*: The PV system has been integrated into the design in a remarkable and beautiful way and plays an important role in the total image of the building (Figures 22.25 and 22.26).
5. *PV system leads to new architectural concepts*: Using PV modules, possibly in combination with other types of solar energy, leads to new designs (Figure 22.27) and new architecture (Figure 22.28). The integration of PV modules was considered on a conceptual level, which gives the project extra value.

Downloaded from https://onlinelibrary.wiley.com/doi/ by <Shibboleth-member@purdue.edu, Wiley Online Library on [25/08/2024]. See the Terms and Conditions (https://onlinelibrary.wiley.com/terms-and-conditions) on Wiley Online Library for rules of use; OA articles are governed by the applicable Creative Commons License



Figure 22.23 The architect integrated the (in total 49 kWp) PV modules into the facades above the windows and produced a combination with the roller blinds. The EMPA office building is located in Sankt Gallen (CH). Reproduced with permission by Electrowatt Eng. Services



Figure 22.24 In this office building in Gouda (NL), the 6.2 kWp PV system is mounted on top of the façade as a canopy that protects the wall. The architect's intention was to show the PV system to his clients when they visit the office. Reproduced with permission by BEAR Architecten T. Reijenga

22.2.6 Brundtland Centre, Toftlund (DK) – a Case Study

The Brundtland Centre in Toftlund opened in 1995, was developed as an education and demonstration center for Denmark [31]. It is part of the "Brundtlandby Project", which designated certain towns, such as Toftlund, to put into practice the goals of low energy consumption and environmental impact, as proposed by the Brundtland Report. The Brundtland Centre was built to exhibit and employ the concept of energy-efficient building strategies combined with well-implemented architectural design. Throughout the

Downloaded from https://onlinelibrary.wiley.com/doi/ by <Shibboleth-member@purdue.edu, Wiley Online Library on [25/08/2024]. See the Terms and Conditions (https://onlinelibrary.wiley.com/terms-and-conditions) on Wiley Online Library for rules of use; OA articles are governed by the applicable Creative Commons License



Figure 22.25 The dwellings at the 5 MW project in the HAL district of Langedijk (NL) have a large PV roof without any perforations. This strengthens the architectural expression of the roof design. Each roof includes a 5.1 kWp BP Solarex PV system. Reproduced with permission by BEAR Architecten M. van Kerckhoven



Figure 22.26 The canteen at the IMEC in Leuven (B) has an entrance with attractive-looking transparent modules in the roof. Reproduced with permission by IMEC

design process, priority was given to strategies that could be achieved through the design of the building itself – its form, orientation and envelope design – rather than "high-tech" strategies. Where the use of "active systems" was necessary, the design team aimed to develop more energy-efficient ways of operating these technologies.

Early consideration of PV within the design process has resulted in an aesthetically and energetically well-integrated PV system within the architectural design (Figure 22.29). Two types of PV systems are used in the building envelope. A PV array is integrated

Downloaded from https://onlinelibrary.wiley.com/doi/ by <Shibboleth-member@purdue.edu, Wiley Online Library on [25/08/2024]. See the Terms and Conditions (https://onlinelibrary.wiley.com/terms-and-conditions) on Wiley Online Library for rules of use; OA articles are governed by the applicable Creative Commons License



Figure 22.27 This shopping mall in Lausanne (CH), includes a louver system with transparent modules mounted above the shop windows, which results in less reflection of sunlight in the windows, making it easier to look into the shops. Reproduced with permission by BEAR Architecten T. Reijenga



Figure 22.28 This zero-energy project in Etten-Leur (NL) combines different sustainable energy techniques. Each house has a roof structure with 6.2 kWp BP Solar PV modules. The aesthetic integration of the PV system is a completely new concept in housing. Reproduced from Reijenga T, "Energy-Efficient And Zero-Energy Building in the Netherlands", *Proc. International Workshop on Energy Efficiency in Buildings in China for the 21st Century*, CBEEA (Beijing, December 2000) with permission by BEAR Architecten M. van de Laan [30]

into the roof of the atrium – a central space connecting the adjacent two-storey building sections. Other PV modules are mounted on the southeast façade of the office section (Figure 2.30).

The atrium roof, incorporating the transparent PV modules, stretches out above the entrance of the building, creating a large canopy. Thus, the PV system mounted on the atrium roof is visible from the inside of the atrium as well as from the outside of the building. Mounting the PV system on the roof had a great impact on the architectural expression, the building layout and internal atmosphere of the center (Figure 22.31).

Downloaded from https://onlinelibrary.wiley.com/doi/ by <Shibboleth-member@purdue.edu, Wiley Online Library on [25/08/2024]. See the Terms and Conditions (https://onlinelibrary.wiley.com/terms-and-conditions) on Wiley Online Library for rules of use; OA articles are governed by the applicable Creative Commons License

Petitioner Canadian Solar (USA) Inc., Ex. 1035, p. 2408



Figure 22.29 Overview of the Brundtland Centre in Toftlund (DK). The glass roof on top of the atrium in the middle of the building has a saw-tooth roof with integrated 9.8 kWp transparent PV modules. Reproduced with permission by BEAR Architecten T. Reijenga



Figure 22.30 PV modules above the windows on the southeast facade. A total of 6 kWp is integrated in the facade. Reproduced with permission by BEAR Architecten T. Reijenga

To achieve the optimum orientation and tilt angle of the PV array (south/60°), the atrium roof has been constructed in a saw-tooth shape that runs diagonally across the space. The steel truss roof, combined with the alternating pattern of dark round cells against transparent glazing, gives the atrium a high-tech atmosphere. Special attention has been paid to provide soft diffused quality of daylight in the interior of the atrium. A thin diffusing glass fabric is integrated into the modules so that sharp edges from the circular solar cells are softened.

In energy terms, the integrated PV system in the atrium roof was designed not only to produce electricity but also to provide shading to prevent the atrium from overheating. The transparent modules allow 20% of the available daylight to enter the atrium. The concrete floors and facades accumulate the heat surplus during the day. At night, the atrium is cooled by natural ventilation, while the mechanically assisted ventilation is used to ventilate the adjacent rooms. Automatic controls stop the ventilation when a sufficiently low temperature has been reached.

Downloaded from https://onlinelibrary.wiley.com/doi/ by <Shibboleth-member@purdue.edu, Wiley Online Library on [25/08/2024]. See the Terms and Conditions (https://onlinelibrary.wiley.com/terms-and-conditions) on Wiley Online Library for rules of use; OA articles are governed by the applicable Creative Commons License



Figure 22.31 Atrium roof of the Brundtland Centre building from the inside. Because the saw-tooth roof casts a shadow on the modules, some of the cells are fake. This solution achieves a more elegant look from the inside. Reproduced with permission by BEAR Architecten T. Reijenga

22.3 BIPV BASICS

22.3.1 Categories and Type of Buildings

Building-integrated PV systems can be divided into different categories according to

1. cell and module type,
2. architectural integration,
3. type of building,
4. mounting technology, and
5. the function of the integration, and possible additional building and architectural functions of the PV system.

It is important that architects know all these categories and their possibilities. The design process consists of translating the brief (program made by the client) into spaces and enclosures, as well as combining functions and materials into constructions. This process is mainly based on experience and knowledge of constructions and materials. New applications based on existing knowledge or techniques are very important in the creative process. New inventions play a minor role in the process.

22.3.1.1 Categories of cells and modules

There is a wide range of cells and modules in the market. There are various types of cell material, types of modules, framed or nonframed laminates, colors of the cells and colors of back sheets and frames; all provide a wide range of possible surfaces [32]. This is a very basic knowledge for architects. Architects will design BIPV systems with a certain image in mind. The choice of monocrystalline or polycrystalline cells will depend on color and not on efficiency [33].

Downloaded from https://onlinelibrary.wiley.com/doi/ by <Shibboleth-member@purdue.edu, Wiley Online Library on [25/08/2024]. See the Terms and Conditions (https://onlinelibrary.wiley.com/terms-and-conditions) on Wiley Online Library for rules of use; OA articles are governed by the applicable Creative Commons License

Downloaded from https://onlinelibrary.wiley.com/doi/ by <Shibboleth>-member@purdue.edu, Wiley Online Library on [25/08/2024]. See the Terms and Conditions (https://onlinelibrary.wiley.com/terms-and-conditions) on Wiley Online Library for rules of use; OA articles are governed by the applicable Creative Commons License

22.3.1.2 Categories of integration

BIPV systems in projects can be divided according to the location of the application: roof systems, facade systems, glass construction (conservatory/atrium) systems and building components such as shading and canopy systems. The main mounting locations are the roof and the façade. There are also many creative solutions available in designing how PV systems can be integrated. All these solutions are grouped as building components.

22.3.1.3 Types of buildings

Different buildings obviously have very different functions, for example, apartments and family houses, public buildings, commercial and industrial buildings and nonoccupied building structures. These can either be newly constructed or renovated buildings [34]. Nonoccupied building structures include shelters (bus stops, canopies, parking structures), kiosks (newsstands, gazebos, pavilions, phone booths), public toilet buildings, car parks, streetlights, parking meters, screens and barriers (fences, noise barriers), road signs and commercial billboards.

All types of building or nonoccupied building structures are a potential location for BIPV systems.

The various commercially available mounting applications can be grouped into 10 types, and can be found on the on-line PV database (*www.pvdatabase.com*).

Location on a building:	Building component(s):	Manufacturers such as:
Sloped roof	Tiles and shingles	LaFarge Braas (Figure 22.12), Atlantis Sunslates [35] (Figure 22.15), Japanese tiles (Figure 22.32), UnisolarStanding Seam panels [36] (Figure 22.20).
	Nonintegrated profiles	BP Sunflower (Figure 22.33), Econergy InterSole [37], Alutec profiles (Figure 22.34)
	Integrated profiles	BOAL/Shell Solar profile system (Figure 22.3), Solrif Solar profile system [38] (Figure 22.35)
Flat roof	Roofing element	Powerlight Powerguard® (Figure 22.8), Alwitra Evalon® roofing foil (Figure 22.36)
	Integrated profiles	Schüco profile system (Figure 22.37)
	Independent support structure	Econergy ConSole [39] (Figure 22.19), Solgreen (Figure 22.38), Sofrel [40] (Figure 22.17), Sobac [41]
Facade	Integrated profiles	Schüco façade profile system (Figure 22.39)
	Cladding system	BP Solface [42] system (Figure 22.40)
	Louvers or sun blinds	ADO louver system (Figure 22.41), Colt Shadovoltaic louver system (Figure 22.9)
	Canopy	Donjon canopy system (Figure 22.42)



Figure 22.32 Prefabricated Japanese tilelike roof panel method with CdTe cells in Nie-ken (JA). Capacity of the system is 1.3 kWp. Reproduced with permission by MSK Corporation

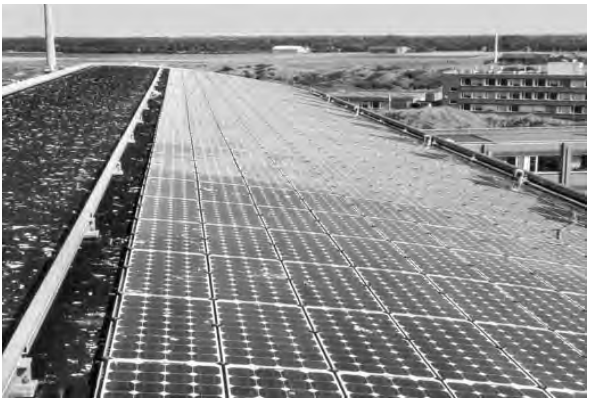


Figure 22.33 BP Sunflower system at the bent roof at ECN building 31, Petten (NL). Capacity 35 kWp. Reproduced with permission by BEAR Architecten H. Lieverse

22.3.1.4 Function of the integration

In addition to generating electricity, PV modules are also used as an integral part of the external skin (roof or façade), as sun protection (Figure 22.43) or as a daylight transmitter. Designing double functions and then integrating PV modules into buildings results in cost reductions on the investment in the building. Several buildings have been built that demonstrate PV systems as part of a passive cooling strategy [14].

The advantages in this specific case are

- the PV modules replace building elements,
- the PV modules are very well ventilated at the back,

Petitioner Canadian Solar (USA) Inc., Ex. 1035, p. 2412

Downloaded from https://onlinelibrary.wiley.com/doi/ by <Shibboleth-member@purdue.edu, Wiley Online Library on [25/08/2024]. See the Terms and Conditions (https://onlinelibrary.wiley.com/terms-and-conditions) on Wiley Online Library for rules of use; OA articles are governed by the applicable Creative Commons License



Figure 22.34 Alutec profile system in a new roof in Langedijk HAL (NL). Capacity of the system is 53 kWp and the project is part of the 5 MW BIPV project. Reproduced with permission by BEAR Architecten M. van Kerckhoven

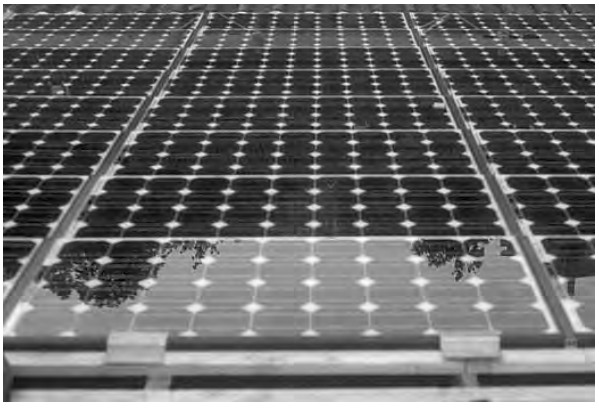


Figure 22.35 Solrif Solar profile system in a roof renovation in Zürich (CH). Capacity of the system is 53 kWp. Reproduced with permission by BEAR Architecten T. Reijenga

- a separate mounting construction is not necessary, and
- the air-conditioning system is eliminated.

22.3.2 Cells and Modules

The PV modules and mounting system are the elements of a PV system that can determine the image of a building. A PV system, particularly the cell material, framing materials, soldering, shape of the modules and the color of cells and back sheets, all influence the image of a building. For architects and designers, these aspects are more important than

Downloaded from https://onlinelibrary.wiley.com/doi/ by <Shibboleth-member@purdue.edu>, Wiley Online Library on [25/08/2024]. See the Terms and Conditions (https://onlinelibrary.wiley.com/terms-and-conditions) on Wiley Online Library for rules of use; OA articles are governed by the applicable Creative Commons License



Figure 22.36 Alwitra Evalon® roofing foil with amorphous silicon cells. Reproduced with permission by O.Ö. Energiesparverband



Figure 22.37 Schüco 1.9 kWp roof profile system with transparent modules in the Energy Forum Center in Bad Oeyenhausen (D). This mounting system can also be used in (difficult) horizontal situations. Reproduced with permission by BEAR Architecten T. Reijenga

the electrical efficiency of a system. Typical efficiencies of today's commercially available solar modules are shown in Table 22.1.

22.3.2.1 Solar cell materials

There are several types of solar cell materials: monocrystalline (single crystal) silicon, polycrystalline silicon (both discussed in Chapters 6 and 7), amorphous silicon (Chapter 12), copper indium gallium diselenide ($CuInGaSe_2$) (Chapter 13), and cadmium

Downloaded from https://onlinelibrary.wiley.com/doi/ by <Shibboleth-member@purdue.edu, Wiley Online Library on [25/08/2024]. See the Terms and Conditions (https://onlinelibrary.wiley.com/terms-and-conditions) on Wiley Online Library for rules of use; OA articles are governed by the applicable Creative Commons License



Figure 22.38 Solgreen flat-roof system for green roofs demonstrated on a roof in Switzerland. Reproduced with permission by SOLSTIS



Figure 22.39 Schüco façade profile system in the Doxford building (UK). See also caption at Figures 22.4 and 22.18. Reproduced with permission by BEAR Architecten T. Reijenga

telluride (CdTe) (Chapter 14). Their characteristics that affect their implementation in BIPV applications are briefly presented here.

Monocrystalline Si cells are initially grown as long cylinders, then sliced into thin discs called wafers (~300 μm thick). Initially round, the wafers often have their edges cut to create a nearly square wafer with slightly rounded corners. This increases their packing density on the module. Typical wafers are presently 10×10 or 12.5×12.5 cm^2 but will be increasing as technology develops. Monocrystalline cells have a very uniform appearance. Their color can be varied (see below) but are typically either dark blue or black since this gives the highest efficiency. (The color of the cell is determined by

Downloaded from https://onlinelibrary.wiley.com/doi/ by <Shibboleth-member@purdue.edu, Wiley Online Library on [25/08/2024]. See the Terms and Conditions (https://onlinelibrary.wiley.com/terms-and-conditions) on Wiley Online Library for rules of use; OA articles are governed by the applicable Creative Commons License



Figure 22.40 BP Solface vertical wall system at the Demosite in Lausanne (CH). Reproduced with permission by EPFL-LESO-PB



Figure 22.41 ADO louver system with integrated transparent PV modules at an apartment building in Amersfoort Nieuwland (NL). The automatic louvers can switch in two positions. The horizontal position at night (left on the figure) and tilted to the sun by day (right on the figure). Reproduced with permission by BEAR Architecten T. Reijenga

the wavelengths that are reflected. The darker the cell looks, the less light that is being reflected. Therefore darker means more absorption of sunlight by the solar cell.)

Polycrystalline silicon wafers are manufactured with a lower cost process than monocrystalline silicon wafers. They are cast in long square ingots. After slicing, polycrystalline wafers are already in the desired square shape. Compared to monocrystalline cells, polycrystalline cells also typically have a bluish color and are the same size, but are slightly less efficient and slightly of lower cost. The main difference between mono and poly wafers as might affect their application for BIPV is their visual

Downloaded from https://onlinelibrary.wiley.com/doi/ by <Shibboleth-member@purdue.edu, Wiley Online Library on [25/08/2024]. See the Terms and Conditions (https://onlinelibrary.wiley.com/terms-and-conditions) on Wiley Online Library for rules of use; OA articles are governed by the applicable Creative Commons License

Petitioner Canadian Solar (USA) Inc., Ex. 1035, p. 2416



Figure 22.42 Canopy at the eaves of a roof. 6.2 kWp PV system at an office building in Gouda (NL). Reproduced with permission by BEAR Architecten T. Reijenga



Figure 22.43 This building, at ECN in Petten (NL) has a 43 kWp PV system integrated into the conservatory roof. The conservatory acts as a parasol in front of the offices, thus eliminating the need for air-conditioning in a moderate climate. The building on the right side has a PV shading system (see caption on Figure 22.11). Reproduced with permission by BEAR Architecten T. Reijenga

appearance: monocrystalline cells are uniform while polycrystalline cells have hundreds of reflective facets, of sizes 0.1–1 cm. Each facet is a separate small crystalline region. Both mono and poly cells have metal grids on the front in a rectangular pattern to collect the electricity and to connect to the next cell. These grids are typically not visible from beyond a few meters away.

Amorphous silicon cells (a-Si) are composed of silicon atoms that are in a thin ($\sim$1 μm) layer and lack crystalline properties. They are commonly referred to as thin film Si PV technology. Amorphous silicon cells are deposited onto substrates like glass window

Downloaded from https://onlinelibrary.wiley.com/doi/ by <Shibboleth-member@purdue.edu, Wiley Online Library on [25/08/2024]. See the Terms and Conditions (https://onlinelibrary.wiley.com/terms-and-conditions) on Wiley Online Library for rules of use; OA articles are governed by the applicable Creative Commons License

Table 22.1 Typical efficiencies for modules. These values are obtained under standard test conditions. Different orientation in BIPV applications may result in lower performance

Cell type	Typical efficiencies [%]
Monocrystalline silicon	12–15
Multicrystalline silicon	11–14
Amorphous silicon	6–8
Cadmium telluride	7–10
Copper indium gallium diselenide	8–12

plates or flexible rolls of stainless steel or plastic, giving a wide range of mechanical strength, weight, and flexibility. The substrate is not visible since it is behind the solar cell. The cells have a uniform typically black appearance. These cells have no grids. Flexible substrates are ideal for curved surfaces and rollable "fold-away" modules. Amorphous silicon modules have lower efficiency than mono or poly silicon (Table 22.1) but better performance at higher temperatures [43, Chapter 12] as often occurs in BIPV applications.

Other thin film PV materials presently include $CuInGaSe_2$ and CdTe. They have a uniform nearly black appearance, indistinguishable visually from amorphous Si modules. They also have lower efficiency compared to mono or poly silicon. $CuInGaSe_2$ cells can be deposited on flexible plastic or metal foils.

Semitransparent cells for BIPV can be manufactured in two ways. Mono silicon wafers can have a series of deep grooves on the front and back which are perpendicular to one another. Where they intersect, light will be transmitted through the holes. Polycrystalline silicon cells with 2% transmission have been reported [44] but higher values should be possible with larger holes. Another approach is to make very thin amorphous silicon layers on glass with transparent contacts so the entire module is semitransparent. However, the transmitted light will have an orange or red tint because the blue and green portion of the spectrum is absorbed in the silicon layers. Such modules could only be used in applications where this color of light was acceptable such as sun-roofs for automobiles. A better method is to selectively remove part of the amorphous silicon layer using laser ablation. Unfiltered white light transmission of 5–15% have been reported for laser scribed amorphous silicon in BIPV applications [43].

22.3.2.2 Module temperature

Module efficiency, therefore electricity produced, decreases as the temperature increases for mono and poly silicon cells but not for amorphous silicon cells. In many non-BIPV applications, modules are mounted on free-standing frames with ambient air on both sides, allowing for cooling on both sides. In contrast, some BIPV applications install the modules in close contact to building material like roofs or wall insulation. The lack of circulating air increases the module temperature. Relative losses of >5% are possible [45]. A good design criterion for mono or poly silicon applications is to allow as much

Downloaded from https://onlinelibrary.wiley.com/doi/ by <Shibboleth-member@purdue.edu, Wiley Online Library on [25/08/2024]. See the Terms and Conditions (https://onlinelibrary.wiley.com/terms-and-conditions) on Wiley Online Library for rules of use; OA articles are governed by the applicable Creative Commons License

cooling as possible by providing for air flow behind the module and minimizing effect of insulation. This is not an issue for amorphous silicon modules [45].

22.3.2.3 Color of the cells and modules

Solar cells are basically blue, dark blue or black after processing. Different colors are possible but these are not manufactured as standard. Some manufacturers sell tailor-made cells in special colors (e.g. gold, gray, green, red-orange and yellow). The cell color is varied by changing the thickness of various optical coatings on top of the cell, which changes their reflection. The blue color produces the highest efficiency solar cells. Current literature gives efficiencies for colored cells as 11.8% and 14.5% compared to optimized cell efficiency of 16.8% [46, 47], which corresponds to around 75% of the power of dark-blue cells [48].

Modules have several sections that can be colored. Besides the cells, the frame and the back sheet will also have a certain color. Older modules had natural aluminum frames and a white back sheet. The shape of the cell was very pronounced because of the contrasting color. However, modern modules have colors that are more in harmony: dark-blue cells with a dark back Tedlar® sheet and a dark-colored frame around the module, which produces a very uniform image. A roof or façade containing these uniform-colored modules will be seen as a single surface. The opposite effect is also possible by using modules in striking colors to attract attention and focus on the PV system.

22.3.2.4 The architecture of modules

Architects select modules based on their shape and composition possibilities. There is a big visual difference between framed and frameless modules.

Frameless modules look very similar to window glass. A surface with frameless modules with a "hidden" mounting system looks very uniform. The seams seem to be hidden and the individual module is hard to recognize. This smooth surface has a high aesthetic value.

Framed modules give a totally different effect. The frames can be heavy and therefore determine the total impression of the surface. The very visible frames divide the surface into modules and every individual module is very recognizable. This is not always the image envisaged by the architect.

To solve this problem, smaller frames in the same (dark or blue) color as the cells can be used and are less visible. The soldering between the cells is a small detail but is an important part of the image for very visible PV systems. In the older techniques the soldering was very visible and not very smooth. However, new techniques mean that the soldering is hidden better and new types of soldering, for example, ECN cells, can be expected in the future.

Modules vary significantly in size. Standard modules are less expensive than applications using tailor-made modules. However, almost every form, shape and dimension is possible with tailor-made modules. The glazing is available as single and double (insulating) glass. Thin-film modules allow greater freedom to select size and color than c-Si modules.

Downloaded from https://onlinelibrary.wiley.com/doi/ by <Shibboleth-member@purdue.edu>, Wiley Online Library on [25/08/2024]. See the Terms and Conditions (https://onlinelibrary.wiley.com/terms-and-conditions) on Wiley Online Library for rules of use; OA articles are governed by the applicable Creative Commons License

22.4 STEPS IN THE DESIGN PROCESS WITH PV

22.4.1 Urban Aspects

The aim of integrating PV systems into buildings is to reduce costs. To generate maximum power from building-integrated systems, certain urban and architectural aspects are important.

The main starting point is the maximum power that can be generated by a system. The primary hindrances can be the (partly) shadowing of a system by other buildings or objects, and the nonoptimum orientation relative to the sun. Reflection can also be a problem for the surrounding buildings.

22.4.1.1 Orientation and angle

The amount of irradiance depends on the latitude. The maximum irradiance corresponds to surfaces, tilted at an angle equal to about the latitude minus 10° (see Chapter 20 for calculations on solar irradiance). At 52° north good results (>90%) can be achieved by orienting the modules between southeast and southwest, with system angles between 30° and 50° from the horizontal. Orientations between east and southeast, and between southwest and west, are fairly reasonable with system angles between 10° and 30° from horizontal. The irradiance will be reduced by around 15% of the maximum.

Flat-roof systems with very low angles (between 5° and 10°) can be a good solution for difficult orientations. The loss of irradiance will be between 5% (south) and 20% (north).

22.4.1.2 Distance between buildings

Shadowing is a critical issue for BIPV. In general, designs in which the PV modules are shaded for much of the year should be avoided. For low-rise areas, the problem is easy to solve. The distance between individual houses can be calculated. For mixed height neighborhoods, it will be more difficult. A high-rise apartment building in a low-rise neighborhood can cause a lot of unwanted shading.

The density of an area also has a lot of influence. In high-density areas (cities) the distances between buildings are often so small that there is significant shadowing throughout a large part of the year.

On a general note, it is worth mentioning that facade systems (vertical) are more sensitive to shading and need longer distances from other buildings than tilted systems (roofs). Horizontal systems have a lower irradiance, as previously mentioned, but will be the best solutions for avoiding shadow. Only neighborhoods with a mixture of low- and high-rise buildings might be unsuitable for horizontal systems.

22.4.1.3 Trees

Greening the area around buildings makes the area look very attractive and the microclimate more comfortable for the inhabitants.

Downloaded from https://onlinelibrary.wiley.com/doi/ by <Shibboleth-member@purdue.edu, Wiley Online Library on [25/08/2024]. See the Terms and Conditions (https://onlinelibrary.wiley.com/terms-and-conditions) on Wiley Online Library for rules of use; OA articles are governed by the applicable Creative Commons License

The shadowing effect of trees is very important, as the trees will be very dense during the summer. Even during the winter, when trees lose their leaves, the branches give too much shade.

The aspect of growth is sometimes underestimated. Planning for the future growth of trees is very important and must be done carefully to avoid problems a few years after the building has been completed or the PV system has been installed.

Solutions can be to

- only plant trees on the north side of buildings,
- plant only small trees up to two stories high,
- prune trees annually to keep them small.

22.4.1.4 Zoning

In future, a special solar zoning will be needed in urban areas with PV systems. The borders of building areas can be clearly marked on three-dimensional maps to prevent future problems. The amount of sunlight can also be determined on these maps.

22.4.1.5 Reflection

Although not a major problem, under certain circumstances, reflection can occur. In low-rise buildings, there are no significant problems, but in mixed low- and high-rise areas residents in high-rise buildings may experience some annoying reflections if all the surrounding houses have (glass-covered) PV modules. The fact that there are certain distances between buildings (for shadowing) may eliminate most of the potential problems.

22.4.2 Practical Rules for Integration

There are a few important rules for integrating modules into buildings. These rules concern the functioning and maintenance of the system, for example:

1. shadow is not allowed on the module,
2. ventilation is required at the back of the modules (not as important for thin film a-Si),
3. make it easy to mount and remove a module,
4. ensure that the module stays clean or can be cleaned,
5. make easy electrical connections,
6. ensure that wiring is sun-proof and weather-proof.

1. As previously mentioned, even partial shadow on the modules will decrease the energy output. Profiled mounting constructions, in particular like awnings, can produce shadows along the edge of the adjacent module that will result in loss of efficiency.
2. Modules with crystalline cells have a higher output when the temperature is lower. With ventilation at the back of the module it is possible to keep the temperature low

Downloaded from https://onlinelibrary.wiley.com/doi/ by <Shibboleth>-member@purdue.edu, Wiley Online Library on [25/08/2024]. See the Terms and Conditions (https://onlinelibrary.wiley.com/terms-and-conditions) on Wiley Online Library for rules of use; OA articles are governed by the applicable Creative Commons License

and avoid a decreasing output. However, thin-film amorphous silicon reacts differently. The higher temperature does not influence the efficiency as much as crystalline silicon.[3]

3. Although the lifetime of modules is proven to be over 20 years, it is better to know how to remove a single module in the middle without removing the whole system. Electrical connections should also be "plug and play".[4] Easy electrical connections are needed for fast installation and for easy replacement of modules. Depending on the local safety regulations, precautionary measures should be taken, for example, using lifelines or moveable safety ladders.
4. The surface of the modules should be clean. Tilted modules will be cleaned by rain in most regions. Modules mounted at low angles can be treated with PV-Guard, a treatment that makes the surface smooth and makes cleaning with rain easier. In dry areas, cleaning should be part of the regular maintenance schedule.
5. Protect wiring against the weather. Rain is not the main problem, though all connections must be waterproof. Long-term influence from water should be avoided. Protection against sun and UV light is needed to ensure that the linesman of the wiring is not reduced. Depending on the area, wiring may also need to be protected from small gnawing animals.

22.4.3 Step-by-step Design

A PV system consists of a number of modules with solar cells, an inverter, batteries or, in most cases, a connection to the grid. A single house with a small installation can be connected through the existing electricity meter. The electricity that is produced will be used primarily in the house. Any surplus will be fed into the grid and the meter will spin backwards. However, not every utility company will allow this and in some cases a second meter is installed. This often happens with larger systems (more than 2 or 3 kWp). Larger systems or combined systems that are maintained by the utilities are connected directly to the grid.

22.4.3.1 Solar design

To design with photovoltaics the first set of questions are, "Why do I want to integrate PV into the building?" and "Is it for general energy supply, to make the building more independent, or to make a statement about the building's inhabitants?"

Large systems will be used for general energy supply. This means large surfaces that can be treated in an architectural way. Different types of modules, shapes, colors or textures can be used to design the look of the building.

The main issues for a more independent building are the efficiency of the system and the generated yearly output. The size of the PV system will depend on this and the designer has to allow for a certain number of modules. The designer will probably design

[3] See Chapter 12.
[4] "Plug and play" refers to very simple wiring and components that fit together like a computer and can easily be replaced.

Downloaded from https://onlinelibrary.wiley.com/doi/ by <Shibboleth-member@purdue.edu>, Wiley Online Library on [25/08/2024]. See the Terms and Conditions (https://onlinelibrary.wiley.com/terms-and-conditions) on Wiley Online Library for rules of use; OA articles are governed by the applicable Creative Commons License

the building around the integrated system, otherwise the system will be something that is connected, but not integrated, into the building.

22.4.3.2 Module placement and shadowing

The first step in the design process will be to look at the number of modules, their dimensions and the total dimensions of the system. All these aspects have to be integrated into the roof or facade. Shadowing of the modules is important. A module that is partly shaded will lose more efficiency than expected. If one row of cells in a module is covered or heavily shaded, this can block the output of the entire string.

Small objects that can cause shading, such as chimneys and fans, are less important. The shadow will move during the day and there maybe indirect light available. Some modules have integrated diodes that allow a short break when a row of cells is covered or shaded.

22.4.3.3 Space required for balance of systems and interconnections

Space is also required for the inverters. The modules have junction boxes at the back that are connected by cables to the inverters. For better efficiency, the best place for these inverters is near the modules. An AC cable has to be fed from the inverters into the grid via the meter.

Space is also required for a junction box at the back. Together with the ventilation required at the back of the module, this means a gap between 20- and 50-mm (depending on the size of the junction box) between the back of the module and the mounting surface that can be used for both functions.

Space for a second utility meter may be required near the first meter, unless a double meter can be used. Safety switches are required near the inverters in order to work on the PV system safely.

22.4.4 Design Process: Strategic Planning

A few procedural steps may be necessary to ensure that the PV system is successfully integrated into the design. A common rule is to integrate the PV system into the building process without disturbing that process.

Step 1: The first step is consultation with the authorities about local regulations, building permits and the electrical connection to the grid.
Step 2: The second step is to consult the utility company about the grid connection, electrical diagrams and the metering system.
Step 3: The third step is the internal meeting with all building partners. A kick-off meeting very early in the process may be useful, to discuss the entire integrated PV system with the building contractor, the roofing company, the electrician and the PV supplier.

There are many unique issues to resolve in installing BIPV. The main points in this meeting concern the responsibilities of each party in the building process. Who is

Downloaded from https://onlinelibrary.wiley.com/doi/ by <Shibboleth-member@purdue.edu>, Wiley Online Library on [25/08/2024]. See the Terms and Conditions (https://onlinelibrary.wiley.com/terms-and-conditions) on Wiley Online Library for rules of use; OA articles are governed by the applicable Creative Commons License

responsible for the waterproofing of the roof – the roofing company or the PV installer? Who is responsible for electrical safety – the electrician or the PV installer? Who is responsible for safety on the site – the general contractor or the PV installer? All these aspects must be clearly defined and noted in advance.

Many PV suppliers offer turnkey contracts. This is easy for clients because they receive a complete working system for their money. However, the client is then responsible for the coordination between PV supplier and building contractor. Placing all responsibility with the building contractor means an extra surcharge of perhaps 10% on the cost of the PV system. A good solution is to make the building contractor (general contractor) responsible for the PV system and negotiate a special fee for coordination and use of equipment (scaffolds and crane) from the building contractor.

22.5 CONCLUSIONS

Building integration aims to reduce costs and minimize the requirement for land. To increase market acceptance it is important to show architecturally elegant, well-integrated systems. Moreover, building owners can show their environmental commitment with highly visible building-integrated PV systems.

This means that there is a large potential for BIPV in the built environment. The main factors for successful integration are suitable buildings [49], (i.e. suitable orientation and lack of shadow) and a reason for building integration. For newly constructed sustainable buildings, BIPV will be part of the energy strategy. However, for existing buildings there must be a valid reason for integrating PV systems. Building renovation, including the roof and façade, often provides an opportune time for selecting BIPV [50, 51].

The building or renovation process plays an important role in the success of BIPV. Can the building owner benefit from BIPV? If so, the owner will be willing to implement PV systems in the building plans. The architect or designer needs to have a good basic knowledge of BIPV and be able to integrate PV into the design. If architects do not understand the basics of PV, they will make mistakes that eventually have to be resolved during the installation process. The worst cases involve mistakes that cannot be resolved at the end of the building process and that result in a lower efficiency and quality of the PV system.

Is the utility company willing to cooperate? If not, the building owner will probably try to avoid difficulties in an already complex construction process.

The architect or designer should use all visible opportunities to integrate PV into the design in a highly aesthetic way. The important issues are the architectural function of a PV module (replacing other building elements) and the visible aspects of modules, such as the dimensions, mounting system, form and color of cells, back sheet and frames.

To recognize these aspects, criteria have been formulated for judging building integration of PV. These criteria are useful for manufacturers and technicians who are involved with building integration from the engineering and technical aspects of the building process.

Downloaded from https://onlinelibrary.wiley.com/doi/ by <Shibboleth-member@purdue.edu>, Wiley Online Library on [25/08/2024]. See the Terms and Conditions (https://onlinelibrary.wiley.com/terms-and-conditions) on Wiley Online Library for rules of use; OA articles are governed by the applicable Creative Commons License

REFERENCES

1. Reijenga T, "The Changing Cities of Europe", *Proc. Sustain '99* (Amsterdam, 1999).
2. EC DG XVII, "White Paper for a Community Strategy and Action Plan; Energy for the Future: Renewable Sources of Energy", *Proc. Sustain '99* (Amsterdam, 1999).
3. Schoen T *et al*., *Proc. 14th Euro. Conf. Photovoltaic Solar Energy Conversion*, 359–364 (1997).
4. Kurokawa K, Kato K, Paletta F, Iliceto A, *Proc. 2nd WC Photovoltaic Solar Energy Conversion*, 2853–2855 (1998).
5. Thomas R, Grainger T, Gething B, Keys M, *Photovoltaics in Buildings – A Design Guide*, Report S/P2/00282/REP, ETSU, DTI, London (1999).
6. Strong S, Lloyd Jones D, *A Renewable Future*, IEA PVPS Task7, Final Task (Feb. 2001).
7. Kiss G, *Proc. 2nd WC Photovoltaic Solar Energy Conversion*, 2452–2455 (1998).
8. Muller A, Roecker C, Bonvin J, *Proc. 14th Euro. Conf. Photovoltaic Solar Energy Conversion*, 889–892 (1997).
9. Reijenga T, *Prog. Photovolt.* **4**, 279–294 (1996).
10. Maycock P *et al*., *Building with Photovoltaics*, 78–81, Ten Hagen & Stam, Den Haag (1995).
11. Reijenga T, Böttger W, *Proc. 2nd WC Photovoltaic Solar Energy Conversion*, 2748–2751 (1998).
12. Lloyd Jones D, Matson C, Pearsall N, *Proc. 2nd WC Photovoltaic Solar Energy Conversion*, 2559–2562 (1998).
13. Wilk H, *OKA-House of the Future*, IEA SHCP Task 19 (1997).
14. Reijenga T, Kaan H, *Proc. 16th Euro. Conf. Photovoltaic Solar Energy Conversion*, 1952–1959 (2000).
15. Hynes K, Pearsall N, Shaw M, Crick F, *Proc. 13th Euro. Conf. Photovoltaic Solar Energy Conversion*, 2203–2205 (1995).
16. Hagemann I, Leppänen J, *Proc. 14th Euro. Conf. Photovoltaic Solar Energy Conversion*, 694–697 (1997).
17. Eiffert P, Kiss G, *Building-Integrated Photovoltaic Designs for Commercial and Institutional Structures – A Sourcebook for Architects*, 7–10, NREL, Golden, CO (2000).
18. Eiffert P, Kiss G, *Building-Integrated Photovoltaic Designs for Commercial and Institutional Structures – A Sourcebook for Architects*, 42–44, NREL, Golden, CO (2000).
19. Pitts A, Tregenza P, Coutts R, *Proc. 16th Euro. Conf. Photovoltaic Solar Energy Conversion*, 1902–1905 (2000).
20. Kaan H, Reijenga T, *Proc. 2nd EuroSun*, V3.2-1–V3.2-6 (1998).
21. Reijenga T, Kaan H, *Proc. 2nd WC Photovoltaic Solar Energy Conversion*, 2740–2743 (1998).
22. Reijenga T, Schoen T, *Proc. 2nd WC Photovoltaic Solar Energy Conversion*, 2744–2745 (1998).
23. Schoen T *et al*., *Proc. 16th Euro. Conf. Photovoltaic Solar Energy Conversion*, 1840–1843 (2000).
24. Reijenga T, "Photovoltaic Building Integration Concepts – What do Architects need?" *Proc. IEA PVPS Task7 Workshop Lausanne Featuring A Review of PV Products*, IEA PVPS Task7, Halcrow Gilbert, Swindon (2000).
25. Reijenga T, "Photovoltaics in the Built Environment", *Proc. 2nd World Solar Electric Buildings Conference*. ESAA, ANZSES (Sydney, 2000).
26. Cace J, *Proc. 14th Euro. Conf. Photovoltaic Solar Energy Conversion*, 698–700 (1997).
27. Vlek F, Schoen T, Iliceto A, *Proc. 16th Euro. Conf. Photovoltaic Solar Energy Conversion*, 1783–1786 (2000).
28. Reijenga T, *Proc. 16th Euro. Conf. Photovoltaic Solar Energy Conversion*, 1793–1796 (2000).
29. Eiffert P, Kiss G, *Building-Integrated Photovoltaic Designs for Commercial and Institutional Structures – A Sourcebook for Architects*, 48, 49, NREL, Golden, CO (2000).
30. Reijenga T, "Energy-Efficient And Zero-Energy Building in the Netherlands", *Proc. International Workshop on Energy Efficiency in Buildings in China for the 21st Century*, CBEEA (Beijing, December 2000).

Downloaded from https://onlinelibrary.wiley.com/doi/ by <Shibboleth-member@purdue.edu>, Wiley Online Library on [25/08/2024]. See the Terms and Conditions (https://onlinelibrary.wiley.com/terms-and-conditions) on Wiley Online Library for rules of use; OA articles are governed by the applicable Creative Commons License

31. Reijenga T, Tuyl L, Schneider A, de Vries G, *Smart Architecture for a Sustainable Future*, IEA-EUREC, Brussels (2000).
32. Ito T, Ishikawa N, Nii T, *Proc. 14th Euro. Conf. Photovoltaic Solar Energy Conversion*, 690–693 (1997).
33. Butson J *et al*., *Proc. 2nd WC Photovoltaic Solar Energy Conversion*, 2571–2574 (1998).
34. Kaan H, Reijenga T, *Proc. ACEEE*, 5.025–5.014 (1998).
35. Posnansky M, Szacsvay T, Dütsch B, Stucki B, *Proc. 14th Euro. Conf. Photovoltaic Solar Energy Conversion*, 1922–1924 (1997).
36. Nath P *et al*., *Proc. 2nd WC Photovoltaic Solar Energy Conversion*, 2538–2541 (1998).
37. Scheijgrond P *et al*., *Proc. 16th Euro. Conf. Photovoltaic Solar Energy Conversion*, 2049, 2050 (2000).
38. Toggweiler P, Ruoss D, Brügger U, Haller A, *16th Euro. Conf. Photovoltaic Solar Energy Conversion*, 1972–1975 (2000).
39. Böttger W, Schalkwijk M, Schoen A, Weiden T, *Proc. 14th Euro. Conf. Photovoltaic Solar Energy Conversion*, 2288–2291 (1997).
40. Roecker C, Bonvin J, Toggweiler P, Ruoss D, *Proc. 14th Euro. Conf. Photovoltaic Solar Energy Conversion*, 701–704 (1997).
41. Bonvin J, Roecker C, Affolter P, Muller A, *Proc. 14th Euro. Conf. Photovoltaic Solar Energy Conversion*, 1849, 1850 (1997).
42. Schnaller F, Roecker C, *Proc. 16th Euro. Conf. Photovoltaic Solar Energy Conversion*, 1945–1947 (2000).
43. Arya R, Carlson D, *Prog. Photovoltaics* **10**, 69–76 (2002).
44. Willeke G, Fath P, *Appl. Physics Lett.* **64**, 1274–1276 (1994).
45. Hunter-Fanney A, Doughtery B, Davis M, *J. Solar Energy Engineering*.
46. Mason N, Bruton T, *Proc. 13th Euro. Conf. Photovoltaic Solar Energy Conversion*, 2218, 2219 (1995).
47. Ishikawa N *et al*., *Proc. 2nd WC Photovoltaic Solar Energy Conversion*, 2501–2506 (1998).
48. Tölle R *et al*., *Proc. 16th Euro. Conf. Photovoltaic Solar Energy Conversion*, 1957–1959 (2000).
49. Frantzis L, Ghosh A, Rogers M, Kern E, *Proc. 2nd WC Photovoltaic Solar Energy Conversion*, 2799–2801 (1998).
50. Gutchner M, Nowak S, *Proc. 2nd WC Photovoltaic Solar Energy Conversion*, 2682–2685 (1998).
51. Reijenga T, Drok M, Oldegarm J, Kampen J van, *PV Systems and Renovation*, TNO, NOVEM, Delft (2001).

Further Reading

Humm O, Toggweiler P, *Photovoltaics in Architecture*, Birkhäuser, Basel (1993).
Lloyd Jones D, Hattersley L, Ager R, Koyama A, *Photovoltaics in Buildings – BIPV Projects*, ETSU, DTI, London (2000).
Muller A, Roecker C, Bonvin J, *Proc. 14th Euro. Conf. Photovoltaic Solar Energy Conversion*, 889–892 (1997).
Schoen T, Prasad D, Toggweiler P, Eiffert P, *Proc. 2nd WC Photovoltaic Solar Energy Conversion*, 2447–2451 (1998).
Strong S, *Photovoltaics in the Built Environment – A Design Guide for Architects and Engineers*, DOE/GO-10097-436, NREL, Golden, CO (1997).
Photovoltaics in the Built Environment (Special Issue) *Prog. Photovoltaics* **4**(4), 237–320 (1996).

Internet
www.pvportal.com
www.task7.org
www.pvdatabase.com
www.demosite.ch
www.lafarge.com

Downloaded from https://onlinelibrary.wiley.com/doi/ by <Shibboleth-member@purdue.edu>, Wiley Online Library on [25/08/2024]. See the Terms and Conditions (https://onlinelibrary.wiley.com/terms-and-conditions) on Wiley Online Library for rules of use; OA articles are governed by the applicable Creative Commons License

Petitioner Canadian Solar (USA) Inc., Ex. 1035, p. 2426

23

Photovoltaics and Development

Jorge M. Huacuz[1] and Lalith Gunaratne[2]

[1]*Instituto de Investigaciones Eléctricas, Cuernavaca, México,*
[2]*Solar Power & Light Co, Ltd, Colombo, Sri Lanka*

23.1 ELECTRICITY AND DEVELOPMENT

23.1.1 Energy and the Early Man

Survival has always been the main preoccupation of mankind. For many thousands of years, food, shelter and protection against harsh weather and wild animals were the primary requirements of early man. In the early days of humanity, people spent most of their time hunting and gathering, and hence, energy cycles in primitive societies were extremely simple: human energy was put into the pursuit of game and the manufacture of tools and weapons; wood collection to keep the fire burning for cooking while at the same time providing warmth and lighting was also an important activity. Food from the hunt was the basic fuel for human energy and the leftover animal grease also contributed to heat and light the shelter to maintain a suitable microclimate.

Over the years, early man incorporated new options to fulfill the basic requirements of survival, and at the same time altered the energy cycles of primitive society. Gardening was added to fishing and hunting as a source of food. Additional human energy had to be put into planting, weeding and harvesting. Products from gardening provided a more predictable source of food energy for humans and the basic feedstock for raising domestic animals, which in turn became the source of high quality protein and eventually an additional source of power. Gardening evolved into agriculture, which, along with animal husbandry, eventually displaced hunting as the main activity for survival. At some point in time, domesticated animals were incorporated to take away from humans the burden of load-pulling and back-carrying.

A time came when technology was developed to simplify everyday productive activities. Along with the dawn of progress came larger and larger requirements for

Handbook of Photovoltaic Science and Engineering. Edited by A. Luque and S. Hegedus
© 2003 John Wiley & Sons, Ltd ISBN: 0-471-49196-9

Downloaded from https://onlinelibrary.wiley.com/doi/ by <Shibboleth-member@purdue.edu, Wiley Online Library on [25/08/2024]. See the Terms and Conditions (https://onlinelibrary.wiley.com/terms-and-conditions) on Wiley Online Library for rules of use; OA articles are governed by the applicable Creative Commons License

energy. It is estimated that early man had a daily energy consumption rate of around 2500 kilocalories [1]. Later on, in primitive agricultural societies, which already had some domestic animals, this rate was around five times as large [2]. By the time of the low-technology industrial revolution in the mid-1800s, per capita daily consumption of energy reached 70 000 kilocalories in England, Germany and the United States [3]. During that period fuel wood and coal constituted the main sources of energy with smaller contributions from petroleum and hydropower. In the last quarter of the twentieth century, the dominant energy sources switched to petroleum, natural gas, nuclear energy and coal, while the average per capita consumption of energy in industrialized nations rose to over 230 000 kilocalories per day [3], two orders of magnitude larger than that of primitive man!

23.1.2 Let There be Electricity

With the early studies on electricity in the nineteenth century and the eventual development of the electric power industry, around 1882, the face of the Earth was changed forever. Electric lighting began flooding the cities at night and electric motors became the main source of power in factories. Earlier, in 1846, long distance communication had been made easier and faster with the introduction of the electric telegraph. Over the years, many inventions based on electricity increased the productivity in factories and made life at home easier and more comfortable.

Modern life became an endless chain of activities and events, fuelled by electricity: the alarm clock to wake people up in the morning, followed by the news on television or on the radio, the electric shaver and the hair dryer, the coffee brewer, the blender and the microwave oven or the electric stove, the refrigerator, the air conditioner, the computer, and so on and so forth. Electricity has also been the main element in improving the quality of basic services for the well being of people, such as clean water, education, medical care, entertainment and modern means of information and communication like the Internet.

23.1.3 One Third of Humanity Still in Darkness

Unfortunately, even today, not everybody has the fortune of enjoying all the benefits of progress: about one-third of humanity lacks access to electricity and, therefore, to a large number of electricity-based services and commodities. Around two billion people, mostly in the so-called developing countries, have remained in the earlier stages of human development, and still rely on wood fire, animal grease or kerosene lamps to light their paths and their homes at night. Modern means of communication and entertainment are either not known to them or are a distant possibility. Millions of people die every year from drinking polluted water, while others suffer from the lack of basic medical services. Illiteracy denies millions of people any possibility of gaining access to better opportunities. As hard as it may seem to believe, at the onset of the twenty-first century, with all the technology mankind has been able to create, survival is still the name of the game for millions and millions of people in remote rural areas of the world.

Reasons for such disparity are manifold, but certainly access to reliable, affordable and high-grade energy sources is one of them. The direct relationship between the

Downloaded from https://onlinelibrary.wiley.com/doi/ by <Shibboleth-member@purdue.edu, Wiley Online Library on [25/08/2024]. See the Terms and Conditions (https://onlinelibrary.wiley.com/terms-and-conditions) on Wiley Online Library for rules of use; OA articles are governed by the applicable Creative Commons License

per capita energy consumption and human development is well established, as can be observed in a number of studies [4, 5]. What is not too clear is what form of energy, how much of it and for what applications, is required to break the vicious circle of underdevelopment. However, experience shows that a little electricity properly applied could help resolve many of these ailments of society.

23.1.4 The Centralized Electrical System

Electricity is certainly the most sophisticated and flexible form of energy in use today around the world. But it has some drawbacks: electricity has to be used almost immediately after it is generated, as storing it may be expensive, time-limited and inefficient, and in the current scheme of supply, it has to be transported over long distances from the point of generation to the point of use, which can be inefficient and unreliable, especially when these two points are too far apart from each other in places lacking support infrastructure.

In the early days of the electric power industry, electricity was generated right at the point of use. Around 1880, even street lights in places like Paris and London had their own individual generators [6]. Electricity was also then mostly generated using local and renewable sources of energy. Water wheels originally used in the factories to mechanically power process machinery, were later retrofitted into prime movers to turn electric generators, which in turn began powering electric motors in the late nineteenth century.

As the demand for electricity increased because of industrial and urban growth, and the distance between the point of generation and that of use became increasingly large, electric companies searched for new ways to deliver their services within good profit margins. Engineering research focused on alternatives to increase the power and hence the scale of the generating stations and the carrying capacity of transmission lines. Thus, the concept of economies of scale was introduced in the electric power industry, which for over one hundred years has influenced decision making for new investments in electric systems.

Since the generating units grew in size, electric companies oftentimes found themselves with excess generating capacity at the end of the construction of a new plant. The need to recover their investment in this excess capacity frequently motivated them strongly to look for new customers. Transmission and distribution lines were extended to reach the new customers, so an extensive grid was eventually created. Sometimes when demand was nonexistent, it was artificially created. For such purpose, donation of appliances was, at times, made by the electric company to the customer.

23.1.5 Rural Electrification

At some point in time, agricultural processes were identified as potential applications for electricity and, consequently, the lines began to be extended into the rural areas. Here, the density of potential clients and the intensity of electricity use was not as large as in the cities or the industrial centers; therefore investments in grid extensions became hard to recover, so new institutional and financing mechanisms were developed to support the operation. Official rural electrification programs were introduced in the most advanced nations, an initiative that eventually trickled down to the developing countries.

Downloaded from https://onlinelibrary.wiley.com/doi/ by <Shibboleth-member@purdue.edu>, Wiley Online Library on [25/08/2024]. See the Terms and Conditions (https://onlinelibrary.wiley.com/terms-and-conditions) on Wiley Online Library for rules of use; OA articles are governed by the applicable Creative Commons License

As rural electrification proved beneficial to developed societies, early policy planners felt that the same or similar benefits could be achieved in developing societies. Thus, a major effort was undertaken in the 1960s and early 1970s to extend the electrical lines into the rural areas of developing countries. However, by the end of the twentieth century only a few developing nations had reached an acceptable degree of electric grid coverage in rural areas. The rest could not advance much as a result of a number of problems faced by the electric utilities, including lack of capital to finance additions of capacity and grid extensions. Thus, the process of rural electrification through grid extensions in many developing nations stalled to the point that the problem of rural electrification again became a major political issue around the world.

23.1.6 The Rural Energy Scene

Life in many rural areas of the world is no different today than it was centuries ago. Even energy cycles resemble those of early man, although with the introduction of some modern elements. Firewood remains the main source of fuel in most rural communities, in spite of the alarming deforestation, dangers to health and the amount of work needed to collect it. In most places firewood is used mainly for cooking followed by shelter heating and lighting. A good reference point at hand is the case of Mexico, one of the most advanced economies in the developing world. Here, firewood consumption in 1997 represented around 2.7% of the total energy supply, a share that is larger than that of coal and nuclear electricity taken together and almost equal to that of hydroelectricity [7].

Candles and votive candles are more convenient than firewood for lighting, as they provide a more steady and whiter light, and can easily be carried from place to place, thus serving as a portable means for lighting pathways at night. Candles are frequently available in nearby towns, are not too heavy to carry in moderate quantities for long distances, and can be stored for long periods of time. Almost the same can be said for kerosene, which can be used in rudimentary lamps for lighting, although its availability may be more geographically restricted than that of candles. Getting either candles or kerosene requires money, which imposes an economic burden on poor rural families, while their use poses the risk of fire due to the flammable nature of the materials oftentimes used in the construction of rural houses.

23.2 BREAKING THE CHAINS OF UNDERDEVELOPMENT

23.2.1 Electricity Applications in the Rural Setting

The current patterns of energy use in rural areas show that the provision of small amounts of energy, especially electricity, changes the lifestyles of the rural population significantly. Energy applied to improve quality of life of the population may be a good first step to break the chains of underdevelopment. Applications such as lighting, clean water supply, entertainment and communications, preservation of vaccines and other medical supplies and means for modern education are usually welcome by governments, aid development agencies and the rural communities themselves. A number of tasks at home, mostly done by women, such as the provisioning of water, grain grinding, clothes sewing and others, could be made easier with the provision of small amounts of electricity.

Downloaded from https://onlinelibrary.wiley.com/doi/ by <Shibboleth-member@purdue.edu, Wiley Online Library on [25/08/2024]. See the Terms and Conditions (https://onlinelibrary.wiley.com/terms-and-conditions) on Wiley Online Library for rules of use; OA articles are governed by the applicable Creative Commons License

Electricity for the household is at the top of the shopping list of rural communities. A house with electricity is a symbol of status. Beyond that, electrical lighting facilitates movement at night inside the house, helps prevent accidents, eliminates the need for kerosene and other combustible materials for illumination (thus avoiding the risk of fire and health-damaging fumes), helps spot poisonous insects and other wild animals that could be a threat to humans, and helps respond instantly to critical situations in case of accidents or illness. Furthermore, illumination of external areas such as the streets and meeting points also helps promote social interaction and a number of after-hours outdoor activities.

Electricity in the house also makes modern means of entertainment a more realistic possibility. The rural telephone system gives people the opportunity to keep in touch with their families in other parts of the world, and to call for help in case of an emergency. Electricity also gives the opportunity to use modern means of getting information and imparting training, using VCRs, satellite links, computers and even the Internet.

23.2.2 Basic Sources of Electricity

With the introduction of the transistor radio and the handheld flashlight dry cells became a favorite means to provide light and entertainment in rural areas. Dry cells can be purchased in many places and are easy to carry. Thus, many rural families spend substantial amounts of money buying them. Transistor radios play an important role in the life of remote communities, not only because they bring music and entertainment, but also because radio broadcasting in many places carry important messages such as warnings of floods, instructions on health practices and other valuable services, such as family to family message delivery. Some countries have even set up radio stations with regional broadcasting in the locally spoken native language or dialect, when it is different from the official national language.

New forms of entertainment, such as portable televisions, VCRs and tape players, have increased the demand for electricity in many rural communities. Because of this, dry cells prove to be expensive and hence many users in rural areas not connected to the grid have resorted to the car battery as the power source for their needs, including home lighting. Car batteries are widely available in rural areas of many developing countries. They are rechargeable, and because of their relatively larger power capacity, they can be applied to a wider variety of services; they last longer and may turn out to be cheaper per unit of service delivered than dry cells. Recharging car batteries, however, requires a primary source of electricity. Where motorcars or tractors are available, people use them to recharge batteries. Otherwise, they are carried over long distances to the nearest source of electricity for recharging. However, batteries are heavy and burdensome to carry, so transport to the point of recharging is sometimes done on the backs of animals and sometimes on the backs of humans. There have been cases of local entrepreneurs setting up micro businesses to offer battery-recharging service. For this, batteries are collected, taken to the point of recharging, recharged and then returned to the owner. This operation however, requires some infrastructure such as roads and means for transportation, not always available in rural areas.

As the economic power of families increases, so does the need for electricity. Dry cells and car batteries are no longer sufficient, so people in many places put political

Downloaded from https://onlinelibrary.wiley.com/doi/ by <Shibboleth-member@purdue.edu, Wiley Online Library on [25/08/2024]. See the Terms and Conditions (https://onlinelibrary.wiley.com/terms-and-conditions) on Wiley Online Library for rules of use; OA articles are governed by the applicable Creative Commons License

pressure on electricity authorities to extend the grid to their communities, or individually resort to the use of small gasoline-fuelled generator sets. Small generator sets have the advantage of supplying alternate current of the right voltage, so that conventional appliances can be used. But their service is usually restricted to a few hours a day, because of the increasing cost of operation and maintenance of the equipment.

Experience shows that even when grid electricity is available, people in rural areas normally use it to light a few bulbs and perhaps to power small radios or typically black and white TV sets. Most people in rural areas lack the money needed to buy larger electric appliances, such as refrigerators and washing machines, or are simply not acquainted with them. Hence, because the number and size of appliances now in use is small, rural electrification represents an important niche of opportunity for the application of photovoltaic technology.

23.3 THE PV ALTERNATIVE

Photovoltaic (PV) technology nowadays is considered one of the most appropriate options to electrify dispersed population in remote places [8]. From an engineering point of view, modularity is perhaps the single most attractive feature of this technology. It allows designers to tailor electricity-generating systems as small in capacity as a few watts, or as large as many megawatts to suit specific needs, just following basic rules of electrical engineering. This feature combined with the suitability of the technology for autonomous operation, producing electricity with locally available sunshine, plus other characteristics such as lightweight, low-maintenance requirements and long useful life, has led people to consider photovoltaics as an attractive option for rural electrification. Ever since the technology was applied to power space satellites in the mid 1950s, the concept of reliable electricity generation for remote applications was firmly established. Terrestrial applications were developed with the basic idea of powering loads in remote places, where the cost of extending the grid was just too high. Today, hundreds of thousands of PV systems have been installed around the world to substitute for candles and kerosene lamps, gasoline- or diesel-powered generating sets, or even for unreliable grid extensions. The types of applications of PV technology in remote areas range from telecommunications, lighthouses and alarm systems in certain industries, to domestic applications and delivery of basic services. Leisure applications, such as sailboats and mountain cottages now carry PV panels to provide the required amounts of electricity, instead of noisy and smoky combustion engines. Even the petroleum industry, which is nowadays the basis for the world's energy supply, is using photovoltaics to supply electricity in offshore rigs or to power remote valve stations in oil and gas ducts.

The advantages of PV technology for rural electrification were demonstrated through a number of early projects in the period between 1968 and 1977 in Niger, Mexico and India. Applications included PV powered educational television, telephones, medical dispensaries and boarding schools for native Indian children. This early work demonstrated not only the technical viability of the systems but also the benefits to the user [9–11]. Some of these installations are still operational and in good condition, although with the limitations of a 30-or-so-year-old technology. Unfortunately, a critical mass of early projects was never achieved as to make a noticeable impact on society, and the lessons derived from the few projects on record have mostly fallen into oblivion. Only the notion that the technology

Downloaded from https://onlinelibrary.wiley.com/doi/ by <Shibboleth-member@purdue.edu, Wiley Online Library on [25/09/2024]. See the Terms and Conditions (https://onlinelibrary.wiley.com/terms-and-conditions) on Wiley Online Library for rules of use; OA articles are governed by the applicable Creative Commons License

was too expensive and not too reliable, has prevailed over the years among many decision makers, in spite of the tremendous progress PV technology has made in recent years in terms of cost, efficiency and reliability.

Progress in materials technology, electronics and PV systems engineering, along with a drop in price of the main components of the PV system and a better understanding of the needs and expectations of the rural people, have resulted in a large variety of ideas, proposals and technological schemes to use photovoltaics as a source of electricity to promote human and economic development in rural areas of the developing world. A large number of applications have been identified for PV systems in rural areas, some more mature than others in technical terms, but all facing similar problems to enter the rural market on a massive scale.

23.3.1 PV Systems for Rural Applications

PV systems for remote applications typically include three basic elements: one PV panel that converts solar radiation into electricity, a means to store the electricity produced by the PV panel, which is normally an electrochemical battery, and an electronic device that helps control the flows of electricity within the system, thus protecting the battery by properly dispatching available energy. A variety of devices capable of using electricity to provide comfort, entertainment and other services for the benefit of the user are then attached to the PV system by means of the electronic charge controller (ECC). Figure 23.1 shows a schematic diagram of a general PV system. Depending on the application, some elements of the PV system may not be necessary, as is the case of the battery in water pumping systems.

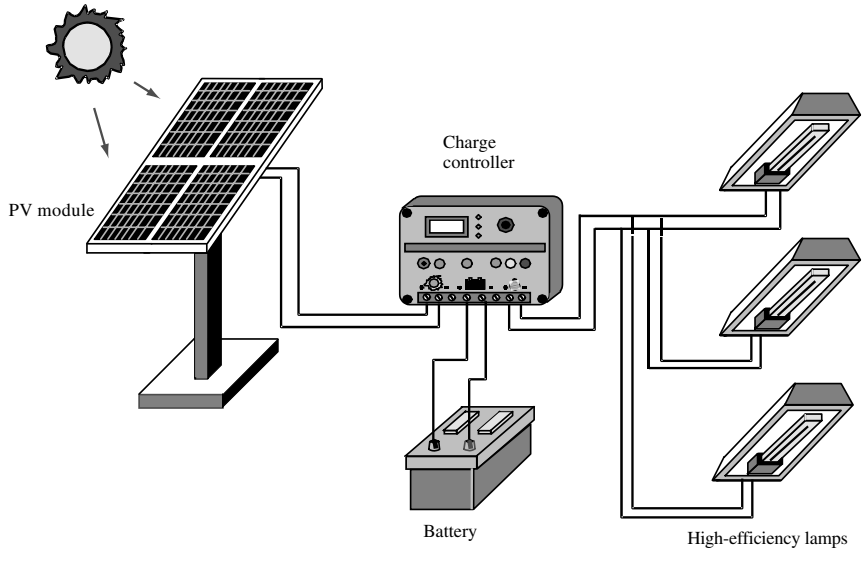


Figure 23.1 Schematic diagram of a general PV system

Downloaded from https://onlinelibrary.wiley.com/doi/ by <Shibboleth-member@purdue.edu>, Wiley Online Library on [25/08/2024]. See the Terms and Conditions (https://onlinelibrary.wiley.com/terms-and-conditions) on Wiley Online Library for rules of use; OA articles are governed by the applicable Creative Commons License

PV systems can be designed and built in the stand-alone mode, in which photovoltaics is the only source of electricity, or as hybrids, in which photovoltaics is combined with other sources of electricity, such as wind generators, small hydropower stations or combustion generators. PV hybrids are normally built to take advantage of other locally available renewable energy resources while at the same time improving the economics of the application. Photovoltaics can be installed in the so-called "disperse" mode, in which each individual application carries a full PV system as its source of electricity (just as it used to be in the very early stages of the electrification process in the late 1800s). Larger PV systems can be built to feed isolated electric minigrids, as is done today with diesel gen-sets in many parts of the world. Since PV panels produce relatively low-voltage direct-current electricity, a minigrid system requires additional components, such as DC/AC inverters and step-up transformers, to yield the right characteristics of the electricity on the user's side of the grid. Hybrid systems are also more complex to integrate, since different types of electricity can be produced by the different generating units that are included in the system. Figure 23.2 shows a number of possible configurations of PV systems, for most of which practical examples can be shown.

Solar home systems (SHS) are perhaps the most popular of all the PV applications. An estimated 500 000 to 1 000 000 such systems have been installed in rural communities around the world [12]. Systems for basic lighting generally include one small, 10 to 40 W PV module and a small battery, enough for one to four points of light (normally compact fluorescent lamps). Larger, 50 to 100 W PV panels and batteries of around 100 Ah open the possibility of feeding other electric appliances, such as transistor radios, tape recorders and small TV sets. Even larger PV systems can support complete sets of domestic electric appliances, just as in any urban house, but the price of such systems is at present prohibitively expensive for a poor family. The smallest SHS are direct substitutes for dry cells and other ancient means of lighting a house, and a form of using electrochemical batteries without the need of sending them elsewhere for recharging.

Quality and efficacy of communal services can substantially be increased when relatively small amounts of electricity are available on site. This can be done by photovoltaics. Schools can be supplied with modern audiovisual means, educational television, and even the Internet, as shown by the project *aldea solar* in Honduras, supported by UNESCO, the Honduras Ministry of Education and the Council for Science and technology (COHCYT) of Honduras. In Mexico, over 13 000 PV powered telephones now link tens of thousands of people in remote communities with the rest of the world, through terrestrial PV powered transmitting stations and satellite links [13]. In Cuba, the Ministry of Health has implemented a system of rural clinics powered by photovoltaics, which has been operational for a number of years [14]. PV powered technologies to disinfect water have already been tested and field-demonstrated in countries of Africa and Latin America in a recent project financed by the European Commission [15]. A large number of PV water-pumping projects have been implemented around the world, and many examples of other PV powered communal services and applications can also be found (see for instance: [16–20]).

A large number of possibilities to apply photovoltaics for productive activities in rural areas of the developing countries can also be envisioned. Small irrigation, cattle watering, grain grinding, small handicrafts shops and other similar activities that require

Downloaded from https://onlinelibrary.wiley.com/doi/ by <Shibboleth-member@purdue.edu, Wiley Online Library on [25/08/2024]. See the Terms and Conditions (https://onlinelibrary.wiley.com/terms-and-conditions) on Wiley Online Library for rules of use; OA articles are governed by the applicable Creative Commons License

Petitioner Canadian Solar (USA) Inc., Ex. 1035, p. 2434

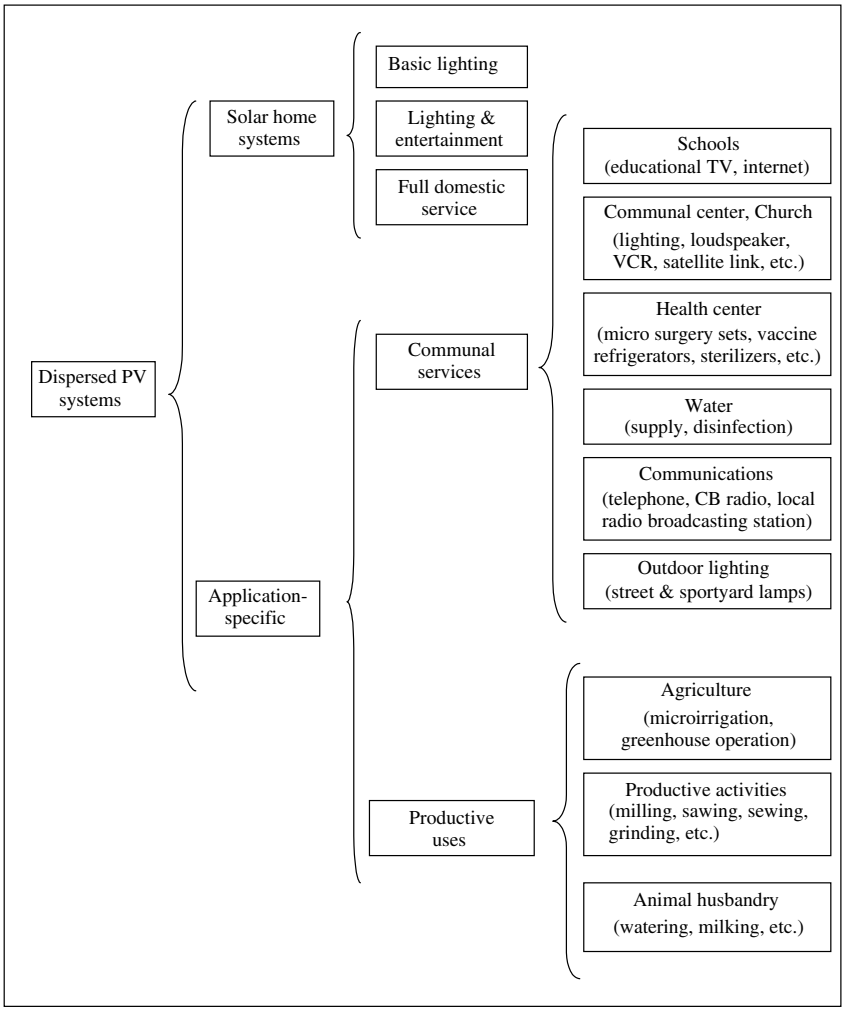


Figure 23.2 Possible configurations of PV systems

relatively small amounts of electricity can now be powered by photovoltaics to increase productivity and foster economic development.

23.3.2 Barriers to PV Implementation

For most urban people around the world, electricity comes into their homes just like magic: it is there, instantly and reliably at the touch of the switch. Few individuals make a conscious connection between their appliances and the electrical pole in the street, so

Downloaded from https://onlinelibrary.wiley.com/doi/ by <Shibboleth-member@purdue.edu, Wiley Online Library on [25/08/2024]. See the Terms and Conditions (https://onlinelibrary.wiley.com/terms-and-conditions) on Wiley Online Library for rules of use; OA articles are governed by the applicable Creative Commons License

paying their monthly bills is perhaps the closest they get to the electricity business. But even fewer people realize the technical and administrative complexities behind the process of generation, transmission and distribution of electricity that allows factories to run and people to enjoy the benefits of modern services.

Understanding the physical principles that turn primary energy into electricity belongs to a small group of technical elite in the universities, research centers and electric companies. For the layman, it makes little difference whether primary energy is hydropower, nuclear power, fossil fuels or solar energy. Thus, the fact that electricity can be locally produced using the sunrays as the primary source of energy, with no wires connecting to remote and unknown places and facilities, would be of significance only to the most knowledgeable people. It is interesting to know that PV users in native communities in many parts of the world make a cosmogonist connection between electricity and their ancient god, the Sun. Thus, for most of these people PV technology is an appealing means to get a long-awaited service.

However, after learning about photovoltaics people are inclined to ask why is it that with so many virtues and so many advocates, PV technology has only reached one-tenth of a percent of the world's rural population with no access to the grid? The answer is found in the number of barriers a new technology such as this has to overcome to fully enter the market. In the case of photovoltaics, some such barriers are well known, others still unknown; some technical in nature and others having to do with institutional, social and financing issues. Just as conventional electricity is generated, in large and distant facilities, transmitted and then distributed to reach the individual consumer, so is PV technology produced in a small number of facilities in Europe, Japan and the United States, transported across the continents and distributed to reach the final user in very remote rural areas. And at each step a number of operations need to take place, which involve different degrees of complexity and cost. Therefore, bringing the PV solution to those sites where the grid has not been able to reach can be a very difficult task, unless such barriers are successfully removed.

23.3.3 Technical Barriers

PV systems are claimed to be reliable and long lasting. This is true and proven insofar as the PV module is concerned, but not every component of the system's balance has the same degree of technological maturity. In both, stand-alone and hybrid systems, batteries are perhaps the weakest links. Batteries are exposed to overcharging and over-discharging, which usually reduce their useful lifetime. Batteries also demand a fair amount of attention and regular maintenance, albeit relatively simple. However, even the simplest technical tasks may prove to be complicated in rural areas where a high degree of illiteracy and a lack of familiarity with modern technology, and with electricity in particular, is more the rule than the exception. The problem with batteries arises in part because of the fact that the lead-acid technology now in use, available for over one hundred years, was not specifically designed for use in PV systems. Adaptations of the current technology into what is now called *solar batteries*, and development of new battery types, such as nickel-metal hydride [21], promise to ease many of the current problems.

SHS also face other problems, mostly in the charge controllers and the lamps, basically as a result of an industry that has until now had an uneven degree of development

Downloaded from https://onlinelibrary.wiley.com/doi/ by <Shibboleth-member@purdue.edu, Wiley Online Library on [25/08/2024]. See the Terms and Conditions (https://onlinelibrary.wiley.com/terms-and-conditions) on Wiley Online Library for rules of use; OA articles are governed by the applicable Creative Commons License

Downloaded from https://onlinelibrary.wiley.com/doi/ by <Shibboleth-member@purdue.edu, Wiley Online Library on [25/08/2024]. See the Terms and Conditions (https://onlinelibrary.wiley.com/terms-and-conditions) on Wiley Online Library for rules of use; OA articles are governed by the applicable Creative Commons License

(for a detailed discussion on charge controllers, see [22]). Two schools of thought seem to underline the issue: simple, sturdy, low-tech, low-purchase-cost devices against high-tech, sometimes a bit complex and perhaps lower life cycle–cost devices. The issue is not easy to resolve, especially with so little systematic information coming from the field on the performance of such devices. Taking into consideration that rural areas in developing countries are far from being mature markets for photovoltaics (and for many other goods) and accounting for the illiteracy of the rural population, consumer choice will hardly be a useful parameter to resolve the issue, especially if one considers that a large number of PV rural electrification projects are still being carried out in the "technology push" mode.

The suitability of photovoltaics as a solution to the rural electrification problem is being taken for granted by many advocates of the technology. Unfortunately, few studies seem to have been carried out to assess the performance of SHS now in the field, in a systematic and comprehensive manner. At this stage of technology implementation, information from the field is vital as a feedback mechanism to gauge the efficacy of the PV solution, to improve the chances of overall success and to assure long-term sustainability. Field surveys, however, tend to be expensive, especially where the most remote and isolated communities are concerned, and availability of funds for monitoring and evaluating SHS projects in the field is not obvious.

A 35-man-month field study was recently completed in Mexico, in which 1740 SHS installations (out of around 60 000 installed with government financing) in most regions and communities included in government programmes were evaluated. The study had a three-fold purpose: to assess the physical and operative condition of the systems, to probe the degree of satisfaction of the users and to evaluate the efficacy of measures previously implemented to make the projects sustainable. Preliminary analysis of the information gathered in the study shows that from the technical point of view things look good with most SHS samples performing well (for more details on these results, see [23]). But there are reasons to believe that as systems age, the results may change, unless corrective measures are taken.

Introducing photovoltaics in rural areas of developing countries is an innovative exercise in society, with the particularity that a space-age technology is being adapted for operation in a sector of society living, in many cases, at least five hundred years in the past. From this perspective, it is hard (and even dangerous for project sustainability) to ignore the strong connection that must be established between the technology (hardware) and the user. For even the most sophisticated, well-designed and perfectly built piece of PV technology is bound to fail sooner than later, if the ground for seeding it is not properly prepared. This means information, training and local capacity building on the user side, as well as user involvement at every step of the process to make them aware of the important role they play in the solution of their own problems. Similar considerations can be made in connection with the environment (social and physical) in which the PV system is bound to be installed. For instance, anecdotic and written information from the field points to the fact that some PV components designed and built with technical criteria prevailing in advanced, cold countries are not performing well in the tropics where it is most needed. Reasons for this are many, but their discussion is outside the scope of this chapter.

Alternative technical schemes to the SHS as a means to provide basic electricity services in rural areas are being tested. Battery-charging stations, where a large central PV array is installed to recharge batteries brought in by the user, who pays a fee for the service, is one such scheme advocated by a number of people. The rationale behind this scheme is that peasants in many parts of the world already use battery-charging points distant from their homes. It is also argued that microbusinesses could develop in remote areas to enhance the chances of sustainability of the electrification process and so, several projects of this kind are underway in various countries. However, recent field studies reveal [24] that this alternative also has several shortcomings, which are forcing project officials and users to switch to SHS as a substitute to the previously used PV battery-charging stations.

The preceding discussion was meant to point out the fact that even though engineers and industries will most likely solve the remaining technical problems facing PV technology for rural applications before this market enters into its mature stage, a number of more complex issues at the technology-user interface remain to be understood and dealt with. The cause–effect diagram of Figure 23.3 is an attempt to show the variety of factors leading to a failed system, and consequently a dissatisfied user. In the long run, the degree of user satisfaction will determine the level of acceptance of PV technology as the solution to the problem of rural electrification.

Technical standards, design guidelines and other elements for quality assurance of PV systems are also important for the sustainability of PV rural electrification projects. A number of these elements are being developed in institutions, professional societies and international organizations around the world. Most of them, however, focus mainly on pure technical (hardware) issues, as is the case of the recommended specifications of the organization Global Approval Program for Photovoltaics (PV GAP) and the standards

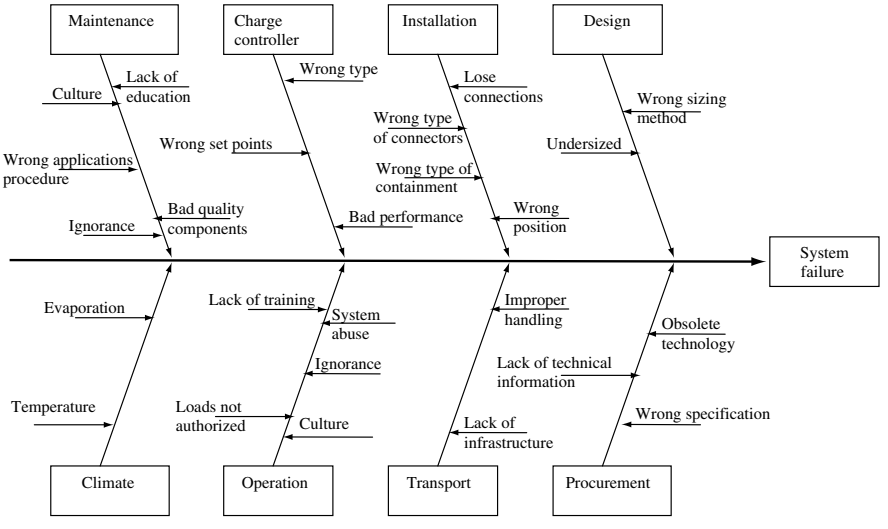


Figure 23.3 Cause–effect diagram showing a variety of factors leading to a failed system

Downloaded from https://onlinelibrary.wiley.com/doi/ by <Shibboleth-member@purdue.edu, Wiley Online Library on [25/08/2024]. See the Terms and Conditions (https://onlinelibrary.wiley.com/terms-and-conditions) on Wiley Online Library for rules of use; OA articles are governed by the applicable Creative Commons License

issued by the International Electrochemical Commission (IEC) Technical Committee 82, and little attention is being given to the soft and organizational aspects of the problem dealt with in other works [25, 26].

23.3.4 Nontechnical Issues

23.3.4.1 Initial cost

It is common knowledge that for a commercial operation to be sustainable in the modern economy, a flow of goods has to be properly matched by a counter flow of money. Sunrays striking on the roofs of houses are free, but equipments to turn solar energy into electricity, and to transform this electricity into needed services, are not. PV manufacturing companies invest in factories and raw materials, pay wages to their workers and taxes to their governments and are obliged to deliver revenues to their shareholders. All expenses plus profits essentially set the base price of their products. In a second step, PV components from different companies are transported to specific points for systems integration. In turn, packaged systems are fed into the distribution channels for retailing and final installation where the end user wants them.

By the time a PV system is installed on the user's premises, its base price has increased a number of times. So, people need money to get their systems installed. Considering the low capacity of the peasants in rural areas to pay for goods, a set of important questions emerge when one considers photovoltaics as the solution to the rural electrification problem. Are people willing to pay for the system? How much can they afford to pay? What mechanisms can be instrumented to make systems more affordable? If people cannot pay, should they remain in darkness or should somebody come to their rescue? What roles can governments and development agencies play? And even when people can pay, should they bear the full system cost, even at this early stage of technology introduction when many companies are still building their infrastructure and learning how to manufacture, integrate and market the systems, so that their transactions costs are a lot higher than they should be? These are not trivial questions considering that, for the miracle of full-scale rural electrification to happen, around 300 000 million US$ must, in principle, flow from the poorest regions of the world to the modern sector of society so that PV systems can flow in the opposite direction.

23.3.4.2 Breaking the initial cost barrier

Consequently, since solar energy, the fuel used by PV systems is free and systems are, at least theoretically, low maintenance and long lasting, system cost is commonly seen as the main stumbling block for the introduction of photovoltaics. A number of schemes have been tried over the past decade in search of an effective way to remove this barrier. Most of them can be grouped into three categories: the *social route*, in which poverty alleviation programs and other socially driven mechanisms are used by governments and bilateral aid organizations to make funds available for the purchase of PV systems in favor of the least privileged people; the *fiscal route*, in which taxes, import duties and other fiscal levies are removed to lower the local price of the PV system, thus making it somewhat more affordable for the final user, while at the same time facilitating the

Downloaded from https://onlinelibrary.wiley.com/doi/ by <Shibboleth-member@purdue.edu>, Wiley Online Library on [25/08/2024]. See the Terms and Conditions (https://onlinelibrary.wiley.com/terms-and-conditions) on Wiley Online Library for rules of use; OA articles are governed by the applicable Creative Commons License

creation of a local market; and the *business route*, in which banks, private companies and entrepreneurs are devising and testing a number of schemes to make financing available for the purchase of the PV system, thus helping to create a market for photovoltaics at the same time. One way or another, currently each of these routes somehow benefit from the intervention of governments, multilateral organizations and lending institutions. On the other hand, boundaries between these routes are not necessarily clear-cut, so that combined or coexisting schemes are not uncommon.

Not everyone in rural areas is necessarily poor or totally dispossessed. Some people live in remote places for convenience, either because their source of income is attached to the natural resources locally available, or because they prefer living in a cleaner and quieter environment than in the city. They do not have electricity from the grid, simply because they are too far away, but they usually rely on gasoline or diesel-fuelled gen-sets for their electrical service. These people, however, could easily purchase a PV system without any financial assistance, if one was made available to them. This is already a good market that is being tapped in a number of countries, such as Spain, Colombia, Mexico and others. On the other hand, some estimates indicate that between 25 and 50% of people living in remote places could purchase a SHS provided some sort of financial assistance was available to them [27]. This is a substantial market in its early stages of development; to tap this market a number of schemes are being tried by private entrepreneurs and multilateral development organizations, as is the case in Kenya, Zimbabwe and the Dominican Republic. However, the poorest of the poor, representing the largest portion of the world's rural population, can hardly ever afford to buy their own PV systems.

23.3.4.2.1 The business route

For those in need of financial assistance, two alternative models are being tested. One focuses on the sale of the PV system (the sales model), the other on the sale of the electricity produced by the system (the service model). Both models have advantages and shortcomings and both involve flows of money beyond the control of the PV user.

In the sales model, the PV system is purchased on credit by the user, who becomes the owner and takes over the responsibility of system maintenance and replacement of parts. Money for the transaction is usually borrowed by the user from a set of different sources, which may include the system supplier, a finance institution, or any other type of credit organization such as a revolving fund or a local microfinance operation. In any case, money is obtained at a cost, which adds to the cost of the PV system, and is paid back in periodic installments under prearranged terms and conditions. However, this additional cost is what entitles the user to the benefits of electricity, albeit in small quantities. This model is preferred by those who like the social status of system ownership and are willing to assume the task of maintaining the equipment and the responsibility for replacing damaged or worn out parts.

People not willing to take any risks, may opt for the service model, in which the supplier retains ownership of the PV system, or of some parts thereof, and then charges some monthly fee for the electricity delivered to the user. The supplier maintains the system and becomes responsible for providing the user with electricity, according to system capacity. Following the current practice, this kind of service can be provided through a regulated concession, an unregulated open market provider or a community-based provider.

Downloaded from https://onlinelibrary.wiley.com/doi/ by <Shibboleth-member@purdue.edu, Wiley Online Library on [25/08/2024]. See the Terms and Conditions (https://onlinelibrary.wiley.com/terms-and-conditions) on Wiley Online Library for rules of use; OA articles are governed by the applicable Creative Commons License

Downloaded from https://onlinelibrary.wiley.com/doi/ by <Shibboleth-member@purdue.edu, Wiley Online Library on [25/08/2024]. See the Terms and Conditions (https://onlinelibrary.wiley.com/terms-and-conditions) on Wiley Online Library for rules of use; OA articles are governed by the applicable Creative Commons License

Needless to say, the risk assumed by the service supplier also has a cost, which reflects on the monthly fee charged. According to some estimates, the added monthly fee for service over a period of 10 years could double the life cycle–costs of the same PV system when purchased on credit [27]. Current PV projects in the fee-for-service model show a large dispersion in the amount of the monthly fee charged to individual users. A number of factors may be responsible for this. For instance, some projects may involve some sort of subsidy, and in other cases, service suppliers may not follow the same rules to define the scope of their responsibility: some may retain responsibility over the PV module and charge controller only (the least troublesome parts of a SHS), while dumping on the user the responsibility of replacing the battery (the weakest link in the system) and the lamps.

Selecting a particular route for a given project is not a matter of personal preference only. The landscape is very important and has to be taken into account, since a number of its elements influence this choice, including local social and energy policies officially established in each country. For instance, some countries do not allow private sale of electricity, so that the fee-for-service model could not be applied, unless prevailing laws and regulations are changed as necessary. Low rural population density, difficult access to the communities, long distances from the supply centers and complex logistics to deliver goods and collect fees, can make both fee-for-service and financed sales schemes difficult to implement and geographically limited. In many cases, monthly fee/payment collection may be an expensive task, due to the time and effort it may take for the supplier or the service men to reach the customer. This fact has already been noted by PV companies operating in Sri Lanka, for instance [27]. Timing is another important factor, considering that people may not be home when the fee collector arrives, and that many peasants have money only during the postharvest period. Such difficulties have led some utilities, for many years, to give up on monthly fee collection from remote clients connected to their grids, basically because of very small bills and comparatively larger billing expenditures. Thus, unless fee collection schemes better adapted to the local conditions can be found, one can theorise that the fee-for-service and purchase models will be applicable basically to the most accessible and higher density rural communities. The fraction of the rural population meeting these criteria in many countries seems to be inversely proportional to the degree of rural electrification by grid extensions.

Local culture and idiosyncrasy are two additional elements to be considered for the choice of a delivery model. The notion of common property embedded in many native communities or the lack of familiarity with commercial practices, or even with money, could lead to unsustainable operations in many rural areas. Some academicians studying the process of introduction of PV systems in rural communities, argue that freedom from any financial burden is one of the most cherished values for rural people, and hence could be an important barrier for them to take on any financial obligations. Hence, government intervention may be indispensable at some point to deliver the PV solution in which the business route cannot be applied.

Over the past ten years delivery models in the business route have been tested through a number of projects financed by the GEF and the World Bank in various countries. A recent review [12] of the GEF solar PV portfolio suggests the following emerging lessons, warning that it is still too early to draw definite conclusions:

- Viable business models must be demonstrated to sustain market development for solar photovoltaics.
- Delivery/business model development, evolution and testing require time and flexibility.
- Institutional arrangements for project implementation can greatly influence the value of the project in terms of demonstrating viable business models and thus achieving sustainability.
- Projects must explicitly recognize and account for the high transaction costs associated with marketing, service and credit collections in rural areas.
- Consumer credit can be effectively provided by microfinance organizations with close ties to the local communities if such organizations already have a strong history and cultural niche in a specific country.
- Projects have not produced adequate experience on the viability of dealer-supplied credit under a sales model, and no project in the portfolio appears set to provide such experience.
- Rural electrification policies and planning have a major influence on project outcome and sustainability, and must be addressed explicitly in project design and implementation.
- Establishing reasonable equipment standards and certification procedures for solar home system components that ensure quality service while maintaining affordability is not difficult, and few technical problems have been encountered with systems.
- Substantial implementation experience is still needed before the success of the service approach can be judged.
- Postproject sustainability of market gains achieved during projects has not yet been demonstrated in any GEF project: it is too early in the evolution of the portfolio.

23.3.4.2.2 The social route

Governments can act in several capacities along the social route. Financing the purchase of SHS for poor people is perhaps the most critical one, although consumer protection and market regulation are also of importance. Government financing of SHS is seen by some as an unnecessary nuisance that distorts the market and creates dependence in the user's minds (users will not buy once the government has provided systems for free, goes the argument). Most critics of government intervention seem to forget that rural electrification has been historically subsidized by governments not only in developing countries but also in some of the most advanced nations. In that sense, there is no reason to think that PV rural electrification has to be different altogether, as it is only the technology base that is changing; the rest of the landscape remains the same.

Direct government financing of photovoltaics for rural electrification is not necessarily a bad thing. Up to now, the largest volume of SHS installed around the world has been realized through government or donor-led programs. Government intervention may help aggregate markets, reduce transaction costs and, if properly done, can create a better setting for quality assurance and local industry development. At least, this has been the experience with government-financed PV projects in Mexico, where proper institutional mechanisms were implemented for this purpose, and as a result, a local industry has also emerged around government-financed projects, which now produces locally and

Downloaded from https://onlinelibrary.wiley.com/doi/ by <Shibboleth-member@purdue.edu, Wiley Online Library on [25/08/2024]. See the Terms and Conditions (https://onlinelibrary.wiley.com/terms-and-conditions) on Wiley Online Library for rules of use; OA articles are governed by the applicable Creative Commons License

exports balance of system components [13, 28–30]. In this case, money provided by the government is seen as an instrument to promote local development. Over 2500 rural communities have been electrified in Mexico with photovoltaics following this model, and it is interesting to note that in many of them people have instrumented a variety of cost-recovery and money-making mechanisms, which allows for system maintenance and additional communal projects.

A number of governments from developing countries are considering the social route to deliver PV-based electricity to rural areas. Policy setting and definition of financing mechanisms are usually the first steps in this direction. Examples can be found in several Latin American countries [31]. Some examples are discussed below.

In Bolivia, Article 61 of the Electrical Law establishes that the State is responsible for the electrification process in smaller localities and in rural areas that cannot be served by private interests. Resources to finance such projects must be provided by the State, through the National Development Fund. The Executive must also propose energy policies and strategies to foster the use of alternative energy sources.

A similar mandate can be observed in Colombia, where Law 143 urges the State to provide basic electrical services to lower-income families in rural areas and to make funds available to cover necessary subsidies in this respect. The Energy and Gas Regulatory Commission is obliged to protect the rights of the lowest-income people, while the Colombian Institute for Electrical Energy has been mandated to prepare the National Energy Plan for regions not served by the grid, including the use of alternative energy systems in substitution of fossil fuelled generating systems.

In Ecuador, the Law of Regime for the Electrical Sector, addresses rural electrification and financing issues for the rural sector. It also assigns priorities for the application of renewable energy in rural electrification projects and describes the structure for project identification, approval, execution and operation. The National Fund for Rural and Urban Marginal Electrification (FERUM) is the body responsible for the administration of financial resources, and is directly regulated by the office of the president.

Similarly, in Nicaragua, the Law for the Electrical Industry holds the State responsible for developing rural electrification in remote areas in lieu of interest from other economic agents. For this, the State must provide the necessary resources through the Fund for Development of the National Electrical Industry. The State is also required by the law to implement policies and strategies for the use of alternative energy sources for electricity generation.

As a last example, in Panama, Article 9 of Executive Decree 22 makes the State responsible for promoting rural electrification and for assigning an annual budget to carry out this task. Consequently, the Office for Rural Electrification was created within the office of the president, and is in charge of promoting the use of renewable energy for rural electrification projects.

23.3.5 Trained Human Resources

Adequate financing and institutional frameworks are necessary but not sufficient conditions to remove the main barriers for PV rural electrification. Properly trained human

Downloaded from https://onlinelibrary.wiley.com/doi/ by <Shibboleth-member@purdue.edu>, Wiley Online Library on [25/08/2024]. See the Terms and Conditions (https://onlinelibrary.wiley.com/terms-and-conditions) on Wiley Online Library for rules of use; OA articles are governed by the applicable Creative Commons License

resources to develop and operate programs, and to carry out projects, are equally important. PV systems and their implementation in rural areas are frequently looked upon in a very simplistic manner by a number of people. However, disregard for the complexities behind the process has resulted in a large number of failures. One would be surprised to learn how many PV projects in rural areas around the world have not lasted but a few years beyond the inauguration date; or how many others are still not complete because a variety of logistic aspects were not given due consideration at project inception; or even how many others are under-performing as a result of faulty engineering and construction practices. Unfortunately, little reliable information from the field is available in this respect as many projects are in their first years of operation so it would be too early to draw any definite conclusions about them.

PV systems packaging is increasingly being carried out by local companies in the developing countries. This practice has its merits, since it promotes the use of local labor and materials, which benefits the local economy. However, workers are not always properly trained to carry out their duties, so that construction and installation guidelines, no matter how precise and elaborate, are not always followed. Sometimes instruction materials are not in the local language, or are translated incorrectly, and at other times they do not properly match the idiosyncratic framework of the local worker. The benefits of training local workers for industry support cannot be overstressed. An example of how far this training could go can be found in the project carried out by the Spanish Cooperation in Bolivia, where native Aymara Indians were successfully trained to assemble electronic charge controllers for SHS. This project is described in greater detail below [32].

Local distributors and vendors of PV systems frequently lack a proper understanding of the products they sell. This leads more often than not to undersized systems, to make the sale easier, or to overselling the attributes of the PV systems to be sold, creating customer expectations beyond the actual capabilities of the system. In any case, the result is customer dissatisfaction. Thus, for the PV business to grow on solid bases, the frontlines that deal with end users must be properly trained in technical, marketing, selling and business practices. This is easier said than done, as many PV businesses in developing countries are small commercial ventures embedded in other lines of activity, such as hardware stores or cattle feed stores.

Photovoltaics being a novel technology for most people, developing and implementing programs for its massive deployment is not necessarily an easy task for program managers. Assistance is oftentimes required for program formulation, and to establish the proper mechanisms for project financing, implementation and monitoring. Multilateral agencies such as the World Bank, the GEF, UNDP and others, organize workshops and seminars around the globe to disseminate best practices that could help solve this problem. Over the past six years, the Network for Rural Electrification with Renewable Energy (RIER) of the Ibero American Program of Science and Technology for Development (CYTED) has been running courses and workshops on strategies for PV rural electrification throughout Latin America. Attendees usually include officials from government agencies in charge of rural electrification, electric utilities, local financing organizations, PV distributors and salespeople, and university professors. Benefits from such training activities often translate into better-formulated programs and projects, and a more appropriate understanding of the critical elements to make PV rural electrification projects sustainable.

Downloaded from https://onlinelibrary.wiley.com/doi/ by <Shibboleth-member@purdue.edu, Wiley Online Library on [25/08/2024]. See the Terms and Conditions (https://onlinelibrary.wiley.com/terms-and-conditions) on Wiley Online Library for rules of use; OA articles are governed by the applicable Creative Commons License

Petitioner Canadian Solar (USA) Inc., Ex. 1035, p. 2444

23.4 FOUR EXAMPLES OF PV RURAL ELECTRIFICATION

It is estimated that by the end of the twentieth century, anywhere between 500 000 and one million small PV systems have been installed to power rural homes in developing countries [12]. On top of that, tens of thousands of PV-powered water lifting pumps and other communal services, such as health centers, schools, telephones, street lamps, have been deployed through government programs, donor-led initiatives and entrepreneurial activities. Many such programs have been subject to in-depth reviews as a means to better understand the process that is taking place in the field and to harvest the lessons learned that can be applied to other projects and programs. For details, the reader is encouraged to consult available reports (see for instance, [33–36]). In this section, a few examples of PV rural electrification projects and programs are described.

23.4.1 Argentina

As part of the reform of the electrical sector in Argentina, the provincial electricity markets were divided into centralized and disperse sectors. Each sector has its own structure, its own mission and its own operational form. Then, the program to supply electricity to the rural and disperse population of Argentina (PAEPRA for its name in Spanish) was established by the government in 1994. This program has the goal of providing electricity to 1.4 million people not yet served by the grid, and to electrify around 6000 public services, all this in areas where the low-population density and the long distance to the electric grid makes it too costly to supply electricity by conventional means [37]. PAEPRA operates at the provincial level through concessions to private companies bound by contract to provide electricity services under the supervision and control of the provincial electricity regulatory body [38]. Provincial concessions are awarded through a public bidding process, in which the winning company is the one that requests the least amount of subsidy money on a per customer basis to operate. This subsidy complements the funds collected from the user under a fee-for-service scheme. Participating companies are required to have experience and technical capabilities (1) to operate and maintain electrical systems and other services, such as water supply and telecommunications in a dispersed rural market; (2) to manage electrical systems based on diesel gen-sets, photovoltaics, wind and microhydro turbines; and (3) to manufacture and supply spare parts and components for this type of system. Furthermore, selected companies must be financially healthy.

The PAEPRA program was conceived to operate supported by a loan from the World Bank, but has not moved forward as fast as originally expected for a number of reasons beyond the scope of this work. Since 1986, the Republic of Argentina has a national PV industry with a capacity to produce balance of system components and about 1 MWp per year of PV modules. The current market is based on rural applications for domestic and communal services, water pumping and telecommunications. The presence of this industry is a good element to support the program.

23.4.2 Bolivia

In Bolivia, the National Rural Electrification Program (PRONER) was established to promote and support economic development in rural areas in order to improve the living

Downloaded from https://onlinelibrary.wiley.com/doi/ by <Shibboleth-member@purdue.edu, Wiley Online Library on [25/08/2024]. See the Terms and Conditions (https://onlinelibrary.wiley.com/terms-and-conditions) on Wiley Online Library for rules of use; OA articles are governed by the applicable Creative Commons License

conditions and the quality of life of the population. The original objective of the program was to provide electrical services to 100 000 households in a time span of five years by means of renewable energy. The process to carry out this task is based on sustainability, by creating an appropriate institutional, financial and technological framework. This program has been under implementation since 1997, supported by an UNDP-GEF grant. The first phase of the program has the goal of installing 3200 SHS through 22 projects in five municipalities and is aimed at removing financial, institutional, technical and human resource barriers to the massive application of photovoltaics.

Bolivia has been a favorite place for international cooperation in the field of PV rural electrification. In 1988, the Spanish Agency for International Cooperation and the Solar Energy Institute of the Polytechnic University of Madrid launched a PV electrification project to bring electricity to the Aymara community in the high Bolivian plateau. Beyond the traditional objectives of a project of this kind, this particular project attempted to foster the development of a users' organization with capabilities to manage and maintain PV installations, and to be responsible for the proper continuation of the project. At the same time, emphasis was put on the creation of an industrial unit in one of the rural communities to manufacture balance of system components using local manpower and Bolivian components as a basis for future projects [39]. By 1993, a total of 1000 SHS had already been installed and the Association for Solar Electrification (AES) had been created. AES included all PV users and was the owner of all the PV installations. An accounting system was established and a team of installers and maintenance crews was trained. This project has been studied thoroughly and important lessons derived thereof [32]. By the end of its fifth year of operation, a demand for about 30 000 SHS had been created, well beyond the financial capabilities of the project. Unfortunately, several problems in the area of financial management developed within the AES once the main implementing agents pulled out from the country and the project stalled.

In another action, the US-based National Rural Electric Cooperatives Association (NRECA, now an incorporated company) launched several pilot PV projects in Bolivia to test different financial schemes. In cooperation with the local organization Rural Electricity Cooperative (CRE), 90 SHS were installed as a preamble to a further 1300 installations. CRE provided complementary financing for the purchase of the PV systems and managed other aspects of project implementation, including the selection of the users and providing technical training [40]. In cooperation with the Cochabamba Electric Company, a privately owned electricity distribution company, NRECA implemented another project to install 300 SHS in remote rural communities. ELFEC finances the purchase of the equipment and provides installation and maintenance services.

The project INTI K'ANCHAY (light from the sun) has been implemented by the local NGO Energética with financial support from the Netherlands. Five hundred SHS were to be installed in the first phase, to test a financing mechanism that eventually could be extended to cover a larger portion of the 150 000 families without electricity in the province of Carrasco [41]. Companies participating in the process are required, among other things, to supply and install the SHS according to technical norms and specifications issued by Energética, to provide guarantees according to the useful life of the individual components and to build a network of representatives at the microregion level for after-sales service. By July 1999, a total of 200 SHS had already been installed, and applications for 350 more were being processed [42].

Downloaded from https://onlinelibrary.wiley.com/doi/ by <Shibboleth-member@purdue.edu, Wiley Online Library on [25/08/2024]. See the Terms and Conditions (https://onlinelibrary.wiley.com/terms-and-conditions) on Wiley Online Library for rules of use; OA articles are governed by the applicable Creative Commons License

Petitioner Canadian Solar (USA) Inc., Ex. 1035, p. 2446

Downloaded from https://onlinelibrary.wiley.com/doi/ by <Shibboleth-member@purdue.edu>, Wiley Online Library on [25/08/2024]. See the Terms and Conditions (https://onlinelibrary.wiley.com/terms-and-conditions) on Wiley Online Library for rules of use; OA articles are governed by the applicable Creative Commons License

On the other hand, the German foreign-aid agency GTZ has promoted and supported several PV projects in Bolivia and has carried out an important promotional campaign in favor of renewable energy through the bilateral program for the diffusion of renewable energy (PROPER). Among other things, PROPER carried out activities to increase the number and capabilities of in-country personnel trained in the field of renewable energy at the professional and technical levels, including microenterprise building [43].

23.4.3 Brazil

PV rural electrification projects in Brazil started around 1992/93 with pilot cooperative projects with Germany and the United States [44]. Around 1500 SHS were installed as part of these projects in Northeast Brazil in cooperation with the local electricity distribution companies, who were responsible for systems installation, maintenance and performance monitoring. In 1994, the Brazilian Government launched an initiative to promote the use of renewable energy and the corresponding *action plan* was established in 1995, with the original goal of installing 50 MWp of PV systems by the year 2005 [45]. The program for energy development in the municipalities and the states (PRODEEM) was also launched in 1994 to deliver electricity by means of renewable energy to rural communities not served by the grid [46]. At the same time, several state governments, including Minas Gerais, Sao Paulo and Parana, launched their own PV rural electrification projects.

The PRODEEM program is coordinated by the National Department for Energy Development of the Ministry of Energy and Mines and is technically supported by the National Center for Electrical Research (CEPEL). Since 1995, three program phases have been implemented [47], with a total number of PV installations close to 2400, basically for water pumping, public lighting and other installations such as communal buildings, schools, health centers and churches. A fourth phase has been under consideration for installing about 1300 additional PV systems [48]. The process for the implementation of PRODEEM is well established and documented in the literature cited here.

The Electric Company of Minas Gerais has been actively involved in deploying PV systems, in spite of owning one of the most extensive electrical grids in Latin America, with a total length of 300 000 km. In 1989, CEMIG launched an experimental project to install PV systems for productive and domestic applications in remote places. Between 1995 and 1997, a demonstration phase of the Program of Assistance for the Rural Development of Brazil took place in cooperation with the US Department of Energy and the US National Renewable Energy Laboratory. PV systems for 70 schools and several pumping systems were installed as part of this program [49]. Plans were made to electrify 2000 regional educational centers and to install about 500 water supply systems, all powered by photovoltaics. By 1987, such pumping systems, with PV capacities between 1 and 2 kW each had already been installed [50]. General criteria for eligibility in the CEMIG program include localities farther than 5 km from the nearest electricity grid and a user density of less than 5 people per kilometer. CEMIG provides financing for 64% of the project cost, the remaining 36% being covered by the community authorities. CEMIG has also established a training center for technicians, who provide regular maintenance of the systems. Monthly salary of the technicians is covered by the municipal authorities of the region they serve [49]. A PV "pre-electrification" program was established by CEMIG in 1998 to stimulate the growth of the electrical demand in remote places, to the point where

grid extensions could become economically viable. Some 500 PV systems were installed for this purpose in 1999 and another 5000 were under consideration for the following years. The rationale of this pre-electrification program is to use photovoltaics as a basis to aggregate electrical demand in rural areas. Once the critical mass has been reached, the grid would be extended to the point of highest demand while the PV installation would be moved to another location for the same purpose.

23.4.4 Mexico

About 5% of the Mexican population (almost 5 million people) has no access to electricity from the grid. A highly dispersed rural population and a rough terrain make grid extensions technically difficult and economically unviable. Several attempts were made in the late 1970s to use photovoltaics to power basic electrical services, as mentioned earlier. In 1989, the Mexican Government launched the PRONASOL program for poverty alleviation, which soon became the platform for a large-scale PV rural electrification activity. Today, over 2500 rural communities have been fully supplied with SHS through government programs, which means there are over 60 000 SHS in the whole territory. It is estimated that another 30 000 SHS have been installed outside government programs on a purely commercial basis. In addition, thousands of other PV-powered rural services have been provided, including rural telephones, schools, health centers and communal buildings.

A distinctive characteristic of the Mexican PV rural electrification program has been the active participation of the national electric utility (CFE) as technical normative agency, a central element for quality assurance and sustainability [29]. Under contract to CFE, the Electrical Research Institute of Mexico developed, in the early 1990s, a set of technical standards and specifications for project implementation. Laboratory testing and field evaluation protocols were also developed and implemented. Government-financed projects are carried out by private companies under the technical supervision of CFE and administered by an implementing agency, usually a government office. Contracts to private companies are awarded through a bidding process within the framework of the law for public works. Companies are required not only to supply the physical equipment but also to install the PV systems and train the user in proper operation and basic maintenance. The winning company must also establish a network of contact points for after-sales services.

Finance to purchase the PV systems has been mostly provided by the Federal Government, with lesser contributions from the state and municipal governments. Communities are requested to contribute to the project according to their own economic capacity. In-kind contributions, such as carrying the PV equipment to the community from the nearest point where vehicles have access, is one of the most frequent services by the community in support of the project. Funds are provided by the government as part of the patrimony for the community and, hence, no *a priori* money repayment mechanisms are established. However, communities are free to implement any fund-raising activities that can help them maintain their systems and purchase additional equipment. A popular mechanism is the so-called communal fund, in which members of the community contribute money or man-hours or both to a common fund managed by the community representatives. The communal fund is then used to maintain the PV installations and/or to implement other projects for the benefit of the community, such as water works repair,

Downloaded from https://onlinelibrary.wiley.com/doi/ by <Shibboleth-member@purdue.edu, Wiley Online Library on [25/08/2024]. See the Terms and Conditions (https://onlinelibrary.wiley.com/terms-and-conditions) on Wiley Online Library for rules of use; OA articles are governed by the applicable Creative Commons License

Petitioner Canadian Solar (USA) Inc., Ex. 1035, p. 2448

Downloaded from https://onlinelibrary.wiley.com/doi/ by <Shibboleth-member@purdue.edu, Wiley Online Library on [25/08/2024]. See the Terms and Conditions (https://onlinelibrary.wiley.com/terms-and-conditions) on Wiley Online Library for rules of use; OA articles are governed by the applicable Creative Commons License

building a new schoolroom and the like. A more detailed description of the Mexican PV rural electrification program can be found in the literature mentioned in References [28, 51, 52].

23.4.5 Sri Lanka

An estimated two million households lack access to grid electricity in this country. Recent studies indicate that at least 10% of these households could afford a SHS at current prices, based on a monthly household income of Rs. 5000 [53]. A market study commissioned by the National Development Bank of Sri Lanka in 1991 indicated that a market of 360 000 households could afford a PV system [54]. However, so far only about 15 000 such systems have been sold commercially for cash through a retail network.

Many reasons have been cited for this low penetration level. As in other places, the biggest barrier for the exploitation of this market has been a lack of consumer financing. Political promises for grid extensions in rural areas and the government sponsored "Electricity for all by the Year 2000" campaign, which was perceived as *grid electricity* for all, have also been major barriers. Lack of government-level endorsement for solar photovoltaics, along with other renewables, was a hindrance to both private sector and NGO promoters. Nevertheless, four companies retail PV systems in Sri Lanka: Shell Renewables, Resco Asia (subsidiary of the US Selco), Alpha Thermal Systems and Access International. Sarvodaya SEEDS, a local NGO, provides microfinancing in partnership with some of these companies.

In the late 1980s, solar PV modules, 12-V lamps and simple electronic charge controllers were assembled in Sri Lanka by Solar Power & Light Company (SPLC), a private venture established as Power & Sun in 1986. However, manufacturing of solar modules ceased as the advantage over imported products was eroded, in part because of the high import duties on raw materials. Thus, SPLC essentially developed into a marketing organization by creating an infrastructure to market, install and maintain PV systems in rural areas. SPLC uses retailers to stock solar home systems; trained technicians and individual agents, called *corresponding agents* (CA), are used to canvass sales, install systems and provide customer service. SPLC, which has just been bought over by Shell International Renewables, has sold over 3000 PV systems directly to consumers, mostly for cash.

Apart from cash sales of SHS, there are examples in Sri Lanka of both successful and "deemed as failed" projects, using loan repayments by the consumer as the measure of success. Projects implemented with total community involvement by NGOs, such as Sarvodaya and Solanka, have been quite successful. Sarvodaya's already successful microcredit operation was adapted to market SHS, and implemented a pilot project with 250 installations through its Rural Technical Services branch, with assistance from the US-based NGO Solar Electric Light Fund (SELF, now the private company Selco) and a seed fund from a US foundation. Further activities by Sarvodaya using funds from a credit line for renewable energy provided to Sri Lanka by the World Bank, led to the installation of 300 more systems. Plans to install 5000 more within the next five years are already drawn. Sarvodaya SEEDS has become a Participating Credit Institution of the Energy Services Delivery Project. It can now access the fund directly and on-lend to customers. In January 2001, it has been reported that Sarvodaya SEEDS' lending portfolio exposure is Rs. 89 million (about US $1 million) for solar photovoltaics.

Solanka Sun Associates, created community level capabilities to do complete projects, including evaluation of potential customers, providing financing; designing, installing and maintaining the solar home systems; collecting repayment and managing the project with the inherent difficulties of managing projects from cities. This model has shown that success can be achieved with proper training and incentives to the operators at the village level. With the lower than commercial rates of interest provided to its customers, Solanka has targeted the lower economic category of the market, having thus far installed two projects, one with 84 solar home systems in the village of Morapathawa, and the other with 77 systems in Thorawa. This has been possible since the funds for lending have been provided as grants. However, it will be difficult to sustain this scheme with commercial level funding, unless interest rates are increased and loan repayment period is reduced. However, this will naturally exclude the current target market of this organization. Thus, the challenge for Solanka is to secure further grant funding to replicate such projects. Its biggest merit has been to prove that the village has the capacity to implement and manage PV electrification projects. Solanka had the provincial government's patronage and support when the selection of areas for implementation was made jointly. The project has an interesting feature in that the 12-V lamp units and the simple electronic controllers are manufactured at the village level. Also, a village level repair unit has been started where defective battery cells can be replaced to lengthen the life of the battery. Loan repayments to date for both projects are 100% due to the grass roots level service that is provided to users. For instance, even when a battery fails, the user immediately gets a replacement while the old one is being repaired or serviced. The Colombo-based head office focuses on long-term strategic planning and also imposes the accounting controls with audits of all accounting operations in the process of selecting recipients and collecting repayments. On the basis of the experience of these two projects, its original promoter has established a commercial solar company called RESCO as a subsidiary of Selco-USA.

A counterexample is the Pansiyagama 1000 homes project, funded by the Sri Lankan and Australian governments, which has a very low repayment rate in spite of the very favorable finance scheme applied. Hence, it can be considered a failure, although technically over 90% of the systems are still operating. This project was politically motivated, and was implemented by the National Housing Development Authority (NHDA) of Sri Lanka, which attempted to implement a "grass roots" level program. However, the top-down manner in which it was done resulted in poor community level involvement and poor management infrastructure. The systems installed were more sophisticated than the normal SHS being installed elsewhere in the country and had a typical cost ranging from Rs. 20 000 (US $571) to Rs. 32 000 (US $914), depending on the size of the module and number of lamps. This led to a monthly payment from Rs. 75 (US $2.14) to Rs. 135 (US $3.85), depending on the cost of the unit (US $1 = Rs. 35 in 1990), which turned out to be unrealistically low. According to a socioeconomic survey conducted by the Marga Institute of Sri Lanka, it was found that most households could afford to pay much more for the system. However, since the payments by households were set at nominal terms, their value has been eroding with inflation. At some point in time, the infrastructure for collecting repayments broke down as a result of bureaucratic problems, and some initial technical problems in the systems set a precedent for nonpayment, which was most difficult to break later. Some of these problems have been fixed after the NHDA handed over the maintenance and money collection duties to Power & Sun in 1991. However, the

Downloaded from https://onlinelibrary.wiley.com/doi/ by <Shibboleth-member@purdue.edu, Wiley Online Library on [25/08/2024]. See the Terms and Conditions (https://onlinelibrary.wiley.com/terms-and-conditions) on Wiley Online Library for rules of use; OA articles are governed by the applicable Creative Commons License

repayments remain around 50%, as the cost of collecting the money is much more than the actual collections due to the low monthly payment. This means that over-subsidizing solar photovoltaics has a negative effect on the dissemination of solar photovoltaics through the business route. This project has demonstrated that solar photovoltaics is an appropriate technology, but the implementing methodology used for the project was not sustainable and as a result was found detrimental to the commercial dissemination process of solar home systems in Sri Lanka.

23.4.6 Water Pumping in the Sahel

The Regional Solar Programme (RSP) was one of the early systematic programs to apply PV technology to solve pressing problems in the Sahel region of sub-Saharan Africa. Financed by a grant of 34 million ECU from the European Commission, to cover the cost of PV equipment and other procedures such as training, information and public awareness activities, regional coordination and technical assistance, this program was launched in 1989. The goal of the RSP was to install almost 1.4 MWp of PV modules (about 3.5% of the world market at that time) in water-pumping systems, vaccine refrigerators, community lighting and battery-charging stations. At the end of the program, a total of 626 pumping systems and 644 community systems had been installed and a wealth of lessons learned.

The principal objectives of the RSP were [55] to improve the accessibility of water in both quantity and quality, to improve the economic condition of the villagers by development of complementary resources through gardening, to reduce the time spent in procuring drinking water, to train personnel for project management, to create management groups for the solar equipment and to develop and adopt a legal framework for operation of the equipment with contractual structure of the relations between users and private companies.

Not all specific goals and objectives originally planned were fully met, but important lessons were derived. The drinking water component of the program took more than 90% of the installed PV power, so the lessons learned apply basically to this application. Solar pumping was found more affordable than diesel motor pumping, by about a factor of two per cubic meter of water. Compared to the per habitant cost of manual water rising pumps (50 ECU), borehole considered, investment on PV pumping systems was slightly higher (55 ECU), but the service quality of PV pumps was superior. Of the total installed cost, 31% was for the supply of the PV system, 11% for installation, 12% for regional activities (including coordination, quality control, tests, monitoring and the like) and 46% for the distribution network, water tower and other reception infrastructure.

One mode of management of the water supply system used in some communities was directly inspired by the management of water points equipped with manual pumps through a village water committee. This management system, however, was not effective owing to a number of difficulties, including an imperfect mastering of the accounting tools and a quasisystematic confusion of the responsibilities assigned to the principal members of the committee. Other communities preferred delegating the management of the entire system to a private-type body on a fee basis or to a communal-type body. These latter forms of management seemed better suited to the local conditions than the water committee scheme.

Downloaded from https://onlinelibrary.wiley.com/doi/ by <Shibboleth>-member@purdue.edu, Wiley Online Library on [25/08/2024]. See the Terms and Conditions (https://onlinelibrary.wiley.com/terms-and-conditions) on Wiley Online Library for rules of use; OA articles are governed by the applicable Creative Commons License

The idea of using PV technology to improve productivity of market gardening and farming was finally abandoned, hence the prospects of PV technology in Sahel were found in meeting specific domestic electrical needs (lighting, radios and TV sets), in pumping drinking water and in telecommunications.

23.5 TOWARD A NEW PARADIGM FOR RURAL ELECTRIFICATION

The problem of rural electrification has been traditionally handled by conventional means in a process of successive approximations. In this process, the most remote and dispersed population is attracted to larger population centers, which are then served by a mini electrical local grid, fed by diesel gen-sets or small hydroelectric generators. As the load increases, a point is reached at which extensions of the main grid become economically viable. This process is known as *pre-electrification* among electric companies and has been the basic growth mechanism of the interconnected system in rural areas. Although effective from a purely technical-economic point of view, this pre-electrification process has several downsides. From the social point of view, it forces people to leave their place of origin to create larger population centers, which in turn induces the need for the central provision of other services and puts a larger stress on the environment.

The term pre-electrification is being used nowadays by some authors in reference to PV rural electrification and, in some cases such as the CEMIG example above, the operational scheme is also being transported. However, there are a number of reasons to think that using the term pre-electrification in the context of photovoltaics is not appropriate. Furthermore, transporting the concept is bound to cancel the advantages offered by photovoltaics to create a new path for rural electrification. First, from the purely technical point of view, photovoltaics offers the possibility of supplying high quality electrical services even to the most remote sites, without the need for relocating people or eventually having to resort to grid extensions. Because of its modular nature PV systems can grow in pace with the load. Furthermore, this vision is compatible with current trends in the electrical sector toward distributed generation systems, and is supported by the development of more efficient electrical appliances, the miniaturization of electrical technologies and the progress being made in electronic devices for system supervision and load management. There are also environmental reasons that lead the notion that the local generation of electricity using renewable and nonpolluting energy resources is more convenient than building kilometers of electricity lines across ecologically sensitive areas. Local generation of electricity also offers the possibility for local management and, hence, for active community participation in the process of self-development.

On the other hand, there is evidence that the traditional electrification process based on the old paradigm of *Delivering electricity to rural people* has frequently lent itself mainly to fulfill the political need to improve the electrification statistics rather than to serve the real needs of people. Thus, it is not uncommon to observe rural communities with access to the grid, where a good portion of the households are not connected, usually because of lack of money to pay for the connection fee, or because the secondary distribution network only reaches the center of the community, leaving the rest of the population unserved. Therefore, if electricity supply is to be used as a tool for development, that is understood as increased life expectancy, more knowledge and a better

Downloaded from https://onlinelibrary.wiley.com/doi/ by <Shibboleth-member@purdue.edu, Wiley Online Library on [25/08/2024]. See the Terms and Conditions (https://onlinelibrary.wiley.com/terms-and-conditions) on Wiley Online Library for rules of use; OA articles are governed by the applicable Creative Commons License

Downloaded from https://onlinelibrary.wiley.com/doi/ by <Shibboleth-member@purdue.edu, Wiley Online Library on [25/08/2024]. See the Terms and Conditions (https://onlinelibrary.wiley.com/terms-and-conditions) on Wiley Online Library for rules of use; OA articles are governed by the applicable Creative Commons License

standard of living [56], then the present rural electrification paradigm must be urgently changed to: "*Increasing the access of the rural poor to electricity-based services*". This set of services includes health, clean water, education, food preservation, entertainment and the possibility of engaging in productive activities.

Under this perspective, current PV rural electrification activities represent a landmark of the transition period into a new rural electrification scheme to substitute the old one with better results. However, the *new electrification* requires among other things, a new culture for electricity supply and use in rural areas, an *ad hoc* legal framework, new business practices within the electrical sector, innovative financial mechanisms, new and better technologies and appropriate institutional schemes. Thus, the actual value of programs and projects currently underway has to be weighted not only in terms of the number of PV users in rural areas, but also in terms of the benefits PV installations are bringing to the population. Also important to gauge the effectiveness of current PV rural electrification projects is the relevance of the lessons learned from them, which will allow the implementation of improved schemes for successful project replication.

This new paradigm for rural electrification should in turn be embedded in the broader concept of rural energy supply, which calls for a timely supply of useful energy in a variety of forms, so that people can have better opportunities to improve their own quality of life, to foster local economic development and to protect the environment.

REFERENCES

1. Kemp W, *The Flow of Energy in a Hunting Society. Energy and Power*, A Scientific American Book, 55–65, W.H. Freeman and Company, San Francisco, CA (1971).
2. Rappaport R, *The Flow of Energy in an Agricultural Society. Energy and Power*, A Scientific American Book, 69–80, W.H. Freeman and Company, San Francisco, CA (1971).
3. Cook E, *The Flow of Energy in an Industrial Society. Energy and Power*, A Scientific American Book, 83–91, W.H. Freeman and Company, San Francisco, CA (1971).
4. *World Energy Assessment: Energy and the Challenge of Sustainability*, United Nations Development Program, United Nations Department of Economic and Social Affairs, World Energy Council (Sept. 2000).
5. *The Challenge of Rural Energy Poverty in Developing Countries*, World Energy Council, Food and Agriculture Organization of the United Nations (Oct. 1999).
6. Bowers B, *A History of Electric Light & Power*, History of Technology Series 3, P. Peregrinus, The Science Museum, London (1982).
7. National Energy Balance 1997. Energy Secretariat of Mexico.
8. Foley G, *Photovoltaic Applications in Rural Areas of the Developing World*, World Bank Technical Paper Number 304, Energy Series (1995).
9. Lorenzo E, Photovoltaic Rural Electrification, *Prog. Photovolt.: Res. Appl.* **5**, 3–27 (1997).
10. Urbano J, "Introduction to the Design, Operation and Application of Photovoltaic Systems – The CIEA Experience (in Spanish)", *Proc. 4th Mexican National Solar Energy Society Meeting* (San Luis Potosi, Mexico, Oct. 1–3, 1980).
11. Urbano J, *Rev. Sol.* **16**, 10–13 (1989).
12. Martinot E, Ramankutty R, Rittner F, *The GEF Solar PV Portfolio: Emerging Experience and Lessons*, Monitoring and Evaluation Working Paper 2, GEF pre-publication draft (Aug. 2000).
13. Huacuz J, Agredano J, "Beyond the Gris: photovoltaic rural electrification in Mexico", *Prog. Photovolt.: Res. Appl.* **6**, 379–395 (1998).

14. Ramos R *et al*., *Photovoltaic Solar Energy: An Option for Rural Electrification in Cuba (in Spanish)*, Solar Energy Research Centre of Cuba (1995).
15. *Clean Water with Clean Energy: Drinking Water Provision in Remote Regions with Decentralised Solar Power Supply*, INCO-DC Project ERBIC18CT960104, Final Report, European Commission, FhG-ISE, Freiburg, Germany (2000).
16. Sapiain R *et al*., *Solar Photovoltaic Pumping in Peasant Communities and New Productive Agricultural Applications in Arid Zones in the North of Chile (in Spanish)*, Renewable Energy Centre, Engineering Faculty, University of Tarapaca (Oct. 1997).
17. Ahm P, "Small PV Powered Medical Equipment", *UNESCO World Solar Summit* (July 1993).
18. Muhopadhyay K, Sensarma B, Saha H, *Sol. Energy Mater. Sol. Cells* **31**, 437–446 (1993).
19. *De l'eau solaire pour la Somalie*, Systemes Solaires, No. 100 (1994).
20. *Les lampes portables solaires*, Systemes Solaires, No. 100 (1994).
21. Flores R *et al*., "Characterization and Evaluation of 30 PV Ovonic-Unisolar Solar Home Systems (in Spanish)". *Proc. ISES Millennium Solar World Forum* (Mexico City, Oct. 2000).
22. Huacuz J, Urrutia M, Eds, *Proceedings of the International Workshop Charge Controllers for Photovoltaic Rural Electrification Systems*, Electrical Research Institute Cuernavaca, Mexico (1998).
23. Nieuwenhout F, *Monitoring and Evaluation of Solar Home Systems: Experiences with Applications of Solar PV for Households in Developing Countries*, Report ECN-C-00-089, Netherlands Energy Research Foundation, Petten (Sept. 2000).
24. dos Santos R, Zilles R, PV Residential Electrification: A Case Study on Solar Battery Charging Stations in Brazil. *Prog. Photovol.: Res. Appl.* **9**(6), 445–453 November/December (2001).
25. European Commission, Directorate General for Energy; Universal Technical Standards for Solar Home Systems. Thermie B: SUP-995-96 (1998).
26. Electrical Research Institute, *Technical Specification for Rural Illumination Photovoltaic Systems (in Spanish)*, Revised Edition. Cuernavaca, Mexico, IIE (1999).
27. Martinot E, Ramankutty R, Rittner F, *Thematic Review of the GEF Solar PV Portfolio: Emerging Experience and Lessons*, Global Environment Facility Working Paper, pre-publication draft (June 2000).
28. Huacuz J, Martinez A, "Renewable Energy Rural Electrification: Sustainability Aspects of the Mexican Programme in Practice", *Nat. Res. Forum* **19**, 223–231 (1995).
29. Huacuz J, Gonzalez C, Uria F, "The role of Comision Federal de Electricidad in the Mexican photovoltaic rural electrification program", *Proc. IERE Workshop Photovoltaic Rural Electrification and the Electric Power Utility*, IIE-EPRI (Cocoyoc, Mexico, May 1995).
30. Flores C, "Expanding PV Rural Electrification with Local Industry and Technology: The Mexican Experience", *Proc. Sustainable Development of the Rural World. Decentralized Electrification Issues* (Marraketch Marruecos, Nov. 13–17, 1995).
31. Huacuz J, "Sustainable Energy in Rural Zones within the Process of Modernization of the Energy Sector in Latin America and The Caribbean (in Spanish)", *Proc. Enerlac '98, IV Energy Conference of Latin America and The Caribbean* (Dominican Republic, 1998).
32. Aguilera T, *Energía Solar Fotovoltaica en el Ambito de la Cooperación al Desarrollo*, Caso de Estudio: El Altiplano Boliviano, Tesis Doctoral, Universidad Politécnica de Madrid, Escuela Superior de Ingenieros en Telecomunicaciones. Madrid (1995).
33. Nieuwenhout F *et al*., *Monitoring and Evaluation of Solar Home Systems. Experiences with Applications of solar PV for Households in Developing Countries*, Report ECN-C-00-089, Netherlands Energy Research Foundation (Sept. 2000).
34. Hankins M, *Solar Rural Electrification in the Developing World*, Four Case Studies: Dominican Republic, Kenya, Sri Lanka and Zimbabwe. Solar Electric Light Fund (1993).
35. Cabraal A *et al*., *Best Practices for Photovoltaic Household Electrification Programs*, Lessons from Experiences in Selected Countries, World Bank Technical Paper Number 324, Asia Technical Department Series, The World Bank (1996).

Downloaded from https://onlinelibrary.wiley.com/doi/ by <Shibboleth-member@purdue.edu, Wiley Online Library on [25/08/2024]. See the Terms and Conditions (https://onlinelibrary.wiley.com/terms-and-conditions) on Wiley Online Library for rules of use; OA articles are governed by the applicable Creative Commons License

Petitioner Canadian Solar (USA) Inc., Ex. 1035, p. 2454

36. Martinot E *et al*., *World Bank/GEF Solar Home Systems Projects: Experiences and Lessons Learned 1993–2000*. Renewable and Sustainable Energy Reviews, **5**, 39–57 (2001).
37. Fabris A, Sotelino E, *Programas de Electrificación Rural en el Cono Sur de América Latina*, Los Recursos Energéticos Renovables y las Políticas de Electrificación Rural, 109–123 (1997).
38. Frigerio A, "Financiamiento del Programa de Abastecimiento Eléctrico a la Población Rural Dispersa de Argentina", *Seminario de Inversiones y Negocios para Energías Renovables en América Latina*, (Quito, Ecuado, 14–16 de septiembre, 1998).
39. Castiella H, *Proyecto de Electrificación Rural Mediante Energía Solar Fotovoltaica en Bolivia*, Agencia Española de Cooperación Internacional (La Paz, Bolivia, 1993).
40. Smith P, International Project CRE *http://www.rsvp.nrel.gov* (1996).
41. INTI K'ANCHAY, Informative Bulletin No. 1. Energética (Sept. 1998).
42. INTI K'ANCHAY, Informative Bulletin No. 2. Energética (July 1999).
43. *Renewable Energy Rural Electrification Projects for the Cochabamba-Bolivia Department (in Spanish)*, Comité de Coordinación Interinstitucional (Cochabamba, April 1995).
44. Barbosa E *et al*., *Toward a Sustainable Future for the Use of SHSs for Rural Electrification in Brazil*.
45. Ribeiro C, Bezerra P, Zilles R, Moskowics M, *Brazilian Strategy on PV Dissemination* (1998) Update.
46. Quintans L, Lima J: *Prodeem: realizaçoes e progressos*, Cresesb Informa, Año III, No. 4 (Diciembre, 1997).
47. Galindo M, Lima J, Quintana L, dos Santos R, *Technical Aspects of the Brazilian PRODEEM Program for Rural Electrification Based on Renewables*.
48. Silva S, *PRODEEM. IV Encontro Forum Permanente de Energias Renovables* (Recife, Pernambuco, Brasil, 6 a 9 de Outubro de, 1998).
49. Diniz A, "Programa de Implantado de Sistemas Fotovoltaicos da CEMIG", *IV Encontro do Fórum Permanente de Energias Renovaveis* (Recife, Pernambuco, Brasil, 6 a 9 de Outubro de, 1998).
50. dos Santos P, "Programa de Implantaçao de Bombeamiento de Agua FV da COPASA", *IV Encontro Forum Permanente de Energias Renovaveis* (Recife, Pernambuco, Brasil, 6 a 9 de Outubro de, 1998).
51. Huacuz J, Martínez A, *ATAS Bull.* **8**, 177–194 (1992).
52. Huacuz J, Martínez A, *Mexico: Rural Electrification Program with Renewable Energy Systems*, EDG, No. 5, 15–20 (1996).
53. Gunaratne L, "Funding and repayment management of PV system dissemination in Sri Lanka", *Proceedings on the Conference on Financial Services for decentralized Solar Energy Applications II*. Harare, Zimbabwe, 20–23 (Oct. 1998).
54. Gunaratne L, Solar PV Market Development in Sri Lanka. GEF Workshop: Making a Difference in Emerging PV Markets. Marrakech, Morocco, September 24–28 (2000).
55. Regional Solar Programme, *Lessons and Perspectives*, European Commission (DGVIII) (Dec. 1999).
56. UNDP, *Human Development Report 2001* (2001).

Downloaded from https://onlinelibrary.wiley.com/doi/ by <Shibboleth-member@purdue.edu, Wiley Online Library on [25/08/2024]. See the Terms and Conditions (https://onlinelibrary.wiley.com/terms-and-conditions) on Wiley Online Library for rules of use; OA articles are governed by the applicable Creative Commons License

24
Financing PV Growth

Michael T. Eckhart[1], Jack L. Stone[2] and Keith Rutledge[3]

[1]*Solar International Management, Inc., Washington DC,* [2]*National Renewable Energy Laboratory, Golden Colorado,* [3]*Renewable Energy Development Institute, Willits, California*

This chapter presents an overview of the financing of photovoltaic PV growth. Solar energy is free, but the equipment to collect it and convert it to electricity is not. PV systems are highly capital intensive, hence the method and cost of financing will affect the economic viability and the affordability of PV systems to the end users (see Reference [1]).

24.1 HISTORICAL DEVELOPMENT OF PV FINANCING

Programs for the financing of photovoltaics began in the late 1980s. The practice of financing photovoltaics has evolved slowly and has not been entirely successful to date:

1987: The Indian Renewable Energy Development Agency (IREDA) was founded; today, it is still the only major national institution that is dedicated solely to the financing of renewable energy.

1989: The World Bank established The Solar Initiative as a way of drawing attention to the environmental and developmental benefits of solar energy (see Reference [2]).

1990: The Solar Electric Light Fund (SELF) began pioneering projects in India, Sri Lanka, Nepal, China, Indonesia, Solomon Islands, Brazil, Zimbabwe, Senegal, Uganda, and South Africa, demonstrating the viability of Solar home systems (SHS) in the developing countries and setting the stage for many PV programs around the world.

1992: The Sustainable Development conference was held in Rio, leading to additional funding of the Global Environment Facility (GEF).

1994: The world's first PV loan program by a bank was established by KM Udupa, chairman of Malaprabha Grameena Bank, the rural lending affiliate of Syndicate Bank, in Hyderabad, India.

Handbook of Photovoltaic Science and Engineering. Edited by A. Luque and S. Hegedus
© 2003 John Wiley & Sons, Ltd ISBN: 0-471-49196-9

Downloaded from https://onlinelibrary.wiley.com/doi/ by <Shibboleth-member@purdue.edu>, Wiley Online Library on [25/08/2024]. See the Terms and Conditions (https://onlinelibrary.wiley.com/terms-and-conditions) on Wiley Online Library for rules of use; OA articles are governed by the applicable Creative Commons License

1995: The Pocantico Conference was convened by the Rockefeller Brothers Fund to debate strategies on mobilizing PV financing in the developing countries.

1996: The Japanese government announced a national PV strategy that included a 50% subsidy for residential rooftop applications, substantial increases in government funding of PV R&D, and government subsidies of interest rates to encourage banks to lend for PV applications. In Europe, Triodos Bank established its Solar Investment Fund (SIF), a $3 million fund focused on end-user financing in the developing countries. In the United States, a joint task force of the World Bank Group and charitable foundations led to plans for the Solar Development Group (SDG) and the proposed SolarBank Program.

1997: The Shell–Eskom joint venture was established in South Africa, providing nongrid electric service to rural households using a "fee-for-service" strategy. The World Bank closed a GEF-supported PV loan facility in Indonesia and laid out plans for PV loan programs in China, Argentina, and other countries.

1998: The PV Market Transformation Initiative (PVMTI) was launched in India, Kenya, and Morocco, sponsored by the International Finance Corporation (IFC) and funded by the Global Environmental Facility (GEF). In the United States, Astropower became the first successful Initial Public Offering (IPO) by a venture capital–backed PV company.

1999: Germany launched its 100 000 Roofs PV Program with a "feed-in tariff" for PV electricity and a national program of low-interest loans, which has been successful.

2000: The IFC's Renewable Energy and Energy Efficiency (REEF) Fund, a $100 million equity fund for such projects in the developing countries, raised its initial capital. In the United States, the Renewable Energy Development Institute (REDI) formalized its PV loan brokerage operation.

2001: The Solar Development Group, including the $20 million Solar Development Foundation (SDF) and the $29 million Solar Development Capital (SDC) fund, was launched by the World Bank, IFC, GEF, US Foundations, and European governments and donor agencies, to fund PV enterprises in the developing countries.

2002: Low-interest loan programs have begun to appear around the world, from California to Kenya.

Historical information from around the world suggests that financing will play a pivotal role in creating and sustaining the growth of PV market demand:

Developing countries: PV companies in India, Indonesia, South Africa, and the Dominican Republic report that only 2 to 5% of prospective purchasers can afford to buy a PV system with cash, while approximately 50% could buy if provided with reasonable third-party financing (please see Section 24.5 for details).

Germany: The KfW made low-interest loans available in conjunction with a DM 0.99 feed-in tariff, igniting a booming PV market that increased from nearly 0 MW in the year 1998, to 40 MW in the year 2000, and an estimated 75 MW in the year 2001 (see Reference [3]).

Indeed, the evidence suggests that market demand for photovoltaics can increase by tenfold with the availability of reasonable end-user credit, from approximately 5% of end users who can pay cash, to 50% of end users who could buy if credit on reasonable terms is made available.

Petitioner Canadian Solar (USA) Inc., Ex. 1035, p. 2457

Downloaded from https://onlinelibrary.wiley.com/doi/ by <Shibboleth-member@purdue.edu, Wiley Online Library on [25/08/2024]. See the Terms and Conditions (https://onlinelibrary.wiley.com/terms-and-conditions) on Wiley Online Library for rules of use; OA articles are governed by the applicable Creative Commons License

24.2 CAPITAL REQUIREMENTS

The worldwide rate of PV installations grew at approximately 15% per year in the early 1990s, and accelerated to an average growth rate of 30% per year in the late 1990s. What will be the future growth rate of PV markets, and how much capital will be needed to fund the growth of PV markets and industry?

24.2.1 Market Drivers

Photovoltaics are becoming a factor in the development of the rural areas of the world where over 35% of the world's population – 56% of the rural population – live without the benefit of electricity from the utility grid, totaling some 2 billion people or 400 million households (see Reference [4]). There, photovoltaics have energy value.

The second major driver of PV growth is the public policy on environment and sustainable development. Climate Change is driving global action through the Kyoto protocol and the separate US Climate Change Strategy. As a result of environmental concerns, we are seeing accelerated growth of PV markets in Japan, Europe and, to a lesser extent, the United States. Much work still needs to be done to monetize environmental values and turn market potential into reality (see Reference [5]).

24.2.2 Growth Outlook

What level of growth can be expected in the future? Scenarios of 25 and 50% annual growth bracket the likely range of outcomes. As illustrated in Figure 24.1, the difference between 25 and 50% compounded growth is substantial:

25% Growth Rate: At a growth rate of 25% between the years 2000 and 2010, the annual amount of PV installations will reach 2500 MW per year by 2010.

50% Growth Rate: At a growth rate of 50% between the years 2000 and 2010, the annual amount of PV installations will increase to over 16 000 MW per year by 2010.

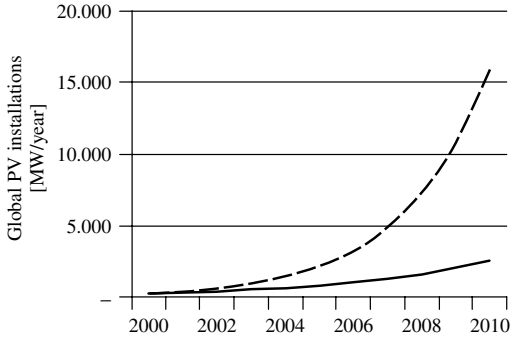


Figure 24.1 PV growth scenarios

Downloaded from https://onlinelibrary.wiley.com/doi/ by <Shibboleth>-member@purdue.edu, Wiley Online Library on [25/08/2024]. See the Terms and Conditions (https://onlinelibrary.wiley.com/terms-and-conditions) on Wiley Online Library for rules of use; OA articles are governed by the applicable Creative Commons License

24.2.3 Capital Requirements

How much capital will be needed? Table 24.1 presents estimates of the amounts of capital that will be required to support the two scenarios of PV market growth. In the year 2010, modules are assumed to cost $1.50/Wp, and systems to cost $3.00/Wp (in 2000 constant dollars). If so, the global PV industry will be doing between $3.8 and $23.8 billion of module shipments, and between $7.7 and $43.6 billion of system installations in the year 2010, under the 25% and 50% growth rate scenarios, respectively. The amounts of capital that will be required to support these levels of growth are estimated as follows:

PV factory investment requirements: The investment cost of PV factory capacity is on the order of $2 to $3 million per MW/year of capacity in the year 2001. This is expected to decline to $1 million per MW/year of capacity as the scale of the new factories continues to increase (i.e. a 100 MW/year factory will cost $100 million to build). Assuming that the PV factory capacity will require an investment of $1 million per MW/year over the next 10 years, the amount of capital to be raised for investment in PV factories will be between $3.1 and $19.0 billion.

Working capital requirements: The operations of the factories and sales distribution channels for PV equipment must also be financed, including inventory and receivables. Assuming that 60 days of work-in-process inventory, 60 days of finished goods inventory, and 90 days of receivables need to be financed, the PV industry will require between $1.9 and $11.9 billion for working capital financing.

End-user financing requirements: Market indicators suggest that as much as 80 to 90% of the PV market will require end-user financing. Assuming that grid-connected systems represent 50% of the world market, and that 80% of the end users receive an average 80% loan, and assuming that off-grid rural electrification represents 30% of the world market, and that 50% of those end users receive an average 80% loan, then the end-user financing requirement to support PV industry growth will be $20.6 to $82.8 billion over the next 10 years.

Table 24.1 Global capital requirements to fund PV growth

	25%/Year growth scenario	50%/Year growth scenario
Annual amounts in 2010:		
PV shipments	2561 MW/year	15 858 MW/year
Module revenues	$3.8 billion/year	$23.8 billion/year
System revenues	$7.7 billion/year	$43.6 billion/year
Cumulative amounts 2000–2010:		
PV shipments	11 700 MW	47 000 MW
Module revenues	$23.4 billion	$94.0 billion
System revenues	$46.8 billion	$188.1 billion
Global capital requirements (US $):		
PV factory investment	$3.1 billion	$19.0 billion
Working capital	$1.9 billion	$11.9 billion
End-user financing	$20.6 billion	$82.8 billion
Total capital required	$25.6 billion	$113.7 billion

Source: Eckhart, Overview, 2001

Downloaded from https://onlinelibrary.wiley.com/doi/ by <Shibboleth-member@purdue.edu, Wiley Online Library on [25/08/2024]. See the Terms and Conditions (https://onlinelibrary.wiley.com/terms-and-conditions) on Wiley Online Library for rules of use; OA articles are governed by the applicable Creative Commons License

Downloaded from https://onlinelibrary.wiley.com/doi/ by <Shibboleth-member@purdue.edu, Wiley Online Library on [25/08/2024]. See the Terms and Conditions (https://onlinelibrary.wiley.com/terms-and-conditions) on Wiley Online Library for rules of use; OA articles are governed by the applicable Creative Commons License

In sum, the PV industry must mobilize at least $25 billion in capital to support a 25% annual growth rate, and as much as $114 billion in capital to support a 50% growth rate, over the next 10 years.

24.3 FINANCIAL CHARACTERISTICS OF PV

This section addresses the characteristics of PV that are essential considerations in the financing of end-use applications, over and above standard lending issues like credit worthiness of the borrower.

Geographic location: The average amount of solar energy hitting the Earth is about 1 kW/m^2. The amount of solar insolation varies by latitude and by regional weather patterns. There is an approximate 2:1 variation in the amount of solar insolation across most of the inhabited world. A 1 kW PV system would generate a 900 to 1000 kWh per year in Germany, and as much as 1800 to 2000 kWh per year in desert locations like Arizona or South Africa. The amount of sunlight varies on an annual cycle, and also as much as +/−10% year to year due to atmospheric and weather conditions (see Reference [6]).

Facility design and cost: The cost of a PV system includes the cost of PV modules (typically 40 to 60% of the total), balance-of-system (BOS) equipment (such as batteries, controllers, inverters, switches, fuses, etc.), and services (design, architecture, engineering, procurement, construction, installation, and postinstallation O&M). PV system costs have come down steadily over the past 25 years, and are now typically $5 to $15 per installed watt. Financiers should be given evidence that the buyer has shopped for a quality system, from a qualified supplier, at a reasonable price.

System efficiency: System efficiency is the key operational characteristic of a PV system, measuring its conversion of solar insolation at the site to output DC or AC electricity. Most of the publicity about PV efficiencies refers to PV cell efficiencies, typically ranging from 5 to 10% for amorphous silicon, 8 to 12% for CIS and CdTe thin-film technologies, 12 to 18% for crystalline silicon, and 25% and higher for cells that are used in concentrator systems (see Reference [7]). The efficiencies of PV cells in research laboratories are even higher and they are improving steadily. But the key for financing is not the latest development in PV cell research; it is the typical, guaranteed output of an entire PV system in its end-use application. The conversion efficiency of the entire system is affected by the efficiency of the cell, reduced somewhat when placed in a module, then further reduced by losses in the wiring and BOS equipment. Thus, PV system efficiencies are about 60 to 80% of PV cell efficiencies (i.e. the efficiency of a system using 16% efficient cells is likely to be in the range of 10 to 13%).

Useful lifetime: The useful lifetime of a PV system is important because it determines the amount of time a financier can allow for repayment of a loan or lease. PV modules typically come with warranties of 10 to 25 years – assuring the owner of 80% to 90% of the module's rated output over the warranty period. From a lender's point of view this is a positive factor in financing. With such guarantees, the modules will have future value as collateral. The weak link in the financing of PV systems is, however, the fact that the useful life of BOS equipment is much shorter and less predictable. BOS equipment often comes with warranties of 90 days to one year, and useful lives

can range from three to five years for batteries, and from 5 to 10 years for electronic inverters, converters, and controllers. The key to the long life of the full system is therefore ongoing maintenance and repair by a qualified supplier.

Operations and maintenance cost: Whereas photovoltaics have a reputation of being "maintenance free," this only applies to the PV modules. PV systems actually require regular checking and maintenance like any electrical system. Financing should be contingent on there being a plan and/or contract for ongoing maintenance service by the installer or another qualified electrical contractor.

Residual value: The residual value of a PV system is the amount that it can be sold for ("liquidated") at the end of the loan or lease. A lender wants assurance that the system's value is never less than the outstanding balance on the loan. A leasing company needs assurance of good residual value, since this is what the leasing company will own at the end of the lease. Lack of evidence on the collateral/residual value of PV equipment is one of the weak points in PV financing today.

Tax treatment: A key issue for financing is how photovoltaics is treated for tax purposes. This typically includes sales and property tax abatements, income tax deductions and credits, and accelerated depreciation schedules. These factors can be instrumental in determining the economic viability of a PV system and the timing of cash returns to the owner.

Regulatory treatment: A factor that is increasingly important is how photovoltaics is treated in government regulations. A key regulatory issue for grid-connected applications is whether photovoltaics qualifies for net metering. That is, whether electricity generated by the PV system can be applied to offset retail electricity purchases from the utility. If photovoltaics qualifies for net metering, then the value of the PV's output electricity equals the retail rate, typically 8 to 15 ¢/kWh in Europe and the United States, and over 20 ¢/kWh in Japan. If photovoltaics do not qualify for net metering, then the electricity is only worth the wholesale "avoided cost" rate, which is typically 2 to 5 ¢ per kWh. As of the year 2002, over 30 US states and several countries like Germany and the Netherlands, have adopted net metering or equivalent regulatory treatment.

Economics of the application: The previous factors related to the PV system. But what really separates photovoltaics from other power-generation technologies is the degree to which photovoltaics becomes an essential element of an end-use application – such as providing "essential electricity" for remote telecommunications, water pumping, home lighting, and other off-grid applications, or providing "clean electricity" for homes, commercial buildings, and other on-grid applications. A key question for the financier is whether the end-use application is economically viable, and the degree to which the use of photovoltaics makes it more or less so. Please see Section 24.4 for additional discussions on PV economics.

Codes and standards: Financing should be conditional on a PV system meeting all applicable codes and standards, and this will vary by end-use application, whether the PV system is integrated into the structure of a building, on the roof of a residential home, or in a field serving a remote application. The key US national standards include the National Electric Code and special standards for interconnection to the utility grid that have been promulgated by the Institute of Electrical and Electronic Engineers (IEEE) and Underwriters Laboratories (U/L). There is also a need to meet all applicable local building and electrical codes, which vary by locality (see Reference [8]). European

Downloaded from https://onlinelibrary.wiley.com/doi/ by <Shibboleth-member@purdue.edu, Wiley Online Library on [25/08/2024]. See the Terms and Conditions (https://onlinelibrary.wiley.com/terms-and-conditions) on Wiley Online Library for rules of use; OA articles are governed by the applicable Creative Commons License

Downloaded from https://onlinelibrary.wiley.com/doi/ by <Shibboleth-member@purdue.edu, Wiley Online Library on [25/08/2024]. See the Terms and Conditions (https://onlinelibrary.wiley.com/terms-and-conditions) on Wiley Online Library for rules of use; OA articles are governed by the applicable Creative Commons License

standards organizations have promulgated a similar set of codes and standards for photovoltaics within the European Union. For solar home systems in the developing countries, the PV Global Acceptance Program (PV/GAP) establishes a testing certification protocol. The adoption of these codes and standards is one of the keys to future financing of PV, as they will build credibility with lenders and investors.

On the basis of the above, one sees that the characteristics of photovoltaics present a complex case. The financial merits of photovoltaics depend on location, cost and quality of the system, efficiency output of the system, useful lifetime, O&M cost, residual value, tax treatment, regulatory treatment, viability of the end-use application, adherence to codes and standards, and credit worthiness of the end user.

24.4 FINANCING PV FOR GRID-CONNECTED RESIDENCES

A major opportunity for PV growth in European, Japanese, and US markets is the grid-connected, residential rooftop system, typically 1.0 to 4.0 kW each. Approximately 110 MW of grid-connected systems were installed in Japan, 75 MW were installed in Germany, and 15 MW were installed in the United States in the year 2001.

24.4.1 Impact of Loan Terms on End-user Cost

Table 24.2 illustrates how the terms of financing can drive monthly payments on a PV system. The example uses a 2.5 kW residential grid-connected PV system costing $8.00 per installed watt (Wac). Credit card type debt (10 year, 18% interest) on a $20 000 residential rooftop PV system would yield payments of $437/month. The monthly payment drops to just $121/month if the PV system is included in a new home mortgage or financed with a low-interest loan.

It is clear from the above analysis that the preferred way to finance a residential PV system is the primary home mortgage loan, if possible. A longer-term loan results in lower monthly payments, but increases interest paid and hence the total amount of money paid for the system. As a rule of thumb, the cost of money is approximately equal to the cost of the PV system with an 11-year, 11% loan. A longer-term loan or a higher interest rate would cause the interest payments to be more than the cost of the PV system, illustrating once again the impact of financing on the viability of photovoltaics.

Table 24.2 Monthly payments on a 2.5-kilowatt rooftop PV system

Loan type	Term [Years]	Interest rate [%]	Monthly payment [$/month]
Credit card	7	18	437
Credit line	10	12	295
Home equity loan	15	8	195
Home mortgage	30	6	121

24.4.2 Types of Residential Financing

There are many financing alternatives available in the residential sector that could be applied to the financing of a PV installation:

Unsecured loan: Credit cards have become a significant source of financing, even though interest rates are typically 12 to 24%. Commercial lenders also provide unsecured signature loans and personal lines of credit at interest rates of 10 to 20%. Terms vary from one to ten years.

Equipment secured loan: There is some use of contractor-originated Retail Installment Contracts that hold security on the equipment until the contracts are paid off.

Home mortgage loan: Real estate secured loans are by far the most common and available form of credit to the residential sector. Loan products range from 5- and 10-year home equity loans, to 15-, 20- and 30-year primary mortgage loans, carrying either fixed or variable interest rates.

Energy-efficient mortgage (EEM) loan: In the United States, the EEM is offered by many of the national residential lenders and is designed to allow additional income credit from energy savings to be used in qualifying for a loan. This program is also called Energy Star. Japan and several European countries have similar programs.

Subsidized and targeted loan programs: Certain population groups – including, for example, low-income, minority, and veterans – are eligible for special terms and rates from a variety of specialized lenders. Also, there are special loan programs for designated locations such as rural areas, economically depressed areas, and inner-city urban areas. Government support for these programs ranges from direct loans, to loan guarantees, to interest subsidies.

Utility financing programs: A number of electric utilities have established special loan programs for energy efficiency and renewable energy. In the United States, the Sacramento Municipal Utility District (SMUD), the Los Angeles Department of Water and Power (LADWP), the Long Island Power Authority (LIPA), and the City of Austin Electric Department – all being nonprofit municipal utilities – have established PV financing programs (see Reference [9]). In Austin, the loans are unsecured, ranging from $1000 to $9000, with terms of three to ten years, at interest rates of 4.00 to 5.99%. The US cooperative utilities are also looking at PV financing programs. In Germany, municipal utilities created the first real market for photovoltaics between the years 1997 and 1998, applying the "Aachen model" of long-term power purchase contracts.

Government loan programs: A number of states in the United States are establishing clean energy funds, typically administered through the in-state utilities and banks. In New York, a $130 million fund has been established. Idaho's Renewable Energy Loan Program finances residential PV in amounts ranging from $1000 to $10 000, subject to the application having a 10-year payback or less. California has established a special alternative energy financing trust and a new Power and Consumer Finance Authority. This is also happening around the world. In Germany, KfW has established a national loan program for residential installations, offering 10-year loans at a 2% interest rate. In Japan, interest rates on loans for residential PV systems are subsidized. In India, IREDA has an ongoing program of lending for photovoltaics and other renewables.

Downloaded from https://onlinelibrary.wiley.com/doi/ by <Shibboleth-member@purdue.edu, Wiley Online Library on [25/08/2024]. See the Terms and Conditions (https://onlinelibrary.wiley.com/terms-and-conditions) on Wiley Online Library for rules of use; OA articles are governed by the applicable Creative Commons License

Downloaded from https://onlinelibrary.wiley.com/doi/ by <Shibboleth-member@purdue.edu, Wiley Online Library on [25/08/2024]. See the Terms and Conditions (https://onlinelibrary.wiley.com/terms-and-conditions) on Wiley Online Library for rules of use; OA articles are governed by the applicable Creative Commons License

24.4.3 Lender's Issues

Decisions about whether to make a loan will depend principally on the borrower's ability and willingness to repay the loan, indicated by past credit history and income. Loans secured by appreciating assets, such as real estate, have the longest terms and lowest interest rates, because the value of the collateral serves as additional protection of the loan. Lenders should ask several key questions in qualifying a loan:

- Is this installation economically advantageous for the borrower? The lender should understand whether the borrower is installing the PV system for economic or for environmental reasons.
- Can the system be easily installed by qualified contractors? Does it meet all of the applicable building codes and safety standards?
- How long will the system perform? Is there a warranty on the system? Is there a guarantee on performance over the life of the system?
- What will be the ongoing or recurring costs of operation, maintenance, repairs, and potential removal of the system?
- What are the energy-cost savings that the borrower will receive from owning the PV system? Are these savings certain enough to count as "income" for loan qualification purposes?
- What is the current market value of the system? How does this change over time? What is the likely residual value of the system at the end of the loan period?
- What are the risks on repayment? Technical? Economic? Others? Are the risks well known and understood?

24.4.4 Borrowers' Experience

A market research report prepared by the Regional Economic Research for the California Energy Commission (see Reference [10]) revealed the following:

- The main concerns singled out by residential consumers ranked system reliability, life, safety, and ongoing costs as more important than the initial cost of the system.
- The majority of residential end users (54%) preferred some form of loan financing over investing their savings – with 35% preferring a home equity loan, 22% a personal loan, and 7% a first mortgage.
- Residential end users were more likely to consider installing a solar system when: roofing the home (60%), remodeling (54%), and purchasing a home (50%) – all times when financing is normally utilized. Only 31% stated that they would be more likely to consider installing a solar system as a "stand-alone" purchase.

Market research by the US National Renewable Energy Laboratory (NREL) indicates that 60% of respondents are willing to pay at least $25 extra per month for a rooftop PV system, 38% are willing to pay an additional $50 per month, and 15% are willing to pay $100 more per month. Regarding financing, 46% prefer long-term loans, while 36% prefer short-term loans (see Reference [11]).

24.4.5 Example Calculation

A 2.5-kW rooftop PV system costing $8.00/Wac installed will cost $20 000. Assuming an excellent location yielding a 22% capacity factor, the system will produce 1927 kilowatt hours per kW installed, per year, or 4818 kWh/year for the 2.5 kW system. The following is a brief assessment of the financial merits under several cases:

No incentives: If the government does not allow net metering, the value of the electricity will only be the wholesale rate that the utility pays for bulk energy. The PV system is not likely to be given capacity credit, so the value will be energy only, or about 2 to 4 ¢/kWh. The value of the output is therefore $96.36/year to $192.72/year. The system will have a simple payback in 103 to 207 years.

Net Metering: If net metering applies, then the value of the electricity is the retail rate (tariff), say, 10 to 15 ¢/kWh. In this case, the value of the output is $481.80/year to $722.70/year. The system will have a simple payback in 28 to 42 years.

Subsidy: If the government now provides a subsidy in the amount of $4.50/Wac, leaving the owner's cost equal to $3.50/Wac or $8750, and net metering still applies, then the value of the output is still $481.80/year to $722.70/year, and the system will have a simple payback of 12 to 18 years, probably within negotiating range for an environmentally motivated end user.

Low-cost financing: The cost of financing will increase the total cost to the end user, and hence lengthen the payback period or rate of return on investment. A 10-year, 12% loan will add 72% to the total outlay by the owner, increasing system cost from $8750 to $15 486. The simple payback will be lengthened from 21 to 32 years. Conversely, if the interest rate is dropped to 5%, the financing will add only 15% to the total outlay by the owner, increasing system cost from $8750 to $10 105. Simple payback will be lengthened to 14 to 21 years, much more favorable than the higher-rate financing. While third-party financing lengthens the payback period, it makes the purchase more affordable by more people, based on monthly payments (see Reference [12]).

The analysis has shown that – with net metering, feed-in tariffs, tax credits, capital cost subsidies, and low-interest financing – residential rooftop PV can yield a payback in the range of 10 to 20 years, potentially enough for those who are motivated by the environment and sustainable development.

24.4.6 Improving the Financing of Residential PV

Several things can be done to improve the fit between photovoltaics and the home-mortgage lending industry. First, the debt/equity ratio should be relaxed, allowing a higher faction of debt on a PV-powered home, reflecting the fact that the owner is prepaying the utility bill for 20 to 30 years. Second, the cost of the PV system should automatically increase the appraised value of the home. Third, the amount of savings on the borrower's utility bill should be added to the income for the purpose of the loan qualification calculation, reflecting the borrower's lower cost of living with the PV option. With these practices, the lending industry would become an enabler of, rather than a constraint on, PV growth.

Downloaded from https://onlinelibrary.wiley.com/doi/ by <Shibboleth-member@purdue.edu, Wiley Online Library on [25/08/2024]. See the Terms and Conditions (https://onlinelibrary.wiley.com/terms-and-conditions) on Wiley Online Library for rules of use; OA articles are governed by the applicable Creative Commons License

24.5 FINANCING PV IN RURAL AREAS OF DEVELOPING COUNTRIES

Financing programs for PV in the rural areas of developing countries is the focus of the World Bank, the IFC, aid agencies from the OECD nations, charitable foundations, and a number of special-purpose funds such as the Solar Development Group and the proposed SolarBank Fund.

24.5.1 Rural Applications

There are four principal applications for photovoltaics in the rural areas of developing countries (see Reference [13]):

Solar home systems (SHS): This basic battery-based electrical system with a solar PV charger includes a PV module – typically 20 Wp in Kenya, 35 Wp in southern India, and 50 Wp in Indonesia and the Philippines – plus a battery, charge controller and wiring, receptacles, outlets, and switches for lighting and communications. Financing can be justified on a cost basis, the monthly payments for the SHS are less than a family's existing costs for kerosene, candles, and dry cell batteries (see Reference [14]), but the stronger basis for lending is the upliftment of family lifestyle and income that generally accompanies rural electrification. A 35-W solar home system costs US $300 to $750, depending on the manufacture, import duties and taxes (if applicable), the quality of components, and installation. Financing is just beginning to be made available through banks, nonbanking finance companies, microcredit lenders, cooperatives, and other sources. Typical financing for an SHS in a developing country is a 1- to 3-year loan at 18 to 36% interest, or a fee-for-service payment that approximates a lease.

Water pumping for irrigation: The financing of a PV-powered water pump for irrigation can be justified on the basis of the economic impact on the farm, typically the addition of a third crop to what was a two-crop farm, or higher yield per acre as a result of irrigation. A 900-W PV pumping system can cost $5000 to $8000, a cost that can be recovered in as little as one year in some extraordinary cases, and can be the least-cost option on a life cycle–basis for many remote farms, especially when compared to the costs of diesel power. PV-powered water pumping is heavily subsidized in most cases today, ranging from 100% grants from European donor agencies to a 50% subsidy from the government of India.

Microenterprise ("Productive Uses"): There are many applications for photovoltaics in small businesses. Financing can be established through microcredit models of group lending, and justified on the basis of the expected cash flows of the microenterprise businesses. PV systems can extend the operating hours with lighting, improve working conditions with lighting and fans, power mechanization and product preservation (drying and refrigeration), and enable communications. PV systems for the microenterprise range in cost from $300 for a minimal PV lighting system to $10 000 or more for a system that is capable of running a significant level of factory motors or refrigeration (see Reference [15]).

Institutional uses: Photovoltaics is being applied for lighting, communications, water supply and refrigeration in schools, health/medical clinics, and community services. A 1000-W PV system for a school or clinic can cost $10 000 or more, fully installed.

Downloaded from https://onlinelibrary.wiley.com/doi/ by <Shibboleth>-member@purdue.edu, Wiley Online Library on [25/08/2024]. See the Terms and Conditions (https://onlinelibrary.wiley.com/terms-and-conditions) on Wiley Online Library for rules of use; OA articles are governed by the applicable Creative Commons License

Such PV systems are typically paid for by government programs, often supported by grants from donor agencies. These applications will require new forms of institutional financing as PV utilization increases in the future beyond the ability of grant agencies to pay.

24.5.2 Impact of Financing on Market Demand

Evidence from Asia, Africa, and Latin America indicates that market demand for PV systems in the developing countries increases by a factor of ten (10x) with the provision of reasonable levels of end-user financing:

Latin America: The pyramid in Figure 24.2 illustrates an estimate that was made by Soluz Inc., a leading PV company operating in Latin America, suggesting a tenfold increase in market demand if financing is available.

Indonesia: A PV developer in Indonesia estimated that the market would expand from 30% of the population for cash sales to 70% for the fee-for-service option (see Reference [16]).

India: A PV company in India has concluded that 5% of rural people in southern India can afford to pay cash, while 50% could afford to buy a PV system if they had a 1 to 2 year loan at market rates (see Reference [17]).

Sri Lanka: A leading microcredit lender in Sri Lanka concludes that over 50% of the people can afford an SHS with reasonable credit (see Reference [18]).

South Africa: The national utility Eskom conducted a field-survey-based market study in preparation for the Shell–Eskom joint venture and found that nearly 50% of the rural families in the Eastern Cape could afford monthly payments of 47 Rand (then about US $10.00) per month, whereas very few could afford to pay for the system up front (see Reference [19]).

The findings are consistent around the world, that at least 50% of all rural households can afford to pay for a PV system given reasonable credit terms or the equivalent through a fee-for-service approach.

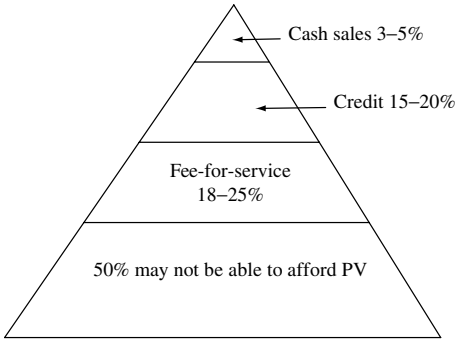


Figure 24.2 Affordability of PV systems by rural people in Latin America

Downloaded from https://onlinelibrary.wiley.com/doi/ by <Shibboleth-member@purdue.edu, Wiley Online Library on [25/08/2024]. See the Terms and Conditions (https://onlinelibrary.wiley.com/terms-and-conditions) on Wiley Online Library for rules of use; OA articles are governed by the applicable Creative Commons License

Downloaded from https://onlinelibrary.wiley.com/doi/ by <Shibboleth-member@purdue.edu, Wiley Online Library on [25/08/2024]. See the Terms and Conditions (https://onlinelibrary.wiley.com/terms-and-conditions) on Wiley Online Library for rules of use; OA articles are governed by the applicable Creative Commons License

24.5.3 Examples of PV Financing in Rural Areas

The financing of photovoltaics is beginning to occur around the world. The following are some current examples.

Bank Lending: SELCO India (Pty) Ltd, a solar PV installation and service company that has installed over 5000 solar home systems in southern India, has built working relationships with a number of area banks such as Syndicate Bank, and nonbanking finance companies (NBFCs) like Manipal Finance. SELCO has provided cash deposits as partial guarantees to several of the lenders, encouraging them to become involved in PV financing, and has provided interest rate buy-downs in other cases. Loans are typically 80% of the system cost, at 14 to 18% interest, repaid over one to three years. Even such short-term lending has sparked a market in southern India.

Microcredit lending: In Sri Lanka, a microcredit lender named Sarvodaya Economic Enterprise Development Services Limited (SEEDS), has embarked on a successful PV-lending program with its members. SEEDS loans 80% of the cost of the system. Loans are repayable in one to five years. Interest rates are in the mid- to upper-twenties (local borrowing rate plus a spread for SEEDS operation). Repayment is flexible – monthly or seasonal, depending on the income stream of the borrower. The loan recovery rate in SEEDS' program has reached 94%. SEEDS expects to finance as many as 50 000 solar home systems between the years 2001 and 2005. This work in Sri Lanka has built upon and perfected the pioneering work by Grameen Bank in Bangladesh (see Reference [20]).

NGO financing: In Bangladesh, Grameen Shakti, the PV affiliate of the Grameen Bank, is an example of a nongovernment organization that is involved in both the financial and technical aspects of PV dissemination. Grameen Shakti offers three financing options (it charges a "service charge" instead of "interest" because of local custom):

- 85% loan, repaid over a period of three years, having a 12% service charge (interest cost);
- 75% loan, repayable over two years, having an 8% service charge;
- Cash: The buyer receives a 4% discount on the system price by paying cash up front (not taking a loan).

Cooperative financing: In Santa Cruz, Bolivia, Cooperativa Rural de Electrificación (CRE) is a rural electric co-op that began installing PV systems in 1995 for customers who could not be reached by the grid. By 1998, CRE was serving 1300 PV customers, charging a flat monthly electric service fee. CRE owns the PV systems and maintains them.

Fee-for-service model: Several pioneering programs are being implemented using a fee-for-service model – charging a flat monthly fee for the use of a solar home system that is owned and maintained by a service company. Prepayment meters are commonly used on the battery's charge controller, which provides a revenue control mechanism. Users purchase prepayment cards each month at a local shop. In Indonesia, Total Energie, the French PV systems integrator, has completed a fee-for-service trial serving some 5000 customers. In South Africa, Shell-Eskom, a 50/50 joint venture of Shell International and Eskom, the national electric utility in South Africa, has installed 6500 solar home systems and is working toward an initial business trial of 50 000 units when

approved as a "concession" by the central government. The model has been adopted as a national strategy by the South African government. South Africa has set a goal of 100% electrification using grid and nongrid (PV) alternatives by the year 2010. A third major application of the fee-for-service model is in Argentina under a World Bank loan.

Rental/Leasing (Entrepreneurial Model): A variation on the fee-for-service approach is leasing. In the Dominican Republic, Soluz Dominicana, an affiliate of the US-based Soluz, Inc., has established a pioneering model using a leasing approach. Soluz charges $10 to $20 per month per SHS. Over 2000 systems are in service. Maintenance is provided by the company.

Tax-driven leasing and other financial engineering: In India, nonbanking finance companies (NBFCs) did some "financial engineering" in the 1997 to 2001 period to create a single-payment lease structure for PV-powered water pumping. The NBFC collected a single, up-front lease payment from the farmer, typically 30% of the system cost. The NBFC then took out a 10-year, 85% loan from IREDA, bearing 2.5% interest. Finally, the NBFC absorbed the 100% first-year depreciation that is available for PV in India, yielding 34% after-tax cash value. The three inflows totaled approximately 150% of the cost of the PV system. The extra 50% was deposited at 12 to 18% interest, from which the IREDA loan is repaid in 6 and 10 years. This model yielded the NBFC a cash-positive deal from day one and a good profit. The net result was a win–win situation: the government's objectives for additional use of photovoltaics were met, the available incentives were fully absorbed by the financial community, and farmers got water-pumping systems that they otherwise could not afford. Nonbanking finance companies such as Sundaram Finance and Srei International participated in this approach. This example illustrates how governments can mobilize private sector capital through tax and loan policy. It also illustrates how unstable government policy can cripple PV markets – financing of PV water pumps through this technique came to a halt when IREDA stopped making PV loans at the 2.5% rate of interest, thus eliminating the interest arbitrage that the NBFCs had built into the model.

As seen above, the financing of photovoltaics in rural areas of the world's developing countries is beginning to occur in a number of ways – bank loans, microcredit lending, NGO programs, cooperative financing, fee-for-service models, rental/leasing, and tax-driven leasing. This is a period of renovation. Considerable efforts will be needed to promulgate the use of successful models and build a higher level of acceptance of PV financing by the financial community.

24.6 SOURCES OF INTERNATIONAL FINANCING

24.6.1 International Aid and Donor Funding

In the past, the programs to fund photovoltaics in the developing countries have been sponsored by donors and aid agencies. OECD countries provide about $50 billion per year in Official Development Assistance (ODA). These amounts include funds channeled by individual countries through multilaterals, such as the United Nations Development Program (UNDP). More recently, in line with GEF grants and World Bank financings, donor agencies have shifted increasingly towards the support of *financing*, rather than

Petitioner Canadian Solar (USA) Inc., Ex. 1035, p. 2469

Downloaded from https://onlinelibrary.wiley.com/doi/ by <Shibboleth-member@purdue.edu, Wiley Online Library on [25/08/2024]. See the Terms and Conditions (https://onlinelibrary.wiley.com/terms-and-conditions) on Wiley Online Library for rules of use; OA articles are governed by the applicable Creative Commons License

Downloaded from https://onlinelibrary.wiley.com/doi/ by <Shibboleth-member@purdue.edu, Wiley Online Library on [25/08/2024]. See the Terms and Conditions (https://onlinelibrary.wiley.com/terms-and-conditions) on Wiley Online Library for rules of use; OA articles are governed by the applicable Creative Commons License

grant *funding*, of solar PV and other renewables. Illustrative examples of such programs include the following:

United States of America: USAID has been funding the Renewable Energy Project Support Operation (REPSO) through Winrock International, resulting in a number of early stage financial support actions in India, Brazil, Indonesia, and elsewhere. USAID explored the possibility of establishing an $18 million fund in South Africa for the Productive Uses of Renewable Energy (PURE Fund), focused on business uses for photovoltaics. In 1999, the US Export–Import Bank established a $50 million allocation to China, earmarked for renewable energy exports, including photovoltaics.

Germany: Kreditanstalt für Wiederaufbau (KfW), the German bank for reconstruction, has extended a DM 120 million loan to India's IREDA including DM 30 million allocation for photovoltaics.

Netherlands: The Ministry of Economic Affairs has supported a number of PV programs around the world, including a 20 000 unit solar home system program in Bolivia and a 30 000 unit program in China, supplied by Shell Solar. A new project in the Philippines is reportedly in the pipeline.

France: The French government had a special tax deduction for investments in the former French colonies, resulting in a subsidized flow of capital to PV projects in such countries. The French electric utility, Electricte de France (EdF) is involved in the financing of fee-for-service programs in Brazil, Indonesia, Morocco, and South Africa.

Spain: In 2001, the Spanish government extended a $48 million soft loan to the Philippines for the installation of 2 MW of photovoltaics in 100 villages, comprising approximately 150 000 homes, all to be supplied by BP Solar Madrid. One-half of the funds will be loaned under the credit conditions of the OECD: a 10-year loan at just-below market rates. The other half will come from the Spanish Development Aid Fund (FAD): a 30-year loan, with a 10-year grace period, with an interest rate less than 1.0% (see Reference [21]).

Australia: USAID extended a $30 million soft loan to Indonesia in 1998 for the installation of 50 000 solar home systems supplied by BP Solar Australia.

Japan: The Japanese aid agency, Overseas Economic Cooperation Fund (OECF), was reported to have begun providing aid in support of photovoltaics in developing countries in the year 2000. Reports suggest that the program might be substantial in scope and scale. OECF has prepared a $100 million funding package for India's IREDA for renewable energy on lending, including photovoltaics.

Others: The aid agencies of Austria, Denmark, Italy, Sweden, Switzerland, and the United Kingdom have funded a variety of PV programs in the developing countries, generally of the grant-for-demonstration kinds of activities. This kind of aid is being coordinated in Europe by the new EC directorate for international aid.

24.6.2 United Nations

UNDP supported demonstrations of solar home systems, PV water pumping, PV-powered health clinics, and other projects in the developing countries, generally with GEF grant support. UNDP-sponsored projects include

Bolivia: rural electrification with renewable energy
China: renewable energy capacity building

Ghana: renewable energy for rural, social, and economic development
Malawi: barrier removal to Malawi renewable energy
Peru: PV-based rural electrification
Sri Lanka: renewable energy capacity building
Uganda: PV pilot project for rural electrification
Zimbabwe: PV for household and community use.

UNEP has recently sponsored a new PV program in Africa, supporting early-stage financing of solar energy ventures (or, "enterprises"). This program has been funded by the UN Foundation, under the guidance of UNDESA.

The World Health Organization (WHO) funds a program for PV-powered refrigeration for storing medicines in remote areas of Africa.

24.6.3 World Bank Solar Home System Projects

The World Bank, with grant support from the GEF, has funded 12 projects around the world providing basic "energy services" such as lighting, radio, television, and operation of small appliances, using solar home systems in rural households that lack access to electricity grids, including

Argentina: renewable energy in rural markets project
Benin: off-grid electrification project
Cape Verde: energy and water sector reform project
China: renewable energy promotion project
India: renewable resources development project, through IREDA
Indonesia: solar home system project
Lao: PDR rural electrification project
Sri Lanka: energy services delivery project
Togo: off-grid electrification.

There are three more projects pending approval of the World Bank:

Peru: PV-based rural electrification
Guinea: rural energy development
Mexico: renewable energy for agriculture.

Most of the World Bank's early experience with photovoltaics and other renewables came from its Asia Alternative Energy Unit ("ASTAE"), funded by a number of donor agencies since 1992. A key finding from ASTAE's early work was that "the lack of term financing was not the sole obstacle to renewable resources or end-use energy efficiency development. The absence of adequate regulatory and institutional arrangements, local technical capacity, and appropriate energy service delivery infrastructure can pose equal or greater barriers to alternative energy development" (see Reference [22]).

On the basis of this experience, the World Bank is concluding that future PV projects will seek to incorporate six elements: support private sector and NGO delivery models, pilot consumer credit delivery mechanisms, pay first-cost subsidies, support policy development and capacity building, enact standards and establish certification, testing, and enforcement institutions, and conduct consumer awareness and marketing programs.

Downloaded from https://onlinelibrary.wiley.com/doi/ by <Shibboleth-member@purdue.edu, Wiley Online Library on [25/08/2024]. See the Terms and Conditions (https://onlinelibrary.wiley.com/terms-and-conditions) on Wiley Online Library for rules of use; OA articles are governed by the applicable Creative Commons License

Downloaded from https://onlinelibrary.wiley.com/doi/ by <Shibboleth-member@purdue.edu, Wiley Online Library on [25/08/2024]. See the Terms and Conditions (https://onlinelibrary.wiley.com/terms-and-conditions) on Wiley Online Library for rules of use; OA articles are governed by the applicable Creative Commons License

24.6.4 International Finance Corporation (IFC)

IFC, an institution of the World Bank Group, promotes economic development by encouraging private sector investment activities in developing countries. With regard to PV financing, the IFC participates in several PV financing programs:

Photovoltaics Market Transformation Initiative (PVMTI): PVMTI is an initiative of the IFC and the GEF to accelerate the sustainable commercialization and financial viability of solar photovoltaic-based energy services in India, Kenya, and Morocco. The IFC has designated Impax Capital and IT Power Ltd, both of the United Kingdom, as the external management team for PVMTI.

Small and Medium Scale Enterprises (SME) Program: This special unit of the IFC's environmental division makes small loans to entrepreneurial ventures and projects in the developing countries, and has made two financings in photovoltaics, in Vietnam and the Dominican Republic.

Solar Development Capital (SDC): SDC is a 10-year, $28.75-million fund that makes minority equity, quasi-equity, and debt investments in PV-related businesses in developing nations. SDC seeks to invest in companies involved in distribution, consumer financing or leasing, manufacturing, or other aspects related to accelerated PV use in rural areas.

Solar Development Foundation (SDF): This is an approximately $19 million nonprofit foundation that provides technical and business assistance to enterprises in preparation for larger-scale private investment, and can provide "seed" finance for business development activities on flexible terms.

Renewable Energy and Energy Efficiency Fund (REEF): REEF was a pioneer financing fund focusing on renewable energy and energy efficiency projects and companies. As of November 2001, REEF was capitalized at a level of $65 million of equity plus a debt facility from the IFC. The external management team was headed by Energy Investors Funds. REEF was disbanded in late-2002.

24.6.5 Global Environment Facility

The Global Environment Facility (GEF) has been a central source of funding for PV in the developing countries. Since 1991, the GEF has provided grant funding for 25 off-grid PV projects in 20 countries, all through the World Bank Group and the United Nations, accounting for about $210 million of GEF allocation, and about $1.4 billion in total project costs, as summarized in Table 24.3. Lessons learned from the GEF's early implementation experience are summarized in a formal review of the program, with several key conclusions (see Reference [23]):

- Local financiers should be encouraged to carry some of the credit risk, not simply act as administrative conduits, in order to increase postproject sustainability and replication.
- Small PV dealers face sufficient business and technology risks that they are reluctant to assume consumer credit risks and incur the costs of credit administration and collections.
- Microfinance may work well in countries that have well-established microfinance institutions, but NGOs do not necessarily have the commercial orientation or business skills for rapid delivery of credit. Scale-up and outreach can become problematic.

Table 24.3 PV projects funded by the Global Environment Facility

Program	Year	Project	Agency	GEF funds [$ millions]	Total funds [$ millions]	Status
India	1991	Alternative energy	WB	26.0	186.0	Implementing
Zimbabwe	1991	PV for households and communities	UNDP	7.0	7.0	Completed
Indonesia	1995	Solar home systems	WB	24.0	118.0	Cancelled
Uganda	1995	PV pilot project, rural electrification	UNDP	1.8	3.6	Implementing
Ghana	1996	Renewable energy rural development	UNDP	2.5	3.1	Implementing
Sri Lanka	1996	Renewable energy capacity building	UNDP	1.5	1.5	Implementing
Sri Lanka	1996	Energy services delivery	WB	5.9	55.0	Implementing
Argentina	1997	Renewables energy in rural markets	WB	10.0	120.0	Implementing
Bolivia	1997	Rural electrification with renewables	UNDP	4.5	8.5	Implementing
China	1997	Capacity building for renewable energy	UNDP	8.8	28.0	Implementing
Lao PDR	1997	South provinces renewables project	WB	0,7	2.1	Implementing
Benin	1998	Decentralized rural energy	WB	1.1	5.7	Pending approval
Cape Verde	1998	Energy & water sector reform	WB	4.9	65	Implementing
China	1998	Renewable energy development	WB	35.0	445.0	Implementing
Peru	1998	PV-based rural electrification	UNDP	4.0	9.2	Implementing
Togo	1998	Decentralized energy	WB	1,1	5.7	Pending approval
Guinea	1999	Rural energy	WB	2.0	10.0	Pending approval
Malawi	1999	Barrier removal for renewables	UNDP	3.4	10.7	Pending approval
Mexico	1999	Renewable energy for agriculture	WB	8.7	26.0	Pending approval
SME	1994	Small and medium scale enterprises	IFC	1.6	4.8	Implementing
PVMTI	1996	PV market transformation initiative	IFC	30.0	120.0	Implementing
REEF	1996	Renewable energy & energy efficiency	IFC	30.0	130.0	Implementing
SDG	1998	Solar development group	IFC	10.0	50.0	Implementing

Source: Martinot, E. *et al*., "The GEF Solar PV Portfolio: Emerging Experience and Lessons," Global Environment Facility, August 2000

- Credit collection can be costly if rural customers are dispersed over large territories with poor transport infrastructure. Businesses organized for marketing, installation, and service may not be well suited for credit collection.
- Some customers with seasonal income (i.e. paddy farmers with semiannual harvests) may require repayment schedules tied to semiannual income rather than to monthly incomes.

Petitioner Canadian Solar (USA) Inc., Ex. 1035, p. 2473

Downloaded from https://onlinelibrary.wiley.com/doi/ by <Shibboleth-member@purdue.edu, Wiley Online Library on [25/08/2024]. See the Terms and Conditions (https://onlinelibrary.wiley.com/terms-and-conditions) on Wiley Online Library for rules of use; OA articles are governed by the applicable Creative Commons License

Downloaded from https://onlinelibrary.wiley.com/doi/ by <Shibboleth-member@purdue.edu>, Wiley Online Library on [25/08/2024]. See the Terms and Conditions (https://onlinelibrary.wiley.com/terms-and-conditions) on Wiley Online Library for rules of use; OA articles are governed by the applicable Creative Commons License

In 2001, the GEF broadened its mandate from a source of primarily grant funds through the United Nations and the World Bank Group, to the possibility of providing a broader array of investments, loans, guarantees, and other forms of financial support through a more diverse network of intermediaries.

24.7 FINANCING THE PV INDUSTRY

The PV industry will need to assemble a substantial amount of capital to support its growth. Capital is needed to expand manufacturing capacity and to fund working capital for inventories and receivables, all of which must be financed ahead of sales and profits in a growing industry. There are several sources of financing for the PV industry:

Major corporations: This is a dynamic time in the PV industry. Approximately 75% of worldwide PV market share is held by the operations and subsidiaries of major corporations – Sharp, Kyocera, BP Solar, Siemens, Sanyo, ASE, Shell, and Mitsubishi. It is typical for such large corporations to require a 20% or greater rate of return on internally invested capital, and this has not been achieved in the past. Many PV businesses have lost money, causing companies to quit the business. Companies that have left the PV business include Westinghouse, IBM, Motorola, Xerox, Texas Instruments, Exxon, Shell (US), Arco, Mobil, and others. More recently, with the global movement towards green energy, several major corporations have increased their commitments, including BP in 1996 and Shell International in 1997. The most recent casualty was Siemens, selling its solar division to Shell. Lacking improved profitability, the industry may see a continuation of entries, exits, and reorganizations by major corporations.

Electric utility companies: There has always been an affinity between photovoltaics and the utility companies. For example, Alabama Power was a major investor in Chronar, which closed. Idaho Power acquired a number of PV-systems integration firms between the years 1997 and 1999, only to exit the business and sell the group to Schott in the year 2001. Siemens Solar was half-owned by a German utility, EoN. The former Mobil Solar was acquired by RWE in 1994, a German utility, creating ASE Americas. General Public Utilities established GPU Solar, a joint venture with Astropower, focusing on grid-connected IPP power projects, commercial systems, and residential rooftop systems. The PV industry can expect to receive additional capital investment from the utility industry.

Capital Markets: The public stock markets in Europe and the US began to show interest in clean energy and distributed power generation in the period between 1998 and 2000. The areas of popular stocks in the United States include fuel cells, microturbines, and photovoltaics. In Europe, where the markets reacted earlier, the favorites have included wind power (in which Denmark and Germany lead the world industry), solar photovoltaics, hydropower, and other renewables. There are three publicly traded PV stocks in the United States: Astropower, Evergreen Solar, and Spire Corporation; and several in Europe. The outlook is positive in the near future, as the supply of money for green energy stocks is increasing, including the formation of mutual funds specializing in clean/green energy, such as Winslow's Green Growth Fund.

Venture Capital: The Venture Capital (VC) industry has invested in PV deals over the past 25 years, generally losing their investments, and never achieving their traditionally accepted financial goal of a 40% rate of return. This may be changing in recent years

with successful Initial Public Offerings (IPOs) by Astropower and Evergreen Solar in the United States and Solar World in Germany. Other venture-capital-backed PV companies, not yet publicly traded, include Solar Electric Light Company (SELCO), First Solar, and Global Solar in the United States, Solar Fabrik in Germany, and Solar Century in the United Kingdom. There is a tremendous influx of new venture start-ups in photovoltaics, especially in Europe and Asia where there are booming markets. Venture capital funds that have invested in photovoltaics include Arete Ventures (the Utech Funds) and Nth Power Technologies in the United States; Swiss Re, the Sarasin Fund, and UBS Energy Fund, all in Switzerland; and Gerling Insurance in Germany. Other US VC funds that have expressed interest in new energy technologies include the Commons Fund, Beacon Energy Funds, Energy Ventures Group, Kinetic Ventures, and Perseus Capital.

24.7.1 Financing Working Capital in the Distribution Channels

One of the more challenging aspects of financing PV growth will be how to capitalize the distribution channels to reach the widely dispersed end-use markets. There are several sources of financing for these firms:

Local lenders: Small business financing is inherently a local lending business. The vast majority of funds for financing the working capital requirements of the PV distributors and dealers will be from local banks, NBFCs, and microcredit lenders.

PV manufacturers: Most of the major PV manufacturers have extended credit programs for their best distributors and dealers.

World Bank/IFC: The IFC and GEF have collaborated on the deployment of two programs, PVMTI and SDG, to finance "PV enterprises" in developing countries. Over 200 such businesses have been identified by SDG as of mid-2001. The number of firms that will be required to support worldwide development of PV markets will, according to E&Co, be as high as 16 000 companies.

24.8 GOVERNMENT INCENTIVES AND PROGRAMS

A wide range of government incentives and programs has been adopted for photovoltaics around the world, stimulating demand for PV systems and affecting the financing of photovoltaics.

24.8.1 Potential Impact of Financing as a Government Policy Option

Looking at financing in the context of government policy shows that low-cost financing programs can actually have more impact on PV markets *in the immediate future* than technology research or manufacturing cost reductions. For example, Figure 24.3 illustrates the monthly payments for the 2.5 kW grid-connected, residential rooftop PV system. The PV system is assumed to cost \$8/watt (\$20 000 total cost), with a total system

Downloaded from https://onlinelibrary.wiley.com/doi/ by <Shibboleth-member@purdue.edu, Wiley Online Library on [25/08/2024]. See the Terms and Conditions (https://onlinelibrary.wiley.com/terms-and-conditions) on Wiley Online Library for rules of use; OA articles are governed by the applicable Creative Commons License

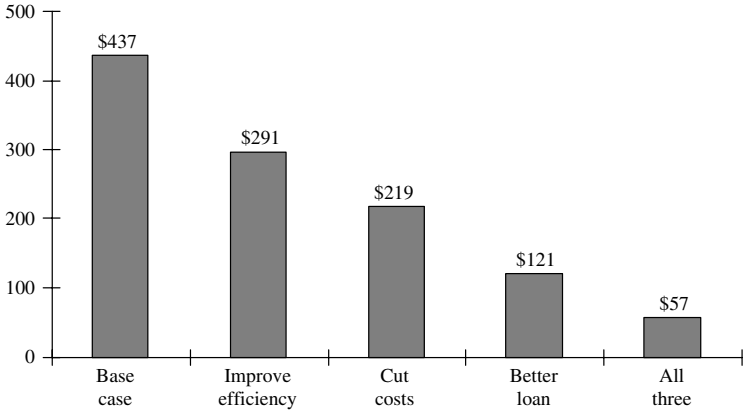


Figure 24.3 Monthly payments on a 2.5 kW residential PV system

efficiency of 10%. In the base case, financing is assumed to be a 7-year 18% loan, resulting in a monthly payment of $437. Then, three improvements are evaluated (see Reference [24]):

Research programs to improve efficiency: By improving the efficiency of the system, its size can be reduced while still generating the same output, thus reducing the cost. For a 50% increase in system efficiency, from 10 to 15%, the monthly payment will be reduced to $291 per month. However, it may take ten years or more before technology research can achieve these results in commercial products.

Cost reduction through manufacturing scale-up: By scaling up manufacturing, automating factories, and generally reducing the production cost per unit, total system costs can be reduced. Assuming a 50% reduction in system cost, from $8.00/Wac to $4.00/Wac, the monthly payment of the system can be reduced to $219 per month. Achieving this result might take approximately five years, as new factories are planned, built, and put into operation.

Better financing: A third way of reducing monthly payments is by applying lower-cost, longer-term financing. Here, the 7-year, 18% loan is replaced with a 30-year, 6% loan. Monthly payments come down to $121 per month, due to the change in financing alone, and this can be done immediately.

All three initiatives: The best public policy will be to accomplish all three cost reductions, but the immediate impact of lower-cost, longer-term financing is apparent.

As shown above, the provision of lower-cost, longer-term financing can have a more immediate impact on the affordability of solar PV systems than research and manufacturing programs, and will probably be the catalyst that creates the jump in demand that, in turn, causes photovoltaics to drive down the learning curve. Thus, financing may be the element that will break photovoltaics out of its long-standing "chicken and egg" dilemma.

Downloaded from https://onlinelibrary.wiley.com/doi/ by <Shibboleth-member@purdue.edu, Wiley Online Library on [25/08/2024]. See the Terms and Conditions (https://onlinelibrary.wiley.com/terms-and-conditions) on Wiley Online Library for rules of use; OA articles are governed by the applicable Creative Commons License

24.8.2 Direct Subsidies ("Buy-downs")

Governments have used different measures to place a value on the public benefits of photovoltaics. Subsidies are tending to be about 30 to 50% of the cost of the PV system. The following is a summary of subsidies that are in use today:

Japan: The program was launched in 1996 with direct subsidies to the amount of 50% of the cost for residential rooftop, grid-connected PV systems. The subsidy is paid to the installation company, not the end user, to foster maximum impact on creating a competitive installation industry and minimum distortion of buyer behavior. The subsidy has since been reduced to 33% in 1999, 25% in 2000, 15% in 2001, and less than 10% in 2002. The Japanese PV market has boomed, reaching over 90 MW or 35% of the world PV market in the year 2000, and there are projections that over 30 000 systems – as much as 130 MW – may be installed in the year 2001 (see Reference [25]).

India: The Ministry of Nonconventional Energy Sources (MNES) has a program in which 10-W to 20-W PV lanterns and 900-W PV water pumps are eligible for a 50% subsidy. The subsidies are distributed through state-level nodal agencies that pass the funds down through the bureaucracy. Thus, it is a matter of working a government "system" to receive the funds. Subsidies are paid only if there is budget available. The net effect has been to create a small market that is "capped" by the availability of subsidy funds. The subsidy program, with its minimum technical specifications, has spawned a subculture PV industry that makes inferior grade equipment just for what is called *the subsidy market*. The Indian subsidy program not only illustrates the power of a subsidy program to create a market but also how to cap it and create distortions (see Reference [26]).

California: The State of California enacted a $3.00/W "buy-down" for PV systems, initially until the year 2002. The subsidy was subsequently increased to $4.50/watt and extended for ten years to 2012, but there were still no financing programs. The program had little effect on the market at first; according to the California Energy Commission, only about 235 residential PV systems were installed in the years 1998 to 2000. A power shortage and sharp increase in electric tariffs in the years 2000 to 2001 created a crisis atmosphere, greater public interest in energy and environmental solutions, and, subsequently, renewed demand for PV systems and other power equipment.

Other countries: Many other countries are adopting PV subsidies. Argentina embarked on a concession approach that included embedded subsidies, but the program has not been fully implemented. Mexico adopted a set of programs that added up to a 90% subsidy for rural photovoltaics. Brazil's PRODEEM program provided massive subsidies, but ended up with a high percentage of nonworking systems. South Africa is considering subsidies as high as 80 to 100% of the cost of a basic 50-W solar home system, in conjunction with the national concession program for nongrid electrification. Morocco's PV program is delayed, awaiting the resolution of the subsidy amount and distribution method, reportedly about 50% of the system cost.

While PV subsidy programs are being implemented around the world, there is a growing body of evidence and opinion that subsidies ultimately do more harm than good for market development. The common argument in favor of subsidies is that they have an immediate impact on demand – which is the mutual goal of the elected officials who enact

Downloaded from https://onlinelibrary.wiley.com/doi/ by <Shibboleth-member@purdue.edu, Wiley Online Library on [25/08/2024]. See the Terms and Conditions (https://onlinelibrary.wiley.com/terms-and-conditions) on Wiley Online Library for rules of use; OA articles are governed by the applicable Creative Commons License

Downloaded from https://onlinelibrary.wiley.com/doi/ by <Shibboleth-member@purdue.edu>, Wiley Online Library on [25/08/2024]. See the Terms and Conditions (https://onlinelibrary.wiley.com/terms-and-conditions) on Wiley Online Library for rules of use; OA articles are governed by the applicable Creative Commons License

them and the companies that lobby for them. The argument against the use of subsidies is that they create artificial markets and the opportunity for corruption while they are in place, that they cap markets to the level of the subsidy budget each year, and that they eventually bring markets to a halt when they are terminated.

24.8.3 Soft Loans (Interest Subsidies)

The use of interest subsidies has been an effective public policy tool for housing. It might also be used for photovoltaics. These are flexible instruments, allowing the sponsoring government or institutions to correct interest rates without severely distorting market forces. They assure financing while spreading the subsidy over the life of the program. This avoids market manipulation and windfall events often related to direct subsidies. A typical soft loan will have low-interest rates, longer terms than normal, grace periods during which payments need not be made, and other features. There are several examples of soft loan incentives in the PV markets today:

India: The Indian Renewable Energy Development Agency (IREDA) offers favorable loans for photovoltaics: 85% of system cost, 10-year repayment period, 2-year grace period, at 2.5 to 5.0% interest rates. The comparable loan from a national bank would be a 5-year loan at 12.5% interest rate with, no grace period. A comparable loan from a nonbanking finance company would be at 18 to 23% interest rate.

Germany: Kreditanstalt für Wiederaufbau (KfW), the German bank for reconstruction, is providing PV loans as part of the country's 100 000 roofs initiative. Loans can be up to 100% of system cost up to 5 kW, and 50% of cost for larger systems. The interest rate is 4% below prevailing market rates. Combined with the national feed-in tariff of DM 0.99 per kWh, users can make a profit through the use of PV in Germany. The program is highly successful.

Japan: In conjunction with its subsidy program, the government of Japan subsidizes the interest rate on PV loans, with subsidy payments going to the lenders. The resulting net interest rate to the end user is near zero percent.

New York: The New York State Energy Research & Development Administration (NYSERDA) began offering interest subsidies for PV loans made by New York banks in the year 2000. NYSERDA buys down the interest rate on loans by making an up-front payment to the lender to the amount of the present value of lost interest. The amount of the interest subsidy is presently 4.0%, bringing interest rates down from 9.5 to 5.5%.

There are precedents for applying interest subsidies. The use of interest subsidies, soft loans, and third-party (government) guarantees has been used extensively in housing finance programs around the world, lowering the real cost of owning a home while minimizing distortions in the home buyer–seller marketplace.

An interest rate subsidy as low as one-half percent (i.e. lowering the mortgage interest rate from 7.0 to 6.5% on a 30-year mortgage) will actually pay for a residential PV system completely, as reported by Alden Hathaway at the Environmental Resources Trust. For example, for a $300 000 home mortgage loan, the interest payments will be $425 277 over 30 years. At the lower rate of 6.5%, total interest payments will be just $389 197. After taking taxes into account, assuming that the interest is tax deductible and

using a 40% combined federal and state tax rate, the difference in after-tax interest cost is $21 648, roughly the full cost of a 2.5 kW PV system.

24.8.4 Income Tax Deductions and Credits

Tax incentives are preferred by many government officials because they can get the intended economic benefits to the intended users without the need to establish an implementing bureaucracy. They are opposed by other officials who see the tax system as a method for raising funds to run the government, not as a means of implementing social policy. They can also be written with sunset provisions, ostensibly to protect the budget from runaway spending, but also to provide elected officials with an opportunity to get publicity for enacting it again and again. Tax credits and deductions therefore appear to be less stable and reliable as market incentives or subsidies. Nonetheless, there are several tax-based incentive programs in place today:

India: PV qualifies for 100% depreciation in the first year for corporate (not individual) taxes. This, in conjunction with IREDA's 2.5% loans, created a PV leasing industry in the period between the years 1997 and 2001.

United States of America: The US tax code allows a 10% tax credit against corporate taxes and five-year accelerated depreciation for photovoltaics. The combination of these incentives will drive the preferred financing of photovoltaics in the United States towards leasing. The US Congress is also considering a 15% tax credit on personal income taxes.

Government subsidies and incentives have increased in recent years with tremendous impacts on the immediate size of PV markets in Japan and Germany. The impacts in India appear to be mixed, with subsidies creating markets but also capping them at the levels of the annual budgets. Likewise, subsidies (tax credits) have had mixed results in the United States.

24.9 FUNDING GOVERNMENT RESEARCH AND DEVELOPMENT

Government funding of research and development (R&D) has traditionally been used to bridge the gap between work that is "too high risk for companies to undertake" and "commercial viability."

Photovoltaics present a case study of a successful publicly funded R&D activity. PV R&D efforts were focused on lowering manufacturing costs in volume production, improving the performance (efficiency) of the devices, and extending the operational lifetime of components and systems. Aggressive goals have been set to make photovoltaics economically competitive with traditional sources of electricity (see Reference [27]). Many countries around the world have been involved in such activities in an effort to supplement traditional energy supplies with renewable energy sources.

24.9.1 PV Programs in the United States

US-government programs in photovoltaics originated from the Conference on PV Conversion of Solar Energy for Terrestrial Applications, sponsored by the National Science

Downloaded from https://onlinelibrary.wiley.com/doi/ by <Shibboleth-member@purdue.edu, Wiley Online Library on [25/08/2024]. See the Terms and Conditions (https://onlinelibrary.wiley.com/terms-and-conditions) on Wiley Online Library for rules of use; OA articles are governed by the applicable Creative Commons License

Foundation (NSF) held in Cherry Hill, New Jersey in October 1973 (see Reference [28]). The program was the responsibility of the National Science Foundation, and then was transferred to the Energy Research and Development Agency (ERDA), which became part of the US Department of Energy (DOE) in 1977.

The first US program was the Low Cost Silicon Solar Array Project, later renamed the Flat-Plate Solar Array Project. The Jet Propulsion Laboratory was assigned management responsibility based on their long experience with space PV power systems. The newly created Solar Energy Research Institute (SERI) was charged in 1978 with the responsibility for thin-film materials and the Sandia National Labs for the concentrator PV programs. The DOE PV Program features significant cost sharing by its industry partners.

SERI became the National Renewable Energy Laboratory (NREL) in 1990, which has championed such programs as the amorphous silicon partnerships, the Photovoltaic Manufacturing Technology (PVMaT), the Thin-film Partnership, the building-integrated (PV-BONUS) program, the Utility Photovoltaic Group (UPVG), and the Million Solar Roofs (MSR) Program. The National Center for Photovoltaics (NCPV) was established to integrate the programs at NREL and Sandia.

US program funding is shown in Figure 24.4, which indicates the rapid buildup of the program in the 1970s, followed by a sharp reduction in the 1980s, and subsequent increase in the 1990s. As reported by DOE, the government's investment in photovoltaics since 1974 is estimated to be $1.7 billion.

24.9.2 PV Programs in Japan

From 1974 to 1983, the Japanese R&D program focused on low-cost solar cell production including mass production of raw silicon (Si) material, poly-Si, ribbon crystal, and amorphous silicon (a-Si).

During the second decade of the program from 1984 to 1993, in addition to material R&D efforts, mass production technologies and solar photovoltaic system technology were pursued, together with cell technology such as a-Si-based stacked solar cell and flexible substrate solar cells.

The New Sunshine Project has been in existence since 1993 in which a variety of new programs have been organized on the promotion and cost reductions of PV systems. Examples include field demonstration and testing of PV systems on public facilities and a subsidy program for private houses. The budget for the R&D portion of the Japanese PV Program is shown in Figure 24.4. It should be pointed out that the R&D portion represents only a small portion of the total Japanese PV effort. In FY 2000, the total effort, including subsidies, was approximately six times the R&D portion of the budget.

24.9.3 PV Programs in Europe

The UNESCO conference "The Sun and the Service of Mankind" held in Paris in 1973 was the starting point for the development of renewable energy in Europe (see Reference [29]). The first European Commission technology program for renewable energy was established by the Council of Ministers in 1975. The European Commission's PV program focused

Downloaded from https://onlinelibrary.wiley.com/doi/ by <Shibboleth-member@purdue.edu>, Wiley Online Library on [25/08/2024]. See the Terms and Conditions (https://onlinelibrary.wiley.com/terms-and-conditions) on Wiley Online Library for rules of use; OA articles are governed by the applicable Creative Commons License

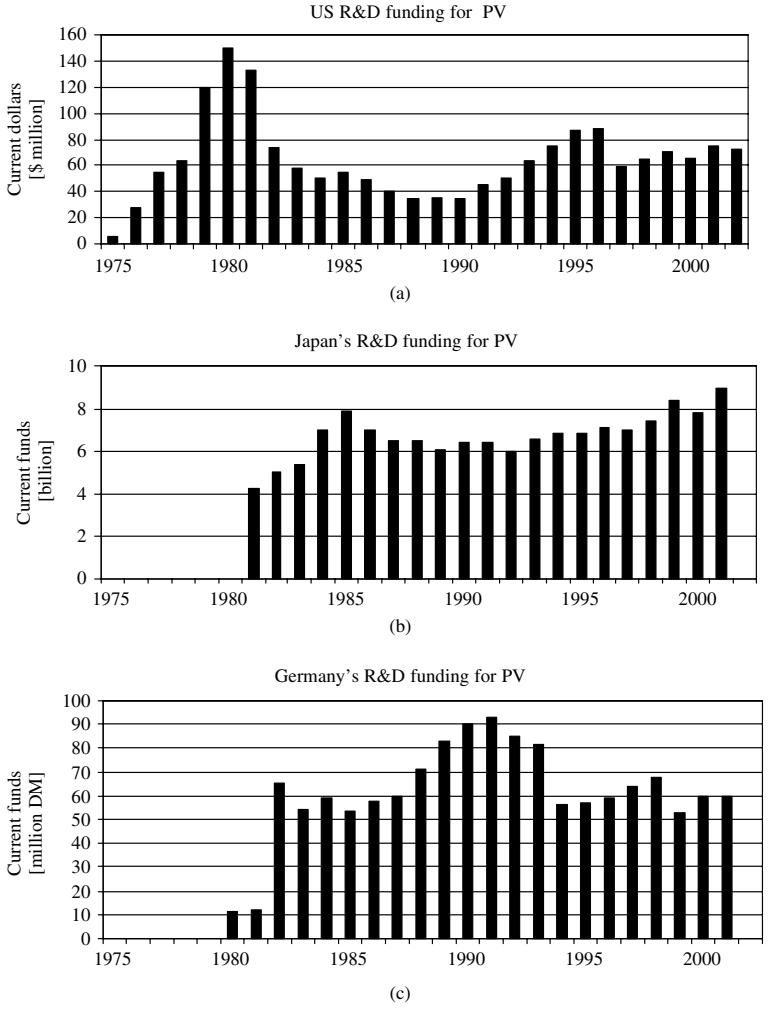


Figure 24.4 Research and development funding for solar photovoltaics. (a) US R&D funding for photovoltaics; (b) Japan's R&D funding for photovoltaics; and (c) Germany's R&D funding for photovoltaics

initially on crystalline silicon and pilot system development. From 1979, the demonstration programs focused on remote and stand-alone applications. Later grid-connected and building-integrated systems were incorporated into the program.

The total budget for EU members on PV R&D between 1974 and the present is about $1.5 billion. Germany has furnished about 65% of the total. Figure 24.4 shows the recent budgets for the German PV R&D program. Like Japan, Germany also budgeted

Petitioner Canadian Solar (USA) Inc., Ex. 1035, p. 2481

Downloaded from https://onlinelibrary.wiley.com/doi/ by <Shibboleth-member@purdue.edu, Wiley Online Library on [25/09/2024]. See the Terms and Conditions (https://onlinelibrary.wiley.com/terms-and-conditions) on Wiley Online Library for rules of use; OA articles are governed by the applicable Creative Commons License

commercialization and subsidy programs. Germany's 1000-roofs program was one of the hallmarks of their efforts. Significant efforts in the Netherlands, Italy, Spain, Switzerland, and France have also contributed to the European PV R&D efforts.

24.9.4 Future PV R&D Programs

Predicting the role for public sector funding of R&D is difficult at best. Fortunately, there appears to be good reason to follow the role of other high-technology programs that have come before. Possibly, the best is what has happened with the development of integrated circuits, which had strong government support during its development. Although one could predict that such support would decline and perhaps be phased out as products came out through the end of the development pipeline, the opposite has occurred. Successful research programs breed future successes in terms of new technologies and approaches. Since research is defined as exploring the unknown, there will always be paths to follow for those technologies that have been shown to be useful and successful. Such is the case for photovoltaics.

24.9.5 Sources of R&D Funding

The R&D programs of each country generally only fund organizations within the respective country. The following are the major funding organizations:

United States:
U.S. Department of Energy
Office of Solar Electric Technologies
1000 Independence Avenue, S. W.
Washington, DC 20585

Japan:
NEDO
Solar Energy Department
Sunshine 60 Bldg.
3-1-1 Higashi Ikebukuro
Toshima-ku
Tokyo 170-6028
Japan

Germany:
Bundesministerium fuer Wirtschaft Technologie
53107 Bonn
Germany

The Netherlands:
Novem
P.O. Box 8242

Downloaded from https://onlinelibrary.wiley.com/doi/ by <Shibboleth-member@purdue.edu>, Wiley Online Library on [25/08/2024]. See the Terms and Conditions (https://onlinelibrary.wiley.com/terms-and-conditions) on Wiley Online Library for rules of use; OA articles are governed by the applicable Creative Commons License

3503 RE Utrecht
The Netherlands

Italy:
ENEA
Renewable Energy Department
CR Casaccia
1300 sp Anguillarese
0006 S M di Galeria (ROMA)
Italy

This chapter has described the financing of PV growth. Financing might be the last "missing link" in the solution to a solar-driven world economy. Our financial systems and practices are built to support a different economic model – central station power plants and the grid system (see Reference [30]). Mobilization of massive amounts of capital to support solar photovoltaics and distributed generation has been, and will for the immediate future be, institutionally complicated. Solutions are coming, though slowly. Now in the year 2002, however, it appears that we are turning the corner towards the financing of a brighter, solar-powered future.

ANNEX

CONTACTS IN PV FINANCING

This Annex exhibit provides a listing of some of the key organizations that are involved in the financing of photovoltaics around the world, by no means covering all, but a list that should prove useful over the coming decade. It is presented by region.

INTERNATIONAL/GLOBAL

Environmental Enterprises Assistance Fund (EEAF)

EEAF, formed in 1990 by USAID, Winrock International and the Rockefeller Foundation, is a specialist in providing debt and equity financing to environmental entrepreneurs in renewable energy and other environmentally beneficial industries.

Contact: Brooks Browne, President
Address: EEAF
1655 N. Fort Myer Drive
Suite 520
Arlington, VA 22209
USA
Phone: 703 522 5928
Fax: 703 522 6450
E-mail: *eeaf@igc.apc.org*

Downloaded from https://onlinelibrary.wiley.com/doi/ by <Shibboleth-member@purdue.edu, Wiley Online Library on [25/08/2024]. See the Terms and Conditions (https://onlinelibrary.wiley.com/terms-and-conditions) on Wiley Online Library for rules of use; OA articles are governed by the applicable Creative Commons License

Global Environment Facility (GEF)

The Global Environment Facility (GEF) is the chief funder of renewable energy in developing countries and, as such, will have a significant impact on expansion of the field. GEF is a major force in promoting renewable energy and the chief driver and catalyst among development agencies.

Contact: Mohamed T. El-Ashry, Chief Executive Officer and Chairman
Address: 1818 H Street, N.W.
Washington, D.C. 20433
U.S.A.
Phone: 202-473-0508
Fax: 202-522-3240
Web site: *www.gefweb.org*
E-mail: *harcher@worldbank.org*

International Finance Corporation (IFC)

IFC is an institution of the World Bank Group and promotes economic development by encouraging private sector investment activities in developing countries.

Address: Corporate Relations Unit
International Finance Corporation
2121 Pennsylvania Avenue, NW,
Washington, DC 20433 USA.
Phone: +202-473-7711
Fax: +202-974-4384
E-mail: *Webmaster@ifc.org*
Web site: *http://www.ifc.org*

Photovoltaics/Market Transformation Initiative (PV/MTI)

PVMTI is an initiative of the International Finance Corporation (IFC) and the Global Environment facility (GEF), to accelerate the sustainable commercialization and financial viability of solar photovoltaic-based energy services in India, Kenya, and Morocco. The IFC has designed Impax capital and IT Power Ltd. as the external management team for PVMTI.

Contact: Vickram Widge
Address: Environment Division
International Finance Corporation
2121 Pennsylvania Avenue, NW
Washington DC 20433

Renewable Energy and Energy Efficiency Fund (REEF)

REEF is a pioneer financing fund focusing on emerging markets, renewable energy, and energy conservation, and efficiency projects and companies. As of April 2001, REEF

Downloaded from https://onlinelibrary.wiley.com/doi/ by <Shibboleth-member@purdue.edu>, Wiley Online Library on [25/08/2024]. See the Terms and Conditions (https://onlinelibrary.wiley.com/terms-and-conditions) on Wiley Online Library for rules of use; OA articles are governed by the applicable Creative Commons License

was capitalized at a level of $65 million equity plus debt facility from the International Finance Corporation.

Contact: Kenneth R. Locklin, Managing Director
Address: Energy Investors Fund
727 Fifteenth St, NW
11th Floor
Washington, DC 20005
USA
Phone: 202 783 4419
Fax: 202 371 5116
E-mail: *klocklin@eifgroup.com*

Solar Development Capital

Solar Development Capital is a 10-year, $28.75 million fund that makes minority equity, quasi-equity and debt investments in solar photovoltaic (PV) and PV-related businesses in developing nations. SDC seeks to invest in companies involved in distribution, consumer financing or leasing, manufacturing, or other aspects related to accelerated PV use in rural areas. Some senior debt may be placed with microcredit institutions. Offices in the United States. and Netherlands:

US Contact: JD Doliner
Address: Solar Development Capital
1655 North Fort Myer Drive
Suite 520
Arlington VA, 22209-3109
Phone: +1-703-522-5928
Fax: +1-703-522-6450
Web site: *www.solardevelopment.org*
E-mail: *sdcf@mindspring.com*

European Contact: Hans Schut
Organization: Solar Development Capital
Address: Utrechtseweg 60
Postbus 55, 3700 AB Zeist,
The Netherlands
Phone: +31-30-693-65-00
Fax: +31-30-693-65-66
Web site: *www.solardevelopment.org*
E-mail: *sdc@triodos.nl*

Solar Development Foundation (SDF)

Solar Development Foundation provides technical and business assistance to enterprises in preparation for larger-scale private investment, and can provide 'seed' finance for business development activities on flexible terms. Business development services may include: market research, communications and market testing (pilot-scale operations); training; business planning assistance; development of end-user financing mechanisms, and so on.

Downloaded from https://onlinelibrary.wiley.com/doi/ by <Shibboleth-member@purdue.edu, Wiley Online Library on [25/08/2024]. See the Terms and Conditions (https://onlinelibrary.wiley.com/terms-and-conditions) on Wiley Online Library for rules of use; OA articles are governed by the applicable Creative Commons License

SDF provides relatively soft debt and grant funding for its business development services with the expectation that the PV and other off-grid renewable electricity businesses that it assists will to attract follow-on investment.

Contact: Candace Smith, Chief Operating Officer, and Phil Covell, Managing Director
Organization: Solar Development Foundation
Address: 1655 North Fort Myer Drive, Suite 520
Arlington VA, 22209-3109 USA
Phone: +1 703-522-5928
Fax: +1 703-522-6450
E-mail: *sdcf@mindspring.com*
Web site: *www.solardevelopment.org*

Solar Electric Light Fund (SELF)

Acting as a catalyst, SELF provides both financial and technical assistance for solar energy and wireless communication systems in the developing world. SELF raises seed funding for in-country NGO's and financial institutions, which provide microloans for the purchase of solar home systems (SHS). SELF has launched solar rural electrification programs and enterprises in India, China, Vietnam, Indonesia, Nepal, South Africa, Brazil, Uganda, Sri Lanka, Tanzania, and the Solomon Islands.

Contact: Robert A. Freling, Executive Director
Address: 1775 K Street, NW Suite 595
Washington, DC 20006
Phone: 202-234-7265
Fax: 202-328-9512
Web site: *http://www.self.org*
E-mail: *solarlight@self.org*

Solar International Management, Inc. (SolarBank Program)

The SolarBank Program is being developed as a future wholesale capital fund with sub-funds within each country. India and South Africa are the prototype countries. SolarBank Funds will supply capital to banks, nonbanking finance companies, cooperatives, societies, microcredit lenders, NGOs, rural finance groups, and others. It will also provide technical support, training, and special programs to its participating lenders.

Contact: Michael T. Eckhart
Address: Suite 400,1825 I Street NW
Washington DC, 20006.
Phone: +1 202-429-2030
Fax: +1 202-429-5532
E-mail: *info@solarbank.com*
Web site: *http://www.solarbank.com*

UNDP Sustainable Energy & Environment Division (SEED)

The Administrator of UNDP made a strategic decision to strengthen UNDP's environment and sustainable development capacity by establishing a new division within the Bureau for

Downloaded from https://onlinelibrary.wiley.com/doi/ by <Shibboleth-member@purdue.edu>, Wiley Online Library on [25/08/2024]. See the Terms and Conditions (https://onlinelibrary.wiley.com/terms-and-conditions) on Wiley Online Library for rules of use; OA articles are governed by the applicable Creative Commons License

Policy and Programme Support (BPPS): the Sustainable Energy and Environment Division (SEED). Since its origin, SEED has worked to support UNDP's overall efforts to help countries successfully design and carry out programs, which integrate the protection and regeneration of the environment and the use of natural resources. Assistance is provided by means of grant aid for technical assistance and investment projects.

Contact: Mr. Roberto Lenton, Director,
Address: SEED,
304 East 45th Street,
New York, N.Y. 10017, USA.
Phone: +1-212-906-5705
Fax: +1-212-906-6973
Web site: *http://www.undp.org/seed/*

UNEP Collaborating Centre on Energy and Environment

Financing Institution. Promotes and facilitates environmentally conscious energy planning throughout the world and especially in developing countries. UCCEE is funded jointly by UNEP, the Danish International Development Agency (DANIDA), and Risoe National Laboratory.

Contact: Mr. Gordon A. Mackenzie, Senior Energy Planner
Address: UCCEE
Risoe National Laboratory, Bldg. 142, Frederiksborgvej 399,
P.O. Box 49,
DK 4000 Roskilde, Denmark.
Phone: +45-46322288
Fax: +45-46321999
E-mail: *gordon.mackenzie@risoe.dk*
Web site: *http://www.uccee.org*

Winrock International

Winrock International is a private, nonprofit organization that works with people in the United States and around the world to increase economic opportunity, sustain natural resources and protect the environment.

Contact: Frank Tugwell, President
Address: 1621 North Kent St. – Suite 1200, Arlington, VA 22209-2134
Phone: 703-525-9430
Fax: 703-243-1175
Web site: *www.winrock.org*
E-mail: *information@winrock.org*

EUROPE

ASN Bank

Banking for renewable energy projects.

Address: PO Box 30502, 2500 GM Den Haag

Downloaded from https://onlinelibrary.wiley.com/doi/ by <Shibboleth-member@purdue.edu, Wiley Online Library on [25/08/2024]. See the Terms and Conditions (https://onlinelibrary.wiley.com/terms-and-conditions) on Wiley Online Library for rules of use; OA articles are governed by the applicable Creative Commons License

Country: Netherlands
Phone: +31 703 569 333
Fax: +31 703 617 948

Clean Energy Fund

Finance for power generation with clean and renewable energy.

Contact: Peter Dunev
Address: 33 St James Street, London SW1A 1HD
Country: UK
Phone: +44 20 7930 1030
Fax: +44 20 7930 1080

D&B Capital

Financial services to the clean and renewable energy sector.

Address: 33 St James's Street, London SW1A 1HD
Country: UK
Phone: +44 20 7 930 1030
Fax: +44 20 7 930 1080

Ernst & Young Renewable Energy Unit

Specialists in RE corporate finance, business planning, taxation, and modeling advice.

Contact: Jonathan H Johns
Address: Broadwalk House, Southernhay West, Exeter EX1 1LF
Country: UK
Phone: +44 1392 284300
Fax: +44 1392 284301

European Bank for Reconstruction and Development

The European Bank for Reconstruction and Development (EBRD) was established in 1991. It exists to foster the transition towards open market-oriented economies and to promote private and entrepreneurial initiative in the countries of central and eastern Europe and the Commonwealth of Independent States (CIS) committed to and applying the principles of multiparty democracy, pluralism, and market economics.

Contact: Beverley Harrison
Address: European Bank for Reconstruction and Development
One Exchange Square
London EC2A 2JN, United Kingdom
Phone: +44 20 7338 6000
Fax: +44 20 7338 6100

Downloaded from https://onlinelibrary.wiley.com/doi/ by <Shibboleth-member@purdue.edu>, Wiley Online Library on [25/08/2024]. See the Terms and Conditions (https://onlinelibrary.wiley.com/terms-and-conditions) on Wiley Online Library for rules of use; OA articles are governed by the applicable Creative Commons License

E-mail: *harrisob@ebrd.com*
Web site: *http://www.ebrd.org*

European Commission DG XVII

Funding Organization. Links to EC energy programs. European Union in collaboration with EBRD has produced a useful publication related to funding issues for energy-related projects.

Address: 200 rue de la Loi, B-1049, Bruxelles, Belgique.
Phone: +32 22991111
Fax: +32 22991111
E-mail: *ener-info@cec.eu.int*
Website: *http://europa.eu.int/en/comm/dg17/dg17home.htm*

European Investment Bank (EIB)

Funding Organization. One of the objectives of EIB is the investment into energy-related projects in Europe as well as in the developing countries outside Europe. Provides funding for assistance with research, development, demonstration, and implementation of projects related to all aspects of renewable energy.

Address: European Investment Bank (EIB),
100 Bd Konrad Adenauer, L-2950 Luxembourg.
Phone: +35-2-43793122
Fax: +35-2-43793189
Web site: *http://www.eib.org*

Impax Capital Corporation Ltd

Finance and strategy for environmental infrastructure and technology. External manager for the IFC's PV market Transformation Program in India, Morocco, and Kenya.

Contact: Melville Haggard
Address: Broughton House, 6–8 Sackville Street, London W1X 1DD
Country: UK
Phone: +44 20 7 434 1122
Fax: +44 20 7 434 1123

IFU

IFU's objective is to promote economic activities in developing countries by promoting investments in these countries in collaboration with Danish trade and industry. IFU participates mostly as a share capital partner holding also a seat on the board of directors together with the Danish company investing in the project company. IFU can also participate as a cofinancing partner, when an existing company is to be expanded or rehabilitated or when state-owned companies are privatized.

Downloaded from https://onlinelibrary.wiley.com/doi/ by <Shibboleth-member@purdue.edu>, Wiley Online Library on [25/08/2024]. See the Terms and Conditions (https://onlinelibrary.wiley.com/terms-and-conditions) on Wiley Online Library for rules of use; OA articles are governed by the applicable Creative Commons License

Downloaded from https://onlinelibrary.wiley.com/doi/ by <Shibboleth-member@purdue.edu, Wiley Online Library on [25/08/2024]. See the Terms and Conditions (https://onlinelibrary.wiley.com/terms-and-conditions) on Wiley Online Library for rules of use; OA articles are governed by the applicable Creative Commons License

Address: Bremerholm 4, DK 1069 Copenhagen K, Denmark.
Phone: +45 33 63 7500
Fax: +45 33 32 2524
E-mail: *ifu-cph@inet.uni2.dk*
Web site: *http://www.ifu.dk/ifu/brief_ifu.htm*

ING Bank Nederland

Banking division of ING Group, specialists in renewable energy project finance.

Address: PO Box 1800, Bijlmerplein 888, 1000 BV Amsterdam
Country: Netherlands
Phone: +31 20 652 39 54
Fax: +31 20 652 39 73

New Century Finance Limited

Innovative finance for specific projects and working capital for manufacturers.

Contact: Richard W Price
Address: Pantiles Chambers, 85 High Street, Tunbridge Wells, Kent TN1 1YG
Country: UK
Phone: +44 1892 618461
Fax: +44 1892 618567

New Energies Invest Ltd.

New Energies Invest Ltd. aims to invest into renewable technologies such as solar, wind, geothermal, biomass, small hydro, and fuel cells. The focus is on nonlisted companies, that is, typically New Energies Invest is providing growth capital as private equity. Geographically, New Energies Invest is covering North America and Europe.

Contact: Andreas Knoerzer, First Vice President
Address: c/o Bank Sarasin & Cie., Elisabethenstrasse 62, 4002 BASEL – Switzerland
Phone: +41 61 277 74 77
Web site: *newenergies.ch*

Rabobank Nederland/Groen Management BV

Specialists in renewable energy project financing. Rabobank is a broad-based financial services provider, founded on cooperative principles. It has been a leading lender to wind power projects and other sustainable development.

Address: PO Box 17100, 3500 HG Utrecht
Country: Netherlands
Phone: +31 302 16 49 83
Fax: +31 302 16 19 76

Triodos Bank NV

Triodos is a social bank with renewable energy, wind, and solar investment funds. Triodos is the leading socially responsible lender in the Netherlands, and is the comanager of Solar Development Capital.

Contact: JF Schut
Address: Postbus 55, 3700 AB Zeist
Country: Netherlands
Phone: +31 30 693 6500
Fax: +31 30 693 6555

VTZ Green Money for the Blue Planet Ltd

Financial services based on environmental, ethical, and financial criteria.

Contact: Martin Brenner
Address: Bahnhofsplatz 9, 8023 Zürich
Country: Switzerland
Phone: +41 1 226 45 45
Fax: +41 1 226 45 46

The Wind Fund Plc

Equity investment fund for wind, hydro, and renewable energy projects.

Contact: Simon Roberts
Address: Brunel House, 11 The Promenade, Clifton, Bristol BS8 3NN
Country: UK
Phone: +44 117 973 9339
Fax: +44 117 973 9303

UNITED STATES

ABN Amro Bank NV

Construction and term financing for independent power projects.

Contact: Joseph C Lane
Address: 135 LaSalle Street, Chicago, Illinois 60603
Country: USA
Phone: +1 312 443 2641
Fax: +1 312 750 6387

Commons Capital LP

Commons Capital LP is a venture capital firm investing in private companies, including renewable energy companies that promise strong financial results and significant contributions to a sustainable future.

Downloaded from https://onlinelibrary.wiley.com/doi/ by <Shibboleth-member@purdue.edu, Wiley Online Library on [25/08/2024]. See the Terms and Conditions (https://onlinelibrary.wiley.com/terms-and-conditions) on Wiley Online Library for rules of use; OA articles are governed by the applicable Creative Commons License

Contact: William Osborn, Manager
Address: Commons Capital Management LLC
115 Buckminster Road
Brookline, MA 02445
Phone: 617-734-1047
Fax: 617-734-3115
E-mail: *wosborn@aol.com*

E&Co

E & Co was established in 1994 as a nonprofit organization with the strategy of providing enterprise development services and modest amounts of money in the form of grants, loans, and equity investments to economically, socially, and environmentally sustainable energy enterprises in developing countries.

Contact: Michael D. Allen, President
Address: E & Co
383 Franklin Street
Bloomfield, NJ 07003 USA
Phone: 973-680-9100
Fax: 973-680-8066
E-mail: *mike@energyhouse.com*

FAC/Equities A Division of First Albany Corporation

Investment bank specializing in rapidly growing companies including alternative energy firms.

Contact: Eric A Prouty
Address: 53 State Street, 29th Floor, Boston, MA 02109–2811
Country: USA
Phone: +1 617 228 3515
Fax: +1 617 228 3515

GE Capital Corporation

Investor in the alternative energy marketplace providing up to 100% of the requirements for the construction and permanent term financing for projects.

Contact: Craig Reynolds
Address: 1600 Summer Street, 5th Floor, Stamford, Connecticut 06927
Country: USA
Phone: +1 203 357 3872
Fax: +1 203 357 4386

Heller Financial Incorporated

Subsidiary of The Fuji Bank, providing structuring advice and financing for alternative energy and industrial projects.

Downloaded from https://onlinelibrary.wiley.com/doi/ by <Shibboleth>-member@purdue.edu, Wiley Online Library on [25/08/2024]. See the Terms and Conditions (https://onlinelibrary.wiley.com/terms-and-conditions) on Wiley Online Library for rules of use; OA articles are governed by the applicable Creative Commons License

Contact: Gar Seifullin
Address: 500 West Monroe Street, Chicago, Illinois 60661
Country: USA
Phone: +1 312 441 7616
Fax: +1 312 441 7827

New Alternatives Fund Inc

Mutual fund emphasizing clean energy and the environment.

Contact: Maurice or David Schoenwald
Address: 150 Broad Hollow Road, Melville, New York 11747
Country: USA
Phone: +1 631 423 7373
Fax: +1 631 423 7393

Nth Power Technologies

Nth Power technologies is a leading venture capital fund focusing on high-growth investment opportunities arising out of the restructuring of the global energy marketplace. Nth Power has investments in distributed generation and storage, communications, control technology, transmission system automation, outsourcing, and power quality management.

Contact: Nancy Floyd, Managing Partner
Address: 50 California Street, Suite 840
San Francisco, CA 94161
Phone: 415-983-9983
Fax: 415-983-9984
E-mail: *info@NthPowers.com*
Web site: *www.Nthpower.com*

SAM Equity Partners Ltd

SAM Equity Partners is the private equity arm of Sustainable Asset Management. SAM Equity Partners invests in ventures that are commercializing PV-related technologies and which have a significant presence in Europe or North America. The fund does not invest in projects or in emerging market economies.

Contact: Nicholas Parker, Principal
Address: 3rd Floor, 8 Faneuil Hall Marketplace
Boston MA 02109, USA
Phone: (+1 617) 973 5112
Fax: (+1 617) 973 6406
E-mail: *nick@sam-group.com*
Web site: *www.sam-group.com*

Downloaded from https://onlinelibrary.wiley.com/doi/ by <Shibboleth-member@purdue.edu, Wiley Online Library on [25/08/2024]. See the Terms and Conditions (https://onlinelibrary.wiley.com/terms-and-conditions) on Wiley Online Library for rules of use; OA articles are governed by the applicable Creative Commons License

US Agency for International Development (USAID)

USAID is the international aid agency of the US. government. The energy and environmental technology (EET) division within the environment center (ENV) funds a number of PV-related programs.

Contact: Dr. Griffin M. Thompson, Director, ENV/EET
Address: USAID
1300 Pennsylvania Avenue
Washington DC 20523
USA
Phone: 202 712 1772
Fax: 202 216 3230
E-mail: *gthompson@usaid.gov*

ASIA

Asian Development Bank (ADB)

ADB is a multilateral development finance institution, engaged in promoting the economic and social progress of its developing countries in the Asian and Pacific region.

Address: 6 ADB Avenue, Mandaluyong,
0401 Metro Manila, P.O. Box 789,
Manila Central Post Office,
0980 Manila, Philippines.
Phone: +632-632-4444
Fax: +632-636-2444
E-mail: *adbhq@mail.asiandevbank.org*
Web site: *http://www.adb.org/mainpage.asp*

Canara Bank (India)

A public sector bank, it offers loans up to Rs. 25 000, repayment up to 5 years, @ 12.5% p.a.(PRIORITY SECTOR LENDING RATE), for purchase of solar home systems in India, through its branch network. The loan sanctioning authority rests with the branch managers.

Address: H.O. 112, JC Road, Bangalore – 560 002 India
Phone: 91-80-222-1581
Fax: 91-80-229-3517

DFCC Bank (Sri Lanka)

A development bank providing fund and fee based services.

Contact: Mr. Jayantha Nagendran
Address: PO Box 1397, 73/5 Galle Road
Colombo 3 Sri Lanka

Downloaded from https://onlinelibrary.wiley.com/doi/ by <Shibboleth-member@purdue.edu, Wiley Online Library on [25/08/2024]. See the Terms and Conditions (https://onlinelibrary.wiley.com/terms-and-conditions) on Wiley Online Library for rules of use; OA articles are governed by the applicable Creative Commons License

Phone: 94 1 440366
Fax: 94 1 440376

IREDA (India)

The financing arm of Ministry of Nonconventional Energy Sources (MNES), Govt. of India, is the principal organization in India, offering a range of services in the renewable energy sector.

Contact: Dr. V. Bakthavatsalam, Managing Director
Address: IREDA-Indian Renewable Energy Development Agency Ltd.,
Core-4A, East Court, 1st floor, India Habitat Center, Lodi Road
New Delhi – 110 003 India
Phone: 91-11-460-1344/66
Fax: 91-11-460-2855.
E-mail: *gen@ireda1.globemail.com*

Grameen Shakti (Bangladesh)

Grameen Shakti (GS) is a not-for-profit rural power company whose purpose is to supply renewable energy to unelectrified villages in Bangladesh.

Country: Bangladesh
Contact: Mr. Dipal Chandra Barua, Managing Director
E-mail: *g_shakti@grameen.net*

IT Power India Pvt. Ltd.

A leading renewable energy consultancy with specialist skills in financing of PV projects. ITPI is the local partner organization for PVMTI. In addition, ITPI assists the Indian PV industry develop financing proposals to IREDA. ITPI has been involved in over 50 renewable energy projects in 17 countries. Areas of interest include financing, business packaging, and technical advisory services.

Contacts: Terence J. Hart and Binu K. Parthan
Company: IT Power Pvt Ltd
Address: #6, Rue Romain Roland
Pondicherry, India
Phone: 91-413-342488/227811
Fax: 91-413-340723
E-mail: *itpi@itpi.co.in*
Web site: *www.itpi.co.in*

Malaprabha Grameena Bank (India)

A public sector bank, it offers loans up to Rs. 25 000, repayment up to 5 years, @ 12.5% p.a.(PRIORITY SECTOR LENDING RATE), for purchase of solar home systems in India, through its branch network. The loan sanctioning authority rests with the branch managers.

Downloaded from https://onlinelibrary.wiley.com/doi/ by <Shibboleth-member@purdue.edu, Wiley Online Library on [25/08/2024]. See the Terms and Conditions (https://onlinelibrary.wiley.com/terms-and-conditions) on Wiley Online Library for rules of use; OA articles are governed by the applicable Creative Commons License

Address: H.O. Post Box No. 111, Belgaum Road, Dharwad – 580 008 India
Phone: 91-836-42861
Fax: 91-836-40393

Manipal Finance Corp. Ltd. (India)

Nonbanking Finance Company (NBFC) offers to lease/finance solar PV systems primarily due to Govt. of India's fiscal incentive of accelerated 100% depreciation on renewable energy systems in the very first year. They are also registered with IREDA as financial intermediaries. The terms of financing vary from project to project and solar PV water pumping systems have particularly benefited from leasing companies.

Address: Manipal House, Manipal – 576 119 India
Phone: 91-8252-70741
Fax: 91-8252-70959.

Nagarjuna Finance Ltd. (India)

Nonbanking Finance Company (NBFC) offers to lease/finance solar PV systems primarily due to Govt. of India's fiscal incentive of accelerated 100% depreciation on renewable energy systems in the very first year. They are also registered with IREDA as financial intermediaries. The terms of financing vary from project to project and solar PV water pumping systems have particularly benefited from leasing companies.

Address: Nagarjuna Hills, Punjagutta, Hyderabad – 500 082, Andhra Pradesh, India
Phone: 91-40-335-4159
Fax: 91-40-335-3805.

Syndicate Bank (India)

A public sector bank, it offers loans up to Rs. 25 000, repayment up to 5 years, @ 12.5% p.a.(PRIORITY SECTOR LENDING RATE), for purchase of solar home systems in India, through its branch network. The loan sanctioning authority rests with the branch managers.

Address: H.O. Manipal – 576 119, D.K. District, Karnataka, India
Phone: 91-8252-70252
Fax: 91-8252-70266.

Winrock International India

Winrock International India (WII) is a nongovernmental organization, an affiliate of Winrock International. WII's mission is to "develop and implement solutions that balance the need for food, income and environmental quality."

Contact: Shyamala Abeyratne, President
Address: 7 Poorvi Marg Vasant Vihar, New Delhi, India 110 057 India
Phone: 91 11 614 2965

Downloaded from https://onlinelibrary.wiley.com/doi/ by <Shibboleth-member@purdue.edu>, Wiley Online Library on [25/08/2024]. See the Terms and Conditions (https://onlinelibrary.wiley.com/terms-and-conditions) on Wiley Online Library for rules of use; OA articles are governed by the applicable Creative Commons License

Fax: 91 11 614 6004
Web site address: *www.winrock.org*
E-mail: *information@winrock.org*

LATIN AMERICA

Inter-American Development Bank (IADB)

The Inter-American Development Bank, the oldest and largest regional multilateral development institution, was established in December of 1959 to help accelerate economic and social development in Latin America and the Caribbean.

Address: 1300 New York Avenue, NW
Washington, DC 20577
United States of America
Phone: 202-623-1000
Web site: *http://www.iadb.org*

AFRICA

African Development Bank

The African Development Bank is the premier financial development institution of Africa, dedicated to combating poverty and improving the lives of people of the continent and engaged in the task of mobilizing resources towards the economic and social progress of its Regional Member Countries.

Address: African Development Bank
01 BP 1387
Abidjan 01, Cote D'Ivoire
Phone: (225) 20.20.44.44
Fax: (225) 20.20.40.06
Web site: *http://www.afdb.org*

REFERENCES

1. Eckhart M, *Financing Solar Energy in the U.S.: Scoping Paper*, REPP (1999).
2. Jechoutec K *et al*., *The Solar Initiative*, World bank (1995).
3. Sickenberger P, "KfW Support Schemes for PV Financing in Germany", 17th *European PV Conf.*, Munich, Germany (2001).
4. World Bank, *Rural Energy and Development: Improving Energy Supplies to 2 Billion People*, WB Rep No 15912, GLB (1996).
5. Greenpeace, *Solar Generation*, for the European PV Industries Assoc (2001).
6. Ball T, Applied Power Corp., Personal Communication (2001).
7. NREL, *PV Technology Performance* (2001).
8. Wiles J, *PV Power Systems and the National Electric Code: Suggested Practices*, SAN2001-0674, Sandia Nat Labs, Albuquerque, NM, USA (2001).
9. Osborn D, *Sustainable Orderly Development: The SMUD Experience*, UPEX (2001).

Downloaded from https://onlinelibrary.wiley.com/doi/ by <Shibboleth-member@purdue.edu, Wiley Online Library on [25/08/2024]. See the Terms and Conditions (https://onlinelibrary.wiley.com/terms-and-conditions) on Wiley Online Library for rules of use; OA articles are governed by the applicable Creative Commons License

10. Regional Economic Research, *Market Research on Energy*, CEC (2001).
11. NREL, *Renewable Energy Market Survey* (2001).
12. Rutledge K, *Financing Solar Energy CD-ROM*, NREL (2001).
13. Gregory J *et al*., *Financing Renewable Energy Projects: A Guide for Development Workers*, Stockholm Environmental Inst. (1997).
14. Cabraal A *et al*., *Best Practices for Photovoltaic Household Electrification Programs*, WB Paper No 324 (1996).
15. Alderslice A, Rogers J, *Renewable Energy for Microenterprise*, NREL (1999).
16. DeLange R, Sudimara P, Indonesia, Personal Communication (1997).
17. Hande H, SELCO India, Personal Communication (2001).
18. Saliya S, *SEEDS Solar Lending Programme*, Shell Solar, Mumbai (2001).
19. Eskom, *Market Research for Solar PV Rural Electric Service* (1998).
20. Wimmer N, "Financing Renewable Energies Through Microcredit", *Financing Renewable Energies*, Eurosolar, Bonn (1999).
21. *Photon Int.* **6**, p. 16 (2000).
22. Cabraal A, Cosgrove-Davies M, Schaeffer L, *Prog. PV Res. Appl.* **6**, 297–306 (1998).
23. Martinot E *et al*., *The GEF Solar PV Portfolio: Emerging Experience and Lessons*, GEF (2000).
24. Eckhart M, *The Solar Bank*, Solar Intl. Mgt. Inc. (1996).
25. Ikki O, *The Current Status of PV Development in Japan*, IRENA, Berlin (2001).
26. Bonda J, *Financing Solar Energy in India*, WIP and TERI for the EC (2000).
27. NREL, *U.S. PV Roadmap* (2000).
28. Donovan P *et al*., *An Assessment of Solar Energy as a National Energy Resource*, NSF/NASA (1972).
29. Palz W, The Photovoltaic Power and Its Applications in Space and on Earth, *Sun in the Service of Mankind*, Paris (1973).
30. Scheer H, *A Solar Manifesto*, James & James Publishers, London, UK (2001).

Downloaded from https://onlinelibrary.wiley.com/doi/ by <Shibboleth-member@purdue.edu, Wiley Online Library on [25/08/2024]. See the Terms and Conditions (https://onlinelibrary.wiley.com/terms-and-conditions) on Wiley Online Library for rules of use; OA articles are governed by the applicable Creative Commons License

Index

a-Si *see* amorphous silicon
a-Si/a-SiGe tandem solar cells 546–51
a-Si/a-SiGe/a-SiGe triple-junction solar cells 546–51
a-Si:H 29
a-Si:H solar cells, optical design 537–40
ABAQUS 245
ABN Amro Bank NV 1108
absorber layer design of *pin* solar cell 533–4
absorber region 87
absorption coefficient 70, 72–4, 341, 507
absorption coefficient spectra 519
acceptors 69–70
accumulator capacity 957–62
activation energy 807
ADO louver system 1032
Advanced Photovoltaic Solar Array (APSA) 435
Advanced Photovoltaics Systems, Inc. 512
African Development Bank 1114
Air Mass 62–3, 914, 916
Air Mass Zero (AM0) spectrum 417
air pollution 997–9
albedo-collecting modules 472
albedo irradiance 931
AlGaAs 360
AlGaAs/GaInP TJIC 397
AlInP window layers 391–2
alternating current (AC) 34
alternative peak power ratings 715
aluminothermic reduction of silica 201
aluminum alloys 158
aluminum back surface field 281
aluminum industry 158
Alwitra Evalon roofing foil 1030
AM/PM method 716
ambient temperature, diurnal variations of 933–4
ambipolar diffusion coefficient 108
Amonix Inc 496
amorphous silicon (a-Si) 21, 27–9, 153, 176, 505
  alloying 518–20
  atomic structure 513–14
  defects 514–15
  deposition, miscellaneous methods 526
  deposition techniques 520–1
  metastability 514–15
  optical properties 518–20
amorphous silicon (a-Si)-based photovoltaics, critical issues for further enhancement and future potential 559
amorphous silicon (a-Si)-based solar cells continuous roll-to-roll manufacturing on stainless steel substrates 553–5
  module manufacturing 553–8
amorphous silicon (a-Si) module 955
  manufacturing cost, safety, and miscellaneous issues 556–7
  performance 557–8
  production on glass superstrate 555–6
amorphous silicon (a-Si) photovoltaics, status and competitiveness 558
amorphous silicon (a-Si) *pin* cells 528–41
amorphous silicon (a-Si)/single-crystalline silicon 176
amorphous silicon (a-Si) solar cells 505–65, 1033–4
  designs for 508–13
  overview 505–13
  substrate and superstrate designs 509–10

Handbook of Photovoltaic Science and Engineering. Edited by A. Luque and S. Hegedus

© 2003 John Wiley & Sons, Ltd

ISBN: 0-471-49196-9

Downloaded from https://onlinelibrary.wiley.com/doi/ by <Shibboleth>-member@purdue.edu, Wiley Online Library on [25/08/2024]. See the Terms and Conditions (https://onlinelibrary.wiley.com/terms-and-conditions) on Wiley Online Library for rules of use; OA articles are governed by the applicable Creative Commons License

ampere-hour efficiency 810
angle of incidence
  effects 934–7
  relative transmittance plotted against 935
angular distribution of sky irradiance 929
angular losses calculation 936
annealing 343–4
annual energy production, economic analysis 983
annual energy value, economic analysis 984
annual performance and energy cost summary for central station plants 36
annual radiation availability 941
ANSYS 245
antireflection (AR) coatings 205, 268–9, 274, 283, 307, 326
  and encapsulation 287
antireflective (AR) coatings, high-efficiency III-V multijunction solar cells 375–6
aperture efficiency 322
Apollo Telescope Mount array 414
Applied Solar Energy Corporation (ASEC) 466
architecture 1005–42
  challenge of photovoltaics 1005–6
  functions of PV modules 1008–10
  see also BIPV
Argentina, rural electrification 1061
Array field 965
ASHRAE model 934–5
Asian Development Bank (ADB) 1111
ASN Bank 1104–5
aspheric lens 486
astronomical unit 907
Atlantis sunslates 1017
atmospheric pressure chemical vapor deposition (APCVD) 547
Auger recombination 76
Australian National University (ANU) 496
autonomous emergency phone and information system 58
autonomous power supply systems 799, 808
  applications 856
  energy-flow diagram 814
  for telecommunications 856
  investment and lifetime costs 857–9
  requirements to electrical storage systems 800
  system designs 801
autumn equinox 907
auxiliary generators 790–1
back reflectors 537, 539
back-surface field (BSF) 88, 258, 281
  recombination velocity 98
balance equation 120
balance of system (BOS) 5, 11, 14, 32–7, 863
Ballistic Missile Defence Organization (BMDO) 416
band diagram of solar cell 120
band gap 37–8, 99–100, 132–4, 516–17, 540
  a-Si alloys 546
  as function of lattice constant 361
  cell efficiencies as function of 415
  grading 546
  narrowing (BGN) 70, 73
  silicon alloys 544–6
bandedges 516–17, 528–9
bandtails 516–17
batteries 33, 54, 1052
  capacity 811–12
  classification of operating conditions 813–17
  for photovoltaic systems 835
  further developments 860
  general concept 801–12
  lifetime 787, 811, 860
  operating conditions 786–7, 811–12
  secondary electrochemical systems with external storage 849–57
  state of charge 811–12
  state of health 811
  system indicators 816
  technical terms and definitions 809–11
  with internal and external storage 807–9
  see also lead acid batteries and specific types
battery chargers 843
battery charging 56
battery charging stations 763
battery currents 810
battery storage 784–7
battery voltage and current during charging 870
beam radiation 913
beginning-of-life (BOL) output 419
belt furnaces 274
bi-directional step-up/step-down conversion 893
bifacial modules 294
BIPV 15, 294, 775–6, 1006, 1014
  basics 1026–35
  categories and type of buildings 1026–35
  categories of cell and modules 1026
  categories of integration 1027

Downloaded from https://onlinelibrary.wiley.com/doi/ by <Shibboleth-member@purdue.edu, Wiley Online Library on [25/08/2024]. See the Terms and Conditions (https://onlinelibrary.wiley.com/terms-and-conditions) on Wiley Online Library for rules of use; OA articles are governed by the applicable Creative Commons License

Petitioner Canadian Solar (USA) Inc., Ex. 1035, p. 2500

cells and modules 1029–35
design process 1036–40
distance between buildings 1036
function of integration 1028–9
module temperature 1034–5
orientation and angle 1036
practical rules 1037–8
reflection 1037
solar cell materials 1030–4
space required for balance of systems and interconnections 1039
step-by-step design 1038–9
strategic planning 1039–40
trees 1036–7
types of buildings and functions 1027
urban aspects 1036
zoning 1037
black body, radiation spectrum for 63
block-casting process 215
body-mounted arrays 432
Bolivia, rural electrification 1061–3
boron back surface field 281
boron-doped *p*-type material 216
Bose–Einstein function 122
boundary condition 338–41
BP Solar 496
BP Solface vertical wall system 1032
Bragg reflectors 124
Brazil, rural electrification 1063–4
Bridgman technology 214–16
Brundtland Centre, Toftlund (DK), case study 1022–6
BSF 266–7, 288
Buck converter 885–7
building integration
definition of 1006–8
well-integrated systems 1014–18
building-integrated PV systems *see* BIPV
built-in voltage 83, 85
bulk multicrystalline silicon 214–23
bulk *p*-type material lifetime 419
bulk silicon crystallization, simulation of 247–9
buried contact solar cell process 289–91
Butler–Volmer equation 804–6

calibration of space solar cells 424–5
Canara Bank (India) 1111
capacitance–voltage ($C-V$) characteristics 398
carbon
as impurity in silicon 187
in multicrystalline silicon 221
carbon dopant 391
carbothermic reduction of quartz 167
carbothermic reduction of silica 161–3, 198
Carnot efficiency 125, 131–2, 148
carrier–carrier scattering 81
carrier mobility 78–9
carrier transport 81
cash flows 974
casting alloys 158–9
cause–effect diagram for failed system 1054
$CdCl_2$ treatment 633–7
CdS/CdTe couples
bulk diffusivities 639
grain-boundary diffusion process 639
CdS/CdTe intermixing 637–42
CdTe 21, 27, 30–1, 64
absorber layer 633–7
band structure 625
cell photon losses and quantum efficiency versus wavelength 648
close-space sublimation (CSS) 628–9
condensation/reaction of Cd and Te vapors on a surface 628–9
crystal structure 624
deposition methods 626–7
electrodeposition 629–30
galvanic reduction of Cd and Te ions at a surface 629–30
high-efficiency 645
material properties and thin-film fabrication methods 621–31
metal organic chemical vapor deposition (MOCVD) 630
optoelectronic properties 622
phase diagram 623
physical vapor deposition (PVD) 628
physiochemical properties 622
potential toxicity 10
precursor reaction at a surface 630–1
screen-print deposition 631
spray deposition 630–1
sputter deposition 629
thin-film deposition techniques 627
vapor transport deposition (VTD) 629
CdTe modules 651–3
CdTe thin-film solar cells 617–62
back contact 642–4
basic structure 632
capacitance measurements and hole-density determination 649
characterization 644–50
development overview 617–21
future 653–7
$J-V$ curves 647
summary of status 650
window layers 631–2
CdTe/CdS 28
bulk-diffusion coefficient versus inverse of treatment temperature 640

Downloaded from https://onlinelibrary.wiley.com/doi/ by <Shibboleth-member@purdue.edu, Wiley Online Library on [25/08/2024]. See the Terms and Conditions (https://onlinelibrary.wiley.com/terms-and-conditions) on Wiley Online Library for rules of use; OA articles are governed by the applicable Creative Commons License

CdTe/CdS (*continued*)
grain-boundary diffusion coefficient versus inverse of treatment temperature 641
CdTe/CdS heterojunction solar cells 619
CdTe/CdS junction band diagrams 644
CdTe/CdS solar cells
current–voltage and relative quantum efficiency curves 621
quantitative assessment of film properties 626
CdTe/CdS thin-film structures, time-progressive X-ray diffraction line profiles 640
CdTe–CdS pseudobinary phase diagram 639
$CdTe_{1-x}S_x$ alloy thin film optical band gap versus composition 638
celestial equator 909
celestial poles 909
celestial sphere 908–9, 911
cell potential 809
cell technology and efficiency, effect on module price 36
cell voltage 809
Central and Southwest Services (CSW) 467
Centre for Sustainability De Kleine Aarde in Boxtel 1017
centrifugal pump system 894
chalcopyrite lattice structure 571
characteristic curve 952
characteristic parameters 951–2
charge controllers 33, 787–8, 843, 864–77
appraisal factors 875–7
compliance to codes 877
design criteria 875–7
efficiency 876–7
linear 865
safety aspects 877
self-regulating PV systems 865
with integrated voltage and current meter 874
see also T-CHEQ system
charge equaliser 843
for long battery strings 877–80
charge transfer between molecular orbitals 39
chemical etchants 397
chemical leaching, post-treatment by 195–6
chemical potential 134, 140, 142, 145
chemical processes 807
chemical texturing 285–7
chemical vapor deposition (CVD) 284, 315
Cherry Hill Conference 13
CHP space-heating applications 855
CIS flat-plate 36
Clean Energy Fund 1105
clearness index 920, 945
close spaced sublimation (CSS) 30
cloudiness index 921
CO_2 emissions 48–9
CO_2 reduction 22
Cold Wall process 246
Colt shading system 1012
Commons Capital LP 1108–9
Communication/Navigation Outage Forecast System (CNOFS) 440
Composited Optics Incorporated (COI) 440
compound parabolic concentrator (CPC) 454, 482–3
concentrating arrays 436–8
concentration PV systems 31–2
concentration ratio 450, 455, 484
concentrator cell and module efficiencies 473
Concentrator Initiative 465–6
concentrators 106–7, 124, 376–80, 406–7, 449–503, 946–7
basic types 452–60
compound parabolic (CPCs) 454, 482–3
current activities 495–500
D-SMTS 494
development dilemma 450–2
dielectric-filled 491–2
early demonstration projects 466–7
historical overview 460–74
history of performance improvements 472–4
innovative 492–4
literature 450
market barriers 449–503
marketing 451
miscellaneous programs 471–2
optics 452–5, 474–95
parabolic 479–82
reflection and refraction 478
reflective trough 494
research 449–503
RXI 494
Sandia National Laboratories program 461–2
schematic representation 475
secondary optics 489–91
static 456–60, 470, 491–2
two-stage 473
types of tracking 456–60
V-trough 483–5

Downloaded from https://onlinelibrary.wiley.com/doi/ by <Shibboleth-member@purdue.edu, Wiley Online Library on [25/08/2024]. See the Terms and Conditions (https://onlinelibrary.wiley.com/terms-and-conditions) on Wiley Online Library for rules of use; OA articles are governed by the applicable Creative Commons License

conduction band (CB) 4, 66–7, 74, 119–21, 129, 144–5, 536
confidence coefficient 918
confidence interval 918
conservation of energy 71
consumer products 57–9
control strategies 870–1
cost break down of solar home system 56
cost distribution for modules and silicon wafers 223
cost model 35
cost of electricity for utility-scale PV plants 990–4
cost projections 50
costs 15–19
  for TFSC 34
  for very high-efficiency 1000 suns-concentrating systems 38
  of construction of PV central plant 35
  of small professional autonomous photovoltaic systems 55
  of stand-alone PV installation 33
  see also economic analysis; system cost
covalent bonds 183
crystal defects 217–19
crystal growth techniques, numerical simulations of 244–51
crystal imperfections, effect of 182–5
crystalline silicon 21, 27–8, 176, 230
  bulk properties 257
  contacting structures 260
  contacts 257–8
  progress and challenges 23–7
  surfaces 256–9
  wafer material for 245
crystalline silicon Cz module 35
crystalline silicon noncontacted surfaces 258–9
crystalline silicon photovoltaic modules 291–302, 948–9, 955
  cell matrix 291–2
  electrical characteristics 295–7
  fabrication spread 297
  field performance 301–2
  lamination and curing 293
  layers of the module 292–3
  lifetime 301
  local shading and hot spot formation 297–9
  mismatch losses 297
  optical properties 300
  postlamination steps 294
  qualification tests 301–2
  special modules 294–5
  thermal characteristics 295–7
  with back contact cells 295
crystalline silicon solar cells 255–91, 948
  back contact print and dry 275
  back surface 266
  back surface passivation 281
  cell structure 259–60
  cofiring of metal contacts 275
  front contact print and dry 274–5
  front surface 263–6
  manufacturing process 271–80
  materials and processing 260–2
  performance comparison 270
  process flow 271–6
  size effects 266–8
  substrate 260–3
  substrate thickness 263
  testing and sorting 275
  throughput and yield 279–80
  variations to basic process 280–3
crystalline silicon technology 40
crystalline silicon wafer PV technology 28
crystallization 193–4, 216–17, 219, 223
  from aluminum melt 194
  from silicon-melt 194
  heat flow in 247
  thermal modeling of 245–7
Cu_2S/CdS thin-film solar cells 568
Cu–In–Se system 571–2
$CuIn_{1-x}$ Ga_xSe_2, complex refractive index 575
$Cu(InGa)Se_2$ 21, 27, 29, 31, 35
$Cu(InGa)Se_2$ solar cells 567–616
  absorption of light with different wavelengths 595
  alternative buffer layers 588–90
  back contact 580
  buffer layers 591–2
  chemical bath deposition (CBD) 585–6
  coevaporation 580–3
  commercial development 570
  composition 571–3
  critical materials with respect to primary supply 608
  current loss 594
  deposition methods 578–84, 587–8
  device completion 592
  device operation 592–602
  efficiency 590, 593
  electrical properties 574–6
  environmental concerns 608–9
  equipment 602–4
  evolution of device record efficiencies 605
  future outlook 609–11
  grain boundaries 576–7
  interface effects 586–7
  junction and device formation 584–92

Downloaded from https://onlinelibrary.wiley.com/doi/ by <Shibboleth-member@purdue.edu, Wiley Online Library on [25/08/2024]. See the Terms and Conditions (https://onlinelibrary.wiley.com/terms-and-conditions) on Wiley Online Library for rules of use; OA articles are governed by the applicable Creative Commons License

Cu(InGa)Se_2 solar cells (*continued*)
lack of comprehensive scientific base 570
light-generated current 593
manufacturing issues 602–9
material properties 570–8
module fabrication 604
module performance 604–7
optical properties 574
outdoor testing results 606
processes 602–4
production costs 607
quantum efficiency 593
recombination 595–8
scanning electron microscopy image 577
schematic cross section 569
structure 571–3
substrates 578–9
surface 576–7
TEM cross section 569
thin films 570
transparent contacts 590–1
two-step processes 583–4
wide and graded band gap devices 600–2
Cu(InGa)Se_2/CdS 28
current–voltage (J–V) behavior 595–6
Cu(InGa)Se_2/CdS interface 599–600
Cu(InGa)Se_2/CdS solar cells
quantum efficiency curves 596
temperature dependence 597
$CuInSe_2$ 570
absorption coefficient 574
complex refractive index 575
electronic levels of intrinsic defects 576
intrinsic defects 576
selected properties 572
$CuInSe_2$ solar cells 567, 569
current density 82, 805
versus voltage 506
current flow, electrode kinetics at 803–7
current matching 548
current–voltage (I–V) characteristics 92–5, 103–4, 122, 335, 701
current–voltage (I–V) measurements 721–38
CVD 321, 343
Czochralski (Cz) cell technology 24, 989–90
Czochralski (Cz) crystal-pulling technique 205, 246
Czochralski (Cz) flat-plate cell 989
Czochralski (Cz)-grown crystalline silicon 206, 261
Czochralski (Cz)-grown crystals and wafers 207–11, 989
Czochralski (Cz) module 987
Czochralski (Cz) web modules 989

daily energy deficit 959
daily irradiation 932–3
on inclined surface 933
daily radiation sequences 937
dangling bonds 514–15, 517
dark saturation current 91–2, 96
daylight control 1013
D&B Capital 1105
DC–AC conversion 37
declination 916
deep discharge protection (DDP) 763, 873–6
Deep Level Transient Spectroscopy (DLTS) 221
Deep Space 1 spacecraft 416, 437
deep trapping 531
defect clustering 334
defect levels 517–18
demand side management options 15
dendritic web (WEB) cells 989
dendritic web (WEB) production 231
dendritic web (WEB) technology 35, 232–5, 239–43, 288
density of state 66–7
depletion approximation 84
depletion region 83–5, 88, 90–1
depth of discharge (DOD) 810, 847–8
developing countries 1074
lack of electricity 1044–5
see also remote areas; rural areas
development 1043–71
device diagnosis 401–3
DFCC Bank (Sri Lanka) 1111–12
diamond lattice 64
diesel generator sets 54
diffuse fraction
of horizontal radiation 920–5
of individual daily global irradiation 922
of mean daily global irradiation 921
diffuse irradiance 928–31
diffuse radiation 913
diffusion 78, 80
diffusion coefficient 81, 185
diffusion length 212–13, 263
diffusion overvoltage 807
diffusion processes 806
digital synthesis, voltage shaping by 890–2
diode ideality factor 103
direct band gap materials 73
direct band gap semiconductors 71, 76

Downloaded from https://onlinelibrary.wiley.com/doi/ by <Shibboleth-member@purdue.edu, Wiley Online Library on [25/08/2024]. See the Terms and Conditions (https://onlinelibrary.wiley.com/terms-and-conditions) on Wiley Online Library for rules of use; OA articles are governed by the applicable Creative Commons License

direct current (DC) 3, 5, 34
direct irradiance 928
direct irradiation 913
direct subsidies (buy-downs) 1094–5
dirt effects 934–7
dirty surfaces 944
Discovery Science Center, Santa Ana, Los Angeles 1018
dislocations 184–5, 218
dispersion parameter 532
dispersive transport 532
displacement current 81
distributed power generation 53
distribution coefficients 182
distribution function of monthly electricity consumption 963
diurnal variations of ambient temperature 933–4
divergence operator 116
doctor blade technique 679
domestic appliances, energy-saving 793–4
donor funding 1086–7
donors 69–70, 186, 220
doping 69, 216, 518
  silicon alloys 528
doping level and type 262–3
double-layer capacitors 824–6, 859
double-sided textured (DT) cells 329, 331
drift 78–9
  of electrons 534
  of holes 531, 534
dummy wafers 178
dust-covered surface 935
dye fixation onto TiO_2 film 680
dye-sensitized solar cells (DSSC) 663–700
  approach to commercialization 691–4
  background 663–4
  cell assembly 681–2
  cell performance 681–2
  characteristics 678
  charge recombination 675
  charge-transfer kinetics 673–8
  counter electrode 669, 681
  efficiency improvement 695–6
  electron injection process 673–5
  fabrication 678–82
  materials 664–70
  metal complex photosensitizers 683–7
  module fabrication 694
  natural dye photosensitizers 687–8
  new developments 682–90
  new dye photosensitizers 683–8
  new electrolytes 688–9
  new oxide semiconductor film photoelectrodes 683
  operating principle 670
  organic dye photosensitizers 687–8
  photovoltaic performance 672–3
  primary processes 670–2
  prospects 695–6
  quasi-solid-state 689–90
  recombination between injected electrons and tri-iodide ions (dark current) 676–7
  redox electrolyte 681
  regeneration of oxidized photosensitizers 676
  sealing materials 670
  solid electrolyte 696
  solid-state 689–90
  stability 691–4
  structure 664–70

E&Co 1109
Earth–Sun position 912
ecliptic plane 907, 909
ecological dimension 48–54
economic analysis 971–1003
  annual energy production 983
  annual energy value 984
  capital recovery factor (CRF) 980
  case studies 984–97
  cash flows 973, 977
  discount rate 975
  discounted payback (DPB) 979, 984
  energy payback 997–9
  financial evaluation of system 976
  general methodology 980–4
  inflationary effects 977
  internal rate of return 979
  key concepts 973
  key technical and financial parameters 986
  levelized bus bar energy cost (LBEC) 980
  levelized energy cost (LEC) 980, 983
  net cash flow 978
  overview 972–3
  payback 984
  payback period in years 979
  present value or present worth 974–7
  return on equity (ROE) 992
  total capital requirements for central station plants 993–4
  value of system 975
  see also cost(s); financing of PV growth
Edge-defined Film-fed Growth (EFG) 230, 232, 234–5, 239–41, 244–5, 251, 288
Edge-Stabilized Ribbon (ESR) 231
Edge-Supported Pulling (ESP) 231
effective concentration 803

Downloaded from https://onlinelibrary.wiley.com/doi/ by <Shibboleth-member@purdue.edu, Wiley Online Library on [25/08/2024]. See the Terms and Conditions (https://onlinelibrary.wiley.com/terms-and-conditions) on Wiley Online Library for rules of use; OA articles are governed by the applicable Creative Commons License

effective distribution function 182
effective recombination velocity 87
efficiency of photovoltaic conversion 113–51
  very high efficiency concepts 132–48
efficiency calculation 125
efficiency forecasts 113
efficiency limit 113, 122–3
efficiency upper limit of solar cell 120
Einstein relationship 80–1, 86
electric current 4
electric field 86
electric field profile 532
Electric Power Research Institute (EPRI) 467–71, 982, 992
electric-vehicle batteries 835
electricity
  and development 1043–6
  applications in rural setting 1046–7
  basic sources 1047–8
  centralized system 1045
  future 2
  lack in developing countries 1044–5
  see also photovoltaic electricity
electricity consumption of household appliances 794
electricity generation 45
  photovoltaics as long-term substitute 48–54
electricity production scenarios 52
electrochemical cells 809
  fundamentals 801–7
electrochemical equilibrium 804
electrochemical potential 122, 143
electrochemical processes 807
electrochemical reactions, energy exchange 802
electrochemical storage 799–862
  schematics 808
electrode kinetics at current flow 803–7
electrodeposition (ED) 30
electrodes 809
electrolyte-agitation systems 844
electrolytic transfer of silicon 201
electromagnetic compatibility (EMC) 867
electromagnetic radiation 61
electron beam-induced current (EBIC) 193
electron behavior 531
electron cyclotron resonance CVD (ECRCVD) 341
electron effective mass 65
electron fluence for silicon solar cell 421
electron-hole pairs 62, 70, 74, 122, 143, 257
electron parameters 531
electron wave function 65
electronic density-of-states 515–16
electronic devices 59
electronic modeling, thin-film silicon solar cells 333–41
electrons
  drift of 534
  thermodynamic function of 119
electrostatic potential difference 84–5
electrostatically clean arrays 439–40
ELYMAT 212–13
emergency telephones 757–8
emitter front 281–2
emitter sheet resistivity 335
emitter structures 264
emitters 87, 93, 258
  homogeneous 264–5
  point 265
  selective 265
end-of-charge voltage 811
end-of-discharge voltage 809
energy and Early Man 1043–4
energy band diagram 66
energy band model 339
energy band structure 65–6
energy collection versus inclination angle 940
energy conversion, characteristics of 45–8
Energy Conversion Devices, Inc (ECD) 553–4
energy efficiency 810
energy flow analysis 812–13
energy gap 516
energy losses in grid-connected systems 966
energy-management systems (EMS) 873, 875
energy market, liberalization 52
energy payback 997–9
energy-saving domestic appliances 793–4
energy storage 55, 799
energy yield of grid-connected systems 965–6
Entech Inc 497
Entech linear-focus Fresnel system 463–5
enthalpy 802
entropy 802
entropy production 116–17, 128
  in Shockley–Queisser solar cell 129–31
environmental considerations 997–9
Environmental Enterprises Assistance Fund (EEAF) 1100
environmental monitoring 10
epilayers, characterization 398–400
epilift technique 320–1

Downloaded from https://onlinelibrary.wiley.com/doi/ by <Shibboleth-member@purdue.edu, Wiley Online Library on [25/08/2024]. See the Terms and Conditions (https://onlinelibrary.wiley.com/terms-and-conditions) on Wiley Online Library for rules of use; OA articles are governed by the applicable Creative Commons License

EPRI 467–71, 992
equilibrium carrier concentration 67–70
equilibrium energy band diagram 86
equilibrium potential 801–3
equilibrium voltage 805, 809
Ernst & Young Renewable Energy Unit 1105
Ethyl Corporation process
  for semiconductor grade silicon 173–5
  simplification 198–201
Euclides linear trough system 497
Europe, PV programs 1097–9
European Bank for Reconstruction and Development (EBRD) 1105–6
European Commission DG XVII 1106
European Investment Bank (EIB) 1106
exchange current density 805
excimer laser annealing (ELA) 350
excimer laser recrystallization (ELR) 350
experience curve 50–1
experience factor 17, 38
Explorer I 414
extensive variables 114
external collection efficiency 95
extraction metallurgy in ladle, post-treatment by 196–8
extraterrestrial applications 59–60
extraterrestrial irradiance 915–16
extraterrestrial radiation 913, 926

FAC/Equities A Division of First Albany Corporation 1109
facade systems 1014
failed system, cause–effect diagram for 1054
Fast Auroral Snapshot (FAST) solar array 440
Fermi energy 68–9, 83, 88, 518
Fermi function 68
Fermi level 119, 529, 535
figures of merit 444–6
fill factor (*FF*) 309
Final Yield 965
financial characteristics 1077–9
financing of PV growth 1073–115
  borrowers experience 1081
  capital requirements 1076–7
  example calculation 1082
  grid-connected residences 1079–82
  growth outlook 1075
  historical development 1073–4
  lenders issues 1081
  market drivers 1075
  organizations involved in 1100–14
  residential sector 1082
  rural areas 1083–6
financing the PV industry 1091–2
financial-support mechanisms 50
fixed surfaces, irradiation on 943–5
Flat Plate Array Project 230
flat-plate, CIS 36
flat-plate conventional PV modules 947
flat-plate solar cells 268, 989
flexible fold-out arrays 433–5
flexible roll-out arrays 435–6
float zone (FZ) monocrystals 205
floating-zone technique 207
flooded batteries 844
flywheels 799
foil *see* silicon ribbon and foil production
forecasts 15–19
  long-term 18
four-junction III-V cells 417
Fourier Transform Infrared Spectroscopy (FTIR) 219
Franz Keldysh effect 73
Fraunhofer-Institut fur Solare Energiesysteme 497–8
free-carrier absorption 74
free enthalpy 802
Fresnel lens 36, 452–3, 462, 464, 466, 474, 485, 487–9, 496
Fresnel module price 992
Fresnel system 990
front-polished and back-textured (FPBT) 329
front-surface recombination velocity 97
front-textured and back-polished (FTBP) 329, 331
fuel cells 854–5
fumed silica 159, 170
functional silanes 160
fundamental absorption 70

GaAs 5, 20, 27, 60, 64, 123–4, 360, 426, 472
  back-surface fields 394
  optical properties 394
  properties at 298K 386
  window layers 394
  see also GaInP/GaAs; GaInP/GaAs/Ge
GaAs cells 393–4, 994–7
  Ge(100) substrates 393–4
GaAs tandem-junction cells 996
GaAsP 360
GaInAs 360
GaInP 5, 20–1, 40, 426, 472
  absorption coefficient 388–9
  optical properties 387–9
  ordering in 387
  properties at 298K 386
GaInP solar cells 383–93
  back-surface barrier 392–3
  characteristics 393

Downloaded from https://onlinelibrary.wiley.com/doi/ by <Shibboleth-member@purdue.edu, Wiley Online Library on [25/08/2024]. See the Terms and Conditions (https://onlinelibrary.wiley.com/terms-and-conditions) on Wiley Online Library for rules of use; OA articles are governed by the applicable Creative Commons License

GaInP solar cells (*continued*)
doping characteristics 389–91
lattice matching 383–7
window layers 391–2
GaInP/GaAs cell efficiencies 361
GaInP/GaAs multijunction solar cell 360
GaInP/GaAs tandem solar cells 360, 362
GaInP/GaAs/Ge concentrator cell 379–80
GaInP/GaAs/Ge solar cells 361, 363
materials issues 382–98
MOCVD 382
refinements to 403–4
GaInP/GaAs/Ge tandem cell 359
Galaxy XI spacecraft 438
gap states 517–18
GaSb 472
GE Capital Corporation 1109
generator capacity 957–62
versus storage capacity 959
Geospace Electrodynamic Connection (GEC) projects 440
geosynchronous Earth orbits (GEO) 420
German 100 000 photovoltaic roofs programme 778–9
germanium
optical properties 394
properties at 298K 386
see also GaInP/GaAs/Ge
germanium cells 394–6, 426–7
III-V heteroepitaxy 395–6
junction formation 394–5
germanium substrates 393–4
Germany 1074
gettering 262, 283
Global Approval Program for Photovoltaics (PV GAP) 1054
Global Environment Facility (GEF) 1089–91, 1101
global horizontal irradiation 918
global irradiance on inclined surface 927–33
global radiation 913, 920–5
global trends in performance and applications 20–3
global warming 48
glow discharge deposition at different frequencies 523–5
goals of current solar cell research and manufacturing 19
government funding of research and development 1096–100
government incentives and programs 1092–6
grain boundaries (GB) 183, 185, 217, 310, 333, 337
categorization 337–8
grain boundary interface recombination velocities 342
grain enhancement, thin-film silicon solar cells 343–50
grain growth 349
grain size 217–18, 340
grain size distribution 349
grains, categorization 337–8
Grameen Shakti (Bangladesh) 1112
grand canonical potential current density 129
grand canonical potential flow for electrons 130
grand potential 115
green design, PV role in 1011
grid-connected systems 754, 779–80
block diagram 775
decentralized 774–9
dependence of annually used solar energy from 792
energy losses in 966
energy yield of 965–6
future developments 796–7
inverters 788–9, 881–902
joint ownership 779–80
grid-independent systems, for small devices and appliances 755–9
Group IB formation in QD arrays 147
Group IB material 144–5
Group IB solar cell
limiting efficiency 147
structure 146
Group III-V semiconductor compounds and alloys 362
Group III-V solar cells, space applications 426–31
Group VB 120–1, 129, 144–5

H-type bridge 892, 895–6
H-type bridge inverter 892
hazard classification 10
Heat Exchange Method (HEM) 246
heat flow in crystallization 247
heat load and daylight control systems 1013
Helios unmanned prototype aircraft 783, 785
Heller Financial Incorporated 1109–10
heterojunction with intrinsic thin-layer (HIT) solar cells 271, 288–9
high-efficiency III-V multijunction solar cells 359–411
antireflective (AR) coating effects 375–6
cell configuration 365–6
chromatic aberration 375
concentration 376–80

Downloaded from https://onlinelibrary.wiley.com/doi/ by <Shibboleth-member@purdue.edu>, Wiley Online Library on [25/08/2024]. See the Terms and Conditions (https://onlinelibrary.wiley.com/terms-and-conditions) on Wiley Online Library for rules of use; OA articles are governed by the applicable Creative Commons License

concentration dependence of efficiency 378
current matching 376
current-matching effect on fill factor and V_{OC} 373
efficiency 382
efficiency versus band gap 370–2
fill factor 382
four-terminal connection 365
growth on other substrates 405–6
implementation into terrestrial systems 406–7
materials availability 398
metallization 378–9
multijunction J–V curves 368–70
overview 359–63
physics of 363–5
series-connected device performance 366–82
series resistance 378–9
single-junction solar cells, physics of 363–5
space applications 363
spectral effects 374–5
spectral fluctuations 374–5
spectrum 377
spectrum splitting 364–5
temperature dependence 380–2
terrestrial energy production 363
theoretical limits to multijunction efficiencies 364
three-terminal voltage-matched interconnections 366
top and bottom subcell QE and J_{SC} 367–8
top-cell thinning 372–3
troubleshooting 398–403
two-terminal series-connected (current matched) 366
high-efficiency multijunction solar cells 551
high-efficiency silicon (HES) cells 415, 426
high-level injection 107–9
high-radiation environment solar arrays 443–4
high specific power arrays 443
high-temperature/intensity arrays 438–9
holes, drift of 531, 534
horizontal radiation, diffuse fraction of 920–5
hot electron solar cells 141–4
band structure 143
hot-wire chemical vapor deposition (HWCVD) 341, 345–7, 525–6
household appliances, electricity consumption of 794
housing projects 1020–1, 1023
HS601 spacecraft 426
HS702 spacecraft 426
Hubble space telescope 436–7
human development index (HDI) 2
hybrid systems 763–6, 768, 860
hydrogen, passivation with 283–5
hydrogen dilution 526–7
hydrogen/oxygen storage systems 852–7
applications 855–7
electrolysers 853
gas storage 853–4
hydrogen storage systems 860
hydrogenated amorphous silicon 507

IFU 1106–7
IMCAP 985
impact ionization 76
Impax Capital Corporation Ltd 1106
impurities 219–23
inclination angle versus latitude 942
inclined surface
daily irradiation on 933
global irradiance on 927–33
solar radiation on 920–33
income tax deductions and credits 1096
indirect band gap semiconductors 72, 76
indium-tin-oxide (ITO) layer 547
ING Bank Nederland 1107
ingot fabrication 214–16
In_2Se_3–Cu_2Se equilibrium phase diagram 573
inside efficiency 322
institutional uses 1083–4
integrated power systems 442–3
integrated PV building *see* BIPV; building integration
intensive variables 114
Inter-American Development Bank (IADB) 1114
interest subsidies 1095–6
interface condition 338–41
intermediate band (IB)
concept 39
solar cell band diagram 145
internal gettering 351
international aid 1086–7
International Finance Corporation (IFC) 1089, 1101
international financing sources 1086–91
International Panel on Climate Change 48–9
International Space Organization 422
International Space Station (ISS) 415–16, 434, 782, 784
interstitial impurities 184
interstitial oxygen 219

Downloaded from https://onlinelibrary.wiley.com/doi/ by <Shibboleth-member@purdue.edu>, Wiley Online Library on [25/08/2024]. See the Terms and Conditions (https://onlinelibrary.wiley.com/terms-and-conditions) on Wiley Online Library for rules of use; OA articles are governed by the applicable Creative Commons License

intragrain defects 333
inverters 5, 788, 881–902
  active quality control in the grid 900
  combination of step-down converter with 890
  general characteristics 881
  grid-connected systems 788–9, 881–902
  H-bridge-type 885
  high-frequency concepts 894–6
  power factor as function of output power 899
  power quality 896–9
  principles 884–96
  safety aspects for grid-connected systems 900–2
  square-wave-type 884–5
  stand-alone operation 883
  stand-alone systems 789–90
  three-phase PWM 894
  with sinusoidal AC output 885–96
Ioffe Physical-Technical Institute 498
ionizing radiation 419
IREDA (India) 1112
iron concentration 222
irradiance 913, 915
irradiance measurements 721–2
irradiance to daily irradiation ratios 926
irradiation 913
  of most widely studied surfaces 940–1
  on fixed surfaces 943–5
IT Power India Pvt. Ltd. 1112
I–V characteristics 92–5, 336
I–V curves 275–6, 299, 867, 949–50
I–V measurements
  cell and module systems 731–6
  multijunction cells 400–1
  simulator-based 722–3
I–V performance 548–9

Japan, PV programs 1097
Japanese residential PV promotion program 777
Jet Propulsion Laboratory (JPL) Flat Plate Array Project 230
joint ownership project 781
JRC Ispra guidelines 965
junction isolation 274
J–V characteristics 544
J–V curves 341–2, 368–70
  for series-connected subcells 369

Kyoto Protocol 22

Lafarge Braas PV 700 roof tile system 1015
Lagrange invariant 118
Landsberg efficiency 148
laser-grooved buried-grid (LGBG) industrial cells 264
laser-grooved buried-grid (LGBG) solar cell process 290–1
laser-induced recrystallization 350
laser-pulse time-of-flight measurements 531
law of the junction 88
lead acid batteries 806, 817, 826–49, 856
  acid stratification 837–9
  ageing processes and their influences of properties 837
  applications 829–35
  charge/discharge process in lead electrode 828
  charging 845–6
  chemistry 827–9
  concepts 829–35
  corrosion 840
  deep-discharge protection 847–9
  discharge capacity 836–7
  discharge curves 849
  erosion 840–1
  fundamentals 829–35
  ice formation 842–3
  operation strategies 844–9
  peripherals 843–4
  reverse charging 842
  short circuits 841–2
  sulphation 839
  technology 829–35
  voltage thresholds 875–6
lead sulphate crystals 807
Legendre's transformation 114–15
less-developed areas 972
light absorption 70–4
light emitting diode (LED) 76, 137–8, 148
light-induced degradation (LID) 212–13
light-soaking effects 541
light-trapping 269–70, 320, 325–7, 333, 537–8
lithium batteries 859
lithium-ion batteries 822–4
lithium-polymer batteries 822–4
local apparent time 909
local horizon 939
long-base approximation 96
Loss of Load Probability (LLP) 956–7, 960–1, 963–4
low intensity low temperature (LILT) cells 441–2
low pressure chemical vapor deposition (LPCVD) method 213
low-Earth orbit (LEO) 414, 420

Downloaded from https://onlinelibrary.wiley.com/doi/ by <Shibboleth-member@purdue.edu>, Wiley Online Library on [25/08/2024]. See the Terms and Conditions (https://onlinelibrary.wiley.com/terms-and-conditions) on Wiley Online Library for rules of use; OA articles are governed by the applicable Creative Commons License

MACD 307–8, 311, 327–31
  influence of bottom angle of texture pits 331–2
  influence of density of texture pits 332
  influence of texture height 331
magnesium dopant 391
Malaprabha Grameena Bank (India) 1112–13
Manipal Finance Corp. Ltd. (India) 1113
MARC 245
market demand 1084
market distribution by technologies 21
market evolution 47
market expansion 39–40
market growth rates 50
market share of monocrystalline and multicrystalline solar cells 256
market volume 56
markets 15–19
Mars Pathfinder Sojourner Rover 432
Mars solar arrays 440
Mars solar electric propulsion (SEP) vehicle 428
Martin Marietta point-focus Fresnel system 462–3
Mataro Library, Barcelona, Spain 776
matching component cells in multijunction designs 550
matching DC/DC converter (MDC) 871
Mathiessen's rule 79
maximum achievable current density *see* MACD
maximum power calculation 950
maximum power point (MPP) 93–4, 866, 881–2, 900, 952–3
  deviations 883
maximum power point tracking (MPPT) 871–3, 881, 894
mean global daily irradiations 917
mechanical stacks 404–5
mechanical texturing 285–6
median cracks 228
MESSENGER Discovery mission 439
metal-induced crystallization (MIC) 344–9
metal-insulator-semiconductor (MIS) contacts 258
metallization techniques 263–4
metallurgical grade silicon 24, 157–8, 161–7, 176–7
  casting 166
  crushing 166
  economics 167
  furnace for production of 164
  refining 163–6
  upgrading purity 194–8
metalorganic chemical vapor deposition (MOCVD) 360
  GaInP/GaAs/Ge solar cells 382
Meteosat weather satellite 783
Mexico, rural electrification 1064–5
microcrystalline silicon solar cells 551–2
microenterprise 1083
micromorph devices 552–3
microwave glow discharge deposition 525
micro-X-ray 347
mid-Earth orbits (MEO) 420
Miller indices 65
minority-carrier diffusion equation 82–3, 89
minority-carrier diffusion length (MCDL) 307, 351
minority-carrier lifetime 77
minority-carrier recombination 185
mobility edges 517
modularity 56
module aperture area 35
module manufacturing, a-Si-based solar cells 553–8
module price for silicon cell technology 985–90
module temperature, BIPV 1034–5
monitoring systems and interfaces 843, 874
monochromatic cell 124–6
monochromatic cell efficiency versus photon energy 125
monocrystalline float zone (FZ-Si) material 260
monocrystalline Si cells 1031–2
monoenergetic membrane 144
morphological defects 401
MOS-FETs 866, 868
multicrystalline silicon (mc-Si) 21, 26, 206
multicrystalline solar cells 256, 283–7
multicrystalline wafers 285
multijunction designs, matching component cells in 550
multijunction III-V cells 427–8
multijunction solar cells 20, 38, 132–5, 510–11, 542–53
  advantages 542–4
  I–V measurements 400–1
  measurement procedures 728–30
  principles and operation 362
  quantum efficiency measurements 549
multilinear Lagrange invariant 118
multi-wire sawing technique 224

n-type material 77, 83
n-type semiconductors 76
n-type side 25

Downloaded from https://onlinelibrary.wiley.com/doi/ by <Shibboleth-member@purdue.edu, Wiley Online Library on [25/08/2024]. See the Terms and Conditions (https://onlinelibrary.wiley.com/terms-and-conditions) on Wiley Online Library for rules of use; OA articles are governed by the applicable Creative Commons License

n-type silicon 184
Nagarjuna Finance Ltd. (India) 1113
nanotechnology 39
National Meteorological Services 916
National Renewable Energy Laboratory (NREL) 323, 360, 498
natural integration 1015
NEDO process 198
Nernst equation 803
New Alternatives Fund Inc. 1110
New Century Finance Limited 1107
New Energies Invest Ltd. 1107
NiCd batteries 818–21
nickel-metal hydride (NiMH) batteries 821–2
Ni-Si phase diagram 190
nominal operating cell temperature (NOCT) 714, 947, 951, 955
noncrystalline semiconductors 517, 532
n-p junction 340
Nth Power Technologies 1110
nucleation 349
numerical modeling of solar cells 109–10
numerical simulations of crystal growth techniques 244–51

off-grid energy supply systems, characteristics of 55
off-grid power supply systems 54–7, 754
  future developments 794–6
  prerequisites 57
off-grid rural electrification 768–71
  categorization of delivery models 773–4
  economic aspects 771–4
  see also rural electrification
open-circuit voltage 309, 529, 534–7, 809, 951, 954
optical confinement 285
optical design, a-Si:H solar cells 537–40
optical generation rate 89
optical properties
  crystalline silicon photovoltaic modules 300
  GaAs 394
  GaInP 387–9
  germanium 394
  thin-film silicon solar cells 328
optics 268–70, 326–36
  concentrators 452–5, 474–95
optimal tilt angle for minimizing solar generator size 793
Orbital Workshop array 414
Ostwald ripening 185
overcast skies, radiance distribution associated with 930
overvoltage 806
oxygen as impurity in silicon 187–8
oxygen segregation 220

p-type material 77, 83
p-type multicrystalline silicon 217, 220
p-type semiconductors 76
p-type side 24
pair formation 185
parallel resistance 953
parasitic power loss 37
parasitic resistance effects of solar cell 102
partial-shunting controller 869
passivated emitter rear contact (PERC) cell 466
passivated emitter rear floating junction (PERF) cells 266
passivated emitter rear locally diffused (PERL) cells 261, 263, 266,270–1, 314–15, 469
passivated emitter rear totally diffused (PERT) cell 266, 314
passivation with hydrogen 283–5
Pathfinder unpiloted prototype 782
$Pb/H_2SO_4/PbO_2$ cell 830
PC1D 334
peak load 51
peak-load-reduction technology 14
performance rating methods, energy-based 716–17
performance ratio (PR) 965
periodic table of elements 64
personal digital assistant 58
phonon absorption 72
phonons 72
phosphorus diffusion 273
phosphorus doping 518
photocarrier drift in absorber layers 530–3
photoconductivity 505
photoluminescence (PL) intensity 400
photon absorption 71–2
photon conversion efficiency, wavelength dependence of 363–4
photon energy 61, 70, 73, 130
  monochromatic cell efficiency versus 125
photon flux 74, 121
photon flux absorption 313
photons 3, 5, 61, 117–18, 127–8, 142, 144
photosynthesis 39
photovoltaic cells 57
  and BIPV modules 1029–35
  manufacturers 22
  measurement and characterization 701–52

Downloaded from https://onlinelibrary.wiley.com/doi/ by <Shibboleth-member@purdue.edu, Wiley Online Library on [25/08/2024]. See the Terms and Conditions (https://onlinelibrary.wiley.com/terms-and-conditions) on Wiley Online Library for rules of use; OA articles are governed by the applicable Creative Commons License

Photovoltaic Concentrator Applications Experiments 462
photovoltaic concentrators *see* concentrators
photovoltaic conversion, efficiency of 113–51
photovoltaic converters 59, 120–31
photovoltaic-diesel-hybrid system 768
photovoltaic efficiency 701
  annual 717
photovoltaic electricity 39
  contribution of 40–1
  technical potential 54
Photovoltaic Energy Project (PEP) 727
photovoltaic engineering problems 925
photovoltaic generator behavior under real operation conditions 947–56
photovoltaic industry 153
photovoltaic integrated as roofing louvres, façades and shading 1011–14
photovoltaic module cell temperature 955
photovoltaic module orientations 925
photovoltaic module placement and shadowing 1039
photovoltaic modules 5, 7, 34, 46, 60
  BIPV 1029–35
  certification 745–6
  energy collection and delivery 905–70
  I–V curve 867
  integration in architecture 1019–21
  measurement and characterization 701–52
  net energy loss 10–11
  qualification 745–6
  rating 947
  solar radiation available for fixed flat-plate conventional 947
  transparent 1009
  world production 22
photovoltaic performance, annual 718
photovoltaic performance rating 701–20
photovoltaic rating criterion 716
photovoltaics 753–98, 972
  advantages and disadvantages 3
  and all of the world's needs 7
  and development 1043–71
  areas of application 45, 754
  as empowering technology 1–2
  as environmentally clean and green technology 9
  as long-term substitute for electricity generation 48–54
  as small-scale cottage industry 7
  basic R&D 19
  components 784–94
  consumer applications 756–7
  development dimension 54–7
  economic assessment 980–4
  experience curve for 1976 to 1998 17
  funding 8–9
  future developments 794–6
  future of emerging technologies 37–9
  future potential 40
  future prospects 999–1002
  history 11–15
  immediate and exclusive use 7
  land area requirement 6–7
  motivation for application and development 45–60
  myths of 5–11
  notable events in history of 12
  overview 753–4
  public funding for R&D 9
  public support 8
  rational decision to develop 972
  status 1
  trend in worldwide applications 8
  use of term 3–5
  Utility-Scale Applications (PVUSA) project 467, 715, 736
Photovoltaics/Market Transformation Initiative (PV/MTI) 1101
pin device, electronic structure 528–30
pin photodiodes 508–9
pin solar cell 109
  absorber layer design 533–4
  band diagram 110
  power output 533
planar cell structures 310
plant cost 34
plasma-deposited silicon thin film 527
plasma-enhanced chemical vapor deposition (PECVD) 28, 243, 258, 284–5,314, 324, 341, 353, 520–1
pn junction 5, 24–5, 29
  n-type 30
  p-type 30
PN-junction diode electrostatics 83–7
point-contact cell design 469
point defects 184
point-focus Fresnel modules and systems 462
point-focus optics 456
Poisson's equation 81, 83
polar tracking 946
polycrystalline silicon 21, 26, 310
polycrystalline silicon wafers 1032–3
polymethyl methacrylate (PMMA) 453, 495
polysilicon 24, 161
  historical processes to manufacture 199
  rejects 178–9
  research projects 199
  see also semiconductor grade silicon

Downloaded from https://onlinelibrary.wiley.com/doi/ by <Shibboleth-member@purdue.edu, Wiley Online Library on [25/08/2024]. See the Terms and Conditions (https://onlinelibrary.wiley.com/terms-and-conditions) on Wiley Online Library for rules of use; OA articles are governed by the applicable Creative Commons License

Polytechnical University of Madrid 496–9
porous-Si layer on single-crystal substrate 317
post-treatment
  by chemical leaching 195–6
  by extraction metallurgy in ladle 196–8
power conditioning 863–903
power distribution of solar irradiation 966
Power Management and Distribution (PMAD) 441
powerguard flat-roof PV system 1012
precipitates in silicon 190–3
precipitation 185
pre-electrification 1068
premature capacity loss 832
price–experience curve 47–8
primary reference cell calibration methods 723–6
Production of High Silicon Alloys 167
professional industrial systems 57
proton exchange membrane fuel cell (PEMFC) 854
pumping stations 56
pumping systems 768
PVUSA 467, 715, 736
PWM controllers 871, 895
pyrogenic silica 170

QD arrays, IB formation in 147
quality-assurance and quality-control (QA/QC) evaluation 555
quantum dot (QD) arrays 148
  IB formation in 147
quantum dot (QD) solar cells 442
quantum efficiency 538
quantum efficiency measurements, multijunction cells 549
quantum efficiency spectra 545
quartz, carbothermic reduction 167
quartz-furnaces 273
quasi-Fermi energy 535–6
quasi-Fermi levels 119–20, 122, 126, 145
quasi-neutral region 83

R&D
  funding sources 1099–100
  future programs 1099
  government funding 1096–100
Rabobank Nederland/Groen Management BV 1107
radiance distribution associated with overcast skies 930
radiation, use of term 913
radiation spectrum for black body 63
Radio Corporation of America (RCA) 506
rapid thermal processes (RTP) 282–3, 314, 350, 353
reactive ion etching (RIE) 286–7
realistic reporting conditions (RRC) 716
receiver position 912
rechargeable alkali mangan (RAM) batteries 822
recombination current 339
recombination mechanisms 113
recombination process 74–7, 121
recombination sites 185
recombinators 844
redox batteries 860
redox electrolyte 667–8
redox-flow batteries 850–2
reference cell calibration procedures
  intercomparison 727–8
  uncertainty estimates 726–7
Reference Year 937
Reference Yield 965
reflective concentrator configurations 454
reflective secondary concentrators 463
refractive lenses 485–9
Regional Solar Programme (RSP) 1067
relative transmittance plotted against angle of incidence 935
reliability, stand-alone systems 953–6
reliability maps 959, 961
remote areas 57, 761–74, 1048
  see also rural electrification
remote low power systems 57
remote (or village) systems 972
renewable energies 54
Renewable Energy and Energy Efficiency Fund (REEF) 1101
renewable energy sources 45
  current use and current potentials 46
repeater station 762–3
residential sector
  financing for 1079–82
  financing of PV growth 1082
  rooftop system 1079
reverse bias 139
RF glow discharge deposition 521–3
Ribbon Growth on Substrate (RGS) 231–2, 236–41, 246, 249–50
RIGES 17
rigid panel planar arrays 432–3
rolling-grain model 227
roof-integrated photovoltaic system 53, 1008
rooftop PV generators 774
Rossi X-Ray Timing Explorer (XTE) 433
Ru complex photosensitizers 666–7, 685–6

Downloaded from https://onlinelibrary.wiley.com/doi/ by <Shibboleth-member@purdue.edu>, Wiley Online Library on [25/08/2024]. See the Terms and Conditions (https://onlinelibrary.wiley.com/terms-and-conditions) on Wiley Online Library for rules of use; OA articles are governed by the applicable Creative Commons License

rural areas 56–7, 1049–51, 1053, 1083–6
financing PV 1083–6
rural electrification 14, 1045–6
advantages of PV technology 1048–9
applications 1046–7
Argentina 1061
barriers to PV implementation 1051–60
Bolivia 1061–3
Brazil 1063–4
initial cost 1055–60
Mexico 1064–5
nontechnical issues 1055–9
Sri Lanka 1065–7
toward a new paradigm 1068–9
trained human resources for 1059–60
see also off-grid
rural energy scene 1046

safety procedures 9–10
Sahel, water pumping 1067–8
SAM Equity Partners Ltd. 1110
Sandia Baseline III point-focus module design 465
Sandia National Laboratories Concentrator Program 461–2
satellites 59–60, 363
SAVANT radiation degradation modeling computer 420
saw damage 271–2
and wafer quality 229–30
Scanning Electron Microscopy (SEM) 193, 221
SCARLET arrays 416, 427–8, 437
Scarlet Deep Space One Satellite 59
scattering mechanisms 79
Schrödinger equation 65
Schüco façade profile system 1031
Schüco roof profile system 1030
screen printing 261, 265, 275–9, 679–80
SEA Corporation 466
second-order effects 953–6
secondary electrochemical accumulators with internal storage 817–49
secondary optical element (SOE) 454
segregation coefficient 219
selenium 505
selenium dopant 389–90
selenization 29
self-discharge 811
self-interstitial 184
self-regulating PV system 865
semiconductor band gap 121, 153
semiconductor equations 81–2
semiconductor grade silicon 24, 176–7
economics and industry 175
Ethyl Corporation process for 173–5
production 167–75
Siemens process for 168–72
Union Carbide process for 172–3
semiconductor lasers 76
semiconductors 5
crystal structure 64–5
electronic grade 64–5
fundamental properties 64–83
n-type 69–70
nondegenerate 68
p-type 69–70
semitransparent cells 1034
series resistance 951
shading structure 1013
shading system 1014
shadows and trajectory maps 939
Shell Solar/BOAL profiles 1008
Shockley–Queisser cell
entrophy production in 129–31
thermodynamic consistence of 126–9
Shockley–Read–Hall (SRH) lifetimes 257, 261
Shockley–Read–Hall (SRH) recombination 75, 620
shopping mall, Lausanne 1024
short-circuit current 92, 422, 540, 951, 953
short-circuit current density 536
shunt resistances 102–4
SiC 163
SiC bond 156
SiC formation 221
Siemens process for semiconductor grade silicon 168–72
Siemens Solar Boron Back Surface Field (BSF) process 213
SiGe alloys 519
silica
aluminothermic reduction of 201
carbothermic reduction of 161–3, 198
silicon 5, 154–61, 182
bulk monocrystalline material 206–13
carbon as impurity in 187
cell technology, module price for 985–90
chemical properties relevant for photovoltaics 156
crystalline 153–4
current feedstock to solar cells 175–9
dopant 390
effect of various impurities 186–93
electrolytic transfer of 201
feedstock for crystalline cells 178
group IIIA impurities 186–7
group VA impurities 186–7
health factors 156–7

Downloaded from https://onlinelibrary.wiley.com/doi/ by <Shibboleth-member@purdue.edu, Wiley Online Library on [25/08/2024]. See the Terms and Conditions (https://onlinelibrary.wiley.com/terms-and-conditions) on Wiley Online Library for rules of use; OA articles are governed by the applicable Creative Commons License

silicon (*continued*)
history 157–61
impurities 155
mechanical properties 155
miscellaneous applications 161
multicrystalline wafers 176
occurrence 154
oxygen as impurity in 187–8
physical properties relevant for photovoltaics 154–5
precipitates in 190–3
refractive index 155
requirements for crystalline solar cells 179
semiconductor material 160–1
single-crystal wafers 154, 176
solar grade feedstock 153–204
solidification 179–82
thermal properties 155
transition-metal impurities in 188–90
ultra-pure 160–1
see also metallurgical grade silicon; semiconductor grade silicon; solar grade silicon routes
silicon alloys 157
band gaps 544–6
doping 528
silicon applications 157–61
in aluminum industry 158–9
in chemistry 159–60
Silicon Film (SF) 230, 239–42, 244, 251
silicon metal 157–8, 161
silicon monoxide 163
silicon multicrystalline sawn wafers 154
silicon nitride 243, 283
passivation 281
silicon ribbon crystal growth technology, productivity comparisons 238–9
silicon ribbon/foil growth techniques 232
silicon ribbon/foil production 230–44
manufacturing technology 239–40
process description 232–8
silicon ribbon/foil technology 231
future directions 243–4
silicon ribbon material properties and solar cells 240–3
silicon ribbon/multicrystalline film 176
silicon ribbon wafer/foil technologies 251
silicon ribbons 288
silicon solar cells 240–3
power density 421
space applications 425–6
temperature coefficients 719
silicon tetrachloride 159, 171
silicon-wafer-based PV module costs 25
silicones 159
SIMS (secondary ion mass spectroscopy) 347
simulation of bulk silicon crystallization 247–9
simulation of silicon ribbon growth 249–51
simulation tools 245
single level trap (SLT) 75
single-crystal silicon 207
single-crystalline solar cells 256
single-junction solar cells 37, 74
physics of 363–5
sizing
stand-alone systems 953–6
system 791–3
sky irradiance, angular distribution of 929
Skylab 1 414
SLI (starting, lighting, ignition) batteries 809, 834
small area champion cells 20
smart cut method 317
Sofrel flat-roof system 1018
soft loans 1095–6
solar altitude 909
solar arrays, space applications 431–41
solar azimuth 909
solar batteries 1052
solar cell 3, 5
spectral response of 100–2
solar cells
back-contact 108
band diagram of 120
basic structure 87
boundary conditions 87–9
circuit model 92, 102
color 1035
cost 26
current-voltage characteristic of 103
design 62
efficiency 99–100, 362
efficiency levels 242
efficiency versus impurity concentration 192
efficiency versus thickness 242
equilibrium conditions 86
fabrication 26
fundamentals 87–99
future-generation 403–6
higher-than-one quantum efficiency 140–1
intermediate band 144–8
lifetime 96–7
manufacturing 26
materials, BIPV 1030–4
model parameters 94
numerical modeling of 109–10
operation 63, 84, 98–9

Downloaded from https://onlinelibrary.wiley.com/doi/ by <Shibboleth-member@purdue.edu, Wiley Online Library on [25/08/2024]. See the Terms and Conditions (https://onlinelibrary.wiley.com/terms-and-conditions) on Wiley Online Library for rules of use; OA articles are governed by the applicable Creative Commons License

parasitic resistance effects of 102
performance 62, 96–8
physics 61–112
power density as function of time 422
properties of 95–6
schematic 4, 62
short-circuit current versus open-circuit voltage 105
silicon current feedstock to 175–9
technology 14
temperature effects on 104–6
Solar Cells and Optics for Photovoltaic Concentration 492, 498
solar constant 912
solar converters, technical efficiency limit for 131–2
solar declination 907
solar design 1038–9
Solar Development Capital 1102
Solar Development Foundation (SDF) 1102–3
solar electric farms 23
Solar Electric Light Fund (SELF) 1103
solar electricity, *see also* photovoltaic electricity
solar energy, availability 799
solar grade silicon 359
solar grade silicon routes 193–201
solar home systems (SHS) 56, 759–60, 813–14, 865, 873, 962–4, 1052, 1054,1083, 1088
cost breakdown 56, 772
solar hour 909
solar illumination 540
Solar International Management Inc. (SolarBank Program) 1103
solar irradiation, power distributions of 966
solar lantern for rural households in developing countries 758–9
solar modules
architecture 1035
color 1035
shipment by technology 176
solar office, Doxford, Sunderland 1019
solar radiation 6
and uncertainty 915–20
available for fixed flat-plate conventional PV modules 947
components 912–15
estimation of hourly irradiation from daily irradiation 925–7
on inclined surfaces 920–33
on surfaces on arbitrary orientation 927–33
parameters 919
Solar Research Corporation Pty Ltd 499
solar shading 1010
solar simulators 736–8
solar spectrum 915
Solar Terrestrial Probe (STP) Program Magnetospheric Multiscale (MMS) 440
solar time 911
solar zenith angle 909
SOLERAS 466–7
Solgreen flat-roof system 1031
solid-phase crystallization 343
solid solutions 184
solidification, silicon 179–82
Solidification by Planar Interface (SOPLIN) processes 246–7, 249
Solrif solar profile system 1029
space applications 780–3
high-efficiency III-V multijunction solar cells 363
silicon solar cells 425–6
solar arrays 431–41
thin-film solar cells 428
space charge region (SCR) 83, 339
space environment 417–20
space solar cells 413–31
calibration and measurement 424–5
challenge for 416–25
history 413
performance 416
technology requirements 418
space vehicles 363
spacecraft 59–60
Spanish National Meteorological Institute 916
specialty markets 7
spectral effects 955
spectral response 100–2
modeling 955
spectral responsivity, versus wavelength characteristics 701
spectral responsivity error sources
for measurement of light power 744
for measurement of photocurrent 743
for monochromatic light 745
spectral responsivity measurements 738–44
filter-based 739–41
grating-based systems 741–2
uncertainty 742–4
Spectrolab Spectrosum Large Area Pulsed Solar Simulator 425, 466, 499
spectrum-splitting 364–5, 406, 510, 543
spherical radiator 476
spray pyrolysis (SP) 30
spring equinox 907
Sri Lanka, rural electrification 1065–7
Staebler–Wronski effect 511–12

Downloaded from https://onlinelibrary.wiley.com/doi/ by <Shibboleth-member@purdue.edu, Wiley Online Library on [25/08/2024]. See the Terms and Conditions (https://onlinelibrary.wiley.com/terms-and-conditions) on Wiley Online Library for rules of use; OA articles are governed by the applicable Creative Commons License

STAMP program 982, 985, 989–90, 992
stand-alone systems 39, 937, 945
  inverters 789–90, 883
  reliability 956–63
  sizing 956–63
standard hydrogen electrode (SHE) 803
standard reporting conditions (SRC) 701–15
standard test conditions (STC) 905, 947, 950, 955
Standard Year 937
Stanford Advanced Back Contact cells 990
STAR 496
starting, lighting, ignition (SLI) battery 809, 834
state of charge (SOC) 809, 849
state-of-charge meters 843
stationary batteries 835
Stefan-Bolzman law 119
step-down converter 885–7, 889
  combination with inverters 890
step-down principle, integration into inverting process 892
step-up converter 887–9
Strategic Analysis of Manufacturing Product and Price *see* STAMP program
String Ribbon (STR) 230, 232, 235–7, 239–40, 243, 245, 288
structural façades 1010
structural glazing 1010
sub-array switching controller 869
substitutional impurities 184, 186
substrate texturing 537
summer solstice 907–8
Sun–Earth movement 906–12
Sun–Earth position 910, 912
Sun-tracking surfaces 945–6
sunlight 5, 40
SunPower Corporation 466, 496, 499–500
sun's rays incidence angle 912
Sun's trajectory maps 939
surface recombination 77, 96–7
surface recombination velocity (SRV) 258–9, 338
Surface Texture and enhanced Absorption with a back Reflector (STAR) cell 321
surface texturing 269
surface to volume relation (SV) 246
Survivable COncentrating Photovoltaic Array (SCOPA) 439
SUrvivable PowER System (SUPER) 439
switching controllers 867–70
Syndicate Bank (India) 1113
synthetic silica 159–60
system cost 980–4
  manufacturing-cost modeling 982–3
system-mounting structure 34
system sizing 791–3

Tafel equation 805
Tafel lines 805
tandem cells 134
T-CHEQ 879
  experimental set-up 880
  operating experience 879
  voltages and currents of 16 series-connected cells during charging 880
technical efficiency limit for solar converters 131–2
telecommunications 761–2
  autonomous power supply system for 856
Telstar 414
temperature coefficients 423
  for module and cell temperature estimation 956
temperature dependence, high-efficiency III-V multijunction solar cells 380–2
temperature determination under considered operating conditions 952
temperature effects on solar cells 104–6
terminal characteristics 89–92
terrestrial applications 363
terrestrial concentrator systems, implementation of multijunction III-V cells 406–7
terrestrial energy production, high-efficiency III-V multijunction solar cells 363
terrestrial spectrum 407
texturing 269, 273, 539
thermal environment 420–3
thermal modeling of crystallization techniques 245–7
thermionic emission model 537
thermodynamic consistence of Shockley–Queisser photovoltaic cell 126–9
thermodynamic converters 790
thermodynamic current densities 115, 117
thermodynamic currents 117
thermodynamic efficiency 125
thermodynamic fluxes 119
thermodynamic functions of electrons 119
thermodynamic functions of radiation 117–19
thermodynamic variables 117–19
thermodynamics
  background 114–19

Downloaded from https://onlinelibrary.wiley.com/doi/ by <Shibboleth-member@purdue.edu, Wiley Online Library on [25/08/2024]. See the Terms and Conditions (https://onlinelibrary.wiley.com/terms-and-conditions) on Wiley Online Library for rules of use; OA articles are governed by the applicable Creative Commons License

basic relationships 114–16
laws of 116, 130
thermoelectric generators (TEG) 790
thermophotonic (TPH) converter 136–40
thermophotovoltaic (TPV) conversion 135–6, 468–9
thermophotovoltaic (TPV) generators 790
thin-film progress and challenges 27–31
thin-film PV materials 1034
thin-film PV modules 53
thin-film silicon solar cells 307–57
carrier collection 316
carrier generation 316
deposition techniques 341
design concepts 324–53
electronic modeling 333–41
generic device structure 325
grain enhancement 343–50
mechanical support 316–17
multicrystalline-Si substrates 320
non-Si substrates 321–4
optical properties 328
overview 307–10
processing considerations 350–3
review of current position 310–24
single-crystal Si substrates 317–20
summary from optical modeling 333
summary of types 318–19
surface structures 312
surface texture 311–12
thermodynamic considerations 311
thin-film solar cells 27–9
CdTe *see* CdTe thin-film solar cells; silicon thin-film solar cells
space applications 428–31
thin-film technology 40
thin-film transistor (TFT) 350
third generation PV converters 148
time variation of generated daily energy 958
TiO_2 274
colloid preparation 678–9
dye fixation onto film 680
electrode preparation 679–80
electron transport 677–8
photoelectrode 666
solar cell, photocurrent–voltage curve 674
Tokyo A&T University 500
total harmonic distortion (THD) 890, 897, 899
total irradiation 958
TPH converter 148–9
TPV converter 139, 148–9
trackers *see* concentrators
traction batteries 835
transition metals (TM) 351
impurities in silicon 188–90
translation equations to reference conditions 719–20
transmission line measurements 400
transparent conducting oxide (TCO) 440, 509–10, 539–40, 555
transparent conducting oxide (TCO)-coated glass substrate 664–6
travel time of electron under short-circuit conditions 531
trichlorosilane 168
tri-crystalline silicon (tri-Si) 211–13, 251
Triodos Bank NV 1108
triple-junction cells 426, 506
triple-junction III-V semiconductor cells 416
triple-junction module 512
triple-junction *nip* substrate-type solar cells 547
Tropical Rainfall Measuring Mission (TRMM) 433
true solar time 909
TU Electric Power Park 467
tubular-plate battery 844
tunnel junction 548
tunnel-junction interconnects (TJICs) 379, 396–7
twin boundaries 183
Typical Meteorological Year (TMY) 937–8, 960

uncertainty
and solar radiation 915–20
spectral responsivity measurements 742–4
uncertainty estimates, reference cell calibration procedures 726–7
uncertainty parameters 919
underdevelopment, breaking the chains of 1046–8
UNDP 1087–8
Sustainable Energy & Environment Division (SEED) 1103–4
UNEP 1088
Collaborating Centre on Energy and Environment 1104
uninterruptible power supplies (UPS) 34, 835
Union Carbide process
for semiconductor grade silicon 172–3
simplification 198–201
United States, PV programs 1096–7
University of New South Wales (UNSW) 324

Downloaded from https://onlinelibrary.wiley.com/doi/ by <Shibboleth-member@purdue.edu, Wiley Online Library on [25/08/2024]. See the Terms and Conditions (https://onlinelibrary.wiley.com/terms-and-conditions) on Wiley Online Library for rules of use; OA articles are governed by the applicable Creative Commons License

University of Reading 500
US Agency for International Development (USAID) 1111
utility systems 779

vacancies 184
valence band (VB) 4, 66–7, 74, 119
valve-regulated lead acid (VRLA) batteries 831–2, 846
Vanguard I 413–16
vapor deposition (VD) 30
VHF glow discharge deposition 524–5
village power supply systems 766–7
vision or view factor 118
volatiles 169
voltage shaping by digital synthesis 890–2
VTZ Green Money for the Blue Planet Ltd. 1108

wafer cost 206xx
wafer material for crystalline silicon 245
wafer quality 205
  and saw damage 229–30
wafering 223–30, 280–1
  cost and size considerations 230
  microscopic process 226–8
  multi-wire technique 224–6
water pumping
  for irrigation 1083
  Sahel 1067–8
water purification systems 768
wavelength dependence of photon conversion efficiency 363–4
WEB *see* dendritic WEB
well-integrated systems 1014–18
Wind Fund Plc, The 1108
window layer 530
Winrock International 1104, 1113–14
winter solstice 908
World Bank solar home system projects 1088
World Photovoltaic Scale (WPVS) 728
wrought alloys 159

xerography 505
X-ray diffraction 345–8

Zentrum fur Sonnenenergie und Wasserstoff Forschung Baden Wurttenberg (ZSW) 500
zero-energy project, Etten-Leur 1024
zinc dopant 390–1
zincblende lattice 64
zone-melting recrystallization (ZMR) 315, 350

Index compiled by Geoffrey Jones.

Downloaded from https://onlinelibrary.wiley.com/doi/ by <Shibboleth-member@purdue.edu>, Wiley Online Library on [25/08/2024]. See the Terms and Conditions (https://onlinelibrary.wiley.com/terms-and-conditions) on Wiley Online Library for rules of use; OA articles are governed by the applicable Creative Commons License

Attachment D-3

LIBRARY OF CONGRESS
0 010 847 836 6







HANDBOOK OF PHOTOVOLTAIC SCIENCE AND ENGINEERING

Edited by
Antonio Luque, *Universidad Politécnica de Madrid, Spain*
Steven Hegedus, *University of Delaware, USA*

You will not find a more comprehensive reference on solar energy!

Handbook of Photovoltaic Science and Engineering **incorporates the most recent technological advances and research developments in photovoltaics. All topics relating to the photovoltaic (PV) industry are discussed and each chapter has been written by an internationally-known expert in the field.**

Each chapter is written to be accessible to both beginners and experts. Encompassing a review of past work and the fundamentals in solar electric science, this outstanding reference provides an invaluable resource to practitioners, consultants, researchers and students in the PV engineering industry.

ISBN 0-471-49196-9
9 780471 491965

WILEY
wiley.com

Detailed treatment covers:

- scientific basis of the photovoltaic effect and solar cell operation.
- the production of solar silicon and of silicon-based solar cells and modules.
- the science and technology of up-and-coming thin film PV technologies.
- how choice of semiconductor materials and their production influence costs and performance.
- high-performance approaches for concentrators and space applications.
- new types of organic dye-based solar cells.
- making measurements on solar cells and modules and how to relate results under standardised test conditions to real outdoor performance.
- photovoltaic system installation and operation of components such as inverters and batteries.
- architectural applications of building-integrated PV.
- finance and the role of investors: public funding and policy in promoting PV world-wide.



(Editors)

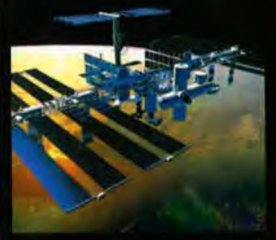




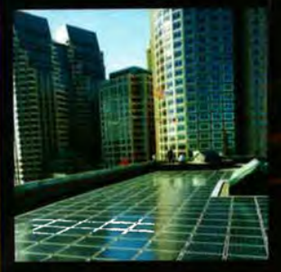
HANDBOOK OF PHOTOVOLTAIC SCIENCE AND ENGINEERING

TK 8322
.H33
2003
Copy 1

WILEY







HANDBOOK OF PHOTOVOLTAIC SCIENCE AND ENGINEERING

Edited by Antonio Luque and Steven Hegedus


LIBRARY OF CONGRESS
1800

Handbook of Photovoltaic Science and Engineering

Edited by

Antonio Luque
Instituto de Energía Solar, Universidad Politécnica de Madrid, Spain

and

Steven Hegedus
Institute of Energy Conversion, University of Delaware, USA



WILEY

Petitioner Canadian Solar (USA) Inc., Ex. 1035, p. 2524

Copyright © 2003

John Wiley & Sons Ltd, The Atrium, Southern Gate, Chichester,
West Sussex PO19 8SQ, England

Telephone (+44) 1243 779777

Email (for orders and customer service enquiries): cs-books@wiley.co.uk
Visit our Home Page on www.wileyeurope.com or www.wiley.com

All Rights Reserved. No part of this publication may be reproduced, stored in a retrieval system or transmitted in any form or by any means, electronic, mechanical, photocopying, recording, scanning or otherwise, except under the terms of the Copyright, Designs and Patents Act 1988 or under the terms of a licence issued by the Copyright Licensing Agency Ltd, 90 Tottenham Court Road, London W1T 4LP, UK, without the permission in writing of the Publisher. Requests to the Publisher should be addressed to the Permissions Department, John Wiley & Sons Ltd, The Atrium, Southern Gate, Chichester, West Sussex PO19 8SQ, England, or emailed to permreq@wiley.co.uk, or faxed to (+44) 1243 770620.

This publication is designed to provide accurate and authoritative information in regard to the subject matter covered. It is sold on the understanding that the Publisher is not engaged in rendering professional services. If professional advice or other expert assistance is required, the services of a competent professional should be sought.

Other Wiley Editorial Offices

John Wiley & Sons Inc., 111 River Street, Hoboken, NJ 07030, USA

Jossey-Bass, 989 Market Street, San Francisco, CA 94103-1741, USA

Wiley-VCH Verlag GmbH, Boschstr. 12, D-69469 Weinheim, Germany

John Wiley & Sons Australia Ltd, 33 Park Road, Milton, Queensland 4064, Australia

John Wiley & Sons (Asia) Pte Ltd, 2 Clementi Loop #02-01, Jin Xing Distripark, Singapore 129809

John Wiley & Sons Canada Ltd, 22 Worcester Road, Etobicoke, Ontario, Canada M9W 1L1

Wiley also publishes its books in a variety of electronic formats. Some content that appears in print may not be available in electronic books.

LIBRARY OF CONGRESS JUL 1 2003

Library of Congress Cataloging-in-Publication Data

Handbook of photovoltaic science and engineering / edited by Antonio Luque and Steven Hegedus.
p. cm.
Includes bibliographical references and index.
ISBN 0-471-49196-9 (alk. paper)
1. Photovoltaic cells. 2. Photovoltaic power generation. I. Luque, A. (Antonio) II. Hegedus, Steven.

TK8322 .H33 2003
621.31'244 – dc21

2002191033

British Library Cataloguing in Publication Data

A catalogue record for this book is available from the British Library

ISBN 0-471-49196-9

Typeset in 10/12 Times by Laserwords Private Limited, Chennai, India
Printed and bound in Great Britain by Antony Rowe Ltd, Chippenham, Wiltshire
This book is printed on acid-free paper responsibly manufactured from sustainable forestry in which at least two trees are planted for each one used for paper production.

xxiii

olar Electricity 1

1
3
5
11
15
Ianufacturing? 19
20
23
27
31
32
37
39
41

nent 45

45
lectricity
ltaics 48
54
ly - The
54
57
- The
57
strial Dimension
59
60

3 The Physics of the Solar Cell **61**
Jeffery L. Gray
3.1 Introduction 61
3.2 Fundamental Properties of Semiconductors 64
3.2.1 Crystal Structure 64
3.2.2 Energy Band Structure 65
3.2.3 Conduction-band and Valence-band Densities of State 66
3.2.4 Equilibrium Carrier Concentrations 67
3.2.5 Light Absorption 70
3.2.6 Recombination 74
3.2.7 Carrier Transport 78
3.2.8 Semiconductor Equations 81
3.2.9 Minority-carrier Diffusion Equation 82
3.3 *PN*-Junction Diode Electrostatics 83
3.4 Solar Cell Fundamentals 87
3.4.1 Solar Cell Boundary Conditions 87
3.4.2 Generation Rate 89
3.4.3 Solution of the Minority-carrier Diffusion Equation 89
3.4.4 Terminal Characteristics 89
3.4.5 Solar Cell $I-V$ Characteristics 92
3.4.6 Properties of Efficient Solar Cells 95
3.4.7 Lifetime and Surface Recombination Effects 96
3.4.8 An Analogy for Understanding Solar Cell Operation: A Partial Summary 98
3.5 Additional Topics 99
3.5.1 Efficiency and Band gap 99
3.5.2 Spectral Response 100
3.5.3 Parasitic Resistance Effects 102
3.5.4 Temperature Effects 104
3.5.5 Concentrator Solar Cells 106
3.5.6 High-level Injection 107
3.5.7 *p-i-n* Solar Cells 109
3.5.8 Detailed Numerical Modeling 109
3.6 Summary 110
References 111

4 Theoretical Limits of Photovoltaic Conversion **113**
Antonio Luque and Antonio Martí
4.1 Introduction 113
4.2 Thermodynamic Background 114
4.2.1 Basic Relationships 114
4.2.2 The Two Laws of Thermodynamics 116
4.2.3 Local Entropy Production 116
4.2.4 An Integral View 117
4.2.5 Thermodynamic Functions of Radiation 117
4.2.6 Thermodynamic Functions of Electrons 119
4.3 Photovoltaic Converters 120

Petitioner Canadian Solar (USA) Inc., Ex. 1035, p. 2527

4.3.1 The Balance Equation of a PV Converter 120
4.3.2 The Monochromatic Cell 124
4.3.3 Thermodynamic Consistence of the Shockley–Queisser Photovoltaic Cell 126
4.3.4 Entropy Production in the Whole Shockley–Queisser Solar Cell 129
4.4 The Technical Efficiency Limit for Solar Converters 131
4.5 Very High Efficiency Concepts 132
4.5.1 Multijunction Solar Cells 132
4.5.2 Thermophotovoltaic Converters 135
4.5.3 Thermophotonic Converters 136
4.5.4 Higher-than-one Quantum Efficiency Solar Cells 140
4.5.5 Hot Electron Solar Cells 141
4.5.6 Intermediate Band Solar Cell 144
4.6 Conclusions 148
References 149

5 Solar Grade Silicon Feedstock 153
Bruno Ceccaroli and Otto Lohne
5.1 Introduction 153
5.2 Silicon 154
5.2.1 Physical Properties of Silicon Relevant to Photovoltaics 154
5.2.2 Chemical Properties Relevant to Photovoltaics 156
5.2.3 Health Factors 156
5.2.4 History and Applications of Silicon 157
5.3 Production of Metallurgical Grade Silicon 161
5.3.1 The Carbothermic Reduction of Silica 161
5.3.2 Refining 163
5.3.3 Casting and Crushing 166
5.3.4 Economics 167
5.4 Production of Semiconductor Grade Silicon (Polysilicon) 167
5.4.1 The Siemens Process 168
5.4.2 The Union Carbide Process 172
5.4.3 The Ethyl Corporation Process 173
5.4.4 Economics and Business 175
5.5 Current Silicon Feedstock to Solar Cells 175
5.6 Requirements of Silicon for Crystalline Solar Cells 179
5.6.1 Solidification 179
5.6.2 Effect of Crystal Imperfections 182
5.6.3 Effect of Various Impurities 186
5.7 Routes to Solar Grade Silicon 193
5.7.1 Crystallisation 193
5.7.2 Upgrading Purity of the Metallurgical Silicon Route 194
5.7.3 Simplification of the Polysilicon Process 198
5.7.4 Other Methods 201
5.8 Conclusions 201
References 202

Petitioner Canadian Solar (USA) Inc., Ex. 1035, p. 2528

6 Bulk Crystal Growth and Wafering for PV **205**
W. Koch, A. L. Endrös, D. Franke, C. Häßler, J. P. Kalejs and H. J. Möller
6.1 Introduction 205
6.2 Bulk Monocrystalline Material 206
6.2.1 Cz Growth of Single-crystal Silicon 207
6.2.2 Tri-crystalline Silicon 211
6.3 Bulk Multicrystalline Silicon 214
6.3.1 Ingot Fabrication 214
6.3.2 Doping 216
6.3.3 Crystal Defects 217
6.3.4 Impurities 219
6.4 Wafering 223
6.4.1 Multi-wire Wafering Technique 224
6.4.2 Microscopic Process of Wafering 226
6.4.3 Wafer Quality and Saw Damage 229
6.4.4 Cost and Size Considerations 230
6.5 Silicon Ribbon and Foil Production 230
6.5.1 Process Description 232
6.5.2 Productivity Comparisons 238
6.5.3 Manufacturing Technology 239
6.5.4 Ribbon Material Properties and Solar Cells 240
6.5.5 Ribbon/Foil Technology – Future Directions 243
6.6 Numerical Simulations of Crystal Growth Techniques 244
6.6.1 Simulation Tools 245
6.6.2 Thermal Modelling of Silicon Crystallisation Techniques 245
6.6.3 Simulation of Bulk Silicon Crystallisation 247
6.6.4 Simulation of Silicon Ribbon Growth 249
6.7 Conclusions 251
6.8 Acknowledgement 252
References 252

7 Crystalline Silicon Solar Cells and Modules **255**
Ignacio Tobías, Carlos del Cañizo and Jesús Alonso
7.1 Introduction 255
7.2 Crystalline Silicon as a Photovoltaic Material 257
7.2.1 Bulk Properties 257
7.2.2 Surfaces 257
7.3 Crystalline Silicon Solar Cells 259
7.3.1 Cell Structure 259
7.3.2 Substrate 260
7.3.3 The Front Surface 263
7.3.4 The Back Surface 266
7.3.5 Size Effects 266
7.3.6 Cell Optics 268
7.3.7 Performance Comparison 270

Petitioner Canadian Solar (USA) Inc., Ex. 1035, p. 2529

7.4 Manufacturing Process 271
7.4.1 Process Flow 271
7.4.2 Screen-printing Technology 276
7.4.3 Throughput and Yield 279
7.5 Variations to the Basic Process 280
7.5.1 Thin Wafers 280
7.5.2 Back Surface Passivation 281
7.5.3 Improvements to the Front Emitter 281
7.5.4 Rapid Thermal Processes 282
7.6 Multicrystalline Cells 283
7.6.1 Gettering in mc Solar Cells 283
7.6.2 Passivation with Hydrogen 283
7.6.3 Optical Confinement 285
7.7 Other Industrial Approaches 288
7.7.1 Silicon Ribbons 288
7.7.2 Heterojunction with Intrinsic Thin Layer 288
7.7.3 Buried Contact Technology 289
7.8 Crystalline Silicon Photovoltaic Modules 291
7.8.1 Cell Matrix 291
7.8.2 The Layers of the Module 292
7.8.3 Lamination and Curing 293
7.8.4 Postlamination Steps 294
7.8.5 Special Modules 294
7.9 Electrical and Optical Performance of Modules 295
7.9.1 Electrical and Thermal Characteristics 295
7.9.2 Fabrication Spread and Mismatch Losses 297
7.9.3 Local Shading and Hot Spot Formation 297
7.9.4 Optical Properties 300
7.10 Field Performance of Modules 301
7.10.1 Lifetime 301
7.10.2 Qualification 301
7.11 Conclusions 302
References 303

8 Thin-film Silicon Solar Cells 307
Bhushan Sopori
8.1 Introduction 307
8.2 A Review of Current Thin-film Si Cells 310
8.2.1 Single-crystal Films Using Single-crystal Si Substrates 317
8.2.2 Multicrystalline-Si Substrates 320
8.2.3 Non-Si Substrates 321
8.3 Design Concepts of TF-Si Solar Cells 324
8.3.1 Light-trapping in Thin Si Solar Cells 326
8.3.2 Description of PV Optics 327
8.3.3 Electronic Modeling 333
8.3.4 Methods of Making Thin-Si Films for Solar Cells 341

Petitioner Canadian Solar (USA) Inc., Ex. 1035, p. 2530

8.3.5 Methods of Grain Enhancement of a-Si/μc-Si Thin Films 343
8.3.6 Processing Considerations for TF-Si Solar Cell Fabrication 350
8.4 Conclusion 353
References 354

9 High-Efficiency III-V Multijunction Solar Cells 359
J. M. Olson, D. J. Friedman and Sarah Kurtz
9.1 Introduction 359
9.2 Applications 363
9.2.1 Space Solar Cells 363
9.2.2 Terrestrial Energy Production 363
9.3 Physics of III-V Multijunction and Single-junction Solar Cells 363
9.3.1 Wavelength Dependence of Photon Conversion Efficiency 363
9.3.2 Theoretical Limits to Multijunction Efficiencies 364
9.3.3 Spectrum Splitting 364
9.4 Cell Configuration 365
9.4.1 Four-terminal 365
9.4.2 Three-terminal Voltage-matched Interconnections 366
9.4.3 Two-terminal Series-connected (Current Matched) 366
9.5 Computation of Series-Connected Device Performance 366
9.5.1 Overview 366
9.5.2 Top and Bottom Subcell QE and J_{SC} 367
9.5.3 Multijunction $J-V$ Curves 368
9.5.4 Efficiency versus Band Gap 370
9.5.5 Top-cell Thinning 372
9.5.6 Current-matching Effect on Fill Factor and V_{OC} 373
9.5.7 Spectral Effects 374
9.5.8 AR Coating Effects 375
9.5.9 Concentration 376
9.5.10 Temperature Dependence 380
9.6 Materials Issues Related to GaInP/GaAs/Ge Solar Cells 382
9.6.1 Overview 382
9.6.2 MOCVD 382
9.6.3 GaInP Solar Cells 383
9.6.4 GaAs Cells 393
9.6.5 Ge Cells 395
9.6.6 Tunnel-junction Interconnects 396
9.6.7 Chemical Etchants 397
9.6.8 Materials Availability 398
9.7 Troubleshooting 398
9.7.1 Characterization of Epilayers 398
9.7.2 Transmission Line Measurements 400
9.7.3 I-V Measurements of Multijunction Cells 400
9.7.4 Evaluation of Morphological Defects 401
9.7.5 Device Diagnosis 401

Petitioner Canadian Solar (USA) Inc., Ex. 1035, p. 2531

9.8 Future-generation Solar Cells 403
9.8.1 Refinements to the GaInP/GaAs/Ge Cell 403
9.8.2 Mechanical Stacks 404
9.8.3 Growth on Other Substrates 405
9.8.4 Spectrum Splitting 406
9.9 Implementation into Terrestrial Systems 406
9.9.1 Economic Issues 406
9.9.2 Concentrator Systems 406
9.9.3 Terrestrial Spectrum 407
References 407

10 Space Solar Cells and Arrays 413
Sheila Bailey and Ryne Raffaelle
10.1 The History of Space Solar Cells 413
10.1.1 Vanguard I to Deep Space I 413
10.2 The Challenge for Space Solar Cells 416
10.2.1 The Space Environment 417
10.2.2 Thermal Environment 420
10.2.3 Solar Cell Calibration and Measurement 424
10.3 Silicon Solar Cells 425
10.4 III-V Solar Cells 426
10.4.1 Thin-film Solar Cells 428
10.5 Space Solar Arrays 431
10.5.1 Body-mounted Arrays 432
10.5.2 Rigid Panel Planar Arrays 432
10.5.3 Flexible Fold-out Arrays 433
10.5.4 Thin-film or Flexible Roll-out Arrays 435
10.5.5 Concentrating Arrays 436
10.5.6 High-temperature/Intensity Arrays 438
10.5.7 Electrostatically Clean Arrays 439
10.5.8 Mars Solar Arrays 440
10.5.9 Power Management and Distribution (PMAD) 441
10.6 Future Cell and Array Possibilities 441
10.6.1 Low Intensity Low Temperature (LILT) Cells 441
10.6.2 Quantum Dot Solar Cells 442
10.6.3 Integrated Power Systems 442
10.6.4 High Specific Power Arrays 443
10.6.5 High-radiation Environment Solar Arrays 443
10.7 Power System Figures of Merit 444
References 446

11 Photovoltaic Concentrators 449
Richard M. Swanson
11.1 Introduction 449
11.1.1 The Concentrator Dilemma 450
11.2 Basic Types of Concentrators 452
11.2.1 Types of Optics 452
11.2.2 Concentration Ratio 455

Petitioner Canadian Solar (USA) Inc., Ex. 1035, p. 2532

11.2.3 Types of Tracking 456
11.2.4 Static Concentrators 456
11.3 Historical Overview 460
11.3.1 The Sandia National Laboratories Concentrator Program (1976 to 1993) 461
11.3.2 The Martin Marietta Point-focus Fresnel System 462
11.3.3 The Entech Linear-focus Fresnel System 463
11.3.4 Other Sandia Projects 465
11.3.5 The Concentrator Initiative 465
11.3.6 Early Demonstration Projects 466
11.3.7 The EPRI High-concentration Program 467
11.3.8 Other Concentrator Programs 471
11.3.9 History of Performance Improvements 472
11.4 Optics of Concentrators 474
11.4.1 Basics 474
11.4.2 Reflection and Refraction 478
11.4.3 The Parabolic Concentrator 479
11.4.4 The Compound Parabolic Concentrator 482
11.4.5 The V-trough Concentrator 483
11.4.6 Refractive Lenses 485
11.4.7 Secondary Optics 489
11.4.8 Static Concentrators 491
11.4.9 Innovative Concentrators 492
11.4.10 Issues in Concentrator Optics 494
11.5 Current Concentrator Activities 495
11.5.1 Amonix 496
11.5.2 Australian National University 496
11.5.3 BP Solar and the Polytechnical University of Madrid 496
11.5.4 Entech 497
11.5.5 Fraunhofer-Institut fur Solare Energiesysteme 497
11.5.6 Ioffe Physical-Technical Institute 498
11.5.7 National Renewable Energy Laboratory 498
11.5.8 Polytechnical University of Madrid 498
11.5.9 Solar Research Corporation 499
11.5.10 Spectrolab 499
11.5.11 SunPower Corporation 499
11.5.12 University of Reading 500
11.5.13 Tokyo A&T University 500
11.5.14 Zentrum fur Sonnenenergie und Wasserstoff Forschung Baden Wurttenberg (ZSW) 500
References 500

12 Amorphous Silicon–based Solar Cells 505
Xunming Deng and Eric A. Schiff
12.1 Overview 505
12.1.1 Amorphous Silicon: The First Bipolar Amorphous Semiconductor 505

Petitioner Canadian Solar (USA) Inc., Ex. 1035, p. 2533

12.1.2 Designs for Amorphous Silicon Solar Cells: A Guided Tour 508
12.1.3 Staebler–Wronski Effect 511
12.1.4 Synopsis of this Chapter 512
12.2 Atomic and Electronic Structure of Hydrogenated Amorphous Silicon 513
12.2.1 Atomic Structure 513
12.2.2 Defects and Metastability 514
12.2.3 Electronic Density-of-states 515
12.2.4 Bandtails, Bandedges, and Band Gaps 516
12.2.5 Defects and Gap States 517
12.2.6 Doping 518
12.2.7 Alloying and Optical Properties 518
12.3 Depositing Amorphous Silicon 520
12.3.1 Survey of Deposition Techniques 520
12.3.2 RF Glow Discharge Deposition 521
12.3.3 Glow Discharge Deposition at Different Frequencies 523
12.3.4 Hot-wire Chemical Vapor Deposition 525
12.3.5 Other Deposition Methods 526
12.3.6 Hydrogen Dilution 526
12.3.7 Alloys and Doping 528
12.4 Understanding a-Si *pin* Cells 528
12.4.1 Electronic Structure of a *pin* Device 528
12.4.2 Photocarrier Drift in Absorber Layers 530
12.4.3 Absorber Layer Design of a *pin* Solar Cell 533
12.4.4 The Open-circuit Voltage 534
12.4.5 Optical Design of a-Si:H Solar Cells 537
12.4.6 Cells under Solar Illumination 540
12.4.7 Light-soaking Effects 541
12.5 Multiple-Junction Solar Cells 542
12.5.1 Advantages of Multiple-junction Solar Cells 542
12.5.2 Using Alloys for Cells with Different Band Gaps 544
12.5.3 a-Si/a-SiGe Tandem and a-Si/a-SiGe/a-SiGe Triple-junction Solar Cells 546
12.5.4 Microcrystalline Silicon Solar Cells 551
12.5.5 Micromorph and Other μc-Si-based Multijunction Cells 552
12.6 Module Manufacturing 553
12.6.1 Continuous Roll-to-roll Manufacturing on Stainless Steel Substrates 553
12.6.2 a-Si Module Production on Glass Superstrate 555
12.6.3 Manufacturing Cost, Safety, and Other Issues 556
12.6.4 Module Performance 557
12.7 Conclusions and Future Projections 558
12.7.1 Status and Competitiveness of a-Si Photovoltaics 558
12.7.2 Critical Issues for Further Enhancement and Future Potential 559
12.8 Acknowledgments 559
References 560

Petitioner Canadian Solar (USA) Inc., Ex. 1035, p. 2534

13 Cu(InGa)Se_2 Solar Cells **567**
William N. Shafarman and Lars Stolt
13.1 Introduction 567
13.2 Material Properties 570
13.2.1 Structure and Composition 571
13.2.2 Optical Properties 574
13.2.3 Electrical Properties 574
13.2.4 The Surface and Grain Boundaries 576
13.2.5 Substrate Effects 578
13.3 Deposition Methods 578
13.3.1 Substrates 579
13.3.2 Back Contact 580
13.3.3 Coevaporation of Cu(InGa)Se_2 580
13.3.4 Two-step Processes 583
13.3.5 Other Deposition Approaches 584
13.4 Junction and Device Formation 584
13.4.1 Chemical Bath Deposition 585
13.4.2 Interface Effects 586
13.4.3 Other Deposition Methods 587
13.4.4 Alternative Buffer Layers 588
13.4.5 Transparent Contacts 590
13.4.6 Buffer Layers 591
13.4.7 Device Completion 592
13.5 Device Operation 592
13.5.1 Light-generated Current 593
13.5.2 Recombination 595
13.5.3 The Cu(InGa)Se_2/CdS Interface 599
13.5.4 Wide and Graded Band Gap Devices 600
13.6 Manufacturing Issues 602
13.6.1 Processes and Equipment 602
13.6.2 Module Fabrication 604
13.6.3 Module Performance 604
13.6.4 Production Costs 607
13.6.5 Environmental Concerns 608
13.7 The Cu(InGa)Se_2 Outlook 609
References 611

14 Cadmium Telluride Solar Cells **617**
Brian E. McCandless and James R. Sites
14.1 Introduction 617
14.2 CdTe Properties and Thin-film Fabrication Methods 621
14.2.1 Condensation/Reaction of Cd and Te_2 Vapors on a Surface 628
14.2.2 Galvanic Reduction of Cd and Te Ions at a Surface 629
14.2.3 Precursor Reaction at a Surface 630
14.3 CdTe Thin-Film Solar Cells 631
14.3.1 Window Layers 631
14.3.2 CdTe Absorber Layer and $CdCl_2$ Treatment 633

14.3.3 CdS/CdTe Intermixing 637
14.3.4 Back Contact 642
14.3.5 Solar Cell Characterization 644
14.3.6 Summary of CdTe-cell Status 650
14.4 CdTe Modules 651
14.5 The Future of CdTe-based Solar Cells 653
14.6 Acknowledgments 657
References 657

15 Dye-sensitized Solar Cells 663
Kohjiro Hara and Hironori Arakawa
15.1 Introduction to Dye-Sensitized Solar Cells (DSSC) 663
15.1.1 Background 663
15.1.2 Structure and Materials 664
15.1.3 Mechanism 670
15.1.4 Charge-transfer Kinetics 673
15.1.5 Characteristics 678
15.2 DSSC Fabrication ($\eta = 8\%$) 678
15.2.1 Preparation of TiO_2 Colloid 678
15.2.2 Preparation of the TiO_2 Electrode 679
15.2.3 Dye Fixation onto the TiO_2 Film 680
15.2.4 Redox Electrolyte 681
15.2.5 Counter Electrode 681
15.2.6 Assembling the Cell and Cell Performance 681
15.3 New Developments 682
15.3.1 New Oxide Semiconductor Film Photoelectrodes 683
15.3.2 New Dye Photosensitizers 683
15.3.3 New Electrolytes 688
15.3.4 Quasi-solid-state and Solid-state DSSCs 689
15.4 Approach to Commercialization 691
15.4.1 Stability of the DSSC 691
15.4.2 Module Fabrication and Other Subjects for Commercialization 694
15.5 Summary and Prospects 695
References 696

16 Measurement and Characterization of Solar Cells and Modules 701
Keith Emery
16.1 Introduction 701
16.2 Rating PV Performance 701
16.2.1 Standard Reporting Conditions 702
16.2.2 Alternative Peak Power Ratings 715
16.2.3 Energy-based Performance Rating Methods 716
16.2.4 Translation Equations to Reference Conditions 719
16.3 Current Versus Voltage Measurements 721
16.3.1 Measurement of Irradiance 721
16.3.2 Simulator-based $I-V$ Measurements: Theory 722

Petitioner Canadian Solar (USA) Inc., Ex. 1035, p. 2536

16.3.3 Primary Reference Cell Calibration Methods 723
16.3.4 Uncertainty Estimates in Reference Cell Calibration Procedures 726
16.3.5 Intercomparison of Reference Cell Calibration Procedures 727
16.3.6 Multijunction Cell Measurement Procedures 728
16.3.7 Cell and Module $I-V$ Systems 731
16.3.8 Solar Simulators 736
16.4 Spectral Responsivity Measurements 738
16.4.1 Filter-based Systems 739
16.4.2 Grating-based Systems 741
16.4.3 Spectral Responsivity Measurement Uncertainty 742
16.5 Module Qualification and Certification 745
Acknowledgements 746
References 747

17 Photovoltaic Systems **753**
Klaus Preiser
17.1 Introduction to PV Systems and Various Forms of Application 753
17.2 Principles of photovoltaic Power System Configuration and their Application 755
17.2.1 Grid-independent Photovoltaic Systems for Small Devices and Appliances 755
17.2.2 Photovoltaic Systems for Remote Consumers of Medium and Large Size 761
17.2.3 Decentralised Grid-connected Photovoltaic Systems 774
17.2.4 Central Grid-connected Photovoltaic Systems 779
17.2.5 Space Application 780
17.3 Components for PV Systems 784
17.3.1 Battery Storage 784
17.3.2 Charge Controller 787
17.3.3 Inverters 788
17.3.4 Auxiliary Generators 790
17.3.5 System Sizing 791
17.3.6 Energy-saving Domestic Appliances 793
17.4 Future Developments in Photovoltaic System Technology 794
17.4.1 Future Developments in Off-grid Power Supply with Photovoltaics 794
17.4.2 Future Developments in Grid-connected Photovoltaic Systems 796
References 797

18 Electrochemical Storage for Photovoltaics **799**
Dirk Uwe Sauer
18.1 Introduction 799
18.2 General Concept of Electrochemical Batteries 801
18.2.1 Fundamentals of Electrochemical Cells 801

Petitioner Canadian Solar (USA) Inc., Ex. 1035, p. 2537

18.2.2 Batteries with Internal and External Storage 807
18.2.3 Commonly Used Technical Terms and Definitions 809
18.2.4 Definitions of Capacity and State of Charge 811
18.3 Typical Operation Conditions of Batteries in PV Applications 812
18.3.1 An Example of an Energy Flow Analysis 812
18.3.2 Classification of Battery-operating Conditions in PV Systems 813
18.4 Secondary Electrochemical Accumulators with Internal Storage 817
18.4.1 Overview 817
18.4.2 NiCd Batteries 818
18.4.3 Nickel-metal Hydride (NiMH) Batteries 821
18.4.4 Rechargeable Alkali Mangan (RAM) Batteries 822
18.4.5 Lithium-ion and Lithium-polymer Batteries 822
18.4.6 Double-layer Capacitors 824
18.4.7 The Lead Acid Battery 826
18.5 Secondary Electrochemical Battery Systems with External Storage 849
18.5.1 Redox-flow Batteries 850
18.5.2 Hydrogen/Oxygen Storage Systems 852
18.6 Investment and Lifetime Cost Considerations 857
18.7 Conclusion 859
References 860

19 Power Conditioning for Photovoltaic Power Systems 863
Jürgen Schmid, Heribert Schmidt
19.1 Charge Controllers and Monitoring Systems for Batteries in PV Power Systems 864
19.1.1 Charge Controllers 864
19.1.2 Charge Equaliser for Long Battery Strings 877
19.2 Inverters 881
19.2.1 General Characteristics of PV Inverters 881
19.2.2 Inverters for Grid-connected Systems 881
19.2.3 Inverters for Stand-alone Operation 883
19.2.4 Inverter Principles 884
19.2.5 Power Quality of Inverters 896
19.2.6 Active Quality Control in the Grid 900
19.2.7 Safety Aspects with Grid-connected Inverters 900
19.3 Acknowledgement 902
References 902

20 Energy Collected and Delivered by PV Modules 905
Eduardo Lorenzo
20.1 Introduction 905
20.2 Movement between Sun and Earth 906
20.3 Solar Radiation Components 912
20.4 Solar Radiation Data and Uncertainty 915
20.4.1 Clearness Index 920
20.5 Radiation on Inclined Surfaces 920

Petitioner Canadian Solar (USA) Inc., Ex. 1035, p. 2538

20.5.1 Estimation of the Direct and Diffuse Components of Horizontal Radiation, Given the Global Radiation 920
20.5.2 Estimation of the Hourly Irradiation from the Daily Irradiation 925
20.5.3 Estimation of the Radiation on Surfaces on Arbitrary Orientation, Given the Components Falling on a Horizontal Surface 927
20.6 Diurnal Variations of the Ambient Temperature 933
20.7 Effects of the Angle of Incidence and of the Dirt 934
20.8 Some Calculation Tools 937
20.8.1 Generation of Daily Radiation Sequences 937
20.8.2 The Reference Year 937
20.8.3 Shadows and Trajectory Maps 939
20.9 Irradiation on Most Widely Studied Surfaces 940
20.9.1 Fixed Surfaces 943
20.9.2 Sun-tracking Surfaces 945
20.9.3 Concentrators 946
20.10 PV Generator Behaviour under Real Operation Conditions 947
20.10.1 The Selected Methodology 949
20.10.2 Second-order Effects 953
20.11 Reliability and Sizing of Stand-alone PV Systems 956
20.12 The Case of Solar Home Systems 962
20.13 Energy Yield of Grid-connected PV Systems 964
20.14 Conclusions 966
Acknowledgements 967
References 967

21 Economic Analysis and Environmental Aspects of Photovoltaic Systems 971
Richard A. Whisnant, Stephen A. Johnston and James H. Hutchby
21.1 Background 972
21.2 Economic Analysis 973
21.2.1 Key Concepts 973
21.2.2 General Methodology 980
21.2.3 Case Studies 984
21.3 Energy Payback and Air Pollution Reduction 997
21.4 Prospects for the Future 999
References 1003

22 PV in Architecture 1005
Tjerk H. Reijenga
22.1 Introduction 1005
22.1.1 Photovoltaics (PV) as a Challenge for Architects and Engineers 1005
22.1.2 Definition of Building Integration 1006

Petitioner Canadian Solar (USA) Inc., Ex. 1035, p. 2539

22.2 PV in Architecture 1008
22.2.1 Architectural Functions of PV Modules 1008
22.2.2 PV as Part of "Green Design" 1011
22.2.3 PV Integrated as Roofing Louvres, Facades and Shading 1011
22.2.4 Well-integrated Systems 1014
22.2.5 Integration of PV Modules in Architecture 1019
22.2.6 Brundtland Centre, Toftlund (DK) – a Case Study 1022
22.3 BIPV Basics 1026
22.3.1 Categories and Type of Buildings 1026
22.3.2 Cells and Modules 1029
22.4 Steps in the Design Process with PV 1036
22.4.1 Urban Aspects 1036
22.4.2 Practical Rules for Integration 1037
22.4.3 Step-by-step Design 1038
22.4.4 Design Process: Strategic Planning 1039
22.5 Conclusions 1040
References 1041
Further Reading 1042

23 Photovoltaics and Development 1043
Jorge M. Huacuz and Lalith Gunaratne
23.1 Electricity and Development 1043
23.1.1 Energy and the Early Man 1043
23.1.2 Let There be Electricity 1044
23.1.3 One Third of Humanity Still in Darkness 1044
23.1.4 The Centralized Electrical System 1045
23.1.5 Rural Electrification 1045
23.1.6 The Rural Energy Scene 1046
23.2 Breaking the Chains of Underdevelopment 1046
23.2.1 Electricity Applications in the Rural Setting 1046
23.2.2 Basic Sources of Electricity 1047
23.3 The PV Alternative 1048
23.3.1 PV Systems for Rural Applications 1049
23.3.2 Barriers to PV Implementation 1051
23.3.3 Technical Barriers 1052
23.3.4 Nontechnical Issues 1055
23.3.5 Trained Human Resources 1059
23.4 Four Examples of PV Rural Electrification 1061
23.4.1 Argentina 1061
23.4.2 Bolivia 1061
23.4.3 Brazil 1063
23.4.4 Mexico 1064
23.4.5 Sri Lanka 1065
23.4.6 Water Pumping in the Sahel 1067
23.5 Toward a New Paradigm for Rural Electrification 1068
References 1069

Petitioner Canadian Solar (USA) Inc., Ex. 1035, p. 2540

24 Financing PV Growth **1073**
Michael T. Eckhart, Jack L. Stone and Keith Rutledge
24.1 Historical Development of PV Financing 1073
24.2 Capital Requirements 1075
24.2.1 Market Drivers 1075
24.2.2 Growth Outlook 1075
24.2.3 Capital Requirements 1076
24.3 Financial Characteristics of PV 1077
24.4 Financing PV for Grid-connected Residences 1079
24.4.1 Impact of Loan Terms on End-user Cost 1079
24.4.2 Types of Residential Financing 1080
24.4.3 Lender's Issues 1081
24.4.4 Borrowers' Experience 1081
24.4.5 Example Calculation 1082
24.4.6 Improving the Financing of Residential PV 1082
24.5 Financing PV in Rural Areas of Developing Countries 1083
24.5.1 Rural Applications 1083
24.5.2 Impact of Financing on Market Demand 1084
24.5.3 Examples of PV Financing in Rural Areas 1085
24.6 Sources of International Financing 1086
24.6.1 International Aid and Donor Funding 1086
24.6.2 United Nations 1087
24.6.3 World Bank Solar Home System Projects 1088
24.6.4 International Finance Corporation (IFC) 1089
24.6.5 Global Environment Facility 1089
24.7 Financing the PV Industry 1091
24.7.1 Financing Working Capital in the Distribution Channels 1092
24.8 Government Incentives and Programs 1092
24.8.1 Potential Impact of Financing as a Government Policy Option 1092
24.8.2 Direct Subsidies ("Buy-downs") 1094
24.8.3 Soft Loans (Interest Subsidies) 1095
24.8.4 Income Tax Deductions and Credits 1096
24.9 Funding Government Research and Development 1096
24.9.1 PV Programs in the United States 1096
24.9.2 PV Programs in Japan 1097
24.9.3 PV Programs in Europe 1097
24.9.4 Future PV R&D Programs 1099
24.9.5 Sources of R&D Funding 1099
Annex 1100
References 1114

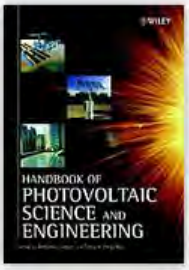
Index **1117**

Attachment D-4

Screen capture created by J L Mullins from WorldCat on August 22, 2024 at URL:
https://search.worldcat.org/title/50912809

WorldCat® Items Search for books, articles, and more

Home Libraries Topics Lists About For Librarians



Handbook of photovoltaic science and engineering

★★★★☆ 0 reviews

Authors: A. Luque, Steven Hegedus

Show more

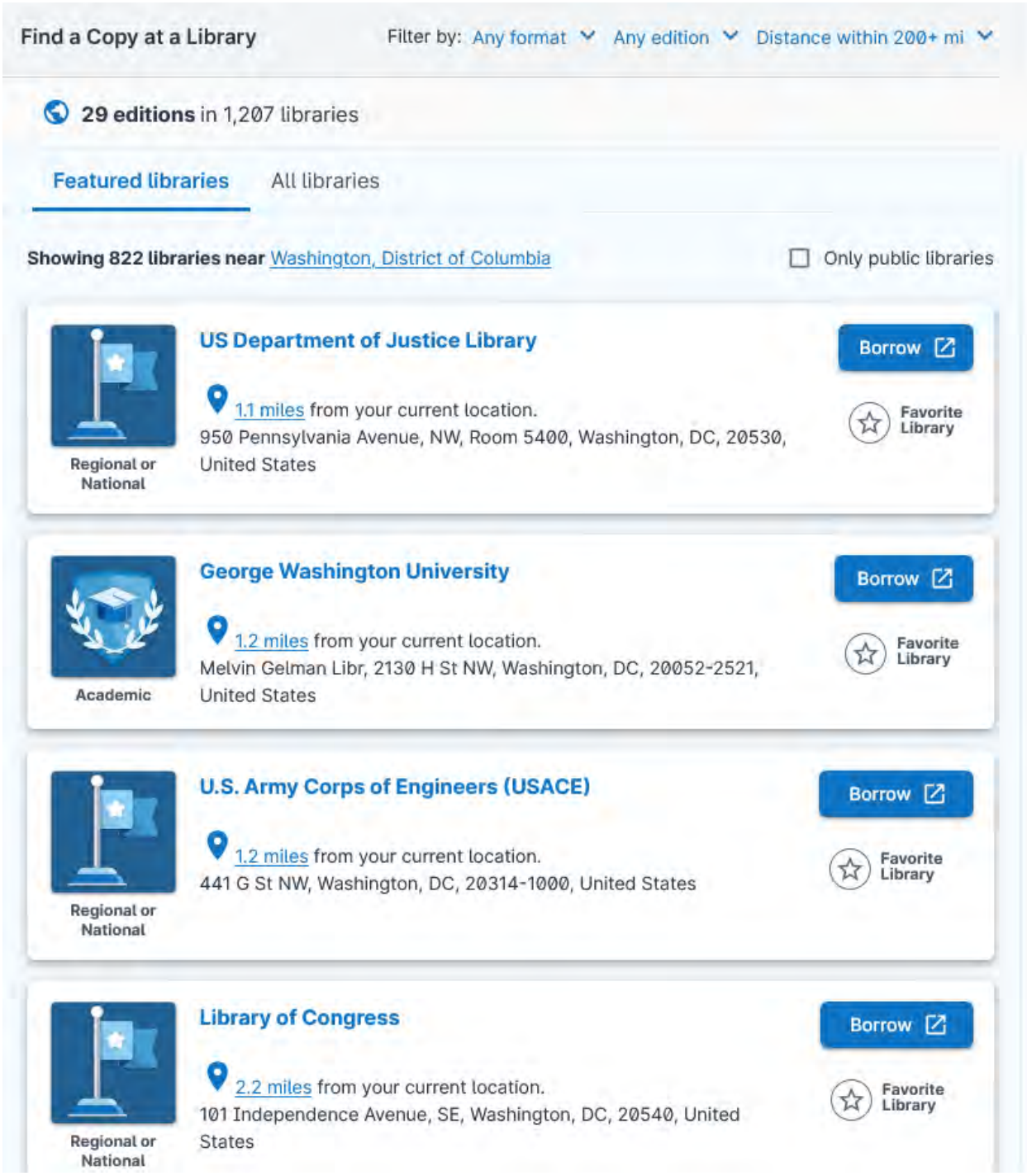
Summary: Handbook of Photovoltaic Science and Engineering incorporates the most recent technological advances and research developments in photovoltaics. All topics relating to the photovoltaic (PV) industry are discussed and each chapter has been written by an internationally-known expert in the field. Detailed treatment covers: scientific basis of the photovoltaic effect and solar cell operation the production of solar silicon and of silicon-based solar cells and modules the science and technology of up-and-coming thin film PV technologies how choice of semiconductor materials and their production in

Show less

Print Book, English, ©2003
Edition: View all formats and editions
Publisher: Wiley, Hoboken, NJ, ©2003

Genre:	Handbooks and manuals
Physical Description:	xxvii, 1138 pages : illustrations ; 26 cm
ISBN:	9780471491965, 0471491969
OCLC Number / Unique Identifier:	50912809
Subjects:	Cellules photovoltaïques Guides, manuels, etc Conversion photovoltaïque Guides, manuels, etc Fotovoltaik Handboeken (vorm) Handbooks and manuals Photovoltaic cells Photovoltaic cells Handbooks, manuals, etc Photovoltaic power generation Photovoltaic power generation Handbooks, manuals, etc Solarzelle

Screen capture created by J L Mullins from WorldCat on August 22, 2024 at URL: https://search.worldcat.org/title/50912809



Attachment D-5

LIBRARY | CATALOG

Search Navigation ▾ < 3 of 3 >

BOOK

Handbook of photovoltaic science and engineering

Full Record MARC Tags

Main title

Handbook of photovoltaic science and engineering / edited by Antonio Luque and Steven Hegedus.

Published/Created

Hoboken, NJ : Wiley, c2003.

Request this Item | LC Find It

Links

Links

Table of contents http://www.loc.gov/catdir/toc/wiley041/2002191033.html
Publisher description http://www.loc.gov/catdir/description/wiley036/2002191033.html
Book review (E-STREAMS) http://www.e-streams.com/es0706/es0706_3291.html

More Information

LCCN Permalink https://lccn.loc.gov/2002191033

Description xxvii, 1138 p. : ill. ; 26 cm.

ISBN	0471491969 (alk. paper)
LC classification	TK8322 .H33 2003
Related names	Luque, A. (Antonio) Hegedus, Steven.
LC Subjects	Photovoltaic cells--Handbooks, manuals, etc. Photovoltaic power generation--Handbooks, manuals, etc.
Browse by shelf order	TK8322
Notes	Includes bibliographical references and index.
LCCN	2002191033
Dewey class no.	621.31/244
Type of material	Book

Item Availability

CALL NUMBER	TK8322 .H33 2003 Copy 1
Request in	Jefferson or Adams Building Reading Rooms
Status	Not Charged

Petitioner Canadian Solar (USA) Inc., Ex. 1035, p. 2547

Attachment E-1

Solid-State Electronics Vol. 30, No. 11, pp. 1121–1125, 1987
Printed in Great Britain

0038-1101/87 $3.00 + 0.00
Pergamon Journals Ltd

N-TYPE SIPOS AND POLY-SILICON EMITTERS

Y. H. KWARK and R. M. SWANSON
Stanford University, Stanford, CA 94305, U.S.A.

Abstract—*N*-type SIPOS and poly-silicon emitters on silicon show potential for improved minority carrier blocking properties over conventional diffused emitters. This paper discusses experiments designed to elucidate the physical mechanisms responsible for this improvement and to optimize the process conditions. Emitters both with and without an intentionally grown chemical oxide under the SIPOS or poly-silicon film are investigated. Both poly-silicon and SIPOS emitters, in their optimized form, can achieve J_{oe} of less than 2×10^{-14} A/cm^2, an improvement of several decades over shallow diffused emitters.

1. INTRODUCTION

SIPOS, for Semi-Insulating Poly-crystalline Silicon, has become the generic acronym for deposited silicon films doped with oxygen. The physical properties can be varied over a wide range by varying oxygen content. Indeed, normal poly-silicon and SiO_2 can be thought of as the limiting cases of no oxygen and full oxidation. The optical and electrical properties can be varied somewhat continuously between Si and SiO_2 by adjusting the oxygen content. *N* and *p*-type conduction can be obtained at low oxygen concentrations by doping with phosphorus and boron. These films, pioneered at Sony, found initial application in their intrinsic form to the passivation of high voltage devices[1]. Later, doped films were successfully applied to emitter contact structures, resulting in a 50-fold reduction of J_{oe} for *n*-type emitters[2,3]. This paper discusses experiments designed to elucidate the physical mechanisms responsible for this improvement and to optimize the process conditions. Further details are available in Ref. [4].

As deposited, SIPOS is usually amorphous. Annealing is necessary to activate the dopant and to produce films suitable for use as emitter contacts. During annealing it has been found that the film morphology changes. Si precipitates into small grains of crystalline Si and the oxygen segregates as SiO_2 on the grain boundaries[5]. One of the salient effects of oxygen incorporation is the suppression of grain growth, typical grain sizes being less than 100 Å. At higher oxygen concentrations, carrier transport is dominated by tunnelling through these thin SiO_2 shells[6].

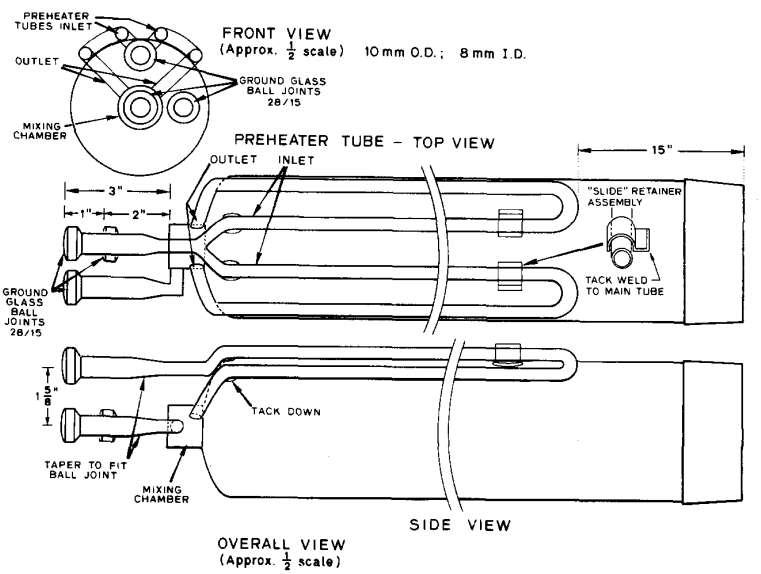


Fig. 1. SIPOS deposition tube—overall view.

Petitioner Canadian Solar (USA) Inc., Ex. 1035, p. 2549

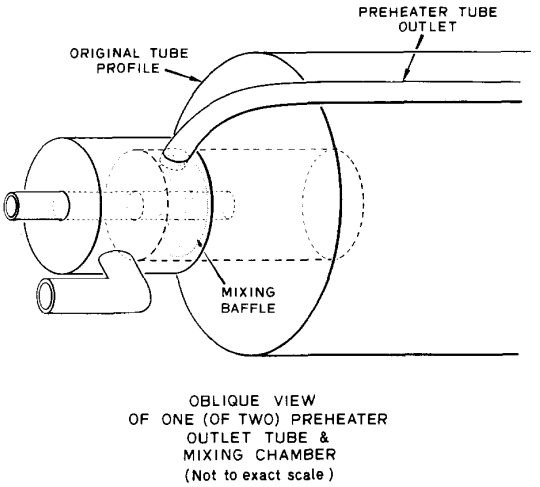


Fig. 2. SIPOS deposition tube—close up to mixing chamber.

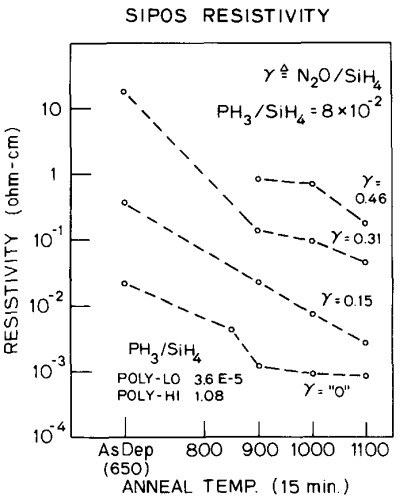


Fig. 3. N + SIPOS film resistivity vs T_A and γ.

2. DEPOSITION

Evaporation, atmospheric CVD, and low pressure CVD have all been used to fabricate SIPOS layers. CVD techniques have been found most successful for device applications. Due to the lack of a low-pressure deposition system, atmospheric CVD was selected as the method for fabricating experimental films. Initial experiments in a cold-wall epitaxial reactor revealed that SIPOS is a difficult material to controllably deposit because of its non-stoichiometric nature. Useable areas of deposition extended only several centimeters over the susceptor. Accurate control of both temperature and flow dynamics was clearly needed. This suggested using a hot-wall system. The final configuration is shown in Fig. 1. A carrier gas preheater is used so that the high flow of nitrogen does not cool the wafers. Figure 2 details the gas-mixing chamber. The design is such that the reactant species are mixed due to turbulance in the gas flows. The end of the tube is purged to minimize stagnant regions and gas-phase reactions. Useful deposition with this system extends over 6 inches on the susceptor.

A plot of film resistivity as determined by four-point probe is shown in Fig. 3, γ is the mol ratio of N_2O to SiH_4. The strong dependence of resistivity on oxygen content is confirmed and anneals at over 900°C are found necessary to fully activate the dopant. It will be shown later that the $\gamma = 0$ films actually contain significant oxygen (as much as several atomic percent), probably due to residual water or oxygen in the deposition ambient; however, resistivities comparable to that of poly-silicon are obtained nevertheless.

3. MEASUREMENT OF J_{oe}

The relevant parameters which characterize the d.c. performance of an emitter are its saturation current, J_{oe}, and specific contact resistance, R_c. This report will concentrate mainly on the saturation current. J_{oe} characterizes the emitter recombination current because it is easily shown that, even in the case of SIPOS emitters, the minority-carrier hole current in low-level injection at the edge of the emitter-base junction space charge region follows the standard relation $J_p = J_{oe}(\exp qV_{be}/kT - 1)$.

In order to measure J_{oe}, transistor test structures, as shown in Fig. 4, were fabricated. These used epitaxially deposited bases with uniform doping concentration to allow extraction of the base-recombination component of the base current through modulating the base width via changes in collector-base voltage. Base recombination current was equivalent to a J_{oe} of 8×10^{-15} A/cm^2 which places a lower limit on the emitter saturation current

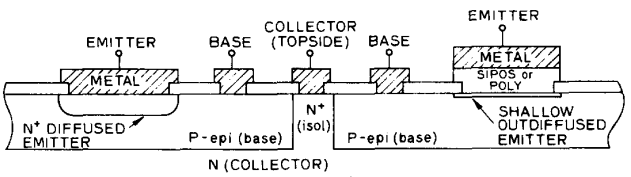


Fig. 4. Cross-section of bipolar test structures.

Petitioner Canadian Solar (USA) Inc., Ex. 1035, p. 2550

which can be reliably determined. The test devices had two diffused emitters of different junction depth, emitters A and B, that were either contacted with aluminum, as a control, or contacted with *in-situ* doped SIPOS or poly-silicon. In addition, emitters of type C with no prediffusion were fabricated. These relied solely on outdiffusion from the *in-situ* doped SIPOS or poly-silicon to provide sufficient surface doping concentration.

The emitter saturation current was measured using standard Gummel plot methods. Devices of two perimeter-to-area ratios were incorporated to allow extraction of the perimeter component of the base current. Temperatures determined using a thermocouple on the wafer chuck agreed with those determined from the slope of the log collector current vs base-emitter voltage, after correcting for base-width modulation effects. Reported saturation currents are "corrected" to 300 K using the relation:

$$J_{oe}(300\text{ K}) = J_{oe}(T_{\text{device}})\frac{n_i^2(300\text{ K})}{n_i^2(T_{\text{device}})}.$$

4. EXPERIMENTAL RESULTS

Three types of emitter contacts were studied, conventional aluminum contacts, SIPOS and polysilicon. In the latter two cases the emitters were fabricated both with and without an interfacial chemical oxide.

4.1. Conventional emitters

The pre-diffused emitter deposition parameters are shown in Table 1. Phosphine at 1100 ppm was used as the dopant source in these conventional predep and drive-in diffusions. Gummel plots for both the large and small devices are shown in Fig. 5. The extracted perimeter- and area-related current components are also shown. The perimeter current shows a strong non-ideal component which was found,through the use of a field plate equipped device, to arise from recombination at the $Si–SiO_2$ interface in the emitter-base space-charge region. Illustrated in Fig. 5 is the method of removing the effect of series resistance by assuming that the collector current continues to follow an ideal exponential form. Any additional voltage is assumed to come from resistive voltage drops and is subtracted from both the collector and base current plots.

Table 2 shows the measured saturation current for an aluminum-contacted conventional emitter. The extracted value varies by less than 4% over 4 decades of base current. This is testimony to the accuracy with which the various parasitics (perimeter current and series resistance) have been accounted for, as well as the precision of the temperature determination. Similar procedures were used for the other emitter structures.

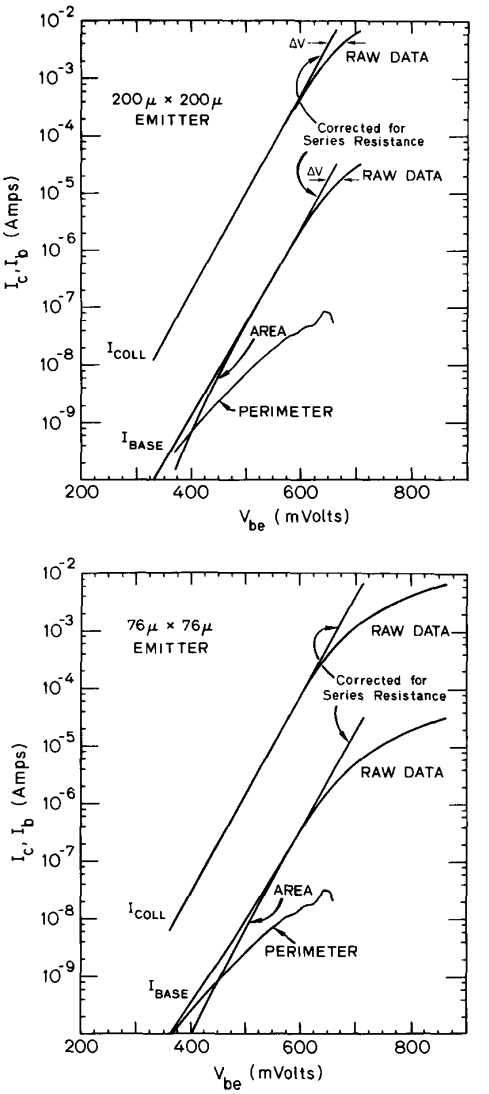


Fig. 5. Gummel plots for aluminum contacted large and small emitter devices.

4.2. SIPOS emitters

4.2.1. Role of oxygen. It has been postulated that the improvement that SIPOS emitters obtain is because SIPOS has a larger band gap than crystalline

Table 1. Deposition parameters for the prediffused emitters

	Predep (T/t)	Drive-in (T/t)	Sheet resistance	Junction depth
EM-A	800°C/30 min	1025°C/90 min	60Ω/□	1.0 μ
EM-B	800°C/30 min	1025°C/30 min	70Ω/□	0.66 μ

Petitioner Canadian Solar (USA) Inc., Ex. 1035, p. 2551

Table 2. Measured J_{oe} vs V_{be} for a conventional aluminum contacted transistor

V_{be} (V)	J_{oe} (10^{-12} A/cm^2)	V_{be} (V)	J_{oe} (10^{-12} A/cm^2)
0.392	1.18	0.545	1.18
0.409	1.21	0.562	1.17
0.426	1.21	0.579	1.17
0.443	1.20	0.596	1.16
0.460	1.19	0.613	1.16
0.477	1.19	0.630	1.15
0.494	1.19	0.647	1.13
0.511	1.19	0.664	1.13
0.528	1.18		

silicon so that the injected minority carriers see a barrier at the SIPOS–Si interface[3]. To test this hypothesis, SIPOS contacts with varying oxygen were fabricated with the results shown in Fig. 6. For these experiments, the SIPOS was annealed at 900°C for 13 min. No out-diffused emitter was incorporated. It is seen that there is no descernable influence of oxygen content on saturation current as would be expected from the heterojunction model. The film with $\gamma = 1.5$ has an oxygen concentration similar to that of the Sony-transistors[3]. Even the $\gamma = 0$ (no intentional oxygen) film has a low saturation current. These films, however, were found to dissolve in HF, indicating the presence of some oxygen.

As seen in Fig. 6, however, the film annealed at 1000°C has J_{oe} nearly an order of magnitude larger than those at 900°C. Clearly, anneal temperature is more important than oxygen concentration in determining saturation current.

4.2.2. J_{oe} vs anneal temperature. A series of experiments was conducted to determine the influence of anneal temperature on saturation current. In addition, it was decided to incorporate an intentional interface oxide on a portion of the devices on each wafer in order to help clarify the roles of interface vs bulk effects in the observed reduction in saturation current under SIPOS contacts. The interface oxide, called "chemox" here, is the result of omitting the final HF dip after an RCA clean. The SIPOS had $\gamma = 0$, or no intentional oxygen. Results are shown in Figs 7 and 8. The results for the aluminum contacted emitters are also shown.

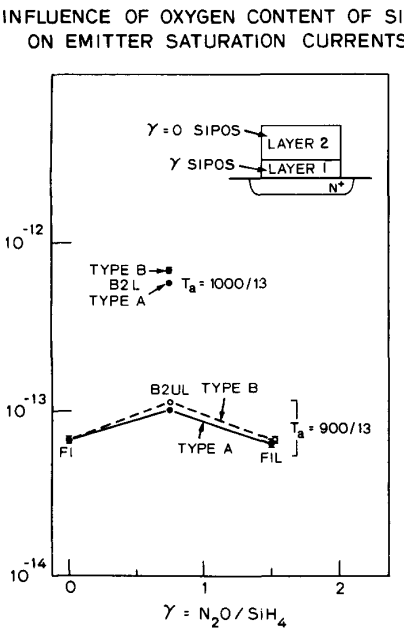


Fig. 6. Influence of oxygen content of SIPOS on J_{oe}.

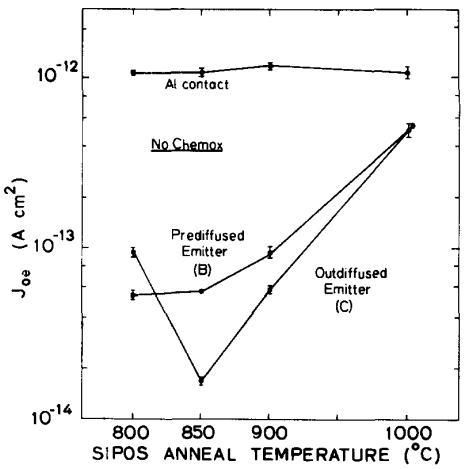


Fig. 7. Influence of anneal temperature on J_{oe} for SIPOS contacted emitters without chemox.

For devices with no chemox and a pre-diffused emitter, Fig. 7, J_{oe} is relatively constant for anneal temperatures less than 850°C at a value of 1/20 that of aluminum contacted emitters. As the temperature increases above 900°C, J_{oe} increases, eventually approaching the value for the conventional emitter at

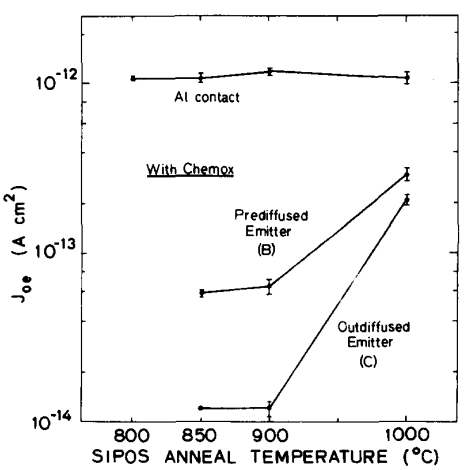


Fig. 8. Influence of anneal temperature on J_{oe} for SIPOS contacted emitters with chemox.

Petitioner Canadian Solar (USA) Inc., Ex. 1035, p. 2552

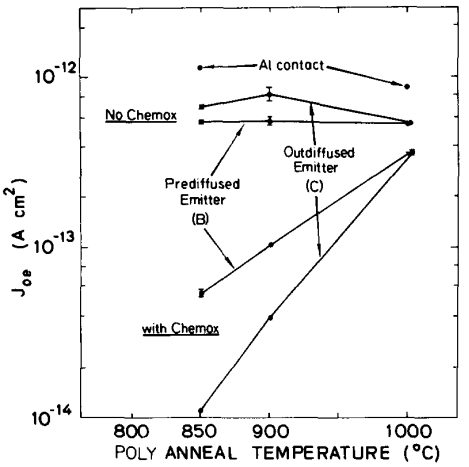


Fig. 9. Experimental J_{oe} vs anneal temperature for poly-silicon contacted emitters.

1000°C. If no pre-diffused emitter exists, J_{oe} starts rather high at 800°C, then exhibits a minimum at 850°C of only 2×10^{-14} A/cm^2. This is 1/50 that of the conventional emitter. Finally, J_{oe} again increases with higher anneal temperatures. Undoubtedly, in the 800°C case the surface of the silicon has not been doped sufficiently in the out-diffused case to limit the minority-carrier concentration at the SIPOS–Si interface, resulting in poor performance.

It is interesting to note that, excluding the 800°C case, J_{oe} for the pre-diffused emitter is 5×10^{-14} A/cm^2 plus that for the out-diffused case. This suggests that the total J_{oe} comes from a constant recombination in the diffused emitter plus that coming from the out-diffused portion. For such to be the case the quasi-Fermi levels throughout the emitter need be constant. This is approximately the case for these devices which have passivated surfaces. The increase in J_{oe} with anneal temperature is then explained as the result of increased doping, and hence reduced lifetime, in the out-diffused portion of the emitter. Alternatively, the increase could be due to the break-up of an interfacial oxide. Such an oxide could form, for example, during the anneal as oxygen segregates from the SIPOS. Perhaps both methods are operative.

When the chemox is incorporated, a slightly different picture emerges. At 800°C J_{oe} could not be extracted due to excessive series resistance. This resistance decreases with higher anneal temperatures suggesting the break-up of the interfacial oxide and an increase in surface doping concentration. At 850°C the results are substantially the same as with no chemox, Fig. 8. Annealing at 900°C, however, does not result in any increase in J_{oe} as was the case without a chemox. This suggests that either the chemox is acting as a barrier to the out-diffusion of phosphorus, and thus prevents lifetime reduction in the surface region, or alternatively, is more resistant to break-up during annealing than whatever oxide exists without the chemox.

4.3. Poly-silicon emitters

When it was discovered that the $\gamma = 0$ SIPOS films actually had significant oxygen, it was decided to compare these results with the case of poly-silicon deposited with a hydrogen carrier in an epi reactor. Such films contain very little oxygen. The results are shown in Fig. 9. In this case the emitters without chemox had J_{oe} only a factor of two less than the aluminum contacted emitters. This reduction can be theoretically accounted for simply from the increase in thickness of the highly doped emitter due to the addition of the poly-silicon. The addition of a chemox causes J_{oe} to be substantially the same as for SIPOS emitters. Once again, there is an additive effect between the pre-diffused and out-diffused emitters.

5. DISCUSSION AND CONCLUSIONS

Both poly-silicon and SIPOS emitters, in their optimized form, can achieve J_{oe} of less than 2×10^{-14} A/cm^2. For poly-silicon contacts this requires an interfacial chemox. The chemox is not necessary for SIPOS contacts. The similarity of results for the chemox poly-silicon contacts and SIPOS contacts suggests that these both obtain their improved performance through incorporating a thin, tunnelable interfacial oxide that impedes the flow of holes rather than as a result of the increased band gap of SIPOS. Preliminary results on p-type SIPOS emitters indicates that they have much poorer performance. This is consistent with a barrier that has a lower electron barrier height than hole barrier height, as does SiO_2.

Acknowledgement—This work was supported by the Department of Energy through Sandia National Laboratories.

REFERENCES

1. T. Matsushita, T. Aoki, T. Ohtsu *et al.*, *IEEE Trans. Electron Dev.* **23,** 826 (1976).
2. T. Matsushita, N. Oh-uchi, H. Hayashi and H. Yamoto, *Appl. Phys. Lett.* **35,** 549 (1979).
3. T. Matsushita, H. Hayashi and N. Oh-uchi, *Jap. J. appl. Phys.* (suppl) **20,** 75 (1981).
4. Y. H. Kwark, Stanford Electronics Laboratory Technical Report, Stanford University (1985).
5. M. Hamasaki, T. Adachi, S. Wakayama and M. Kikuchi, *J. appl. Phys.* **49,** 3987 (1978).
6. J. Ni and E. Arnold, *Appl. Phys. Lett.* **39,** 554 (1981).

Petitioner Canadian Solar (USA) Inc., Ex. 1035, p. 2553

Attachment E-2

VOLUME 30 NUMBER 11
NOVEMBER 1987

SOLID-STATE ELECTRONICS

An International Journal

Editor-in-Chief
W. CRAWFORD DUNLAP
West Newton, Mass.

Regional Editors

U.K.
R. W. BRANDER
Suffolk, England

EUROPE
F. M. KLAASSEN
Eindhoven

JAPAN and FAR EAST
W. CRAWFORD DUNLAP

LINDA HALL LIBRARY
DEC 9 1987

SPECIAL ISSUE

New Developments in the PHYSICS OF HOMO- AND HETEROJUNCTIONS

Guest Editors: R. J. VAN OVERSTRAETEN
R. P. MERTENS
A. NEUGROSCHEL

PERGAMON PRESS
OXFORD · NEW YORK
BEIJING · FRANKFURT · SÃO PAULO
SYDNEY · TOKYO · TORONTO

Petitioner Canadian Solar (USA) Inc., Ex. 1035, p. 2555

SOLID-STATE ELECTRONICS

EDITORS

Dr W. Crawford Dunlap (*Editor-in-Chief*), *126 Prince Street, West Newton, MA 02165, U.S.A.*
R. W. Brander, *British Telecom, Anzani House, Felixstowe, Suffolk IP11 8XB, England*
Dr F. M. Klaassen, *Philips Research Laboratories, Eindhoven, The Netherlands*

HONORARY EDITORIAL ADVISORY BOARD

J. R. Brews, *Murray Hill, NJ*
R. H. Bube, *Stanford, CA*
H. C. Card, *Winnipeg, Man.*
D. K. Ferry, *Tempe, AZ*
J. G. Fossum, *Gainesville, FL*
S. K. Ghandhi, *Troy, NY*
R. N. Hall, *Schenectady, NY*
H. K. Henisch, *University Park, PA*
N. Holonyak Jr, *Urbana, IL*
L. P. Hunter, *Rochester, NY*
A. C. Ipri, *Princeton, NJ*
R. W. Knepper, *East Fishkill, NY*
A. G. Milnes, *Pittsburgh, PA*
B. R. Nag, *Calcutta*
H. C. Nathanson, *Pittsburgh, PA*
J. Nishizawa, *Tohoku*
A. Nussbaum, *Minneapolis, MN*
W. G. Oldham, *Berkeley, CA*
J. I. Pankove, *Boulder, CO*
R. F. Pierret, *W. Lafayette, IN*
D. L. Pulfrey, *Vancouver, B.C.*
E. H. Rhoderick, *Manchester*
D. J. Roulston, *Waterloo, Ont.*
C. A. T. Salama, *Toronto, Ont.*
R. Stratton, *Dallas, TX*
Y. Takeishi, *Kawasaki*
R. Van Overstraeten, *Louvain*
C. A. Varker, *Phoenix, AZ*
J. Walling, *Redhill*
M. Watanabe, *Tokyo*
B. H. L. Wilson, *Towcester*
G. T. Wright, *Birmingham*
M. Zerbst, *Munich*

Publishing Office: Journals Production Unit, Pergamon Journals Ltd, Hennock Road, Marsh Barton, Exeter, Devon EX2 8NE, England (*Tel.* Exeter (0392) 51558; *Telex* 42749). *Subscription and Advertising Offices:* Enquiries from customers in North America should be sent to: Pergamon Journals Inc., Maxwell House, Fairview Park, Elmsford, NY 10523, U.S.A., and from the remainder of the world to: Pergamon Journals Ltd, Headington Hill Hall, Oxford OX3 0BW, England.

Annual Subscription Rates for 1988: Annual institutional subscription rate (1988) DM 940.00; 2-year institutional rate (1988/89) DM 1786.00; personal subscription rate for those whose library subscribes at the regular rate (1988) DM 213.00. Prices are subject to amendment without notice.

Microform Subscriptions and Back Issues: Back issues of all previously published volumes are available in the regular editions and on microfilm and microfiche. Current subscriptions are available on microfiche simultaneously with the paper edition and on microfilm on completion of the annual index at the end of the subscription year.

Copyright © 1987 · Pergamon Journals Limited *Published monthly*

It is a condition of publication that manuscripts submitted to this journal have not been published and will not be simultaneously submitted or published elsewhere. By submitting a manuscript, the authors agree that the copyright for their article is transferred to the publisher if and when the article is accepted for publication. However, assignment of copyright is not required from authors who work for organizations which do not permit such assignment. The copyright covers the exclusive rights to reproduce and distribute the article, including reprints, photographic reproductions, microform or any other reproductions of similar nature and translations. No part of this publication may be reproduced, stored in a retrieval system or transmitted in any form or by any means, electronic, electrostatic, magnetic tape, mechanical, photocopying, recording or otherwise, without permission in writing from the copyright holder.

Photocopying information for users in the USA
The Item-Fee Code for this publication indicates that authorization to photocopy items for internal or personal use is granted by the copyright holder for libraries and other users registered with the Copyright Clearance Center (CCC) Transactional Reporting Service, provided the stated fee for copying beyond that permitted by Section 107 or 108 of the U.S. Copyright Law is paid. The appropriate remittance of $3.00 per copy per article is paid directly to the Copyright Clearance Center Inc., 27 Congress Street, Salem, MA 01970.

Permission for other use
The copyright owner's consent does not extend to copying for general distribution, for promotion, for creating new works or for resale. Specific written permission must be obtained from the publisher for such copying.

The Item-Fee Code for this publication is: 0038-1101/87 $3.00 + 0.00

AIMS AND SCOPE

It is the function of this Journal to bring together in one publication outstanding papers reporting original work in the following areas: (1) applications of solid-state physics in such fields as transistor technology, including theory and design, crystal growth, measurement and evaluation, preparation of junctions and measurement techniques; (2) applications of computer and numerical methods to the modeling of and simulation of solid-state devices; (3) physics and design of ultra-small (submicron) microelectronic devices (VLSI), including methods of processing, measurement and evaluation. Also of interest are applications of intermetallic and binary and ternary semiconductors, the design and performance of power semiconductor devices, solar cells, photoconductors, thermoelectric and ferroelectric devices, galvanomagnetic devices, and electroluminescent devices, including semiconductor lasers. Of particular interest are solid-state optical devices for storage and transfer of information. Papers covering novel topics extending the frontiers of solid-state technology are of course invited. Review papers covering important topics in solid-state electronics will be presented at intervals. Papers will be published in the formats of short camera-ready Communications, regular Research Papers, Notes, and Letters to the Editor.

It is expected that, because of its international scope and because it emphasizes the association of theory and practice, the Journal will promote further progress in the ever-widening borderland between solid-state physics and circuit engineering.

CONTENTS

R. J. Van Overstraeten, R. P. Mertens and A. Neugroschel: Foreword and Introduction v

Roger J. Van Overstraeten and Robert P. Mertens: Heavy doping effects in silicon 1077

Alan H. Marshak: Transport equations for highly doped devices and heterostructures 1089

Hilmi Unlu and Allen Nussbaum: A review of models for heterojunction band offsets 1095

A. G. Milnes: Heterojunctions: some knowns and unknowns 1099

Peter T. Landsberg: The band–band Auger effect in semiconductors 1107

Joachim Wagner: Optical characterization of heavily doped silicon 1117

Y. H. Kwark and R. M. Swanson: *N*-Type SIPOS and poly-silicon emitters 1121

Jesús A. del Alamo and Richard M. Swanson: Modelling of minority-carrier transport in heavily doped silicon emitters 1127

Herbert S. Bennett: Modeling silicon emitters for VLSI transistors 1137

J. Symons, M. Ghannam, A. Neugroschel, J. Nijs and R. Mertens: Silicon heterojunction bipolar transistors with amorphous and microcrystalline emitters 1143

Moustafa Y. Ghannam: Characterization of the heavily (non-degenerate) boron-doped Si–SiO_2 interface 1147

B. Benna, T. F. Meister and H. Schaber: The role of the interfacial layer in bipolar (poly-Si)-emitter transistors 1153

J. P. Bailbe, A. Marty and G. Rey: III, V Heterojunction bipolar transistors 1159

Arnost Neugroschel: Emitter injection efficiency in heterojunction bipolar transistors 1171

R. Baets: Heterostructures in III–V optoelectronic devices 1175

Dieter Fritzsche: Heterostructures in MODFETs 1183

Dany Loret: Two-dimensional numerical model for the high electron mobility transistor 1197

Joseph J. Loferski: Optimization of II–VI based heterojunctions 1205

P. De Visschere, M. Burgelman and H. Pauwels: II–VI Heterojunction device physics 1215

Software Survey Section I

Petitioner Canadian Solar (USA) Inc., Ex. 1035, p. 2557

Solid-State Electronics Vol. 30, No. 11, pp. 1121–1125, 1987
Printed in Great Britain

0038-1101/87 $3.00 + 0.00
Pergamon Journals Ltd

N-TYPE SIPOS AND POLY-SILICON EMITTERS

Y. H. KWARK and R. M. SWANSON
Stanford University, Stanford, CA 94305, U.S.A.

Abstract—*N*-type SIPOS and poly-silicon emitters on silicon show potential for improved minority carrier blocking properties over conventional diffused emitters. This paper discusses experiments designed to elucidate the physical mechanisms responsible for this improvement and to optimize the process conditions. Emitters both with and without an intentionally grown chemical oxide under the SIPOS or poly-silicon film are investigated. Both poly-silicon and SIPOS emitters, in their optimized form, can achieve J_{oe} of less than 2×10^{-14} A/cm^2, an improvement of several decades over shallow diffused emitters.

1. INTRODUCTION

SIPOS, for Semi-Insulating Poly-crystalline Silicon, has become the generic acronym for deposited silicon films doped with oxygen. The physical properties can be varied over a wide range by varying oxygen content. Indeed, normal poly-silicon and SiO_2 can be thought of as the limiting cases of no oxygen and full oxidation. The optical and electrical properties can be varied somewhat continuously between Si and SiO_2 by adjusting the oxygen content. *N* and *p*-type conduction can be obtained at low oxygen concentrations by doping with phosphorus and boron. These films, pioneered at Sony, found initial application in their intrinsic form to the passivation of high voltage devices[1]. Later, doped films were successfully applied to emitter contact structures, resulting in a 50-fold reduction of J_{oe} for *n*-type emitters[2,3]. This paper discusses experiments designed to elucidate the physical mechanisms responsible for this improvement and to optimize the process conditions. Further details are available in Ref. [4].

As deposited, SIPOS is usually amorphous. Annealing is necessary to activate the dopant and to produce films suitable for use as emitter contacts. During annealing it has been found that the film morphology changes. Si precipitates into small grains of crystalline Si and the oxygen segregates as SiO_2 on the grain boundaries[5]. One of the salient effects of oxygen incorporation is the suppression of grain growth, typical grain sizes being less than 100 Å. At higher oxygen concentrations, carrier transport is dominated by tunnelling through these thin SiO_2 shells[6].

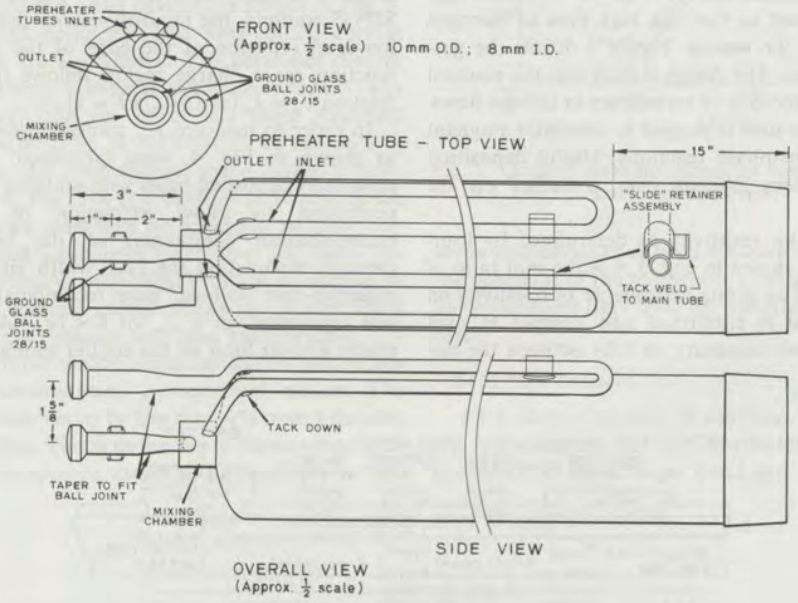


Fig. 1. SIPOS deposition tube—overall view.

Petitioner Canadian Solar (USA) Inc., Ex. 1035, p. 2558

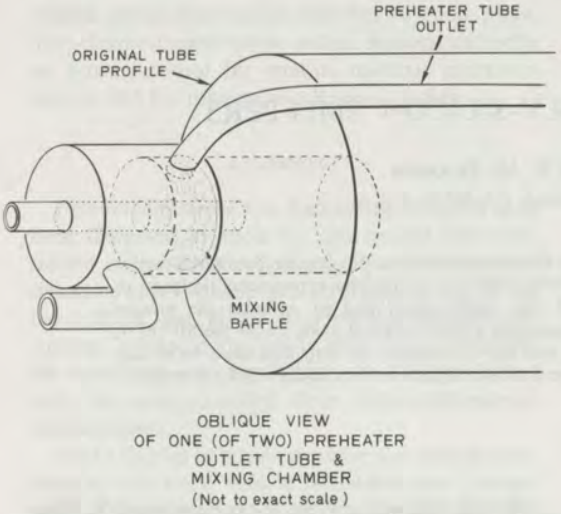


Fig. 2. SIPOS deposition tube—close up to mixing chamber.

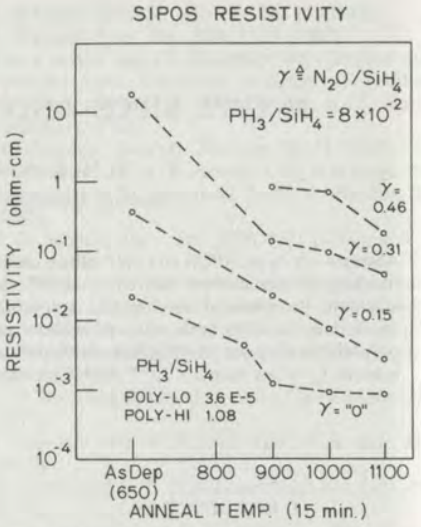


Fig. 3. $N+$ SIPOS film resistivity vs T_A and γ.

2. DEPOSITION

Evaporation, atmospheric CVD, and low pressure CVD have all been used to fabricate SIPOS layers. CVD techniques have been found most successful for device applications. Due to the lack of a low-pressure deposition system, atmospheric CVD was selected as the method for fabricating experimental films. Initial experiments in a cold-wall epitaxial reactor revealed that SIPOS is a difficult material to controllably deposit because of its non-stoichiometric nature. Useable areas of deposition extended only several centimeters over the susceptor. Accurate control of both temperature and flow dynamics was clearly needed. This suggested using a hot-wall system. The final configuration is shown in Fig. 1. A carrier gas preheater is used so that the high flow of nitrogen does not cool the wafers. Figure 2 details the gas-mixing chamber. The design is such that the reactant species are mixed due to turbulance in the gas flows. The end of the tube is purged to minimize stagnant regions and gas-phase reactions. Useful deposition with this system extends over 6 inches on the susceptor.

A plot of film resistivity as determined by four-point probe is shown in Fig. 3, γ is the mol ratio of N_2O to SiH_4. The strong dependence of resistivity on oxygen content is confirmed and anneals at over 900°C are found necessary to fully activate the dopant. It will be shown later that the $\gamma = 0$ films actually contain significant oxygen (as much as several atomic percent), probably due to residual water or oxygen in the deposition ambient; however, resistivities comparable to that of poly-silicon are obtained nevertheless.

3. MEASUREMENT OF J_{oe}

The relevant parameters which characterize the d.c. performance of an emitter are its saturation current, J_{oe}, and specific contact resistance, R_c. This report will concentrate mainly on the saturation current. J_{oe} characterizes the emitter recombination current because it is easily shown that, even in the case of SIPOS emitters, the minority-carrier hole current in low-level injection at the edge of the emitter-base junction space charge region follows the standard relation $J_p = J_{oe}(\exp qV_{be}/kT - 1)$.

In order to measure J_{oe}, transistor test structures, as shown in Fig. 4, were fabricated. These used epitaxially deposited bases with uniform doping concentration to allow extraction of the base-recombination component of the base current through modulating the base width via changes in collector-base voltage. Base recombination current was equivalent to a J_{oe} of 8×10^{-15} A/cm^2 which places a lower limit on the emitter saturation current

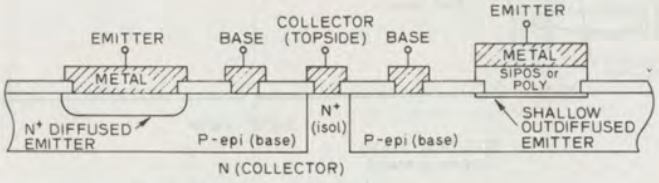


Fig. 4. Cross-section of bipolar test structures.

Petitioner Canadian Solar (USA) Inc., Ex. 1035, p. 2559

which can be reliably determined. The test devices had two diffused emitters of different junction depth, emitters A and B, that were either contacted with aluminum, as a control, or contacted with *in-situ* doped SIPOS or poly-silicon. In addition, emitters of type C with no prediffusion were fabricated. These relied solely on outdiffusion from the *in-situ* doped SIPOS or poly-silicon to provide sufficient surface doping concentration.

The emitter saturation current was measured using standard Gummel plot methods. Devices of two perimeter-to-area ratios were incorporated to allow extraction of the perimeter component of the base current. Temperatures determined using a thermocouple on the wafer chuck agreed with those determined from the slope of the log collector current vs base-emitter voltage, after correcting for base-width modulation effects. Reported saturation currents are "corrected" to 300 K using the relation:

$$J_{oe}(300\ \mathrm{K}) = J_{oe}(T_{\mathrm{device}})\frac{n_i^2(300\ \mathrm{K})}{n_i^2(T_{\mathrm{device}})}.$$

4. EXPERIMENTAL RESULTS

Three types of emitter contacts were studied, conventional aluminum contacts, SIPOS and polysilicon. In the latter two cases the emitters were fabricated both with and without an interfacial chemical oxide.

4.1. Conventional emitters

The pre-diffused emitter deposition parameters are shown in Table 1. Phosphine at 1100 ppm was used as the dopant source in these conventional predep and drive-in diffusions. Gummel plots for both the large and small devices are shown in Fig. 5. The extracted perimeter- and area-related current components are also shown. The perimeter current shows a strong non-ideal component which was found,through the use of a field plate equipped device, to arise from recombination at the Si–SiO_2 interface in the emitter-base space-charge region. Illustrated in Fig. 5 is the method of removing the effect of series resistance by assuming that the collector current continues to follow an ideal exponential form. Any additional voltage is assumed to come from resistive voltage drops and is subtracted from both the collector and base current plots.

Table 2 shows the measured saturation current for an aluminum-contacted conventional emitter. The extracted value varies by less than 4% over 4 decades of base current. This is testimony to the accuracy with which the various parasitics (perimeter current and series resistance) have been accounted for, as well as the precision of the temperature determination. Similar procedures were used for the other emitter structures.

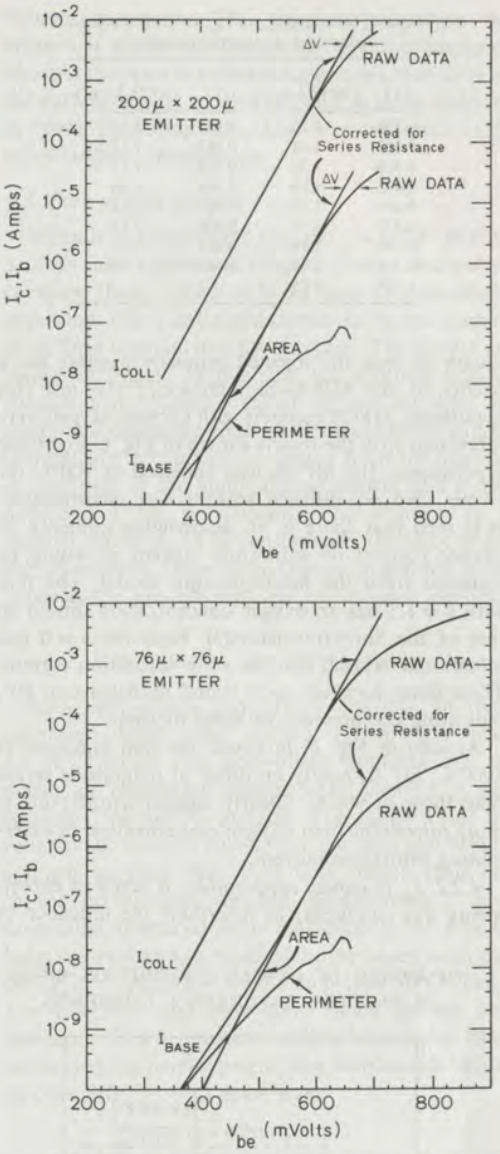


Fig. 5. Gummel plots for aluminum contacted large and small emitter devices.

4.2. SIPOS emitters

4.2.1. Role of oxygen. It has been postulated that the improvement that SIPOS emitters obtain is because SIPOS has a larger band gap than crystalline

Table 1. Deposition parameters for the prediffused emitters

	Predep (T/t)	Drive-in (T/t)	Sheet resistance	Junction depth
EM-A	800°C/30 min	1025°C/90 min	60Ω/□	1.0 μ
EM-B	800°C/30 min	1025°C/30 min	70Ω/□	0.66 μ

Petitioner Canadian Solar (USA) Inc., Ex. 1035, p. 2560

Table 2. Measured J_{oe} vs V_{be} for a conventional aluminum contacted transistor

V_{be} (V)	J_{oe} (10^{-12} A/cm^2)	V_{be} (V)	J_{oe} (10^{-12} A/cm^2)
0.392	1.18	0.545	1.18
0.409	1.21	0.562	1.17
0.426	1.21	0.579	1.17
0.443	1.20	0.596	1.16
0.460	1.19	0.613	1.16
0.477	1.19	0.630	1.15
0.494	1.19	0.647	1.13
0.511	1.19	0.664	1.13
0.528	1.18		

silicon so that the injected minority carriers see a barrier at the SIPOS–Si interface[3]. To test this hypothesis, SIPOS contacts with varying oxygen were fabricated with the results shown in Fig. 6. For these experiments, the SIPOS was annealed at 900°C for 13 min. No out-diffused emitter was incorporated. It is seen that there is no descernable influence of oxygen content on saturation current as would be expected from the heterojunction model. The film with $\gamma = 1.5$ has an oxygen concentration similar to that of the Sony-transistors[3]. Even the $\gamma = 0$ (no intentional oxygen) film has a low saturation current. These films, however, were found to dissolve in HF, indicating the presence of some oxygen.

As seen in Fig. 6, however, the film annealed at 1000°C has J_{oe} nearly an order of magnitude larger than those at 900°C. Clearly, anneal temperature is more important than oxygen concentration in determining saturation current.

4.2.2. J_{oe} vs anneal temperature. A series of experiments was conducted to determine the influence of anneal temperature on saturation current. In addition, it was decided to incorporate an intentional interface oxide on a portion of the devices on each wafer in order to help clarify the roles of interface vs bulk effects in the observed reduction in saturation current under SIPOS contacts. The interface oxide, called "chemox" here, is the result of omitting the final HF dip after an RCA clean. The SIPOS had $\gamma = 0$, or no intentional oxygen. Results are shown in Figs 7 and 8. The results for the aluminum contacted emitters are also shown.

For devices with no chemox and a pre-diffused emitter, Fig. 7, J_{oe} is relatively constant for anneal temperatures less than 850°C at a value of 1/20 that of aluminum contacted emitters. As the temperature increases above 900°C, J_{oe} increases, eventually approaching the value for the conventional emitter at

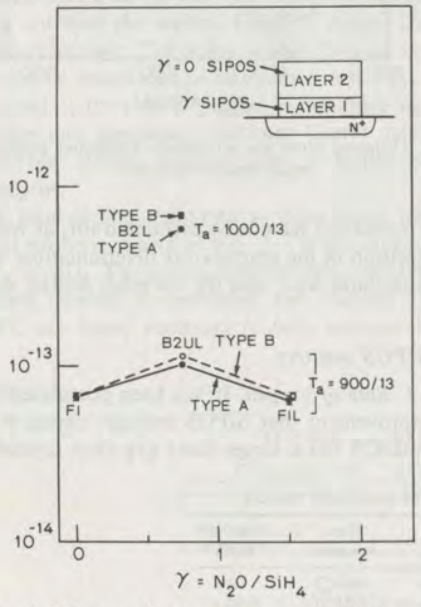


Fig. 6. Influence of oxygen content of SIPOS on J_{oe}.

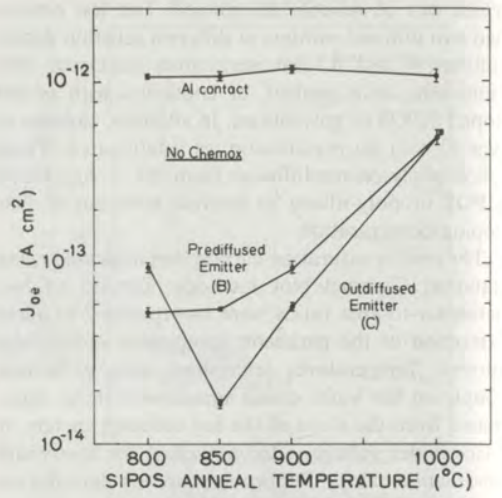


Fig. 7. Influence of anneal temperature on J_{oe} for SIPOS contacted emitters without chemox.

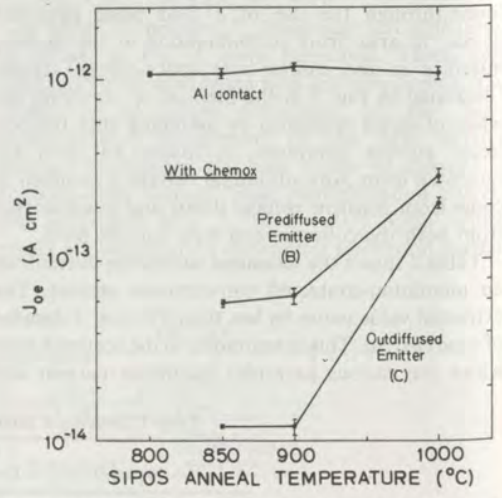


Fig. 8. Influence of anneal temperature on J_{oe} for SIPOS contacted emitters with chemox.

Petitioner Canadian Solar (USA) Inc., Ex. 1035, p. 2561

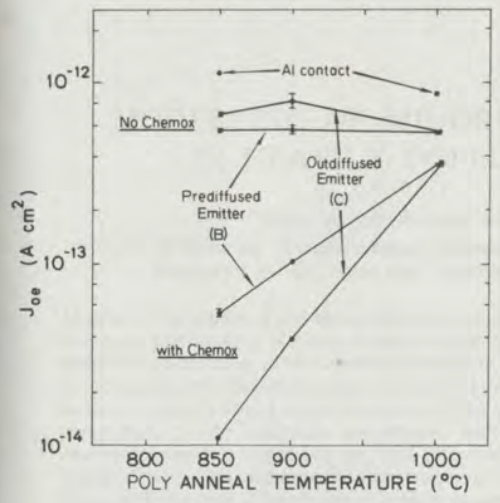


Fig. 9. Experimental J_{oe} vs anneal temperature for poly-silicon contacted emitters.

1000°C. If no pre-diffused emitter exists, J_{oe} starts rather high at 800°C, then exhibits a minimum at 850°C of only 2×10^{-14} A/cm^2. This is 1/50 that of the conventional emitter. Finally, J_{oe} again increases with higher anneal temperatures. Undoubtedly, in the 800°C case the surface of the silicon has not been doped sufficiently in the out-diffused case to limit the minority-carrier concentration at the SIPOS–Si interface, resulting in poor performance.

It is interesting to note that, excluding the 800°C case, J_{oe} for the pre-diffused emitter is 5×10^{-14} A/cm^2 plus that for the out-diffused case. This suggests that the total J_{oe} comes from a constant recombination in the diffused emitter plus that coming from the out-diffused portion. For such to be the case the quasi-Fermi levels throughout the emitter need be constant. This is approximately the case for these devices which have passivated surfaces. The increase in J_{oe} with anneal temperature is then explained as the result of increased doping, and hence reduced lifetime, in the out-diffused portion of the emitter. Alternatively, the increase could be due to the break-up of an interfacial oxide. Such an oxide could form, for example, during the anneal as oxygen segregates from the SIPOS. Perhaps both methods are operative.

When the chemox is incorporated, a slightly different picture emerges. At 800°C J_{oe} could not be extracted due to excessive series resistance. This resistance decreases with higher anneal temperatures suggesting the break-up of the interfacial oxide and an increase in surface doping concentration. At 850°C the results are substantially the same as with no chemox, Fig. 8. Annealing at 900°C, however, does not result in any increase in J_{oe} as was the case without a chemox. This suggests that either the chemox is acting as a barrier to the out-diffusion of phosphorus, and thus prevents lifetime reduction in the surface region, or alternatively, is more resistant to break-up during annealing than whatever oxide exists without the chemox.

4.3. *Poly-silicon emitters*

When it was discovered that the $\gamma = 0$ SIPOS films actually had significant oxygen, it was decided to compare these results with the case of poly-silicon deposited with a hydrogen carrier in an epi reactor. Such films contain very little oxygen. The results are shown in Fig. 9. In this case the emitters without chemox had J_{oe} only a factor of two less than the aluminum contacted emitters. This reduction can be theoretically accounted for simply from the increase in thickness of the highly doped emitter due to the addition of the poly-silicon. The addition of a chemox causes J_{oe} to be substantially the same as for SIPOS emitters. Once again, there is an additive effect between the pre-diffused and out-diffused emitters.

5. DISCUSSION AND CONCLUSIONS

Both poly-silicon and SIPOS emitters, in their optimized form, can achieve J_{oe} of less than 2×10^{-14} A/cm^2. For poly-silicon contacts this requires an interfacial chemox. The chemox is not necessary for SIPOS contacts. The similarity of results for the chemox poly-silicon contacts and SIPOS contacts suggests that these both obtain their improved performance through incorporating a thin, tunnelable interfacial oxide that impedes the flow of holes rather than as a result of the increased band gap of SIPOS. Preliminary results on p-type SIPOS emitters indicates that they have much poorer performance. This is consistent with a barrier that has a lower electron barrier height than hole barrier height, as does SiO_2.

Acknowledgement—This work was supported by the Department of Energy through Sandia National Laboratories.

REFERENCES

1. T. Matsushita, T. Aoki, T. Ohtsu *et al.*, *IEEE Trans. Electron Dev.* **23,** 826 (1976).
2. T. Matsushita, N. Oh-uchi, H. Hayashi and H. Yamoto, *Appl. Phys. Lett.* **35,** 549 (1979).
3. T. Matsushita, H. Hayashi and N. Oh-uchi, *Jap. J. appl. Phys.* (suppl) **20,** 75 (1981).
4. Y. H. Kwark, Stanford Electronics Laboratory Technical Report, Stanford University (1985).
5. M. Hamasaki, T. Adachi, S. Wakayama and M. Kikuchi, *J. appl. Phys.* **49,** 3987 (1978).
6. J. Ni and E. Arnold, *Appl. Phys. Lett.* **39,** 554 (1981).

Attachment E-3

Solid-State Electronics Vol. 30, No. 11, pp. 1121–1125, 1987
Printed in Great Britain

0038-1101/87 $3.00 + 0.00
Pergamon Journals Ltd

N-TYPE SIPOS AND POLY-SILICON EMITTERS

Y. H. KWARK and R. M. SWANSON
Stanford University, Stanford, CA 94305, U.S.A.

Abstract—*N*-type SIPOS and poly-silicon emitters on silicon show potential for improved minority carrier blocking properties over conventional diffused emitters. This paper discusses experiments designed to elucidate the physical mechanisms responsible for this improvement and to optimize the process conditions. Emitters both with and without an intentionally grown chemical oxide under the SIPOS or poly-silicon film are investigated. Both poly-silicon and SIPOS emitters, in their optimized form, can achieve J_{oe} of less than 2×10^{-14} A/cm^2, an improvement of several decades over shallow diffused emitters.

1. INTRODUCTION

SIPOS, for Semi-Insulating Poly-crystalline Silicon, has become the generic acronym for deposited silicon films doped with oxygen. The physical properties can be varied over a wide range by varying oxygen content. Indeed, normal poly-silicon and SiO_2 can be thought of as the limiting cases of no oxygen and full oxidation. The optical and electrical properties can be varied somewhat continuously between Si and SiO_2 by adjusting the oxygen content. *N* and *p*-type conduction can be obtained at low oxygen concentrations by doping with phosphorus and boron. These films, pioneered at Sony, found initial application in their intrinsic form to the passivation of high voltage devices[1]. Later, doped films were successfully applied to emitter contact structures, resulting in a 50-fold reduction of J_{oe} for *n*-type emitters[2,3]. This paper discusses experiments designed to elucidate the physical mechanisms responsible for this improvement and to optimize the process conditions. Further details are available in Ref. [4].

As deposited, SIPOS is usually amorphous. Annealing is necessary to activate the dopant and to produce films suitable for use as emitter contacts. During annealing it has been found that the film morphology changes. Si precipitates into small grains of crystalline Si and the oxygen segregates as SiO_2 on the grain boundaries[5]. One of the salient effects of oxygen incorporation is the suppression of grain growth, typical grain sizes being less than 100 Å. At higher oxygen concentrations, carrier transport is dominated by tunnelling through these thin SiO_2 shells[6].

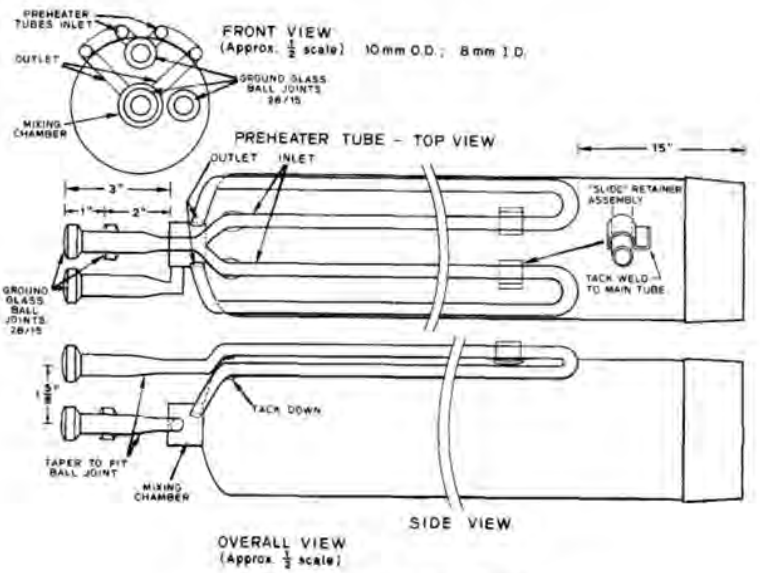


Fig. 1. SIPOS deposition tube—overall view.

Petitioner Canadian Solar (USA) Inc., Ex. 1035, p. 2564

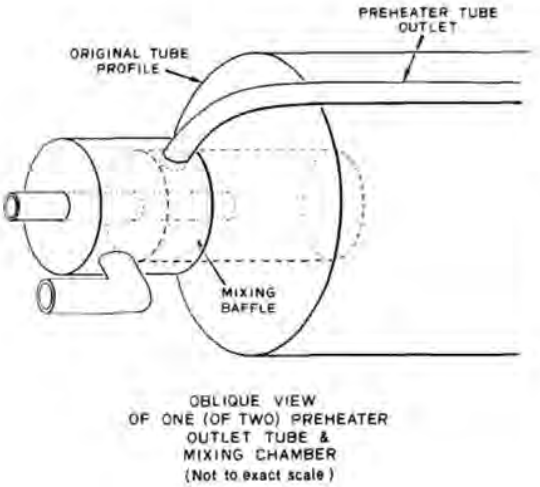


Fig. 2. SIPOS deposition tube—close up to mixing chamber.

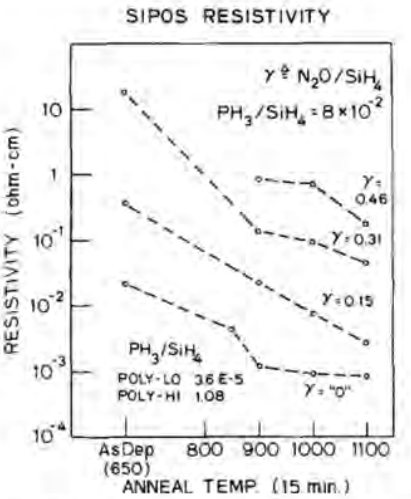


Fig. 3. $N+$ SIPOS film resistivity vs T_A and γ.

2. DEPOSITION

Evaporation, atmospheric CVD, and low pressure CVD have all been used to fabricate SIPOS layers. CVD techniques have been found most successful for device applications. Due to the lack of a low-pressure deposition system, atmospheric CVD was selected as the method for fabricating experimental films. Initial experiments in a cold-wall epitaxial reactor revealed that SIPOS is a difficult material to controllably deposit because of its non-stoichiometric nature. Useable areas of deposition extended only several centimeters over the susceptor. Accurate control of both temperature and flow dynamics was clearly needed. This suggested using a hot-wall system. The final configuration is shown in Fig. 1. A carrier gas preheater is used so that the high flow of nitrogen does not cool the wafers. Figure 2 details the gas-mixing chamber. The design is such that the reactant species are mixed due to turbulance in the gas flows. The end of the tube is purged to minimize stagnant regions and gas-phase reactions. Useful deposition with this system extends over 6 inches on the susceptor.

A plot of film resistivity as determined by four-point probe is shown in Fig. 3, γ is the mol ratio of N_2O to SiH_4. The strong dependence of resistivity on oxygen content is confirmed and anneals at over 900°C are found necessary to fully activate the dopant. It will be shown later that the $\gamma = 0$ films actually contain significant oxygen (as much as several atomic percent), probably due to residual water or oxygen in the deposition ambient; however, resistivities comparable to that of poly-silicon are obtained nevertheless.

3. MEASUREMENT OF J_{oe}

The relevant parameters which characterize the d.c. performance of an emitter are its saturation current, J_{oe}, and specific contact resistance, R_c. This report will concentrate mainly on the saturation current. J_{oe} characterizes the emitter recombination current because it is easily shown that, even in the case of SIPOS emitters, the minority-carrier hole current in low-level injection at the edge of the emitter-base junction space charge region follows the standard relation $J_p = J_{oe}(\exp qV_{be}/kT - 1)$.

In order to measure J_{oe}, transistor test structures, as shown in Fig. 4, were fabricated. These used epitaxially deposited bases with uniform doping concentration to allow extraction of the base-recombination component of the base current through modulating the base width via changes in collector-base voltage. Base recombination current was equivalent to a J_{oe} of 8×10^{-15} A/cm^2 which places a lower limit on the emitter saturation current

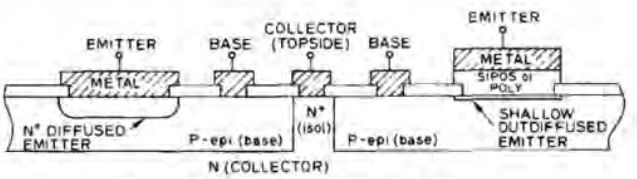


Fig. 4. Cross-section of bipolar test structures.

Petitioner Canadian Solar (USA) Inc., Ex. 1035, p. 2565

which can be reliably determined. The test devices had two diffused emitters of different junction depth, emitters A and B, that were either contacted with aluminum, as a control, or contacted with *in-situ* doped SIPOS or poly-silicon. In addition, emitters of type C with no prediffusion were fabricated. These relied solely on outdiffusion from the *in-situ* doped SIPOS or poly-silicon to provide sufficient surface doping concentration.

The emitter saturation current was measured using standard Gummel plot methods. Devices of two perimeter-to-area ratios were incorporated to allow extraction of the perimeter component of the base current. Temperatures determined using a thermocouple on the wafer chuck agreed with those determined from the slope of the log collector current vs base-emitter voltage, after correcting for base-width modulation effects. Reported saturation currents are "corrected" to 300 K using the relation:

$$J_{oe}(300\ \mathrm{K}) = J_{oe}(T_{\mathrm{device}})\frac{n_i^2(300\ \mathrm{K})}{n_i^2(T_{\mathrm{device}})}.$$

4. EXPERIMENTAL RESULTS

Three types of emitter contacts were studied, conventional aluminum contacts, SIPOS and polysilicon. In the latter two cases the emitters were fabricated both with and without an interfacial chemical oxide.

4.1. Conventional emitters

The pre-diffused emitter deposition parameters are shown in Table 1. Phosphine at 1100 ppm was used as the dopant source in these conventional predep and drive-in diffusions. Gummel plots for both the large and small devices are shown in Fig. 5. The extracted perimeter- and area-related current components are also shown. The perimeter current shows a strong non-ideal component which was found,through the use of a field plate equipped device, to arise from recombination at the $Si–SiO_2$ interface in the emitter-base space-charge region. Illustrated in Fig. 5 is the method of removing the effect of series resistance by assuming that the collector current continues to follow an ideal exponential form. Any additional voltage is assumed to come from resistive voltage drops and is subtracted from both the collector and base current plots.

Table 2 shows the measured saturation current for an aluminum-contacted conventional emitter. The extracted value varies by less than 4% over 4 decades of base current. This is testimony to the accuracy with which the various parasitics (perimeter current and series resistance) have been accounted for, as well as the precision of the temperature determination. Similar procedures were used for the other emitter structures.

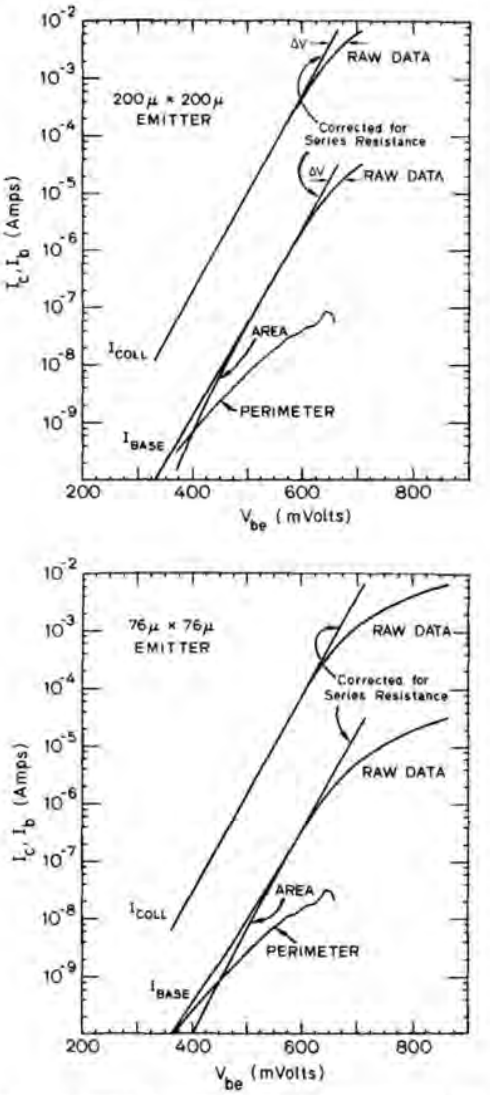


Fig. 5. Gummel plots for aluminum contacted large and small emitter devices.

4.2. SIPOS emitters

4.2.1. Role of oxygen. It has been postulated that the improvement that SIPOS emitters obtain is because SIPOS has a larger band gap than crystalline

Table 1. Deposition parameters for the prediffused emitters

	Predep (T/t)	Drive-in (T/t)	Sheet resistance	Junction depth
EM-A	800°C/30 min	1025°C/90 min	60Ω/□	1.0 μ
EM-B	800°C/30 min	1025°C/30 min	70Ω/□	0.66 μ

Petitioner Canadian Solar (USA) Inc., Ex. 1035, p. 2566

Table 2. Measured J_{oe} vs V_{be} for a conventional aluminum contacted transistor

V_{be} (V)	J_{oe} (10^{-12} A/cm^2)	V_{be} (V)	J_{oe} (10^{-12} A/cm^2)
0.392	1.18	0.545	1.18
0.409	1.21	0.562	1.17
0.426	1.21	0.579	1.17
0.443	1.20	0.596	1.16
0.460	1.19	0.613	1.16
0.477	1.19	0.630	1.15
0.494	1.19	0.647	1.13
0.511	1.19	0.664	1.13
0.528	1.18		

silicon so that the injected minority carriers see a barrier at the SIPOS–Si interface[3]. To test this hypothesis, SIPOS contacts with varying oxygen were fabricated with the results shown in Fig. 6. For these experiments, the SIPOS was annealed at 900°C for 13 min. No out-diffused emitter was incorporated. It is seen that there is no descernable influence of oxygen content on saturation current as would be expected from the heterojunction model. The film with $\gamma = 1.5$ has an oxygen concentration similar to that of the Sony-transistors[3]. Even the $\gamma = 0$ (no intentional oxygen) film has a low saturation current. These films, however, were found to dissolve in HF, indicating the presence of some oxygen.

As seen in Fig. 6, however, the film annealed at 1000°C has J_{oe} nearly an order of magnitude larger than those at 900°C. Clearly, anneal temperature is more important than oxygen concentration in determining saturation current.

4.2.2. J_{oe} vs anneal temperature. A series of experiments was conducted to determine the influence of anneal temperature on saturation current. In addition, it was decided to incorporate an intentional interface oxide on a portion of the devices on each wafer in order to help clarify the roles of interface vs bulk effects in the observed reduction in saturation current under SIPOS contacts. The interface oxide, called "chemox" here, is the result of omitting the final HF dip after an RCA clean. The SIPOS had $\gamma = 0$, or no intentional oxygen. Results are shown in Figs 7 and 8. The results for the aluminum contacted emitters are also shown.

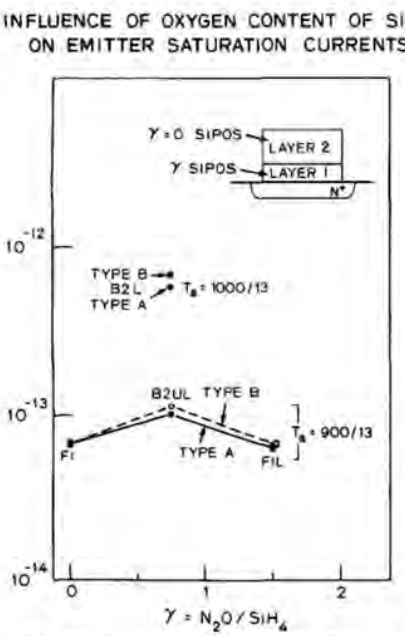


Fig. 6. Influence of oxygen content of SIPOS on J_{oe}.

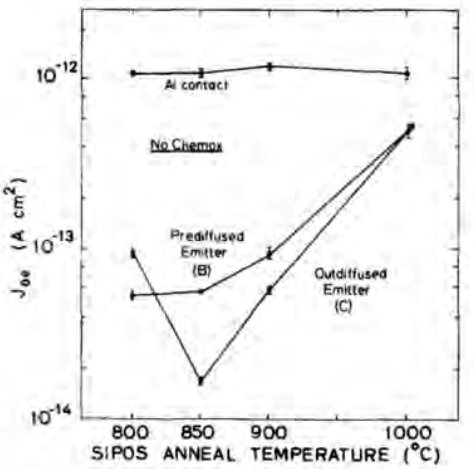


Fig. 7. Influence of anneal temperature on J_{oe} for SIPOS contacted emitters without chemox.

For devices with no chemox and a pre-diffused emitter, Fig. 7, J_{oe} is relatively constant for anneal temperatures less than 850°C at a value of 1/20 that of aluminum contacted emitters. As the temperature increases above 900°C, J_{oe} increases, eventually approaching the value for the conventional emitter at

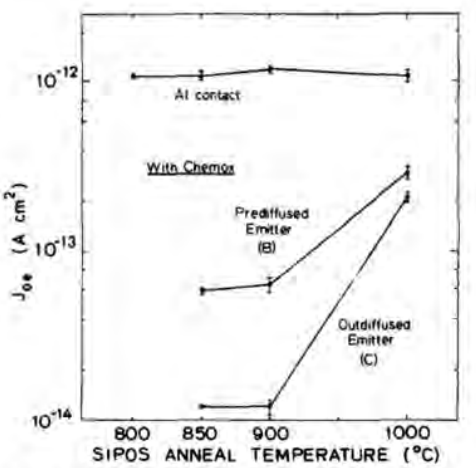


Fig. 8. Influence of anneal temperature on J_{oe} for SIPOS contacted emitters with chemox.

Petitioner Canadian Solar (USA) Inc., Ex. 1035, p. 2567

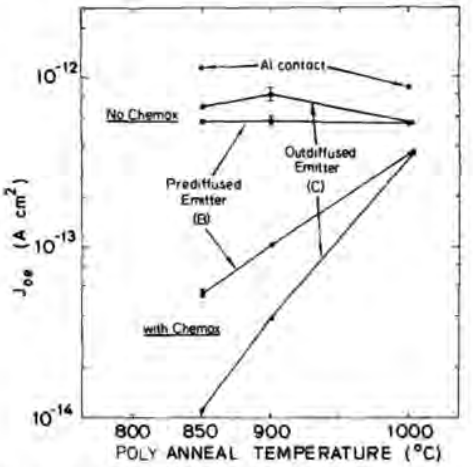


Fig. 9. Experimental J_{oe} vs anneal temperature for poly-silicon contacted emitters.

1000°C. If no pre-diffused emitter exists, J_{oe} starts rather high at 800°C, then exhibits a minimum at 850°C of only 2×10^{-14} A/cm^2. This is 1/50 that of the conventional emitter. Finally, J_{oe} again increases with higher anneal temperatures. Undoubtedly, in the 800°C case the surface of the silicon has not been doped sufficiently in the out-diffused case to limit the minority-carrier concentration at the SIPOS–Si interface, resulting in poor performance.

It is interesting to note that, excluding the 800°C case, J_{oe} for the pre-diffused emitter is 5×10^{-14} A/cm^2 plus that for the out-diffused case. This suggests that the total J_{oe} comes from a constant recombination in the diffused emitter plus that coming from the out-diffused portion. For such to be the case the quasi-Fermi levels throughout the emitter need be constant. This is approximately the case for these devices which have passivated surfaces. The increase in J_{oe} with anneal temperature is then explained as the result of increased doping, and hence reduced lifetime, in the out-diffused portion of the emitter. Alternatively, the increase could be due to the break-up of an interfacial oxide. Such an oxide could form, for example, during the anneal as oxygen segregates from the SIPOS. Perhaps both methods are operative.

When the chemox is incorporated, a slightly different picture emerges. At 800°C J_{oe} could not be extracted due to excessive series resistance. This resistance decreases with higher anneal temperatures suggesting the break-up of the interfacial oxide and an increase in surface doping concentration. At 850°C the results are substantially the same as with no chemox, Fig. 8. Annealing at 900°C, however, does not result in any increase in J_{oe} as was the case without a chemox. This suggests that either the chemox is acting as a barrier to the out-diffusion of phosphorus, and thus prevents lifetime reduction in the surface region, or alternatively, is more resistant to break-up during annealing than whatever oxide exists without the chemox.

4.3. Poly-silicon emitters

When it was discovered that the $\gamma = 0$ SIPOS films actually had significant oxygen, it was decided to compare these results with the case of poly-silicon deposited with a hydrogen carrier in an epi reactor. Such films contain very little oxygen. The results are shown in Fig. 9. In this case the emitters without chemox had J_{oe} only a factor of two less than the aluminum contacted emitters. This reduction can be theoretically accounted for simply from the increase in thickness of the highly doped emitter due to the addition of the poly-silicon. The addition of a chemox causes J_{oe} to be substantially the same as for SIPOS emitters. Once again, there is an additive effect between the pre-diffused and out-diffused emitters.

5. DISCUSSION AND CONCLUSIONS

Both poly-silicon and SIPOS emitters, in their optimized form, can achieve J_{oe} of less than 2×10^{-14} A/cm^2. For poly-silicon contacts this requires an interfacial chemox. The chemox is not necessary for SIPOS contacts. The similarity of results for the chemox poly-silicon contacts and SIPOS contacts suggests that these both obtain their improved performance through incorporating a thin, tunnelable interfacial oxide that impedes the flow of holes rather than as a result of the increased band gap of SIPOS. Preliminary results on p-type SIPOS emitters indicates that they have much poorer performance. This is consistent with a barrier that has a lower electron barrier height than hole barrier height, as does SiO_2.

Acknowledgement—This work was supported by the Department of Energy through Sandia National Laboratories.

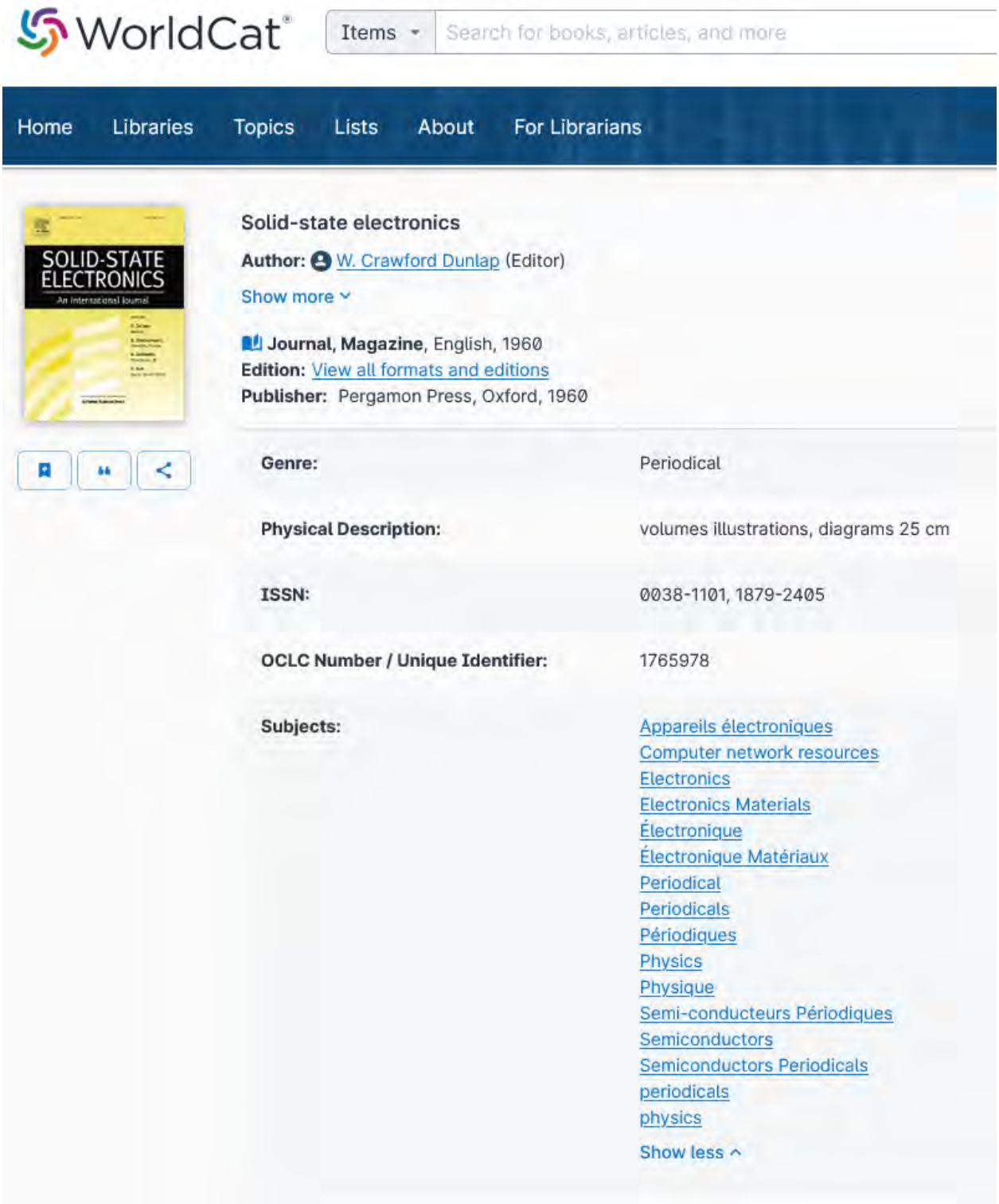
REFERENCES

1. T. Matsushita, T. Aoki, T. Ohtsu *et al.*, *IEEE Trans. Electron Dev.* **23**, 826 (1976).
2. T. Matsushita, N. Oh-uchi, H. Hayashi and H. Yamoto, *Appl. Phys. Lett.* **35**, 549 (1979).
3. T. Matsushita, H. Hayashi and N. Oh-uchi, *Jap. J. appl. Phys.* (suppl) **20**, 75 (1981).
4. Y. H. Kwark, Stanford Electronics Laboratory Technical Report, Stanford University (1985).
5. M. Hamasaki, T. Adachi, S. Wakayama and M. Kikuchi, *J. appl. Phys.* **49**, 3987 (1978).
6. J. Ni and E. Arnold, *Appl. Phys. Lett.* **39**, 554 (1981).

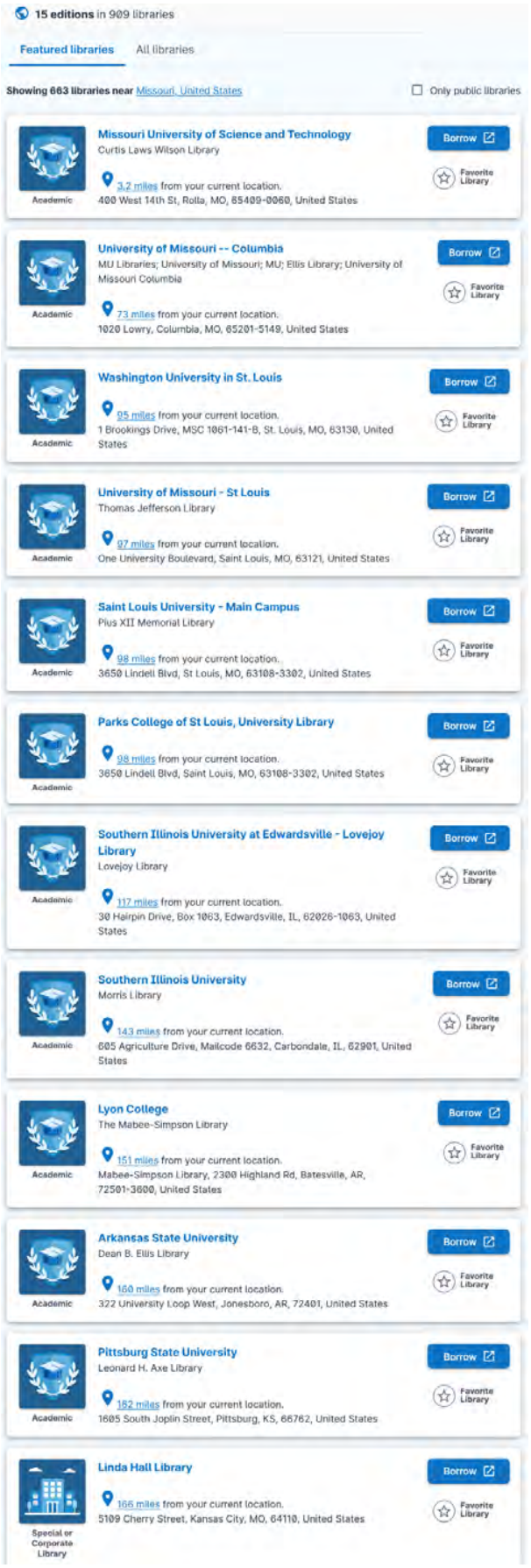
Petitioner Canadian Solar (USA) Inc., Ex. 1035, p. 2568

Attachment E-4

Screen capture completed by J L Mullins from WorldCat on August 24, 2024 at URL:
https://search.worldcat.org/title/1765978?oclcNum=1765978



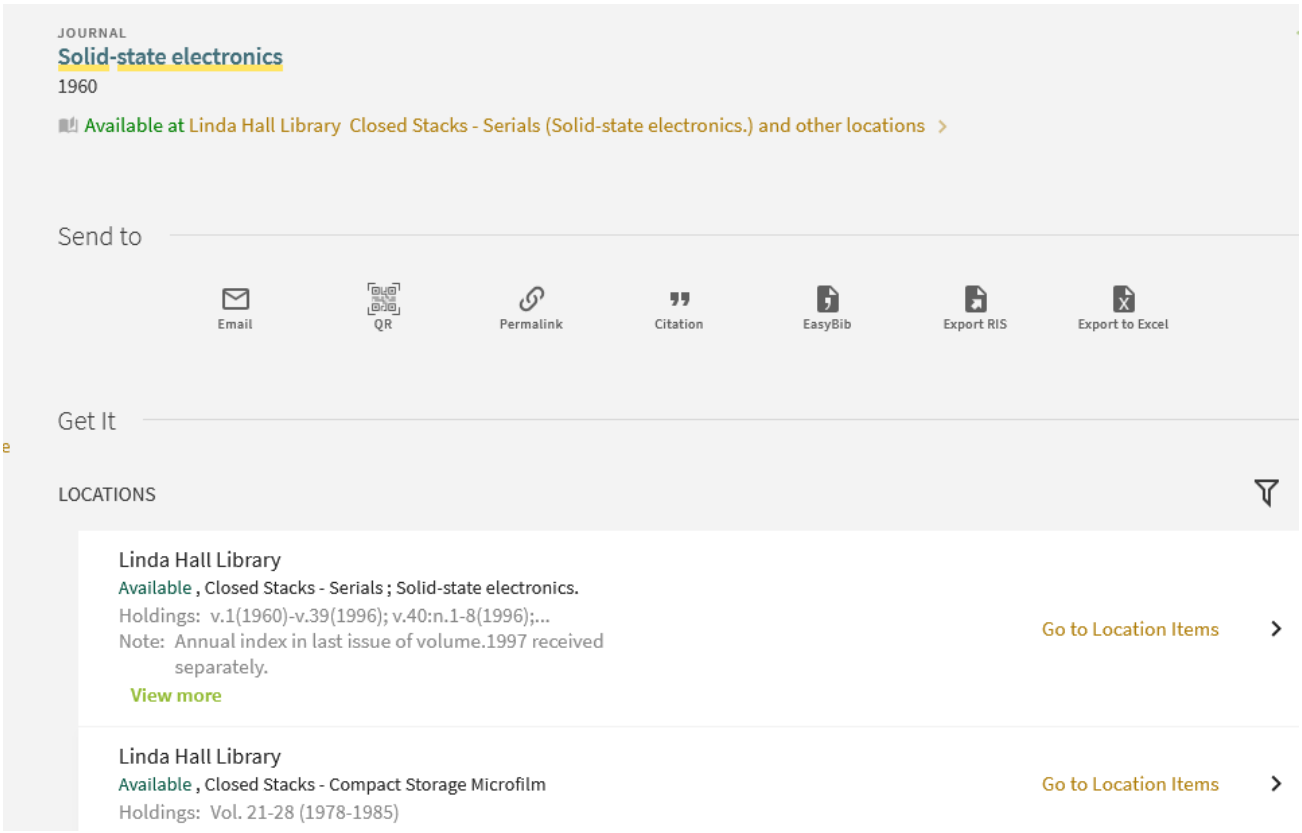
Screen capture completed by J L Mullins from WorldCat on August 24, 2024 at URL: https://search.worldcat.org/title/1765978?oclcNum=1765978



Attachment E-5

Screen capture created by J L Mullins from Linda Hall Library OPAC on August 24, 2024 at URL: https://catalog.lindahall.org/discovery/fulldisplay?docid=alma992683223405961&context=L&vid=01LINDAHALL_INST:LHL&lang=en&search_scope=MyInstitution&adaptor=Local%20Search%20Engine&tab=LibraryCatalog&query=any,contains,solid%20state%20electronics&mode=simple&offset=0





Screen capture created by J L Mullins from Linda Hall Library OPAC on August 24, 2024 at URL: https://catalog.lindahall.org/discovery/fulldisplay?docid=alma992683223405961&context=L&vid=01LINDAHALL_INST:LHL&lang=en&search_scope=MyInstitution&adaptor=Local%20Search%20Engine&tab=LibraryCatalog&query=any,contains,solid%20state%20electronics&mode=simple&offset=0

Details

Title	Solid-state electronics
Other title	Solid-state electron. Solid-state electronics Solid state electronics Applied superconductivity.
Subjects	Semiconductors ›
Identifier	ISSN : 0038-1101 OCLC : (OCoLC)1765978
Related title	Later title : Applied superconductivity. › Later title : Materials science in semiconductor processing. ›
Publisher	Oxford, New York, Pergamon Press. v. 1- Mar. 1960-
Creation date	1960
Format	v. ill., diagrs. 25 cm.
Frequency	Monthly, <Nov. 1975->
General notes	May and October 1998 include a section, Materials science in semiconductor processing, vol. 1, no. 1-2; v.1, no.3- published separately, which see for Library's holdings. Editor: Mar. 1960-<Nov. 1975> W.C. Crawford. Section on superconduction issued in separate publication: Applied superconductivity.
Citations/References	Applied science & technology index, Computer & control abstracts, Electrical & electronics abstracts, Physics abstracts, Chemical abstracts, Engineering index annual (1968), Engineering index bioengineering abstracts, Engineering index energy abstracts, Engineering index monthly (1984), International aerospace abstracts, Engineering index monthly, Nuclear science abstracts,

Attachment F-1

SIPOS HETEROJUNCTION CONTACTS TO SILICON

Young H. Kwark, Ron Sinton, Richard M. Swanson

110 McCullough Building, Stanford Electronics Laboratories
Stanford, CA. 94305 (415)497-0503

Abstract: Using SIPOS films (SiO_x, x <2) as an emitter contact has been previously shown to reduce the emitter saturation current, J_{oe}, by at least a factor of fifty when compared to a conventional emitter structure with a metallic contact. Previous attempts to explain this J_{oe} reduction have focused on the bulk properties of the SIPOS films. Experimental results of this study which attained J_{oe} values of $2 \times 10^{-}14$ A/cm^2, suggest that an interfacial layer between the SIPOS and underlying silicon may play an important, if not dominant, role with the implication that the high oxygen concentrations previously used may not be essential for J_{oe} reduction. This would permit the use of lower oxygen content SIPOS films whose lower bulk resistivities would allow utilization of these films in structures such as scaled VLSI bipolar devices and high concentration point contact solar cells where series resistance is detrimental to device performance.

Introduction: Deliberate introduction of controlled amounts of an oxygen bearing species such as nitrous oxide into the deposition ambient normally used for chemical vapor deposition of polysilicon produces SIPOS, a class of silicon oxides which exhibits a wide range of physical properties (1). It is possible to tailor film characteristics such as the refractive index, by altering the oxygen partial pressure in the deposition ambient. The addition of a dopant species converts these films from semi-insulating to a form that can be made sufficiently conductive after annealing to make them interesting for electronic applications (2). Incorporation of these films into the emitter structure of an NPN bipolar transistor had been found to reduce the emitter saturation current fifty fold (3); this translates into potential improvements of energy conversion efficiency for solar cells and enhanced high frequency performance of bipolar structures.

Matsushita (3) hypothesized that large amounts of oxygen in his SIPOS films produce a bandgap larger than for monocrystalline silicon. In N-type SIPOS emitter contacts the lining up of the equilibrium Fermi levels results in a barrier in the valence band which blocks hole transport and accounts for the reduction in J_{oe}. Simplified density of states calculations using small clusters of SiO_x lend qualitative support to this scenario; namely the gap in the density of states increases in a continuous manner as the oxygen content in SiO_x is increased (4). However, it is important to note that these clusters were constructed assuming a uniform and random distribution of oxygen throughout the film. While this may apply to films prepared at low temperatures (e.g. evaporation or sputtering), the CVD deposited SIPOS films used in these devices require a high temperature anneal in order to activate the dopant. A phase precipiation which results in a fine dispersion of silicon microcrystallites embedded in an oxygen rich matrix appears to be the result of such anneals (5). Such a heterogeneous structure would indicate that a model based on an effective bandgap and diffusion length may be oversimplified.

Experimental Results: Bipolar test structures and measurement techniques were refined to allow measurement of the emitter saturation current at these low levels; a sample Gummel plot showing the area related component from which J_{oe}, the emitter saturation current, was extracted is shown in Fig. 1. Devices with differing area/perimeter ratios were used in conjunction with the definition

$$I_{base} = Area * J_{area} + Perimeter * J_{peri}$$

to effect this separation. By utilizing various SIPOS emitter contact configurations, these measurements, after correcting to 300°K, allowed determination of which film parameters were relevant in determining the hole blocking action of the films.

The first set of experiments investigated the effect of varying the oxygen content on J_{oe}. These films were deposited in a hot wall APCVD reactor using nitrogen as the carrier gas. Varying γ, the ratio of nitrous oxide to silane in the deposition ambient, from $\gamma = 0$ (which should produce POLY) to $\gamma = 1.5$ (which should produce films comparable to ref. (3)) should display a monotonically decreasing J_{oe} as hole transport is increasingly impeded by the increasing bandgap in the bulk SIPOS. In fact for devices annealed at 900°C/13 min, there is very little dependence on γ as seen in Fig. 2, although increasing the anneal temperature to 1000°C adversly affected J_{oe}. That the γ=0 films produced such good results was surprising since POLY films of comparble thickness should yield a J_{oe} an order of magnitude larger. In fact it was discovered that these $\gamma = 0$ films

CH2099-0/84/0000-0742 $1.00 © 1984 IEDM

Authorized licensed use limited to: Sidley Austin LLP. Downloaded on March 26,2024 at 22:45:30 UTC from IEEE Xplore. Restrictions apply.

Petitioner Canadian Solar (USA) Inc., Ex. 1035, p. 2576

incorporated significant (several atomic %) amounts of oxygen as indicated from electron microprobe and the fact that they etched, albeit slowly, in buffered HF. This insensitivity to bulk film properties implies that other mechanisms, in this case the formation of an interfacial oxide layer as a result of the annealing process (Fig. 3), may be primarily responsible for the reduced hole currents. This conclusion suggests that the mechanism of hole suppression is akin to that for polysilicon SIS contacts, and that the distinguishing feature of SIPOS may be its built-in source of oxygen which aids in the formation and/or maintainence of this interfacial layer.

In order to establish unambiguous results for a relatively oxygen free film, POLY films doped insitu in an RF heated cold wall APCVD reactor using a hydrogen carrier were used in the next set of emitter contacts; these films did not etch in BHF. Fig. 4 displays the resulting J_{oe} as a function of annealing temperature for emitter B which had a Gaussian (3×10^{19} surface concentration, 1 micron depth into 5×10^{16} background) emitter diffused prior to the POLY deposition and emitter C which relied solely on outdiffusion from the doped POLY to form the base-emitter junction. For both structures, devices were prepared with and without a chemically grown oxide (chemox) by dipping half of the wafer which underwent a full RCA clean in dilute HF. The value for emitter B with a conventional aluminum contact is shown for reference. Addition of POLY without the chemox does not greatly impact J_{oe} as would be expected since the heavily doped POLY acts essentially as an extension of the monocrystalline emitter. Addition of the chemox greatly decreases the J_{oe} as has been previously reported (6). "Prediffused" emitter B displays a baseline J_{oe} of 5×10^{-14} A/cm^2 due to recombination in the bulk of the emitter. To this is added a component due to outdiffusion from the heavily doped POLY which becomes increasingly significant for annealing temperatures above 900°C. This is apparent if one notes that the increase in J_{oe} for emitter B can be accounted for by the J_{oe} of emitter C at the same temperature. At 1000°C, this outdiffusion is severe enough to dominate the J_{oe} which accounted for the lack of difference between emitters B and C.

In Fig. 5, J_{oe} for a $\gamma = 0$ SIPOS film (which recall has several at% oxygen) without the chemox is shown. The behavior above 850°C strongly resembles the POLY case with chemox. Addition of the chemox to the SIPOS contact structure does not greatly affect the lowest values of J_{oe} attained. However, the increase in J_{oe} at higher temperatures is not as severe as for the devices in Fig. 4 and 5. Furthermore, devices annealed at 850°C, while displaying the same J_{oe} as the SIPOS devices without the chemox, also suffered from greatly increased series resistance.

Discussion: Emitter saturation currents of $1 - 2 \times 10^{-14}$ A/cm^2 have been attained for POLY with chemox and for both SIPOS contact structures. That there was little difference in J_{oe} between the SIPOS contacted emitters with and without the chemox would indicate that the interface between SIPOS and monocrystalline silicon is similar in both cases. Postulating the formation of a thin tunnelable interfacial oxide as a consequence of the high temperature annealing step is consistent with the observed similarities in J_{oe}. The smaller increase in J_{oe} for the SIPOS device with chemox can be explained by assuming that the chemox simply adds an additional thickness to the oxide layer resulting from the anneal step. This would act as a more robust diffusion barrier and would limit the extent of outdiffusion of dopants from the SIPOS thus reducing bulk recombination in the monocrystalline emitter region. This is also consistent with the increased series resistance which would arise from a thicker interfacial layer. The possibilty remains that a thin thermal oxide is growing during the thermal equilibration phase prior to deposition of the SIPOS films; although standard precautions were taken to minimze the presence of oxygen and water vapor in the deposition ambient, the apparatus currently available can not be used to rule out this possibility.

A key figure of merit which has not been discussed is the specific resistivity of the emitter contact structure. For the SIPOS films mentioned in ref. (3), a specific contact resistivity of 1×10^{-3} ohm-cm^2 would result for a 1000 angstrom thick film. This is far too high to permit use in scaled bipolar or in high concentration point contact solar cells. If the hole barrier mechanism operative in SIPOS contacts is indeed associated with the formation of interfacial layers, then there is no apriori need for such high oxygen concentrations in the bulk of the films with their attendant high resistivity. The focus, in this case, would shift to the kinetics of the annealing process and to the morphology of the near interface region, much as is the case with POLY SIS structures. For the $\gamma = 0$ SIPOS contacts, an upper limit to the specific resistivity can be set at 1×10^{-4} ohm-cm^2 from device Gummel plots; although the actual value is quite likely to be far below this, the presence of other parasitic resistances does not allow a more refined determination from the device data. The ability to directly measure the voltage drop at the interface is being incorporated into the next mask set.

References:

(1) D. Dong, E. Irene, et al "Preparation and Some Properties of CVD Si-rich SiO_2 and Si_3N_4 Films", J. Electrochemical Soc. 125(5), May 1978, p819

(2) H. Yamoto, N. Oh-uchi , et al "New Technology by the Use of Doped SIPOS Films", ECS Abstracts, #168, 1979

(3) T. Matsushita, "A Silicon Heterojunction Transistor," Appl. Phys. Lett., vol 35(7), p 549, 1979

(4) A. Bennet, L. Roth "Calculation of the Optical Properties of Amorphous SiO_x Materials" Phys. Rev. B 4(8), Oct. 15, 1971, p 2686

(5) M. Hamasaki, "Crystallographic Study of SIPOS Doped with Oxygen Atoms,"J. Appl. Phys. 49(7), p 3987, 1978

(6) B. Soerowirdjo, P. Ashburn, et al "The Influence of Surface Treatments on the Electrical Characteristics of Polysilicon Emitter Bipolar Transistors" Tech. Digest IEDM, 1982, p 668

Authorized licensed use limited to: Sidley Austin LLP. Downloaded on March 26,2024 at 22:45:30 UTC from IEEE Xplore. Restrictions apply.

Petitioner Canadian Solar (USA) Inc., Ex. 1035, p. 2577

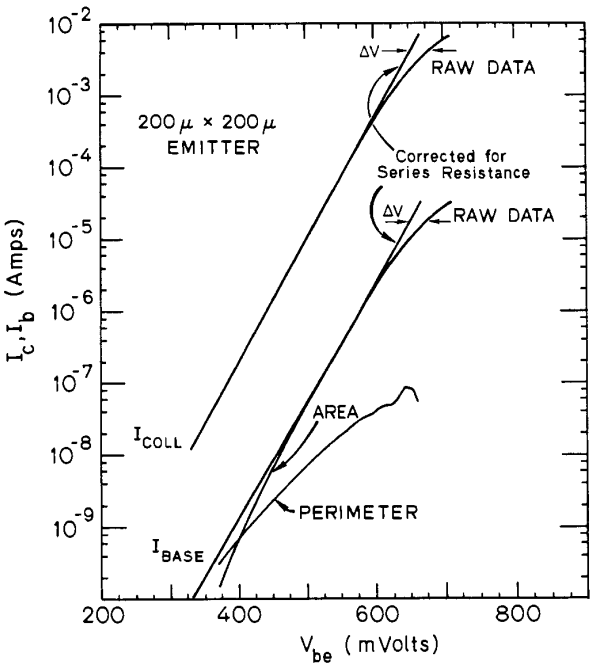


Fig. 1: Gummel plot of test bipolar structure showing area and perimeter related components.

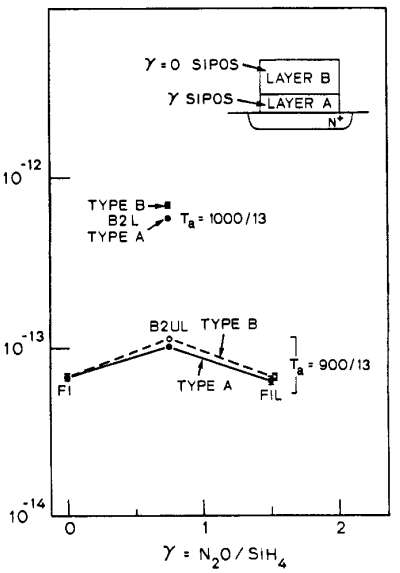


Fig.2: γ is the ratio of nitrous oxide to silane in the SIPOS deposition ambient, T_a is the anneal temperature (followed by a slash and anneal time in minutes). Layer B is a 2000 angstrom capping layer; layer A is the "active layer" ranging from 1000 to 1600 angstroms.

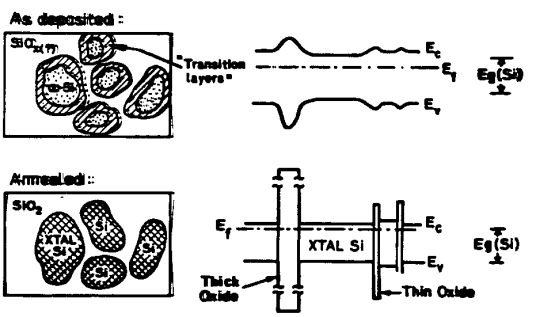


Fig. 3: (A) postulated structure of as-deposited SIPOS (B) and after annealing; the "oxide-like" regions become more SiO_2-like, accompanied by crystallization of the silicon crystallites.

Authorized licensed use limited to: Sidley Austin LLP. Downloaded on March 26,2024 at 22:45:30 UTC from IEEE Xplore. Restrictions apply.

Petitioner Canadian Solar (USA) Inc., Ex. 1035, p. 2578

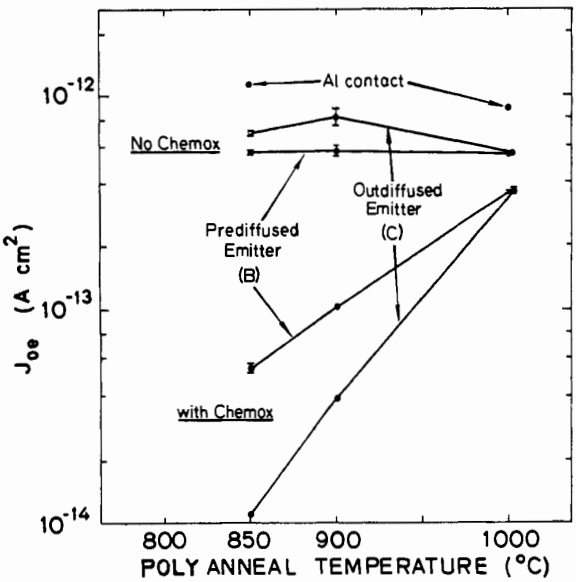


Fig. 4: emitter saturation current for POLY contacts with and without a chemically grown interfacial layer vs. anneal temperature. Thicknesses range from 3000-3600 angstroms. Note the large difference when the interfacial oxide is missing.

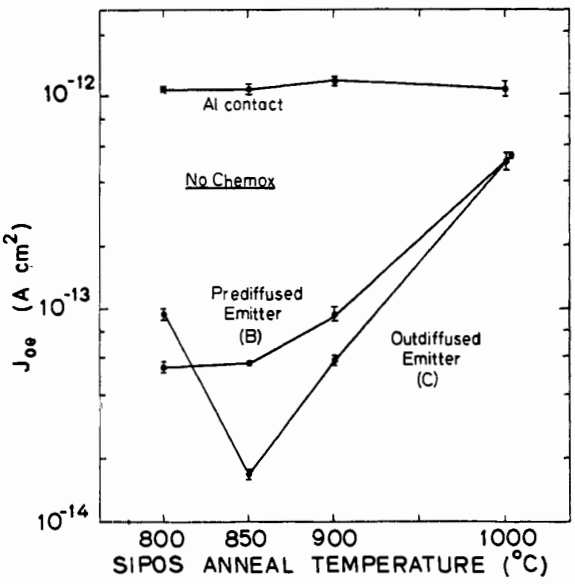


Fig. 5: emitter saturation current vs. anneal temperature for SIPOS contacts without a chemically grown interfacial oxide. The $\gamma = 0$ SIPOS layer is 3300 angstroms thick.

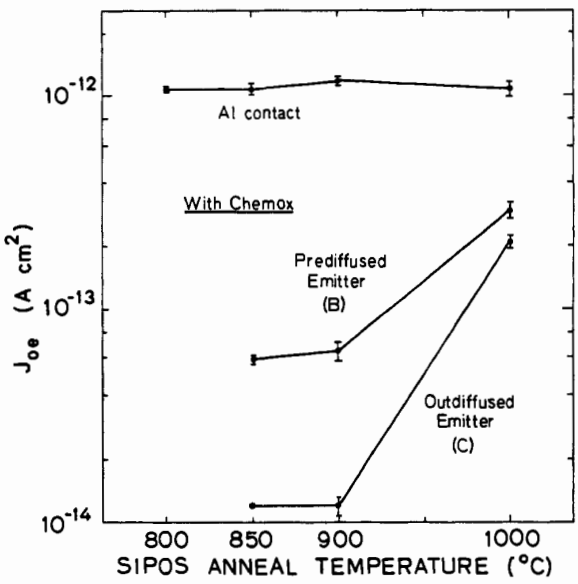


Fig. 6: emitter saturation current vs. anneal temperature for SIPOS contacts with a chemically grown interfacial oxide. The $\gamma = 0$ SIPOS layer is 3300 angstroms thick.

Authorized licensed use limited to: Sidley Austin LLP. Downloaded on March 26,2024 at 22:45:30 UTC from IEEE Xplore. Restrictions apply.

Petitioner Canadian Solar (USA) Inc., Ex. 1035, p. 2579

Attachment F-2

SIPOS HETEROJUNCTION CONTACTS TO SILICON

Young H. Kwark, Ron Sinton, Richard M. Swanson

110 McCullough Building, Stanford Electronics Laboratories
Stanford, CA. 94305 (415)497-0503

Abstract: Using SIPOS films (SiO_x, x <2) as an emitter contact has been previously shown to reduce the emitter saturation current, J_{oe}, by at least a factor of fifty when compared to a conventional emitter structure with a metallic contact. Previous attempts to explain this J_{oe} reduction have focused on the bulk properties of the SIPOS films. Experimental results of this study which attained J_{oe} values of $2 \times 10^{-}14$ A/cm^2, suggest that an interfacial layer between the SIPOS and underlying silicon may play an important, if not dominant, role with the implication that the high oxygen concentrations previously used may not be essential for J_{oe} reduction. This would permit the use of lower oxygen content SIPOS films whose lower bulk resistivities would allow utilization of these films in structures such as scaled VLSI bipolar devices and high concentration point contact solar cells where series resistance is detrimental to device performance.

Introduction: Deliberate introduction of controlled amounts of an oxygen bearing species such as nitrous oxide into the deposition ambient normally used for chemical vapor deposition of polysilicon produces SIPOS, a class of silicon oxides which exhibits a wide range of physical properties (1). It is possible to tailor film characteristics such as the refractive index, by altering the oxygen partial pressure in the deposition ambient. The addition of a dopant species converts these films from semi-insulating to a form that can be made sufficiently conductive after annealing to make them interesting for electronic applications (2). Incorporation of these films into the emitter structure of an NPN bipolar transistor had been found to reduce the emitter saturation current fifty fold (3); this translates into potential improvements of energy conversion efficiency for solar cells and enhanced high frequency performance of bipolar structures.

Matsushita (3) hypothesized that large amounts of oxygen in his SIPOS films produce a bandgap larger than for monocrystalline silicon. In N-type SIPOS emitter contacts the lining up of the equilibrium Fermi levels results in a barrier in the valence band which blocks hole transport and accounts for the reduction in J_{oe}. Simplified density of states calculations using small clusters of SiO_x lend qualitative support to this scenario; namely the gap in the density of states increases in a continuous manner as the oxygen content in SiO_x is increased (4). However, it is important to note that these clusters were constructed assuming a uniform and random distribution of oxygen throughout the film. While this may apply to films prepared at low temperatures (e.g. evaporation or sputtering), the CVD deposited SIPOS films used in these devices require a high temperature anneal in order to activate the dopant. A phase precipiation which results in a fine dispersion of silicon microcrystallites embedded in an oxygen rich matrix appears to be the result of such anneals (5). Such a heterogeneous structure would indicate that a model based on an effective bandgap and diffusion length may be oversimplified.

Experimental Results: Bipolar test structures and measurement techniques were refined to allow measurement of the emitter saturation current at these low levels; a sample Gummel plot showing the area related component from which J_{oe}, the emitter saturation current, was extracted is shown in Fig. 1. Devices with differing area/perimeter ratios were used in conjunction with the definition

$$I_{base} = Area * J_{area} + Perimeter * J_{peri}$$

to effect this separation. By utilizing various SIPOS emitter contact configurations, these measurements, after correcting to 300°K, allowed determination of which film parameters were relevant in determining the hole blocking action of the films.

The first set of experiments investigated the effect of varying the oxygen content on J_{oe}. These films were deposited in a hot wall APCVD reactor using nitrogen as the carrier gas. Varying γ, the ratio of nitrous oxide to silane in the deposition ambient, from $\gamma = 0$ (which should produce POLY) to $\gamma = 1.5$ (which should produce films comparable to ref. (3)) should display a monotonically decreasing J_{oe} as hole transport is increasingly impeded by the increasing bandgap in the bulk SIPOS. In fact for devices annealed at 900°C/13 min, there is very little dependence on γ as seen in Fig. 2, although increasing the anneal temperature to 1000°C adversly affected J_{oe}. That the γ=0 films produced such good results was surprising since POLY films of comparble thickness should yield a J_{oe} an order of magnitude larger. In fact it was discovered that these $\gamma = 0$ films

CH2099-0/84/0000-0742 $1.00 © 1984 IEDM

Authorized licensed use limited to: Purdue University. Downloaded on August 22,2024 at 14:10:08 UTC from IEEE Xplore. Restrictions apply.

Petitioner Canadian Solar (USA) Inc., Ex. 1035, p. 2581

incorporated significant (several atomic %) amounts of oxygen as indicated from electron microprobe and the fact that they etched, albeit slowly, in buffered HF. This insensitivity to bulk film properties implies that other mechanisms, in this case the formation of an interfacial oxide layer as a result of the annealing process (Fig. 3), may be primarily responsible for the reduced hole currents. This conclusion suggests that the mechanism of hole suppression is akin to that for polysilicon SIS contacts, and that the distinguishing feature of SIPOS may be its built-in source of oxygen which aids in the formation and/or maintainence of this interfacial layer.

In order to establish unambiguous results for a relatively oxygen free film, POLY films doped insitu in an RF heated cold wall APCVD reactor using a hydrogen carrier were used in the next set of emitter contacts; these films did not etch in BHF. Fig. 4 displays the resulting J_{oe} as a function of annealing temperature for emitter B which had a Gaussian (3×10^{19} surface concentration, 1 micron depth into 5×10^{16} background) emitter diffused prior to the POLY deposition and emitter C which relied solely on outdiffusion from the doped POLY to form the base-emitter junction. For both structures, devices were prepared with and without a chemically grown oxide (chemox) by dipping half of the wafer which underwent a full RCA clean in dilute HF. The value for emitter B with a conventional aluminum contact is shown for reference. Addition of POLY without the chemox does not greatly impact J_{oe} as would be expected since the heavily doped POLY acts essentially as an extension of the monocrystalline emitter. Addition of the chemox greatly decreases the J_{oe} as has been previously reported (6). "Prediffused" emitter B displays a baseline J_{oe} of 5×10^{-14} A/cm^2 due to recombination in the bulk of the emitter. To this is added a component due to outdiffusion from the heavily doped POLY which becomes increasingly significant for annealing temperatures above 900°C. This is apparent if one notes that the increase in J_{oe} for emitter B can be accounted for by the J_{oe} of emitter C at the same temperature. At 1000°C, this outdiffusion is severe enough to dominate the J_{oe} which accounted for the lack of difference between emitters B and C.

In Fig. 5, J_{oe} for a $\gamma = 0$ SIPOS film (which recall has several at% oxygen) without the chemox is shown. The behavior above 850°C strongly resembles the POLY case with chemox. Addition of the chemox to the SIPOS contact structure does not greatly affect the lowest values of J_{oe} attained. However, the increase in J_{oe} at higher temperatures is not as severe as for the devices in Fig. 4 and 5. Furthermore, devices annealed at 850°C, while displaying the same J_{oe} as the SIPOS devices without the chemox, also suffered from greatly increased series resistance.

Discussion: Emitter saturation currents of $1 - 2 \times 10^{-14}$ A/cm^2 have been attained for POLY with chemox and for both SIPOS contact structures. That there was little difference in J_{oe} between the SIPOS contacted emitters with and without the chemox would indicate that the interface between SIPOS and monocrystalline silicon is similar in both cases. Postulating the formation of a thin tunnelable interfacial oxide as a consequence of the high temperature annealing step is consistent with the observed similarities in J_{oe}. The smaller increase in J_{oe} for the SIPOS device with chemox can be explained by assuming that the chemox simply adds an additional thickness to the oxide layer resulting from the anneal step. This would act as a more robust diffusion barrier and would limit the extent of outdiffusion of dopants from the SIPOS thus reducing bulk recombination in the monocrystalline emitter region. This is also consistent with the increased series resistance which would arise from a thicker interfacial layer. The possibilty remains that a thin thermal oxide is growing during the thermal equilibration phase prior to deposition of the SIPOS films; although standard precautions were taken to minimze the presence of oxygen and water vapor in the deposition ambient, the apparatus currently available can not be used to rule out this possibility.

A key figure of merit which has not been discussed is the specific resistivity of the emitter contact structure. For the SIPOS films mentioned in ref. (3), a specific contact resistivity of 1×10^{-3} ohm-cm^2 would result for a 1000 angstrom thick film. This is far too high to permit use in scaled bipolar or in high concentration point contact solar cells. If the hole barrier mechanism operative in SIPOS contacts is indeed associated with the formation of interfacial layers, then there is no apriori need for such high oxygen concentrations in the bulk of the films with their attendant high resistivity. The focus, in this case, would shift to the kinetics of the annealing process and to the morphology of the near interface region, much as is the case with POLY SIS structures. For the $\gamma = 0$ SIPOS contacts, an upper limit to the specific resistivity can be set at 1×10^{-4} ohm-cm^2 from device Gummel plots; although the actual value is quite likely to be far below this, the presence of other parasitic resistances does not allow a more refined determination from the device data. The ability to directly measure the voltage drop at the interface is being incorporated into the next mask set.

References:

(1) D. Dong, E. Irene, et al "Preparation and Some Properties of CVD Si-rich SiO_2 and Si_3N_4 Films", J. Electrochemical Soc. 125(5), May 1978, p819

(2) H. Yamoto, N. Oh-uchi , et al "New Technology by the Use of Doped SIPOS Films", ECS Abstracts, #168, 1979

(3) T. Matsushita, "A Silicon Heterojunction Transistor," Appl. Phys. Lett., vol 35(7), p 549, 1979

(4) A. Bennet, L. Roth "Calculation of the Optical Properties of Amorphous SiO_x Materials" Phys. Rev. B 4(8), Oct. 15, 1971, p 2686

(5) M. Hamasaki, "Crystallographic Study of SIPOS Doped with Oxygen Atoms,"J. Appl. Phys. 49(7), p 3987, 1978

(6) B. Soerowirdjo, P. Ashburn, et al "The Influence of Surface Treatments on the Electrical Characteristics of Polysilicon Emitter Bipolar Transistors" Tech. Digest IEDM, 1982, p 668

Authorized licensed use limited to: Purdue University. Downloaded on August 22,2024 at 14:10:08 UTC from IEEE Xplore. Restrictions apply.

Petitioner Canadian Solar (USA) Inc., Ex. 1035, p. 2582

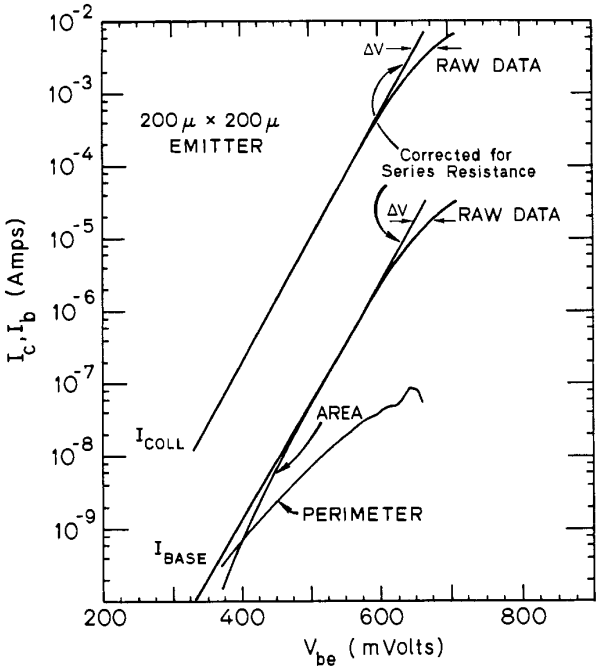


Fig. 1: Gummel plot of test bipolar structure showing area and perimeter related components.

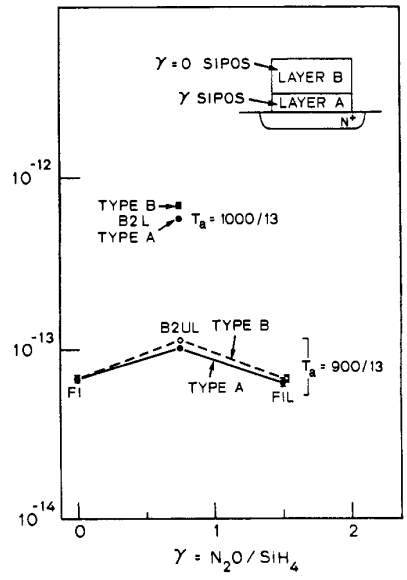


Fig.2: γ is the ratio of nitrous oxide to silane in the SIPOS deposition ambient, T_a is the anneal temperature (followed by a slash and anneal time in minutes). Layer B is a 2000 angstrom capping layer; layer A is the "active layer" ranging from 1000 to 1600 angstroms.

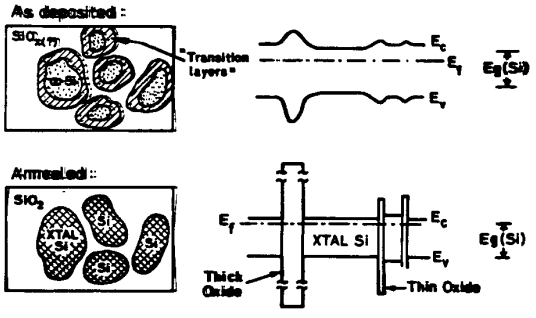


Fig. 3: (A) postulated structure of as-deposited SIPOS (B) and after annealing; the "oxide-like" regions become more SiO_2-like, accompanied by crystallization of the silicon crystallites.

Authorized licensed use limited to: Purdue University. Downloaded on August 22,2024 at 14:10:08 UTC from IEEE Xplore. Restrictions apply.

Petitioner Canadian Solar (USA) Inc., Ex. 1035, p. 2583

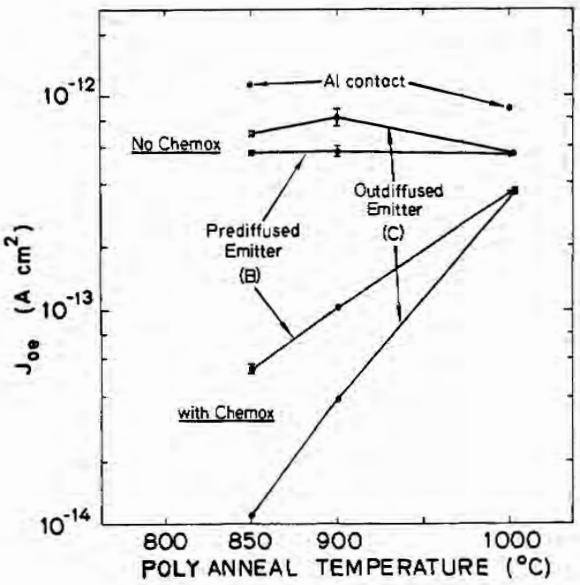


Fig. 4: emitter saturation current for POLY contacts with and without a chemically grown interfacial layer vs. anneal temperature. Thicknesses range from 3000-3600 angstroms. Note the large difference when the interfacial oxide is missing.

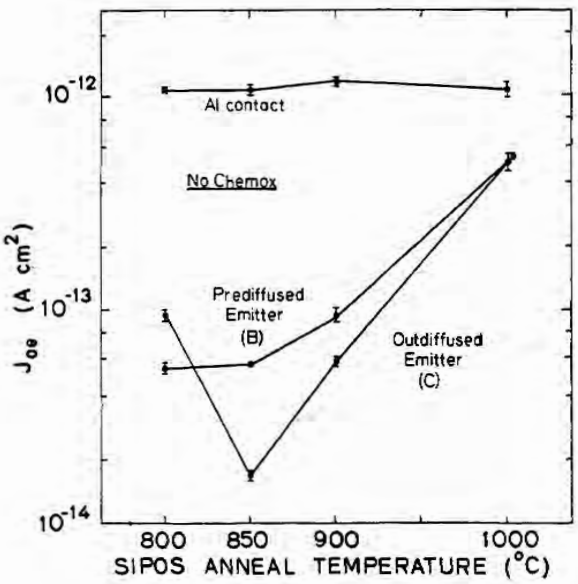


Fig. 5: emitter saturation current vs. anneal temperature for SIPOS contacts without a chemically grown interfacial oxide. The $\gamma = 0$ SIPOS layer is 3300 angstroms thick.

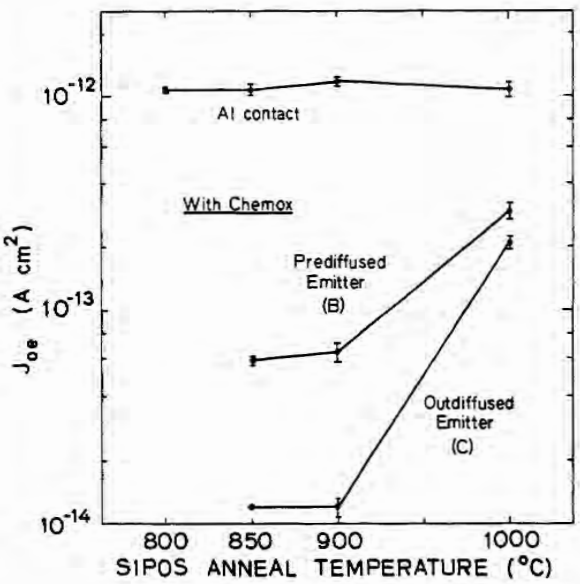


Fig. 6: emitter saturation current vs. anneal temperature for SIPOS contacts with a chemically grown interfacial oxide. The $\gamma = 0$ SIPOS layer is 3300 angstroms thick.

Authorized licensed use limited to: Purdue University. Downloaded on August 22,2024 at 14:10:08 UTC from IEEE Xplore. Restrictions apply.

Petitioner Canadian Solar (USA) Inc., Ex. 1035, p. 2584